THROUGH-BOND ENERGY TRANSFER CASSETTES FOR MULTIPLEXING AND DEVELOPMENT OF METHODS FOR PROTEIN MONO-LABELING

A Dissertation

by

YUICHIRO UENO

Submitted to the Office of Graduate Studies of
Texas A&M University
in partial fulfillment of the requirements for the degree of

DOCTOR OF PHILOSOPHY

May 2009

Major Subject: Chemistry

THROUGH-BOND ENERGY TRANSFER CASSETTES FOR MULTIPLEXING AND DEVELOPMENT OF METHODS FOR PROTEIN MONO-LABELING

A Dissertation

by

YUICHIRO UENO

Submitted to the Office of Graduate Studies of
Texas A&M University
in partial fulfillment of the requirements for the degree of

DOCTOR OF PHILOSOPHY

Approved by:

Chair of Committee,	Kevin Burgess
Committee Members,	Eric E. Simanek
	Daniel A. Singleton
	Robert C. Burghardt
Head of Department,	David H. Russell

May 2009

Major Subject: Chemistry

ABSTRACT

Through-bond Energy Transfer Cassettes for Multiplexing and
Development of Methods for Protein Mono-labeling.
(May 2009)
Yuichiro Ueno, B.S., Fukuoka University, Japan; M.S., Fukuoka University, Japan
Chair of Advisory Committee: Dr. Kevin Burgess

A set of three through-bond energy transfer cassettes based on BODIPY as a donor and cyanine dyes as acceptors has been prepared via Sonogashira couplings, and their photophysical properties were examined. These cassettes fluoresce around 600 to 800 nm and are resolved by approximately 100 nm. This property is an important factor for multiplexing study in cellular imaging. Several useful fluorescent probes such as 5- and 6-carboxyfluorescein, water-soluble BODIPY, and water-soluble Nile Blue dyes, have also been synthesized and their photophysical properties studied.

We have also attempted to develop a method for protein mono-labeling via a solid-phase approach. The labeling of protein with one fluorescent dye facilitates quantification and single molecule imaging in biological applications. Various solid-supports such as PEGA, CPG, and BSA-coated CPG, were tested. Photolabile and chemically cleavable linkers were prepared to connect solid-supports and fluorophores. Unfortunately, our approach to the fluorescent mono-labeling of native proteins did not give us any conclusive results.

ACKNOWLEDGEMENTS

I would like to thank Professor Kevin Burgess, my research advisor, for providing a conducive environment to independent research. I really appreciate him for his helpful advice and guidance.

Thanks to Professors Eric Simanek, Daniel Singleton, and Robert Burghardt for serving on my graduate advisory committee.

Thanks to Mingchien Li, Roy Estrada, and Professor Gyula Vigh for CE analyses of my samples and Dr. Shane Tichy for LCMS and MALDI analyses.

Thanks to Jill Powers, Angie Medina, Lauren Kulpa, and Sandy Manning for assistance with office related work.

Thanks to Jiney Jose and Dr. Aurore Loudet for lots of valuable discussions and corrections regarding my dissertation.

Thanks to Liangxing Wu, Cliferson Thivierge, Lingling Li, and Eunhwa Ko for providing useful compounds and to Dr. Jing Liu and Dr. Andrey Malakhov for helpful discussions on solid-phase syntheses.

Thanks to everyone in the Burgess group, especially, the Dyes group.

Finally, thanks to my mother and brothers for their encouragement and to my wife and son for their patience and love.

TABLE OF CONTENTS

Page

ABSTRACT iii

ACKNOWLEDGEMENTS iv

TABLE OF CONTENTS v

LIST OF FIGURES vii

LIST OF TABLES x

LIST OF SCHEMES xi

NOMENCLATURE xiv

CHAPTER

I INTRODUCTION 1

1.1 Fluorescence and Phosphorescence 1
1.2 Fluorescence Resonance Energy Transfer (FRET) 2
1.3 Through-bond Energy Transfer (TBET) 4
1.4 Multiplexing in Cellular Imaging 5
1.5 Specific Labeling of Proteins 7

II SYNTHESIS OF WATER-SOLUBLE FLUORESCENT PROBES 8

2.1 Introduction 8
2.2 Fluorescein Derivatives 9
2.3 Water-soluble BODIPY™ Dyes 19
2.4 Water-soluble Nile Blue Derivatives 31

III THROUGH-BOND ENERGY TRANSFER CASSETTES FOR MULTIPLEXING 45

3.1 Introduction 45
3.2 Donor Fragments (BODIPY Dyes) 50
3.3 Acceptor Fragments (Cyanine Dyes) 54
3.4 Synthesis of TBET Cassettes 66
3.5 Dye-doped Nanoparticles for Bioimaging in Cells 71

CHAPTER Page

IV DEVELOPMENT OF METHODS FOR PROTEIN MONO-LABELING 87

4.1 Introduction 87
4.2 System A: Nile Red Based Photolabile System 98
4.3 System B: Activated Photolabile-protecting Group 104
4.4 System C: Photolabiling System Based on BSA-coated CPG 113
4.5 System D: Chemically Cleavable Linker, Azobenzene 126
4.6 Summary for Each Approach and Reactions 131
4.7 Conclusion 138

V CONCLUSIONS AND OUTLOOK 140

5.1 Water-soluble Fluorescent Probes 140
5.2 Through-bond Energy Transfer Cassettes 142
5.3 Solid-phase Approach Towards Protein Mono-labeling 143

REFERENCES 145

APPENDIX A: EXPERIMENTAL DATA FOR CHAPTER II 155

APPENDIX B: EXPERIMENTAL DATA FOR CHAPTER III 191

APPENDIX C: EXPERIMENTAL DATA FOR CHAPTER IV 235

APPENDIX D: PROCEDURES OF SOLID-PHASE SYNTHESIS AND PHOTOLYSIS FOR CHAPTER IV 293

APPENDIX E: FLUORESCENT DYE TERMINATORS FOR DNA SEQUENCING 312

APPENDIX F: RELATED ATTEMPTED REACTIONS 324

APPENDIX G: EXPERIMENTAL DATA FOR APPENDIX E & F 330

VITA 407

LIST OF FIGURES

		Page
Figure 1.1	Jablonski diagram	1
Figure 1.2	The concept of through-bond energy transfer cassette	4
Figure 1.3	Through-space energy transfer (concept for FRET)	5
Figure 1.4	Plausible multiplexing imaging of the cell	6
Figure 2.1	Structure of Alexa Fluor series	8
Figure 2.2	Different ionic forms of fluorescein in various pH's	10
Figure 2.3	Structures of fluorescein and halogenated-fluorescein derivative	11
Figure 2.4	a; Structures of O^6-benzylguanine-Pennsylvania and Oregon green, b; reaction mechanism of SNAP-tag assay	12
Figure 2.5	Structures of 5- and 6-carboxyfluorescein	13
Figure 2.6	Formation of CrAsH-QD nanohybrids	15
Figure 2.7	Structures of intermediate 5 and cyclic lactone form 6a	17
Figure 2.8	Aromatic ^{1}H NMR (CD_3OD) regions of: a, compound 4a; and, b, compound 6a formed from treatment of 4a with NaOH then HCl	18
Figure 2.9	a: Dehaen's nucleophilic and Pd-catalyzed reaction systems, b: nucleophilic reaction systems studied in our group	20
Figure 2.10	Water-soluble BODIPY derivatives 10, 11, and 12	21
Figure 2.11	Structure of target functionalized ethylene glycol 14	22
Figure 2.12	Structures of BODIPY 12 and 23	26
Figure 2.13	Normalized UV absorption and fluorescence emission spectra of dyes 12 and 23 in MeOH and pH 7.4 phosphate buffer	26
Figure 2.14	Normalized UV absorption and fluorescence emission spectra of 12-BSA and 23-BSA in pH 7.4 phosphate buffer	28
Figure 2.15	Series of benzophenoxazine-based dye	31
Figure 2.16	Water-soluble Nile Red derivatives	31
Figure 2.17	Photophysical properties of Nile Blue 27 in various solvents	32
Figure 2.18	Water-soluble Nile Blue derivatives in literature (28 and 29) and from our group (30 and 31)	33

Page

Figure 2.19	Absorption (dashed lines) and fluorescence (solid lines) of a: 30a and 31a in methanol and 30a,b and 31a,b in b: phosphate buffer (pH 7.4), c: phosphate buffer (pH 7.4) with 3% Triton X-100, and d: borate buffer (pH 9.0)	37
Figure 2.20	Aggregation studies	41
Figure 2.21	Absorption and fluorescence spectra of covalently and non-covalently bonded dye-protein conjugates	42
Figure 3.1	NIR fluorescent probes based on BODIPY dyes	46
Figure 3.2	TBET cassettes 41-44 and acceptor synthons 45-48 of those cassettes	47
Figure 3.3	Fluorescence of equimolar EtOH solutions of 41-48 excited at 488 nm	48
Figure 3.4	Structure of cassette 49 (left) and fluorescence spectra of 49, donor fluorescein and acceptor rosamine (right)	49
Figure 3.5	Structures of cyanine series	54
Figure 3.6	General structures of cyanine dye	55
Figure 3.7	Most commonly used NIR dyes	56
Figure 3.8	Structures of cyanine dyes 73 and 74 used in this research	59
Figure 3.9	Absorption and fluorescence spectra of cyanine dyes 73 in EtOH	64
Figure 3.10	Absorption and fluorescence spectra of cassettes 75a-c	68
Figure 3.11	General synthesis of calcium phosphate nanoparticle	74
Figure 3.12	Absorption and fluorescence of cyanine acceptors 73a-c doped silica nanoparticles in 0.1 M phosphate buffer (pH 7.4)	75
Figure 3.13	Absorption and fluorescence of TBET cassettes 75a,b doped silica nanoparticles in 0.1 M phosphate buffer (pH 7.4)	76
Figure 3.14	TEM images of silica nanoparticles	79
Figure 3.15	Absorption and fluorescence of cyanine 73a-c doped calcium phosphate (CP) nanoparticles in 0.1 M phosphate buffer (pH 7.4)	80
Figure 3.16	Absorption and fluorescence of cassettes 75a-c doped calcium phosphate nanoparticles in 0.1 M phosphate buffer (pH 7.4)	82
Figure 3.17	AFM images of calcium phosphate nanoparticles	85
Figure 4.1	Francis' selective labeling of tyrosine	89

		Page
Figure 4.2	Design of molecule in this work	90
Figure 4.3	Overall scheme for protein mono-labeling process	91
Figure 4.4	Cleavage of azobenzene linker with $Na_2S_2O_4$	95
Figure 4.5	Mechanism of photocleavage reaction	96
Figure 4.6	MacBeath's work based on BSA-coated glass slide	97
Figure 4.7	*o*-Nitrobenzyl alcohol linker based solid-support (System A)	98
Figure 4.8	Activated photolinker based solid-support (System B)	104
Figure 4.9	Fluorescence emission spectra from the photochemical reaction of 117 upon excitation at 498 nm	108
Figure 4.10	Activated photolinker based BSA-coated CPG (System C)	113
Figure 4.11	CE results a: ubiquitin, b: sample 141, c: spiked of Ubq and 141	119
Figure 4.12	CE results; ubiquitin and ubiquitin with ethanolamine	120
Figure 4.13	Structure of BODIPY-ubiquitin conjugate 141	121
Figure 4.14	a; Ester system (138), and b; ether (148) system	122
Figure 4.15	Amino acid sequence of small peptide used in this study	125
Figure 4.16	Azobenzene linker based solid-support (System D)	126
Figure 5.1	5- and 6-Carboxyfluorescein 3	140
Figure 5.2	Photophysical properties of water-soluble BODIPY derivative 23 and its dye-BSA conjugate 23-BSA	141
Figure 5.3	Water-soluble Nile Blue derivatives 30 and 31	141
Figure 5.4	Iodo-cyanine series 74a-c, and novel TBET cassettes 75a-c	142
Figure 5.5	Alternative design for this project	143
Figure 5.6	Antibody immobilization process onto the luminophore-doped silica nanoparticle's surface	144
Figure 6.1	Structures of deoxynucleotides and dideoxynucleotides	312
Figure 6.2	Representative autoradiogram of electrophoresis gel	313
Figure 6.3	Structures of four iodo-dideoxynucleosides	314
Figure 6.4	Triphosphorylation of dideoxynucleosides via *Eckstein* or *Kovacs* method	317

LIST OF TABLES

		Page
Table 2.1	Photophysical properties of free dyes and dye-protein conjugates	30
Table 2.2	Spectroscopic properties of the Nile Blue and its derivatives under different conditions	38
Table 3.1	Photophysical properties of cyanine dyes 73a-c	65
Table 3.2	Photophysical properties of TBET cassettes 75a-c	70
Table 3.3	Photophysical properties of cyanine 73a-c doped silica nano-particles in 0.1 M phosphate buffer (pH 7.4)	78
Table 3.4	Photophysical properties of TBET cassettes 75a,b doped silica nanoparticles in 0.1 M phosphate buffer (pH 7.4)	78
Table 3.5	Photophysical properties of cyanine 73a-c doped CP nano-particles in 0.1 M phosphate buffer (pH 7.4)	83
Table 3.6	Photophysical properties of cassettes 75a-c doped CP nano-particles in 0.1 M phosphate buffer (pH 7.4)	84
Table 4.1	Summary of this project	131

LIST OF SCHEMES

		Page
Scheme 2.1	Synthesis of TP5-FAM	14
Scheme 2.2	Synthesis of CrAsH	15
Scheme 2.3	Synthesis of 5- and 6-carboxyfluorescein 3	16
Scheme 2.4	An iterative route to functionalized ethylene glycol	22
Scheme 2.5	Synthesis of first ethylene glycol unit 17	23
Scheme 2.6	Synthesis of second ethylene glycol unit 19	23
Scheme 2.7	Cu-catalyzed cycloaddition reaction of tosylate 17 and ester 19	24
Scheme 2.8	Synthesis of water-soluble ethylene glycol 14	24
Scheme 2.9	Propargylation of BODIPY 9	25
Scheme 2.10	Click reaction of BODIPY 22 and ethylene glycol 14	25
Scheme 2.11	Syntheses of dye-protein conjugates 12-BSA and 23-BSA	28
Scheme 2.12	Syntheses of functionalized aminophenol 34 and 36	34
Scheme 2.13	Syntheses of aminonaphthol components 37	35
Scheme 2.14	Syntheses of water-soluble Nile Blue derivatives	36
Scheme 3.1	Synthesis of 4-iodo-2-methoxybenzaldehyde 52	50
Scheme 3.2	Synthesis of 4-ethynyl tetramethyl-BODIPY 55	51
Scheme 3.3	Synthesis of 4-iodo tetramethyl-BODIPY 58	52
Scheme 3.4	Synthesis of 5-ethynyl tetramethyl-BODIPY 63	53
Scheme 3.5	General synthesis of cyanine dyes	57
Scheme 3.6	Solid-phase “Catch-and-Release” synthesis	58
Scheme 3.7	Synthesis of TBET cassette 75 via Sonogashira coupling	60
Scheme 3.8	Alkylation of 2,3,3-trimethylindolenine	60
Scheme 3.9	Syntheses of Cy3 73a and iodo-Cy3 74a	61
Scheme 3.10	Synthesis of Cy7 73c via two steps condensation reaction	62
Scheme 3.11	Synthesis of iodo-Cy7 74c via two steps condensation	63
Scheme 3.12	Synthesis of TBET cassette 75a	66

		Page
Scheme 3.13	Synthesis of TBET cassette 75c	67
Scheme 3.14	General synthetic scheme for silica nanoparticle formation	73
Scheme 4.1	Synthesis of photolabile-protected benzylbromide 91	98
Scheme 4.2	Synthesis of photolabile-protected Nile Red derivative 94	99
Scheme 4.3	Attachment of compound 94 on PEGA resin or aminopropyl-CPG	100
Scheme 4.4	Synthesis of TBDPS-protected benzylbromide 99	102
Scheme 4.5	Synthesis of Nile Red derivative 102 as a control compound	102
Scheme 4.6	Photocleavage reaction of compound 96-CPG	103
Scheme 4.7	Synthesis of activated photolabile-protecting group 108	105
Scheme 4.8	Insertion of alkyne functionality	105
Scheme 4.9	Control experimental for photochemical reaction	106
Scheme 4.10	Attachment of photolinker 110a onto glass beads	107
Scheme 4.11	Synthesis of control compound 117 and its photochemical reaction	108
Scheme 4.12	Synthesis of CPG-support triazole 123	109
Scheme 4.13	Attachment of Nile Red to solid-support	110
Scheme 4.14	Photolysis of dye-protein conjugates on solid-support 127	112
Scheme 4.15	Synthesis of photolinker on BSA-coated CPG	114
Scheme 4.16	Synthesis of BODIPY derivative 137	115
Scheme 4.17	Click reaction of solid-support 133 and BODIPY 137	116
Scheme 4.18	Coupling reaction with ubiquitin	116
Scheme 4.19	Photochemical reaction of compound 139	117
Scheme 4.20	Synthesis of ether based photolinker 146	123
Scheme 4.21	Synthesis of solid-support photolinker with BODIPY 148	124
Scheme 4.22	Synthesis of solid-support 149 via Sonogashira coupling	125
Scheme 4.23	Synthesis of BSA-coated CPG with azolinker (154)	127
Scheme 4.24	Synthesis of BSA-coated azobenzene-linked BODIPY 155	128
Scheme 4.25	Activation of carboxylic acid for compound 155	129
Scheme 4.26	Synthesis of solid-support azobenzene-linked BODIPY 157	130

		Page
Scheme 6.1	Synthesis of 2',3'-dideoxy-5-iodouridine 163	315
Scheme 6.2	Synthesis of 2',3'-dideoxy-5-iodocytidine 162	316
Scheme 6.3	Triphosphorylation of dideoxyiodo adenosine, cytidine, and uridine	318
Scheme 6.4	Synthesis of fluorescein derivative 182	319
Scheme 6.5	Synthesis of model nucleotide compound 183	320
Scheme 6.6	Synthesis of TBDMS-protected amino-hexaethylene glycol 186	320
Scheme 6.7	Synthesis of modified ethylene glycol linker 188	321
Scheme 6.8	Synthesis of 5-ethynylfluorescein diacetate 191	322
Scheme 6.9	Synthesis of precursor 192 for TBET cassette	323
Scheme 7.1	Synthesis of cyclized anisidine 194	324
Scheme 7.2	Synthesis of 5-iodo rosamine derivative 199	325
Scheme 7.3	Synthesis of triazole-decorated oligoethylene glycol 203	326
Scheme 7.4	Synthesis of functionalized aminonaphthol derivative 206	327
Scheme 7.5	Plan for the synthesis of water-soluble Nile Blue derivative 209	328
Scheme 7.6	Synthesis of triazole 212 and its photolysis	329

NOMENCLATURE

BOC	*tert*-butoxycarbonyl
BODIPY	4,4-difluoro-4-bora-3a,4a-diaza-*s*-indacene
BSA	Bovine Serum Albumin
CE	capillary electrophoresis
CH_2Cl_2	dichloromethane
CH_3CN	acetonitrile
CPG	control pore glass
Cy	cyanine
DIC	*N,N'*-diisopropylcarbodiimide
DMAP	4-dimethylaminopyridine
DMF	*N,N*-dimethylformamide
EDCI	1-ethyl-3-(3-dimethylaminopropyl)carbodiimide hydrochloride
ETE	energy transfer efficiency
EtOAc	ethylacetate
EtOH	ethanol
FAM	carboxyfluorescein
FRET	fluorescence resonance energy transfer
MeOH	methanol
NHS	*N*-hydroxysuccinimide
ONB	*o*-nitrobenzyl
PCC	pyridinium chlorochromate
PEG	polyethylene glycol
PEGA	polyethylene glycol polyacrylamide
TBAF	tetrabutylammonium fluoride
TBET	through-bond energy transfer
TFA	trifluoroacetic acid
THF	tetrahydrofuran

CHAPTER I

INTRODUCTION

1.1 Fluorescence and Phosphorescence

Luminescence takes place from electronically excited states to ground states. It is categorized in terms of *fluorescence* and *phosphorescence*, and the mechanism of those emissions are explained by the Jablonski diagram (Figure 1.1). For fluorescence, the electron is usually excited to singlet states S_1 or S_2 levels from the ground states by the absorption of photons. The electron occasionally rapidly relaxes to lower level, S_1, and this process is called internal conversion and the general rate is 10^{-12} s or less. When the electron relaxes to ground states, fluorescence occurs by releasing light energy and the rate is 10^{-8} s. The electron of S_1 level can also go to triplet state (T^1) via spin conversion (called intersystem crossing). The emission from T^1 level to ground state is known as phosphorescence, and this emission process is usually observed at relatively longer wavelengths. The rate of phosphorescence is therefore slower than that of fluorescence. The heavy atoms such as halogens are known to facilitate intersystem crossing and this process also involves the fluorescence quenching mechanism.

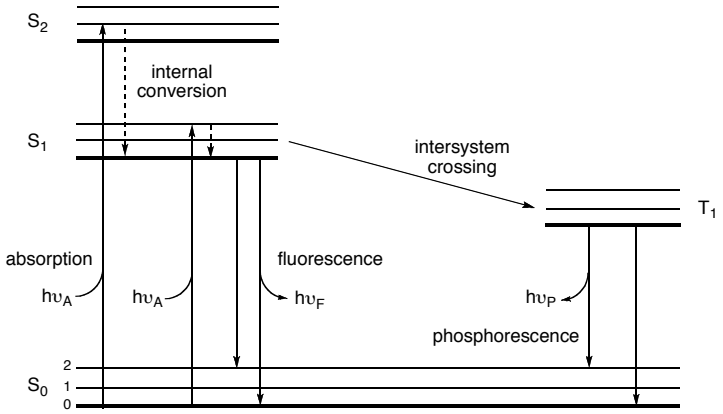

Figure 1.1. Jablonski diagram.[1]

This dissertation follows the style of *The Journal of Organic Chemistry*.

1.2 Fluorescence Resonance Energy Transfer (FRET)

Fluorescence resonance energy transfer (FRET) is an electrodynamic phenomenon which occurs between a donor fluorophore (D) in the excited state and an acceptor fluorophore (A) in the ground state. For FRET to occur the distance between both fluorophores should be less than 100 nm. The most important factor for FRET is the requirement of the overlap between the emission of a donor and the absorption of an acceptor. The less overlapping integral decreases the FRET efficiency. FRET was first reported by Theodor Förster in 1946.[2] FRET is now widely used in various biological application such as medical diagnostics, DNA analysis, and cell imaging. The energy transfer (ET) which takes place between the donor and the acceptor separated by a distance *r*, is given by the following equation:

$$k_T(r) = \frac{Q_D \kappa^2}{\tau_D r^6} \left(\frac{9000(\ln 10)}{128\pi^5 N n^4} \right) \int_0^\infty F_D(\lambda)\varepsilon_A(\lambda)\lambda^4 d\lambda \qquad \text{(i)}$$

where Q_D is quantum yield of the donor in the absence of the acceptor, and κ^2 is orientation factor (range from 0 to 4, usually assumed to be 0.67 for dynamic random averaging). When the transition dipole moments of the donor and the acceptor are perfectly parallel, then κ^2 is 4. If the dipole moments of both fluorophores are orthogonal, κ^2 is given by 0. *N* is Avogadro's number (6.02×10^{23}), *n* is the refractive index of the medium, τ_D is the lifetime of the donor in the absence of acceptor. $F_D(\lambda)$ is the integral of the corrected fluorescence intensity of the donor and $\varepsilon_A(\lambda)$ is the extinction coefficient of the acceptor at wavelength λ. The rate of ET is inversely proportional to the sixth power of the distance *r*, between the donor and the acceptor. The overlap integral $J(\lambda)$ is given as:

$$J(\lambda) = \int_0^\infty F_D(\lambda)\varepsilon_A(\lambda)\lambda^4 d\lambda \qquad \text{(ii)}$$

The Förster radius, R_0, is the distance r, at which the rate of ET is equal to the rate of decay of the donor ($1/\tau_D$) in the absence of the acceptor. Therefore it is also the distance at which FRET is 50 % efficient. At r = R_o, $k_T = (1/\tau_D)$ and equation (i) can be written as:

$$R_0^6 = \frac{9000(\ln 10)Q_D\kappa^2}{128\pi^5 N n^4} \int_0^\infty F_D(\lambda)\varepsilon_A(\lambda)\lambda^4 d\lambda \qquad \text{(iii)}$$

R_0 is typically in the range of 20 to 60 Å for organic fluorophores. The ET rate can be calculated by:

$$k_T(r) = \frac{1}{\tau_D}\left(\frac{R_0}{r}\right)^6 \qquad \text{(iv)}$$

The efficiency of ET, E, is the fractions of photons absorbed by the donor that are transferred to the acceptor. E is given by:

$$E = \frac{k_T(r)}{\tau_D^{-1} + k_T(r)} \qquad \text{(v)}$$

which is the ratio of the energy transfer rate to the total decay rate of the donor. Hence the ET efficiency can be easily calculated from the fluorescence emission intensity of the donor in the absence and in the presence of the acceptor or from the fluorescence lifetime of the excited donor in the presence and absence of the donor (equation vi).[1]

$$E = \frac{\tau_D - \tau_{DA}}{\tau_D} \qquad \text{(vi)}$$

1.3 Through-bond Energy Transfer (TBET)

The idea of through-bond energy transfer was reported by Lindsey and co-workers in 1994.[3] They used a boron-dipyrromethene (BODIPY) as a donor and zinc-coordinated porphyrin as an acceptor. The concept of TBET cassettes is that when donor and acceptor systems are connected *via* conjugated linkers that do not allow them to become planar, then rapid energy transfer from the donor to the acceptor may occur in through bonds (Figure 1.2). Through-bond energy transfer is mechanistically different to FRET (Figure 1.3), and there is no known requirement of overlapping of the emission of the donor fragment with the absorption of the acceptor part. Therefore, appropriately designed through-bond energy transfer cassettes could absorb photons via a donor part, or parts, at a convenient wavelength (*eg* 488 nm: excitation from an argon-laser), transfer the energy rapidly through the conjugated linker to the acceptor fragment that emits at a far longer wavelength. There is no constraint on the difference between the donor absorption and the acceptor emission wavelengths in this system. Consequently it is possible to design dyes that absorb strongly at a short wavelength and emit brightly with very similar intensities at several wavelengths (governed by the chemical nature of the acceptor) that are many wavenumbers apart, *ie* with excellent resolution. Coupling more than one donor in a conjugated system with an acceptor facilitates absorption of more light thereby increasing the intensity of the emission. In summary, through bond energy transfer cassettes have the potential to increase both the resolution and fluorescence intensities obtained from several probes excited by a laser source operating at a single wavelength.

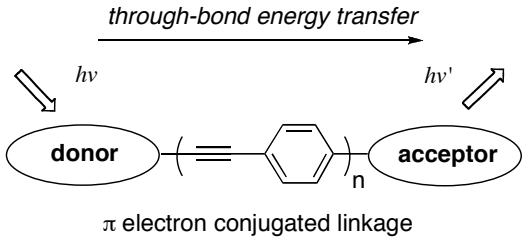

Figure 1.2. The concept of through-bond energy transfer cassette.

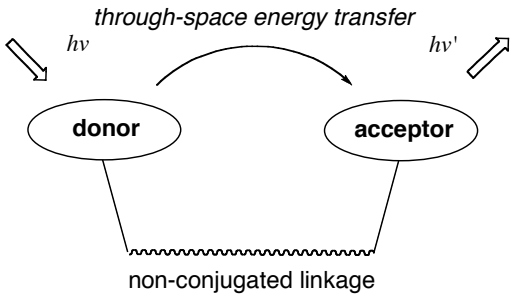

Figure 1.3. Through-space energy transfer (concept for FRET).

1.4 Multiplexing in Cellular Imaging

Cellular imaging has become essential to obtain information about protein expression and molecular dynamics of protein in cells. Various techniques for fluorescence imaging of cells have been reported.[4] Multiplexing is useful for gaining information simultaneously from the different parts of the cell. Multiplexed observation of fluorescently tagged biochemical components is simplest when all the tags are excited using the same laser source; the equipment required is less complex and all the labels receive the same input power. However, fluorescent dyes that emit close to the excitation source tend to absorb light most efficiently since they have the greatest absorption at that wavelength, while those dyes that emit further into the red have red-shifted absorption spectra and harvest less photons at the excitation wavelength. Combinations of dyes arranged to maximize FRET only partially alleviate this problem[5,6] because poor overlap of donor emission with acceptor dye absorption gives inefficient energy transfer.

The use of TBET cassettes will probably facilitate multiplexing study in the cells because only single excitation wavelength is required to obtain multiple fluorescent colors. Figure 1.4 demonstrates the plausible multiplexing for protein interaction in the cell. Each TBET cassettes are conjugated with different proteins and those dye-protein conjugates will be imported to corresponding places of the cell (*eg*: nucleus, golgi, mitochondria, lysosome...) with carrier protein. The excitation at single wavelength will hypothetically give multiple colors at the same time from the places to which cassette-

protein conjugates were imported. It is possible to obtain simultaneous fluorescent signals from the cells, and therefore it is very time efficient. Thus TBET-cassettes can be used to obtain information about protein-protein interaction *in vitro* and *ex vivo*. The number of false positives can also be reduced to a greater extend by using TBET-cassettes instead of FRET based systems.

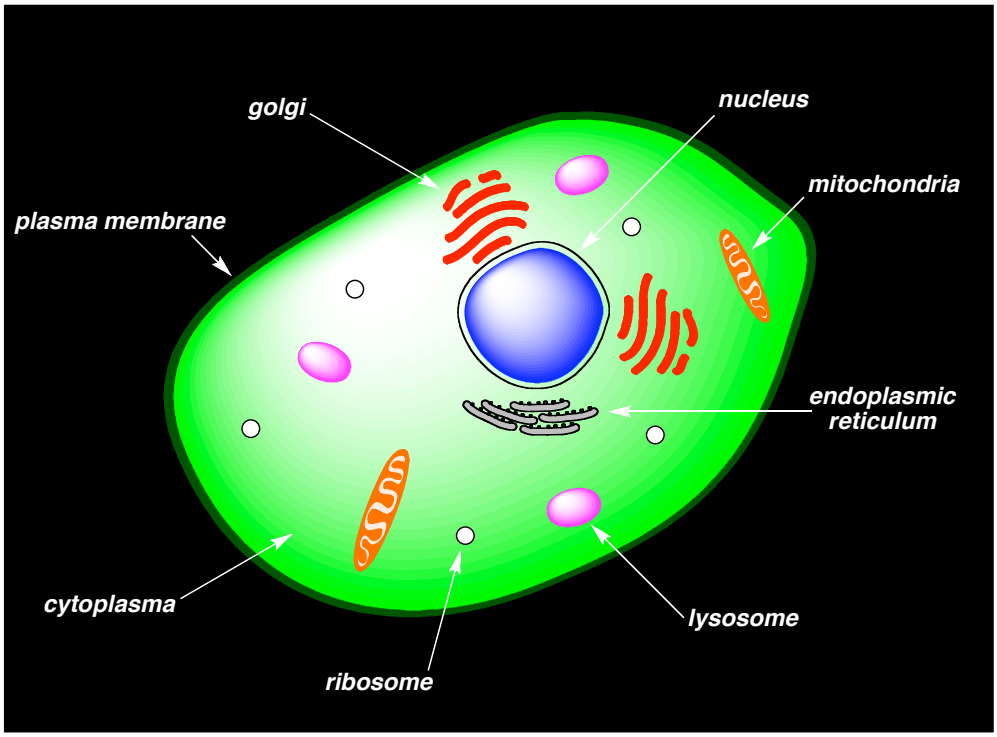

Figure 1.4. Plausible multiplexing imaging of the cell.

1.5 Specific Labeling of Proteins

Fluorescent labeling of proteins has become an essential tool in biological assays. Amino acids containing reactive functional groups such as thiol (cysteine) and primary amine (lysine), are usually reacted with succinimidyl esters or maleimides of dyes to label proteins. However these labeling methods are non-specific. The site-specific labeling of tetra-cysteines was reported by Tsien and co-workers.[7] Recombinant proteins containing tetra-cysteines was successfully tagged by bisarsenical fluorophore (FlAsH tag) and this small tag is membrane permeable and binds with high affinity. The small peptide containing tetra-cysteines were also selectively tagged by Cy3 based bisarsenical dyes.[8] Di-cysteine of recombinant protein was labeled by dimaleimide fluorogens, but the distance between two cysteines must be *ca.* 10 Å which is almost similar to two maleimide groups.[9] In recent years, the specific labeling of recombinant proteins which contains an unnatural amino acid have been reported by some groups. Tirrell *et al* reported the specific dye-labeling between a terminal alkyne on protein and an azide on coumarin via 2+3 cycloaddition reaction.[10] The *C*-terminus of green fluorescent protein (GFP) was modified with aniline derivative and this aromatic amine was specifically reacted with rhodamine analogue via oxidative coupling and this work was done by Francis' group.[11] More recently, Schultz, Deniz *et al* reported the synthesis of recombinant T4 lysozyme (T4L*) containing one cysteine residue and one ketone functionality which is formed by the incorporation of unnatural amino acid, *p*-acetylphenylalanine. The dual-labeling of cysteine (thiol-group) and ketone were performed with Alexa594-maleimide and Alexa488-ONH_2, respectively. The resulting dyes-T4L* conjugate had a desired FRET efficiency.[12] There are many reports about site-specific labeling of recombinant biomolecules as shown above. The application of such techniques to native proteins could be possible via the slight modification of natural biomolecules.

CHAPTER II

SYNTHESIS OF WATER-SOLUBLE FLUORESCENT PROBES

2.1 Introduction

Water-soluble fluorescent probes are essential tools in intracellular imaging. These dyes must have significant water solubilities and high quantum yields at physiological pH. The most widely used fluorescent probes are the Alexa Fluor series (developed by Molecular Probes, Inc. Figure 2.1).[13] The core structures of these dyes are based on coumarin and rhodamine, and each dye has one or two sulfonic acids to enhance water solubility and carboxylic acids to conjugate with biomolecules. All Alexa Fluor dyes tend to be more fluorescent and photostable than other commonly used dyes, *e.g.* fluorescein, rhodamine 6G, and Texas Red. Alexa Fluor dyes are pH insensitive in the range of 4 to 10, and they have high quantum yields in aqueous media. Their dye-protein conjugates also tend to have relatively high quantum yields. Moreover, absorption and emission wavelengths of Alexa Fluor series cover from UV-vis to NIR regions, but the structures of NIR Alexa dyes have not been published.

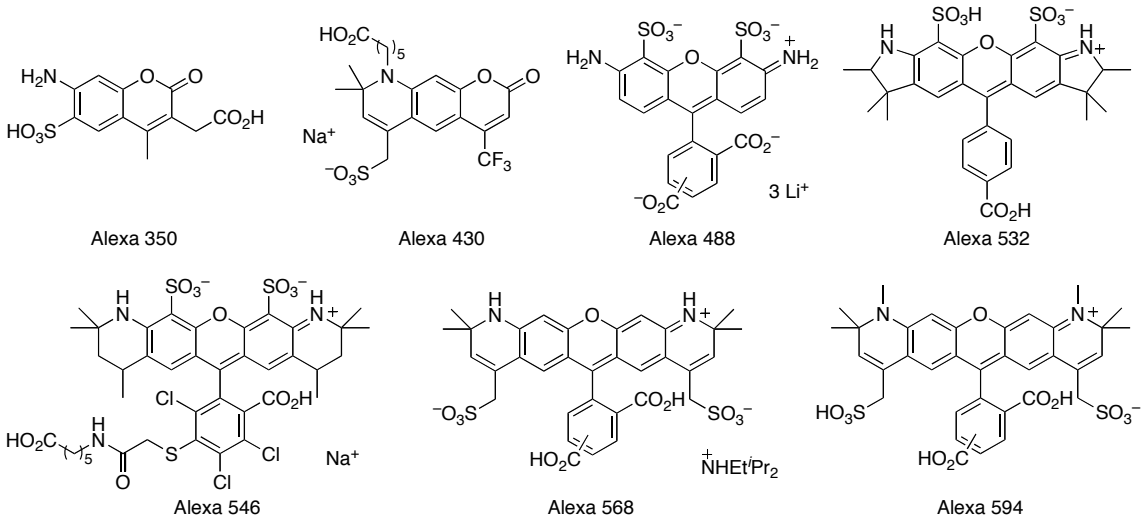

Figure 2.1. Structure of Alexa Fluor series. The numbers in the Alexa names correspond to the approximate $\lambda_{abs\ max}$ of each dyes.

All the Alexa Fluor dyes are sulfonated; this helps in improving water-solubility and preventing aggregation with good photophysical properties. Purification of water-soluble fluorescent dyes are usually difficult due to the high polarities of dyes. Some cases require a reverse phase preparative HPLC and this is unsuitable for large scale syntheses. In those cases, a better synthetic approach is required and purification procedures have to be modified. Therefore, the specific aims for synthesizing fluorescent probes are as follows:

(i) design of molecules which absorb and fluoresce in the desired wavelengths;
(ii) convenient synthesis and easy purification of fluorophores; and,
(iii) high quantum yields and water-solubilities at physiological pH.

We will describe three fluorescent dyes: carboxyfluorescein, water-soluble BODIPY dye, and water-soluble Nile Blue derivatives. Syntheses of these dyes and their photophysical properties will be discussed and some biological applications of BODIPY and Nile Blue dyes will also be shown.

2.2 Fluorescein Derivatives

Fluorescein is a highly fluorescent molecule that absorbs at 492 nm and emits at 517 nm in water, with a quantum yield of 0.92 at pH > 8. The synthesis of fluorescein *via* condensation reaction of resorcinol with phthalic anhydride catalyzed by zinc chloride was first reported in 1871 by von Baeyer.[14] Despite their widespread use in biological studies, fluorescein has some remarkable deficiencies. First and foremost, fluorescein-based dyes cause irreversible photobleaching, which results in a rapid decrease of fluorescent signal. Second, in aqueous media, it can exist as cationic, neutral, anionic and dianionic forms, making its absorption and fluorescence properties highly pH dependent (Figure 2.2).[15] Third, the dye-protein conjugates usually tend to show a fluorescence quenching relative to that of the free fluorophore. This leads to the protein-

dye conjugates exhibiting less fluorescence even with increasing number of dye molecules conjugated to protein,[16,17] reducing the sensitivity that is possible for assays using fluorescein conjugates.

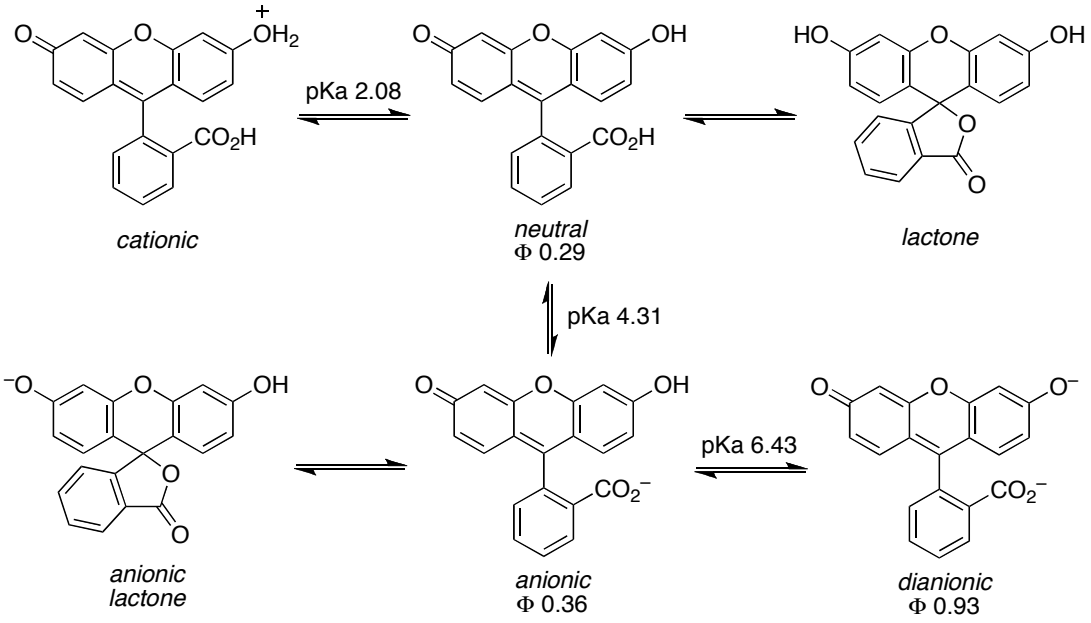

Figure 2.2. Different ionic forms of fluorescein in various pH's.

2',7'-Halogenated fluorescein derivatives have been synthesized and used in biological studies by many researchers (Figure 2.3). These halogen atoms dramatically change the electron density of xanthene part of fluorescein because of highly electronegative nature and small van der Waals radius. These features make the dyes exist as anionic forms at lower pH, resulting in higher quantum yield and photostability in acidic media. A chlorine substituted fluorescein, 4',5-alkylated-2',7'-dichlorofluorescein derivative was used as a cell-permeable fluorescent probe for zinc sensor by Lippard.[18,19] The functionalized 2',7'-dichlorofluorescein derivatives were well studied as metal (palladium[20] and mercury[21]) and specific RNA[22-24] sensors by Koide.

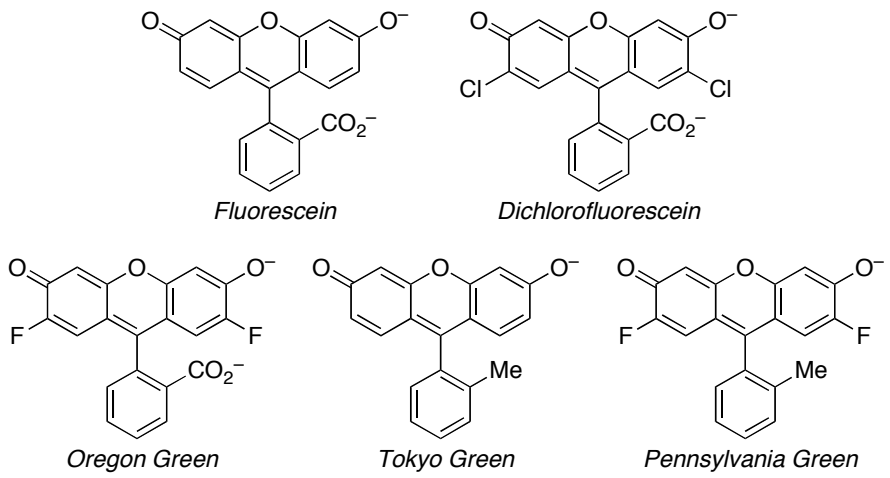

Figure 2.3. Structures of fluorescein and halogenated-fluorescein derivative.

The synthesis and photophysical properties of 2',7'-difluorofluorescein (also called Oregon Green, with pKa of 4.8) were first described in 1997 by Sun and co-workers.[15] This probe has a similar quantum yield (Φ 0.97, pH 9.0) to fluorescein, but with superior photostability. In 2005, Nagano and co-workers reported a novel series of fluorescein derivatives where benzene moiety was functionalized by methyl or methoxy group (called Tokyo Greens).[25] Tokyo Green showed almost the same fluorescent properties as fluorescein and has less pH dependence than that of fluorescein. Moreover, the synthesis of Tokyo Green was carried out via Grignard coupling of substituted bromobenzenes and xanthone and this reaction yielded a single isomer in high yield of 96 %. More recently, Peterson and co-workers reported a novel fluorophore (called Pennsylvania Green) which has similar pH-insensitivity and photostability as compared to Oregon Green and hydrophobicity similar to Tokyo Green.[26] At pH 9.0, 5-carboxy-Pennsylvania Green and 5-carboxy-Tokyo Green have similar quantum yields of 0.91 and 0.93, respectively. However, at pH 5.0, more acidic media, 5-carboxy-Pennsylvania Green was substantially brighter with a quantum yield of 0.68 compared with 0.39 for the 5-carboxy-Tokyo Green. Further, Pennsylvania Green is more photostable than Tokyo Green, which makes it a very useful fluorophore in biological assays.

One of the most interesting applications of Pennsylvania Green is as a SNAP-Tag[27] based biological assays. Fluorescent probes **1** and **2** derived from O^6-benzylguanine were described by Peterson (Figure 2.4a).[28] O^6-Benzylguanine derivatives (SNAP-Tag substrates) are useful molecular probes for cellular study because they selectively alkylate the DNA repair protein O^6-alkylguanine DNA alkyltransferase (AGT), and it produces the covalent labeling of AGT fusion proteins (SNAP-Tag fusion protein). AGT is an important protein because the lack of AGT causes apoptosis and mutagenesis of cell.

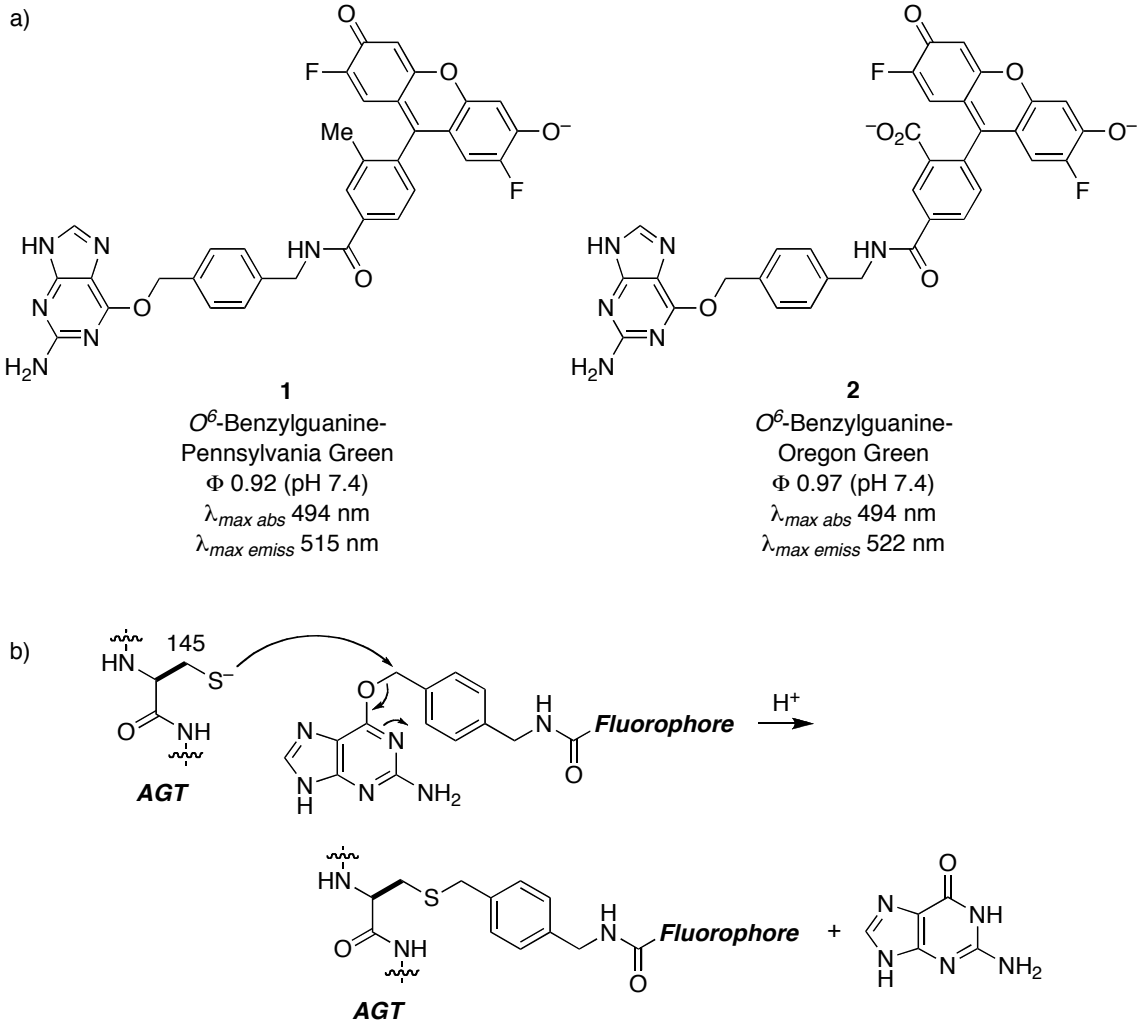

Figure 2.4. **a**; Structures of O^6-benzylguanine-Pennsylvania and Oregon green, **b**; reaction mechanism of SNAP-tag assay.

The reaction mechanism of SNAP-Tag involves the nuclephilic attack of cysteine residue-145 of AGT on alkylguanine and the fluorescent labeled fusion protein is formed by releasing a guanine molecule (Figure 2.4b). Next, to compare the cellular permeability of **1** and **2**, Chinese hamster ovary-K1 (CHO) cells were used for this biological assay. For the imaging of cellular plasma membrane, AGT was fused to a C-terminal CAAX peptide sequence from a human Ras protein and treated with probes **1** or **2**. On the other hand, AGT was fused to the C-terminus of the human histone 2B (H2B) protein and treated with fluorescent probes **1** or **2** to image the localization inside of cell nucleus. For molecular probe **1**, the clear labeling of cellular plasma membrane was observed, but only punctate fluorescence was detected in the cytoplasm of the subset of transfected cells for probe **2**. A strong fluorescence output was observed in the cell nucleus for probe **1**, however, only weak nuclear fluorescence signal was detected for probe **2**.

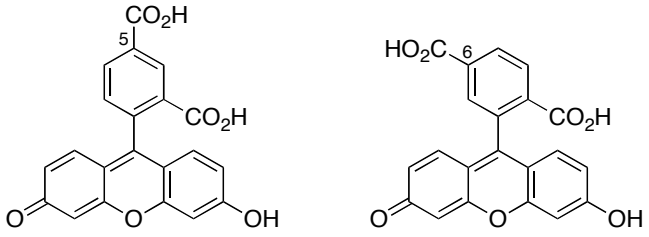

3a *5-carboxyfluorescein* **3b** *6-carboxyfluorescein*

Figure 2.5. Structures of 5- and 6-carboxyfluorescein.

Although fluorescein has some deficiencies like pH sensitivity and poor photostability as shown in previous chapter, the derivatives of fluorescein, 5- and 6-carboxyfluorescein **3** (also called FAM) are still widely used in biological imaging studies (Figure 2.5). Many researchers use these compounds in biochemistry and medicinal chemistry and many papers have been published. In 2006, Onoue and co-

wokers reported the synthesis of *C*-terminally coupled 5-carboxyfluorescein TP5 (TP5-FAM) as a fluorescent probe for thymopoietin receptor via solid-phase synthesis (Scheme 2.1).[29] TP5 (thymopentin) is a synthetic pentapeptide fragment which has a specific amino acid sequence (Arg-Lys-Asp-Val-Tyr). This sequence corresponds to the 32-36 fragment of thymic polypeptide thymopoietin. The fluorescent cellular imaging shows a specific binding of TP5-FAM to the thymopoietin receptor in MOLT-4 (human acute lymphoblastic leukemia cell line) with a dissociation constant (K_d) of 33.3 μM.

Scheme 2.1. Synthesis of TP5-FAM.

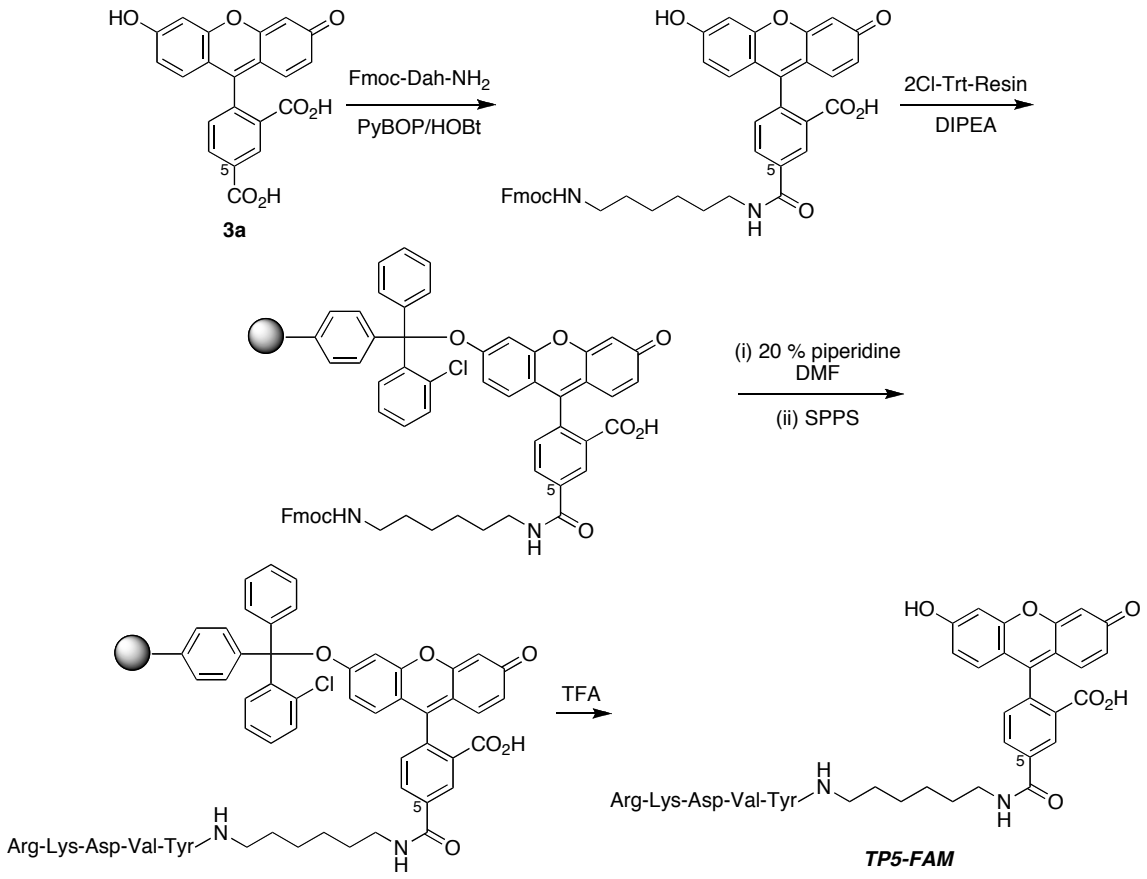

In 2008, Dubertret, Doris and co-workers reported the synthesis of new nanohybrids that consists of quantum dots (QDs) and CrAsH which is a FlAsH analogue.[30] FlAsH (Fluorescein Arsenical Helix binder) is known as a fluorescein tag that specifically bind to tetra-cysteine of protein.[7,31] The synthesis of CrAsH is shown in Scheme 2.2; mercuration of 6-carboxyfluorescein followed by transmetalation with $AsCl_3$ and ligand exchange with ethanedithiol gave CrAsH (overall yield: 30 %). Next, QD based on CdSe/CdZnS was encapusulated with poly(ethylene glycol) phospholipids to give hydrophilic and biocompartible QD micelles and this QD was further reacted with CrAsH *via* EDC-coupling to form CrAsH-QD nanohybrids (Figure 2.6).

Scheme 2.2. Synthesis of CrAsH.

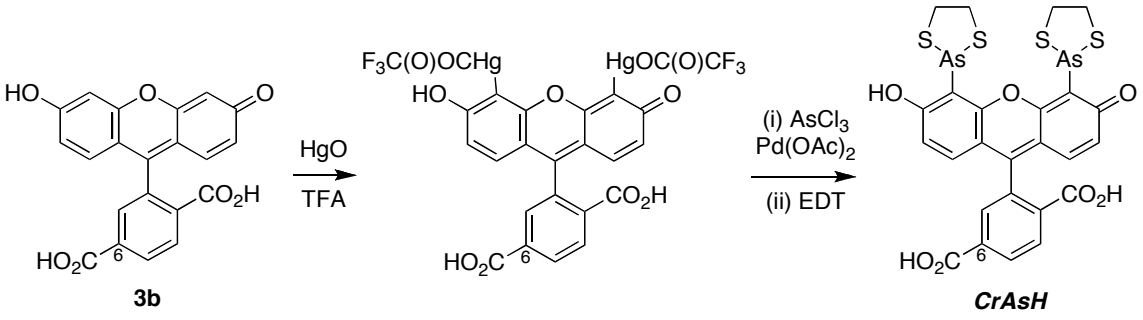

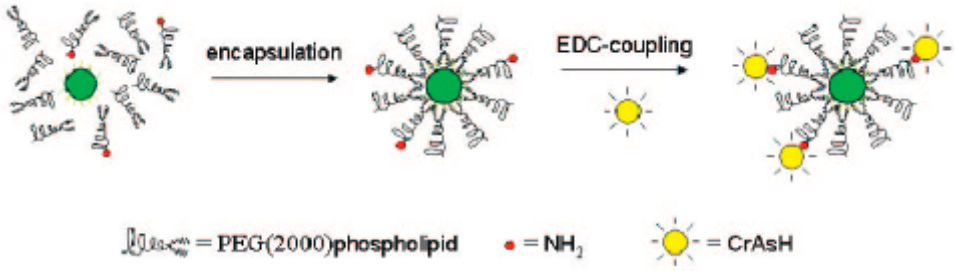

Figure 2.6. Formation of CrAsH-QD nanohybrids.

The affinity of this CrAsH-QD nanohybrids was then tested for the tetra-cysteine tagged proteins. This nanohybrid was treated with a viral lysate containing target cysteines and the increase of fluorescence intensity was observed when the concentration

of lysate was increased. On the other hand, this nanohybrid was also treated with a viral lysate without target tetra-cysteine as a control experimental, and it resulted in a weak fluorescent signal. These data shows that CrAsH-QD specifically binds to tetra-cysteine residues of protein.

2.2.1 Results and Discussion (*Preparation of 5- and 6-Carboxyfluorescein*)

Despite the widespread applications of 5- and 6-carboxyfluorescein[32] as molecular probes,[33-35] it is surprisingly difficult to obtain these compounds as pure regioisomers. These mixtures can be usually separated via preparative HPLC and such separation is not suitable for the large scale synthesis. The commercial samples of these isomers are very expensive. Therefore procedure for large-scale preparation of these fluorescein derivatives would definitely be preferred. We have reported a fractional crystallization procedure for the preparation of pure 5- and 6-carboxyfluorescein isomers in mult-gram amounts. (Scheme 2.3).[36]

Scheme 2.3. Synthesis of 5- and 6-carboxyfluorescein **3**.

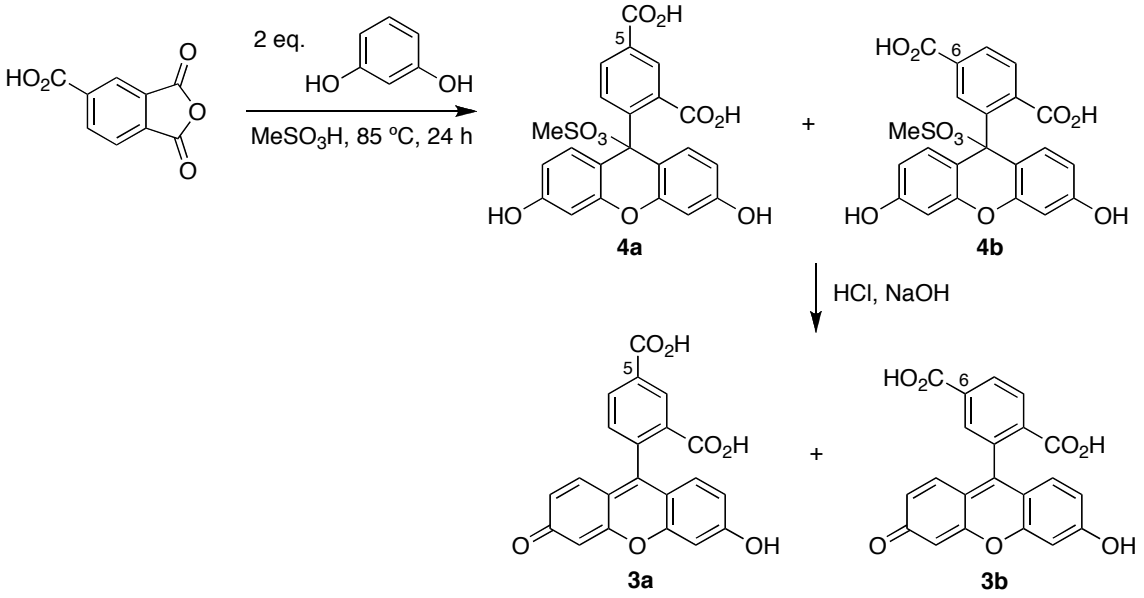

The approach of purification *via* fractional crystallization is used for halogenated fluoresceins,[15,37,38] and also for 5- and 6-carboxyfluorescein *via* a procedure that involves intermediates **5** (Figure 2.7).[39] However, the latter procedure is not easily reproducible,[34] and resorted to reduction of the 5- or 6-carboxylic acid functionality and separation of the regioisomers of this material instead.

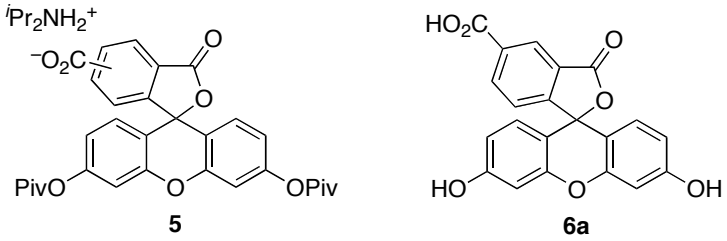

Figure 2.7. Structures of intermediate **5** and cyclic lactone form **6a**.

The key observation that led to the our procedure is that the compound formed from condensation of 4-carboxyphthalic anhydride with resorcinol in the presence of methanesulfonic acid was different to that formed when other acids were used (Scheme 2.3). Figure 2.8a shows the aromatic region of the ^{1}H NMR spectrum of the product **4a** formed from the condensation reaction, then purified via fractional crystallization. Treatment of this **4a** with sodium hydroxide, then protonation with HCl affords a different material (Figure 2.8b): this compound is assumed to be cyclic lactone **6a**. Conversely, product **4a** was regenerated when **6a** was treated with excess methanesulfonic acid. Characterization of structures **4a** and **4b** to the products of the initial reaction was certified by data from elemental analyses.

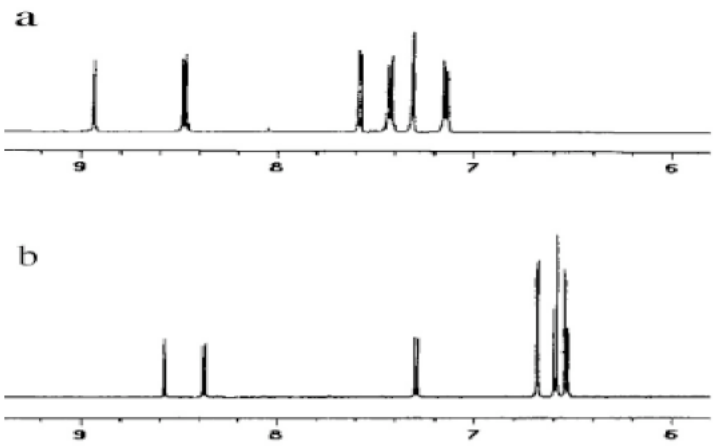

Figure 2.8. Aromatic ^{1}H NMR (CD_3OD) regions of: **a**, compound **4a**; and, **b**, compound **6a** formed from treatment of **4a** with NaOH then HCl.

The reaction shown in Scheme 2.3 affords compounds **4a** and **4b** in approximately a 1:1 ratio. Recrystallization of 20 g of that mixture from methanol/hexanes (3:1, 800 mL total) at –18 ºC gave a crude sample of compound **4b**. A second recrystallization gave 1.0 g of this material in over 98 % regioisomeric purity by HPLC analysis. Combination of the mother liquors, removal of the solvent, then two recrystallizations from a similar solvent system, ethanol/hexanes (3:1, 800 mL total), gave 3.2 g of the 5-carboxy isomer **4a** in over 98 % purity (anal. HPLC). The mother liquors were again combined, the solvents were removed, and two recrystallizations of the residues from methanol/hexanes system afforded another 3.0 g of the 6-isomer **4b**. As a result, the 5- and 6-isomers were isolated in 3.2 and 4.0 g amounts corresponding to 32 and 40 % yields, respectively. The methanesulfonic acid adducts **4a** and **4b** were easily converted to the 5- and 6-carboxyfluorescein **3a** and **3b** by treatment with sodium hydroxide solution then neutralizing with aq. HCl in quantitative yields.

2.2.2 Conclusion

We synthesized 5- and 6-carboxyfluorescein **3** in multi-gram scale and high purity (> 98 % by anal. HPLC) *via* a fractional crystallization with methanol/hexanes or ethanol/hexanes systems. The procedures are reproducible and extremely convenient syntheses to produce pure 5- and 6-isomers. In recent years, halogenated fluorescein derivatives such as Oregon, Tokyo, and Pennsylvania Greens have often used because of their excellent photostability. However, 5- and 6-carboxyfluorescein are still powerful tools as fluorescent probes in biological application, and actually our fractional crystallization method has been often used by many other groups.

2.3 Water-soluble BODIPY™ Dyes

4,4-Difluoro-4-bora-3a,4a-diaza-*s*-indacene (BODIPY™) dyes are the widely used fluorescent probes in biological assays such as labeling of proteins[40-44] or DNA.[45] In spite of their small core structure, they tend to be strongly UV-absorbing and emit sharp fluorescence peaks with high quantum yields in the range of 500–700 nm. These dyes are relatively photostable, and insensitive to the polarity and pH of their environment. Moreover, BODIPYs are reasonably stable to physiological conditions. The modification of BODIPY core (*i.e.* extended conjugation) and functionalization of the benzene moiety have been described by many researchers[46-49] and our group has also reported syntheses of functionalized BODIPY dye including water-soluble fluorophore in recent years.[50-53]

Dehaen *et al* reported the useful selective functionalization of 3-chloro or 3,5-dichloro BODIPY **7** by replacing chlorine with various nucleophiles *via* S_NAr reaction[54,55] or aromatic substituents *via* Pd-catalyzed cross-coupling reactions (Figure 2.9a).[56] The member in our group reported the synthesis of BODIPY **8** and **9**, and studied the reactivity of S_NAr reaction (Figure 2.9b).[57] S_NAr reaction of dye **9** smoothly worked because of the enhancement of reactivity by the trifluoro-group and the member in our group even succeeded the direct attachment of this dye **9** to protein (avidin was used), but the quantum yield of dye-protein conjugate was not reported. The water-

soluble derivatives of dye **9** were also made, compounds **10**, **11** and **12**, and their quantum yields in pH 7.4 buffer were quite high (Figure 2.10).[57] Therefore, the modification of BODIPY **9** by different water-solubilizing groups can produce a variety of useful fluorescent probes for biological studies. In this section, the synthesis of new water-soluble BODIPY derivative based on dye **9** and its photophysical properties will be covered. The quantum yield of this new dye conjugated with protein in aqueous medium will also be discussed.

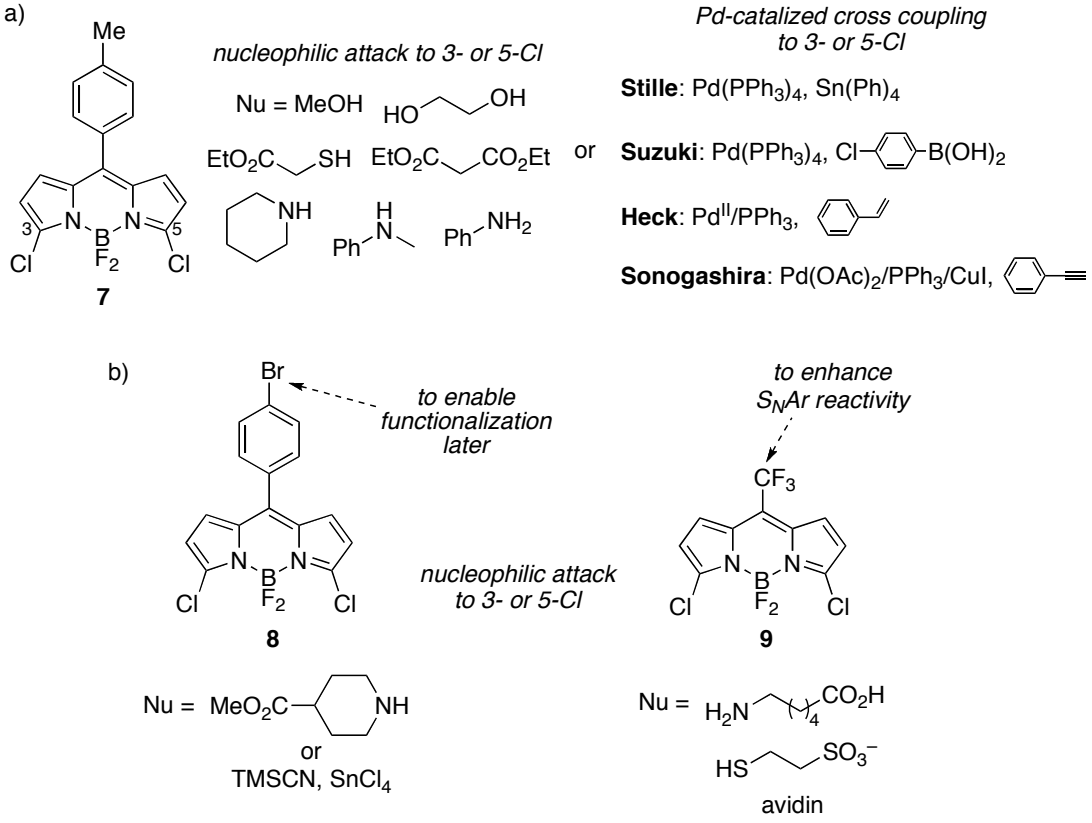

Figure 2.9. **a**: Dehaen's nucleophilic and Pd-catalyzed reaction systems, **b**: nucleophilic reaction systems studied in our group.

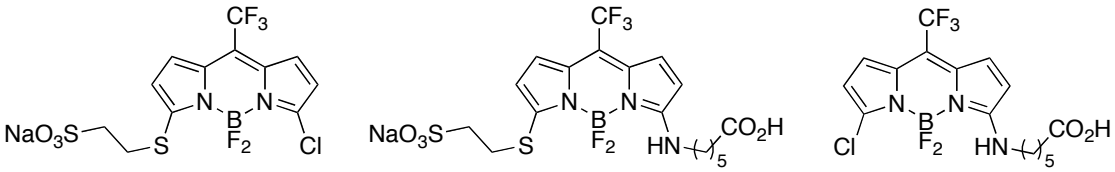

10
pH 7.4
Φ 0.95
λ_{abs} = 569 nm
λ_{em} = 584 nm
ε 57,000

11
pH 7.4
Φ 0.70
λ_{abs} = 477 nm
λ_{em} = 584 nm
ε 41,800

12
pH 7.4
Φ 0.74
λ_{abs} = 468 nm
λ_{em} = 541 nm
ε 24,900

Figure 2.10. Water-soluble BODIPY derivatives **10**, **11**, and **12**.

The water-soluble fluorescent dyes are definitely preferred for bioimaging studies and the use of oligoethylene glycol is one of the best strategies for synthesizing this class of dyes. There are many advantages for using oligoethylene glycol, (i) increases water-solubility, (ii) prevents aggregation because of its random orientation, (iii) serves dual purpose of increasing quantum yield in aqueous media and acting as a surfactant Triton X-100, and (iv) easy to work-up compared to other water-solubilizing groups (*eg*: sulfonic acid or phosphoric acid). A few methods for preparing oligoethylene glycol units have been reported so far, however, even the best method requires a long reaction time and several chromatographic separations.[58] In fact, the routes that feature iterative S_N2 ether-bond-forming steps are vulnerable to formation of vinyl ether side-products *via* competing elimination reactions. In 2006, the member in our group reported an iterative route to functionalized ethylene glycol units using copper-catalyzed [2+3] cycloaddition of azides to alkynes (also called "click" chemistry).[59] This new methodology provided the triazole-decorated oligoethylene glycol with several end groups, and only one chromatographic separation in the closing stage gave the pure product **13** in moderate yield (overall 39 % yield, Scheme 2.4).

Scheme 2.4. An iterative route to functionalized ethylene glycol.

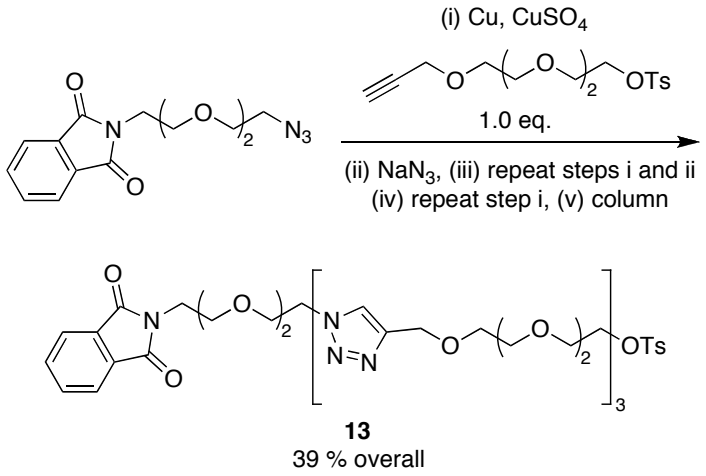

2.3.1 Results and Discussion (*Synthesis of Water-soluble BODIPY Derivative*)

We chose the above strategy to synthesize the new water-soluble oligoethylene glycol linker **14** (Figure 2.11). Two hexaethylene glycol units are connected with triazole ring, and one end of ethylene glycol has a carboxylic acid for conjugation with biomolecules and the other end, an azido-group which will be used to form a triazole ring with alkyne on BODIPY dye *via* click chemistry.

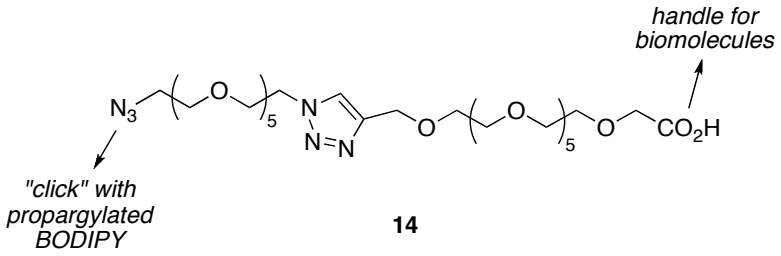

Figure 2.11. Structure of target functionalized ethylene glycol **14**.

To synthesize our target molecule **14**, we needed two ethylene glycol units. For the first unit, mono-tosylation[58] of a hexaethylene glycol followed by the replacement with azido-group gave the mono-azido hexaethylene glycol **16**. This **16** was tosylated[60] to afford an azido-hexaethylene glycol tosylate **17** (Scheme 2.5).

Scheme 2.5. Synthesis of first ethylene glycol unit **17**.

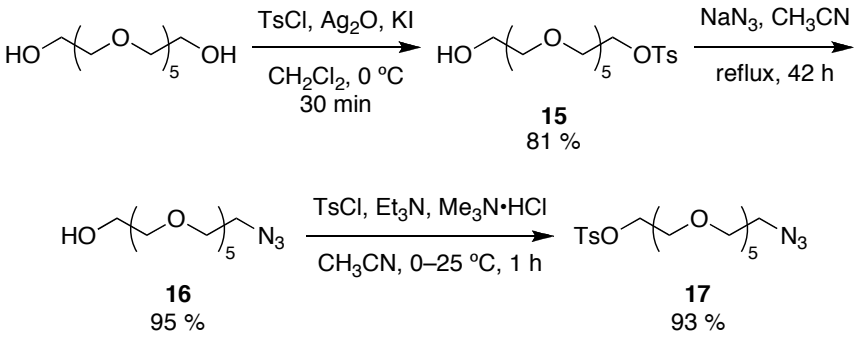

The synthesis of second unit involves the two steps. Hexaethylene glycol was mono-propargylated with propargyl bromide to give **18**. Compound **18** was then reacted with *tert*-butylbromo acetate to afford propargylated-ethylene glycol *tert*-butyl ester **19** (Scheme 2.6).

Scheme 2.6. Synthesis of second ethylene glycol unit **19**.

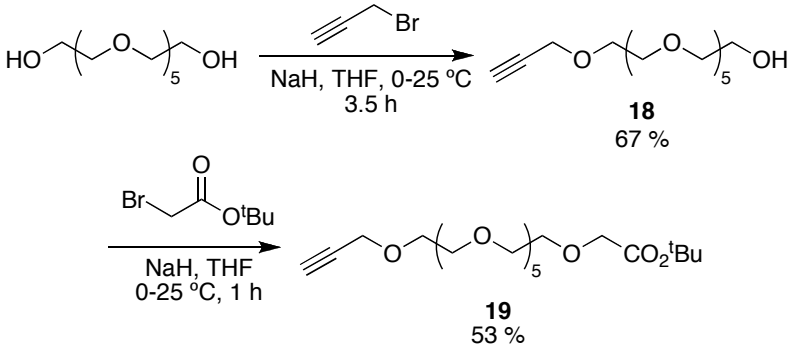

The azido-ethylene glycol tosylate **17** and propargylated ethylene glycol ester **19** were then reacted *via* a copper-catalyzed [2+3] cycloaddition to give triazole **20**. The tosyl group of **20** was replaced with azide to afford ester **21** in 95 % yield without chromatographic separation (Scheme 2.7).

Scheme 2.7. Cu-catalyzed cycloaddition reaction of tosylate **17** and ester **19**.

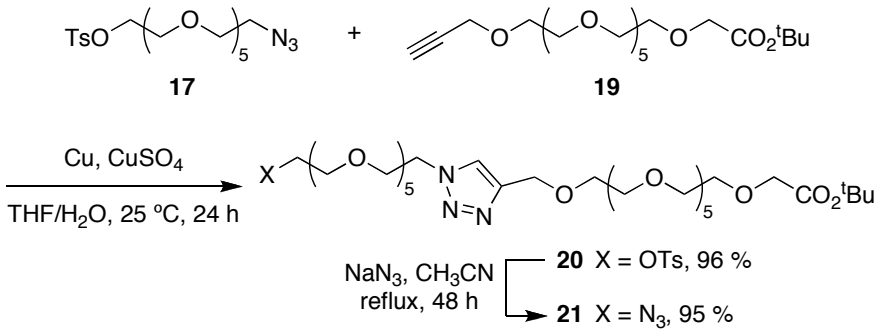

Ester **21** was then deprotected under mild reaction conditions (TFA/CH_2Cl_2, 25 ºC, 2 h). Trifluoroacetic acid and CH_2Cl_2 were removed and virtually pure target molecule **14** was obtained in 99 % yield (Scheme 2.8).

Scheme 2.8. Synthesis of water-soluble ethylene glycol **14**.

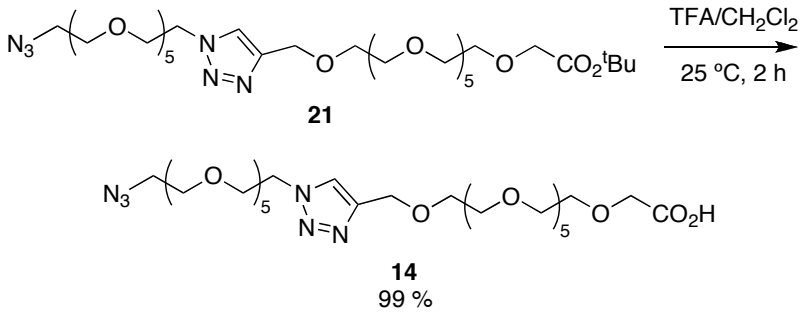

The nucleophilic reaction of propargylamine to dichloro-BODIPY **9**[57] which was synthesized by Mrs. Lingling Li in our group, selectively gave the desired mono-propargylated BODIPY **22** in 99 % yield at room temperature (Scheme 2.9). Similar nucleophilic reaction at higher temperature (acetonitrile, reflux) gave di-substituted BODIPY derivative and this was done by Dehaen *et al*.[55]

Scheme 2.9. Propargylation of BODIPY **9**.

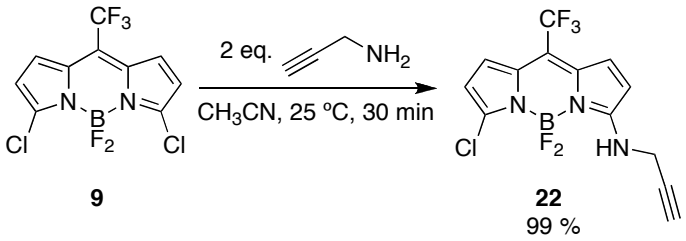

Building on the above results, a copper-catalyzed [2+3] cycloaddition of BODIPY **22** with ethylene glycol linker **14** gave the target water-soluble BODIPY **23** in 76 % yield (Scheme 2.10). Photophysical properties of dye **23** will be shown in the next section.

Scheme 2.10. Click reaction of BODIPY **22** and ethylene glycol **14**.

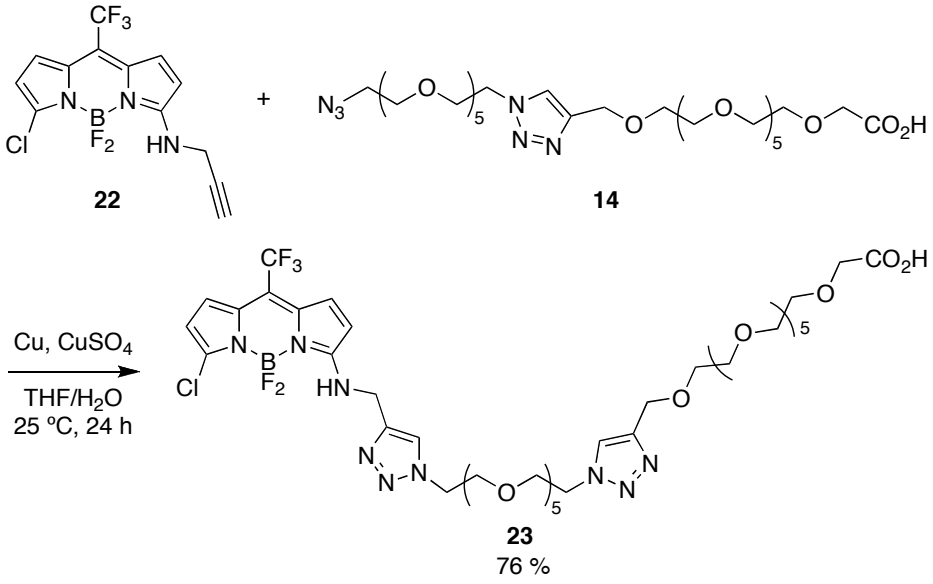

Figure 2.12 represents the structure of BODIPY **12** and **23**. Dye **12** was synthesized by Mrs. Lingling Li and used as a control compound against dye **23** to compare their photophysical properties. Figure 2.13 shows the UV absorption and fluorescence emission spectra for dye **12** and **23** in MeOH and pH 7.4 buffer. Almost similar UV absorption and emission maxima were obtained for both dyes in MeOH. UV absorption

of **23** resulted in a slight red-shift compared to that of **12** in pH 7.4 phosphate buffer. This is due to the enhanced water-solubility of dye **23**; however, the fluorescence emission maxima of dye **12** and **23** were quite similar. More details concerning the photophysical properties for these dyes are presented in the table on page 30.

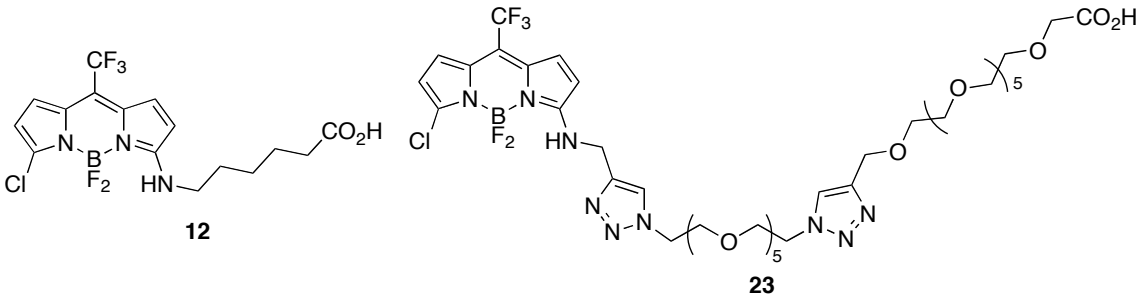

Figure 2.12. Structures of BODIPY **12** and **23**.

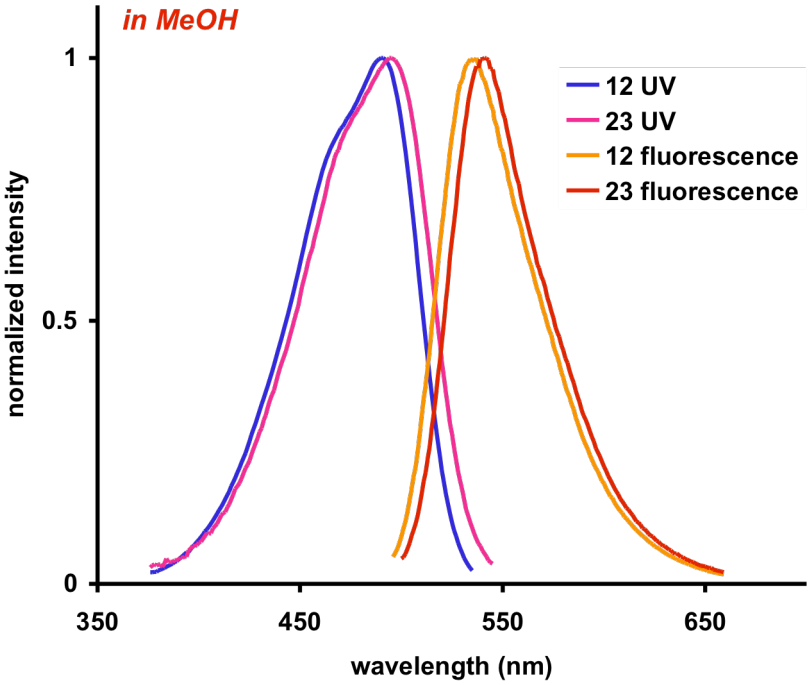

Figure 2.13. Normalized UV absorption and fluorescence emission spectra of dyes **12** and **23** in MeOH and pH 7.4 phosphate buffer.

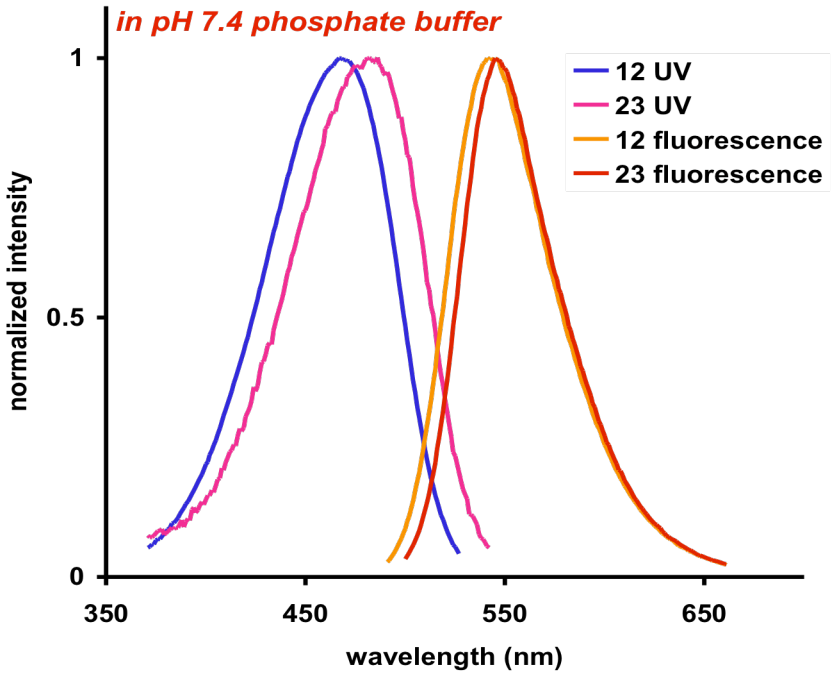

Figure 2.13. Continued.

We next studied the effects of linker length on the photophysical properties of dye-protein conjugates **12** and **23**. To perform this study, we first made dye-protein conjugates **12-BSA** and **23-BSA** (Scheme 2.11). The carboxylic acid of dye **12** or **23** were activated using NHS and DIC in DMF at 25 ºC. The subsequent coupling reaction of activated dye **12** and **23** with BSA in pH 8.3 buffer followed by size exclusion column chromatography and lyophilization of the solvents afforded the dye-protein conjugates **12-BSA** and **23-BSA** as a light yellow powder. The dye:protein ratio for **12-BSA** and **23-BSA** were calculated[61] to be 2.5 and 1.3, respectively. Figure 2.14 shows the normalized UV absorption and fluorescence spectra for dye-protein conjugates in pH 7.4 buffer.

Scheme 2.11. Syntheses of dye-protein conjugates **12-BSA** and **23-BSA**.

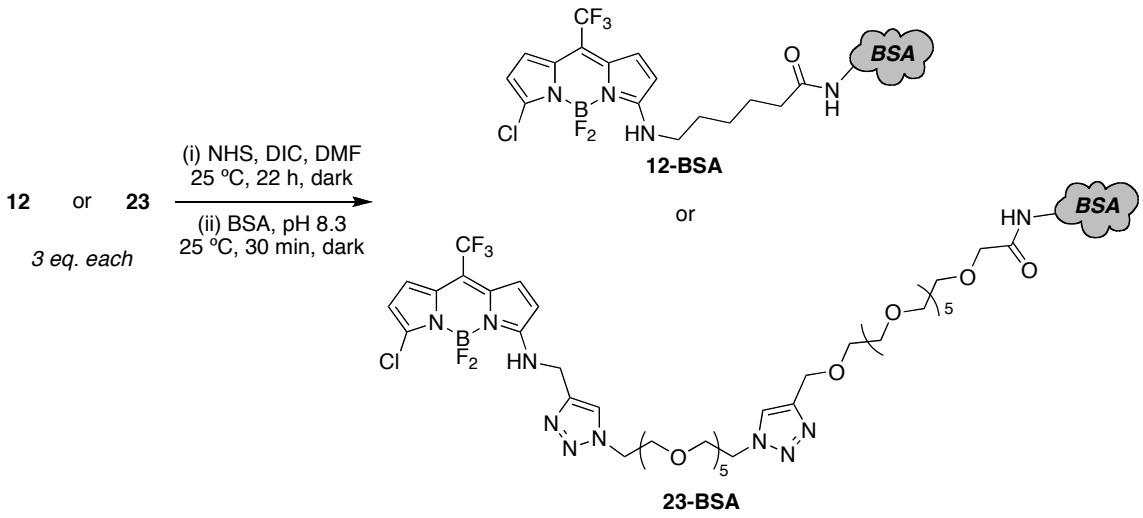

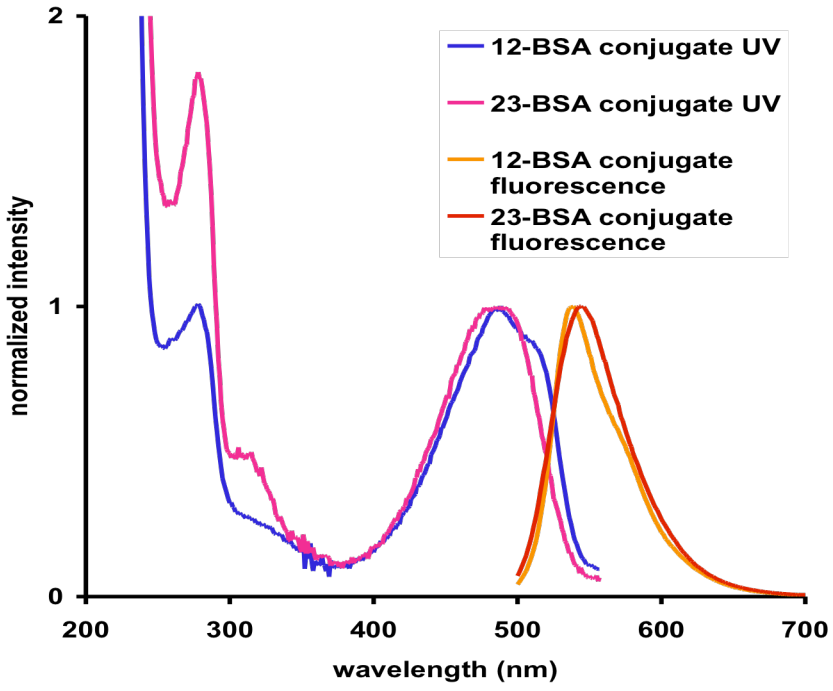

Figure 2.14. Normalized UV absorption and fluorescence emission spectra of **12-BSA** and **23-BSA** in pH 7.4 phosphate buffer.

Steady-state fluorescence spectroscopic studies were performed on a Cary Eclipse fluorometer for the determination of quantum yields. The slit width was 5 nm for both excitation and emission. The relative quantum yield of the samples were obtained by comparing the area under the corrected emission spectrum of the test sample with that of a solution of fluorescein in 0.1 N NaOH, which has a quantum yield of 0.92 according to the literature.[62] The quantum efficiencies of fluorescence were obtained from multiple measurements (N = 3) with the following equation:

$$\Phi_x = \Phi_{st} (I_x/I_{st}) (A_{st}/A_x) (\eta_x^2/\eta_{st}^2)$$

Where Φ_{st} is the reported quantum yield of the standard, **I** is the area under the emission spectra, **A** is the absorbance at the excitation wavelength and η is the refractive index of the solvent used, measured on a pocket refractometer from ATAGO. **X** subscript denotes unknown, and **st** denotes standard.[63]

Table 2.1 shows the photophysical properties for free dyes, hexanoic acid BODIPY **12** and oligoethylene glycol BODIPY **23**, and dye-protein conjugates **12-BSA** and **23-BSA**. In MeOH, UV absorption and fluorescence maximum for **12** and **23** were almost the same (**12**: λ_{abs} 490 nm, λ_{emiss} 537 nm, **23**: λ_{abs} 494 nm, λ_{emiss} 541 nm). The quantum yield of dye **12** in MeOH (Φ 0.70) is slightly higher than that of **23** (Φ 0.65). Similar photophysical properties were obtained when the UV and fluorescence were measured in pH 7.4 except for extinction coefficient. The extinction coefficient of dye **23** in MeOH and pH 7.4 were decreased by about one-third and by half of those of dye **12**, in respective solvents. The quantum yield of dye **23** was increased by 0.1 in pH 7.4 compared to MeOH. This is due to the increasing water-solubility of fluorophore; actually dye **23** is highly water-soluble in aqueous media. The quantum yields of **12-BSA** and **23-BSA** in pH 7.4 were decreased by 30 and 41 % from those of free dyes, respectively.

Table 2.1. Photophysical properties of free dyes and dye-protein conjugates.

dye	solvent	$\lambda_{max\ abs}$ (nm)	ε ($M^{-1}cm^{-1}$)	$\lambda_{max\ emiss}$ (nm)	fwhm (nm)	Φ^c
12	MeOH	490	34300	537	56	0.70
12	pH 7.4[a]	468	24900	541	61	0.74
12-BSA	pH 7.4	488	–	538	56	0.52
23	MeOH	494	11700	541	54	0.65
23	pH 7.4	482	14000	545	56	0.74
23-BSA	pH 7.4	489	–	544	59	0.44

[a] sodium phosphate buffer; [b] fluorescein was used as a standard (Φ 0.92 in 0.1 N NaOH).

2.3.2 Conclusion

We synthesized two water-soluble BODIPY derivatives with short (**12**) and long chains (**23**). The absorption and fluorescence maxima of dye **12** were similar to those of dye **23**. Dye **12** had good photophysical properties in MeOH and pH 7.4 phosphate buffer with quantum yields of 0.70 and 0.74, respectively. The BODIPY with the PEG chain (**23**) had a quantum yield of 0.65 in MeOH, and in aqueous medium the quantum yield improved by a factor of 0.1 to 0.74. This phenomenon is due to the enhancement of water-solubility of dye **23**. Moreover, dye-protein conjugates of **12** and **23** were synthesized and their photophysical properties were studied in aqueous medium. The quantum yields of dye-protein conjugates **12** and **23** were decreased only by 30 and 41 % from those of free dyes, respectively. The quantum yield of dye-protein conjugates dramatically decreases compare to those of free dyes in most cases. Thus the quantum yields of 0.52 for **12-BSA** and 0.44 for **23-BSA** are highly desirable data at physiological pH.

2.4 Water-soluble Nile Blue Derivatives

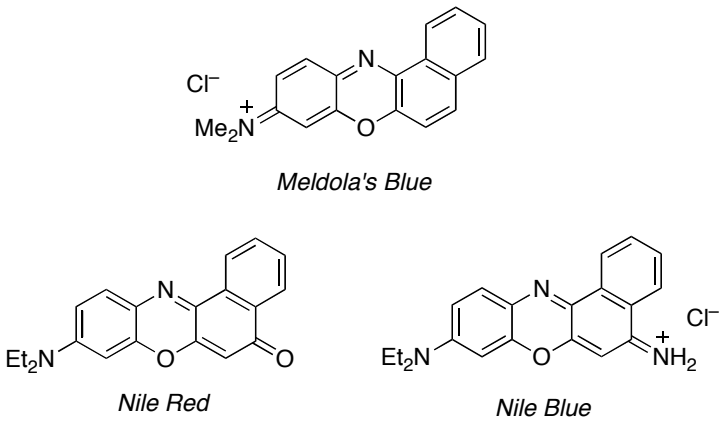

Figure 2.15. Series of benzophenoxazine-based dye.

Benzophenoxazine-based dyes like Meldola's Blue, Nile Red[64], and Nile Blue[64] have some desirable attributes as fluorescent probes (Figure 2.15).[65] Nile Red and Nile Blue have reasonably high quantum yields in apolar organic solvents and they fluoresce at relatively long wavelengths. However, none of these dyes are significantly soluble in aqueous media and their quantum yields are dramatically reduced. One of the big challenges in the production of fluorescent dyes is to produce water-soluble probes that fluoresce strongly in aqueous media, particularly above 600 nm or at even longer wavelengths.

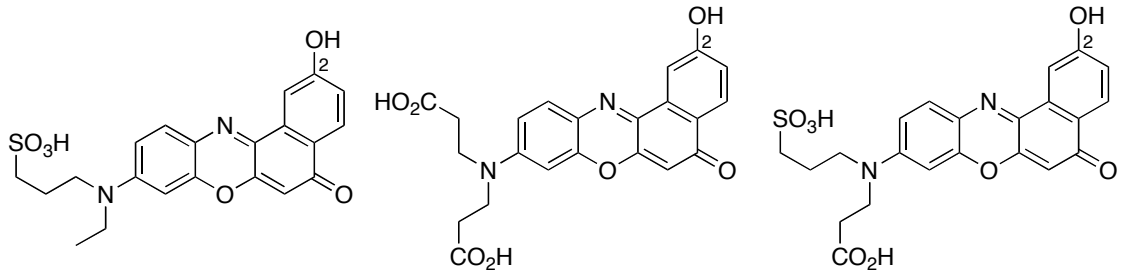

Briggs — *Burgess*

24	**25**	**26**
MeOH	pH 7.4	pH 7.4
$\lambda_{max\ abs}$ 547 nm	Φ 0.33	Φ 0.37
$\lambda_{max\ emiss}$ 618 nm	$\lambda_{max\ abs}$ 560 nm	$\lambda_{max\ abs}$ 558 nm
	$\lambda_{max\ emiss}$ 648 nm	$\lambda_{max\ emiss}$ 652 nm

Figure 2.16. Water-soluble Nile Red derivatives.

The first synthesis of water-soluble Nile Red derivative **24** was described by Briggs and co-workers, but the data for photophysical properties were shown only in methanol (λ_{abs} 547 nm, λ_{emiss} 632 nm).[66,67] Our group has reported functionalized water-soluble Nile Red derivatives **25** and **26**, and their photophysical properties were shown in aqueous media (pH 7.4 and pH 9.0).[68,69] Dyes **25** and **26** have excellent water-solubilities and reasonable quantum yields in aqueous media (>0.3). Moreover, they emit fluorescence around 650 nm and have reasonably sharp peaks (Figure 2.16).

Nile Blue **27** is a fluorescent probe that has been known for over 110 years (Figure 2.17).[64,69] In polar media, its absorption and emission maxima shift to the red, which is indicative of stabilized charge separation in the excited state; consequently, this dye has been used to monitor events that depend upon solvent polarity.[70-72] It has also been used for FRET studies.[73,74] Nile Blue tends to have a higher affinity for cancerous cells than healthy ones[75] and it is a photosensitizer for oxygen;[76,77] these two properties together can be useful in photodynamic therapy.[78] However, two properties of Nile Blue in aqueous media are limiting for many applications, specifically (i) low solubility and (ii) low quantum yield.

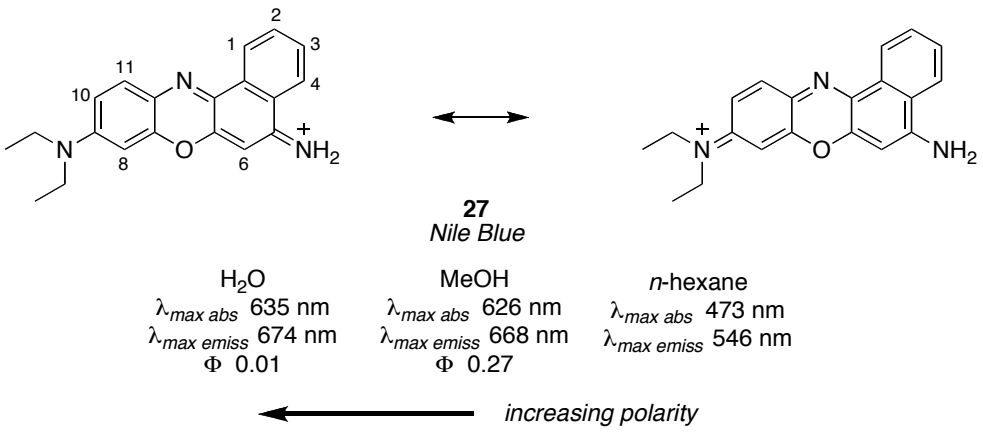

Figure 2.17. Photophysical properties of Nile Blue **27** in various solvents.

Some work has been reported on Nile Blue derivatives with improved water solubilities.[79-82] The aggregation of inherently flat, lipophilic aromatic dyes is disfavored when they are functionalized with water-solubilizing substituents and their quantum yields can improve as a result. Consequently, Nile Blue derivatives with hydrophilic groups can have improved solubilities and fluorescence outputs. Derivatives **28** and **29** are the most interesting probes to arise from these studies (Figure 2.18).[79] Their quantum efficiencies are improved by as much as a factor of ten, however, they have no carboxylic acid handle for attachment to biomolecules, and the sharpness of their emissions broadens as the solvent is changed from methanol to water, which is perhaps indicative of aggregation.

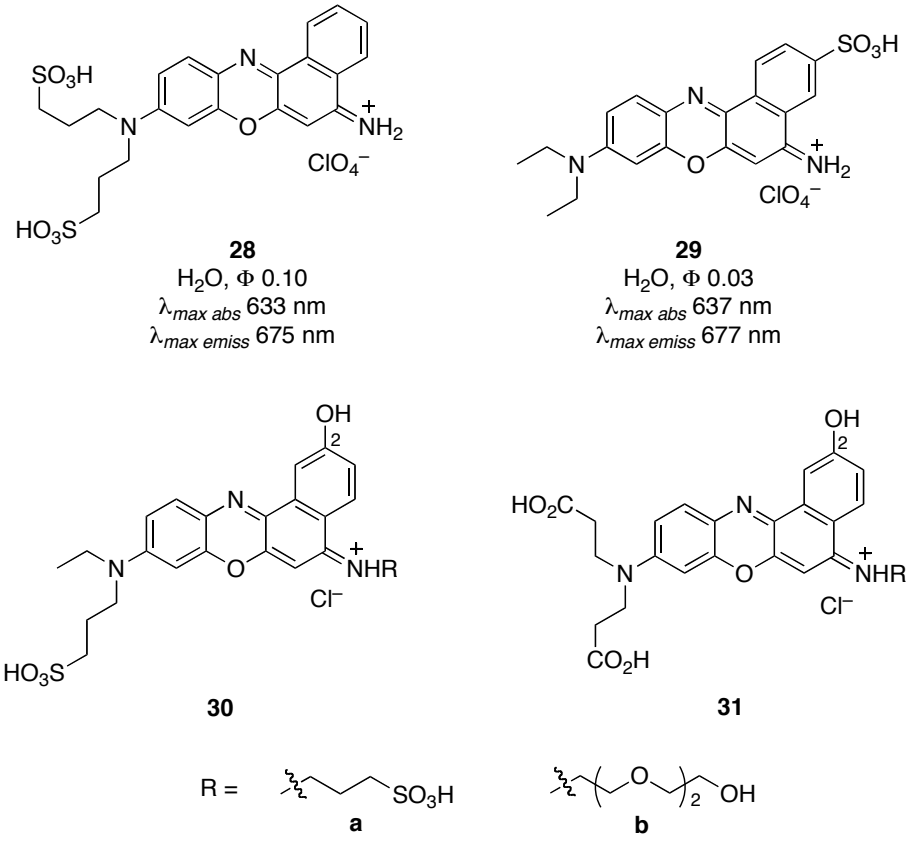

Figure 2.18. Water-soluble Nile Blue derivatives in literature (**28** and **29**) and from our group (**30** and **31**).

2.4.1 Results and Discussion (*Synthesis of Water-soluble Nile Blue Derivatives*)

In this section, we discuss the synthesis of 2-hydroxy Nile Blue derivatives **30** and **31**[83] and compares their fluorescence properties with those of **28** and **29**. For both probes, a 2-hydroxy substituent was incorporated to enhance water solubility and other hydrophilic groups are situated on both ends of the molecule to reduce the potential for aggregation. Not all possible applications of these dyes require functional groups for attachment to biomolecules, but many do, and compounds **31a** and **31b** were designed for that purpose.

The western part of targets **30** and **31** were formed from functionalized nitrosophenols; these were prepared as outlined in Scheme 2.12. Nitroso compound **36** was formed via nitrosylation of phenol **35**, a starting material previously used in our laboratories for syntheses of Nile Red derivatives.[68] The 3-(*N*-ethylamino)phenol **32** and derivative **33** have been previously described in a patent that gives the experimental procedures.[84] Nitrosylation of phenol **33** gave the nitroso compound **34**.

Scheme 2.12. Syntheses of functionalized aminophenol **34** and **36**.

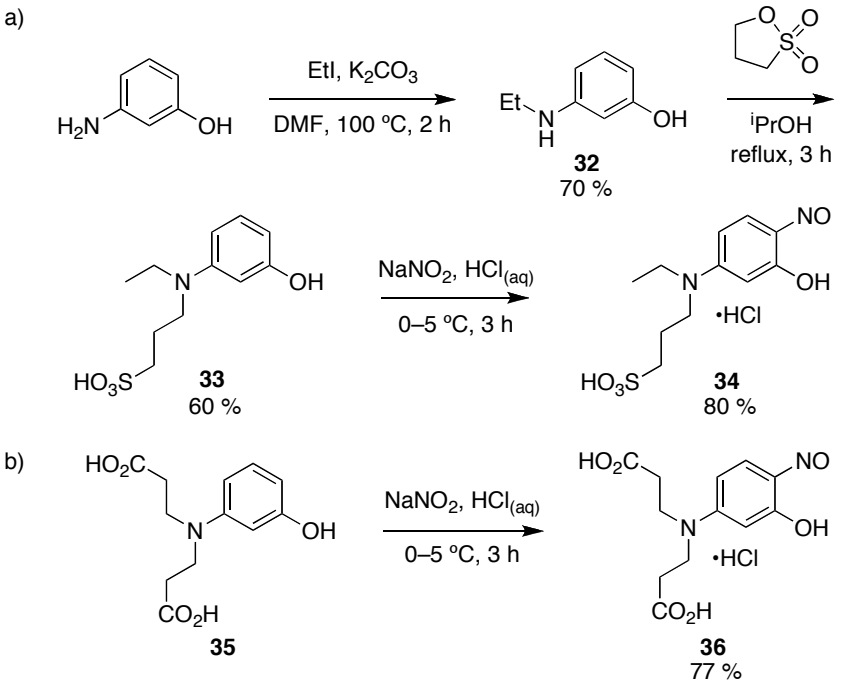

Both the aminonaphthol components **37** required for the eastern half of these molecules were made via alkylation reactions. Compound **37a** was obtained via alkylation with propane sultone (Scheme 2.13a). The triethylene glycol derivative **39** was conveniently made via TBDMS-protection and tosylation of the parent diol, then this was used to *N*-alkylate 5-amino-2-naphthol to give compound **40**. Aminonaphthol **40** was then deprotected to afford compound **37b** as shown (Scheme 2.13b).[60,85,86]

Scheme 2.13. Syntheses of aminonaphthol components **37**.

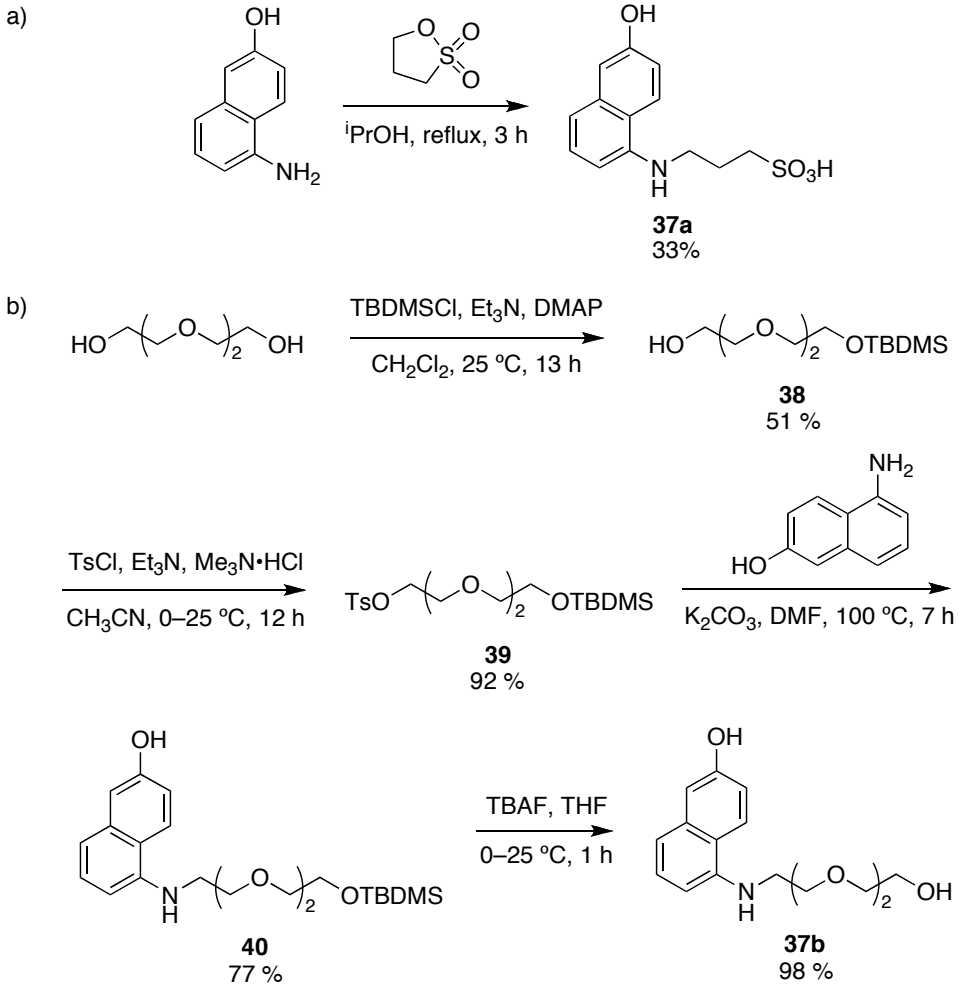

Previous syntheses of Nile Blue derivatives required relatively high temperatures and/or strong acids. Compounds **30** and **31** were made via condensation at a relatively low temperature (90 °C) without addition of any additional acids. The blue products were isolated by using medium-pressure liquid chromatography (MPLC) on a reverse phase C18 column (Scheme 2.14).

Scheme 2.14. Syntheses of water-soluble Nile Blue derivatives.

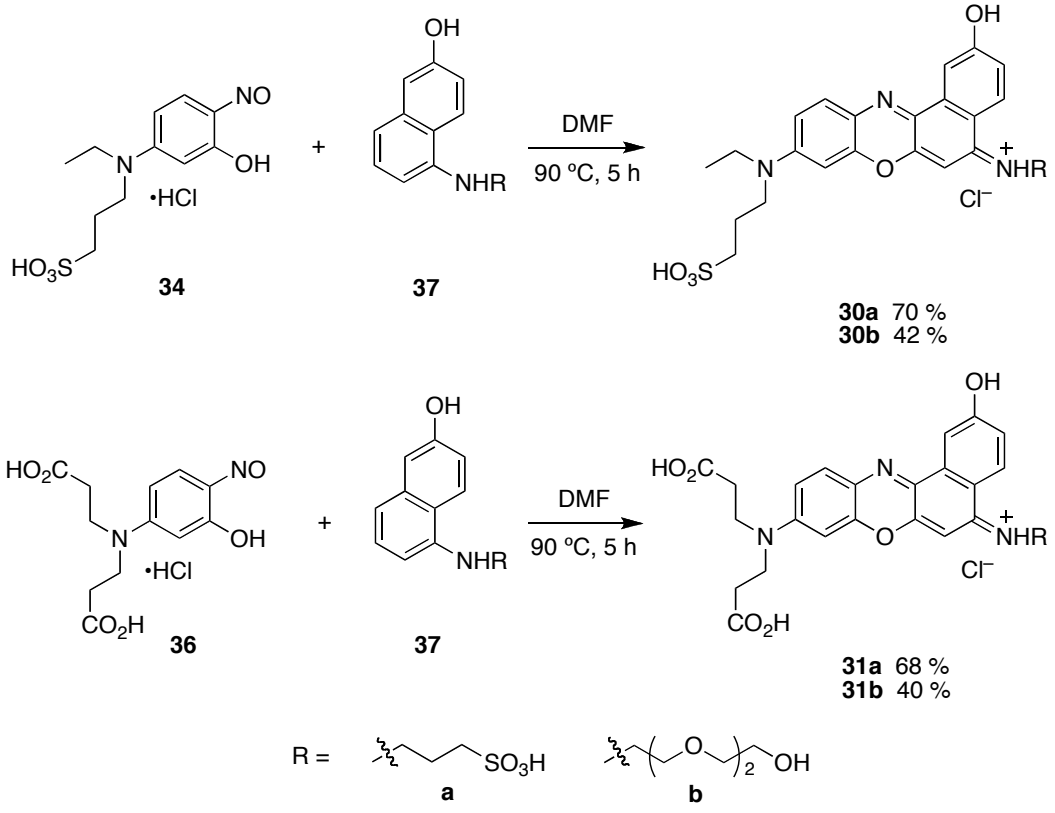

The electronic spectra (Figure 2.19) of the dyes were recorded in methanol (as a representative polar organic solvent), in 0.1 M phosphate buffer at pH 7.4 (PB, Table 2.2), in the same buffer but with 3 % Triton X-100 (TX), and in 0.1 M pH 9.0 borate buffer (BB). Only **30a** and **31a** were soluble in MeOH; data for **30b** and **31b** could not be obtained in this medium. The effects of adding Triton X-100 to the medium are

ambiguous; this reagent changes the solvent polarity, but might also prevent aggregation effects.[71,87,88] In borate buffer at pH 9.0, the phenolic hydroxyl of the dyes will be predominately in the anionic form.

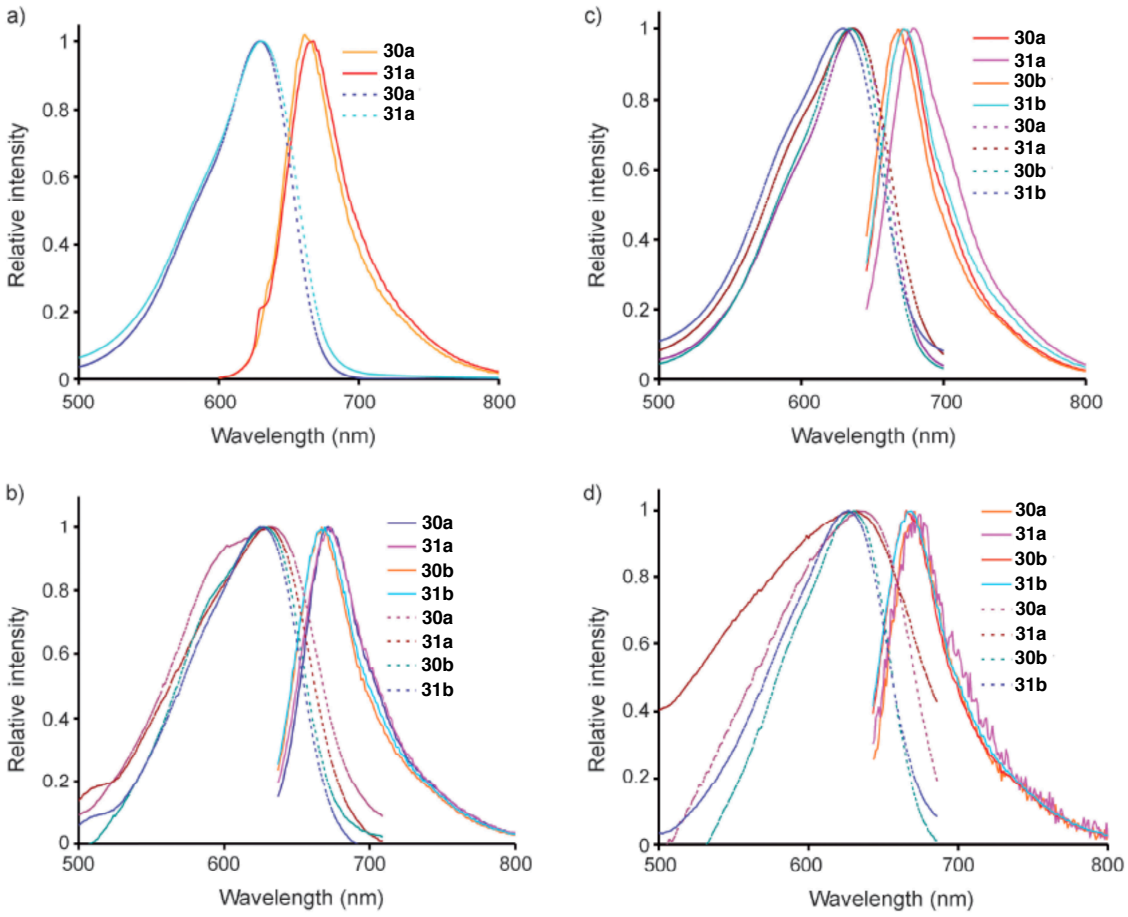

Figure 2.19. Absorption (dashed lines) and fluorescence (solid lines) of **a**: **30a** and **31a** in methanol and **30a,b** and **31a,b** in **b**: phosphate buffer (pH 7.4), **c**: phosphate buffer (pH 7.4) with 3% Triton X-100, and **d**: borate buffer (pH 9.0). All dyes (2×10^{-6} M) were excited at their corresponding λ_{max}.

Table 2.2. Spectroscopic properties of the Nile Blue and its derivatives under different conditions.

dye	λ_{abs} (nm)	ε ($M^{-1}cm^{-1}$)	$\lambda_{em.}$ (nm)	fwhm (nm)	Φ[a]	solvent
30a	628	14400	662	47	0.56	MeOH
30a	630	42400	671	52	0.14	PB[b]
30a	631	51200	669	49	0.24	TX[c]
30a	630	28400	670	56	0.02	BB[d]
31a	629	58800	666	50	0.32	MeOH
31a	630	30300	670	58	0.10	PB[b]
31a	629	64100	669	56	0.11	TX[c]
31a	631	34500	670	73	0.02	BB[d]
30b	629	33600	671	55	0.14	PB[b]
30b	628	44400	670	47	0.23	TX[c]
30b	630	21800	672	51	0.13	BB[d]
31b	632	38100	673	56	0.13	PB[b]
31b	631	14700	672	54	0.26	TX[c]
31b	630	38000	670	54	0.08	BB[d]
27[e]	635	4000	675	115	0.01	water
28[e]	633	36000	675	86	0.10	water
29[e]	637	11000	677	93	0.03	water

[a] standard used for quantum yield measurement: Nile Blue in MeOH (Φ : 0.27), quantum yield measurements were repeated three times and extinction coefficients were measured at 10^{-6} M; [b] pH 7.4 phosphate buffer; [c] 3 % Triton X-100 in pH 7.4 phosphate buffer; [d] pH 9.0 borate buffer; [e] values obtained from ref. [79].

All the dyes under any of the conditions described above, had absorption maxima between 628 – 632 nm; consequently, there is little variation of this parameter with solvent polarity. Extinction coefficients for the molecules, however, were in the range 14,400 – 64,100. For **30a**, **31a**, and **30b**, the maximum values corresponded to the media that includes Triton X-100; such enhancement effects have been observed for fluorescent dyes,[87,88] including Nile Blue.[71] Fluorescent emission maxima for the dyes varied between 662 – 673 nm. The fact that compounds **30a** and **31a** had fluorescence emission maxima in MeOH that were within 9 nm of the values obtained in aqueous buffers means that the solvatochromic effects for these two materials are much less than for Nile Red. Further, the lack of significant variations between the emission wavelengths in the various buffers indicates that changing the pH away from physiological levels and adding lipophilic co-solvents have little effect on these dyes. The sharpness of the fluorescent emissions are expressed in terms of full width at half maximum peak heights (fwhm; where smaller is sharper). All the dyes **30** and **31** emitted with sharper fluorescence peaks than Nile Blue or the more water-soluble forms **28** and **29** (data shown in Table 2.2 for these dyes is taken from the literature reference). Further, in aqueous media the quantum yields for these emissions were in all cases better for **30** and **31** relative to Nile Blue and its derivatives **28** and **29**.[79]

Figure 2.20 outlines experiments performed to explore aggregation of the dyes in aqueous media. Plots of the normalized UV absorbance versus concentration reveal that the $\lambda_{max\ abs}$ for compound **30a** at 4 μM occurs at 671 nm, with an inflection on the blue side of the peak at approximately 600 nm (Figure 2.20a). This inflection point grows as the concentration of the dye was increased; at 16 μM there are two distinct absorption maxima, and at higher concentrations, the shorter wavelength absorption becomes dominant. Figure 2.20b shows that at concentrations of up to 4.0 μM the absorbance of **30a** varies in a near linear way with concentration. Above that concentration, the absorbance deviated markedly from linear concentration dependence. Overall, these data may be interpreted to mean that the dye is aggregating at concentrations above *ca* 4.0 μM. Similar analyses using UV absorption indicate that dye **30a** deviates from Beer-Lambert behavior above this concentration. Probably the dyes are forming fluorescent J-aggregates at concentrations above *ca* 4.0 μM, rather than the non-fluorescent H-forms. Analyses for dyes **30b**, **31a**, and **31b** (Figures 2.20c – h) indicate very similar behavior. Concentration versus absorbance studies indicate that these materials tend to aggregate above 4.0 μM.

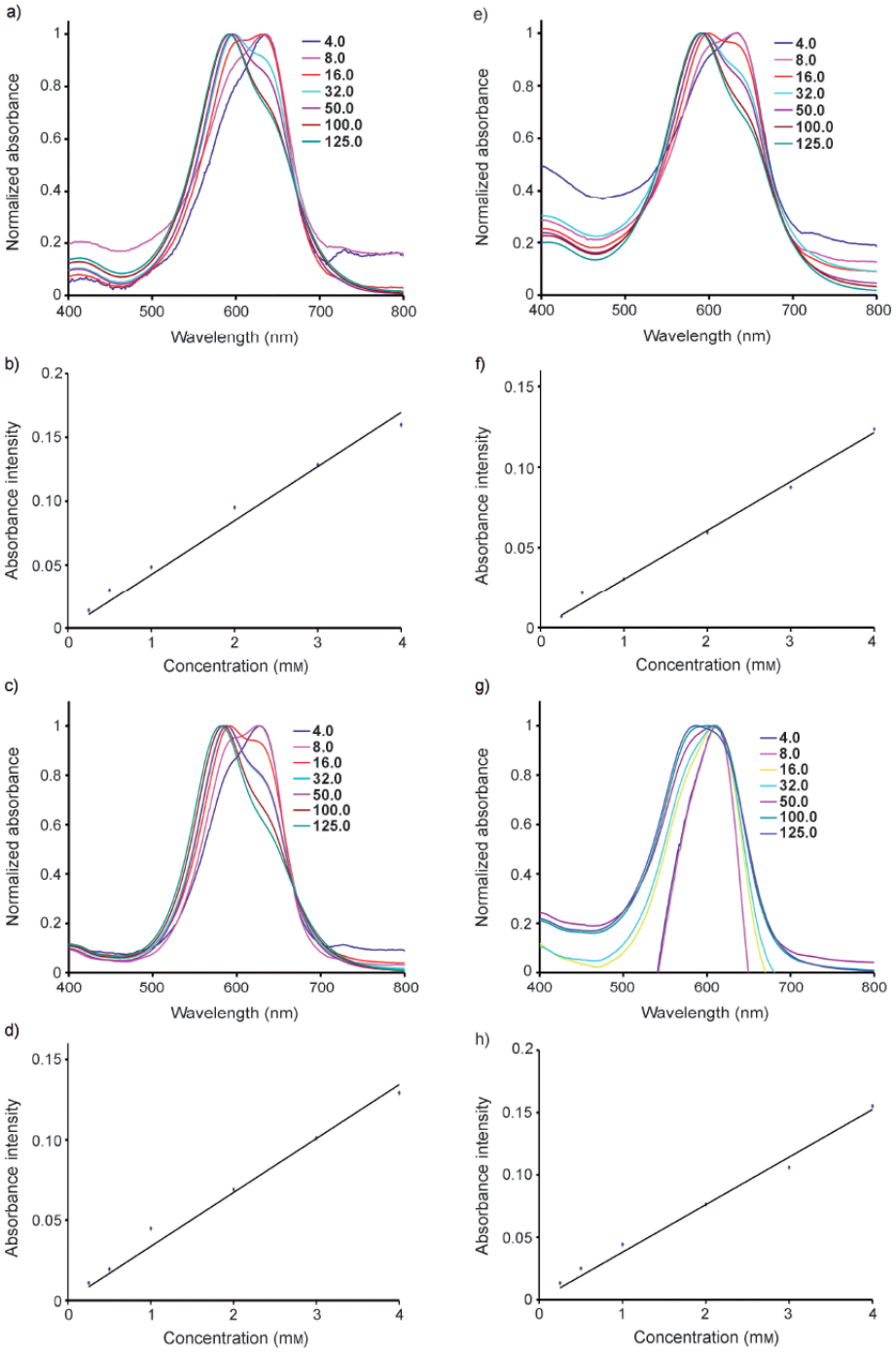

Figure 2.20. Aggregation studies. Normalized absorption for various concentrations of **30a** (a), **30b** (c), **31a** (e), and **31b** (g) in phosphate buffer at pH 7.4, and plots of absorbance intensity vs. concentration of **30a** (b), **30b** (d), **31a** (f), and **31b** (h).

Finally the Nile Blue derivative, **31a** was used to label ovalbumin by activation of the dye-dicarboxylic acids (*N*-hydroxysuccinimide and *N*,*N*'-diisopropylcarbodiimide in DMF) followed by addition of this activated probe to protein in 0.1M $NaHCO_3$ solution (pH 8.3). The dye:protein ratio was calculated[61] to be 1.1 when 5 eq. of dye was used; this corresponds to 22 % labeling efficiency. This sample was used to obtain the spectral data shown in Figure 2.21a. The wavelengths for the absorption and fluorescence maxima for the free dye **31a** and the **31a**-ovalbumin conjugate were observed to be almost identical, but the fluorescence intensity was much less.

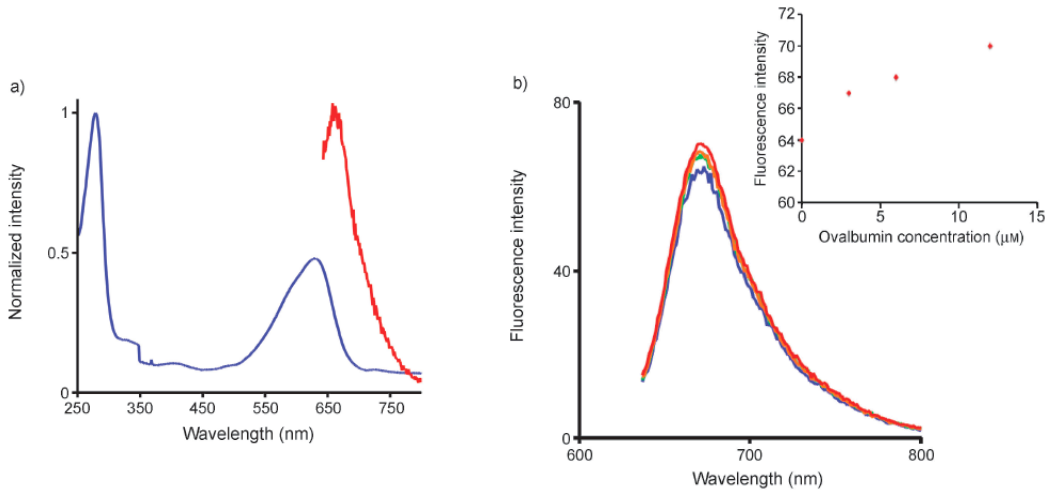

Figure 2.21. Absorption and fluorescence spectra of covalently and non-covalently bonded dye-protein conjugates. **a**: Absorbance (blue) and fluorescence (red) spectra of **31a**-ovalbumin in 0.1 M phosphate buffer (pH 7.4). **b**: Fluorescence spectra of **31a** (5 x 10^{-7} M) and blue: 0, green: 3.0, orange: 6.0, and red: 12.0 μM ovalbumin in phosphate buffer (pH 6.8), λ_{ex} = 630 nm. Inset: Variation in the fluorescence intensity of **31a** vs. ovalbumin concentration.

One application of Nile blue derivatives is to measure protein concentrations; this is possible because the fluorescence intensities of Nile blue derivatives tend to increase with protein concentration.[70] However, one limitation of this method is that the solubility of Nile Blue derivatives can be problematic. Herein, the Nile Blue derivative

31a was mixed with increasing concentrations of ovalbumin in pH 6.8 phopsphate buffer. The fluorescence data for this set of experiments are shown in Figure 2.21b. The measurements were performed at different pH values because in one case a covalent interaction was formed by using a protocol at pH 8.3, whereas the other was a simple addition at a more standard pH. The fluorescence intensity of **31a** was increased when the protein was added. These increases were small, but the concentrations of ovalbumin were only varied between 3 – 12 μM, *ie* also small changes in protein concentration that are hard to detect. Furthermore, unlike in some previous works with lipophilic Nile Blue derivatives, use of the water-soluble form **31a** circumvented the need for any detergent additives.

2.4.2 Conclusion

The Nile Blue derivatives **30** and **31** have sharper fluorescence emissions (fwhm 30 nm less), and improved quantum yields in pH 7.4 phosphate buffer relative to the known water-soluble Nile Blue derivatives **28** and **29**. They are formed via condensation reactions that do not require additional acids or very harsh reaction conditions (DMF, 90 °C); this is in marked contrast to the syntheses of most other Nile Blue derivatives. Preparative HPLC purification of the products was not necessary: they were isolated by using reverse phase MPLC with acetonitrile/water as the eluent. The phenolic OH functionalities of dyes **30** and **31** almost certainly increase the water solubilities of these compounds. Alternatively, the phenolic group provides a potential avenue for further derivatization of the dyes (*eg* via triflation and organometallic couplings, or for attachment of a handle to enable dyes **30** to be conjugated to proteins). Three other groups that promote water solubilities were included in these studies: a sulfonic acid, dicarboxylic acids, and a triethylene glycol fragment. Despite this, the fluorescence properties of the dyes, and presumably their aggregation states at elevated concentrations, did not vary significantly. All the dyes showed little tendency to aggregate below 1 – 4 μM; this characteristic would tend to make them useful for biochemical studies when used in relatively dilute solutions, but would exclude

applications where quantitation is required at higher concentrations. Probably the most useful spectroscopic parameter of the dyes is their fluorescence at relatively long wavelengths, 670-680 nm, in aqueous media. Probes that emit above 650 nm are relatively few, yet they tend to be the most useful ones for tissue and intracellular imaging applications.[89,90]

CHAPTER III

THROUGH-BOND ENERGY TRANSFER CASSETTES FOR MULTIPLEXING

3.1 Introduction

Through-bond energy transfer (TBET) cassettes consist of donor and acceptor dyes connected by π-electron conjugated linkers (*e.g.* alkene, alkyne, or benzene moiety). As described in Chapter I, a set of TBET cassettes based on one donor and different acceptors, simultaneously provides multiple fluorescence by the single excitation of donor part and this makes it possible to perform multiplexing.

Fluorophores which have absorption maxima in the range of 450–530 nm can be used as donors. Coumarin, fluorescein, and BODIPY dyes are some examples of dyes that can be used as donors. However most coumarins tend to have short wavelength absorption maxima and thus high energy is required to excite them, and this leads to cell damage in biological studies. Fluorescein and BODIPY dyes are superior because they can be excited at 488 nm and emit strong fluorescence. In fact, we have been focusing on these fluorophores as donors for synthesizing TBET cassettes in our laboratory for several years.[53,91-93]

Acceptor dyes for cassettes, must fluoresce above 600 nm with relatively high quantum yields. The commonly used BODIPY dyes emit around 520 nm, however, these dyes with extended conjugation fluoresce above 600 nm, some even in near IR region and these were reported by Ziessel as bisisoindolomethene dyes[48], Suzuki as furan-fused BODIPYs (also called Keio Fluors)[49], and Burgess and O'Shea as *B*,*O*-chelated aza-BODIPYs[94] (Figure 3.1). Rosamine dyes are photostable and tend to have high quantum yields, but purification of these dyes are usually difficult and gives low product yields. Previous group members attempted the microwave-assisted syntheses of 5-bromo rosamine derivatives and this approach improved the yields of rosamine dye

syntheses compared to syntheses under thermal conditions.[95] However, the emission maxima of rosamine dyes cannot be easily extended beyond 650 nm.

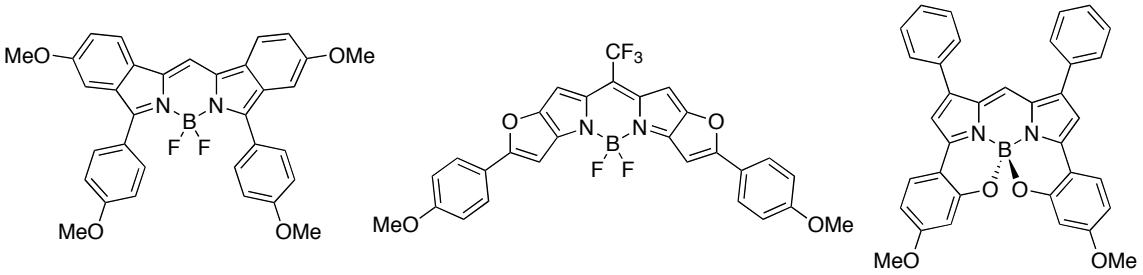

Ziessel
CH_2Cl_2
$\lambda_{max\ abs}$ 673 nm
$\lambda_{max\ em}$ 704 nm
ε 118600
Φ 0.49

Suzuki
$CHCl_3$
$\lambda_{max\ abs}$ 723 nm
$\lambda_{max\ em}$ 738 nm
ε 253000
Φ 0.56

Burgess & O'Shea
toluene
$\lambda_{max\ abs}$ 765 nm
$\lambda_{max\ em}$ 782 nm
ε –
Φ 0.18

Figure 3.1. NIR fluorescent probes based on BODIPY dyes.

We are interested in TBET cassettes which fluoresce near IR region. Cyanine dyes fluoresce in the range of 600 to 800 nm with distinct emission maxima and there are no reports of TBET cassettes based on these dyes in literature. Therefore, the specific aims for synthesizing TBET cassettes for multiplexing studies are as follows:

(i) study the photophysical properties of cyanine dyes;
(ii) design and synthesis of a series of TBET cassettes which can be excited at single wavelength and fluoresce at multiple wavelengths; and,
(iii) enhancement of water-solubility and photostability by the encapsulation of cassettes with silica or calcium phosphate nanoparticles.

We will discuss the synthesis of BODIPY derivatives as a donor in section 3.2, the structural and photophysical properties of cyanine dyes in section 3.3 and the syntheses of three TBET cassettes based on BODIPY and cyanine dyes in section 3.4. The general synthetic approaches of encapsulating TBET cassettes in hydrophilic silica or calcium phosphate nanoparticles will also be described as applications in section 3.5.

3.1.1 Preliminary Through-bond Energy Transfer (TBET) Cassettes

As a proof of concept, previous group members reported the syntheses and photophysical properties of four TBET cassettes **41-44** in 2003 (Figure 3.2).[91] These cassettes **41-44** were synthesized *via* Sonogashira coupling between one 5-ethynyl fluorescein derivative as a donor and four different 5-bromo rosamine dyes **45-48** as acceptors. Each cassettes fluoresce at different emission wavelengths (538, 582, 603, and 616 nm, respectively), when excited at fluorescein donor. Their emissions are dispersed over a 78 nm wavelength range (Figure 3.3), and their fluorescence signals are easily differentiated. When the donor fluorescein of each cassettes was excited at 488 nm, these four cassettes **41-44** produce four different colors because of their different emission wavelengths, thus this property possibly serves for multiplexing study in DNA sequencing and cell imaging.

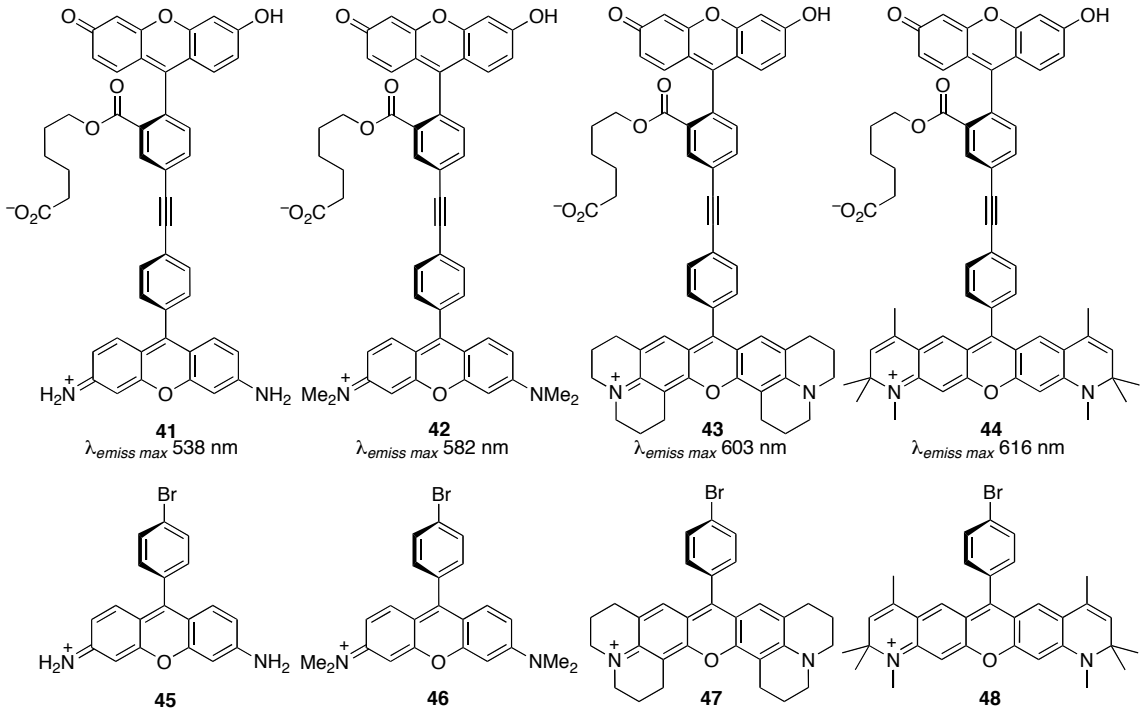

Figure 3.2. TBET cassettes **41-44** and acceptor synthons **45-48** of those cassettes.

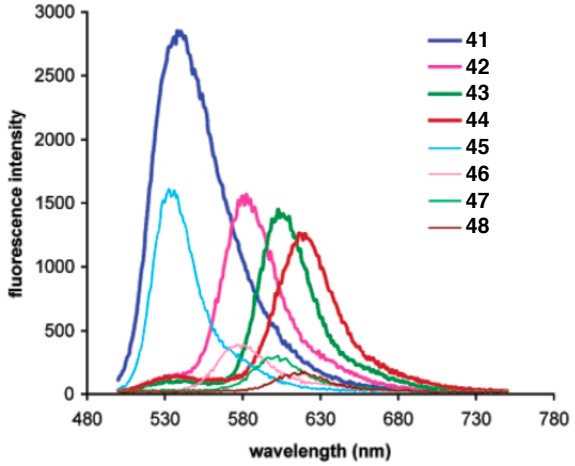

Figure 3.3. Fluorescence of equimolar EtOH solutions of **41**-**48** excited at 488 nm.

These four TBET cassettes **41-44** were not water soluble and water-soluble cassettes are preferred in biological studies. To address this issue, previous group members attached four carboxylic groups to rosamine component of cassette **41** and synthesized water-soluble TBET cassette **49** for intracellular imaging (Figure 3.4).[92,96] Cassette **49** was prepared via Sonogashira coupling between 5-ethynyl fluorescein derivative and 5-bromo rosamine tetracarboxylic acids derivative.

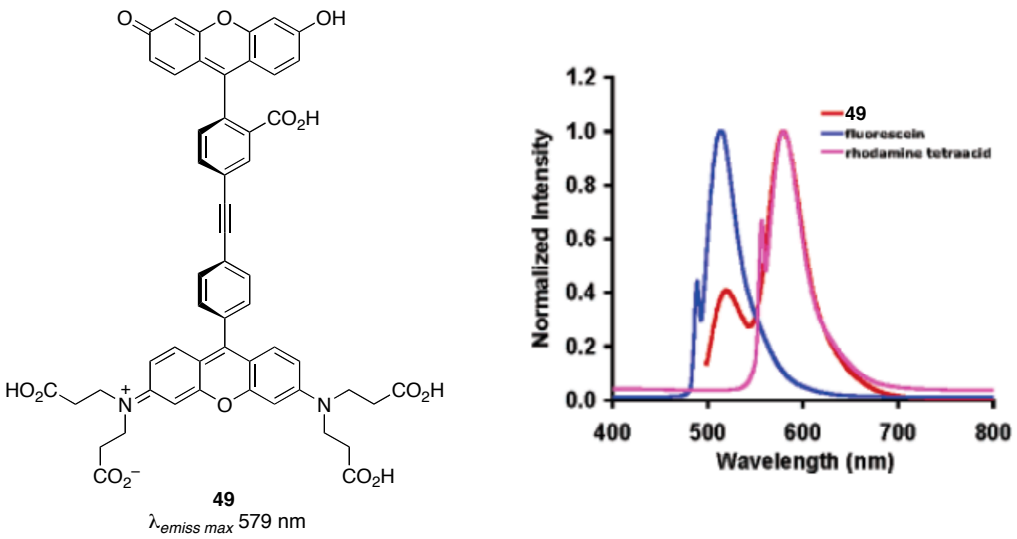

Figure 3.4. Structure of cassette **49** (left) and fluorescence spectra of **49**, donor fluorescein and acceptor rosamine (right).

Cassette **49** shows approximately 80 % energy transfer in pH 8 phosphate buffer when cassette is excited at 488 nm which corresponds to the excitation wavelength of donor fluorescein (red line, Figure 3.4). For cellular imaging studies, cassette **49** was attached to ACBP (mouse acyl-coenzyme A binding protein) and this dye-protein conjugate was imported into COS-7 cells with Chariot which is a cell-penetrating peptide. Chariot is unique insofar as it binds nonselectively and noncovalently to extracellular proteins and mediates their transfer into cells. Cellular imaging of ACBP-**49** conjugate in COS-7 cells showed colocalization around the nuclei. When the cells were excited at 488 nm (excitation of donor fluorescein), the fluorescence signals from the acceptor (a filter at 598 nm) were observed and this signal was brighter than that of acceptor when it was excited at 520 nm (excitation of acceptor). According to these data, ACBP-**49** conjugate in the cell is more visible when the cassette **49** is irradiated at the donor excitation; hence, the function of the energy-transfer cassette is demonstrated *ex vivo*.

3.2 Donor Fragments (BODIPY Dyes)

As described in Chapter II, most BODIPY dyes have excellent photophysical properties in organic and aqueous media. Therefore, BODIPY dyes were chosen as donor parts for synthesizing TBET cassettes.

3.2.1 Results and Discussion (*4-Halogenated and Ethynyl-BODIPY Derivatives*)

Syntheses of BODIPY dyes involve condensation of two equivalents of pyrrole with one equivalent of an aliphatic or aromatic aldehyde, and their syntheses and photophysical properties were reviewed by Burgess[50] and Ziessel.[97] These dyes can be easily derivatized to their corresponding halogenated and ethynylated form. As a starting material for BODIPY synthesis, 2-hydroxy-4-iodobenzoic acid was alkylated with iodomethane followed by DIBAL reduction to afford primary alcohol **51**. This alcohol **51** was oxidized back to iodobenzaldehyde **52** with pyridinium chlorochromate in 91 % yield (Scheme 3.1).

Scheme 3.1. Synthesis of 4-iodo-2-methoxybenzaldehyde **52**.

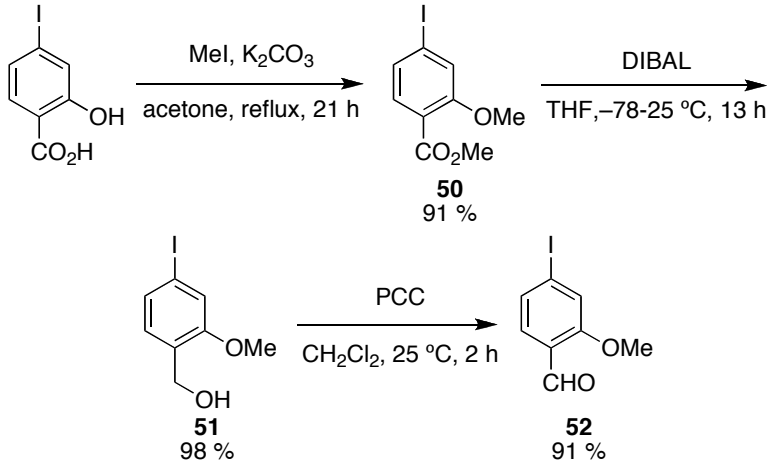

4-Iodo-2-methoxybenzaldehyde **52** was condensed with 2.2 eq. of 2,4-dimethylpyrrole followed by oxidation and BF_2-chelation to afford BODIPY **53** in moderate yield. This was coupled with trimethylsilyl acetylene *via* Sonogashira coupling to give TMS-protected BODIPY dye **54** and the TMS-group of this dye was deprotected with tetrabutylammonium fluoride to afford 4-ethynyl-BODIPY **55** in 92 % yield (Scheme 3.2). Uses of BODIPY **55** to TBET cassette syntheses will be shown in section 3.4.

Scheme 3.2. Synthesis of 4-ethynyl tetramethyl-BODIPY **55**.

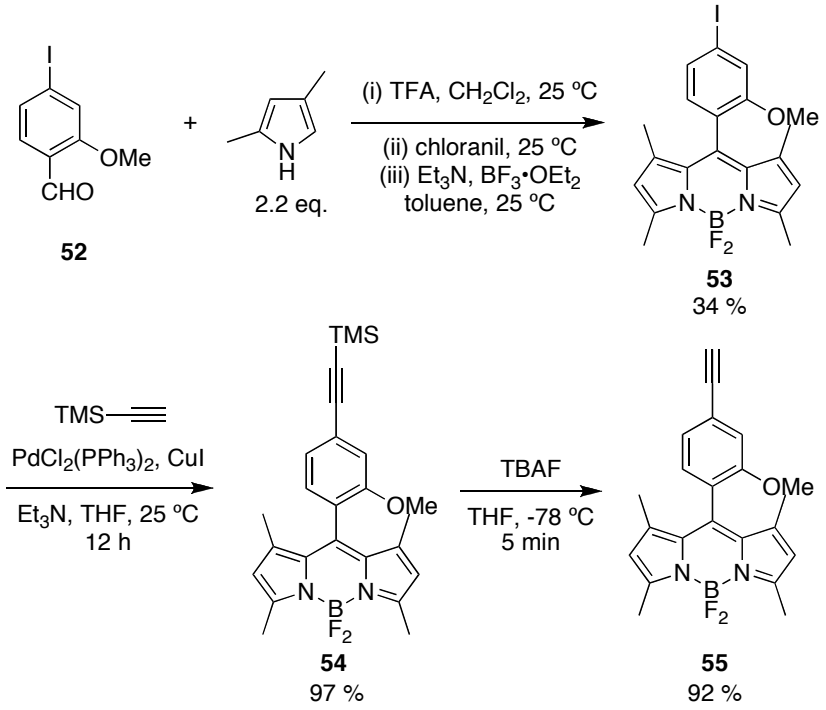

4-Iodo tetramethyl BODIPY with carboxylic acid (**58**) was next synthesized. 4-Iodobenzaldehyde **56** (*provided by Mr. Liangxing Wu*) was condensed with 2,4-dimethylpyrrole (2.2 eq.) followed by oxidation and BF_2-chelation to afford BODIPY **57**. Methyl ester of this dye was deprotected under mild condition (K_2CO_3,

MeOH/THF/H_2O, 25 ºC) and an aqueous work-up gave pure BODIPY **58** (99 % yield) as a control compound for TBET cassette syntheses (Scheme 3.3).

Scheme 3.3. Synthesis of 4-iodo tetramethyl-BODIPY **58**.

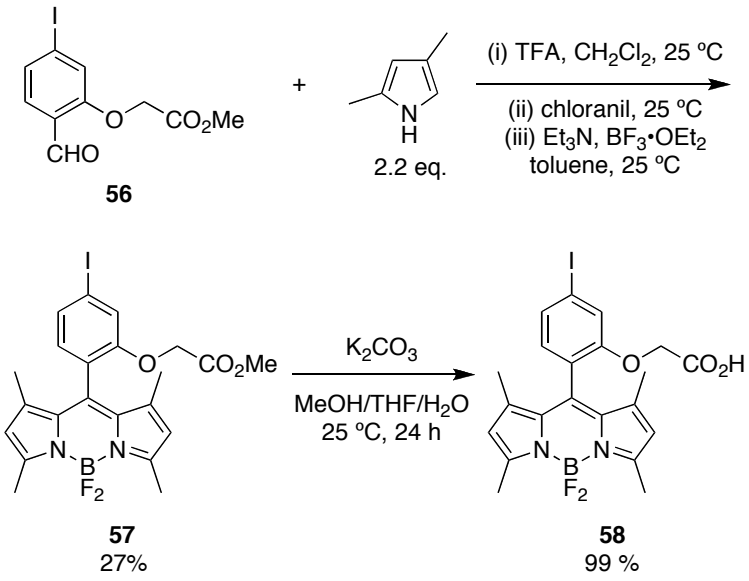

Finally, 5-ethynyl tetramethyl BODIPY with carboxylic acid (**63**) was synthesized. 5-Iodobenzaldehyde **59** (*provided by Mr. Liangxing Wu*) was condensed with 2.2 eq. of 2,4-dimethylpyrrole followed by oxidation and BF_2-chelation to afford BODIPY **60**. BODIPY **60** was coupled with trimethylsilyl acetylene *via* Sonogashira coupling to give TMS-protected BODIPY dye **61** and TMS-group of this dye was deprotected with tetrabutylammonium fluoride to afford 5-ethynyl-BODIPY **62**. Finally the deprotection of methyl ester with K_2CO_3 gave final product **63** (Scheme 3.4). BODIPY **63** was used for the protein mono-labeling (Chapter IV).

Scheme 3.4. Synthesis of 5-ethynyl tetramethyl-BODIPY **63**.

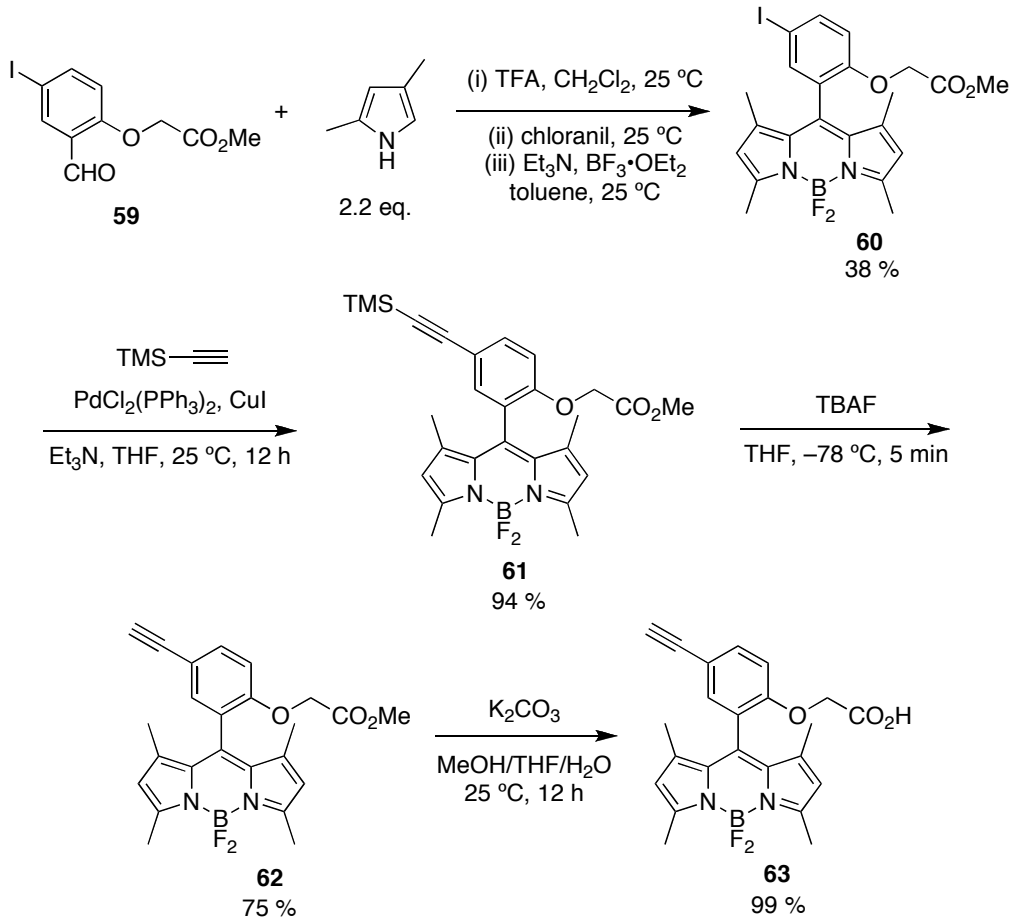

3.2.2 Conclusion on Donor Synthesis

In conclusion, we synthesized two useful 4-ethynyl-BODIPY derivatives **55** and **63**. We also obtained three 4-halogenated derivatives **53**, **58** and **60** as an intermediate for ethynyl-derivative, and these dyes can be used as donors for TBET cassettes syntheses. Similar BODIPY dyes were used to prepare cassettes in our group.

3.3 Acceptor Fragments (Cyanine Dyes)

Cyanine dyes as acceptor fragments for TBET cassettes are promising because they have near IR emissions (typically 650-800 nm). This section outlines structures, syntheses, and photophysical properties of general cyanine dyes in literature. On the basis of this knowledge, we attempted to synthesize three iodinated-cyanine dyes. The photophysical properties of these cyanine dyes will also be evaluated.

3.3.1 Cyanine Dyes

Cyanine dyes have been known for more than 150 years (first synthesized by C. H. G. Williams in 1856).[98] These dyes tend to have long absorption and emission wavelengths (>550 nm) because of its unique structure. Only few fluorescent probes emitting in the near-IR (NIR) region with high quantum yields are reported so far.[89,94,99] Such probes are valuable for intracellular imaging because auto-fluorescence in cells tends to obscure the fluorescence emission at wavelengths below *ca.* 550 nm, but this phenomenon becomes less at longer wavelengths. Fluorescent probes that emit in the 700–900 nm region are, therefore, relatively easy to visualize *in vivo,*[90] and cyanine dye is the most widely used NIR fluorescent probes. Futher, cyanine dyes are the least cyctotoxic dyes known till date,[90] thus the use of cyanines is highly suitable for the biological assays.

Cyanine dyes are categorized into three major groups: streptocyanines (or open cyanines), hemicyanines and closed cyanines (Figure 3.5). Each two nitrogens are joined by polymethine chain (n = 0, 1, 2). The heteroaromatic parts for hemicyanines and closed cyanines can be replaced with a variety of heterocyclic components.

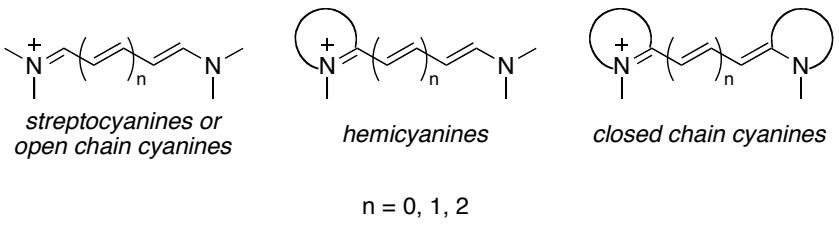

Figure 3.5. Structures of cyanine series.

Figure 3.6 demonstrates the general structures and photophysical properties of cyanine dyes. The numbers Cy3, Cy5 and Cy7 correspond to the number of carbons in polymethine chain. The extended structures of aromatic parts are known as Cy3.5 and Cy5.5 where the benzene ring is replaced with naphthalene. As shown in Figure 3.6, all cyanine dyes have extremely well separated UV absorption and fluorescence emission maxima. The brightness of cyanine dyes increases with increasing conjugation, and dyes tend to have high extinction coefficient with moderate quantum yields. Remarkably, Cy3, Cy5 and Cy7 have *ca.* 100 nm difference in their absorption and emission; this is a useful attribute in multiplexing studies for cellular imaging.

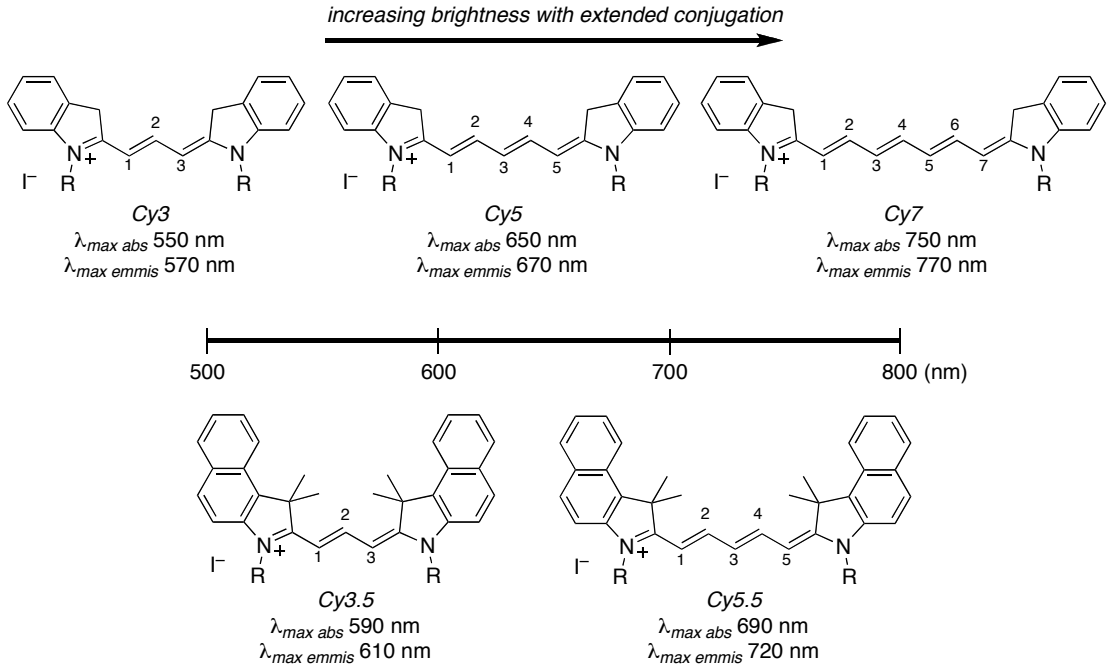

Figure 3.6. General structures of cyanine dye.

Cyanines suffer from low photostabilities and their synthetic manipulations are limited due to reactive alkene chain, modification of which may result in loss of extended conjugation. However, there are few frequently used NIR fluorescent probes based on cyanine dye in biological assays. Figure 3.7 shows the structure of those

compounds. Indocyanine green (ICG) is most widely used in biological application because it does not have aggregation problem.[90] Moreover ICG is one of the least toxic fluorescent probes ever administered to humans, with the only known undesirable reaction being rare anaphylaxis. In recent years, some modification of indocyanine series have been attempted and the improved fluorophore IRDye78 was synthesized and commercialized as its *N*-hydroxysuccinimide ester to conjugate with biomolecules. This dye has tetra-sulfonic acids and these groups increase water-solubility and also quantum yield in aqueous media.

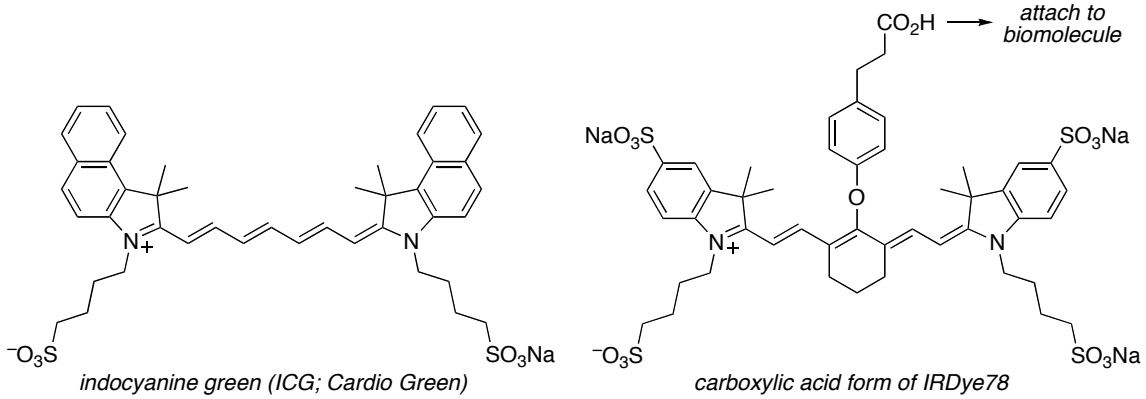

Figure 3.7. Most commonly used NIR dyes.

Cyanine dyes can also act as pH sensitive fluorescent probes. Cooper *et al* reported synthesis of water-soluble Cy5 pH probe and studied its fluorescent property in the range of pH 4.5-9.[100] In this study, one of alkyl groups on nitrogen of heterocyclic ring is replaced with hydrogen. In acidic media, this nitrogen is protonated and cyanine dye exists as fluorescent form. On the other hand, this hydrogen is deprotonated in basic media and it showed almost no fluorescence above pH 8. In fact, protonated form (cyanine dye) and deprotonated form (base form) resulted in different characteristic absorption maximum at 645 nm and 480 nm, respectively. In basic media, the absorption maximum at 645 nm is greatly reduced as a new peak evolves at 480 nm. Recently similar pH probe based on cyanine dye was described by Hilderbrand's group

and they studied ratiometric pH imaging in the cells and biological tissues.[101] More recently, a new type of pH probe based on cyanine dye was reported by Achilefu *et al* and this probe was synthesized *via* barbituric acid mediated synthesis.[102]

3.3.2 General Synthesis of Cyanine Dyes

Both symmetric and unsymmetric cyanine dyes can be synthesized from heterocyclic compounds, and their syntheses and photophysical properties were reviewd by Behera.[103] Scheme 3.5 shows a general synthesis of cyanine dyes. This reaction is usually done by either one-pot or two steps reactions. The advantages of cyanine dye synthesis are the relatively short reaction time and easy work-up procedure. After the reaction, cyanine dyes are usually precipitated by addition of ether and most impurities can be removed with ether.[104] At first, the indole **64** reacts with *N,N'*-diphenylformamidine to form hemicyanine intermediate **65**. This intermediate can also be isolated. Second, an another molecule of indole **66** reacts with intermediate **65** under mild condition (pyridine, 25 ºC) to afford a desired cyanine dye **67**.

Scheme 3.5. General synthesis of cyanine dyes.

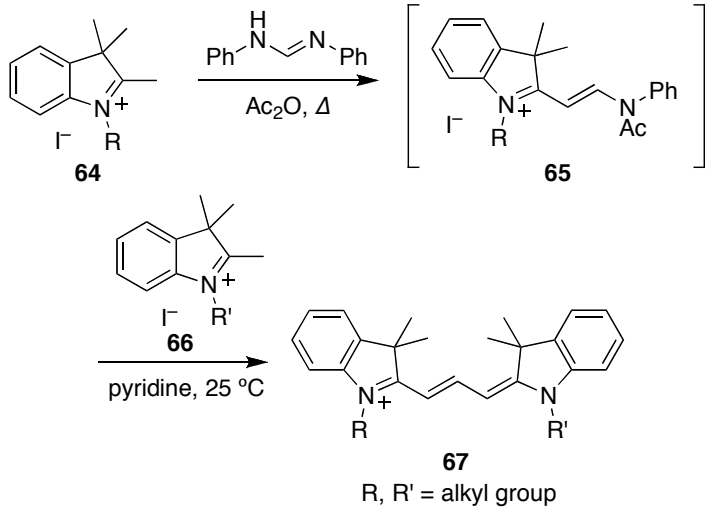

Solution phase syntheses of cyanine dyes sometimes require laborious chromatographic separation of intermediates or the final dye products. To avoid this, solid-phase approaches to cyanine dyes were described by Balasubramanian (Scheme 3.6).[105,106] Hemicyanine **69** was synthesized from indole **68** and malonaldehyde bisphenylimine hydrochloride, then attached to a solid-support using sulfonyl chloride resin (PS-SO_2Cl) to afford compound **70**. Nucleophilic attack of another benzthiazole **71** to the sp^2 carbon produces the desired product **72** in high purity (>95 %) by releasing the solid-support which acts as a leaving group; this concept is called "Catch-and-Release". They reported preparation of more than ten different compounds where the heteroaromatic pairs are different, with high purities and moderate yields. Syntheses of some water-soluble unsymmetric cyanines were also described using this method.

Scheme 3.6. Solid-phase "Catch-and-Release" synthesis.

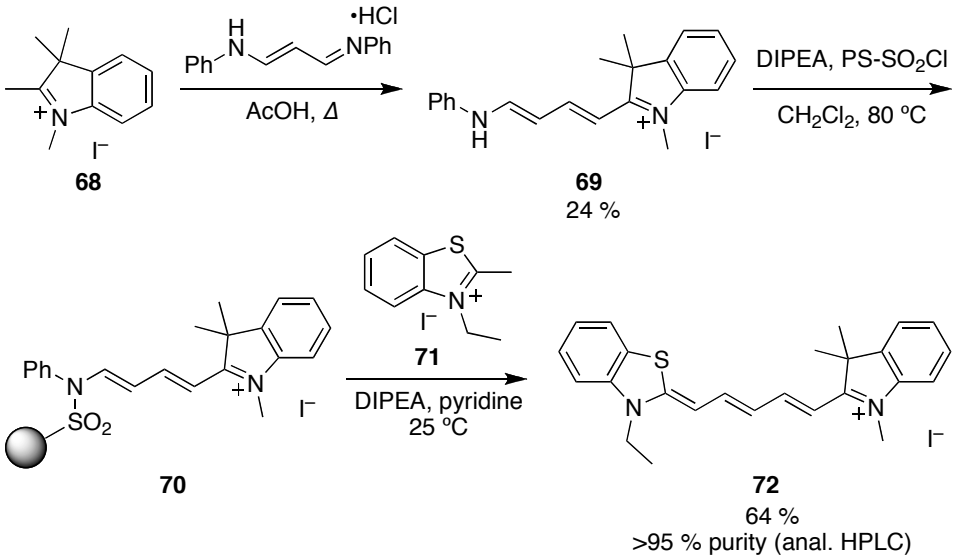

3.3.3 Results and Discussion (*Synthesis of Cyanine Dyes as Acceptors for TBET Cassettes*)

We designed three novel 5-iodo cyanine dyes **74a-c** as acceptor precursors and three known cyanine dyes **73a-c** as their control compounds (Figure 3.8). Two different indolium salts were condensed with three polymethine chain with varying length to synthesize dyes **73** and **74**. Finally, dyes **74** were coupled with 4-ethynyl BODIPY **55** as a donor fragment *via* Sonogashira coupling to afford TBET cassettes **75** (Scheme 3.7).

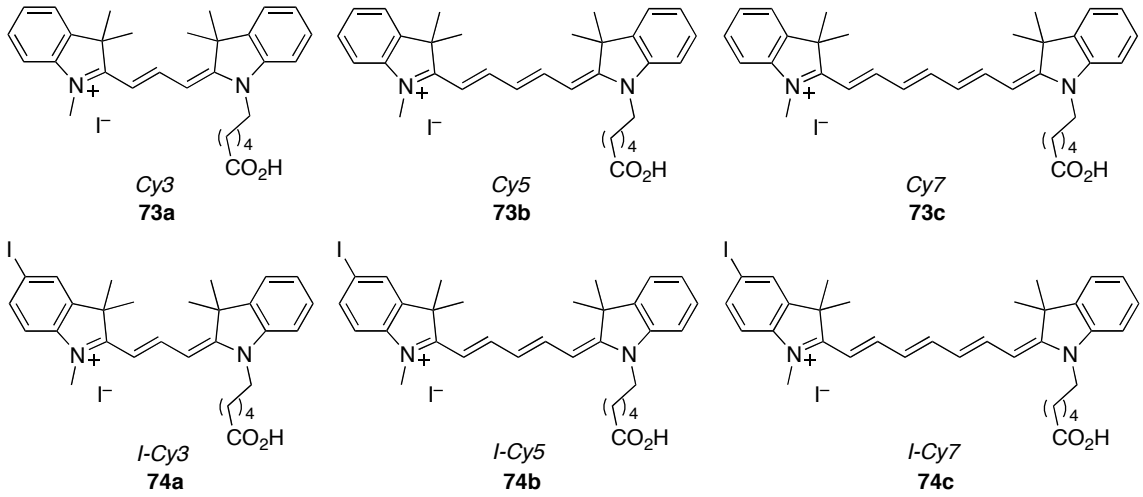

Figure 3.8. Structures of cyanine dyes **73** and **74** used in this research. *I-Cy* stands for iodo-cyanine.

Scheme 3.7. Synthesis of TBET cassette **75** via Sonogashira coupling.

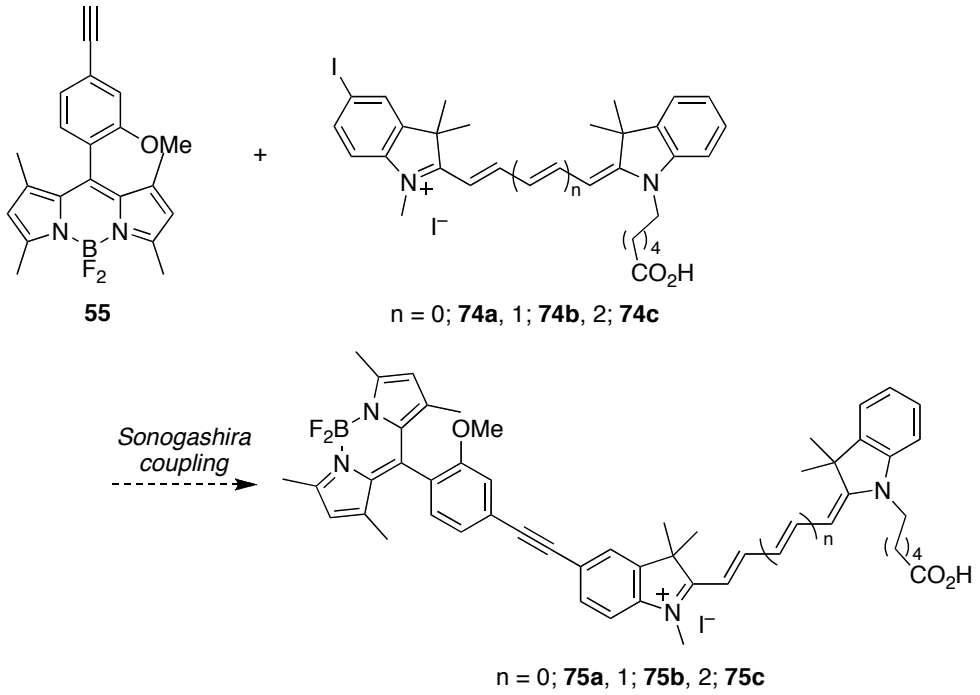

Two indolium salts were synthesized as starting materials for the synthesis of cyanine dyes (Scheme 3.8). The alkylation of 2,3,3-trimethylindolenine by iodomethane or 6-bromohexanoic acid at 80 ºC afforded iodide salt **68**[107] and bromide salt **76**[108], respectively, using previously reported procedures.

Scheme 3.8. Alkylation of 2,3,3-trimethylindolenine.

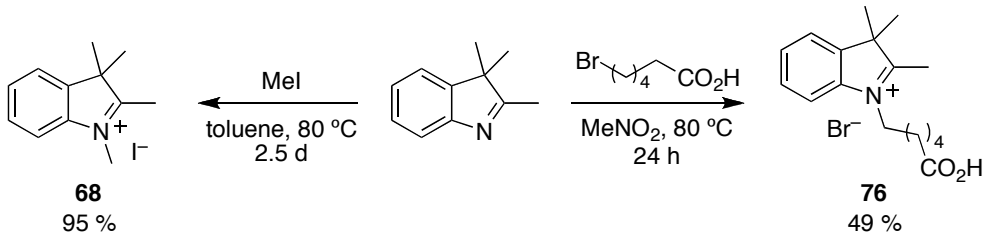

Convenient one-pot syntheses of Cy3 and Cy5 derivatives on a multi-gram scale were described by Shmanai, Korshun, *et al*[108] and their method was used for the cyanine dye syntheses in our group. A solution of bromide salt **76** and *N*,*N*'-

diphenylformamidine in acetic anhydride was heated at 120 ºC for 30 min to generate hemicyanine **77** *in situ*. This hemicyanine intermediate **77** was used for making two cyanine dyes **73a** and **74a** (Scheme 3.9). After the addition of iodide salt **68** with pyridine, the reaction was completed in 1 h and ether was added to the reaction mixture to precipitate the crude product. The addition of ether also helps to wash away acetic anhydride and pyridine. After the chromatographic separation of crude materials, pure Cy3 **73a** was obtained and this will be using as a control compound. On the other hand, the reaction with iodo-indolium salt **78** afforded iodo-Cy3 **74a** and the same work-up procedure was used, but it took a longer reaction time. This is because of the poor solubility of salt **78** in pyridine. Cy5 **73b** and iodo-Cy5 **74b** were synthesized by Mr. Jiney Jose using similar reaction conditions and obtained in 74 and 65 % yields, respectively.

Scheme 3.9. Syntheses of Cy3 **73a** and iodo-Cy3 **74a**.

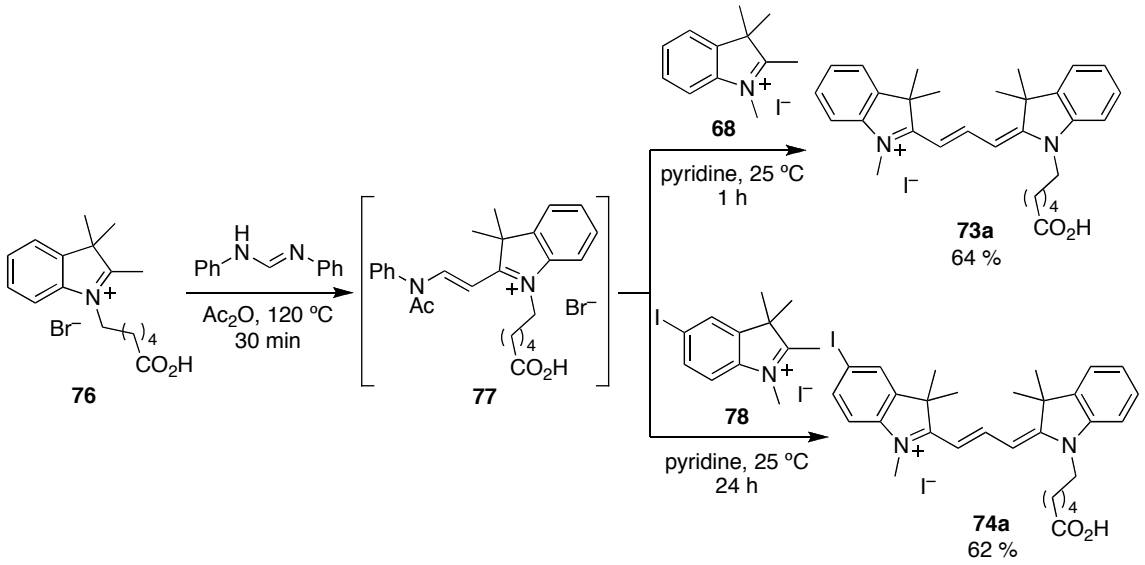

Cy7 **73c** and iodo-Cy7 **74c** were synthesized in two steps because the attempted one-pot synthesis for Cy7 resulted in a messy reaction and low yields. Therefore, we decided to isolate hemicyanine intermediates. The condensation of iodide salt **68** and glutaconaldehydedianil hydrochloride afforded pure hemicyanine intermediate **79** in 90

% yield after the chromatographic separation and, this intermediate was quite isolable and stable. The second condensation of hemicyanine **79** with bromide salt **76** at 50 ºC gave pure Cy7 **73c** in 78 % yield (Scheme 3.10). This **73c** was used as a control compound.

Scheme 3.10. Synthesis of Cy7 **73c** via two steps condensation reaction.

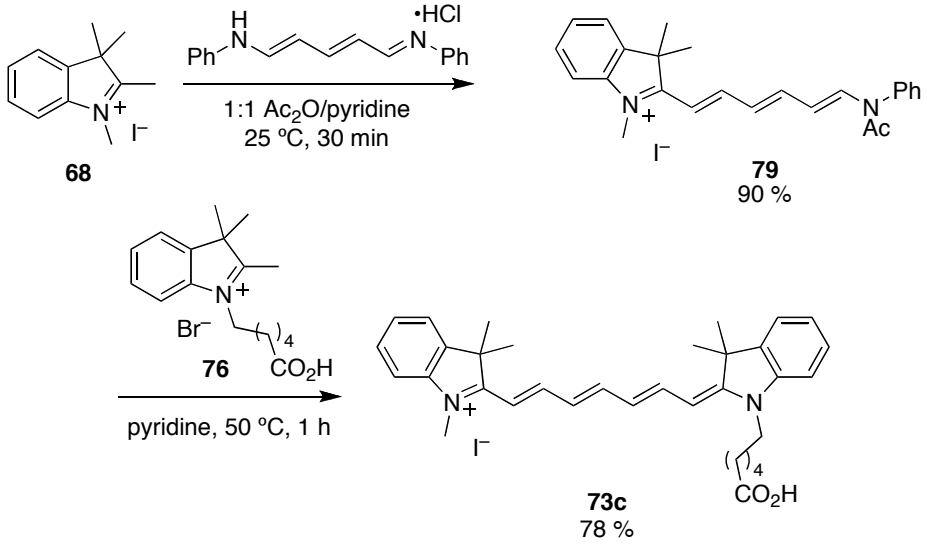

The hemicyanine intermediate **80** was synthesized in 81 % yield *via* the condensation of iodo-indolium salt **78** and glutaconaldehydedianil hydrochloride. The second condensation of intermediate **80** with boromide salt **76** at 50 ºC afforded pure iodo-Cy7 **74c** in 72 % yield (Scheme 3.11). This iodo-Cy7 **74c** was used for the synthesis of TBET cassette, as described in the next section.

Scheme 3.11. Synthesis of iodo-Cy7 **74c** via two steps condensation.

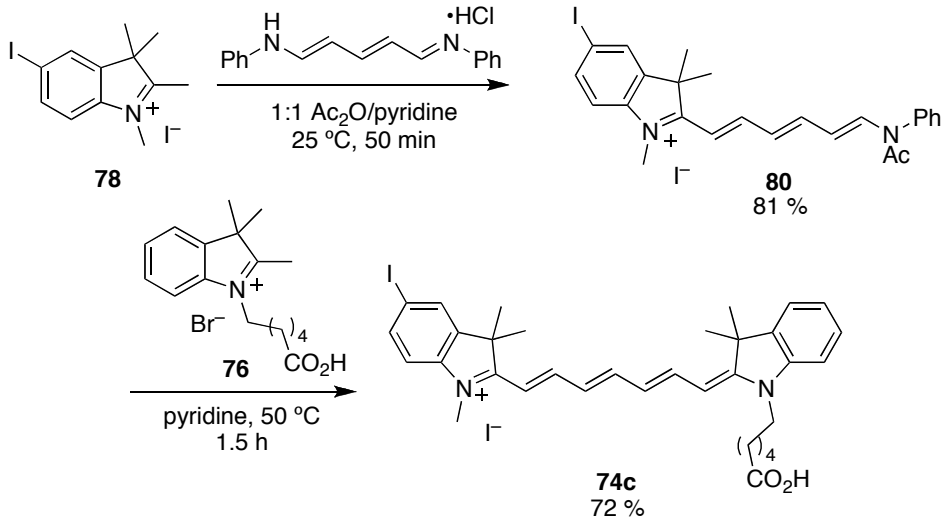

The UV absorption and fluorescence emission spectra of Cy3 **73a**, Cy5 **73b**, and Cy7 **73c** were recorded in EtOH with the concentration of 10^{-7} and 10^{-8} M, respectively (Figure 3.9). These three cyanine dyes have well-separated UV absorption and fluorescence emissions.

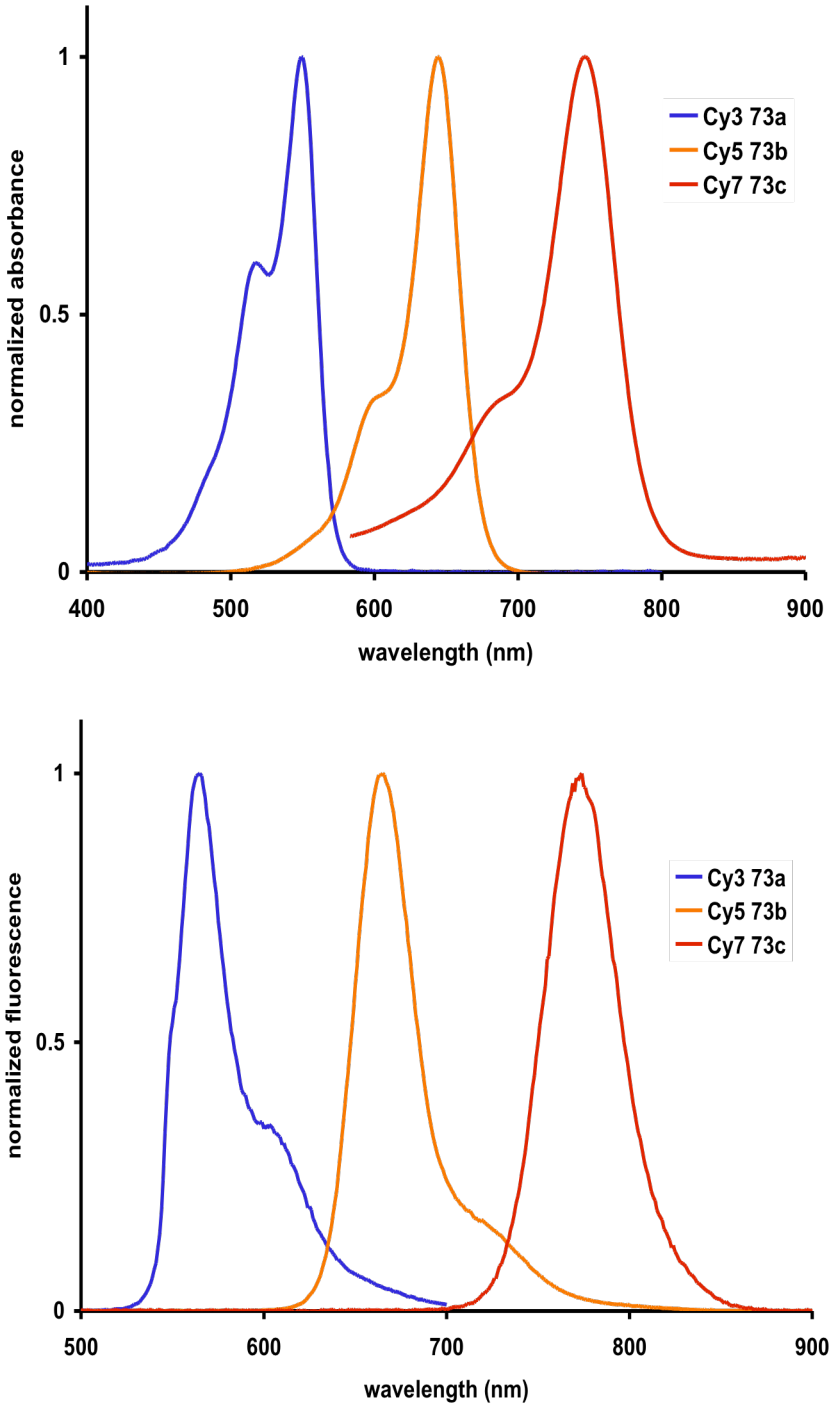

Figure 3.9. Absorption and fluorescence spectra of cyanine dyes **73** in EtOH. Fluorescence spectra: excited at corresponding excitation wavelengths.

Table 3.1 summarizes the photophysical properties of Cy3 **73a**, Cy5 **73b**, and Cy7 **73c**. Remarkably, the extinction coefficients (ε) of those dyes were extremely high. Surprisingly, the insertion of another methine chain into cyanine dye led to approximately twice the ε value because of its extended conjugation. This kind of phenomenon has not been seen for any other fluorescent dyes. Cy3 **73c** had a quantum yield (Φ) of 0.085 in EtOH, and this **73c** was slightly soluble in water and the measurement of Φ in pH 7.4 phosphate buffer gave 0.039. Quantum yields of Cy5 **73b** and Cy7 **73c** in EtOH were also measured and these resulted in Φ of 0.31 and 0.13, respectively. Quantum yields of those dyes in pH 7.4 were not measured because of their poor solubilities in aqueous media.

Table 3.1. Photophysical properties of cyanine dyes **73a-c**.

dye	solvent	$\lambda_{max\ abs}$ (nm)	ε ($M^{-1}cm^{-1}$)	$\lambda_{max\ emiss}$ (nm)	fwhm (nm)	*Φ*
Cy3 73a	EtOH	549	92100	565	35	0.085[b]
Cy3 73a	pH 7.4[a]	542	–	–	–	0.039
Cy5 73b	EtOH	644	164500	665	38	0.31[c]
Cy7 73c	EtOH	747	292000	774	48	0.13[d]

[a] sodium phosphate buffer; [b] Rhodamine 101 was used as a standard (*Φ* 1.0 in EtOH); [c] Nile Blue (*Φ* 0.27 in EtOH); [d] Cardiogreen (*Φ* 0.04 in MeOH).

3.4 Synthesis of TBET Cassettes

We next synthesized three novel TBET cassettes **75a-c** consisting of BODIPY donors and cyanine acceptors. Scheme 3.12 represents the synthesis of TBET cassette **75a** which is based on Cy3. Palladium (0)-catalyzed Sonogashira coupling[109] of BODIPY derivative **55** and iodo-Cy3 **74a** was completed in 45 min. The use of Pd^{II} catalyst resulted in a messy reaction and the reaction was not completed. After the reaction, ether was added into the reaction mixture to wash away Et_3N and DMF. The obtained crude product was purified with flash chromatography to afford TBET cassette **75a** in 45 % yield. TBET cassette **75b** based on Cy5 was synthesized by Mr. Jiney Jose using similar reaction conditions and obtained in 26 % yield.

Scheme 3.12. Synthesis of TBET cassette **75a**.

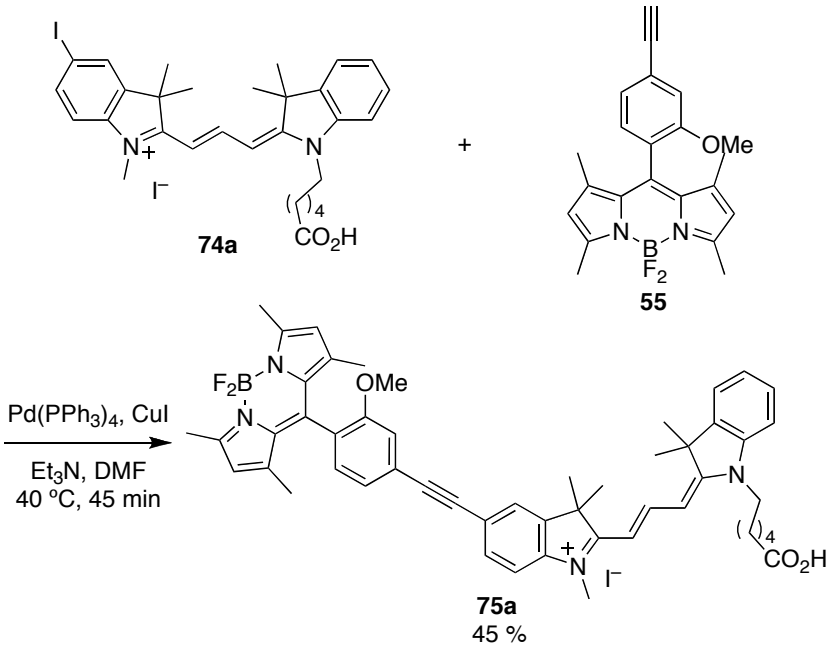

Similar reaction conditions were used for synthesizing TBET cassette **75c** based on Cy7. In this process, Cy7 **74c** and BODIPY **55** were reacted *via* Sonogashira coupling to afford TBET cassette **75c** in 33 % yield (Scheme 3.13). The reaction was not clean for Cy5 and Cy7 based cassettes, and we expect this is due to the side-reaction of reactive polymethine chain with palladium catalyst. Palladium could be coordinated to polymethine chain and it results in decomposition of this chain. The reactions between cyanine dyes with longer methine chains (Cy5 and Cy7) and palladium catalyst are more prone to this type of decomposition. In fact, the purification was harder for cassettes **75b** and **75c** compared to cassette **75a**, and we obtained some other fractions containing unknown compounds.

Scheme 3.13. Synthesis of TBET cassette **75c**.

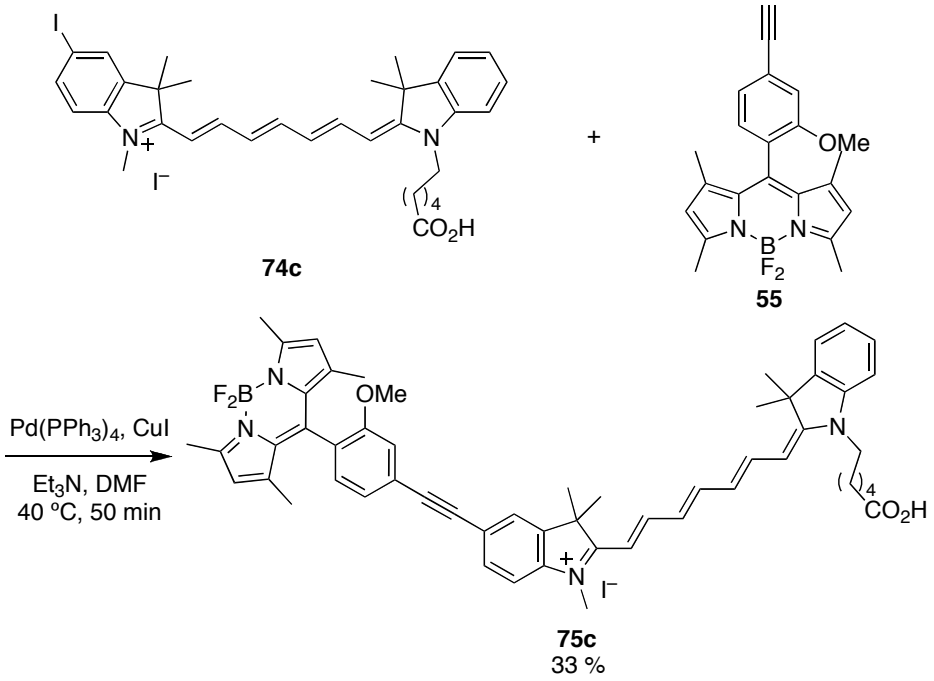

The UV absorption and fluorescence emission spectra of cassettes **75a-c** were recorded in EtOH with the concentration of 10^{-6} and 10^{-7} M, respectively (Figure 3.10). For cassette **75c** based on Cy3, some spectral overlap of UV absorption between BODIPY donor and Cy3 was observed because their excitation wavelengths are near to each other and their absorption intensities are almost the same. As we expected, the higher UV absorption intensities from Cy5 and Cy7 compared to those of BODIPY donor were observed for cassettes **75b** and **75c**, and this is reasonable because of their high extinction coefficients. In the fluorescence spectra, TBET cassettes **75a-c** had emission wavelengths that are extremely well-separated from the cyanine parts. According to UV and fluorescence measurements of cassettes, we observed *ca.* 100 nm difference in their absorptions and emissions for the acceptor fragments.

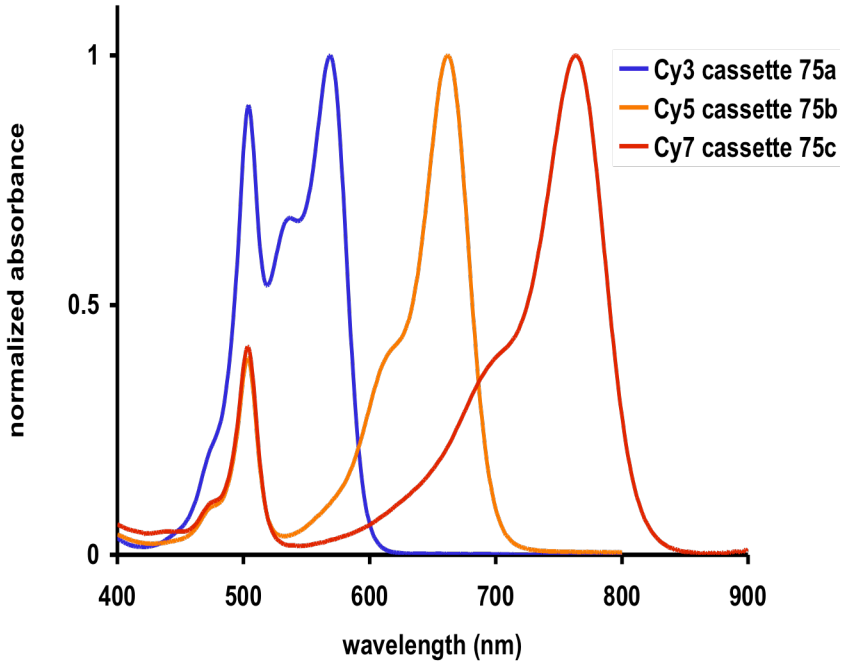

Figure 3.10. Absorption and fluorescence spectra of cassettes **75a-c**. Fluorescence spectra: excited at 504 nm which corresponds to excitation wavelength of BODIPY.

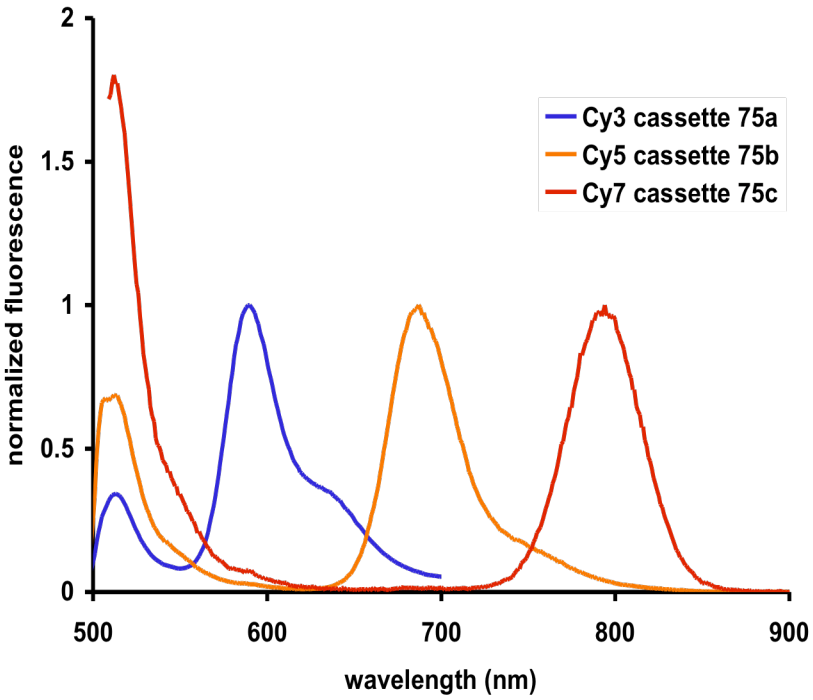

Figure 3.10. Continued.

The summary of photophysical properties for the cassettes are shown in Table 3.2. The UV absorption maxima from BODIPY parts were seen at 504 nm. As described above, the fluorescence emission from cyanine part of cassettes **75a-c** showed approximately 100 nm difference *i.e.* 590, 687, and 794 nm, respectively. Energy transfer efficiency (ETE) was calculated by the equation below. For this, the quantum yields of a donor and an acceptor fragments are first needed and finally ETE of cassette **75a** (Cy3) and **75b** (Cy5) were calculated to be 90 and 88 %, respectively. A quantum yield for cassette **75c** was not measured due to lack of a proper standard. The correction curve for our fluorescence spectrometer covers only the 200–800 nm range, but the fluorescence of **75c** is broadly centered on 794 nm, extending beyond 800 nm as shown in Figure 3.10. This feature causes a huge error in quantum yield calculations in this region.

Table 3.2. Photophysical properties of TBET cassettes **75a-c**.

cassette	solvent	$\lambda_{max\ abs}$ (nm)	$\lambda_{max\ emiss}$ (nm)	Φ[a] *ex. at donor*	Φ[b] *ex. at acceptor*	ETE (%)
75a (Cy3)	EtOH	504, 569	590	0.20	0.22	90
75b (Cy5)	EtOH	504, 662	687	0.35	0.40	88
75c (Cy7)	EtOH	504, 763	794	–	–	–

[a] Rhodaime 6G was used as a standard (Φ 0.92 in EtOH); [b] Rhodamine 101 for Cy3 (Φ 1.0 in EtOH); Nile Blue for Cy5 (Φ 0.27 in EtOH).

$$\text{energy transfer efficiency (ETE) (\%)} = \frac{\Phi_{\text{excited at donor}}}{\Phi_{\text{excited at acceptor}}} \times 100$$

3.4.1 Conclusions for Cyanine Dyes and Their TBET Cassettes

In conclusion, we synthesized three cyanine dyes **73a-c** as control compounds, three novel iodo-cyanine dyes **74a-c**, and three novel through-bond-energy-transfer cassettes

75a-c consist of BODIPY as a donor and cyanine dyes as acceptors. Synthesis of cyanine dye series were carried out using the reported one-pot reaction or two steps. Cassettes **75a-c** were prepared via Sonogashira couplings; they were obtained in moderate yields. The control compound **73a** was slightly water soluble, however, other materials including cassettes **75a-c** had poor water-solubility, thus photophysical properties of those dyes were not measured in aqueous media. Each control compounds **73a-c** had about 100 nm difference in their absorption and emission spectra in EtOH and gave reasonable quantum yields. Energy transfer efficiencies of cassettes **75a** (based on Cy3) and **75b** (based on Cy5) were found to be 90 and 88 %, respectively. Moreover the well-separated fluorescence spectra were observed for all cassettes **75a-c**. This is one of the most important factors in multiplexing studies and these cassettes will be possible candidates for the same. Further modification of these cassettes, *e.g.* coating by silica or calcium phosphate, can produce water-soluble materials and higher photostabilities. Water-soluble fluorescent probes with good photophysical properties are more preferred when biological studies are performed. Therefore silica- or calcium-coated cassettes may possibly be useful for multiplexing studies. The syntheses of nanoparticles will be described in the next section and this research is currently in progress in our laboratory.

3.5 Dye-doped Nanoparticles for Bioimaging in Cells

One of the requirements for bioimaging is that the fluorescent probe should be sufficiently water soluble because imaging is preferred to be done at physiological pH. Moreover cells are not stable in organic solvents. Many water soluble fluorescent probes are described in the literature[68,83,90,110,111] but their brightnesses in aqueous media tend to be much less than in organic media. This effect can be attributed to aggregation[112,113] of dyes in aqueous media, and this cannot be prevented completely even if water solubilizing groups are present on the dyes. Further, most organic dyes have low photostabilities,[114] therefore fluorescent signal cannot be observed for longer

duration. The dye-protein conjugates always tend to be less brighter than the parent dye itself which again causes problem in signal detection.

In the past decade, quantum dots (QDs) have been widely investigated in nanotechnology for cell imaging study because of their excellent properties such as tunable emission wavelengths from UV-Vis to near IR region, photostable, and highly fluorescent.[115-117] However, the core shell of QDs consists of toxic atoms such as cadmium, selenium, and lead.[114] The toxicity of QDs have not well-proven yet and this may cause a cell damage when QDs are imported into cells.

Several research groups have encapsulated fluorescent probes into nanoparticles to improve their photophysical properties. These improvements are due to suppressing interactions between the fluorescent probe and the outside environment. Two prominent ways to achieve this are to coat the fluorescent probe with silica[118-120] or calcium phosphate.[121-123] Syntheses of such nanoparticles are well documented in the literature. Photostabilities of such nanoparticles are higher than the dye by itself. Surface modifications of these nanoparticles are possible[124-126] and therefore this too is advantageous for cellular imaging. One of the most important criteria while dealing with nanoparticles is their cytoxicity. Silica nanoparticles are biocompartible when used at or below concentration of 0.1 mg/mL.[114] There is no known cytoxicity for calcium nanoparticles and they are bioresorbable.[121] Thus these nanoparticles are less harmful to cells compared to QDs.

Syntheses of such nanoparticles were achieved by forming a dye core and then covering it with an outside shell. The shell thickness usually ranges between 10–30 nm which gives sufficient protection to the dye core from the outside environment. Microemulsion is widely used for formation of nanoparticles, but the dye may leach out after a week or two. To overcome this issue, covalent attachment of the dye core to the shell has been developed. Both water soluble and insoluble dyes can be encapsulated inside nanoparticles.[127] These nanoparticles are well dispersed in aqueous media and therefore can be used for biological studies.

3.5.1 Syntheses of Dye-doped Silica and Calcium Phosphate Nanoparticles

Scheme 3.14 illustrates a general synthetic scheme for formation of fluorescent dye-doped silica nanoparticles as in a reported procedure.[128] The carboxylic acid of fluorescent dye reacts with aminopropyl silicate *via* EDCI-coupling to give triethyl-silicate **81**. Compound **81** is then hydrolyzed under basic conditions to afford silicate **82**, and finally this **82** is treated with tetraethyl-silicate to form silica nanoparticle **83**.

Scheme 3.14. General synthetic scheme for silica nanoparticle formation.

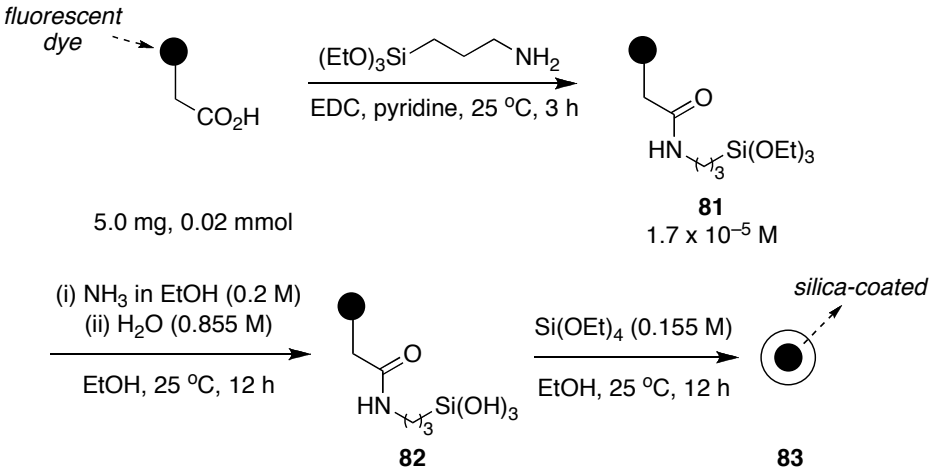

A general synthesis of calcium phosphate nanoparticle is shown in Figure 3.11.[123] Two microemulsion A and B are separately formed with a cyclohexane/Igepal CO-520/water system. Typically, 650 μL of 1 x 10^{-2} M $CaCl_2$ in CO_2-free deionized water is added to 14 mL of a 29 vol % solution of Igepal CO-520 in cyclohexane to form microemulsion A. Similarly, 650 μL of 6 x 10^{-3} M disodium phosphate with 8 x 10^{-4} M disodium silicate in CO_2-free deionized water (pH 7.4) is added to 14 mL of a 29 vol % solution of Igepal CO-520 in cyclohexane to form microemulsion B. Disodium silicate is present to act as a nucleation agent for the calcium phosphate. The addition of the aqueous solution to the cyclohexane/Igepal CO-520 solution forms a self-assembled, reverse micelle suspension. Dyes which are insoluble in water can be added in ethanol

or ethanol/water solution after the microemulsion is formed. A dispersant is then added to microemulsion C. For carboxy-functionalized particles, 225 μL of 1 x 10^{-3} M sodium citrate is added and allowed to react for 15 min.

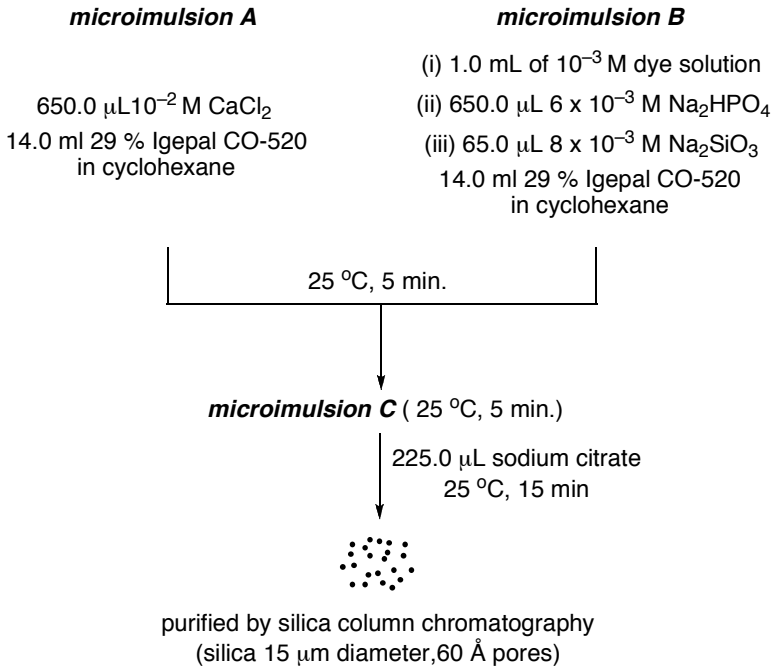

Figure 3.11. General synthesis of calcium phosphate nanoparticle.

3.5.2 Cyanine 73a-c and TBET cassettes 75a,b doped Silica Nanoparticles

The encapsulations of cyanine dyes **73a-c** and TBET cassettes **75a-c** with silica were performed by Mr. Jiney Jose in our group using the procedure[128] described in Scheme 3.14. Figure 3.12 shows UV absorption and emission spectra of cyanine dyes **73a-c** doped silica nanoparticles in pH 7.4 phosphate buffer. The absorption and emission maxima for dye-doped nanoparticles were quite similar to those of free cyanine dyes **73a-c** in ethanol.

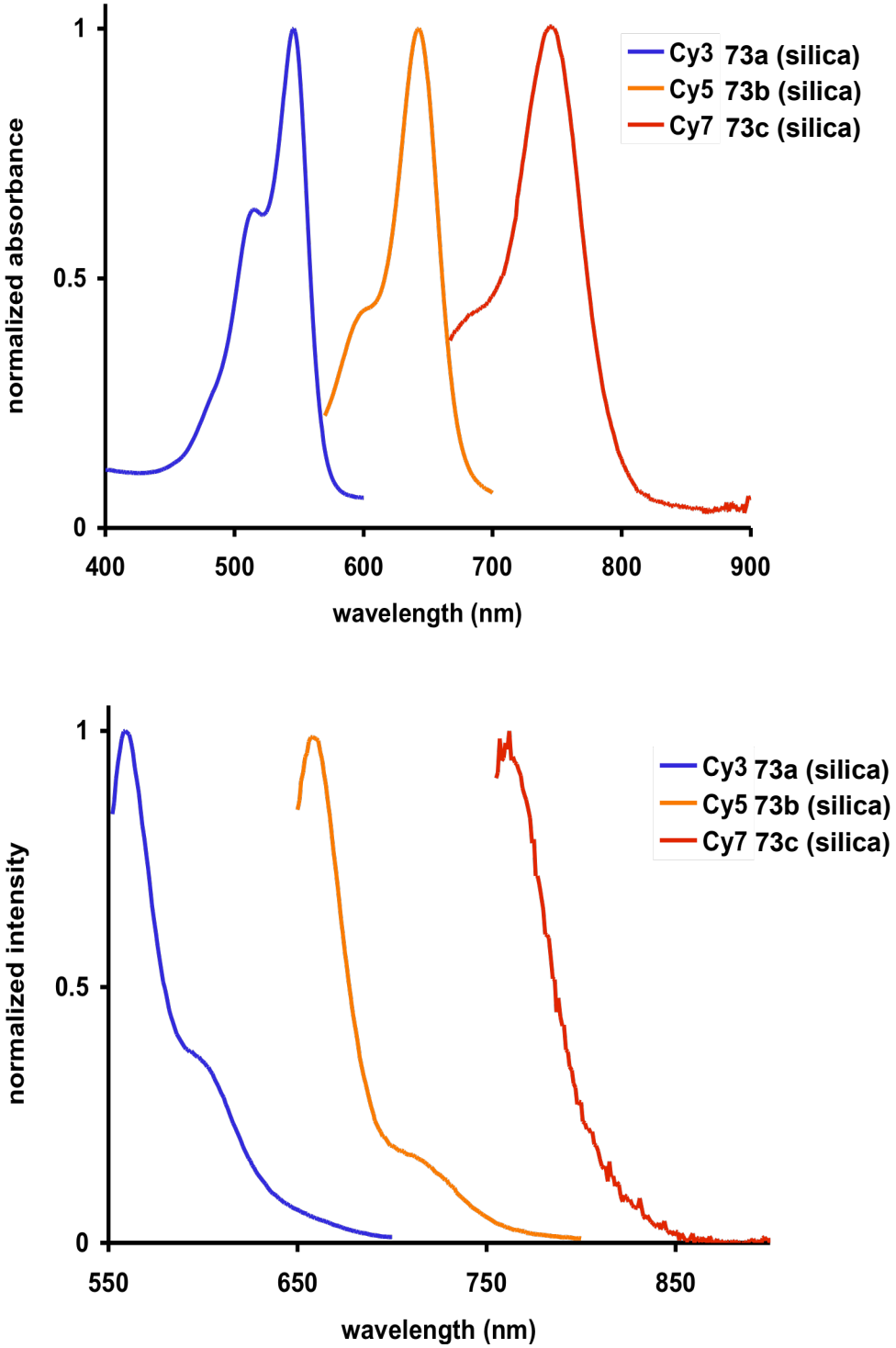

Figure 3.12. Absorption and fluorescence of cyanine acceptors **73a-c** doped silica nanoparticles in 0.1 M phosphate buffer (pH 7.4).

The absorption and emission spectra of TBET cassettes **75a**,**b** doped silica nanoparticles were also similar to those of free cassettes **75a** and **75b** (Figure 3.13) (see Figure 3.10 for free cassettes **75a** and **75b** in ethanol). The attempted encapsulation of cassette **75c** with silica resulted in the decomposition of cassette, therefore no photophysical properties were obtained.

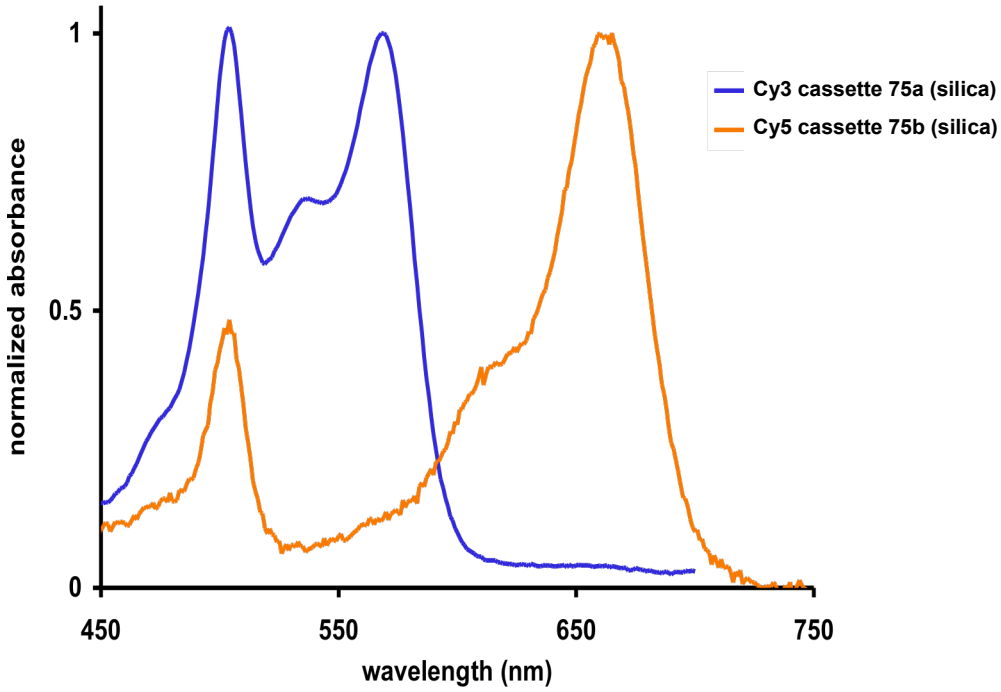

Figure 3.13. Absorption and fluorescence of TBET cassette **75a**,**b** doped silica nanoparticles in 0.1 M phosphate buffer (pH 7.4).

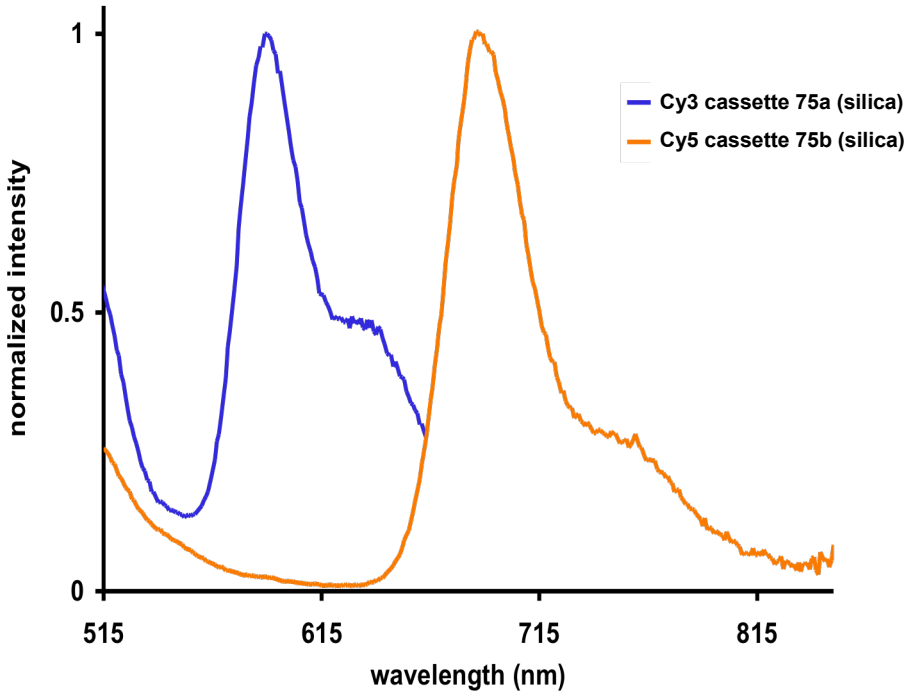

Figure 3.13. Continued.

The photophysical properties of cyanine **73a-c** doped silica nanoparticles in pH 7.4 phosphate buffer are shown in Table 3.3. Quantum yields of cyanine **73a**,**73b**, and **73c** in silica nanoparticles were calculated to be 0.30, 0.15, and 0.09, respectively. For cyanine **73a** in pH 7.4 buffer, Φ of silica-coated **73a** was increased by *ca.* 7-fold compared to that of free dye **73a** (Φ 0.039 in pH 7.4, see Table 3.1). This improvement was because of the less interactions between the dyes inside the silica particle and the outside environment. Table 3.4 summarizes the photophysical properties of silica-coated TBET cassettes **75a** and **75b** in pH 7.4 buffer. Energy transfer efficiencies (ETE %) were calculated by the equation showed in Table 3.2. Both silica-coated cassettes **75a** and **75b** gave good ETE of 91 and 81 %, respectively, but quantum yields were quite low.

Table 3.3. Photophysical properties of cyanine **73a-c** doped silica nanoparticles in 0.1 M phosphate buffer (pH 7.4).

dye	$\lambda_{max\ abs}$ (nm)	$\lambda_{max\ emiss}$ (nm)	Φ
Cy3 73a in silica	550	566	0.30[a]
Cy5 73b in silica	646	666	0.15[b]
Cy7 73c in silica	751	776	0.09[c]

[a] Rhodamine 101 was used as a standard (Φ 1.0 in EtOH); [b] Nile Blue (Φ 0.27 in EtOH); [c] Cardiogreen (Φ 0.04 in MeOH).

Table 3.4. Photophysical properties of TBET cassettes **75a**,**b** doped silica nanoparticles in 0.1 M phosphate buffer (pH 7.4).

cassette	$\lambda_{max\ abs}$ (nm)	$\lambda_{max\ emiss}$ (nm)	Φ^a *ex. at donor*	Φ^b *ex. at acceptor*	ETE (%)
75a in silica	504, 568	592	0.04	0.044	91
75b in silica	504, 659	687	0.021	0.026	81

[a]Rhodamine 6G was used as a standard (Φ 0.92 in EtOH); [b]Rhodamine 101 for Cy3 (Φ 1.0 in EtOH); [b]Nile Blue for Cy5 (Φ 0.27 in EtOH).

The transmission electron microscope (TEM) images for silica-nanoparticles were also measured and this was performed by Dr. Hansoo Kim (TAMU, MIC lab). As shown in Figure 3.14, all the silica-nanoparticles were spherical in shape, and the average particle size for each compounds were in the range of 22 to 25 nm.

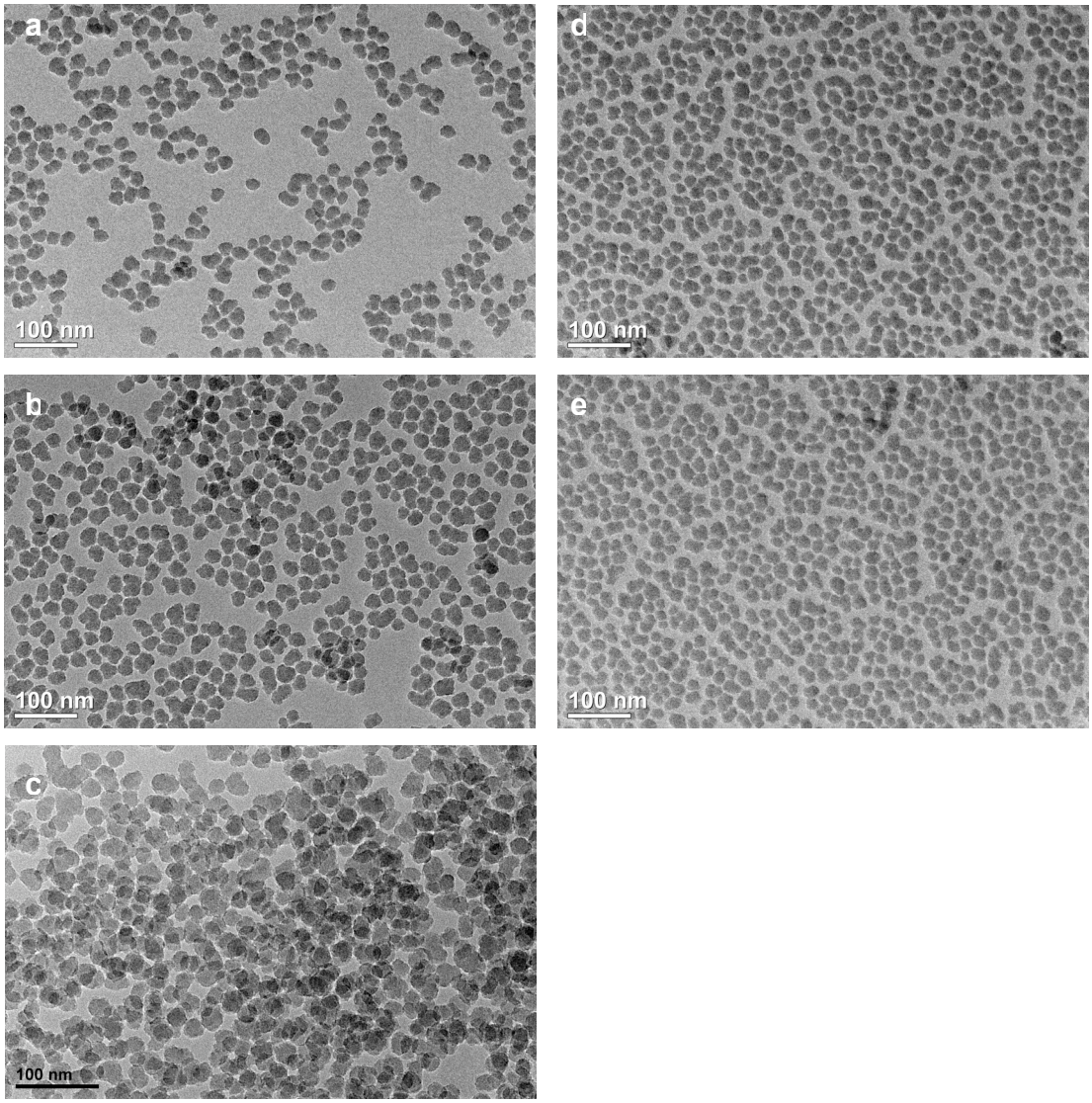

Figure 3.14. TEM images of silica nanoparticles. **a**, Cy3 **73a**; **b**, Cy5 **73b**; **c**, Cy7 **73c**; **d**, Cy3 cassette **75a**; and **e**, Cy5 cassette **75b**; average particle size: 22, 25, 22, 24, and 24 nm, respectively.

3.5.3 Cyanine 73a-c and TBET cassettes 75a-c doped Calcium Phosphate Nanoparticles

Calcium phosphate (CP) nanoparticles of cyanine dyes **73a-c** and TBET cassettes **75a-c** were synthesized by Mr. Jiney Jose using the procedure[123] described in Figure 3.11. Figure 3.15 shows UV absorption and emission spectra of cyanine dyes **73a-c** doped calcium phosphate nanoparticles in pH 7.4 phosphate buffer. Each dye doped CPs had well distinguished absorption and emission maxima separated by approximately 100 nm.

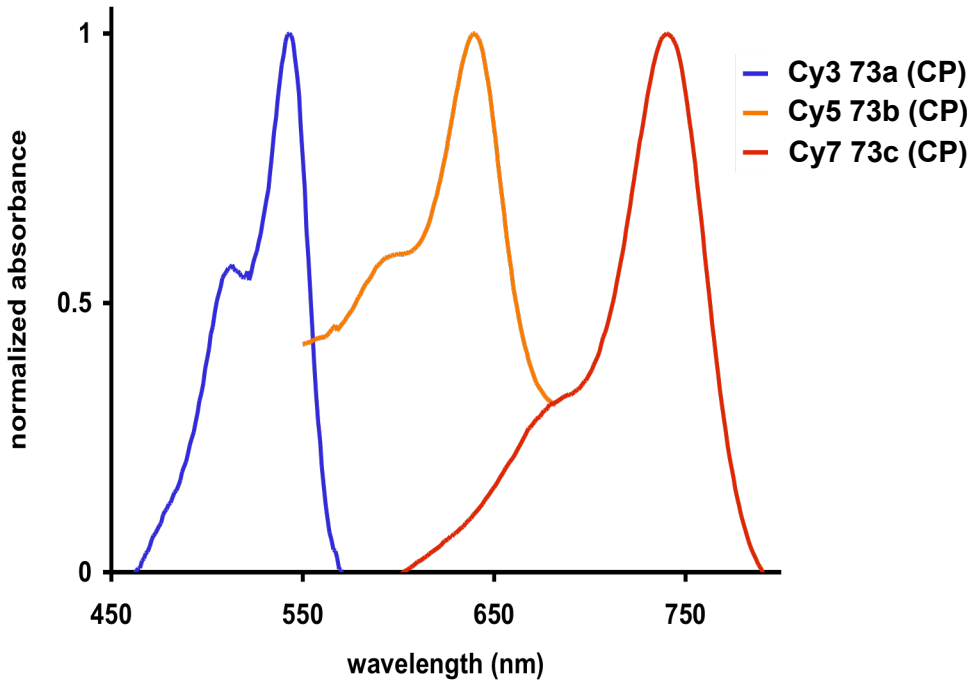

Figure 3.15. Absorption and fluorescence of cyanine **73a-c** doped calcium phosphate (CP) nanoparticles in 0.1 M phosphate buffer (pH 7.4).

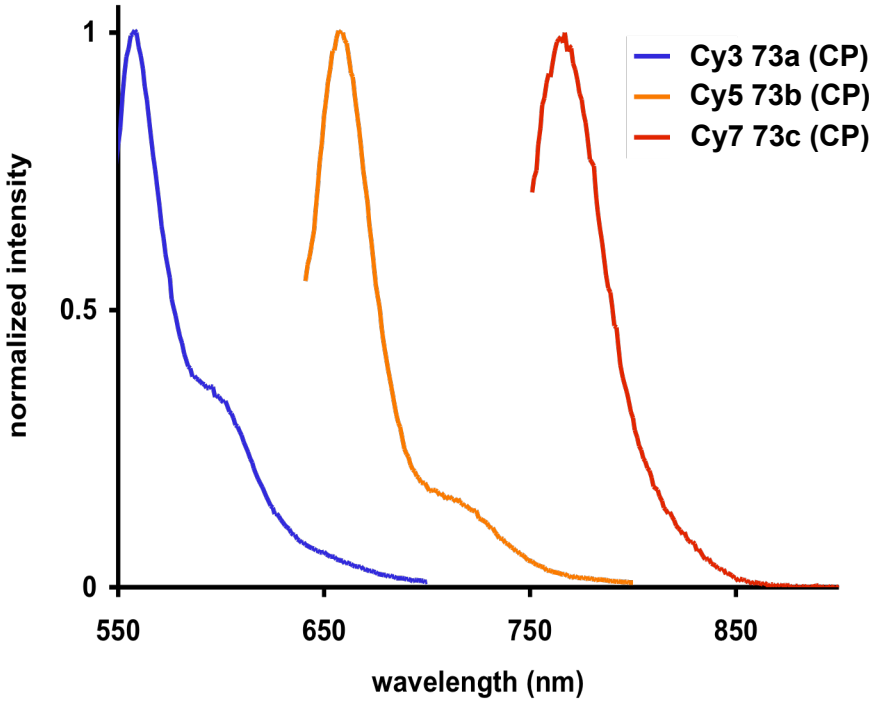

Figure 3.15. Continued.

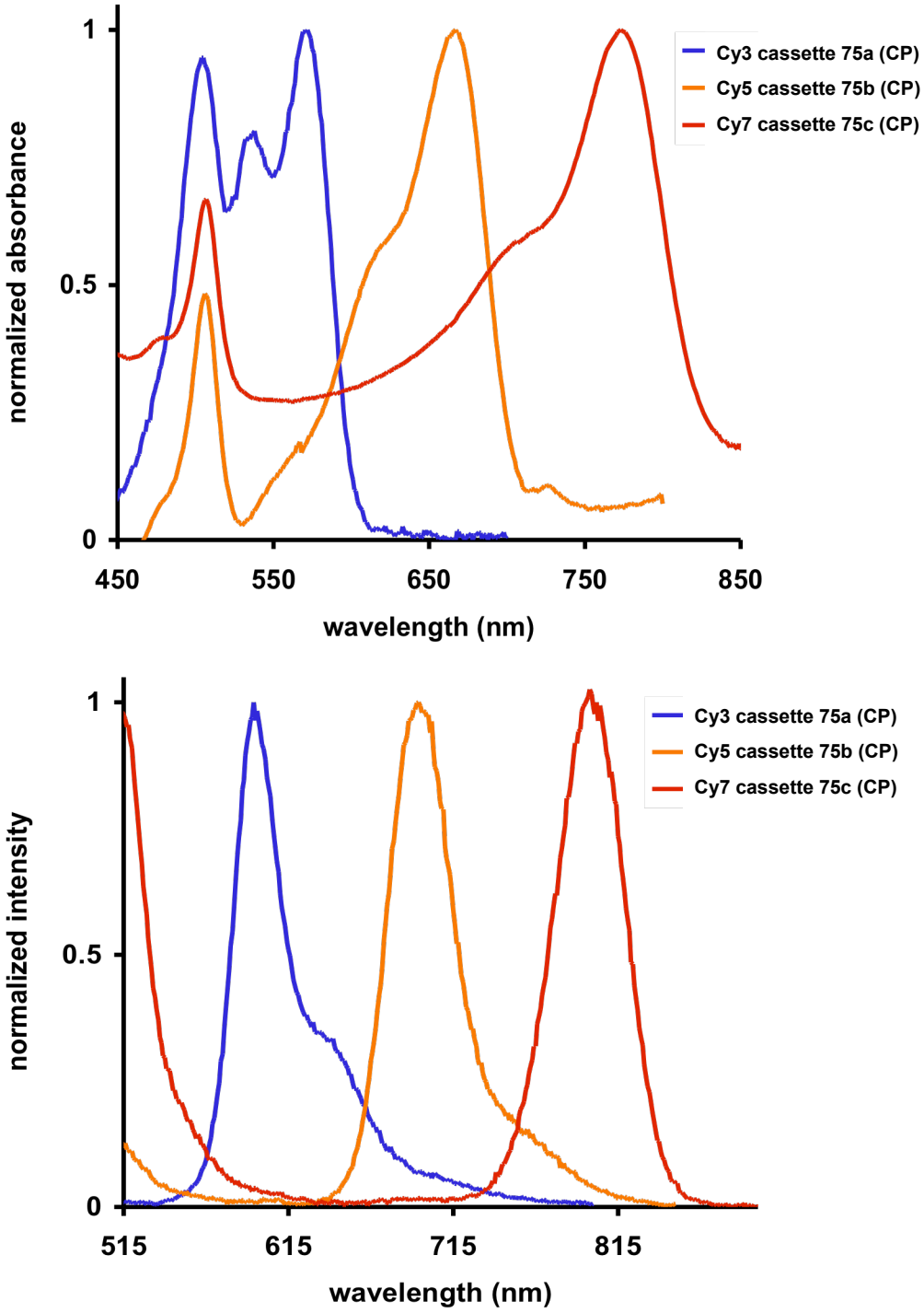

Figure 3.16. Absorption and fluorescence of cassettes **75a-c** doped calcium phosphate nanoparticles in 0.1 M phosphate buffer (pH 7.4).

Figure 3.16 shows absorption and emission spectra of cassettes **75a-c** doped CP nanoparticles. We did not observe decomposition of Cy7 cassette **75c** under the reaction conditions for the formation of CP nanoparticles.

The photophysical properties of cyanine **73a-c** doped CP nanoparticles in pH 7.4 phosphate buffer are shown in Table 3.5. Both absorption and emission maxima of CP particles were again quite similar to those of free cyanine dyes in ethanol. Quantum yields of cyanine dyes **73a**, **73b**, and **73c** in CP nanoparticles were calculated to be 0.07, 0.21, and 0.14, respectively. The quantum yields of Cy5 **73b** and Cy7 **73c** coated by CP were slightly higher than those of **73b** and **73c** coated by silica (Φ 0.15 and 0.09, see Table 3.3). However we obtained Φ of 0.07 for Cy3 CP particle **73a**, and this was *ca.* one forth of silica-coated **73a** (Φ 0.30).

Table 3.5. Photophysical properties of cyanine **73a-c** doped CP nanoparticles in 0.1 M phosphate buffer (pH 7.4).

dye	$\lambda_{max\ abs}$ (nm)	$\lambda_{max\ emiss}$ (nm)	Φ
Cy3 73a in CP	543	564	0.07[a]
Cy5 73b in CP	643	663	0.21[b]
Cy7 73c in CP	748	774	0.14[c]

[a]Rhodamine 101 was used as a standard (Φ 1.0 in EtOH); [b]Nile Blue (Φ 0.27 in EtOH); [c]Cardiogreen (Φ 0.04 in MeOH); CP stands for *calcium phosphate*.

Table 3.6. Photophysical properties of cassettes **75a-c** doped CP nanoparticles in 0.1 M phosphate buffer (pH 7.4).

cassette	$\lambda_{max\ abs}$ (nm)	$\lambda_{max\ emiss}$ (nm)	Φ^a *ex. at donor*	Φ^b *ex. at acceptor*	ETE (%)
Cy3 75a in CP	504, 569	590	0.037	0.041	90
Cy5 75b in CP	504, 659	687	0.051	0.057	90
Cy7 75c in CP	504, 764	793	0.039	–	–

[a]Rhodaime 6G was used as a standard (Φ 0.92 in EtOH); [b]Rhodamine 101 for Cy3 (Φ 1.0 in EtOH); [b]Nile Blue for Cy5 (Φ 0.27 in EtOH). CP stands for *calcium phosphate*.

Figure 3.17 shows atomic force microscopy (AFM) images for cyanine dyes **73a-c** and TBET cassettes **75a-c** doped calcium phosphate nanoparticles. As shown in figure, all the CP nanoparticles were spherical in shape, and the average particle size were 14–29 nm. TEM images could not be obtained because CP particles were not stable to electron beam.

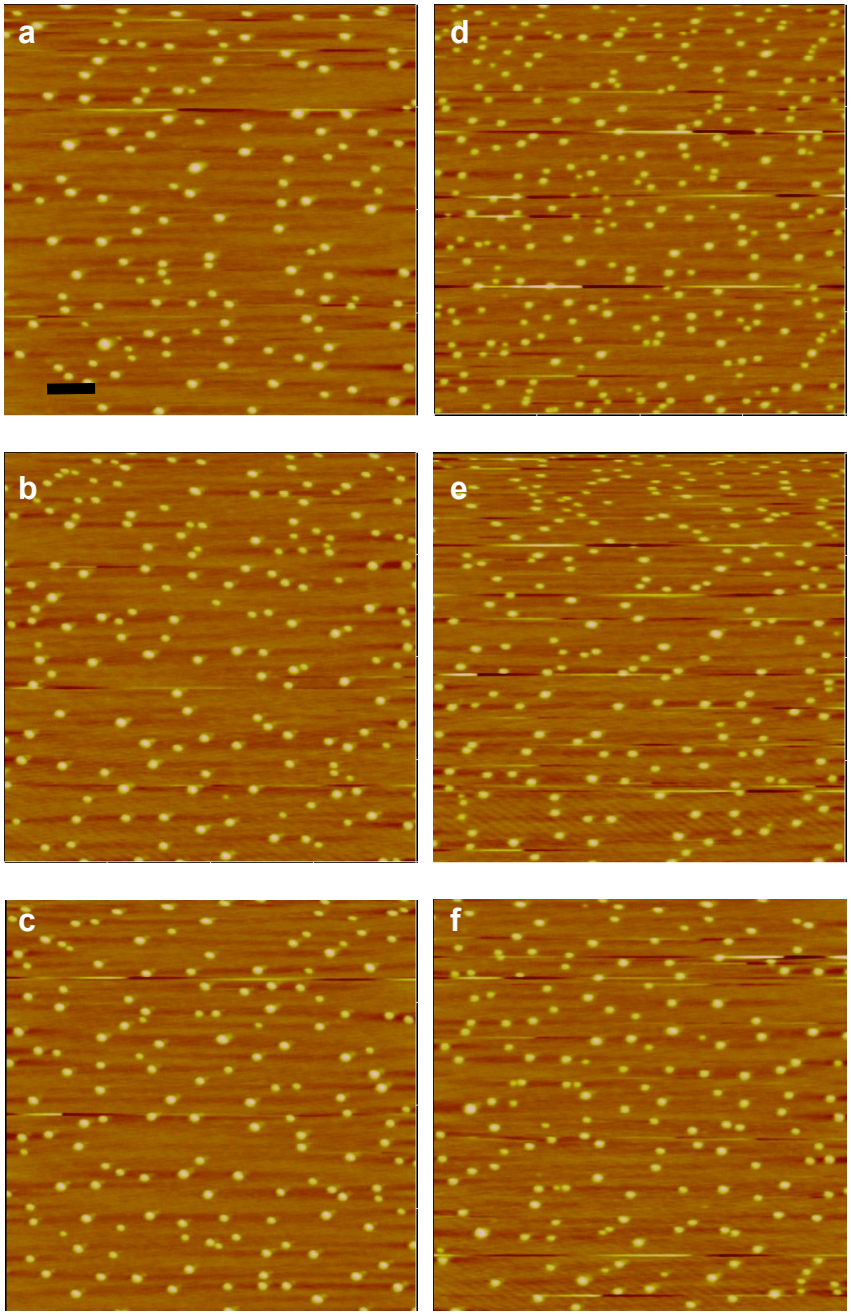

Figure 3.17. AFM images of calcium phosphate nanoparticles. **a**, Cy3 **73a**; **b**, Cy5 **73b**; **c**, Cy7 **73c**; **d**, Cy3 cassette **75a**; **e**, Cy5 cassette **75b**; and **f**, Cy7 cassette **75c**; average particle size: 14-29 nm; scale: 100 nm.

3.5.2 Conclusion on Silica and Calcium Phosphate Nanoparticles

Cyanine dyes **73a-c** as control compounds and TBET cassettes **75a**,**b** were covalently coated by silica to form corresponding nanoparticles and their photophysical properties were studied in aqueous media. These silica nanoparticles were well dispersed in phosphate buffer (pH 7.4) and silica-coated cassette **75a**,**b** showed moderate energy transfer efficiencies (ETE) with low quantum yields, but we expect these values to be better than those of free dyes in water. Cyanine **73a-c** and cassettes **75a-c** were also non-covalently coated by calcium phosphate, and their photophysical properties were studied at pH 7.4 phosphate buffer. These nanoparticles were highly water-soluble and the ETE of cassettes **75a**,**b** doped CP nanoparticles were about 90 %. Again both silica and CP nanoparticles had well-resolved absorption and emission maxima separated by *ca.* 100 nm. Further the formation of silica and calcium phosphate nanoparticles were confirmed by measuring TEM and AFM images, respectively, and both particles were spherical in shape. The photo-stabilities of silica nanoparticles **73a-c** (cyanine) and **75a**,**b** (cassette) are currently being measured by Dr. Son's group (TAMU) and will be compared to those of the free cassettes and cyanine dyes. As a future work, we will study multiplexing of TBET cassettes **75a-c** doped calcium phosphate nanoparticles in intracellular imaging.

CHAPTER IV

DEVELOPMENT OF METHODS FOR PROTEIN MONO-LABELING

4.1 Introduction

Single molecule imaging has become an important tool in the cell studies. It provides information about molecular dynamics, distribution, and protein-protein interactions. The most widely used technique is a total internal reflection fluorescence microscopy (TIRFM) which makes possible to visualize individual interactions *in vivo* and *in vitro*.[129,130] On the other hand, the uses of single-fluorescent-labeled biomolecules could also be powerful tools for such studies. It is valuable if a protein of interest can be selectively mono-labeled with only one fluorescent dye, then this leads to the quantification of protein and makes possible to perform single molecule studies in cell imaging.

Lysine residues are commonly used to label natural proteins because most proteins have several number of lysines and primary amines are quite reactive with succinimidyl ester of fluorophores, but this is not specific. The mono-labeling of lysine residues in natural proteins is extremely difficult. To overcome this drawback, we propose a new method for mono-fluorescent labeling of protein using a solid-phase approach and a photo-cleavable system. The specific aims for mono-labeling of natural protein are as follows:

(i) design and synthesis of cleavable linkers and fluorescent dyes;
(ii) focus on the nature of resin (the number of reactive sites on the resin and the particle sizes); and,
(iii) label one lysine residue in natural protein with one fluorescent dye on solid-support.

4.1.1 Background: Selective Labeling of Protein

Specific labeling of protein with fluorescent tags requires the modification of protein under study either chemically or genetically incorporating an unnatural amino acid.[10,12] The later method is most widely used because any functional groups can be introduced into the protein which can then selectively react with the fluorescent tags. Site-specific labeling of cysteine residues in recombinant proteins[7,9,12] is a well known method for mono-labeling as shown in Chapter I.

There are very few reports on the selective modification of natural proteins. Francis' group reported a selective labeling of tyrosine residues in natural protein via a Pd-catalyzed alkylation (Figure 4.1).[131] The key features in this work are the uses of reactive π-allyl species and the tyrosine residues for the conjugation. The π-allyl Pd-complex **B** was formed from rhodamine-allylic acetate **A** in aqueous buffer, this **B** was readily available to conjugate with protein (Chymotrypsinogen A was used for this study). Excess **A** was converted to diene **C**, and this was easily removed using gel-filtration or extraction. Two tyrosine residues are available for reactions; tyrosine (Y)-171 and -146. The Y171 is more accessible for conjugation than Y146. The single-dye-labeled protein **D** and double-labeled protein were observed from ESI analyses, indicating that this Pd-catalyzed reaction is effective for bioconjugations.

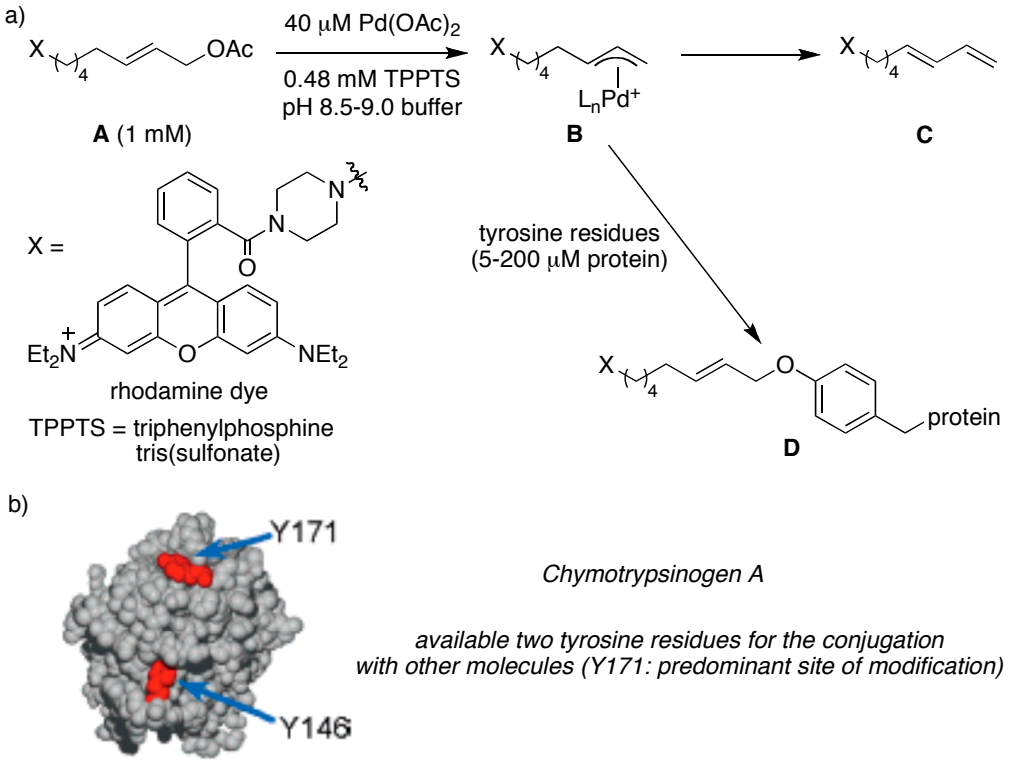

Figure 4.1. Francis' selective labeling of tyrosine. **a**; Pd-catalyzed alkylation, and **b**; structure of Chymotrypsinogen A.[131]

The selective modification of tryptophan in the natural protein was reported by the same group.[132] A similar approach was attempted for this study. The tryptophan residues in myoglobin (two tryptophan residues are available for the conjugation) were alkylated with rhodium carbenoids and this afforded mono- and di-alkylated protein by ESI-MS. However quantification of dye-protein conjugate cannot be determined by mass spectrometry analyses alone. Even though mono- and di-alkylated proteins were obtained via a Pd-catalyzed alkylation or an alkylation with rhodium carbenoids, these methods need further modification to achieve site-specific mono-labeling.

4.1.2 Our Approach: The Process of Protein Mono-labeling

Other members in our group have reported work involving photocleavable linkers,[133-135] a similar strategy was chosen for this project. The essential components are the solid-support, photolabile linker, fluorescent dye, and carboxylic acid for the attachment of biomolecules (Figure 4.2). The photolabile linker is attached on solid-support. The fluorescent dye and carboxylic acid are connected to this photolinker with or without another spacer. There are two ways to synthesize the target molecule; (i) the traditional solid-phase synthesis, and (ii) the solution phase synthesis of the photolabile linker with fluorescent dye and attachment of this functionalized dye to solid-support in the final step. In the solution-phase synthesis, the characterization of each compounds is easier than in the traditional solid-phase synthesis.

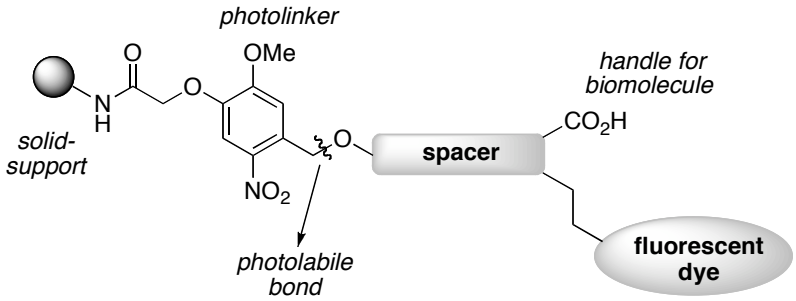

Figure 4.2. Design of molecule in this work.

Figure 4.3 shows the overall scheme for protein mono-labeling process and some key features. a) *the state of functionalized solid-support and proteins*: Solid-support is modified with the cleavable linker and fluorescent dye, and all carboxylic acids on the support are activated with succinimidyl esters. The attachment of protein is carried out in diluted conditions to prevent further reactions (protein di- or tri-labeling). b) *dye-protein conjugates on solid-support*: The mono-labeling of protein could be achieved because other active (reactive) sites on resin are far apart from protein. c) *cleavage of dye-protein conjugate*: The cleavable linker is cleaved to release a mono-fluorescent dye labeled protein and unreacted fluorescent dyes; these are separated by size-exclusion column and analyzed by CE, MALDI, and LCMS.

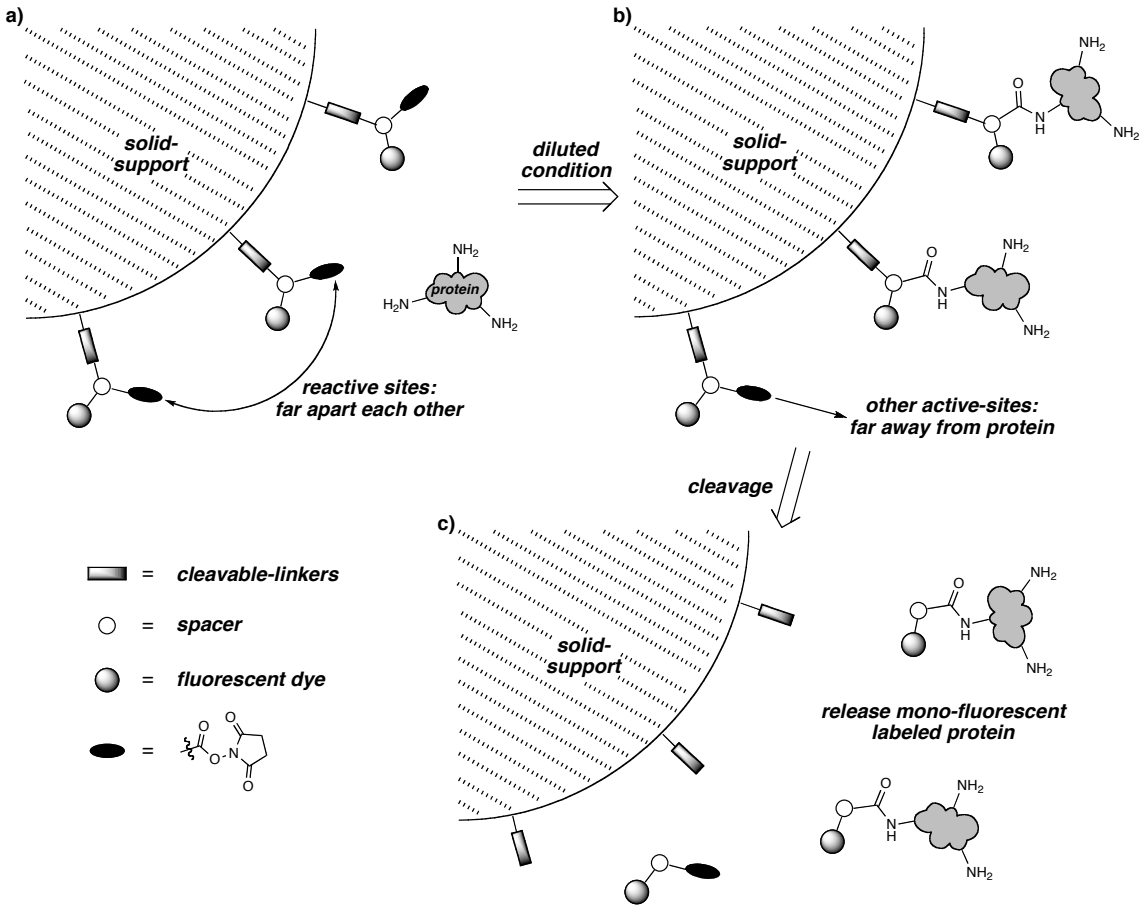

Figure 4.3. Overall scheme for protein mono-labeling process.

Based on this idea, four different strategies for this project were attempted:

section 4.2: photolinker based on *o*-nitrobenzyl alcohol derivative, PEGA resin, CPG, and Nile Red as a fluorescent tag (System A);

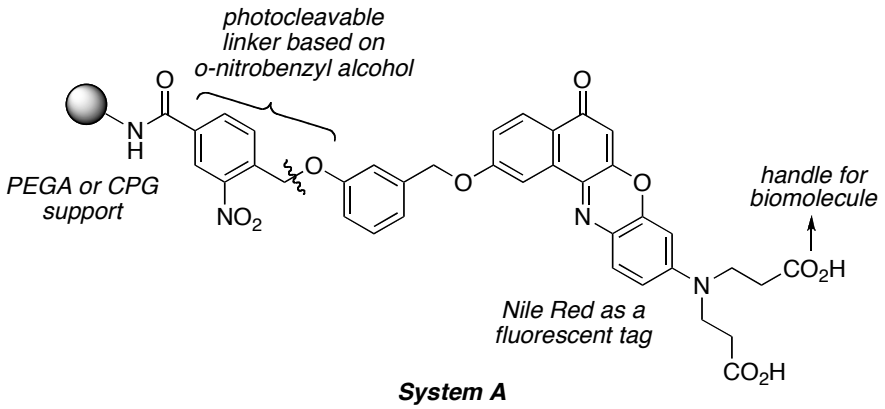

System A

section 4.3: an activated photolinker based on a modification of *o*-nitrobenzyl alcohol derivative, CPG, Nile Red and BODIPY as fluorescent tags (System B);

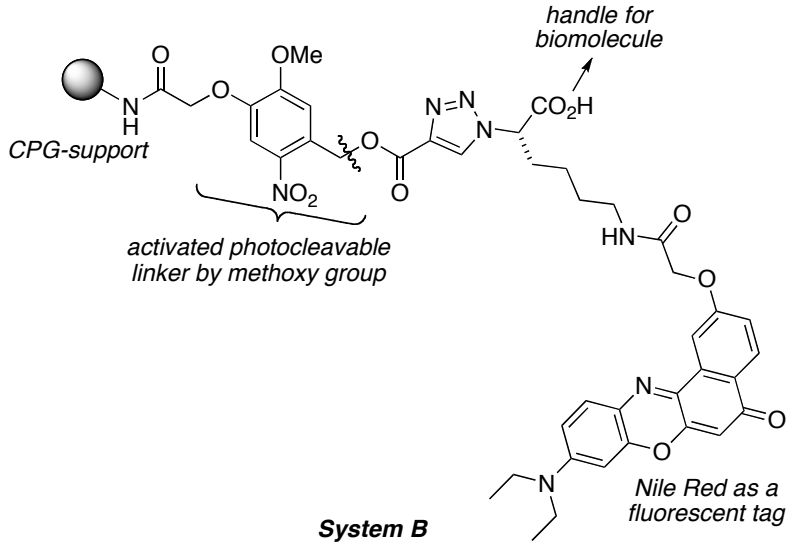

System B

section 4.4: an activated photolinker with BSA-coated CPG, and BODIPY as a fluorescent probe (System C);

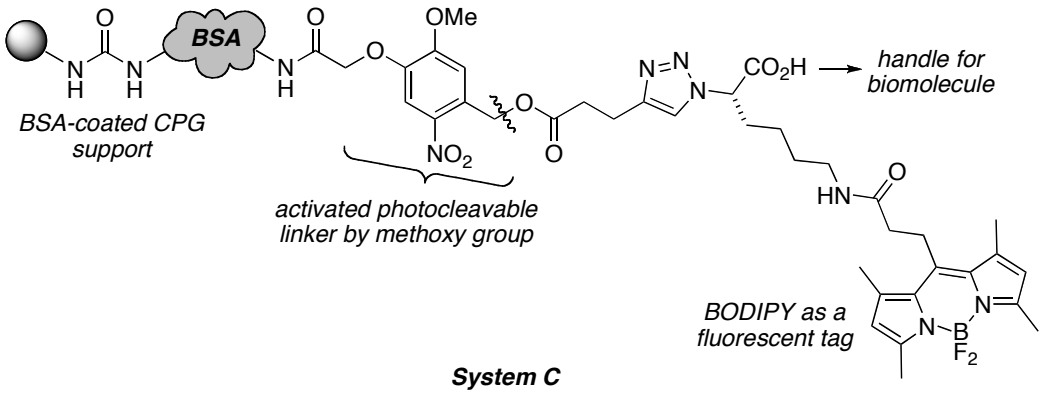

System C

section 4.5: chemically cleavable linker, azobenzene (System D).

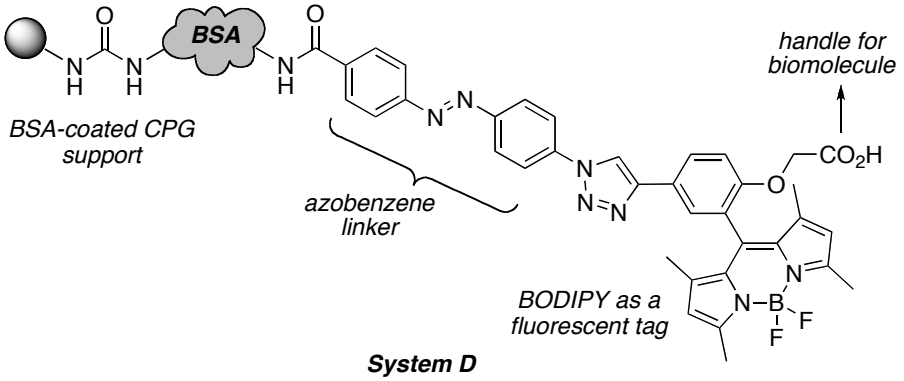

System D

Unfortunately, the above strategies on protein mono-labeling did not work. We will describe problems which we observed and how we tried to overcome these. This project is a collaboration between Prof. Burgess (synthesis of fluorescent dye and production of mono-labeled protein), Prof. Vigh (analysis of dye-protein sample using capillary

electrophoresis; CE), and Dr. Shane Tichy (analysis of dye-protein sample using MALDI and LCMS).

Prof. Vigh's group uses capillary electrophoresis (CE) for single molecule detection and purification of proteins. They are currently studying specific mono-labeling of natural protein using this technique. Overall concept is similar to our approach; use of reactive sites on solid-support for the protein conjugation (see Figure 4.3 for our approach). They attach fluorescent-tags and cleavable linkers inside of a capillary tube; this acts as a solid-support. The reactive sites on the support are far apart from each other, thus mono-labeling of protein could occur inside of capillary. Then the cleavage of linkers affords mono-labeled protein molecule and this can be directly analyzed by CE. If proteins are labeled with one or two fluorescent tags, these dye-protein conjugates can be separated by CE and quantified.

In theory for detection purposes, if a protein is labeled with large number of fluorescent tags, this leads to more signal intensity, however, this may cause quenching of signals because of the close proximity of fluorescent tags on protein surface. Therefore labeling of protein with a single dye molecule is more advantageous. Before the results and discussion, we will describe short background about cleavable linkers (section 4.1.3) and some key reports involving our research (section 4.1.4).

4.1.3 Cleavable Linkers

Linker syntheses and the cleavage of linkers are the most important factors in solid-phase organic synthesis (SPOS). The linkers should not only be stable to perform SPOS, but also must be easy to cleave. Moreover, cleaner reaction conditions for cleavage are preferred, because chromatographic purifications are usually not attempted after the cleavage of linkers. There are many strategies for the cleavage of linkers from the solid-support.[136] Merrifield resin, Wang linker, and Trityl linker are widely used in solid-phase peptide synthesis (SPPS). These linkers are quite stable under basic conditions and are usually cleaved with TFA in CH_2Cl_2 at room temperature to release the product. Another useful method for cleavage is the palladium-catalyzed cleavage of allylic

linkers. The main drawback for solid-phase synthesis is that the use of metals are invasive and it is difficult to remove. Therefore, these methods are more preferred in solution-phase synthesis, in fact, this method was previously used in our group for the cleavage of nucleotides in solution-phase.[135] However, the use of acid even weak acid like TFA or any other chemicals for the cleavages, are not suitable when proteins are used for some studies, because it may cause damage to the biomolecules and also denature the proteins. Bogyo and co-workers reported a mild chemically cleavable linker for which the cleavage conditions are compatible with biochemical systems (Figure 4.4).[137] This linker is based on an azobenzene derivative and the azo bond can be cleaved under mild reaction condition by sodium dithionite. The activity-based probe **SV1** is the analogue of a general papain-family-probe DCG04.

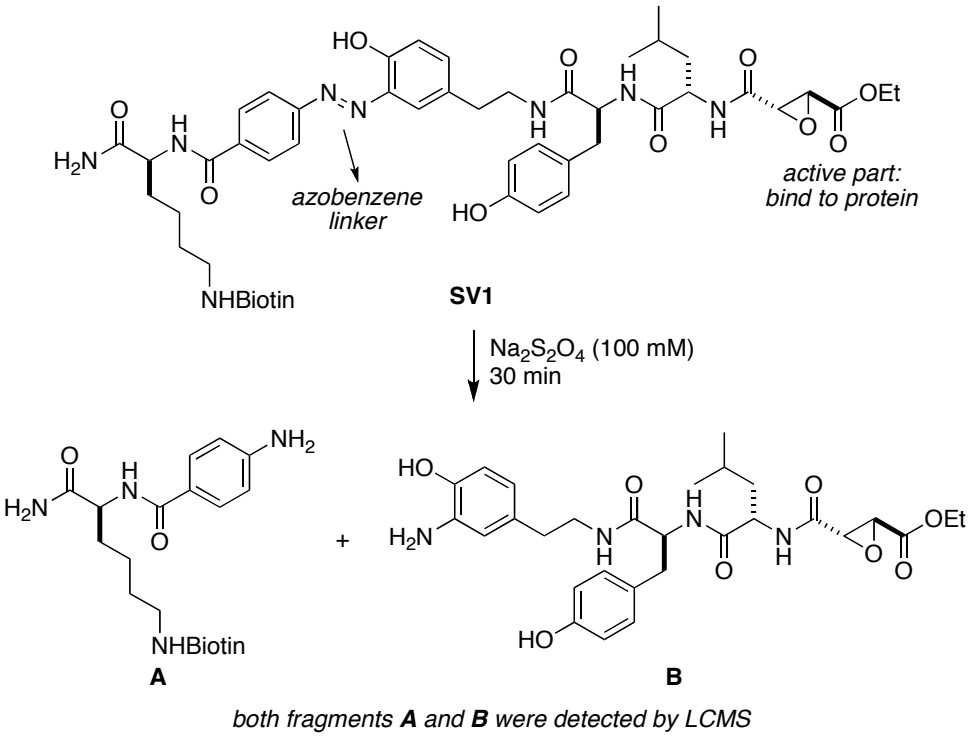

Figure 4.4. Cleavage of azobenzene linker with $Na_2S_2O_4$.

Photolysis produces a mild and orthogonal method of cleavage that takes place under neutral conditions, and tends to be suitable for biomolecules. Photolabile protecting groups were reviewed by Bochet in 2002.[138] The most widely used photocleavable linkers are *o*-nitrobenzyl alcohol derivatives. Photochemically-induced photoisomerisation of this compound produces its cleaved product, *o*-nitrosobenzaldehyde. The mechanism of photolysis is based on Norrish-type II reaction (Figure 4.5). The excitation of *o*-nitrobenzyl alcohol derivative **84** can generate a highly reactive diradical species **85**. The radical on oxygen in nitro-group abstracts γ-hydrogen to form another diradical species **86a**. The resonance structure of **86a**, non-radical form **86b**, cyclizes to form five-membered ring **87** and the ring opening leads to *o*-nitrosobenzaldehyde **88** as a cleaved product. Amide, ester, carbamate and ether can be used for this photolysis system.

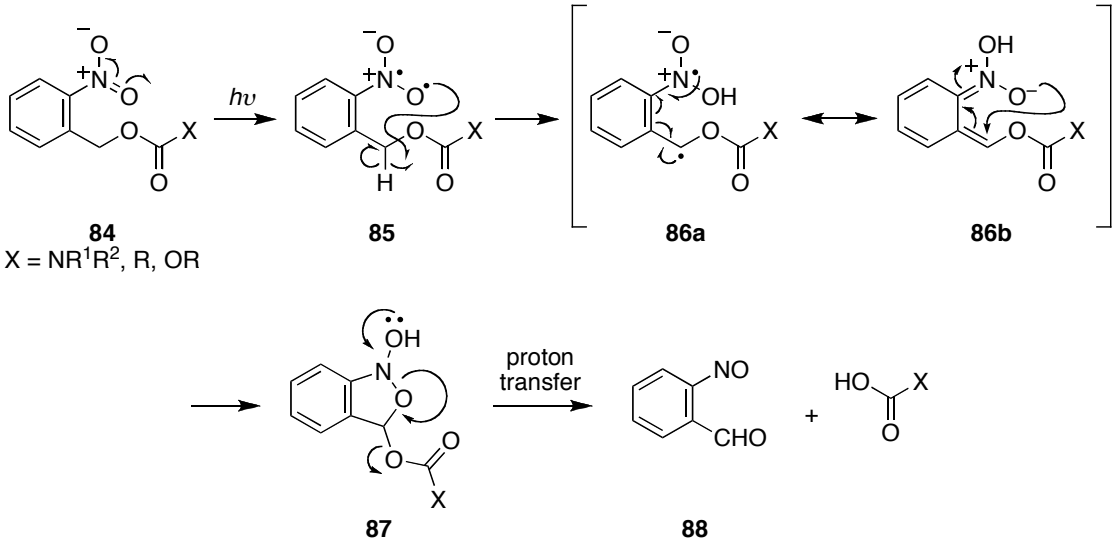

Figure 4.5. Mechanism of photocleavage reaction.

4.1.4 Key Reports Involving Our Research

One of the most important features in this project is the choice of solid-support. Bradley and co-workers studied enzyme accessibility to some solid-supports like TentaGel, PEGA, and CPG (control pore glass).[139] These solid-supports were loaded with peptide 4-CBA-Gly-Pro-Leu-Gly-Leu-Phe-Ala-Arg-OH (4-CBA: 4-cyanobenzoic acid) and incubated with five different enzymes with a range of molecular weights (22–90 kDa). The absence or presence of CN signal (2230 cm^{-1}) was recorded by Raman spectroscopy. When TentaGel and PEGA were treated with most enzymes, a CN signal was clearly seen at 2230 cm^{-1}. This indicated that the peptide sequence was not cleaved by the enzyme. On the other hand, the CN signal was not detected when CPG was incubated with all enzymes, the peptide was cleaved by the enzymes and this result proved that the accessibility of the enzyme to CPG was the best in these solid-supports.

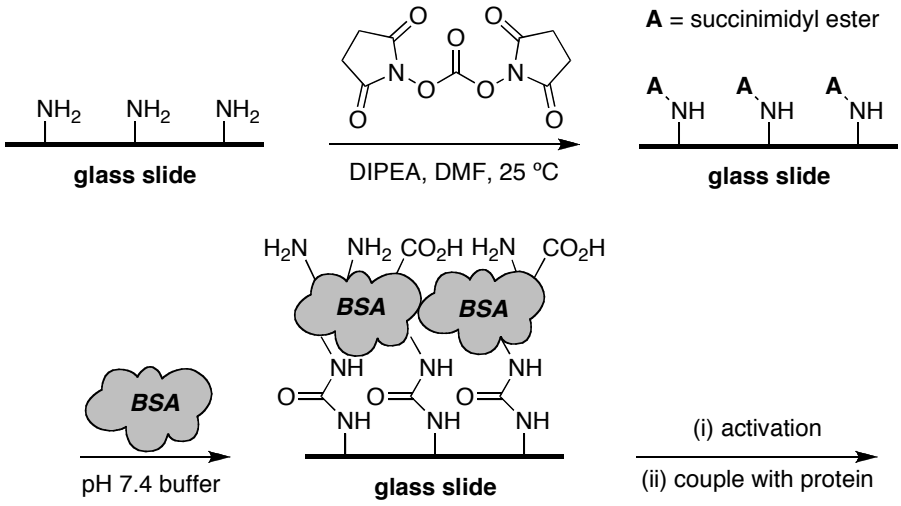

Figure 4.6. MacBeath's work based on BSA-coated glass slide.

MacBeath and Schreiber reported an innovative biological study for protein-protein interaction by modifying the surface of glass slide (Figure 4.6).[140] They uniformly coated the surface of glass slide with BSA and used those coated slides for biological assays such as screening for protein-protein interactions, and identifying the substrates of protein kinases or the protein targets of small molecules. Their work produced that

the BSA-coated glass slide made possible to do the direct protein-protein interactions on solid-support, indicating the increases of bioaccessibilities to solid-support.

4.2 System A: Nile Red Based Photolabile System

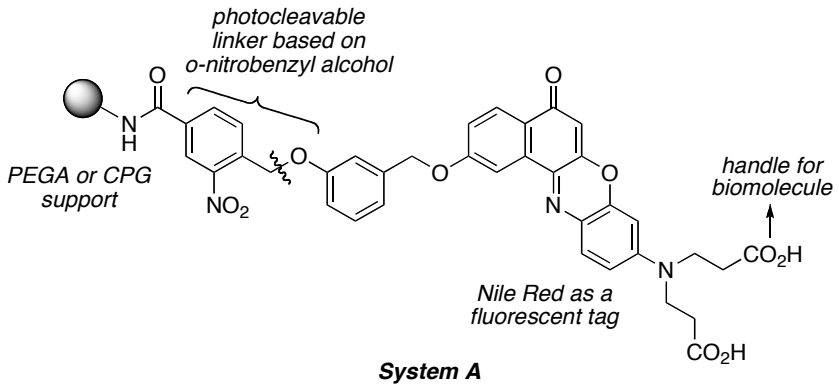

Figure 4.7. *o*-Nitrobenzyl alcohol linker based solid-support (System A).

Our first system was designed with an *o*-nitrobenzyl alcohol derivative photolabile linker and Nile Red as a fluorescent dye (Figure 4.7). 4-Bromomethyl-3-nitrobenzoic acid was first protected with ^{t}BuOH, DIC and DMAP to afford the *tert*-butyl ester **89**. Ester **89** was reacted with 3-hydroxybenzyl alcohol and brominated (CBr_4, PPh_3) to give the photolabile-protected benzyl bromide **91** (Scheme 4.1).

Scheme 4.1. Synthesis of photolabile-protected benzylbromide **91**.

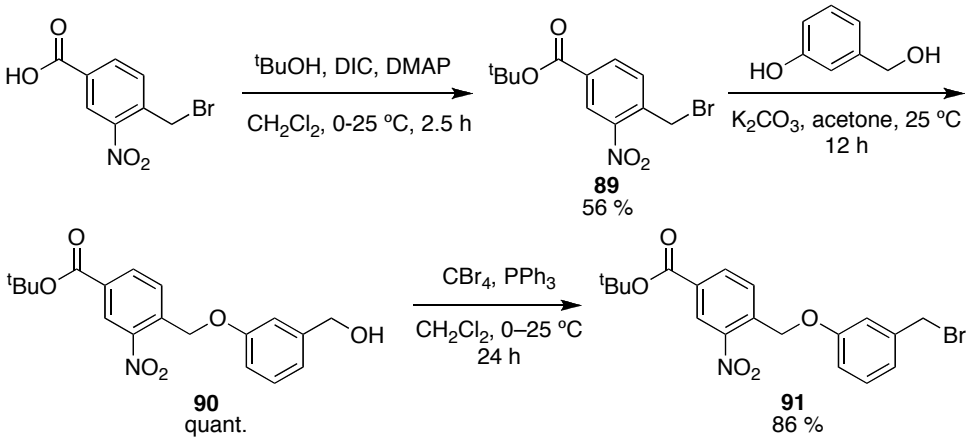

Nucleophilic attack of 2-hydroxy Nile Red dimethyl ester **92** (*provided by Mr. Jiney Jose*) to benzylbromide **91** afforded compound **93**. Deprotection of the ^{t}Bu-group under normal reaction condition (TFA, CH_2Cl_2, 25 ºC) resulted in the decomposition of molecule. Fortunately, compound **94** could be obtained in 77% yield using conditions (TMSOTf, 2,6-lutidine, CH_2Cl_2, 25 ºC) which had previously been reported for the deprotection of Boc-protected amino acid on TFA-sensitive resins by our group (Scheme 4.2).[141]

Scheme 4.2. Synthesis of photolabile-protected Nile Red derivative **94**.

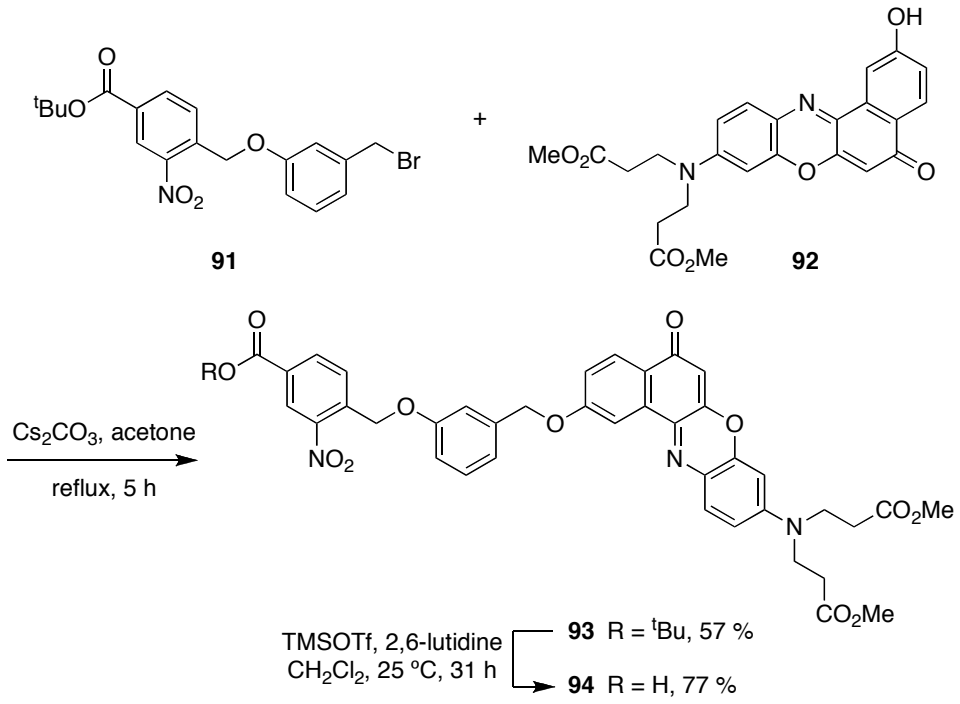

The PEGA (polyethylene glycol polyacrylamide copolymers) resin[142] was the first solid-support used to synthesize the target molecule. Although Bradley reported that the accessibilities of enzymes to PEGA resins are lesser,[139] swelling of PEGA resins is excellent in solvents of various polarities ranging from dichloromethane to water[143] and this is widely used in peptide synthesis.[144,145] The photolabile-protected Nile Red **94** was reacted with PEGA resin for 24 h, and the ninhydrin test was positive (purple beads)

after the reaction. This resin was then capped using normal capping conditions for primary amines (Ac_2O, pyridine, CH_2Cl_2) and the ninhydrin test was negative (brown beads). The dimethyl ester **95-PEGA** was deprotected under the mild reaction conditions (K_2CO_3, MeOH/H_2O, 40 ºC, 24 h) to afford diacid **96-PEGA** as purple beads (Scheme 4.3). Nile Red dimethyl ester **92** was previously deprotected under these conditions to afford the corresponding diacid in solution phase, thus we assume that **96-PEGA** was formed.

Scheme 4.3. Attachment of compound **94** on PEGA resin or aminopropyl-CPG.

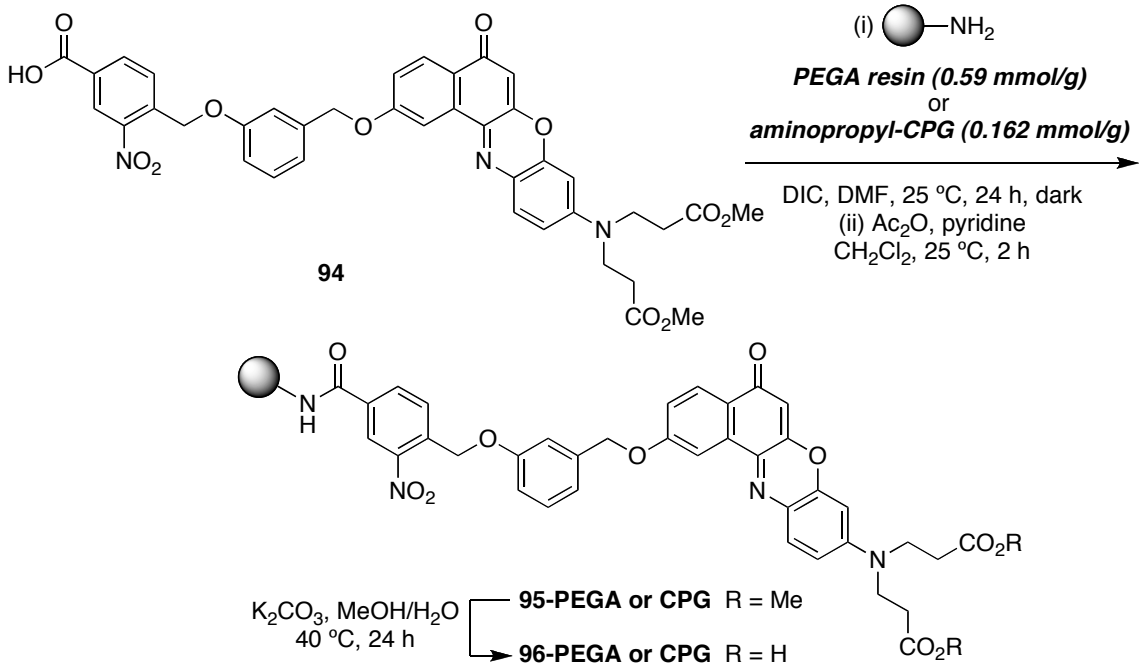

We made **96-PEGA** and thought this could help coupling reaction between **96-PEGA** and biomolecules in aqueous medium because PEGA has excellent swelling in water. However, there are two problematic issues: (i) the sticky nature of PEGA resin makes it difficult to handle, and (ii) the loading of PEGA resin is too high (0.59 mmol/g). It was difficult to continue the synthesis using this material (**96-PEGA**) because of above issues, therefore, we decided to use CPG as a solid support.

Following the synthetic approach outlined in Scheme 4.3, we tried to prepare **96-CPG** from aminopropyl-CPG (*control pore glass*, 0.162 mmol/g). CPG-supported dimethyl ester **95-CPG** was obtained as dark purple beads and K_2CO_3 was used for the deprotection of dimethyl ester (Scheme 4.3). However, we obtained very light pink beads after the deprotection, indicating the loss of some Nile Red. We were supposed to get purple beads because Nile Red has a reddish purple color. When TMSOK was used for the deprotection of the methyl ester,[146] brown beads were obtained. Decomposition of **95-CPG** or **96-CPG** might have occurred under those conditions and we were not sure how. However, at least if some of **96-CPG** were formed, then we could try some studies using this material.

It is important to confirm if photolysis of compounds work when photolabile linkers are synthesized. To do this, there are some possible analytical methods, *eg* anal. HPLC, mass spectrometry, and UV and fluorescence spectrometry. A control study was performed to confirm the photolysis of compound **96-CPG** using anal. HPLC. The aim was that we tried to compare the retention time between the product **102** obtained from the photolysis of **96-CPG** and compound **102** synthesized via solution phase. If the retention time of those peaks match, then this is strong evidence that the photolysis of **96-CPG** worked.

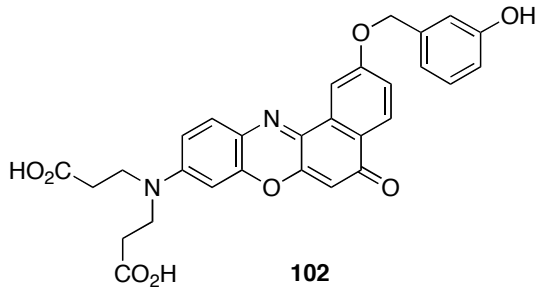

102

For the synthesis of control compound **102**, 3-hydroxybenzaldehyde was protected with TBDPS-group followed by sodium borohydride reduction to give alcohol **98**. This alcohol **98** was then brominated to afford compound **99** in overall 73 % yield (Scheme 4.4). Compound **99** was reacted with 2-hydroxy Nile Red dimethylester **92** *via* nucleophilic attack to form protected-Nile Red **100**. The deprotection of TBDPS-group

with TBAF and dimethyl ester with K_2CO_3 afforded a control compound **102** in 77 % yield (Scheme 4.5).

Scheme 4.4. Synthesis of TBDPS-protected benzylbromide **99**.

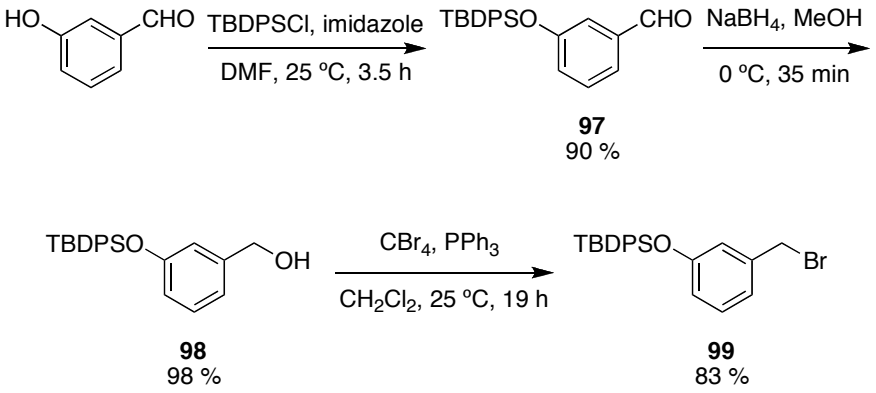

Scheme 4.5. Synthesis of Nile Red derivative **102** as a control compound.

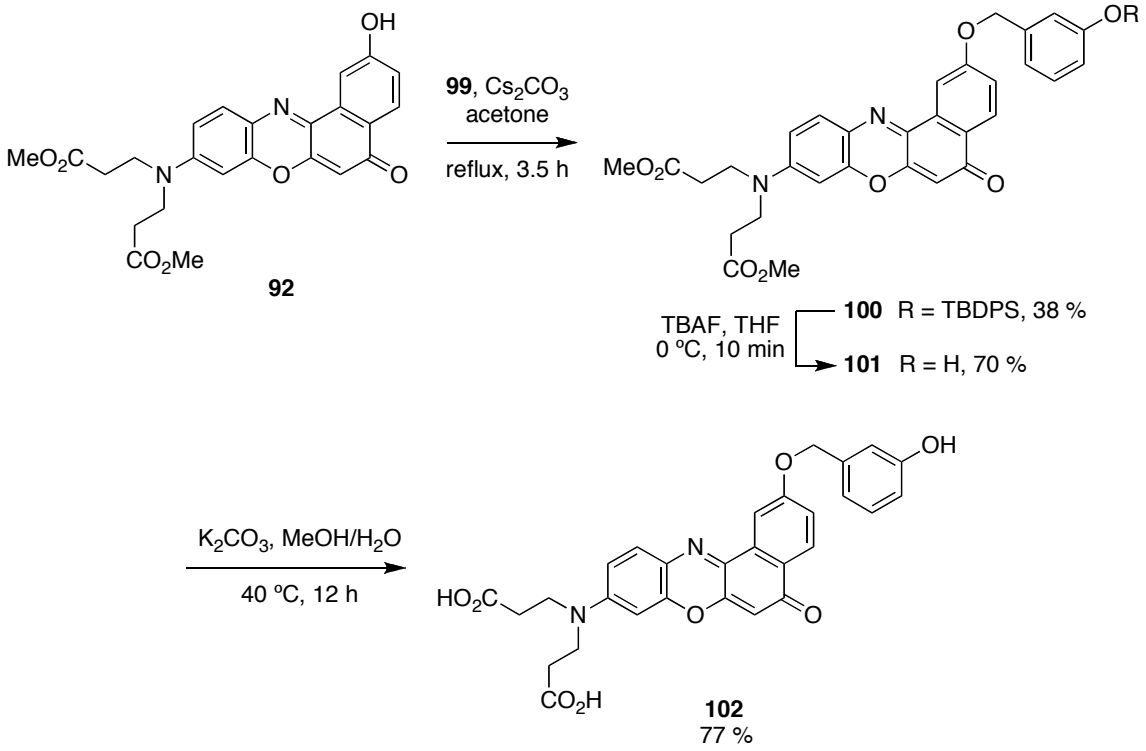

The photocleavage reactions of compound **96-CPG** obtained from K_2CO_3 and TMSOK deprotections were performed using our previously reported method (Scheme 4.6).[135] Ethanolamine was necessary for the photolysis since without it the deprotection was only partial,[102] and compound **103** is the cleaved solid-support part. Both samples from photolysis and control compound **102** (made by solution-phase synthesis, Scheme 4.5), were analyzed by anal. HPLC. However, the samples from photolysis showed several peaks and the retention time of those peaks did not match with the retention time of the control compound **102**. Thus it was difficult to analyze those samples and this control experement did not work.

Scheme 4.6. Photocleavage reaction of compound **96-CPG**.

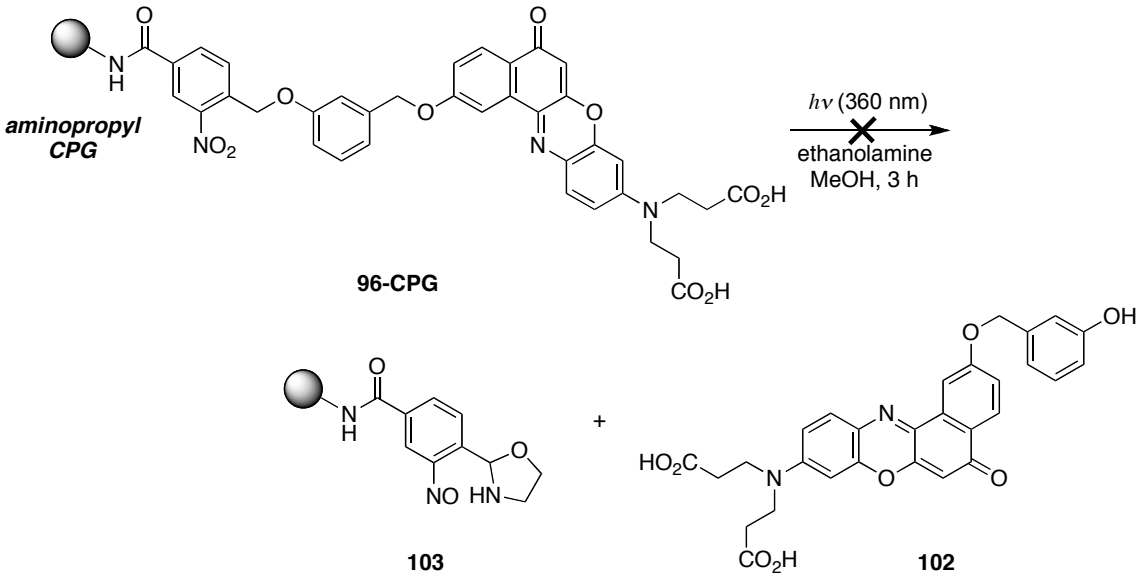

In summary, PEGA resin was difficult to handle because of its sticky nature and the accessibility of biomolecules to PEGA was presumably not good (Bradley's work).[139] For the CPG-supported compound, deprotection of the dimethyl esters lead to decomposition upon treatment with TMSOK and substantial loss of the dye from the CPG upon treatment with K_2CO_3. Furthermore, due to their lesser reactivities, *o*-

nitrobenzyl alcohol based photolinker required longer reaction time and harsh conditions for the photolysis making the substrate more prone to decomposition. In the next section, the synthesis and the uses of an activated photolinker will be described.

4.3 System B: Activated Photolabile-protecting Group

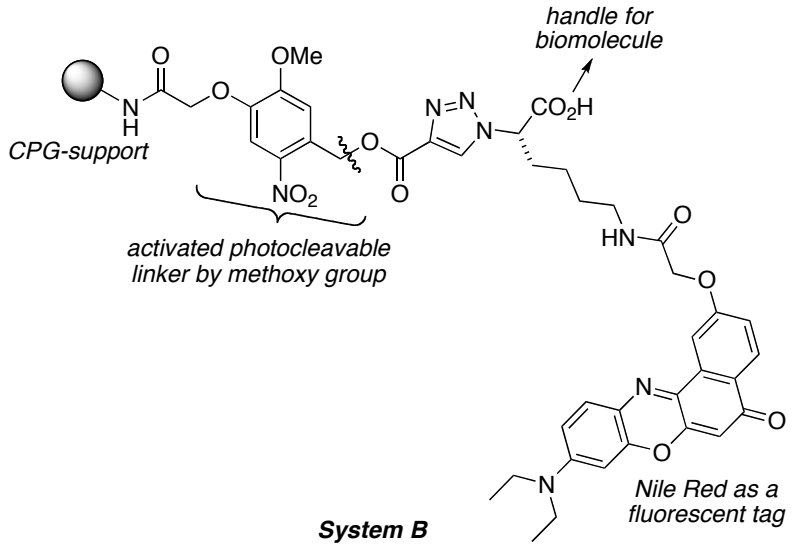

Figure 4.8. Activated photolinker based solid-support (System B).

Activation of photolinkers by introduction of a methoxy-group is often used in organic synthesis and in biological applications.[135,136,138,147,148] This methoxy group is incorporated onto the benzene ring (*p*-position with respect to nitro-group) and can serve to enhance the photocleavage rate, *ie* methoxy group increases quantum yields of photolinkers. This results in cleaner and faster reaction than the less-activated *o*-nitrobenzyl linker, however, several steps are required to synthesize this type of photolinkers.

The synthesis of activated photolinkers from vanillin was described by Klinman and co-worker.[149] Protection of vanillin with benzyl bromide, followed by nitration gave *O*-benzyl-6-nitrovanillin **105** and deprotection of *O*-benzyl-group with HBr/AcOH afforded 3-methoxy-6-nitrovanillin **106**. Aldehyde **106** was then reduced to the

corresponding alcohol **107** using sodium borohydride.[135] This primary alcohol was reacted with *tert*-butylbromoacetate to afford the photolinker **108** in 96 % yield (Scheme 4.7). In fact, the photolinker **107** is a very useful compound because many modifications of phenol and primary alcohol functionality are possible. Photolinker **108** was reacted with propiolic acid or 4-pentynoic acid using DIC-coupling to insert alkyne functionality. Compound **109a** and **109b** were then deprotected with TFA to afford carboxylic acid **110a** and **110b** in quantitative yields (Scheme 4.8).

Scheme 4.7. Synthesis of activated photolabile-protecting group **108**.

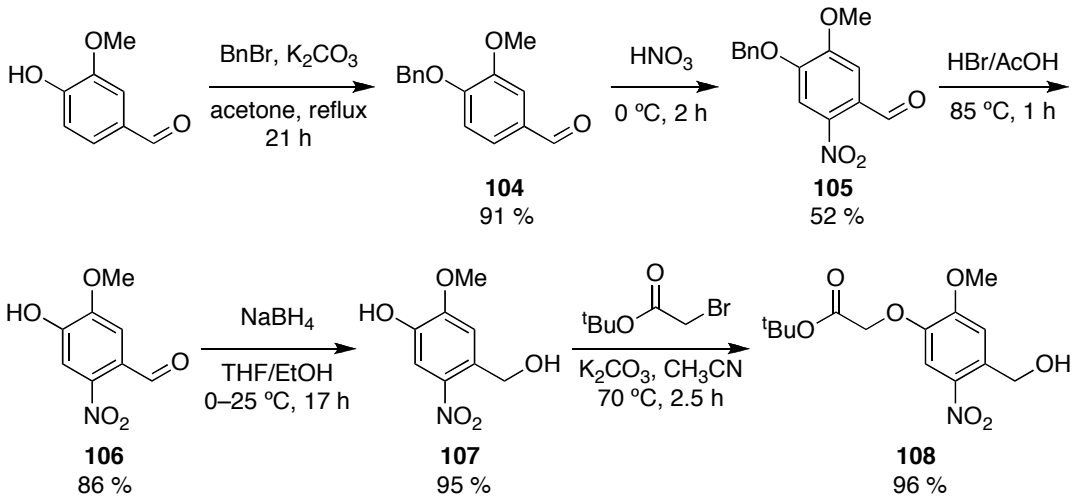

Scheme 4.8. Insertion of alkyne functionality.

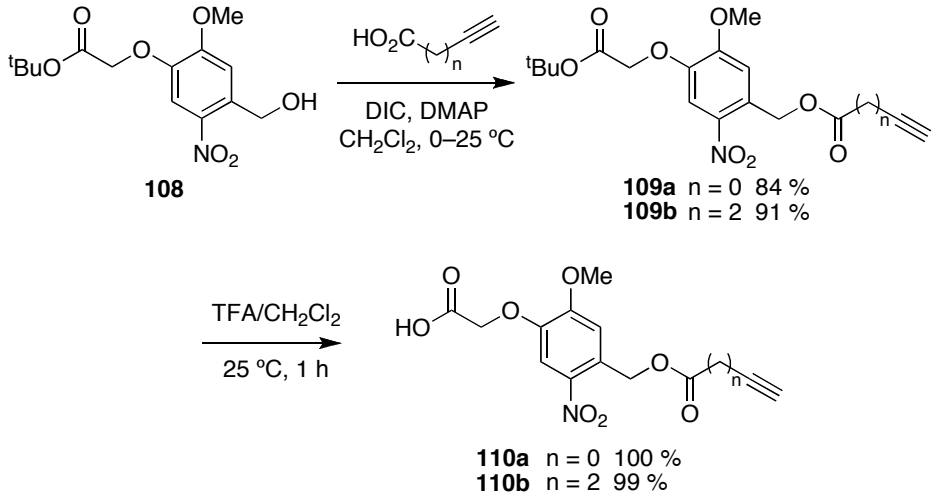

First, we examined whether this new photolinker **109** was cleavable. For a solution-phase control, alkyne **109a** was cyclized with benzyl azide **111**[150] to afford triazole **112**. This triazole **112** was then irradiated under UV (strip UV light designed to emit at 360 nm; Southern New England Ultraviolet Company); the reaction was complete in 1 h (TLC, >95 % conversion, Scheme 4.9). Samples from the photolyses were analyzed by mass spectrometry and triazole **112** and the photo-cleaved product **114** were detected. Compound **113** was not detected presumably because of its instability.

Scheme 4.9. Control experimental for photochemical reaction.

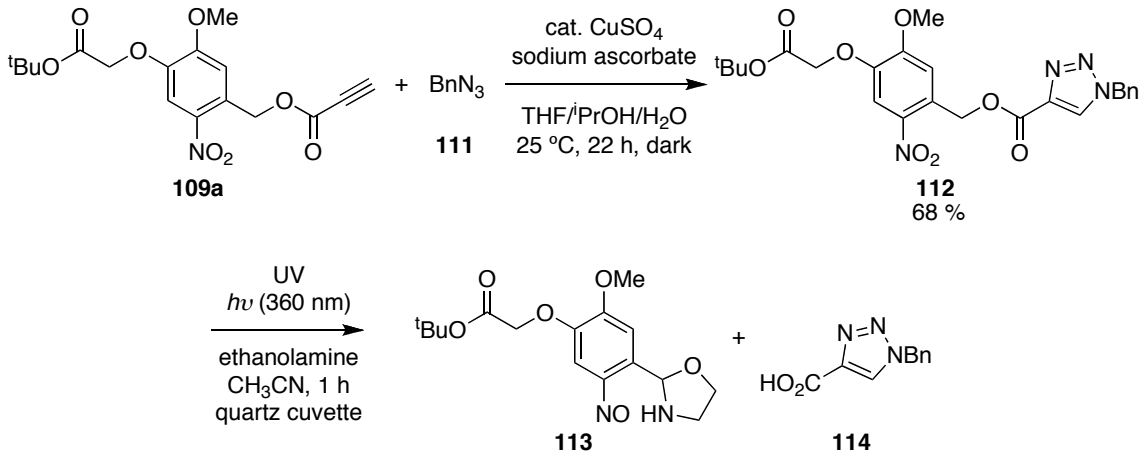

For the control photolysis study on solid-phase, alkyne **110a** was first attached onto glass beads (GB) using DIC and DMAP to give **115** (Scheme 4.10). The ninhydrin test of compound **115** resulted in negative (brown beads), indicating no primary amine functionality were left on the solid support.

Scheme 4.10. Attachment of photolinker **110a** onto glass beads.

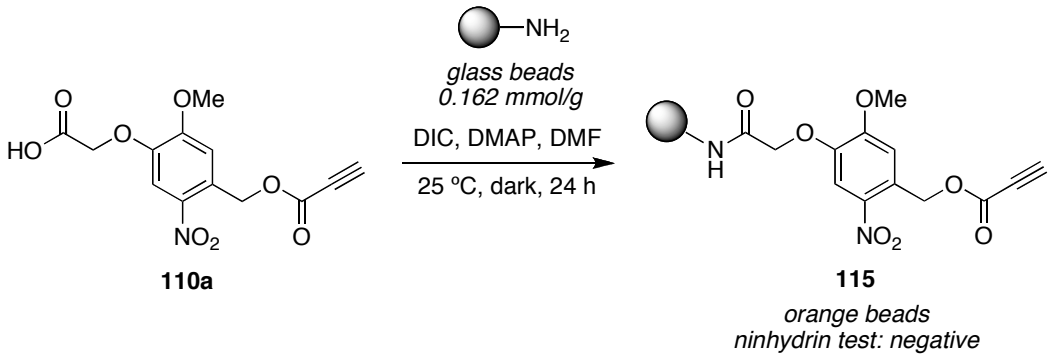

Next, alkyne **115** was clicked with 4-azido-BODIPY **116** (*provided by Mrs. Lingling Li*) to form triazole **117** (Scheme 4.11). This triazole **117** was then photo-cleaved in a quartz cuvette under UV (360 nm). The fluorescence intensity in the solution above the beads was measured every 5 min over a period of time of 80 min. As shown in Figure 4.9, the fluorescence intensity increased from 0 to 80 min, indicating that the photocleavage reaction of compound **117** occurred. Some fluorescence was detected at 0 min, probably due to the small amounts of photolysis of compound **117**.

Scheme 4.11. Synthesis of control compound **117** and its photochemical reaction.

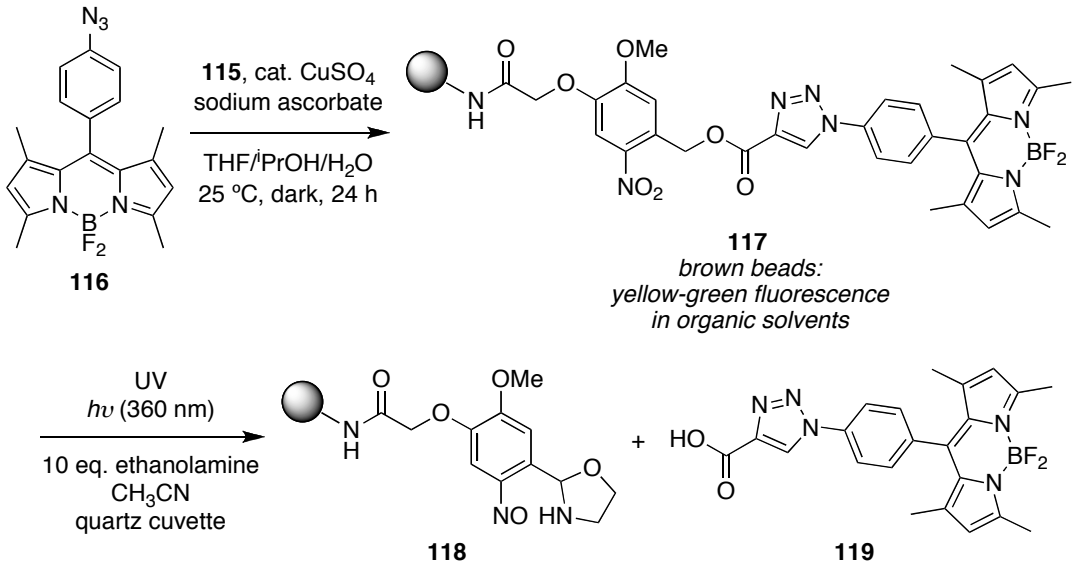

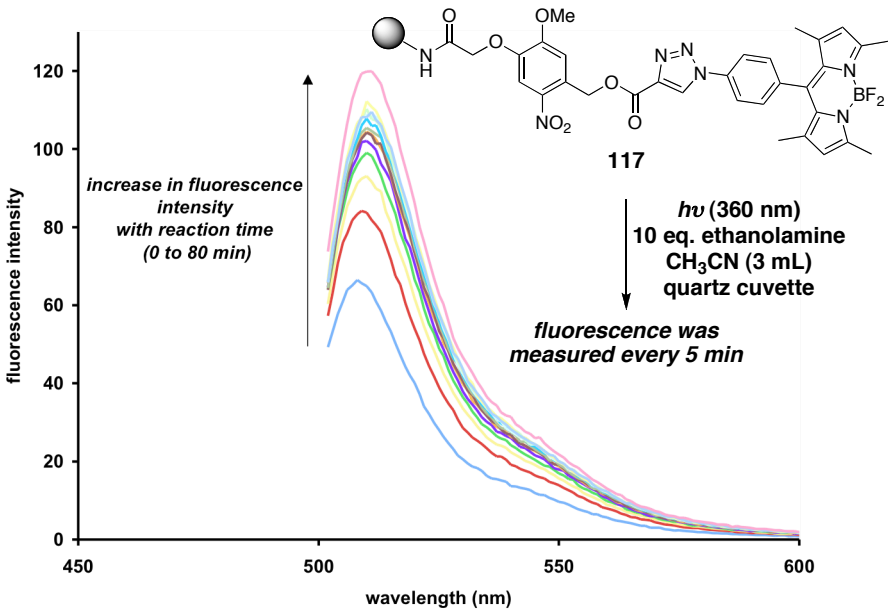

Figure 4.9. Fluorescence emission spectra from the photochemical reaction of **117** upon excitation at 498 nm.

In conclusion, we proved that photolysis of the new photolinker **109** works well in a short reaction time with good conversion (>95 %); (mass spectrometry analysis; *solution-phase*). We also observed the increase of fluorescence intensity of BODIPY dye **119** at around 515 nm from a *solid-phase* synthesis. Unfortunately, glass beads (loading: 0.162 mmol/g) were no longer available from Sigma at this time. Therefore, we purchased another CPG (*controlled pore glass*) from 3-Prime and used it.

Photolinker **110a** was reacted with CPG (pore size: 1000 Å, loading: 0.082 mmol/g) to give solid-support **120**. This alkyne **120** was cyclized with lysine-derivative **121** (*provided by Ms. Eunhwa Ko*) *via* click reaction to afford triazole **122**. Deprotection of the Boc-group with TFA gave the primary amine **123** and positive ninhydrin test for these beads indicated that the amino-functionalities were on the surface of the CPG (Scheme 4.12).

Scheme 4.12. Synthesis of CPG-support triazole **123**.

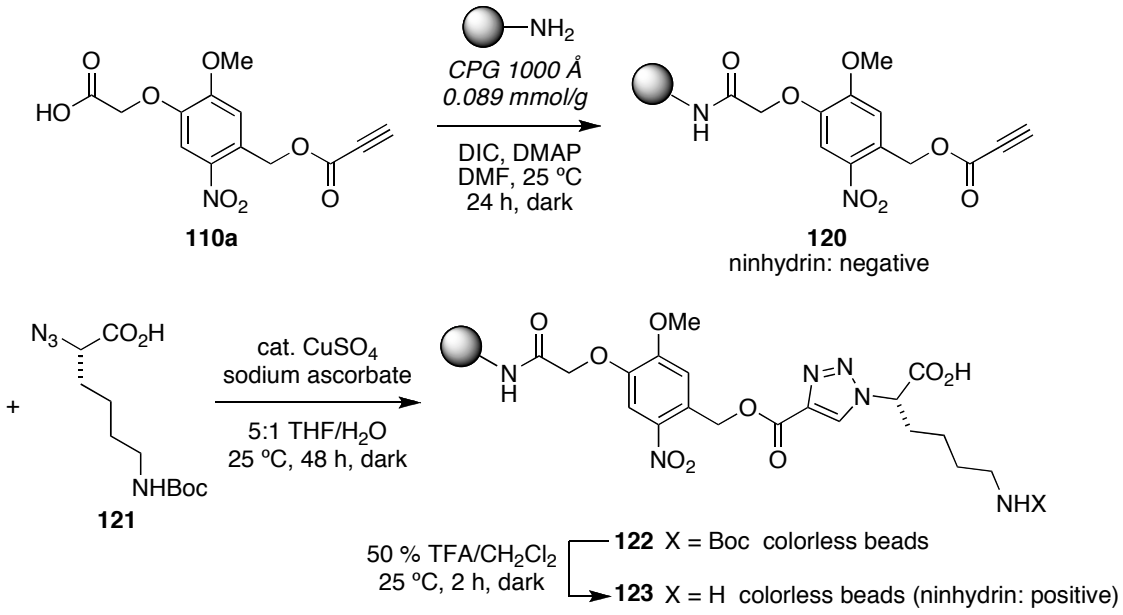

Nile Red derivative **124** (*provided by Mr. Jiney Jose*) was activated with NHS (*N*-hydroxysuccinimide) and DIC (diisopropylcarbodiimide), and used without purification for the coupling reaction with solid-support **123**, and the carboxylic acid was activated with NHS to afford product **126** (Scheme 4.13). Compound **126** had a red fluorescence in organic solvents (DMF, MeOH, and CH_2Cl_2).

Scheme 4.13. Attachment of Nile Red to solid-support.

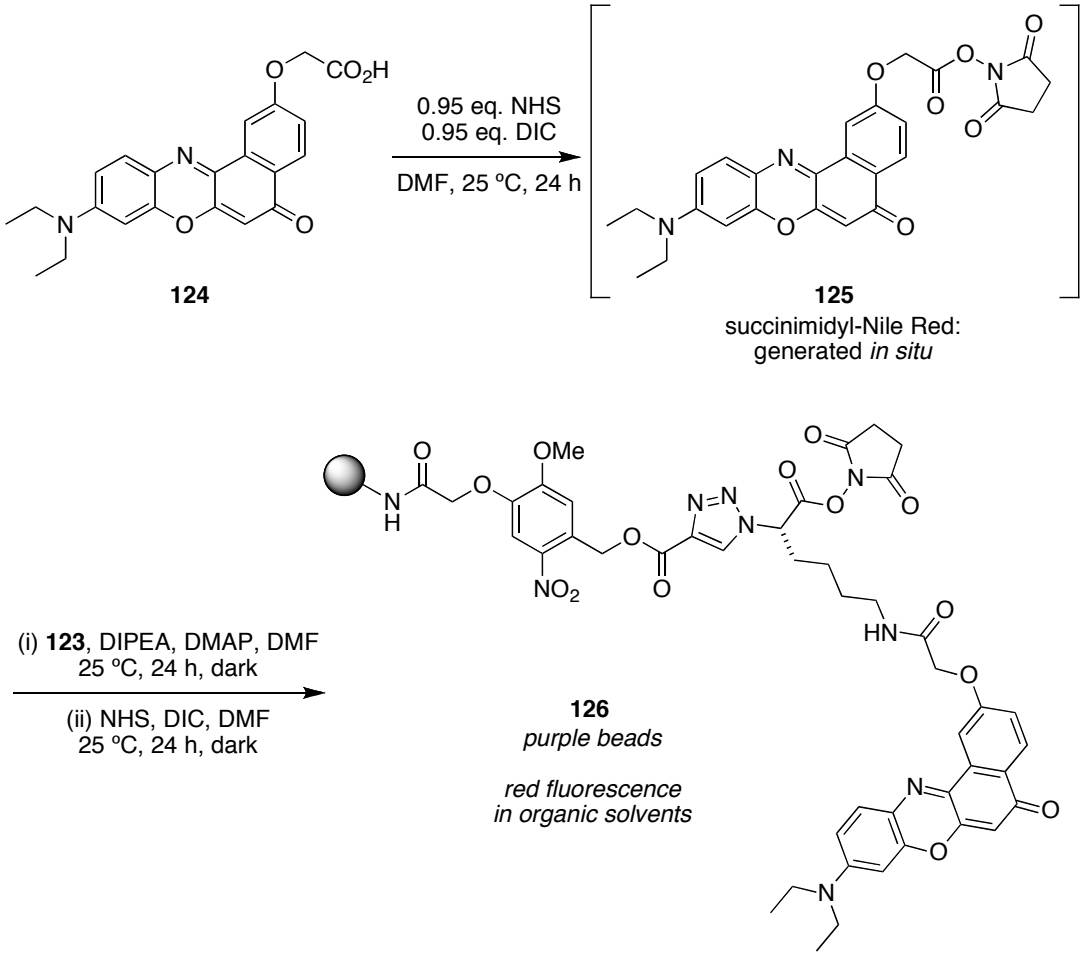

With the supported dye **126** in hand, we could investigate mono-labeling of proteins. Two important factors concerning the protein were: (i) the number of lysine residues; and (ii) the protein molecular weight (MW). The smaller molecular weight is preferred, because the distinction of one or two dyes on the protein by MALDI is more difficult when a protein of big molecular weight is used since the molecular weight of the dye is comparatively small (~550 MW). Therefore, ubiquitin was chosen for mono-labeling with molecule **126**. Ubiquitin has seven lysines and all of them are surface exposed and available to conjugate with other molecules. The molecular weight of ubiquitin is 8565 Da, and can be analyzed by MALDI.

Compound **126** was coupled with ubiquitin under basic conditions (pH 8.3 buffer). Excess ubiquitin was washed away after the reaction and photolysis of dye-protein conjugate on solid-support **127** was performed (Scheme 4.14). However, when the dye-protein conjugate **129** was purified using size-exclusion column, we did not see any purple band. UV absorption spectra for each fraction were taken and we observed only a small peak at 268 nm instead of 280 nm, a characteristic peak for protein. Furthermore, only a small absorption band characteristic of Nile Red at around 548 nm was observed. Similarly, a weak fluorescence emission at 648 nm was observed for each fraction. MALDI analysis for **129** did not show any dye-protein conjugates. According to these observations, no dye-protein conjugate or at least no detectable functional, non-denatured, unfolded protein was obtained. It is also important to mention that it was difficult to measure UV absorption and fluorescence emission spectra of lipophilic Nile Red in water because of its poor photophysical properties in aqueous media. Therefore we decided to study a similar system using BODIPY dye which has good photophysical properties even in aqueous media.

Scheme 4.14. Photolysis of dye-protein conjugates on solid-support **127**.

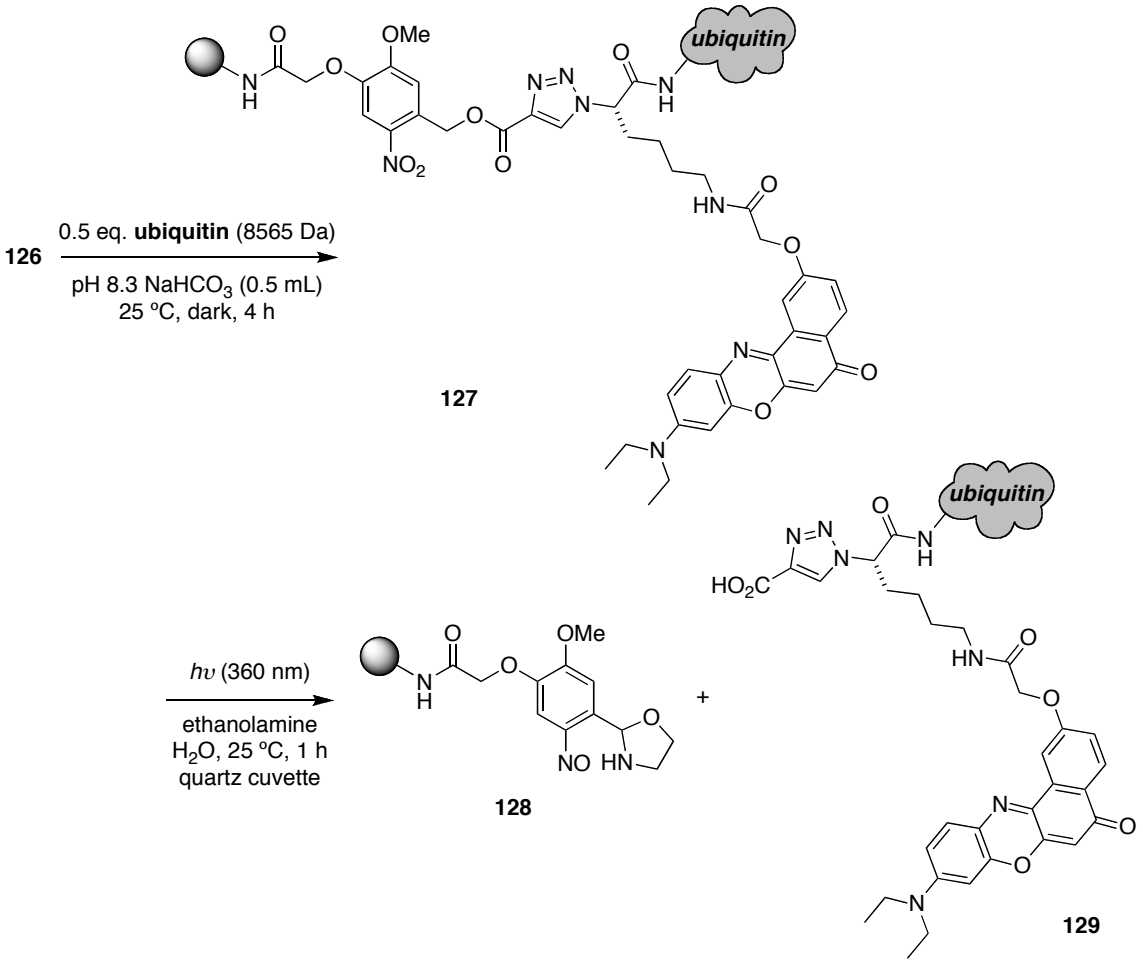

4.4 System C: Photolabiling System Based on BSA-coated CPG

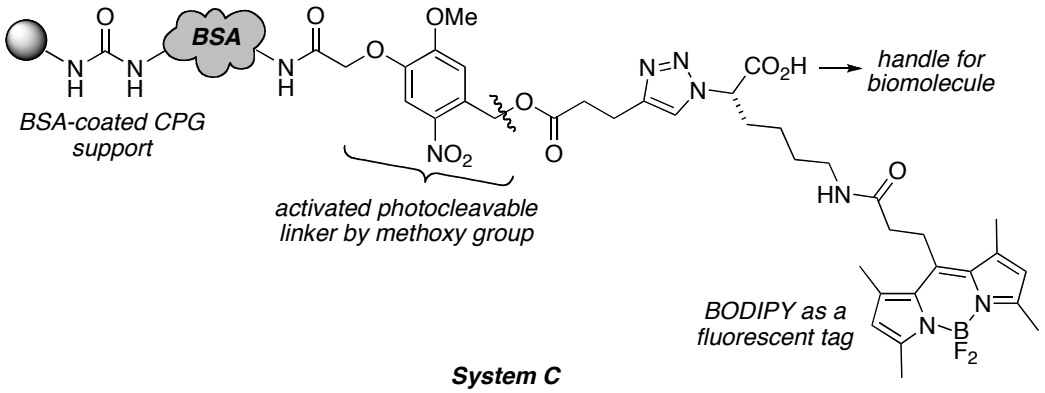

Figure 4.10. Activated photolinker based BSA-coated CPG (System C).

MacBeath and Schreiber described interesting biological studies as shown in section 4.1.4,[140] and we could use their method to our research to enhance the accessibility of biomolecules against CPG. Using their method, we prepared BSA-coated glass beads. The CPG was activated with *N,N'*-disuccinimidyl carbonate to afford NHS-CPG **130,** and this was then coupled with an excess amount of BSA in pH 7.4 buffer at 25 ºC. Ninhydrin test for BSA-coated CPG **131** showed positive result (purple beads). Next the photolinker **110b** was attached on BSA-coated CPG **131** under the mild conditions (DIC, DMAP, DMF, 25 ºC) to form alkyne **132**. Ninhydrin test for these beads gave a negative (brown beads). Finally, aspartic acid and glutamic acid residues on BSA were capped by activation of acids with NHS followed by coupling with ethanolamine to afford product **133** (Scheme 4.15).

Scheme 4.15. Synthesis of photolinker on BSA-coated CPG.

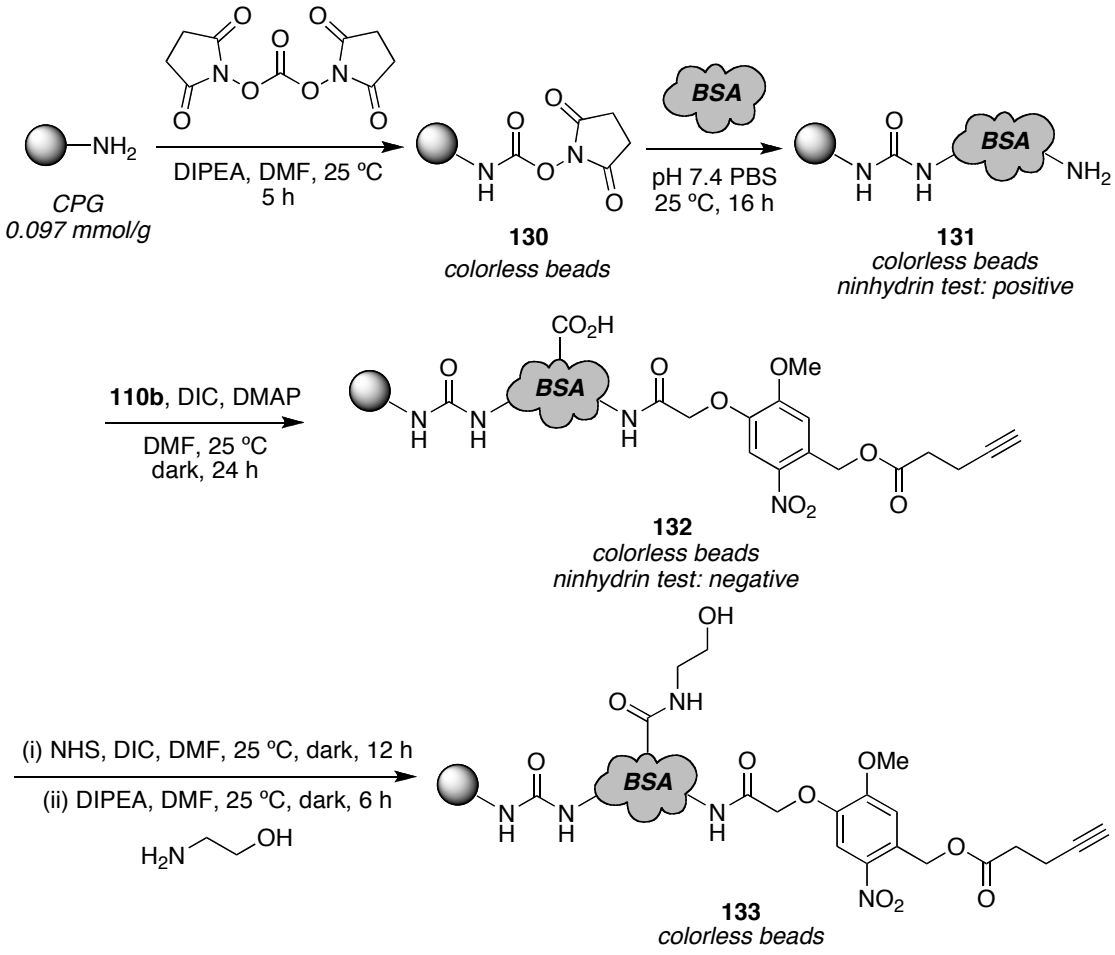

The Boc-protected azido lysine **121** was deprotected with TFA to give lysine derivative **134** in quantitative yield (Scheme 4.16a). Next, BODIPY dye **135** (*provided by Mr. Cliferson Thivierge*) was activated using NHS followed by coupling reaction with compound **134** to afford BODIPY derivative **137** (Scheme 4.16b).

Scheme 4.16. Synthesis of BODIPY derivative **137**.

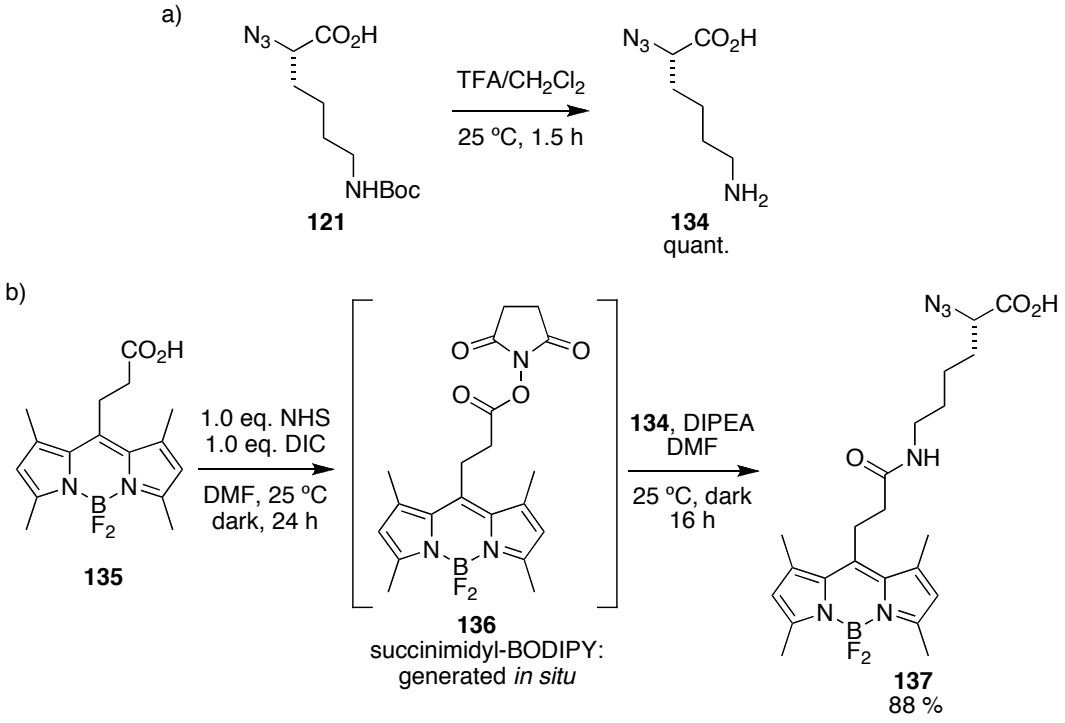

The BSA-coated CPG **133** and BODIPY **137** were then cyclized to form triazole **138** *via* a 2+3 cycloaddition. After the reaction, the beads were washed with several organic solvents and the resulting light orange beads showed a yellow-green fluorescence in organic solvents (Scheme 4.17). The carboxylic acid of triazole **138** was then activated with NHS and DIC in DMF at 25 ºC. After washing off excess chemicals, this activated material was coupled with ubiquitin in pH 8.3 buffer at 25 ºC. The ubiquitin-conjugated beads **139** had a quite strong yellow-green fluorescence in water (Scheme 4.18).

Scheme 4.17. Click reaction of solid-support **133** and BODIPY **137**.

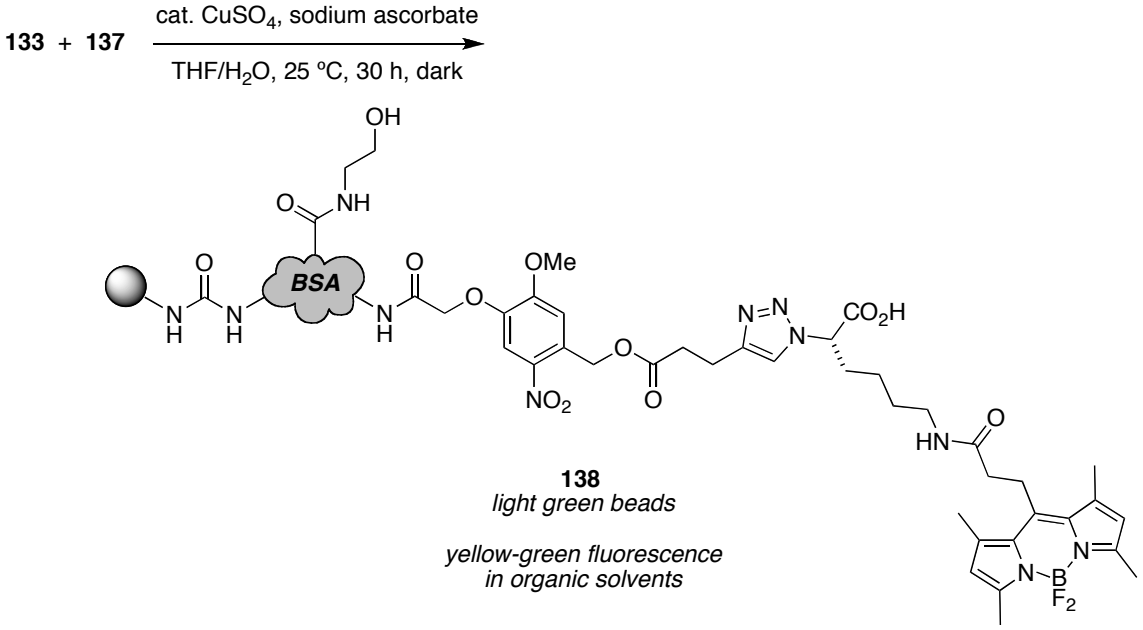

Scheme 4.18. Coupling reaction with ubiquitin.

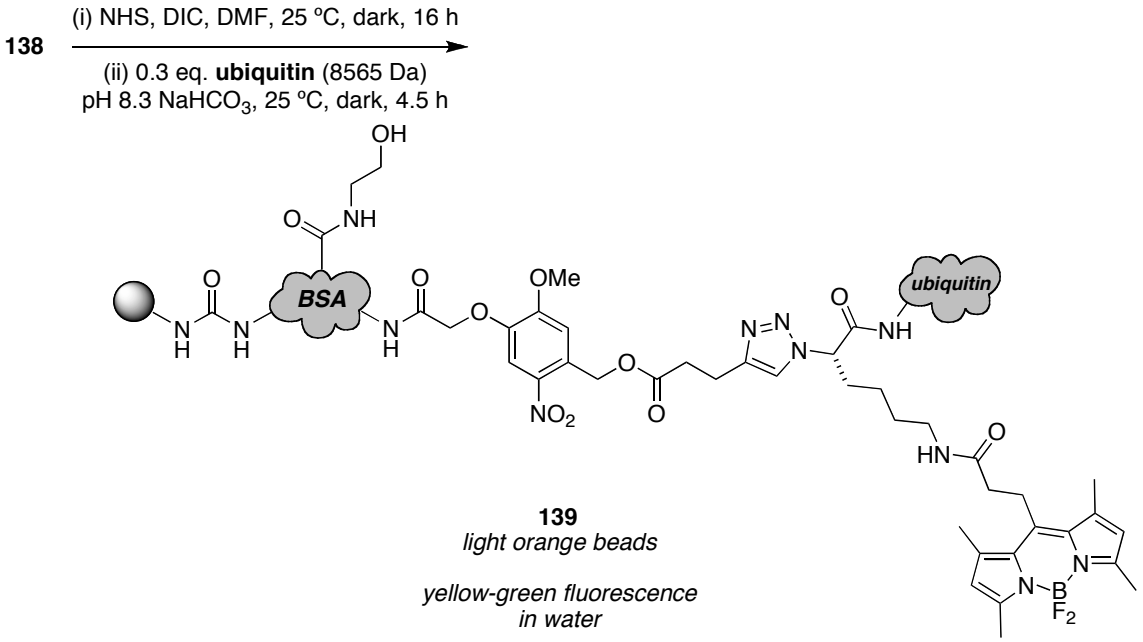

Photolysis of dye-protein conjugate on solid-support **139** was attempted, and as we expected a strong yellow-green fluorescent solution was obtained after the reaction (Scheme 4.19). The sample of compound **141** was directly analyzed by CE (*capillary electrophoresis* using UV and fluorescence detectors, Dr. Vigh's group), MALDI and LCMS (Dr. Tichy). The results of MALDI and LCMS analyses will be shown on page 121.

Scheme 4.19. Photochemical reaction of compound **139**.

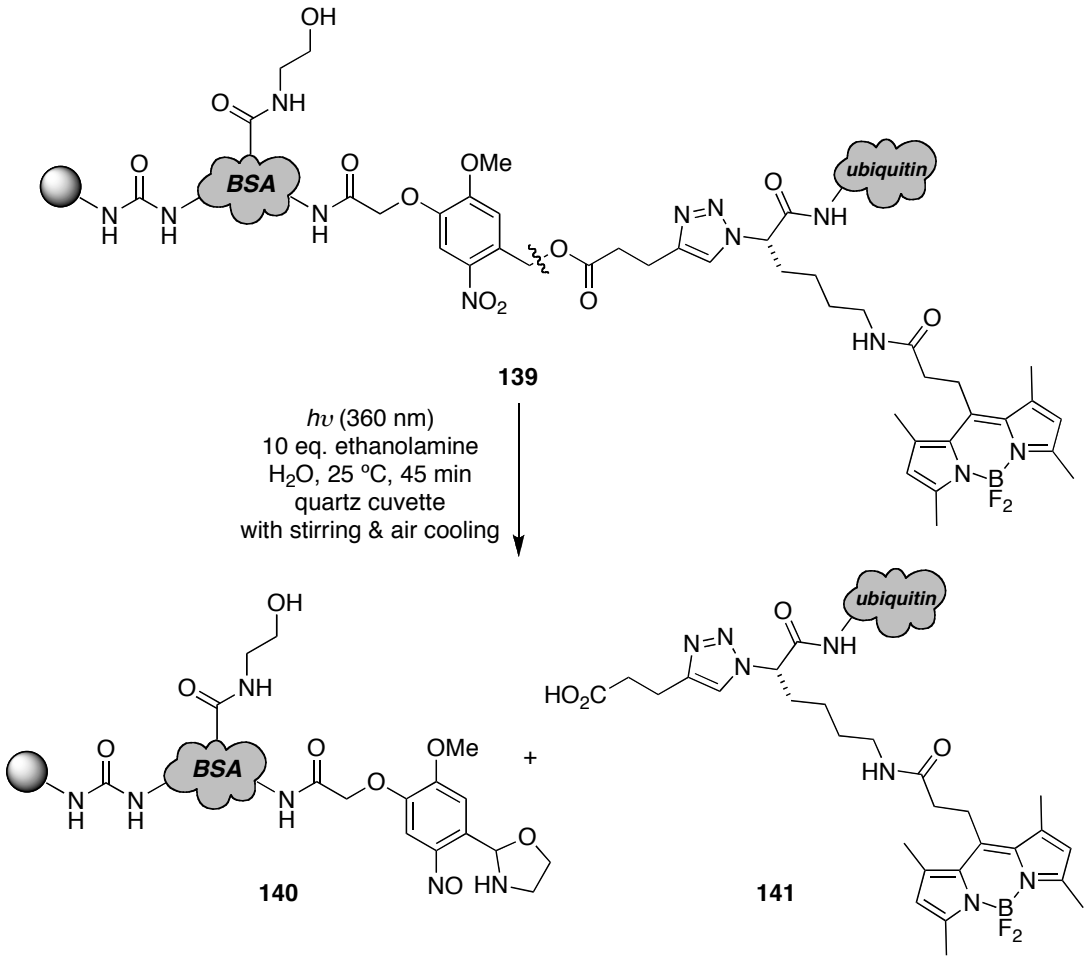

Figure 4.11 shows the electropherogram from CE analyses with UV detection (uncoated capillary was used for these studies). DMSO was used as a mobility marker; effective mobility (μ_{eff}) of the sample was calculated by comparing retention time between sample and marker. At first, native ubiquitin (a solution of 5 mg/mL in H_2O, E = 18 kV) was injected as a control study and it showed a single peak of μ_{eff} = 14 (Figure 4.11a). A single peak was also detected when the sample **141** (a solution of 1 mg/mL in background electrolyte: 10 mM acetic acid/10 mM β-alanine at pH 4.11) obtained from the photocleavage reaction of compound **139** was injected (μ_{eff} = 8.5, Figure 4.11b). Figure 4.11c shows an electropherogram spiked with native ubiquitin and sample **141**, and two different peaks with a mobility of 7.8 and 6.9, respectively, were observed. However, the effective mobility of spiked peaks did not match with any control experimental data (μ_{eff} = 14 for native ubiquitin or 8.5 for sample **141**). This sample **141** was also analyzed by CE with fluorescence detection, but several peaks were observed and characterization was therefore very difficult. Effective mobilities were obtained by the equations given below.

$$\mu_{eff} = \mu_{obs} - \mu_{EOF}$$

μ_{eff} = effective mobility

μ_{EOF} = effect of flow (marker: DMSO)

μ_{obs} = observed (sample)

$$\mu_{obs} \text{ or } \mu_{EOF} = \frac{L_T \times L_D}{T \times V}$$

L_T = total length of capillary

L_D = length of detection

T = time (min)

V = volt (kV)

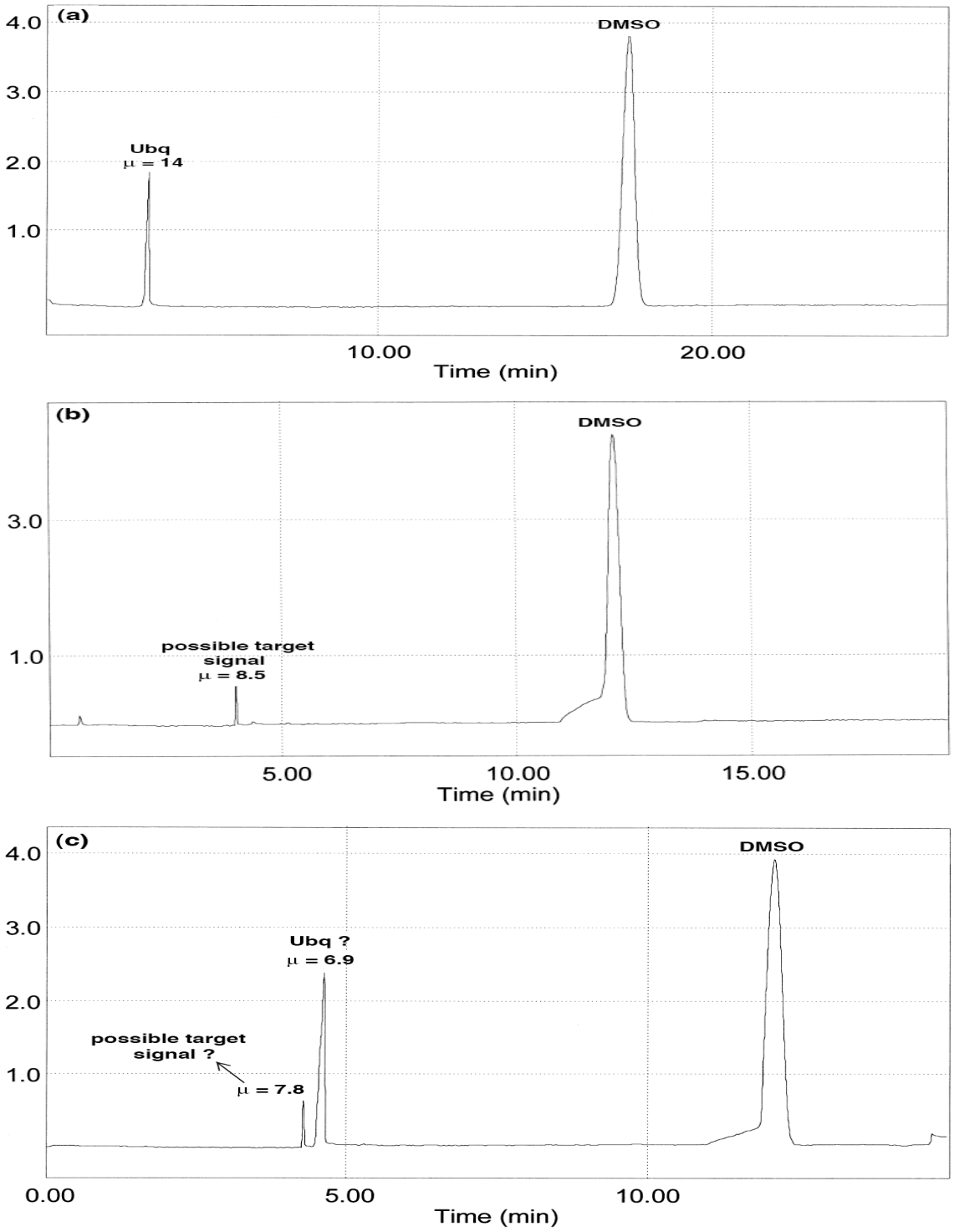

Figure 4.11. CE results **a**: ubiquitin, **b**: sample **141**, and **c**: spiked of ubiquitin and **141**.

Electro-osmotic flow in a capillary varies with the pH of background electrolyte. We used ethanolamine as a trapping agent in our photolysis system and this probably changes the mobility of the injected sample. A control experiment was performed to confirm this hypothesis. Two samples were injected, one native ubiquitin and the other native ubiquitin with ethanolamine (10 μL). We tried to compare the μ_{eff} of ubiquitin and DMSO (marker), however those were obviously different between two samples, *i.e.* the difference of retention time between Ubq and DMSO with ethanolamine was closer compared to that of Ubq and DMSO without ethanolamine (Figure 4.12). To solve this problem, the sample from the photolysis (**141**) was purified using size-exclusion column to remove excess ethanolamine, however, most of the dye-protein sample was lost in the column because of small amount of sample.

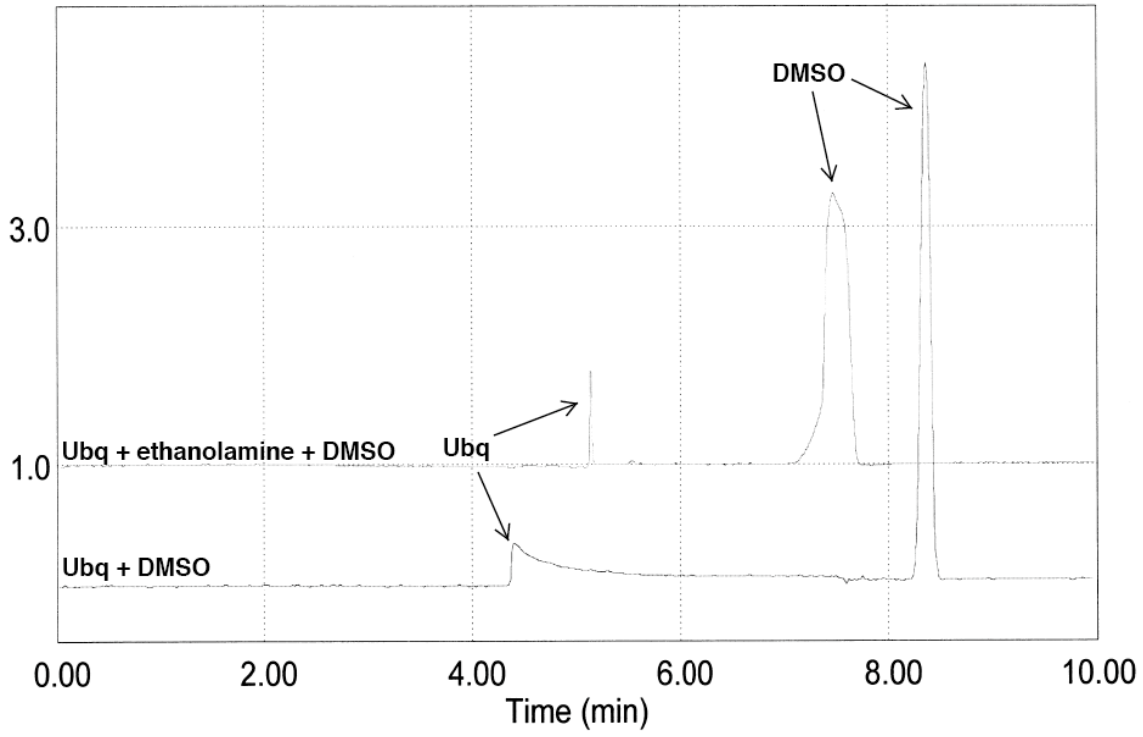

Figure 4.12. CE results, ubiquitin and ubiquitin with ethanolamine.

The compound **141** (predicted mono-dye labeled protein) was also analyzed by MALDI and LCMS (by Dr. Tichy). A solution of this sample in H_2O had a slightly yellow color and a strong yellow-green fluorescence under UV irradiation. According to our hypothesis, if one dye (MW: 555.27) was conjugated with ubiquitin (MW: ~8565 Da), then the molecular weight of dye-ubiquitin conjugate (total MW: ~9120.27 Da) should be detected by LCMS and MALDI. A maximum of seven dyes can be possibly conjugated with ubiquitin which will correspond to a dye-protein conjugate with a MW of *ca.* 12400 Da (Figure 4.13). Data from both LCMS and MALDI showed a single peak at 8570 Da. As a control experimental, LCMS and MALDI analyses of native ubiquitin gave a single peak at 8570 Da. Therefore, we could conclude that the photolysis product of **139** contained only ubiquitin and free BODIPY dyes, no dye-protein conjugates were observed in these experiments.

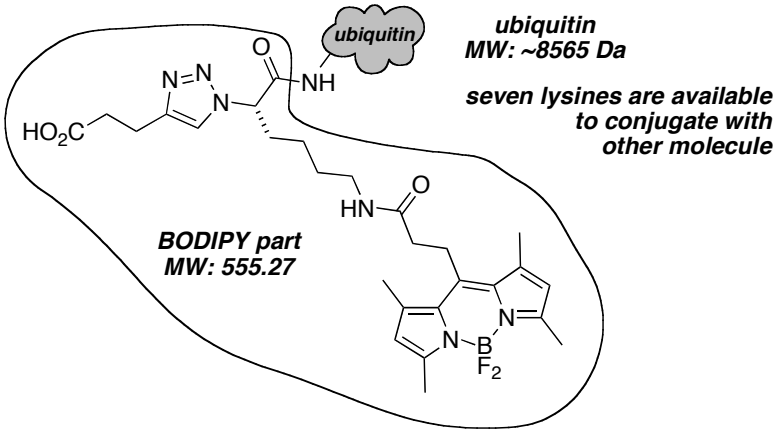

Figure 4.13. Structure of BODIPY-ubiquitin conjugate **141**.

Interestingly, a yellow-green fluorescent solution was obtained during the activation and coupling steps between **138** and ubiquitin. This indicates that some BODIPY dyes were being cleaved from the solid-support under those conditions. A possible reason for this decomposition is the stability of the ester bond between the photolinker and the triazole under basic condition (Figure 4.14a). If the hydrolysis of the ester occurred with bases, BODIPY dye can be released from the resin and this leads to a strong yellow-green fluorescence. To prevent this possible side reaction and improve the overall stability of our system, we designed a new system with an ether based spacer (Figure 4.14b).

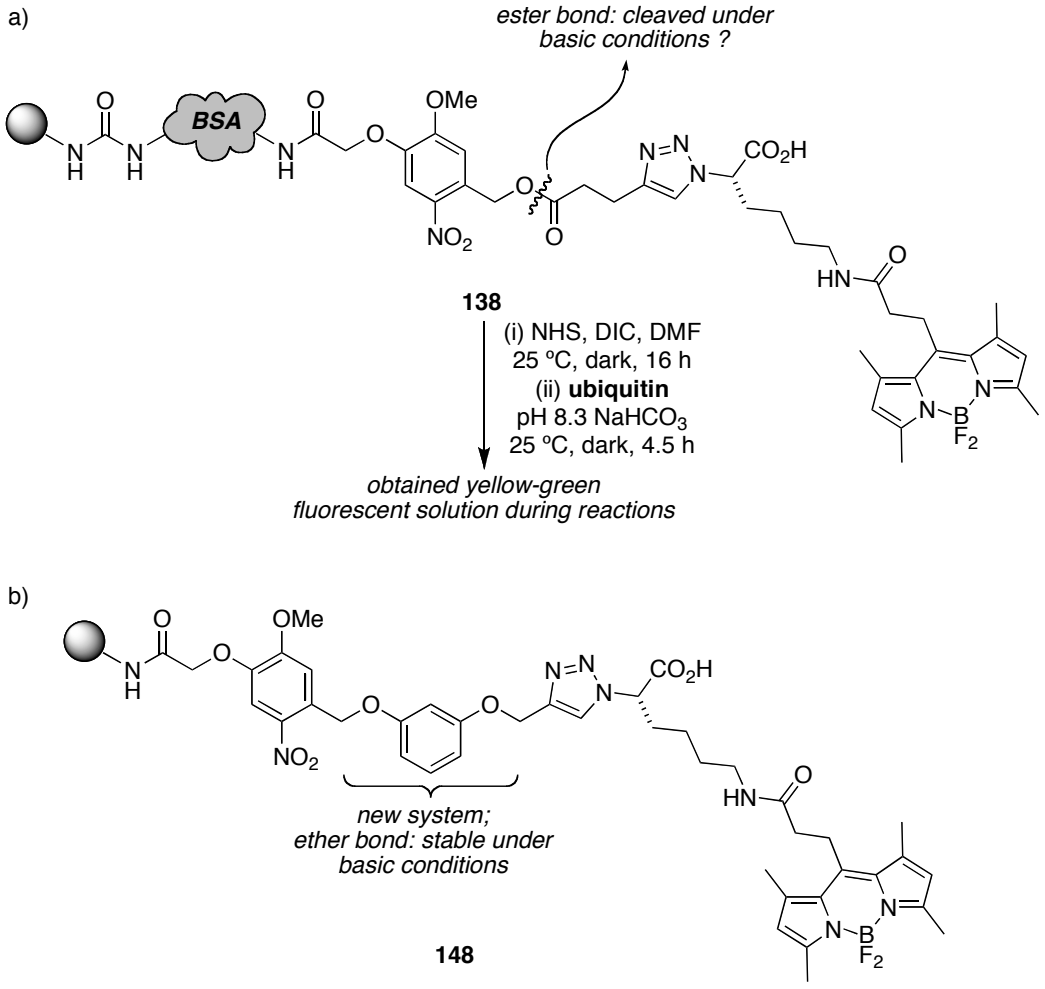

Figure 4.14. **a**; Ester system (**138**), and **b**; ether (**148**) system.

Resorcinol was chosen as a spacer and mono-propargylic resorcinol **143**[151] was first synthesized via the mono-alkylation of resorcinol with propargyl tosylate **142**[152] (Scheme 4.20a). Next, photolinker **108** was tosylated to give tosylate **144** in 99 % yield without chromatographic purification. This tosylate **144** was then alkylated with compound **143** to form the ether **145**. The *tert*-butyl-group was deprotected with TFA/CH_2Cl_2 conditions to afford the desired product **146** in 99 % yield (Scheme 4.20b).

Scheme 4.20. Synthesis of ether based photolinker **146**.

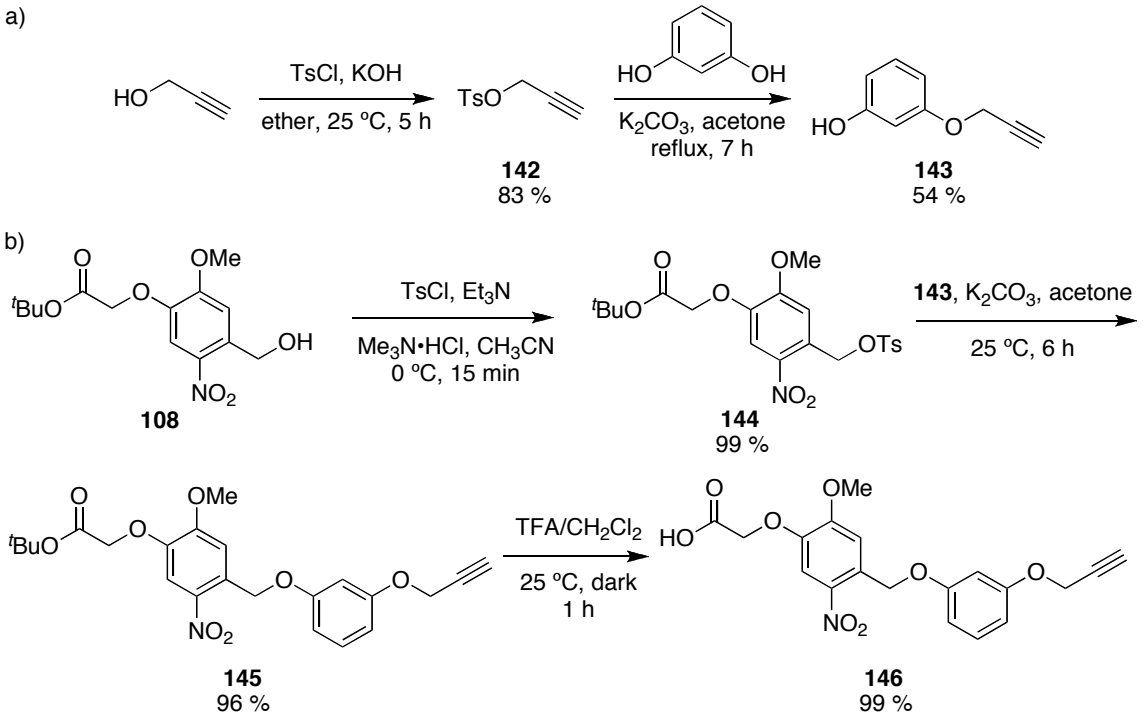

Photolinker **146** was attached on the solid-support (CPG; 0.097 mmol/g) *via* DIC coupling. After the reaction, ninhydrin test of compound **147** gave a positive result (purple beads). Those beads were then capped using normal conditions (Ac_2O, pyridine, CH_2Cl_2) and the ninhydrin test gave a negative result (brown beads). The alkyne **147** was then cyclized with BODIPY **137** *via* click reaction to afford compound **148** as

orange beads (Scheme 4.21). These beads showed a strong yellow-green fluorescence in organic solvents (DMF, THF, MeOH and CH_2Cl_2) and aqueous solution.

Scheme 4.21. Synthesis of solid-support photolinker with BODIPY **148**.

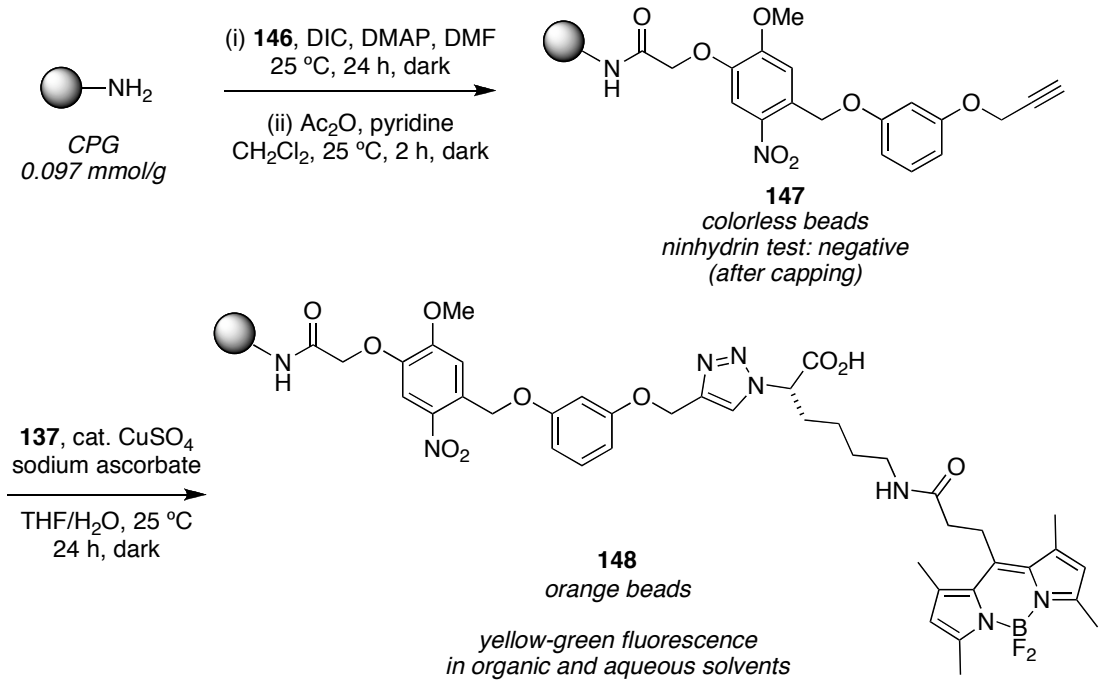

Several different conditions (EDCI in pH 7.4, NHS with DIC in DMF, iso-butylchloroformate with Et_3N in CH_2Cl_2) for the activation of the carboxylic acid of ether system (**148**) were attempted to study its stability. However, a strong yellow-green fluorescent solution was immediately observed in all cases after the addition of the reagents. Washing the beads with several organic and aqueous solvents many times before the activation reaction also gave a fluorescent solution. Therefore, the decomposition process does not involve the ester and ether bonds, and probably a more complicated mechanism is happening in the cleavage of the dye.

Although we knew some BODIPY's docomposed during the activation step, we tried to couple it with a small peptide (Figure 4.15) using EDCI activated molecule **148**. The molecular weight of the small peptide used was 1652 g/mol and this was easier to react

with the dyes on solid-support than the ubiquitin. After the photocleavage reaction, the sample was analyzed by Dr. Tichy using LCMS and MALDI, however, both experiments showed only a peptide peak (MW: 1652). No dye-peptide conjugates were observed in this study.

Lys-Pro-Val-Gly-Lys-Lys-Arg-Arg-Pro-Val-Lys-Val-Tyr-Pro

***small peptide*: MW 1652**

Figure 4.15. Amino acid sequence of small peptide used in this study.

Another synthesis was also attempted *via* Sonogashira coupling (Scheme 4.22). This idea is structurally more simple than the previous one. The alkyne **147** was directly coupled with 4-iodo-BODIPY **58** (*synthesis was described in Chapter 3.2.1*) to form compound **149**. The obtained beads had a slightly yellow-green fluorescence in organic solvents. The activation of the carboxylic acid in **149** (NHS with DIC in DMF, and *N,N'*-disuccinimidyl carbonate with 1-methylimidazole in CH_2Cl_2) led to similar results. As soon as we treated the beads with the chemicals, we obtained a strong yellow-green fluorescent solution.

Scheme 4.22. Synthesis of solid-support **149** via Sonogashira coupling.

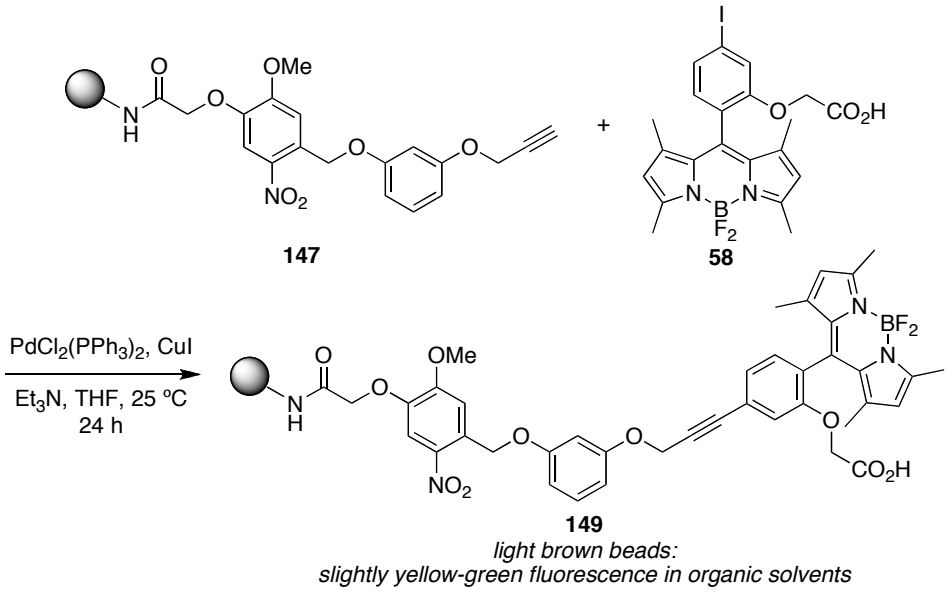

4.5 System D: Chemically Cleavable Linker, Azobenzene

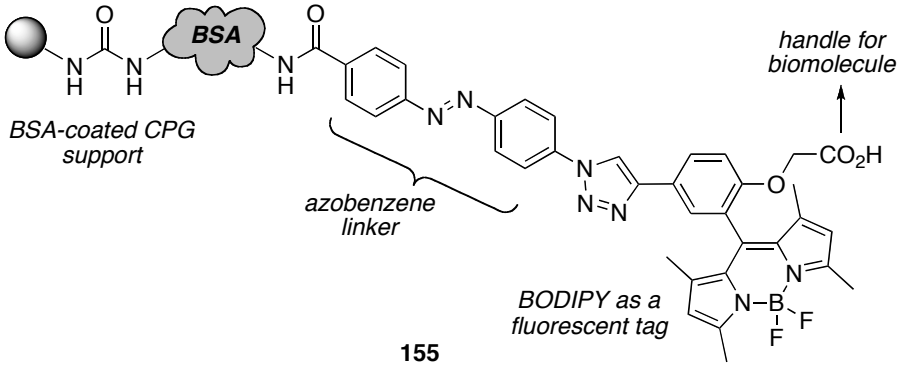

Figure 4.16. Azobenzene linker based solid-support (System D).

There are many chemically cleavable linkers, however, acids or bases are usually required for a cleavage and those systems are not suitable to biomolecules. As shown in section 4.1.3, Bogyo's azobenzene linker is cleaved under mild reaction conditions and this is biocompartible.[137] Thus, we used the linker **152** (previously synthesized by Mr. Jiney Jose and used for other research) to design the new solid-supported compound **155** (Figure 4.16) and studied its stability for the activation step. A carboxylic acid was attached on solid-support and an azide was cyclized with an ethynylated BODIPY dye.

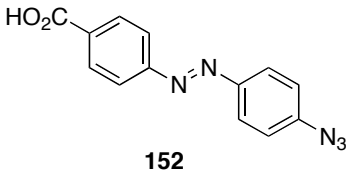

Scheme 4.23 illustrates the synthesis of BSA-coated CPG with a azobenzene linker (**154**). The amine-functionality of CPG (pore size: 500 Å) was activated with *N,N'*-disuccinimidyl carbonate followed by BSA coating to afford BSA-coated CPG **151**. The azobenzene compound **152** was then coupled with BSA-CPG **151** to give azide **153** as orange beads and the ninhydrin test of **153** gave negative (brown beads). Aspartic acids and glutamic acids of BSA were capped *via* the activation of acids with NHS followed by coupling with ethanolamine to afford product **154**.

Scheme 4.23. Synthesis of BSA-coated CPG with azolinker (**154**).

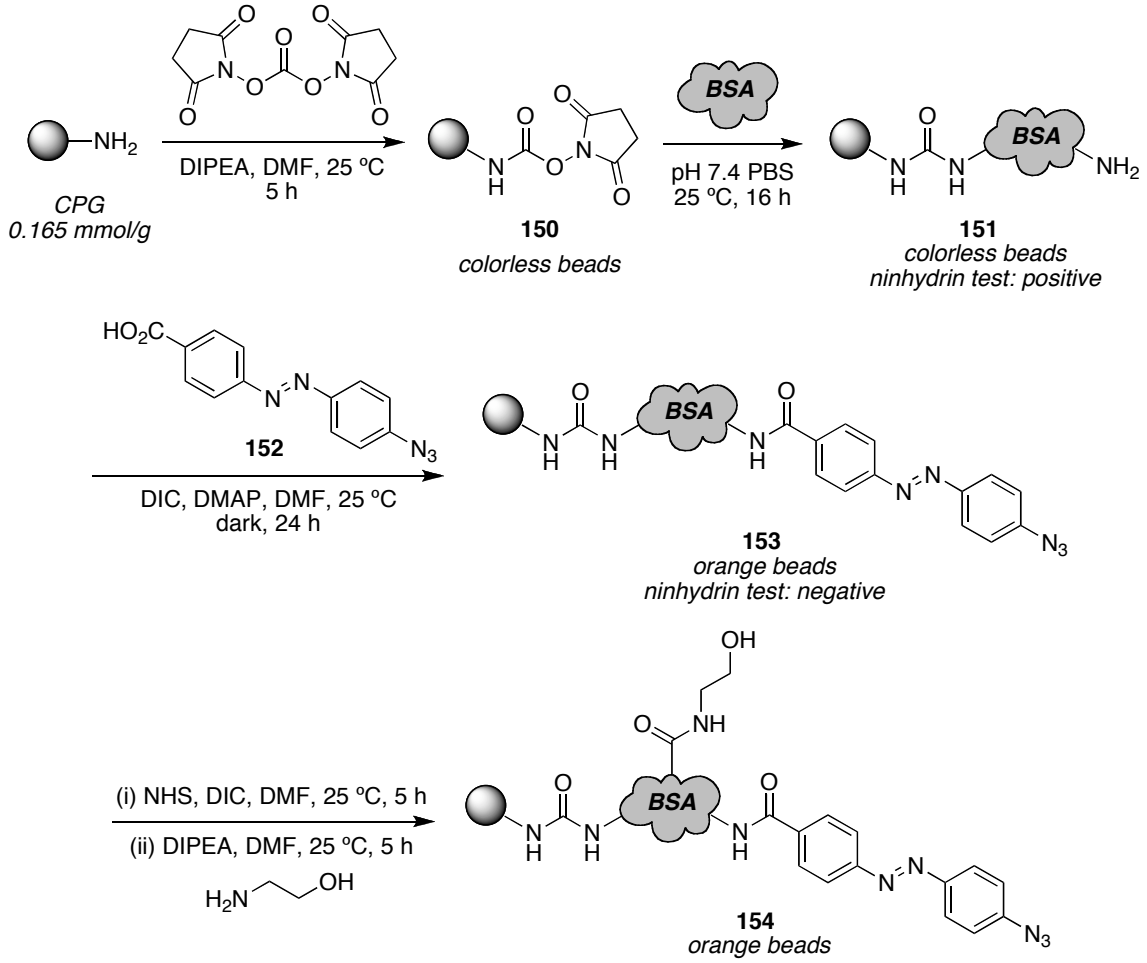

The compound **155** was synthesized from azide **154** and BODIPY derivative **63** (*synthesis was described in Chapter III, section 3.2.1*) *via* a 2+3 cycloaddition reaction (Scheme 4.24). These beads had a slightly yellow-green fluorescence in organic solvents (DMF, EtOH).

Scheme 4.24. Synthesis of BSA-coated azobenzene-linked BODIPY **155**.

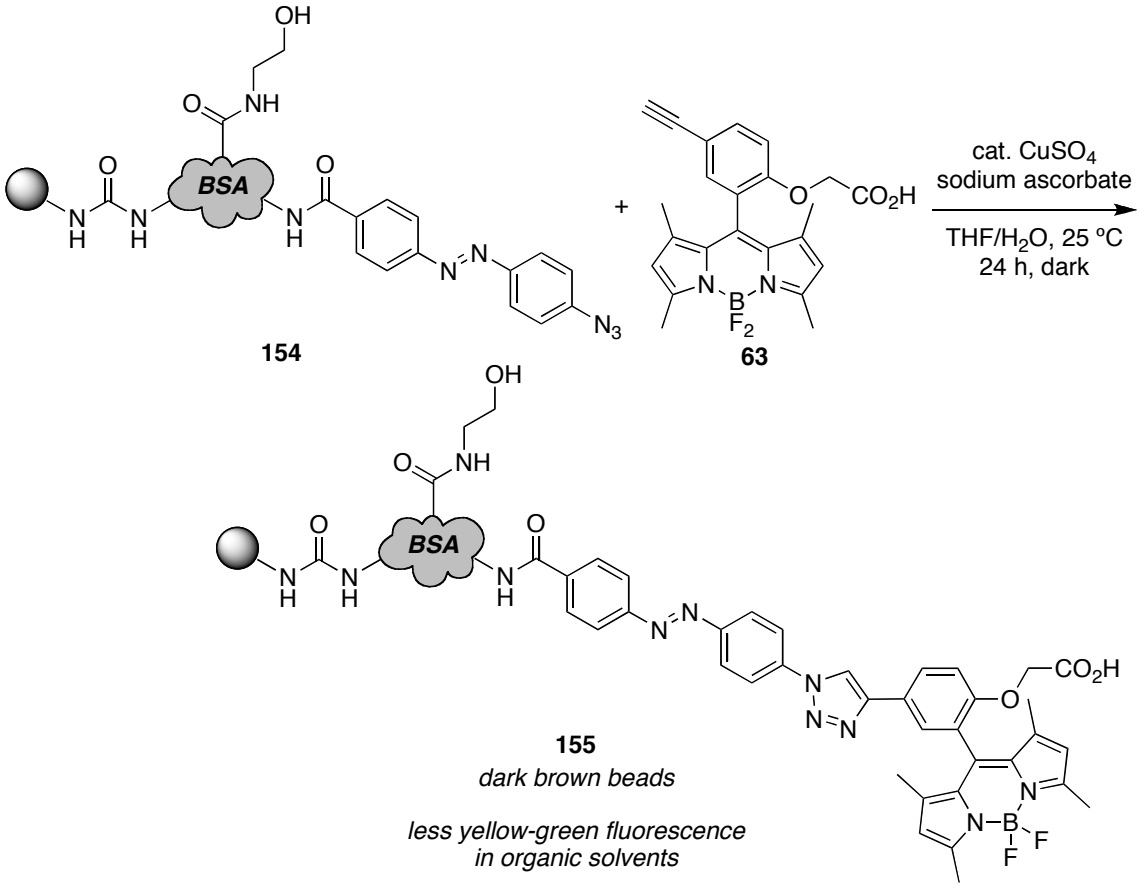

Next, two activation methods for the carboxylic acid of compound **155** were attempted. However, both the methods (NHS, DIC, DMF, 25 ºC or EDCI, pH 7.4 PBS, 25 ºC) led to the decomposition of the molecule again, because the starting colorless solution turned to a strong yellow-green fluorescent solution immediately after the addition of chemicals in both cases (Scheme 4.25). The decomposition process is not clear since there are no clevable bonds under those activating conditions.

Scheme 4.25. Activation of carboxylic acid for compound **155**.

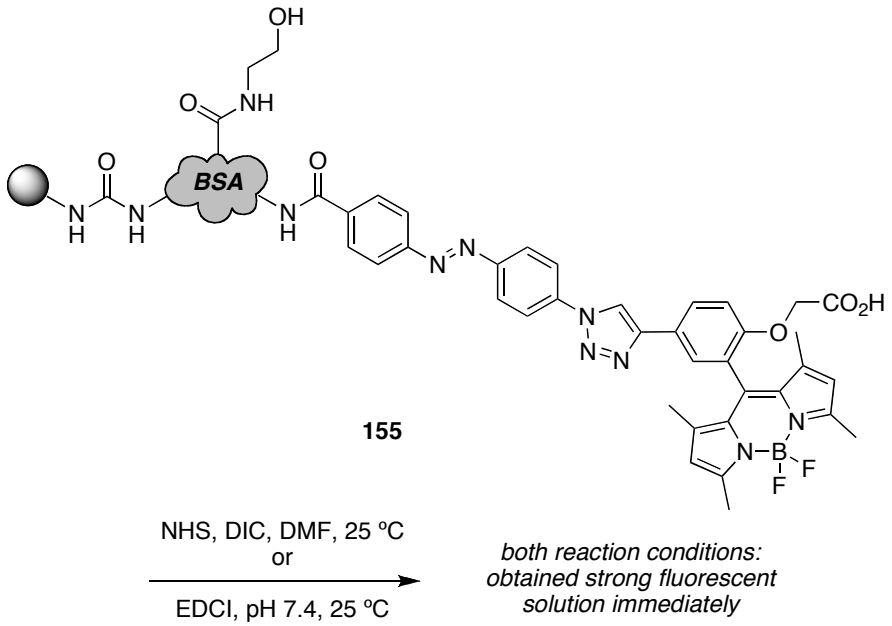

The non-BSA-coated CPG **157** was also synthesized to study how the reaction works without BSA (Scheme 4.26). The CPG (pore size; 500 Å) were directly coupled with the azo compound **152** followed by click chemistry with BODIPY **63** to afford compound **157** as reddish brown beads. Activation of the carboxylic acid using the same method as above (NHS, DIC or EDCI, pH 7.4) resulted in the decomposition of the molecule again (appearance of a strong yellow-green fluorescence in solution). On the other hand, the cleavage reaction of the azobenzene linker (**157**) was tried using 100 mM sodium dithionite (25 ºC, 12 h) to confirm whether the reaction work or not. However, the mass spectrometry analysis of the sample from this reaction did not detect compound **159**, but this could be because BODIPY **159** containing a free amine and a carboxylic acid is probably quite unstable. Moreover the obtained beads (**158**) were still reddish brown color and the ninhydrin test of these beads gave a negative result (brown bead) indicating that the reaction was not completed even after 12 h.

Scheme 4.26. Synthesis of solid-support azobenzene-linked BODIPY **157**.

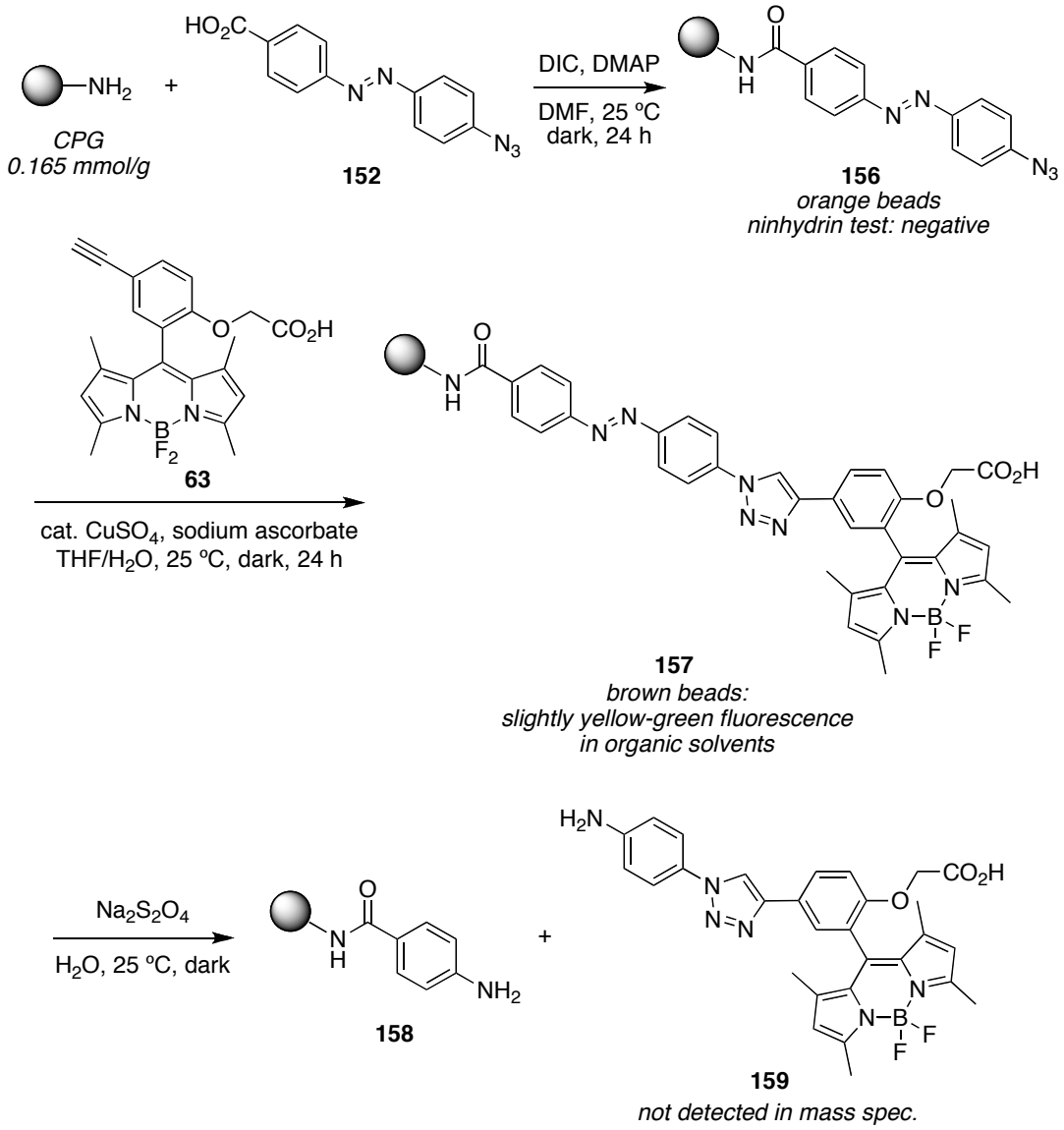

4.6 Summary for Each Approach and Reactions

Table 4.1 shows the summary for each compounds and reactions which we have attempted in this project.

Table 4.1. Summary of this project.

strategy	cpd.	solid-support	dye	cleavable-linker	protein[d]	results
1	**96**	PEGA	Nile Red	photo (ONB[a])	–	difficult to handle, swelling too much
2	**96**	CPG	Nile Red	″	–	decomposed during deprotection
3	**112**	″	BODIPY	photo (MNB[b])	–	photolysis was confirmed (solution-phase)
4	**117**	″	″	″	–	photolysis was confirmed (solid-phase)
5	**127**	″	Nile Red	″	Ubq	not detected by MALDI
6	**139**	BSA-CPG	BODIPY	″	Ubq	not detected by CE, MALDI and LCMS
7	**148**	CPG	″	″	small peptide	decomposition in activation step, not detected by MALDI and LCMS
8	**149**	″	″	″	–	decomposition in activation step
9	**155**	BSA-CPG	″	chemical[c]	–	decomposition in activation step
10	**157**	CPG	″	″	–	decomposition in activation step

a; *o*-nitrobenzyl, **b**; 5-methoxy-2-nitrobenzyl, **c**; azobenzene, and **d**; Ubq = ubiquitin.

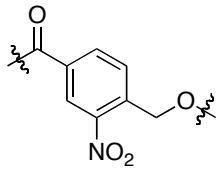

a: *o*-nitrobenzyl (ONB)

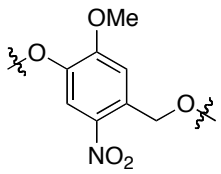

b: 5-methoxy-2-nitrobenzyl (MNB)

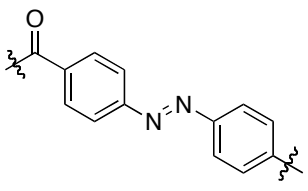

c: azobenzene

Strategy 1:

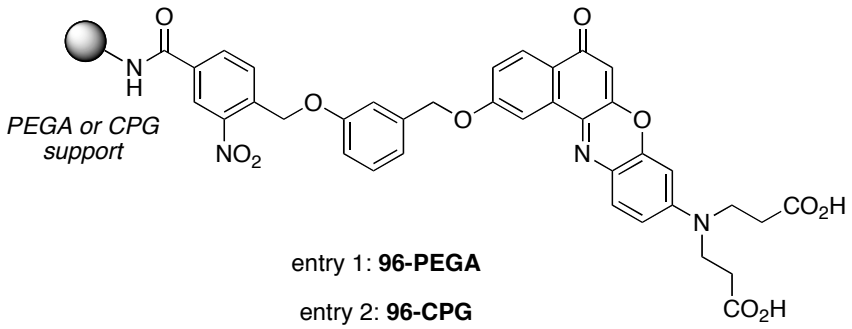

entry 1: **96-PEGA**

entry 2: **96-CPG**

Molecule **96** based on *o*-nitrobenzyl linker, Nile Red, and PEGA-support was synthesized, but PEGA resin swelled too much in these solvents and was difficult to handle due to its sticky nature. PEGA resin also has a limited accessibility for protein.

Strategy 2:

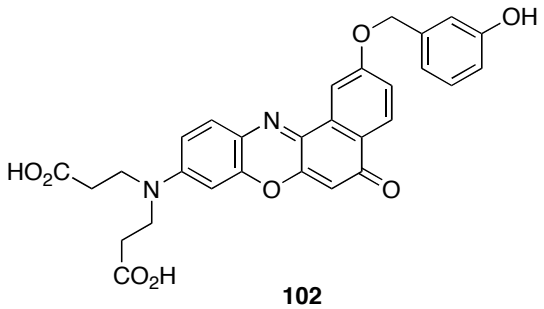

102
control compound

For compound **96** with CPG, decomposition occurred during the deprotection of the methyl ester with K_2CO_3 or TMSOK as indicated by the dramatic color change of the beads. Photolysis of **96** was performed and analyzed by HPLC to compare to its cleaved-product (control compound **102** which was made via solution-phase synthesis), however, the retention time for both samples did not match.

Strategy 3:

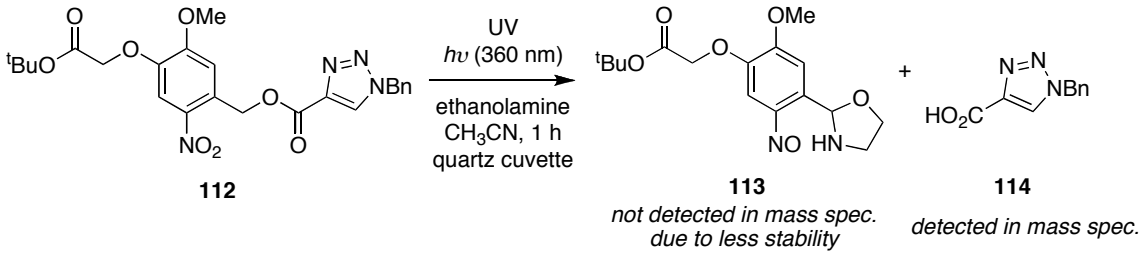

Model study for photolysis was performed in solution-phase. Compound **112** was irradiated under UV and the desired photo-cleaved product **114** was obtained and observed by mass spectrometry. We confirmed that the photolysis works.

Strategy 4:

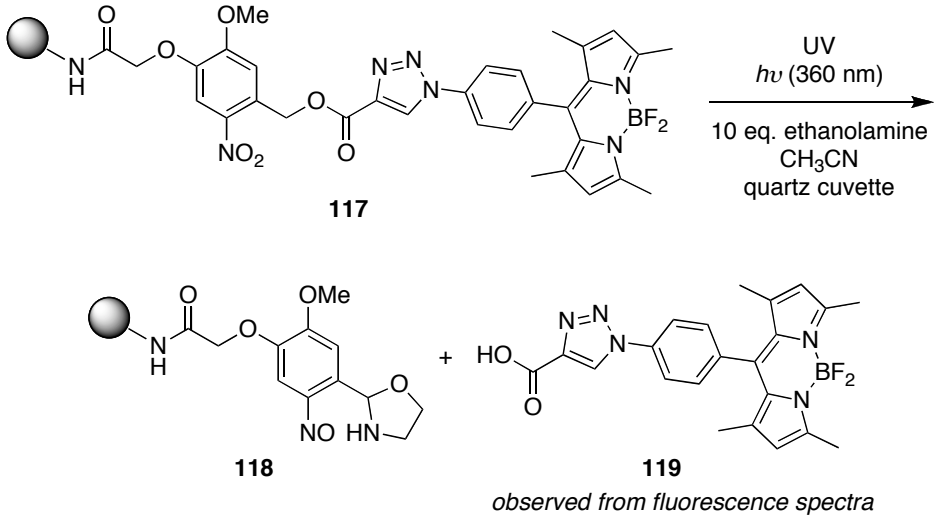

Model study for photolysis was performed in solid-phase. Compound **117** was irradiated under UV, and UV absorption and fluorescence emission spectra were recorded and these λ_{max} matched with those of parent BODIPY.

Strategy 5:

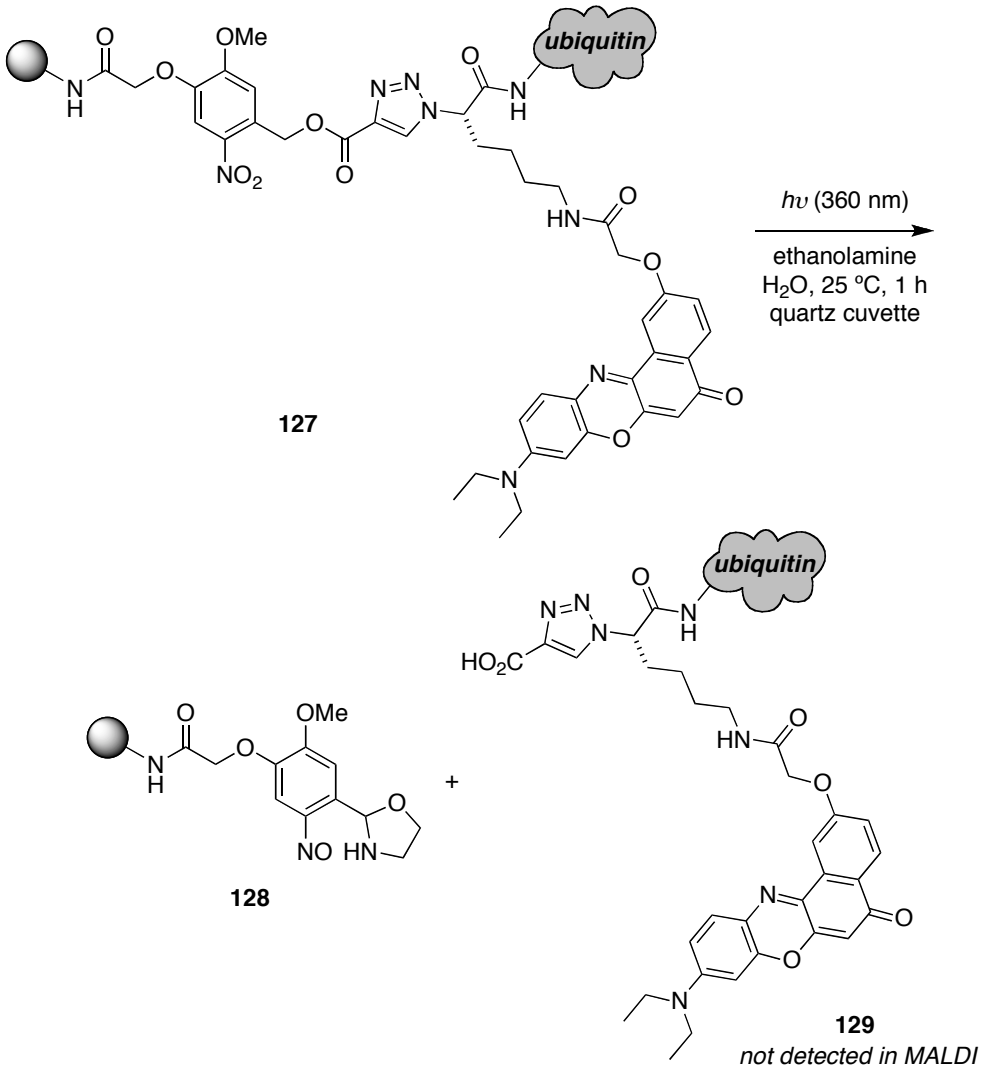

Compound **127** was photo-cleaved and the dye-protein conjugate **129** was analyzed by measuring UV and fluorescence spectra. However, we did not see a peak at 280 nm which is a characteristic peak of protein.

Strategy 6:

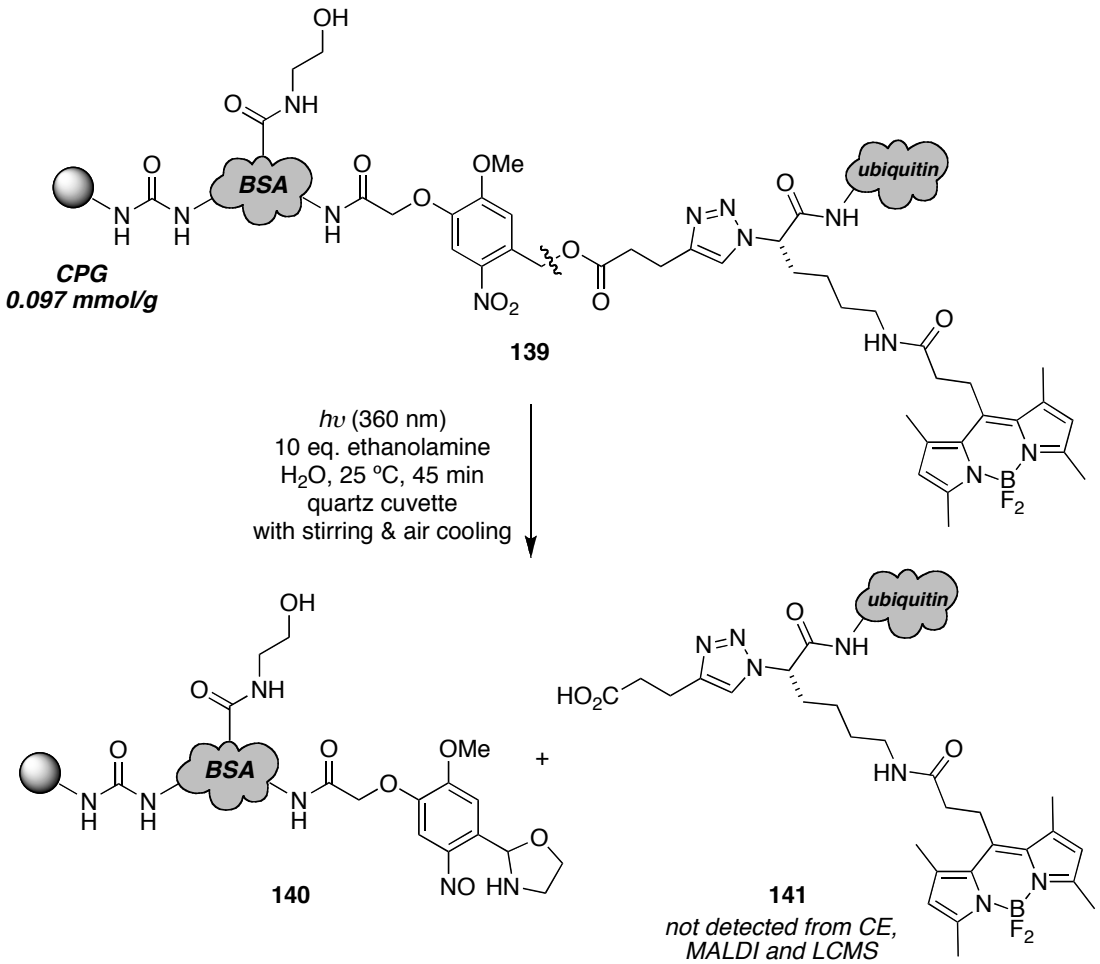

Photolysis of dye-protein conjugate **139** was performed and the sample was analyzed by CE, MALDI, and LCMS. Products from CE analysis could not be easily assigned because the presence of ethanolamine affected the mobility of the compounds. For MALDI and LCMS analyses of compound **141**, only a peak at 8570 Da (corresponding to the MW of native ubiquitin) was observed. No dye-protein conjugates were detected from these analyses.

Strategy 7:

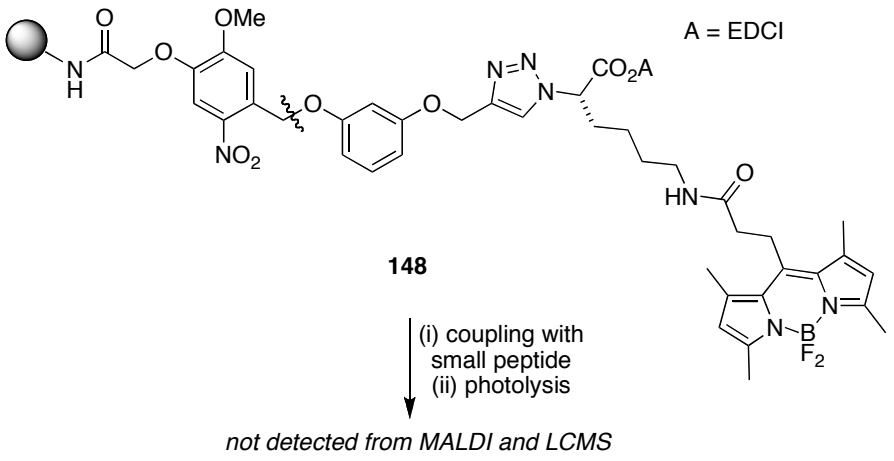

Compound **148** was activated and coupled with a small peptide. The sample from the photolysis was analyzed by MALDI and LCMS, however, we obtained only a small peptide with MW of 1652. There was no dye-peptide conjugate in the sample.

Strategy 8:

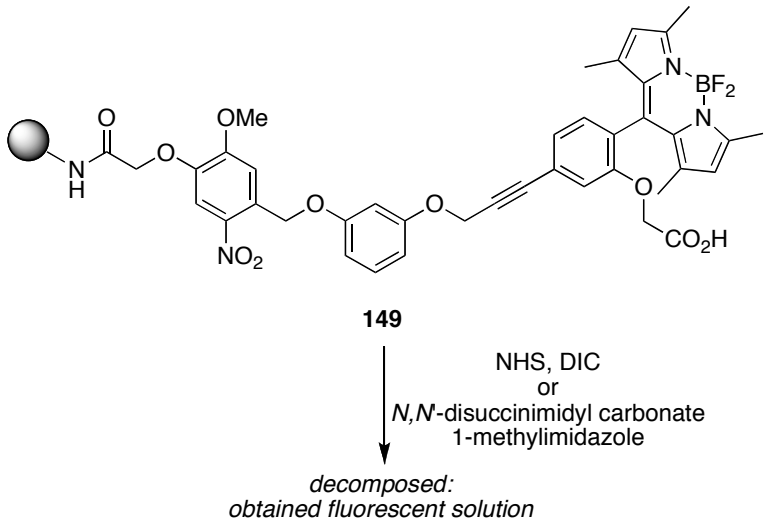

The activation of compound **149** led to the decomposition of the molecule: rapid appearance of a strong yellow-green fluorescence in solution after the addition of the reagents.

Strategy 9:

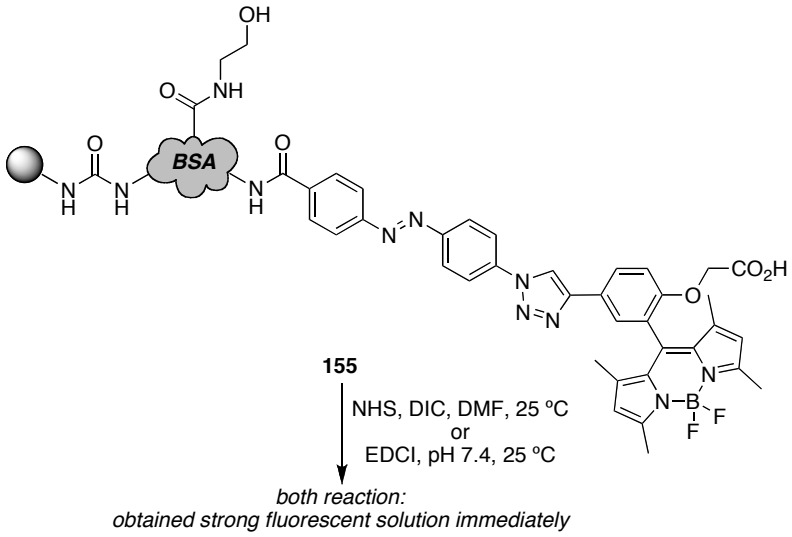

Chemically cleavable linker, azobenzene, was used for compound **155** (based on BSA-CPG). Again a strong yellow-green fluorescent solution was obtained after the addition of the reagents.

Strategy 10:

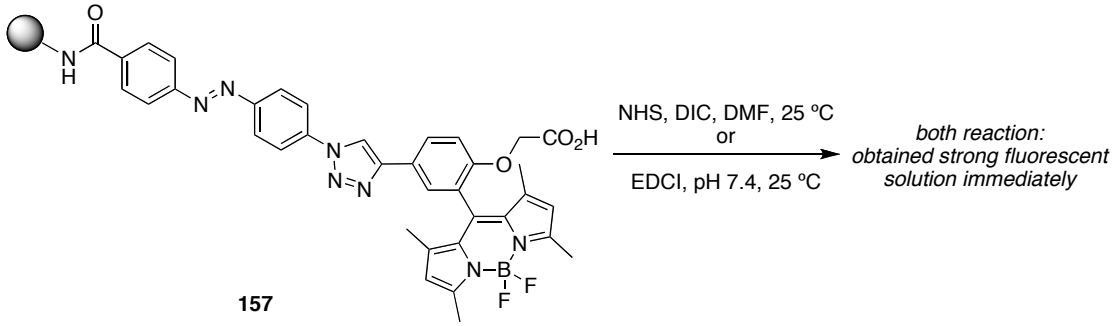

Chemically cleavable linker, azobenzene, was used for compound **157** (based on CPG). In the activation step of the carboxylic acid, a strong yellow-green fluorescent solution was immediately obtained after the addition of the chemicals. The cleavage of azobenzene linker was also performed using sodium dithionite, but the cleaved product **159** was not detected in mass spectrometry.

4.7 Conclusion

There are two possible explanations for the decomposition process. First, the photolinker may not be stable even when the reactions are carried out in dark. Chemically cleavable linkers can be used instead of photolabile linker, but cleavage conditions must be mild to prevent protein damage. A chemically cleavable linker, azobenzene derivative, was used for this study because it is cleaved under mild reaction condition. Nevertheless, we obtained a strong yellow-green fluorescent solution during the activation of carboxylic acid and also did not confirm the cleavage of azobenzene linker with 100 mM sodium dithionite (25 ºC, 12 h) by mass spectrometry. Second, the dye must be carefully chosen. It is very important that the dye used be stable under strong acid or basic conditions. The BODIPY dye chosen in these studies might have been a poor choice as it is known that the BF_2 group can fall off under strong basic conditions. Furthermore, the high energy irradiation (360 nm) required to cleave off the photolinker, could also damage the protein or the dye. Therefore, other chemically and photostable dyes such as halogenated-fluorescein or rhodamine derivatives may be a better choice for this project.

For the dye-protein conjugation on solid-phase, the coupling reaction between large beads and biomolecules may not be efficient. Thus further screening for different size of beads will be required, *e.g.* the use of smaller CPGs. Second, we selected the amide-coupling between carboxylic acid on bead (succinimidyl ester) and amine-group (from lysine) of protein to make dye-protein conjugates. Succinimidyl esters are not stable in basic media, *i.e.* they do not survive for a long time. In this solid-phase synthesis, the succinimidyl ester was on the bead and its stability might have been less than that of one in solution-phase synthesis. If this succinimidyl ester was decomposed before coupling with protein, then no dye-protein conjugates will be formed. In fact, this might occur in the coupling stage between the dye on solid-support and ubiquitin (Ubq) because only Ubq was observed after photolysis instead of any dye-protein conjugates, or dye-peptide conjugates from MALDI and LCMS analyses. However, the reason why we obtained Ubq is not clear since excess Ubq was washed away in the previous stage (coupling

between Ubq and dye on resin). A plausible reason for this is that Ubq was stuck on the beads without forming amide bond. Instead of amide-coupling, click reaction might be a good idea, and this 2+3 cycloaddition is usually efficient in solution and solid-phase. The insertion of azido or alkyne functionality onto beads is easy, however, the problem is the functionalization of native protein surface. There is literature for the insertion of alkyne-functionality into recombinant protein, and this was successfully cyclized with azido-coumarin.[10] Therefore if the functionalization of protein surface is achieved, then this could produce more efficient strategy for coupling reaction in solid-phase synthesis.

CHAPTER V

CONCLUSIONS AND OUTLOOK

5.1 Water-soluble Fluorescent Probes

We synthesized regioisomerically pure 5- and 6-carboxyfluorescein **3a** and **3b** *via* fractional crystallization (*MeOH/hexanes* or *EtOH/hexanes* system) on multi-gram scale (Figure 5.1). This method is very convenient because no expensive chemicals are required and it produces both isomers in high purity (>98 %). In fact, both commercial samples are expensive. Dyes **3a** and **3b** cannot be directly used to synthesize TBET cassette but they are very useful to couple to proteins. Their derivatives, 5- and 6-bromofluorescein which were previously synthesized in our lab, are used for cassettes synthesis.[38]

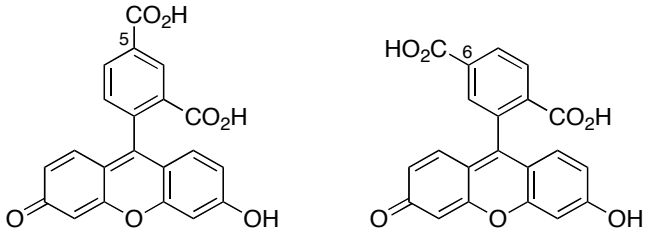

3a *5-carboxyfluorescein* **3b** *6-carboxyfluorescein*

Figure 5.1. 5- and 6-Carboxyfluorescein **3**.

Water-soluble BODIPY derivative **23** and dye-protein conjugate **23-BSA** were synthesized and their photophysical properties in aqueous medium were studied. As shown in Figure 5.2, dye **23** and its dye-protein conjugate **23-BSA** had quantum yields (0.74 and 0.44) in pH 7.4 phosphate buffer. Further functionalization of chlorine on dye **23** was tested via nucleophilic attack of taurine. However the reaction was not

completed and resulted in difficult purification due to the high porality of dye **23**. Fluorescent probe **23** has excellent photophysical properties at physiological pH.

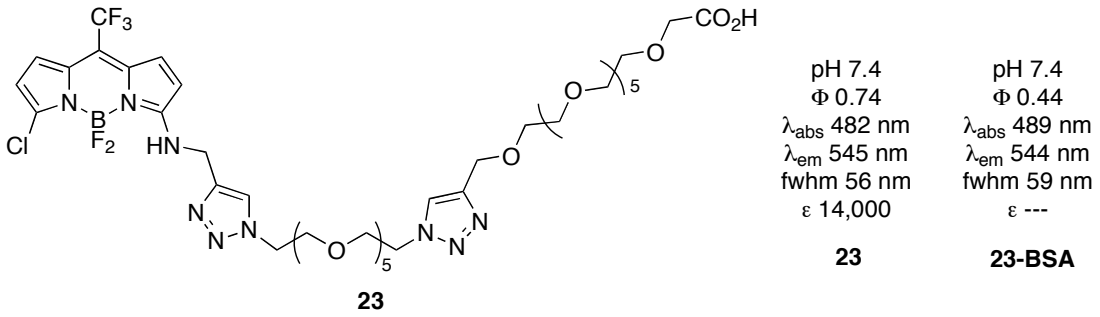

Figure 5.2. Photophysical properties of water-soluble BODIPY derivative **23** and its dye-BSA conjugate **23-BSA**.

Water-soluble Nile Blues **30a,b** and **31a,b** were synthesized and their quantum yields were improved in aqueous medium compared to the reported Nile Blues **28** and **29** (Figure 5.3). Dyes **30** and **31** were synthesized via condensation reaction (DMF, 90 ºC) that do not require additional acids or very harsh conditions. Further functionalization of **30** and **31** is possible *e.g.* via triflation of the 2-hydroxy substituent and organometallic cross-coupling. All the dyes showed little tendency to aggregate below 4 μM, this property is useful when biological studies are performed in dilute conditions. Moreover, dyes **30** and **31** have relatively long emission wavelengths (670-680 nm) and therefore these dyes are suitable probes for tissue and intracellular imaging.

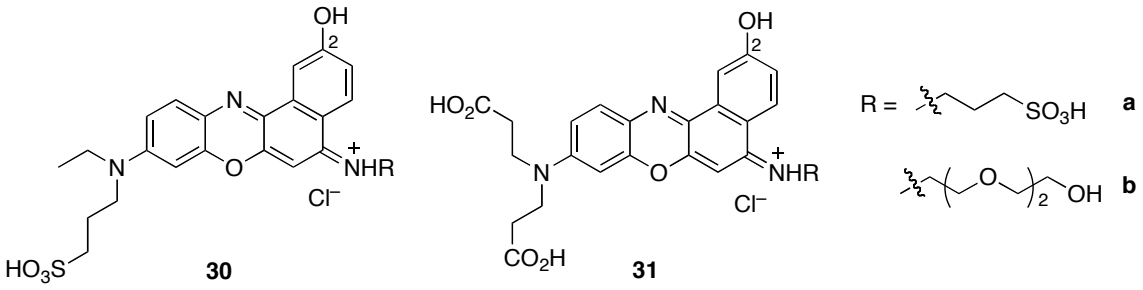

Figure 5.3. Water-soluble Nile Blue derivatives **30** and **31**.

5.2 Through-bond Energy Transfer Cassettes

Three novel iodo-cyanine dyes **74a-c** were synthesized as acceptor fragments for synthesizing TBET cassettes. Syntheses of these dyes are relatively straightforward via two steps condensation. All cyanine dyes had well-distinguished absorption and emission maxima (*ca.* 100 nm). We synthesized a series of TBET cassettes **75a-c** (26-45 % yields) from the corresponding iodo-cyanine dyes **74a-c** and 4-Ethynyl BODIPY *via* Sonogashira coupling (Figure 5.4). The fluorescence emission maxima of these cassettes were extremely well-separated in EtOH by approximately 100 nm and this is very useful for multiplexing study in cellular imaging.

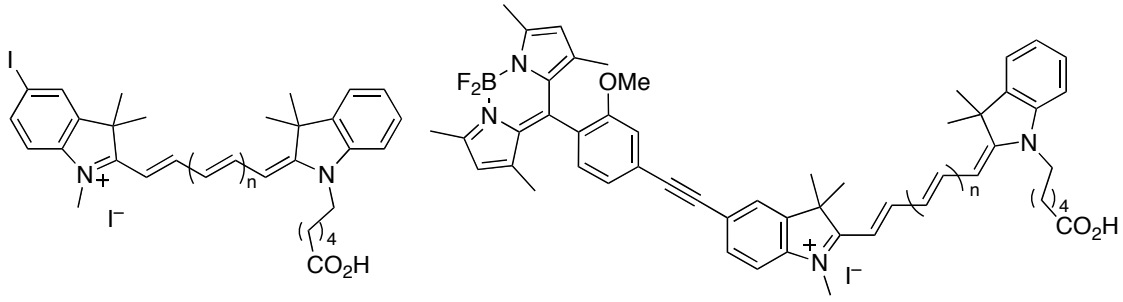

n = 0; **74a**, 1; **74b**, 2; **74c** n = 0; **75a**, 1; **75b**, 2; **75c**

Figure 5.4. Iodo-cyanine series **74a-c**, and novel TBET cassettes **75a-c**.

We are particularly interested in incorporating these cassettes into silica or calcium phosphate (CP) nanoparticles to improve their photostabilities and solubilities in aqueous media. These three cassettes were coated with silica via covalent bonding or calcium phosphate by non-covalent bonding, and the corresponding both nanoparticles were water soluble. The cassettes doped nanoparticles had moderate ETE (about 85 %) with low quantum yields in aqueous media. Further the formation of silica and CP nanoparticles were confirmed by TEM and AFM images, respectively. Their photostabilities are being studied by Dr. Son's group and we will also work multiplexing in intracellular imaging in future.

5.3 Solid-phase Approach Towards Protein Mono-labeling

Different designs (surmmarized in Table 4.1 in Chapter IV) for protein mono-labeling were prepared on various solid supports, but no dye-protein conjugates could be detected after photolysis by CE, MALDI, and LCMS. There are some plausible reasons for this; (i) lower reactivity between large beads and biomolecules, (ii) stability of the photolabile linker, and (iii) stability of the succinimidyl ester on solid-support. As described in Chapter IV, succinimidyl esters are not very stable under basic conditions, and different coupling strategies must be envisaged *i.e.* click reaction.

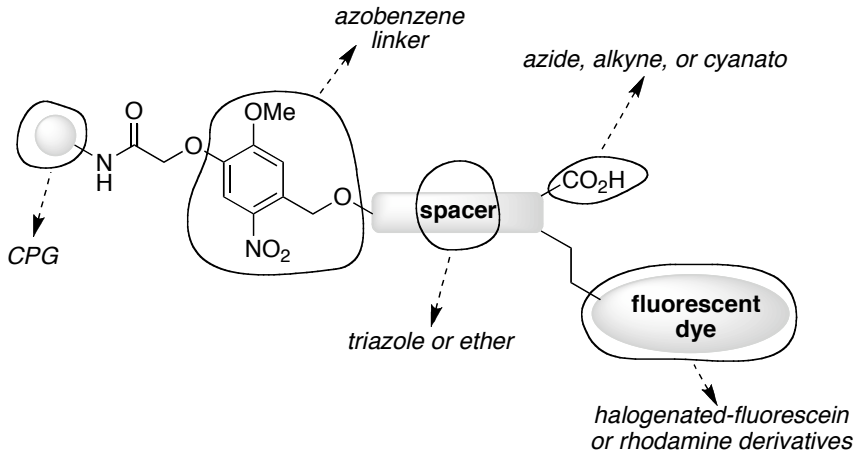

Figure 5.5. Alternative design for this project.

Figure 5.5 illustrates an alternative design for this project. Each fragments will be replaced with other functional groups or compounds as shown in Figure 5.5. The use of chemically cleavable linker instead of photolabile one is preferred to perform this research because irradiation at 360 nm may cause damage to protein and fluorophores. Azobenzene linker which can be cleaved under mild condition,[137] was one of the first chemically cleavable linkers investigated by us in this project. However, we did not detect the cleaved products when 100 mM sodium dithionite was used. This reaction has only been done once, thus further exploration of reaction condition *e.g.* increasing

concentration of sodium dithionite and reaction time, will be necessary to optimize cleavage condition. For the fluorescent dye part, halogenated-fluorescein or rhodamine dyes will be more suitable because they are much more photo- and chemically stable than BODIPY. Finally, coupling to the biomolecules could be done via click chemistry. This could solve some of the problems we encountered during the activation step of carboxylic acid. However, the handle for attachment of biomolecules would have to be replaced with an azide or alkyne and this might be difficult to do.

Without modification of the protein surface, Tan and co-worker's method may be an other good idea.[153] They modified the surface of silica nanoparticles using cyanogen bromide (CNBr) to form a cyanato-group. This was then coupled with antibody to afford antibody immobilized silica nanoparticle (Figure 5.6). There are big advantages in this method; (i) it is not necessary to isolate a compound activated with cyanato-group, (ii) short activating reaction time, and (iii) possibility to add biomolecules directly into the solution containing activated materials. These issues make it more efficient bioconjugations and this could be an alternative method to our project.

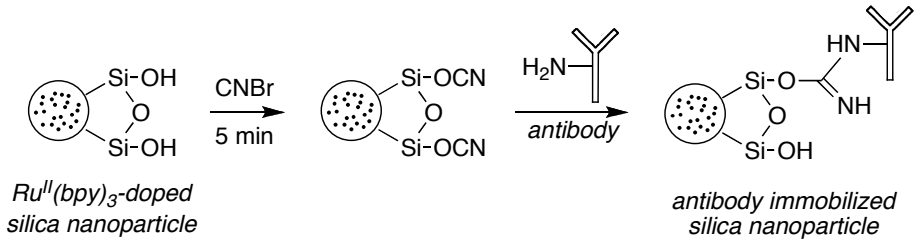

Figure 5.6. Antibody immobilization process onto the luminophore-doped silica nanoparticle's surface.

REFERENCES

(1) Lakowicz, J. R. *Principles of Fluorescence Spectroscopy*; 3rd ed.; Springer: New York, 2006.

(2) Förster, T. *Naturwissenschaften* **1946**, *6*, 166-175.

(3) Wagner, R. W.; Lindsey, J. S. *J. Am. Chem. Soc.* **1994**, *116*, 9759-60.

(4) Lang, P.; Yeow, K.; Nichols, A.; Scheer, A. *Nat. Rev. Drug Discovery* **2006**, *5*, 343-356.

(5) Ju, J.; Glazer, A. N.; Mathies, R. A. *Nature Med.* **1996**, *2*, 246-9.

(6) Metzker, M. L.; Lu, J.; Gibbs, R. A. *Science* **1996**, *271*, 1420-2.

(7) Griffin, B. A.; Adams, S. R.; Tsien, R. Y. *Science* **1998**, *281*, 269-272.

(8) Cao, H.; Xiong, Y.; Wang, T.; Chen, B.; Squier, T. C.; Mayer, M. U. *J. Am. Chem. Soc.* **2007**, *129*, 8672-8673.

(9) Girouard, S.; Houle, M.-H.; Grandbois, A.; Keillor, J. W.; Michnick, S. W. *J. Am. Chem. Soc.* **2005**, *127*, 559-566.

(10) Beatty, K. E.; Xie, F.; Wang, Q.; Tirrell, D. A. *J. Am. Chem. Soc.* **2005**, *127*, 14150-14151.

(11) Hooker, J. M.; Esser-Kahn, A. P.; Francis, M. B. *J. Am. Chem. Soc.* **2006**, *128*, 15558-15559.

(12) Brustad, E. M.; Lemke, E. A.; Schultz, P. G.; Deniz, A. A. *J. Am. Chem. Soc.* **2008**, *130*, 17664-17665.

(13) Panchuk-Voloshina, N.; Haugland, R. P.; Bishop-Stewart, J.; Bhalgat, M. K.; Millard, P. J.; Mao, F.; Leung, W.-Y.; Haugland, R. P. *J. Histochem. Cytochem.* **1999**, *47*, 1179-1188.

(14) Baeyer, A. v. *Chem. Ber.* **1871**, *5*, 255.

(15) Sun, W.-C.; Gee, K. R.; Klaubert, D. H.; Haugland, R. P. *J. Org. Chem* **1997**, *62*, 6469-75.

(16) Chapple, M. R.; Johnson, G. D.; Davidson, R. S. *J Microsc* **1990**, *159*, 245-53.

(17) Chen, R. F.; Knutson, J. R. *Anal Biochem* **1988**, *172*, 61-77.

(18) Walkup, G. K.; Burdette, S. C.; Lippard, S. J.; Tsien, R. Y. *J. Am. Chem. Soc.* **2000**, *122*, 5644-5.

(19) Tomat, E.; Nolan, E. M.; Jaworski, J.; Lippard, S. J. *J. Am. Chem. Soc.* **2008**, *130*, 15776-15777.

(20) Song, F.; Garner, A. L.; Koide, K. *J. Am. Chem. Soc.* **2007**, *129*, 12354-12355.

(21) Song, F.; Watanabe, S.; Floreancig, P. E.; Koide, K. *J. Am. Chem. Soc.* **2008**, *130*, 16460-16461.

(22) Sparano, B. A.; Shahi, S. P.; Koide, K. *Org. Lett.* **2004**, *6*, 1947-1949.

(23) Sparano, S.; Koide, K. *J. Am. Chem Soc.* **2005**, *127*, 14954-55.

(24) Sparano, B. A.; Koide, K. *J. Am. Chem. Soc.* **2007**, *129*, 4785-4794.

(25) Urano, Y.; Kamiya, M.; Kanda, K.; Ueno, T.; Hirose, K.; Nagano, T. *J. Am. Chem. Soc.* **2005**, *127*, 4888-4894.

(26) Mottram, L. F.; Boonyarattanakalin, S.; Kovel, R. E.; Peterson, B. R. *Org. Lett.* **2006**, *8*, 581-584.

(27) Keppler, A.; Pick, H.; Arrivoli, C.; Vogel, H.; Johnsson, K. *Proc. Nat. Acad. Sci. U.S.A.* **2004**, *101*, 9955-9959.

(28) Mottram, L. F.; Maddox, E.; Schwab, M.; Beaufils, F.; Peterson, B. R. *Org. Lett.* **2007**, *9*, 3741-3744.

(29) Onoue, S.; Liu, B.; Nemoto, Y.; Hirose, M.; Yajima, T. *Anal. Sci.* **2006**, *22*, 1531-1535.

(30) Genin, E.; Carion, O.; Mahler, B.; Dubertret, B.; Arhel, N.; Charneau, P.; Doris, E.; Mioskowski, C. *J. Am. Chem. Soc.* **2008**, *130*, 8596-8597.

(31) Thorn, K. S.; Naber, N.; Matuska, M.; Vale, R. D.; Cooke, R. *Protein Sci.* **2000**, *9*, 213-217.

(32) Orndorff, W. R.; Hemmer, A. J. *J. Am. Chem. Soc.* **1927**, *49*, 1272-1280.

(33) Adamczyk, M.; Fishpaugh, J. R.; Heuser, K. J. *Bioconjugate Chem.* **1997**, *8*, 253-5.

(34) Adamczyk, M.; Chan, C. M.; Fino, J. R.; Mattingly, P. G. *J. Org. Chem.* **2000**, *65*, 596-601.

(35) Fischer, R.; Mader, O.; Jung, G.; Brock, R. *Bioconjugate Chem.* **2003**, *14*, 653-660.

(36) Ueno, Y.; Jiao, G.-S.; Burgess, K. *Synthesis* **2004**, 2591-2593.

(37) Lyttle, M. H.; Carter, T. G.; Cook, R. M. *Org. Process Res. Dev.* **2001**, *5*, 45-9.

(38) Jiao, G.-S.; Han, J. W.; Burgess, K. *J. Org. Chem.* **2003**, *68*, 8264-7.

(39) Rossi, F. M.; Kao, J. P. Y. *Bioconjugate Chem.* **1997**, *8*, 495-7.

(40) Karolin, J.; Johansson, L. B. A.; Strandberg, L.; Ny, T. *J. Am. Chem. Soc.* **1994**, *116*, 7801-6.

(41) Haugland, R. P. *Handbook of Fluorescent Probes and Research Chemicals*; 6th ed.; Molecular Probes: Eugene, OR, 1996.

(42) Wagner, R. W.; Lindsey, J. S. *Pure Appl. Chem.* **1996**, *68*, 1373-80.

(43) Tan, K.; Jaquinod, L.; Paolesse, R.; Nardis, S.; Di Natale, C.; Di Carlo, A.; Prodi, L.; Montalti, M.; Zaccheroni, N.; Smith, K. M. *Tetrahedron* **2004**, *60*, 1099-1106.

(44) Yee, M.-c.; Fas, S. C.; Stohlmeyer, M. M.; Wandless, T. J.; Cimprich, K. A. *J. Biol. Chem.* **2005**, *280*, 29053-29059.

(45) Metzker, M. L. Substituted 4,4-Difluoro-4-bora-3a,4a-diaza-*s*-indacene Compounds for 8-Color DNA Sequencing. WO Patent 2003066812, August 14, 2003.

(46) McDonnell, S. O.; O'Shea, D. F. *Org. Lett.* **2006**, *8*, 3493-3496.

(47) Ueno, T.; Urano, Y.; Kojima, H.; Nagano, T. *J. Am. Chem. Soc.* **2006**, *128*, 10640-10641.

(48) Ulrich, G.; Goeb, S.; De Nicola, A.; Retailleau, P.; Ziessel, R. *Synlett* **2007**, 1517-1520.

(49) Umezawa, K.; Nakamura, Y.; Makino, H.; Citterio, D.; Suzuki, K. *J. Am. Chem. Soc.* **2008**, *130*, 1550-1551.

(50) Loudet, A.; Burgess, K. *Chem. Rev.* **2007**, *107*, 4891-4932.

(51) Wu, L.; Burgess, K. *J. Am. Chem. Soc.* **2008**, *130*, 4089-4096.

(52) Li, L.; Han, J.; Nguyen, B.; Burgess, K. *J. Org. Chem.* **2008**, *73*, 1963-1970.

(53) Han, J.; Gonzalez, O.; Aguilar-Aguilar, A.; Pena-Cabrera, E.; Burgess, K. *Org. Biomol. Chem.* **2009**, *7*, 34-36.

(54) Baruah, M.; Qin, W.; Vallee, R. A. L.; Beljonne, D.; Rohand, T.; Dehaen, W.; Boens, N. *Org. Lett.* **2005**, *7*, 4377-4380.

(55) Rohand, T.; Baruah, M.; Qin, W.; Boens, N.; Dehaen, W. *Chem. Commun.* **2006**, 266-8.

(56) Rohand, T.; Qin, W.; Boens, N.; Dehaen, W. *Eur. J. Org. Chem.* **2006**, 4658-4663.

(57) Li, L.; Nguyen, B.; Burgess, K. *Bioorg. Med. Chem. Lett.* **2008**, *18*, 3112-3116.

(58) Loiseau, F. A.; Hii, K. K.; Hill, A. M. *J. Org. Chem.* **2004**, *69*, 639-647.

(59) Lu, G.; Lam, S.; Burgess, K. *Chem. Commun.* **2006**, 1652-54.

(60) Yoshida, Y.; Sakakura, Y.; Aso, N.; Okada, S.; Tanabe, Y. *Tetrahedron* **1999**, *55*, 2183-2192.

(61) Molecular Probes; http://probes.invitrogen.com. Invitrogen Corporation: Eugene, OR, 2006.

(62) Melhuish, W. H. *J. Phys. Chem.* **1960**, *64*, 762-4.

(63) Williams, A. T. R.; Winfield, S. A.; Miller, J. N. *Analyst* **1983**, *108*, 1067-71.

(64) Mohlau, R.; Uhlmann, K. *Justus Liebigs Ann. Chem.* **1896**, *289*, 94-128.

(65) Wichmann, C. F.; Liesch, J. M.; Schwartz, R. E. *J. Antibiot.* **1989**, *42*, 168-73.

(66) Briggs, M. S. J.; Bruce, I.; Miller, J. N.; Moody, C. J.; Simmonds, A. C.; Swann, E. *J. Chem. Soc., Perkin Trans. 1* **1997**, *7*, 1051-1058.

(67) Simmonds, A.; Miller, J. N.; Moody, C. J.; Swann, E.; Briggs, M. S. J.; Bruce, I. E. Benzophenoxazine Dyes. WO Patent 9729154, August 14, 1997.

(68) Jose, J.; Burgess, K. *J. Org. Chem.* **2006**, *71*, 7835-7839.

(69) Jose, J.; Burgess, K. *Tetrahedron* **2006**, *62*, 11021-11037.

(70) Lee, S. H.; Suh, J. K.; Li, M. *Bull. Korean Chem. Soc.* **2003**, *24*, 45-48.

(71) Das, K.; Jain, B.; Patel, H. S. *Spectrochim. Acta, Part A* **2004**, *60A*, 2059-2064.

(72) Krihak, M.; Murtagh, M. T.; Shahriari, M. R. *J. Sol-Gel Sci. Technol.* **1997**, *10*, 153-163.

(73) Maliwal, B. P.; Kusba, J.; Lakowicz, J. R. *Biopolymers* **1995**, *35*, 245-255.

(74) Lakowicz, J. R.; Piszczek, G.; Kang, J. S. *Anal. Biochem.* **2001**, *288*, 62-75.

(75) Nikas, D. C.; Foley, J. W.; Black, P. M. *Lasers Surg. Med.* **2001**, *29*, 11-7.

(76) Lin, C. W.; Shulok, J. R.; Wong, Y. K.; Schanbacher, C. F.; Cincotta, L.; Foley, J. W. *Cancer Research* **1991**, *51*, 1109-16.

(77) Lin, C.-W.; Shulok, J. R. *Photochem. Photobiol.* **1994**, *60*, 143-6.

(78) Juzeniene, A.; Peng, Q.; Moan, J. *Photochem. Photobiol. Sci.* **2007**, *6*, 1234-1245.

(79) Ho, N.-h.; Weissleder, R.; Tung, C.-H. *Tetrahedron* **2006**, *62*, 578-585.

(80) Frade, V. H. J.; Coutinho, P. J. G.; Moura, J. C. V. P.; Goncalves, M. S. T. *Tetrahedron* **2007**, *63*, 1654-1663.

(81) Lopez-Calle, E.; Fries, J. R.; Mueller, A.; Winkler, D. *Innovation and Perspectives in Solid Phase Synthesis & Combinatorial Libraries: Peptides, Proteins and Nucleic Acids--Small Molecule Organic Chemistry Diversity, Collected Papers, International Symposium, 7th,* Southampton, UK, MD, Sep. 18-22, 2001; pp 129-136.

(82) Yan, X.; Yuan, P. M. Sulfonated [8,9]Benzophenoxazine Dyes and The Use of Their Labelled Conjugates. US Patent 7238789, November 8, 2001.

(83) Jose, J.; Ueno, Y.; Burgess, K. *Chem. Eur. J.* **2009**, *15*, 418-423.

(84) Kina, K.; Horiguchi, D. Novel Water-soluble Nitrosophenolic Compound and Its Application. JP Patent 57091969, August 6, 1982.

(85) Hansen, T. M.; Engler, M. M.; Forsyth, C. J. *Bioorg. Med. Chem. Lett.* **2003**, *13*, 2127-30.

(86) Burns, C. J.; Field, L. D.; Petteys, B. J.; Ridley, D. D. *Aust. J. Chem.* **2005**, *58*, 738-748.

(87) Mishra, V. N.; Datt, N. *Indian J. Chem., Sect. A: Inorg., Phys., Theor. Anal. Chem.* **1985**, *24A*, 597-600.

(88) Mathur, A. K.; Agarwal, C.; Pangtey, B. S.; Singh, A.; Gupta, B. N. *Int. J. Cos. Sci.* **1988**, *10*, 213-18.

(89) Sun, C.; Yang, J.; Li, L.; Wu, X.; Liu, Y.; Liu, S. *J. Chromatogr. B* **2004**, *803*, 173-190.

(90) Frangioni, J. V. *Curr. Opin. Chem. Biol.* **2003**, *7*, 626-634.

(91) Jiao, G.-S.; Thoresen Lars, H.; Burgess, K. *J. Am. Chem. Soc.* **2003**, *125*, 14668-9.

(92) Bandichhor, R.; Petrescu, A. D.; Vespa, A.; Kier, A. B.; Schroeder, F.; Burgess, K. *J. Am. Chem. Soc.* **2006**, *128*, 10688-10689.

(93) Han, J. W.; Castro, J. C.; Burgess, K. *Tetrahedron Lett.* **2003**, *44*, 9359-62.

(94) Loudet, A.; Bandichhor, R.; Burgess, K.; Palma, A.; McDonnell, S. O.; Hall, M. J.; O'Shea, D. F. *Org. Lett.* **2008**, *10*, 4771-4774.

(95) Jiao, G.-S.; Castro, J. C.; Thoresen, L. H.; Burgess, K. *Org. Lett.* **2003**, *5*, 3675-7.

(96) Bandichhor, R.; Petrescu, A. D.; Vespa, A.; Kier, A. B.; Schroeder, F.; Burgess, K. *Bioconjugate Chem.* **2006**, *17*, 1219-1225.

(97) Ulrich, G.; Ziessel, R.; Harriman, A. *Angew. Chem., Int. Ed.* **2008**, *47*, 1184-1201.

(98) Williams, C. H. G. *Trans. R. Soc. Edinburg* **1856**, *21*, 377.

(99) Kiyose, K.; Kojima, H.; Nagano, T. *Chem.--Asian J.* **2008**, *3*, 506-515.

(100) Briggs, M. S.; Burns, D. D.; Cooper, M. E.; Gregory, S. J. *Chem. Commun.* **2000**, 2323-4.

(101) Hilderbrand, S. A.; Kelly, K. A.; Niedre, M.; Weissleder, R. *Bioconjugate Chem.* **2008**, *19*, 1635-1639.

(102) Lee, H.; Berezin, M. Y.; Guo, K.; Kao, J.; Achilefu, S. *Org. Lett.* **2009**, *11*, 29-32.

(103) Mishra, A.; Behera, R. K.; Behera, P. K.; Mishra, B. K.; Behera, G. B. *Chem. Rev.* **2000**, *100*, 1973-2011.

(104) Lindsey, J. S.; Brown, P. A.; Siesel, D. A. *Tetrahedron* **1989**, *45*, 4845-66.

(105) Mason, S. J.; Balasubramanian, S. *Org. Lett.* **2002**, *4*, 4261-4264.

(106) Mason, S. J.; Hake, J. L.; Nairne, J.; Cummins, W. J.; Balasubramanian, S. *J. Org. Chem.* **2005**, *70*, 2939-2949.

(107) Tomasulo, M.; Sortino, S.; Raymo, F. M. *J. Org. Chem.* **2008**, *73*, 118-126.

(108) Kvach, M. V.; Ustinov, A. V.; Stepanova, I. A.; Malakhov, A. D.; Skorobogatyi, M. V.; Shmanai, V. V.; Korshun, V. A. *Eur. J. Org. Chem.* **2008**, 2107-2117.

(109) Sonogashira, K.; Tohda, Y.; Hagihara, N. *Tetrahedron Lett.* **1975**, *16*, 4467-70.

(110) Thivierge, C.; Bandichhor, R.; Burgess, K. *Org. Lett.* **2007**, *9*, 2135-2138.

(111) Atilgan, S.; Ozdemir, T.; Akkaya, E. U. *Org. Lett.* **2008**, *10*, 4065-4067.

(112) Vickerstaff, T.; Lemin, D. R. *Nature* **1946**, *157*, 373.

(113) Wang, J. C. *Adv. Color. Sci. Technol.* **2000**, *3*, 20-31.

(114) Choi, J.; Burns, A. A.; Williams, R. M.; Zhou, Z.; Flesken-Nikitin, A.; Zipfel, W. R.; Wiesner, U.; Nikitin, A. Y. *J. Biomed. Optics* **2007**, *12*, 064007.

(115) Chan, W., CW.; Maxwell, D. J.; Gao, X.; Bailey, R. E.; Han, M.; Nie, S. *Curr Opin Biotechnol* **2002**, *13*, 40-6.

(116) Bailey, R. E.; Smith, A. M.; Nie, S. *Physica E* **2004**, *25*, 1-12.

(117) Medintz, I. L.; Uyeda, H. T.; Goldman, E. R.; Mattoussi, H. *Nat. Mater.* **2005**, *4*, 435-446.

(118) Burns, A.; Ow, H.; Wiesner, U. *Chem. Soc. Rev.* **2006**, *35*, 1028-1042.

(119) Burns, A.; Sengupta, P.; Zedayko, T.; Baird, B.; Wiesner, U. *Small* **2006**, *2*, 723-726.

(120) Kim, S. H.; Jeyakumar, M.; Katzenellenbogen, J. A. *J. Am. Chem. Soc.* **2007**, *129*, 13254-13264.

(121) Altinoglu, E. I.; Russin, T. J.; Kaiser, J. M.; Barth, B. M.; Eklund, P. C.; Kester, M.; Adair, J. H. *ACS Nano* **2008**, *2*, 2075-2084.

(122) Kester, M.; Heakal, Y.; Fox, T.; Sharma, A.; Robertson, G. P.; Morgan, T. T.; Altinoglu, E. I.; Tabakovic, A.; Parette, M. R.; Rouse, S.; Ruiz-Velasco, V.; Adair, J. H. *Nano Lett.* **2008**, *8*, 4116-4121.

(123) Morgan, T. T.; Muddana, H. S.; Altinoglu, E. I.; Rouse, S. M.; Tabakovic, A.; Tabouillot, T.; Russin, T. J.; Shanmugavelandy, S. S.; Butler, P. J.; Eklund, P. C.; Yun, J. K.; Kester, M.; Adair, J. H. *Nano Lett.* **2008**, *8*, 4108-4115.

(124) Santra, S.; Bagwe, R. P.; Dutta, D.; Stanley, J. T.; Walter, G. A.; Tan, W.; Moudgil, B. M.; Mericle, R. A. *Adv. Mater.* **2005**, *17*, 2165-2169.

(125) Wu, C.; Hong, J.; Guo, X.; Huang, C.; Lai, J.; Zheng, J.; Chen, J.; Mu, X.; Zhao, Y. *Chem. Commun.* **2008**, 750-752.

(126) Sokolov, I.; Naik, S. *Small* **2008**, *4*, 934-939.

(127) Ow, H.; Larson, D. R.; Srivastava, M.; Baird, B. A.; Webb, W. W.; Wiesner, U. *Nano Lett.* **2005**, *5*, 113-117.

(128) Larson, D. R.; Ow, H.; Vishwasrao, H. D.; Heikal, A. A.; Wiesner, U.; Webb, W. W. *Chem. Mater.* **2008**, *20*, 2677-2684.

(129) Funatsu, T.; Harada, Y.; Tokunaga, M.; Saito, K.; Yanagida, T. *Nature* **1995**, *374*, 555-9.

(130) Weiss, S. *Science* **1999**, *283*, 1676-83.

(131) Tilley, S. D.; Francis, M. B. *J. Am. Chem. Soc.* **2006**, *128*, 1080-1081.

(132) Antos, J. M.; Francis, M. B. *J. Am. Chem. Soc.* **2004**, *126*, 10256-10257.

(133) Burgess, K.; Jacutin, S. E.; Lim, D.; Shitangkoon, A. *J. Org. Chem.* **1997**, *62*, 5165-8.

(134) Burgess, K.; Martinez, C. I.; Russell, D. H.; Shin, H.; Zhang, A. J. *J. Org. Chem.* **1997**, *62*, 5662-3.

(135) Lu, G.; Burgess, K. *Bioorg. Med. Chem. Lett.* **2006**, *16*, 3902-3905.

(136) Guillier, F.; Orain, D.; Bradley, M. *Chem. Rev.* **2000**, *100*, 2091-157.

(137) Verhelst, S. H. L.; Fonovic, M.; Bogyo, M. *Angew. Chem. Int. Ed.* **2007**, *46*, 1284-1286.

(138) Bochet, C. G. *J. Chem. Soc., Perkin Trans. 1* **2002**, 125-42.

(139) Kress, J.; Zanaletti, R.; Amour, A.; Ladlow, M.; Frey, J. G.; Bradley, M. *Chem. Eur. J.* **2002**, *8*, 3769-72.

(140) MacBeath, G.; Schreiber, S. L. *Science* **2000**, *289*, 1760-3.

(141) Zhang, A. J.; Russell, D. H.; Zhu, J.; Burgess, K. *Tetrahedron Lett.* **1998**, *39*, 7439-42.

(142) Meldal, M. *Tetrahedron Lett.* **1992**, *33*, 3077-80.

(143) Auzanneau, F.-I.; Meldal, M.; Bock, K. *J. Pep. Sci.* **1995**, *1*, 31-44.

(144) Meldal, M.; Auzanneau, F.-I.; Hindsgaul, O.; Palcic, M. M. *J. Chem. Soc., Chem. Commun.* **1994**, 1849-50.

(145) Nielsen, T. E.; Le Quement, S.; Meldal, M. *Org. Lett.* **2005**, *7*, 3601-3604.

(146) Laganis, E. D.; Chenard, B. L. *Tetrahedron Lett.* **1984**, *25*, 5831-4.

(147) Holmes, C. P. *J. Org. Chem.* **1997**, *62*, 2370-2380.

(148) Kostiainen, M. A.; Smith, D. K.; Ikkala, O. *Angew. Chem. Int. Ed.* **2007**, *46*, 7600-7604.

(149) Tsai, S.-C.; Klinman, J. P. *Bioorg. Chem.* **2003**, *31*, 172-190.

(150) Alvarez, S. G.; Alvarez, M. T. *Synthesis* **1997**, 413-414.

(151) Srinivasan, M.; Sankararaman, S.; Hopf, H.; Dix, I.; Jones, P. G. *J. Org. Chem.* **2001**, *66*, 4299-4303.

(152) Srinivasan, R.; Uttamchandani, M.; Yao, S. Q. *Org. Lett.* **2006**, *8*, 713-716.

(153) Santra, S.; Zhang, P.; Wang, K.; Tapec, R.; Tan, W. *Anal. Chem.* **2001**, *73*, 4988-4993.

(154) Maxam, A. M.; Gilbert, W. *Proc. Natl. Acad. Sci.* **1977**, *74*, 560-4.

(155) Sanger, F.; Nicklen, S.; Coulson, A. R. *Proc. Natl. Acad. Sci.* **1977**, *74*, 5463-5467.

(156) Corey, E. J.; Hopkins, P. B. *Tetrahedron Lett.* **1982**, *23*, 1979-82.

(157) Chu, C. K.; Bhadti, V. S.; Doboszewski, B.; Gu, Z. P.; Kosugi, Y.; Pullaiah, K. C.; Van Roey, P. *J. Org. Chem.* **1989**, *54*, 2217-25.

(158) Saito, Y.; Zevaco, T. A.; Agrofoglio, L. A. *Tetrahedron* **2002**, *58*, 9593-9603.

(159) McGuigan, C.; Pathirana, R. N.; Snoeck, R.; Andrei, G.; De Clercq, E.; Balzarini, J. *J. Med. Chem.* **2004**, *47*, 1847-1851.

(160) Watanabe, K. A.; Fox, J. J. *Angew. Chem. Inter. Ed.* **1966**, *5*, 579-80.

(161) Manchand, P. S.; Belica, P. S.; Holman, M. J.; Huang, T. N.; Maehr, H.; Tam, S. Y. K.; Yang, R. T. *J. Org. Chem.* **1992**, *57*, 3473-8.

(162) Marcuccio, S. M.; Elmes, B. C.; Holan, G.; Middleton, E. J. *Nucleosides & Nucleotides* **1992**, *11*, 1695-701.

(163) Clive, D. L. J.; Wickens, P. L.; Sgarbi, P. W. M. *J. Org. Chem.* **1996**, *61*, 7426-7437.

(164) Kovács, T.; Ötvös, L. *Tetrahedron Lett.* **1988**, *29*, 4525-8.

(165) Ludwig, J.; Eckstein, F. *J. Org. Chem.* **1989**, *54*, 631-5.

(166) Thoresen, L. H.; Jiao, G.-S.; Haaland, W. C.; Metzker, M. L.; Burgess, K. *Chem. Eur. J.* **2003**, *9*, 4603-4610.

(167) Jiang, Z.-Y.; Wang, Y.-G. *Tetrahedron Lett.* **2003**, *44*, 3859-3861.

(168) Jiao, G.-S.; Castro, J. C.; Thoresen, L. H.; Burgess, K. *Org. Lett.* **2003**, *5*, 3675-3677.

(169) Wang, Z.-Q.; Diwu, Z.; Francisco-Reyes, J.; Yi, G. G. *Chem. Lett.* **2005**, *34*, 404-405.

(170) Kalbag, S. M.; Roeske, R. W. *J. Am. Chem. Soc.* **1975**, *97*, 440-1.

(171) Rai, D.; Johar, M.; Srivastav, N. C.; Manning, T.; Agrawal, B.; Kunimoto, D. Y.; Kumar, R. *J. Med. Chem.* **2007**, *50*, 4766-4774.

(172) Lam, S. Q. M.S. Thesis, Texas A&M University, 2005.

(173) Quiclet-Sire, B.; Zard, S. Z. *Synthesis* **2005**, 3319-3326.

APPENDIX A

EXPERIMENTAL DATA FOR CHAPTER II

General Experimental Procedures

All reactions were carried out under an atmosphere of dry nitrogen. Glasswares were oven-dried prior to use. Unless otherwise indicated, common reagents or materials were obtained from commercial source and used without further purification. All solvents were dried prior to use with appropriate drying agents. Dry distilled DMF was obtained from Acros and used as such. Flash column chromatography was performed using silica gel 60 (230-400 mesh). Analytical thin layer chromatography (TLC) was carried out on Merck silica gel plates with QF-254 indicator and visualized by UV. Fluorescence spectra were obtained on a Varian Cary Eclipse fluorescence spectrophotometer at room temperature. Absorbance spectra were obtained on a Varian 100 Bio UV-Vis spectrophotometer at room temperature. IR spectra were recorded on a Bruker Tensor 27 spectrometer.

Nuclear Magnetic Resonance (NMR) spectra were recorded on a Varian 300 (^{1}H at 300 MHz; ^{13}C at 75 MHz; ^{31}P at 121 MHz), Mercury 300 (^{1}H at 300 MHz; ^{13}C at 75 MHz) or Inova 500 (^{1}H at 500 MHz; ^{13}C at 125 MHz) spectrometer at room temperature. Chemical shifts were reported in ppm (parts per million) relative to the residual $CDCl_3$ (δ 7.26 ppm ^{1}H; δ 77.0 ppm ^{13}C), CD_3OD (δ 3.31 ppm ^{1}H; δ 49.0 ppm ^{13}C), acetone-d_6 (δ 2.09 ppm ^{1}H; δ 205.87 & 30.6 ppm ^{13}C) or DMSO-d_6 (δ 2.54 ppm ^{1}H; δ 40.45 ppm ^{13}C). Coupling constants (*J*) were reported in Hertz.

Analytical HPLC were run on a Beckman System Gold 125 solvent module and 166 UV-vis detector using a Vydac analytical (4.6 x 250 mm) C-18 column. Gradient elution was used (A = water, B = CH_3CN, both with 0.1 % v/v TFA) with a constant flow rate of 1.0 mL/min. Preparative HPLC were run on a Beckman System Gold 125P solvent module and 166P UV-vis detector using a Vydac semi-preparative C-18 column (22 x 250 mm), the solvent system described above, and a flow rate of 10 mL/min.

5- and 6-Carboxyfluorescein (3a) and (3b),
and their methanesulfonic acid adducts (4a) and (4b)

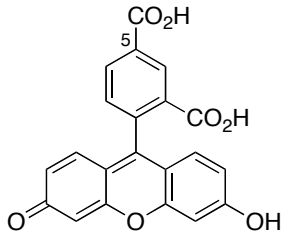

3a
5-carboxyfluorescein

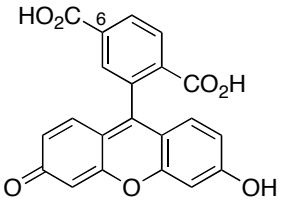

3b
6-carboxyfluorescein

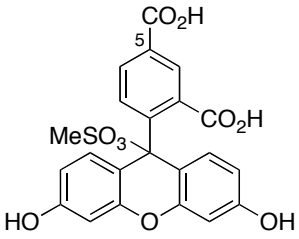

4a
5-carboxyfluorescein
methanesulfonic acid adduct

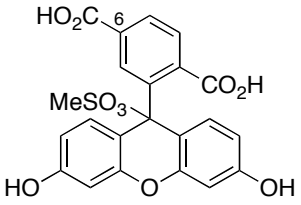

4b
6-carboxyfluorescein
methanesulfonic acid adduct

1,2,4-Benzenetricarboxylic anhydride (also called 4-carboxyphthalic anhydride, 25.0 g, 0.13 mol) was added to a solution of 1,3-dihydroxybenzene (also called resorcinol, 28.6 g, 0.26 mol) in methanesulfonic acid (130 mL, 1 M against to 4-carboxyphthalic anhydride [0.13 mol]). An air condenser was attached to the flask and the reaction was heated at 85 ºC in an open vessel for 24 h. After cooling to room temperature, the reaction mixture was poured into 7 volumes of ice-H_2O (900 mL). An orange-yellow precipitate formed; this was collected by filtration and dried in an oven at 200 ºC for 10 h to afford 67.2 g of mixture. 20 g of this material was recrystallized from MeOH-hexanes (2 times: 1st recrystallization: 600 mL of MeOH and 200 mL of hexanes, 2nd recrystallization: 120 mL of MeOH and 40 mL of hexanes) at –18 ºC to give 6-carboxyfluorescein methanesulfonic acid adduct **4b** (1.0 g, >98 % purity by anal. HPLC). The mother liquors from this procedure were collected, the solvent was removed in vacuo, and the residues were recrystallized from EtOH-hexanes (2 times: 1st

recrystallization: 600 mL of EtOH and 200 mL of hexanes, 2nd recrystallization: 120 mL of EtOH and 40 mL of hexanes) to give 5-carboxyfluorescein methanesulfonic acid adduct **4a** (3.2 g, 32 %, >98 % purity by anal. HPLC). Finally, the mother liquors from this experiment were combined, evaporated to dryness, and recrystallized from MeOH-hexanes (2 times: 1st recrystallization: 600 mL of MeOH and 200 mL of hexanes, 2nd recrystallization: 120 mL of MeOH and 40 mL of hexanes) to give another 3.0 g of 6-isomer **4b**, making a total yiled of 4.0 g (40 %). Careful dropwise addition of concd. aq. HCl to solutions of these methanesulfonic esters **4a** and **4b** in 4 M NaOH gave 5- and 6-carboxyfluorescein **3a** and **3b**, respectively in near quantitative yield.

Notes for recrystallization

1: The ratio of solvents must be 3:1 (MeOH/hexanes or EtOH/hexanes).

2: Small amount of methanesulfonic acid was added to solution dropwise when the material was not soluble in MeOH or EtOH. The solution can also be heated to dissolve material in MeOH or EtOH completely.

3: MeOH or EtOH and hexanes are immiscible at room temperature and this is important. Because the yellow solids started precipitating from the solvent interphase between MeOH of EtOH and hexanes in freezer.

3a: mp 385-388 ºC; ^{1}H NMR (300 MHz, NaOD-D_2O) δ 8.26 (d, 1H, J = 1.9 Hz), 8.07 (dd, 1H, J = 7.8, 1.7 Hz), 7.33 (d, 1H, J = 7.7 Hz), 7.20 (d, 2H, J = 9.1 Hz), 6.66 (dd, 2H, J = 9.4, 2.2 Hz), 6.56 (d, 2H, J = 2.5 Hz); ^{13}C NMR (75 MHz, NaOD-D_2O) δ 176.4, 174.57, 174.55, 158.5, 158.0, 139.7, 137.8, 133.9, 131.7, 130.1, 129.9, 128.8, 121.7, 114.2, 103.4; MS (ESI) m/z 375 $(M–H)^-$; Anal. Calcd for $C_{21}H_{12}O_7$•1.5H_2O: C, 62.53; H, 3.75. Found: C, 62.70; H, 3.49.

3b: mp 372-374 ºC; ^{1}H NMR (300 MHz, NaOD-D_2O) δ 8.09 (dd, 1H, J = 8.1, 1.5 Hz), 7.89 (s, 1H), 7.86 (d, 1H, J = 1.1 Hz), 7.24 (d, 2H, J = 9.4 Hz), 6.68 (m, 4H); ^{13}C NMR (75 MHz, NaOD-D_2O) δ 175.3, 174.6, 174.3, 158.2, 157.9, 141.7, 137.5, 131.9, 131.1,

130.4, 130.2, 128.6, 121.3, 115.0, 103.3; MS (ESI) m/z 375 $(M–H)^-$; Anal. Calcd for $C_{21}H_{12}O_7$•1.5H_2O: C, 62.53; H, 3.75. Found: C, 62.43; H, 3.36.

4a: mp 196-198 ºC; ^{1}H NMR (300 MHz, NaOD-D_2O) δ 8.23 (d, 1H, *J* = 1.2 Hz), 8.02 (dd, 1H, *J* = 9.0, 1.8 Hz), 7.21 (d, 1H, *J* = 7.8 Hz), 7.13 (d, 2H, *J* = 9.3 Hz), 6.60 (dd, 2H, *J* = 9.6, 2.4 Hz), 6.53 (d, 2H, *J* = 2.1 Hz), 2.80 (s, 3H); ^{13}C NMR (75 MHz, NaOD-D_2O) δ 180.7, 174.9, 174.7, 158.8, 158.7, 139.8, 137.5, 134.2, 131.5, 130.2, 129.6, 128.6, 123.1, 112.3, 103.8, 38.57; MS (ESI) m/z 471 $(M–H)^-$; Anal. Calcd for $C_{22}H_{16}O_{10}S$•H_2O: C, 53.88; H, 3.70; S, 6.54. Found: C, 53.66; H, 3.86; S, 6.61.

4b: mp 318-321 ºC; ^{1}H NMR (300 MHz, NaOD-D_2O) δ 8.06 (dd, 1H, *J* = 9.0, 1.2 Hz), 7.84 (d, 1H, *J* = 8.1 Hz), 7.76 (s, 1H), 7.19 (d, 2H, *J* = 9.6 Hz), 6.61 (m, 4H), 2,79 (s, 3H); ^{13}C NMR (75 MHz, NaOD-D_2O) δ 177.2, 174.8, 174.4, 158.3, 141.9, 137.5, 131.9, 131.2, 130.5, 130.1, 128.5, 121.9, 114.2, 103.5, 38.58; MS (ESI) m/z 471 $(M–H)^-$; Anal. Calcd for $C_{22}H_{16}O_{10}S$•2H_2O: C, 51.97; H, 3.96; S, 6.31. Found: C, 52.30; H, 4.02; S, 6.23.

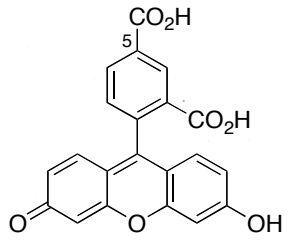

3a

5-carboxyfluorescein

^{1}H NMR (NaOD-D_2O)

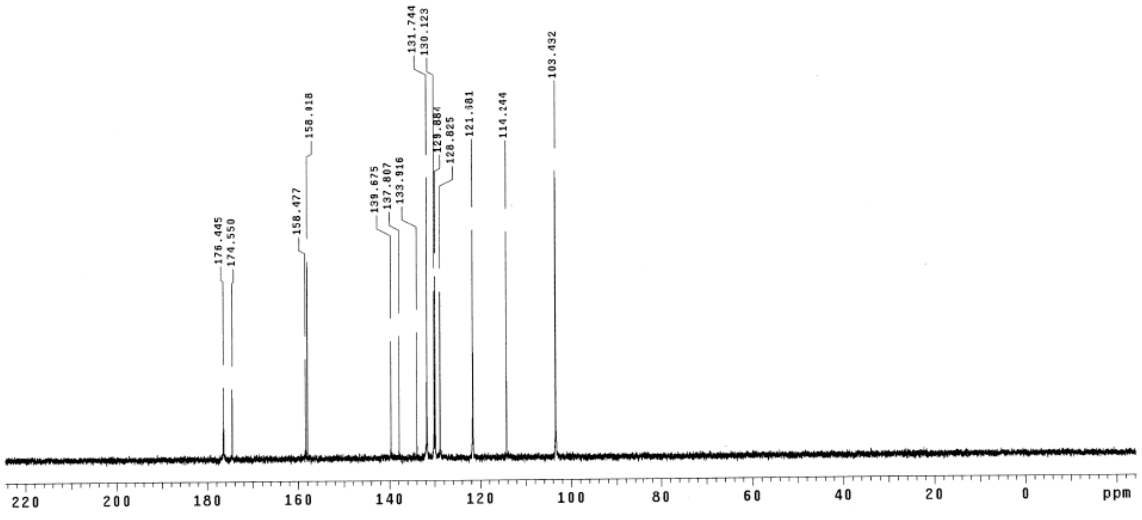

^{13}C NMR (NaOD-D_2O)

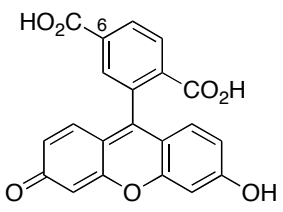

3b

6-carboxyfluorescein

^{1}H NMR (NaOD-D$_2$O)

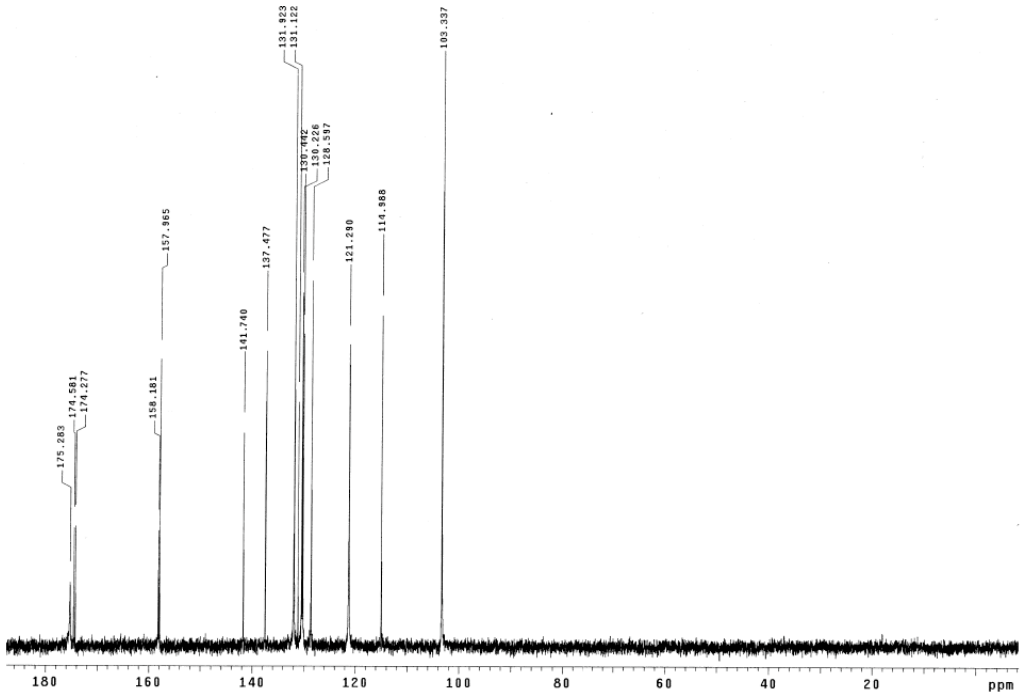

^{13}C NMR (NaOD-D$_2$O)

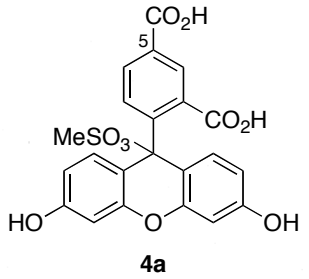

4a

5-carboxyfluorescein methanesulfonic acid adduct

^{1}H NMR (NaOD-D_2O)

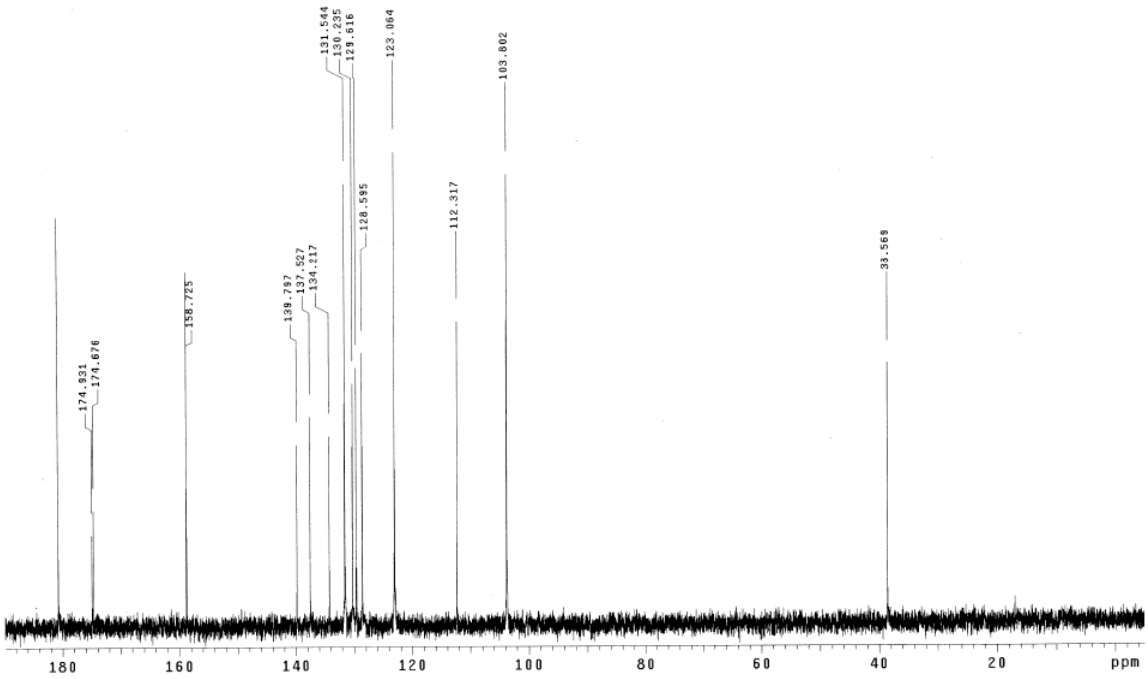

^{13}C NMR (NaOD-D_2O)

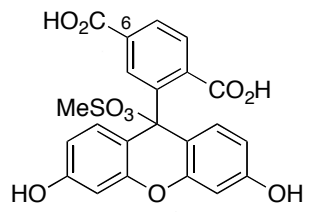

4b

6-carboxyfluorescein methanesulfonic acid adduct

^{1}H NMR (NaOD-D_2O)

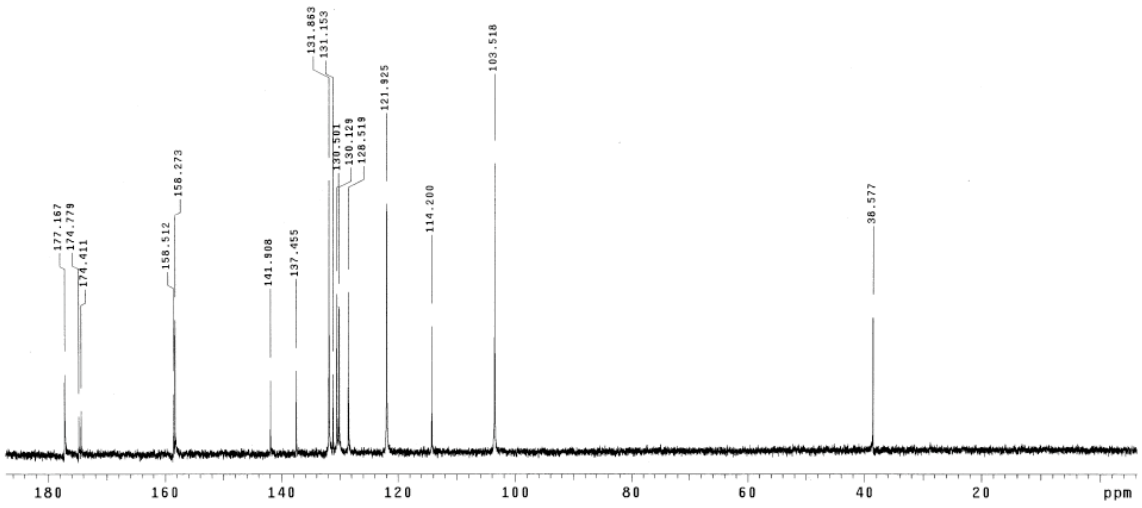

^{13}C NMR (NaOD-D_2O)

Hexaethylene glycol mono-tosylate (15)[58]

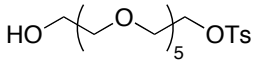

Silver oxide (6.2 g, 26.6 mmol), *p*-toluenesulfonyl chloride (3.7 g, 19.5 mmol) and potassium iodide (588 mg, 3.5 mmol) were added to a solution of hexaethylene glycol (5 g, 17.7 mmol) in CH_2Cl_2 (50 mL) at 0 ºC. The reaction mixture was stirred at 0 ºC for 30 min then filtrated through celite and washed with EtOAc. The solvents were concentrated under the reduced pressure and the residue was purified by flash chromatography eluting with 100 % EtOAc then 30 % acetone/EtOAc to afford product as a colorless oil (6.2 g, 81 %). R_f 0.3 (15 % acetone/EtOAc with iodine stain). ^{1}H NMR (500 MHz, $CDCl_3$) δ 7.78 (d, 2H, J = 8.0 Hz), 7.33 (d, 2H, J = 8.0 Hz), 4.14 (t, 2H, J = 5.0 Hz), 3.71-3.57 (m, 20H), 3.28 (bs, 2H), 2.43 (s, 3H); ^{13}C NMR (125 MHz, $CDCl_3$) δ 144.8, 132.8, 129.8, 127.9, 72.6, 70.6, 70.5 (2C), 70.41, 70.40, 70.35, 70.34, 70.1, 69.3, 68.6, 61.6, 21.6.

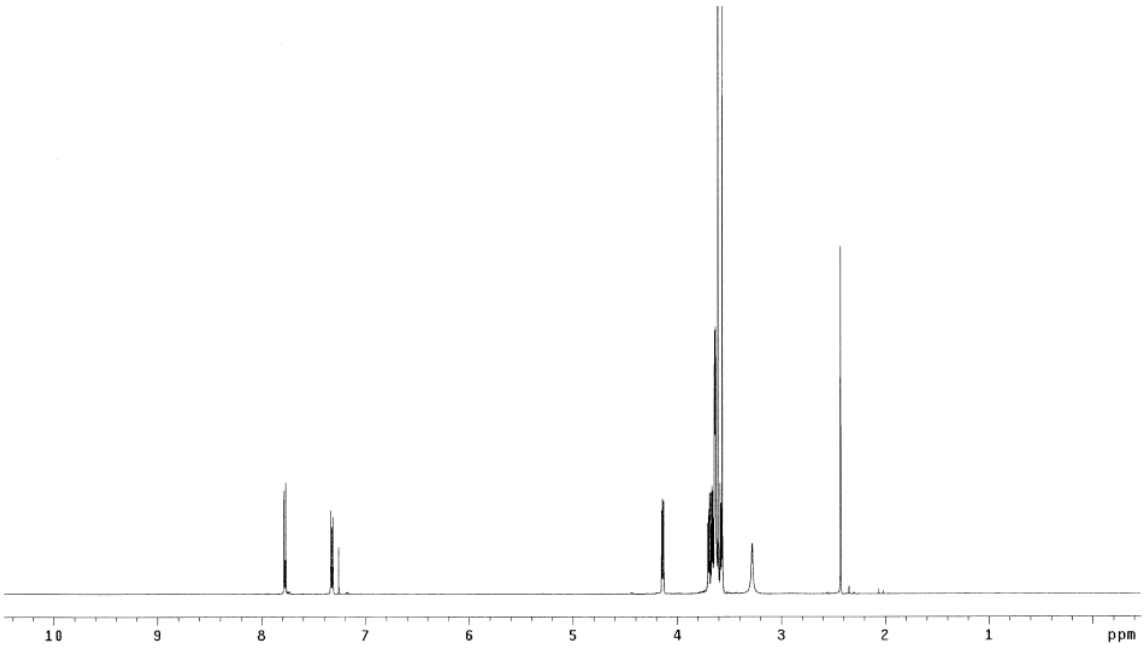

^{1}H NMR ($CDCl_3$)

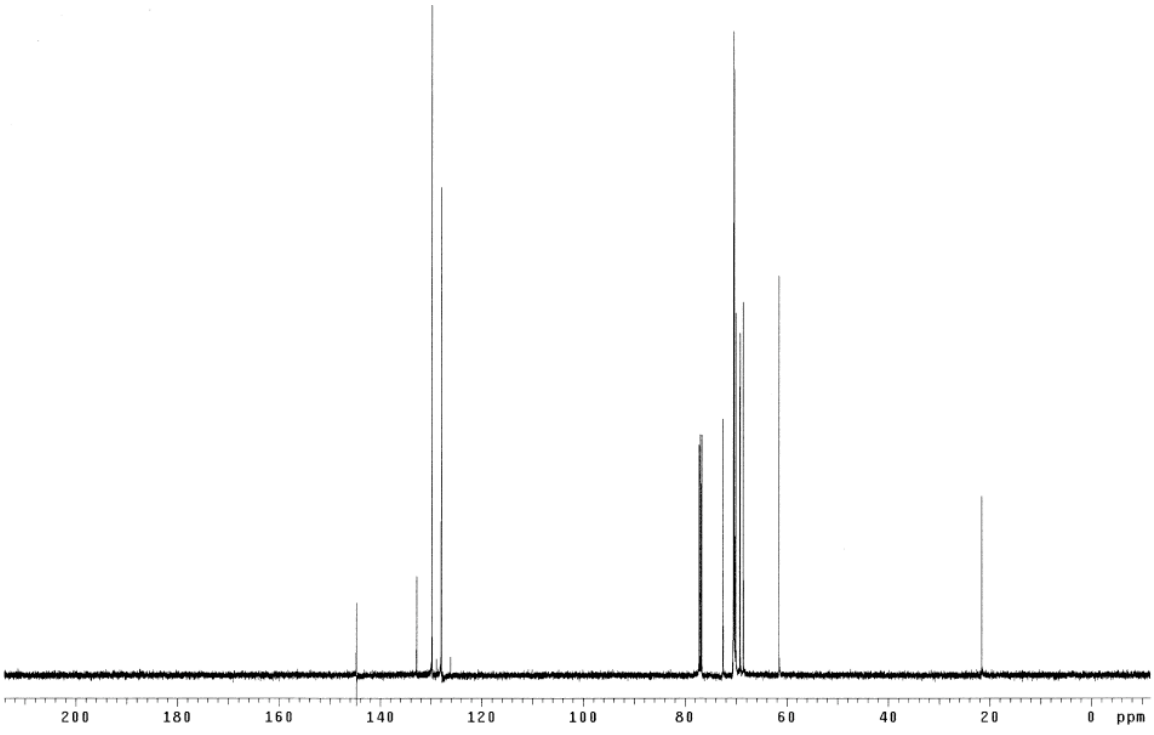

^{13}C NMR ($CDCl_3$)

Mono-azido hexaethylene glycol (16)[135]

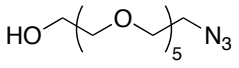

A solution of hexaethylene glycol mono-tosylate **15** (5.75 g, 13.2 mmol) and sodium azide (1.46 g, 22.4 mmol) in CH_3CN (70 mL) was refluxed at 85 ºC for 42 h. The reaction mixture was cooled down to room temperature and diluted with water (100 mL) and extracted with CH_2Cl_2 (5 x 50 mL). The combined organic layer was dried over $MgSO_4$ and concentrated under the reduced pressure to afford pure product as a colorless oil (3.8 g, 95 %). R_f 0.1 (100 % EtOAc with iodine stain). ^{1}H NMR (500 MHz, $CDCl_3$) δ 3.67 (t, 2H, J = 4.5 Hz), 3.64-3.60 (m, 16H), 3.55 (t, 2H, J = 4.5 Hz), 3.35 (t, 2H, J = 5.5 Hz), 3.25 (s, 2H); ^{13}C NMR (125 MHz, $CDCl_3$) δ 72.6, 70.43, 70.42, 70.40, 70.39, 70.31, 70.28, 70.26, 69.96, 69.85, 61.4, 50.5.

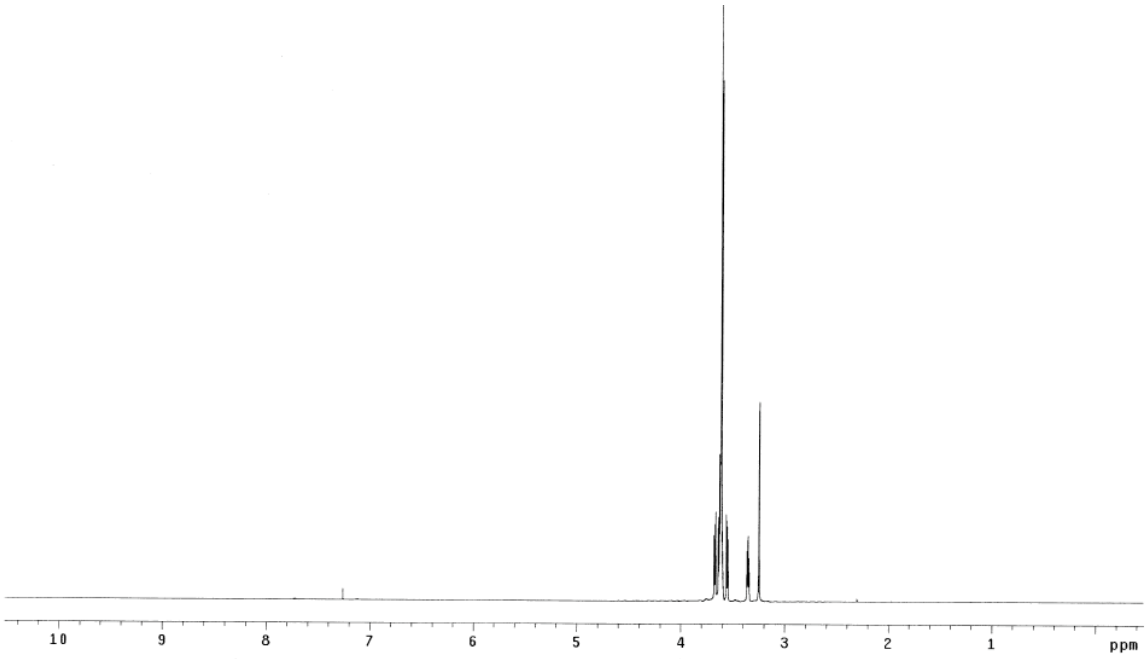

^{1}H NMR ($CDCl_3$)

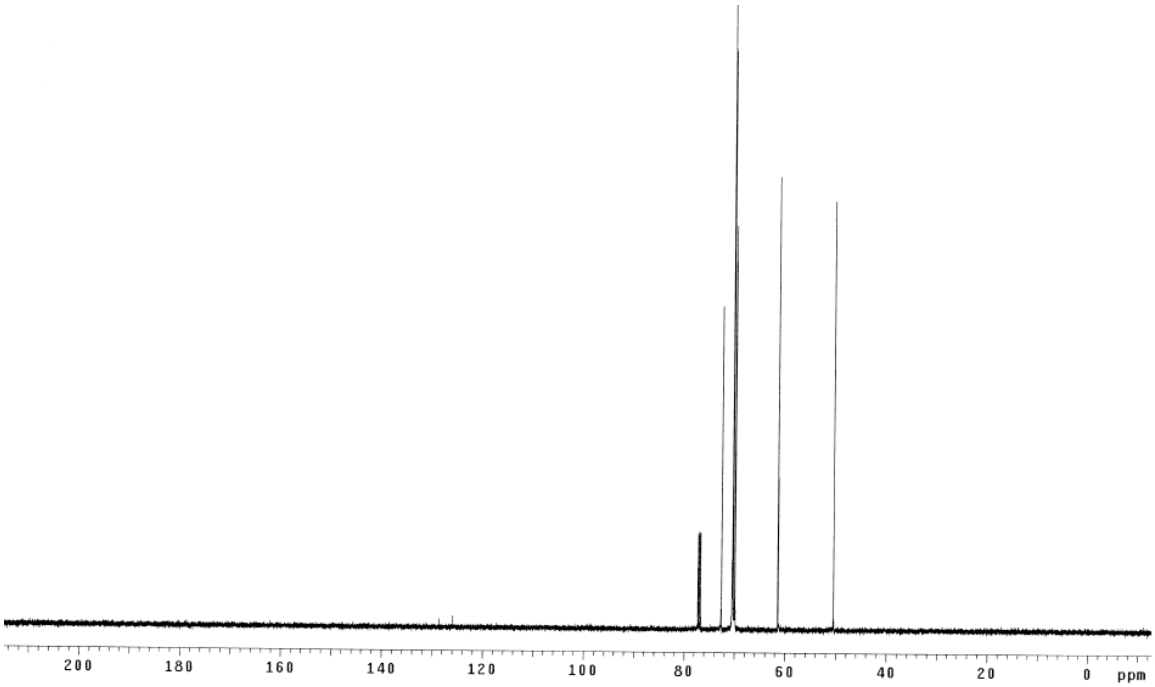

^{13}C NMR ($CDCl_3$)

Mono-azido hexaethylene glycol tosylate (17)[135]

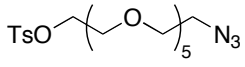

Hexaethylene glycol mono-azide **16** (1.8 g, 5.86 mmol), Et_3N (1.6 mL, 11.7 mmol) and Me_3N•HCl (56 mg, 0.59 mmol) were added in CH_3CN (20 mL) at 0 ºC. A solution of TsCl (1.67 g, 8.79 mmol) in CH_3CN (10 mL) was then added by syringe and the reaction mixture was stirred at 0 ºC for 10 min and 1 h at 25 ºC. The reaction was quenched with water (30 mL) and the aqueous layer was extracted with EtOAc (3 x 30 mL). The combined organic layer was dried over $MgSO_4$ and solvents were concentrated under the reduced pressure. The residue was purified by flash chromatography eluting with 50 % EtOAc/hexanes then 100 % EtOAc to afford product as a yellow oil (2.5 g, 93 %). R_f 0.7 (100 % EtOAc with iodine stain). ^{1}H NMR (500 MHz, $CDCl_3$) δ 7.76 (d, 2H, J = 6.0 Hz), 7.31 (d, 2H, J = 6.0 Hz), 4.14-4.11 (m, 2H), 3.67-3.57 (m, 16H), 3.56-3.55 (m, 4H), 3.37-3.34 (m, 2H), 2.42 (s, 3H); ^{13}C NMR (125 MHz, $CDCl_3$) δ 144.7, 132.8, 129.7, 127.8, 70.6, 70.53, 70.51, 70.46 (2C), 70.43, 70.40, 70,36, 69.9, 69.2, 68.5, 50.5, 21.5; MS (ESI) m/z 468.19 $(M+Li)^+$.

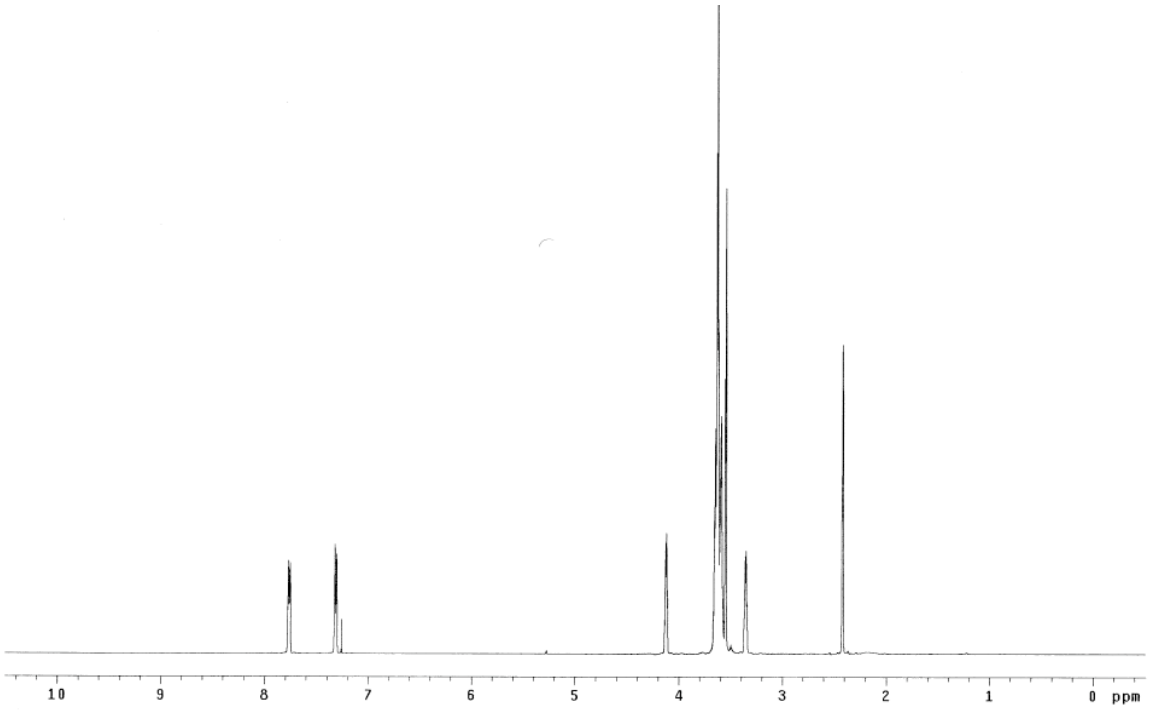

^{1}H NMR ($CDCl_3$)

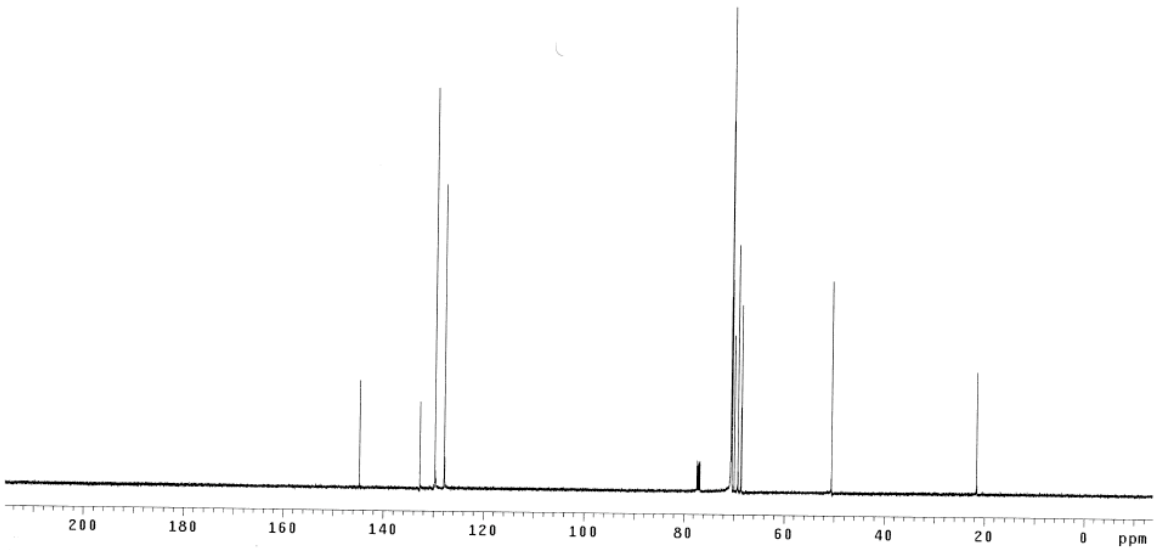

^{13}C NMR ($CDCl_3$)

Mono-propargyl hexaethylene glycol (18)

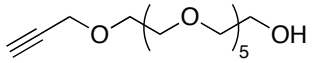

Sodium hydride (460 mg, 11.5 mmol, 60 % in mineral oil) was slowly added to a solution of hexaethylene glycol (5.0 g, 17.7 mmol) in THF (25 mL) at 0 ºC. The reaction was stirred at 0 ºC for 30 min, then propargyl bromide (1.3 g, 8.9 mmol, 80 % w/w in toluene) was added dropwise. After the stirring at 0 ºC for 30 min, the reaction mixture was warmed to room temperature and stirred at 25 ºC for additional 1.5 h. Water (25 mL) was slowly added at 0 ºC and extracted with CH_2Cl_2 (3 x 20 mL). The combined organic layer was dried over $MgSO_4$ and concentrated under the reduced pressure. The residue was purified by flash chromatography eluting with 100 % EtOAc then 30 % acetone/EtOAc to afford product as a yellow oil (1.9 g, 67 %). R_f 0.3 (30 % acetone/EtOAc with iodine stain). ^{1}H NMR (300 MHz, $CDCl_3$) δ 4.20 (d, 2H, J = 2.4 Hz), 3.74-3.59 (m, 24H), 2.43 (t, 1H, J = 2.4 Hz); ^{13}C NMR (75 MHz, $CDCl_3$) δ 74.5, 72.5, 70.6 (2C), 70.5 (6C), 70.4, 70.3, 69.1, 61.7, 58.4; MS (ESI) m/z 327.19 $(M+Li)^+$.

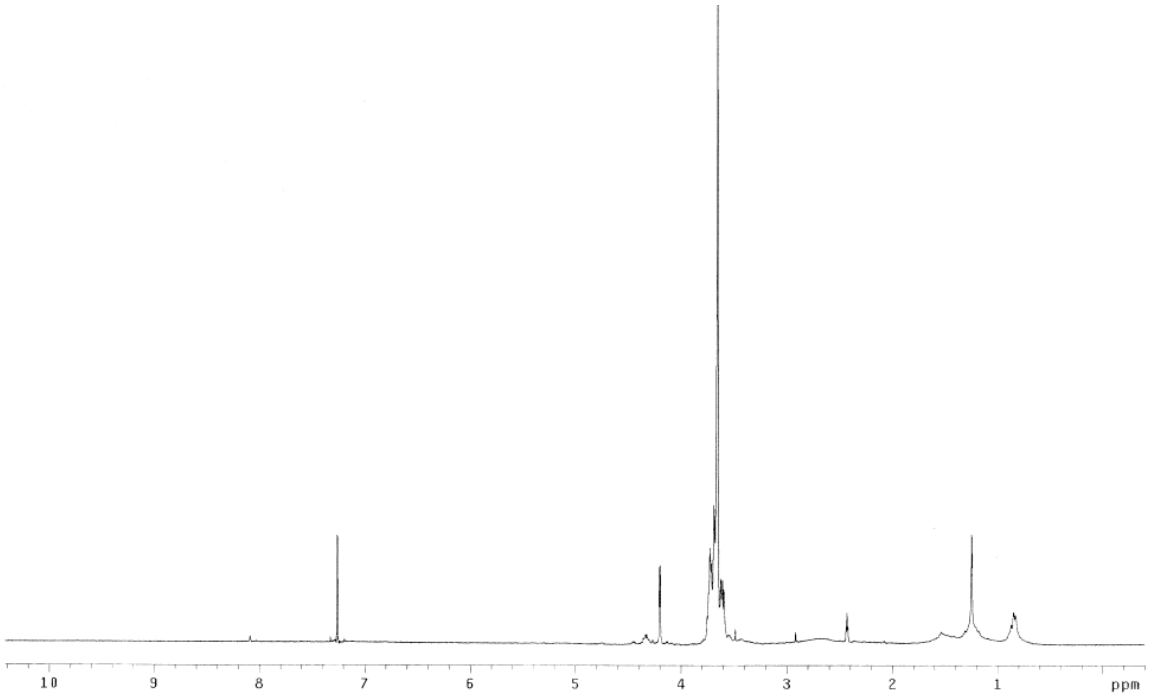

^{1}H NMR ($CDCl_3$)

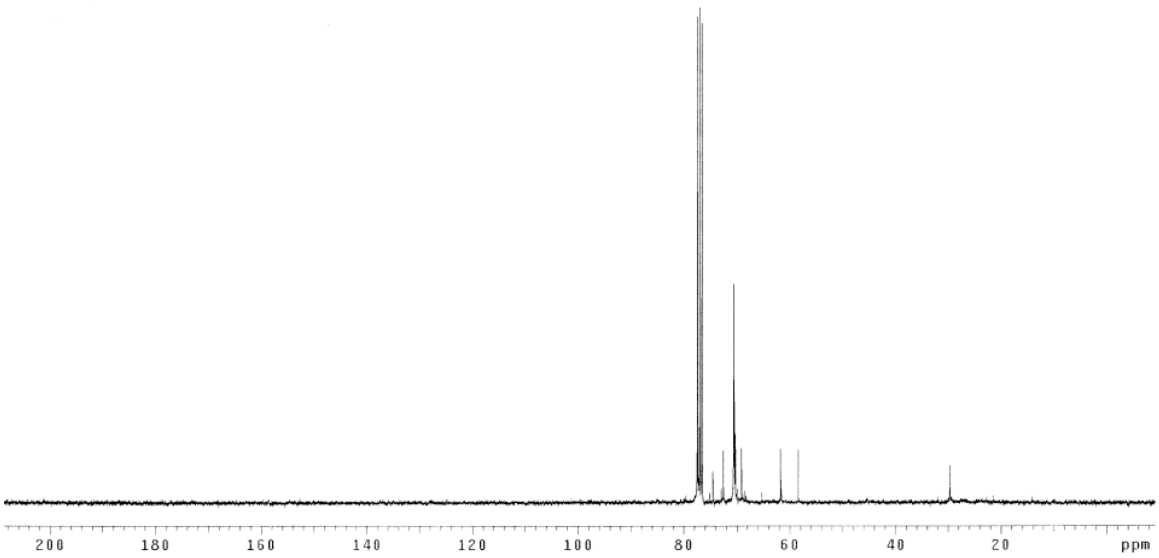

^{13}C NMR ($CDCl_3$)

Mono-propargyl hexaethylene glycol *tert*-butyl ester (19)

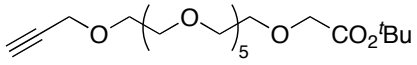

Sodium hydride (177 mg, 4.4 mmol, 60 % in mineral oil) was slowly added to a solution of mono-propargylated hexaethylene glycol **18** (942 mg, 2.9 mmol) in THF (10 mL) at 0 ºC. The reaction was stirred at 0 ºC for 30 min, then *tert*-butylbromoacetate (0.87 mL, 5.9 mmol) was added dropwise at 0 ºC. The reaction mixture was warmed to room temperature and stirred at 25 ºC for additional 40 min. Water (10 mL) was slowly added at 0 ºC and extracted with CH_2Cl_2 (5 x 10 mL). The combined organic layer was dried over $MgSO_4$ and concentrated under the reduced pressure. The residue was purified by flash chromatography eluting with 100 % EtOAc then 20 % acetone/EtOAc to afford product as a colorless oil (673 mg, 53 %). R_f 0.7 (20 % acetone/EtOAc with iodine stain). ^{1}H NMR (500 MHz, $CDCl_3$) δ 4.17 (d, 2H, J = 2.5 Hz), 3.99 (s, 2H), 3.71-3.58 (m, 24H), 2.42 (t, 1H, J = 2.5 Hz), 1.44 (s, 9H); ^{13}C NMR (125 MHz, $CDCl_3$) δ 169.6, 94.6, 81.5, 79.6, 75.3, 74.5, 70.6, 70.5 (3C), 70.41, 70.36, 70.3, 70.2, 69.0, 68.9, 63.7, 58.3, 28.0; MS (ESI) m/z 441.25 $(M+Li)^+$.

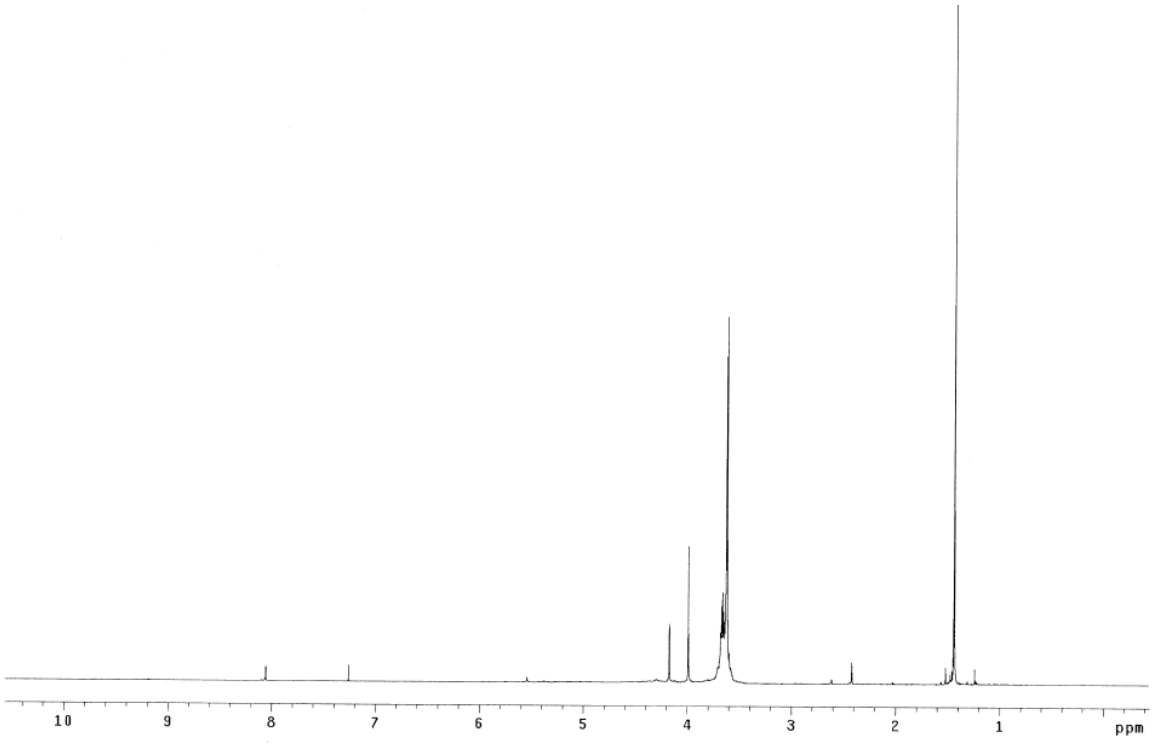

^{1}H NMR ($CDCl_3$)

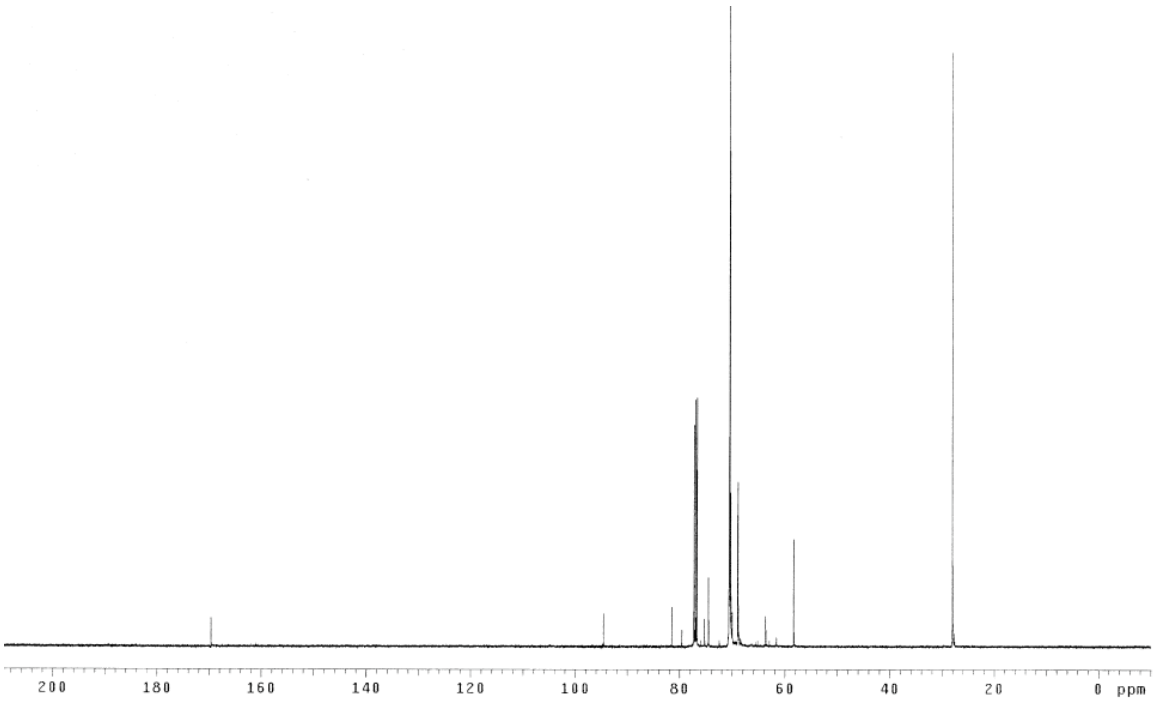

^{13}C NMR ($CDCl_3$)

Triazole-decorated oligoethylene glycol mono-tosylate (20)

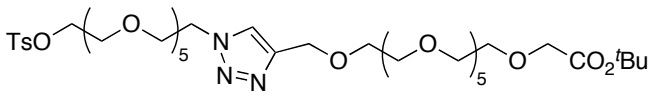

Copper powder (94 mg, 1.48 mmol), $CuSO_4$ (0.3 mL, 0.30 mmol, 1M in H_2O) and H_2O (8.0 mL) were added to a solution of mono-azido hexaethylene glycol **17** (680 mg, 1.48 mmol) and alkylated ethylene glycol **19** (771 mg, 1.77 mmol) in THF (8.0 mL). The reaction mixture was stirred at 25 ºC for 24 h under nitrogen. The solvents were evaporated under reduced pressure and the residual material was purified by flash chromatography eluting with 40 to 90 % acetone/EtOAc then 100 % acetone to afford product as a yellow oil (1.27 g, 96 %). R_f 0.2 (40 % acetone/EtOAc with iodine stain). ^{1}H NMR (500 MHz, $CDCl_3$) δ 7.77 (d, 2H, J = 8.5 Hz), 7.73 (s, 1H), 7.32 (d, 2H, J = 8.5 Hz), 4.65 (s, 2H), 4.51 (t, 2H, J = 5.0 Hz), 4.13 (t, 2H, J = 5.0 Hz), 4.00 (s, 2H), 3.85 (t, 2H, J = 5.5 Hz), 3.70-3.59 (m, 40H), 3.56 (s, 2H), 2.43 (s, 3H), 1.45 (s, 9H); ^{13}C NMR (125 MHz, $CDCl_3$) δ 169.6, 144.78, 144.76, 132.8, 129.8, 127.9, 123.8, 81.5, 70.7, 70.6, 70.5, 70.48 (3C), 70.45 (10C), 70.41, 70.40, 70.38, 69.5, 69.4, 69.2, 68.9, 68.6, 64.5, 50.1, 28.0, 21.6; MS (ESI) m/z 896.45 $(M+H)^+$.

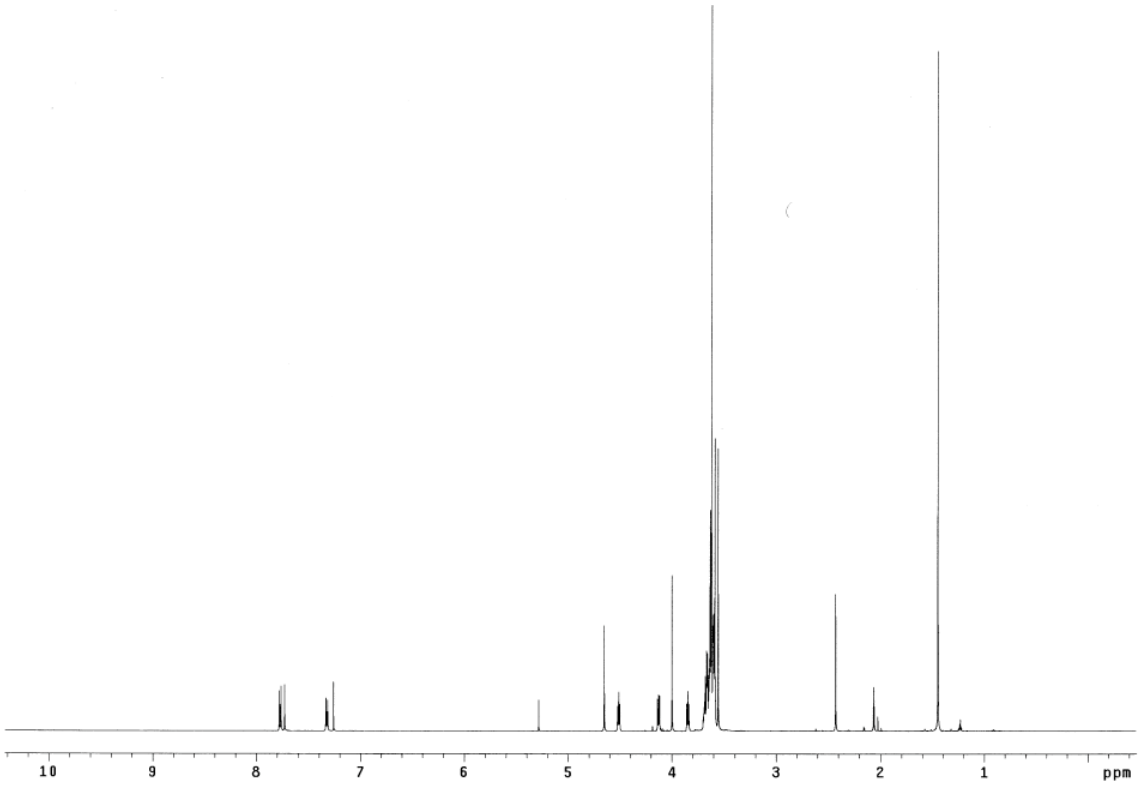

^{1}H NMR ($CDCl_3$)

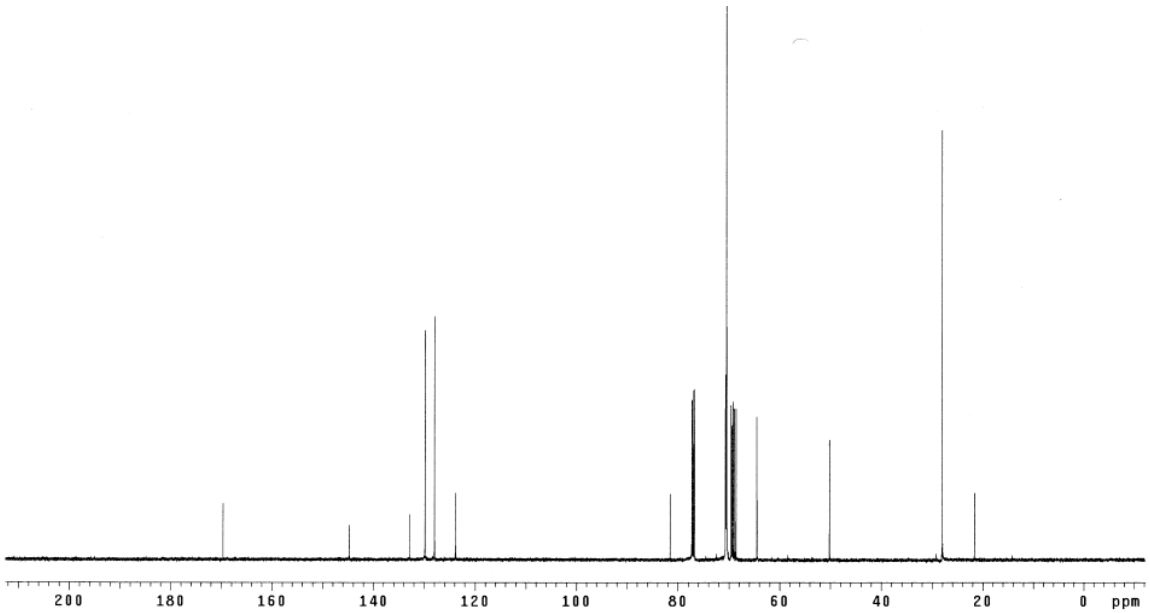

^{13}C NMR ($CDCl_3$)

Triazole-decorated oligoethylene glycol mono-azide (21)

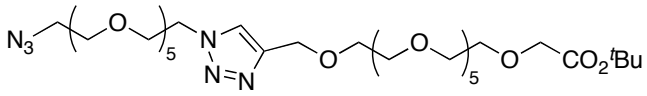

Sodium azide (0.46 g, 7.09 mmol) was added to a solution of triazole-decorated ethylene glycol **20** (1.27 g, 1.42 mmol) in CH_3CN (20 mL) and the reaction mixture was refluxed at 88 ºC for 48 h under nitrogen. The reaction mixture was cooled to room temperature and diluted with H_2O (25 mL). The aqueous layer was extracted with CH_2Cl_2 (5 x 20 mL) and the combined organic layer was dried over $MgSO_4$. The solvents were concentrated under the reduced pressure at below 40 ºC to afford pure product as a brown oil (1.04 g, 95 %). R_f 0.2 (50 % acetone/EtOAc with iodine stain). ^{1}H NMR (500 MHz, $CDCl_3$) δ 7.73 (s, 1H), 4.66 (s, 2H), 4.52 (t, 2H, J = 5.0 Hz), 4.01 (s, 2H), 3.86 (t, 2H, J = 5.0 Hz), 3.71-3.59 (m, 42H), 3.37 (t, 2H, J = 5.0 Hz), 1.46 (s, 9H); ^{13}C NMR (125 MHz, $CDCl_3$) δ 169.6, 144.8, 123.8, 81.5, 70.64, 70.63, 70.60, 70.55 (4C), 70.52 (6C), 70.49 (4C), 70.44, 70.41, 70.0, 69.6, 69.4, 69.0, 64.5, 50.6, 50.2, 28.1; MS (ESI) m/z 767.44 $(M+H)^+$.

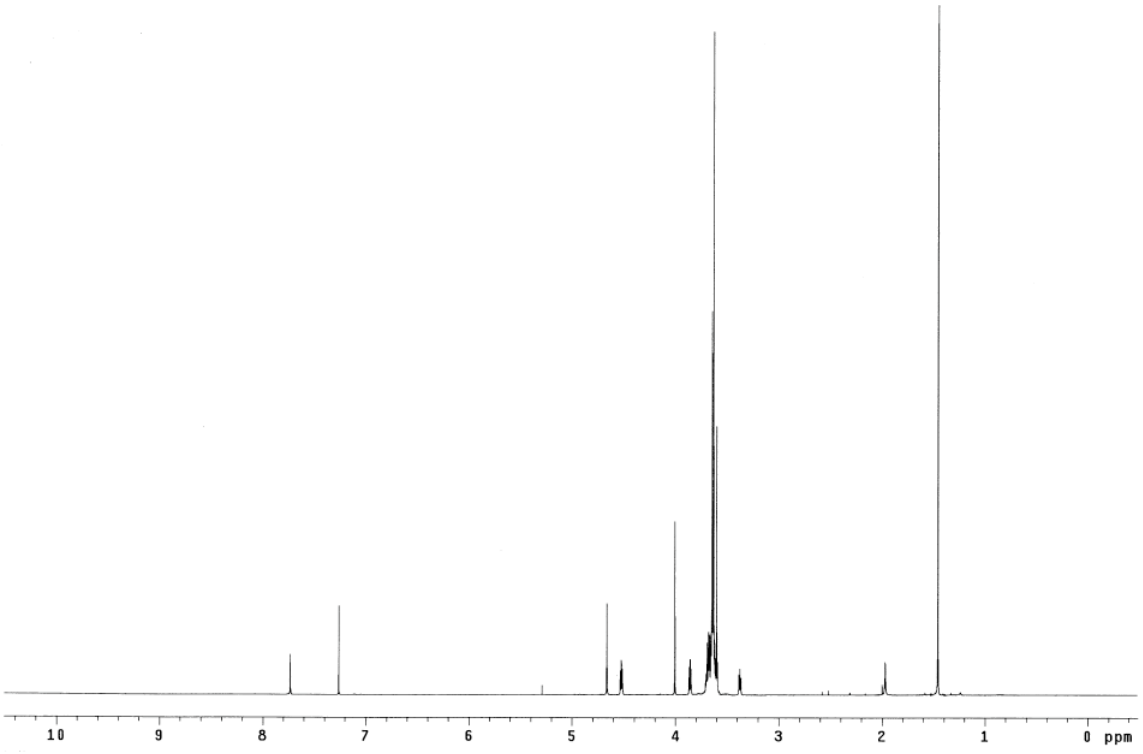

^{1}H NMR ($CDCl_3$)

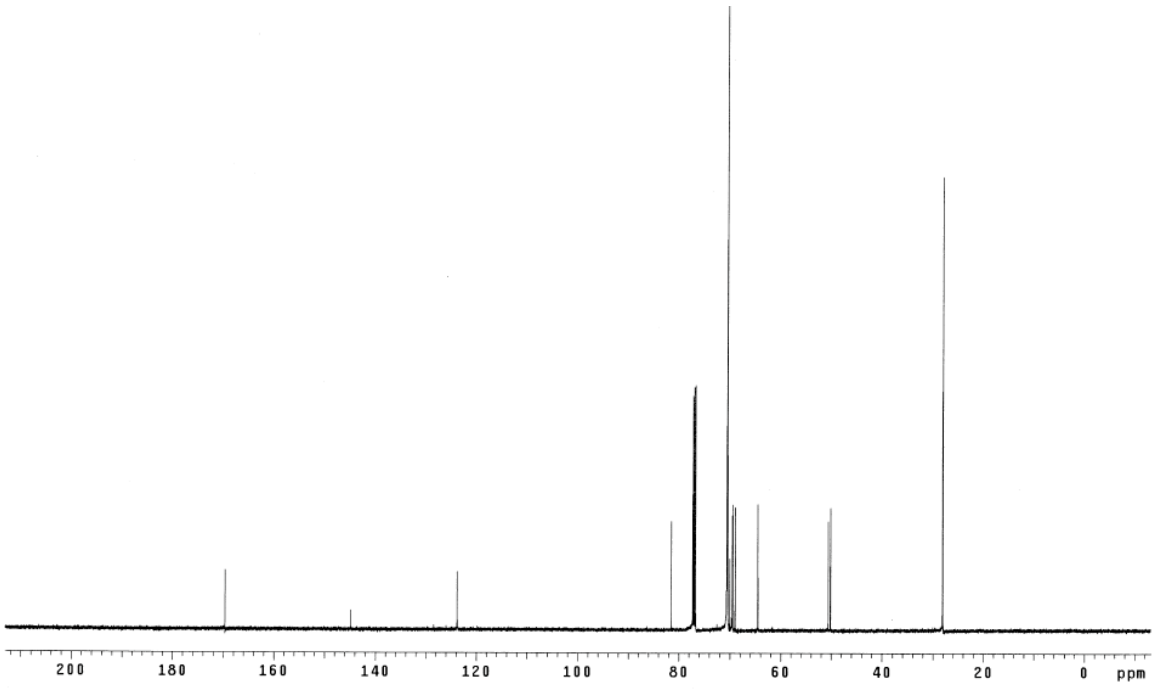

^{13}C NMR ($CDCl_3$)

Triazole-decorated oligoethylene glycol mono-carboxylic acid (14)

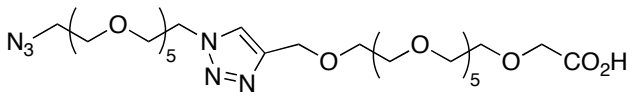

A solution of ethylene glycol *tert*-butyl ester **21** (700 mg, 0.91 mmol) in 1:1 TFA/CH_2Cl_2 (1.5 mL: 1.5 mL) was stirred at 25 ºC for 2h under nitrogen. The reaction mixture was flashed with nitrogen for overnight to remove TFA/CH_2Cl_2. Pure product was obtained as a brown oil (649 mg, 99 %). R_f 0.1 (50 % acetone/EtOAc with iodine stain). ^{1}H NMR (300 MHz, DMSO-d_6) δ 8.09 (s, 1H), 4.57-4.53 (m, 4H), 4.05 (s, 2H), 3.85 (t, 2H, J = 5.0 Hz), 3.65-3.47 (m, 42H), 3.42 (t, 2H, J = 5.0 Hz); ^{13}C NMR (75 MHz, DMSO-d_6) δ 172.6, 144.8, 125.2, 70.7 (16C), 70.64, 70.58, 70.5, 70.2, 69.9, 69.7, 68.5, 64.5, 50.9, 50.3; MS (ESI) m/z 711.37 $(M+H)^+$.

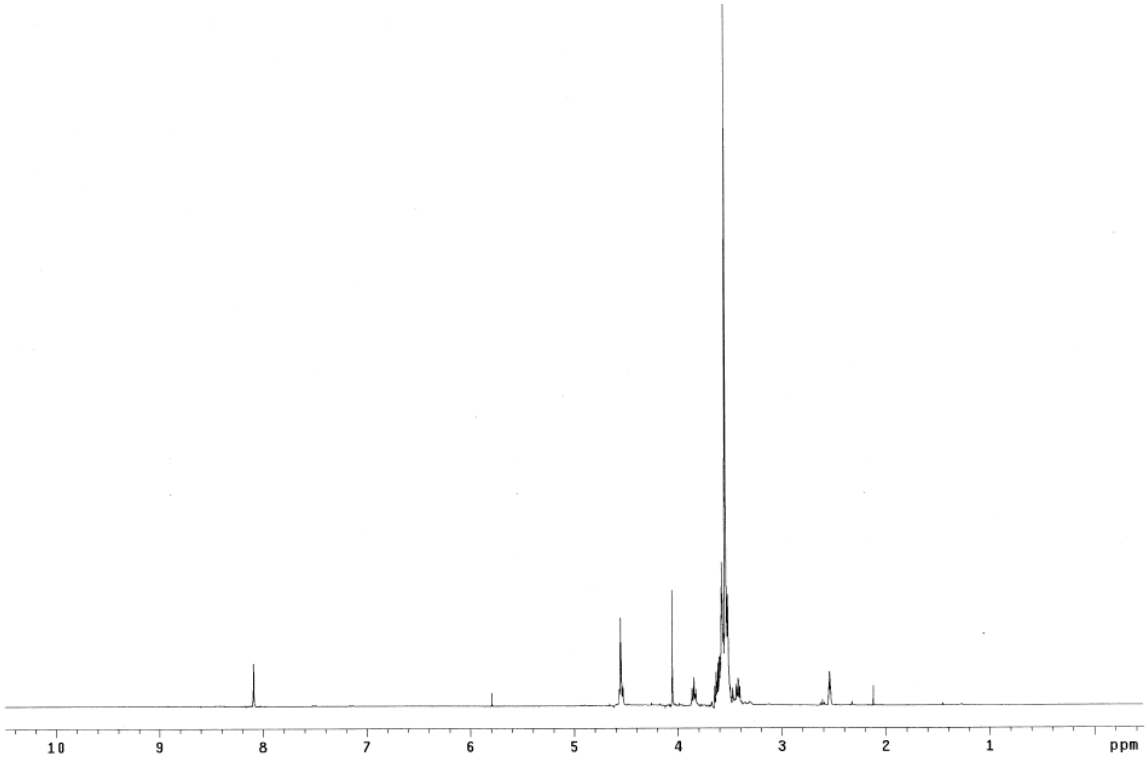

^{1}H NMR (DMSO-d_6)

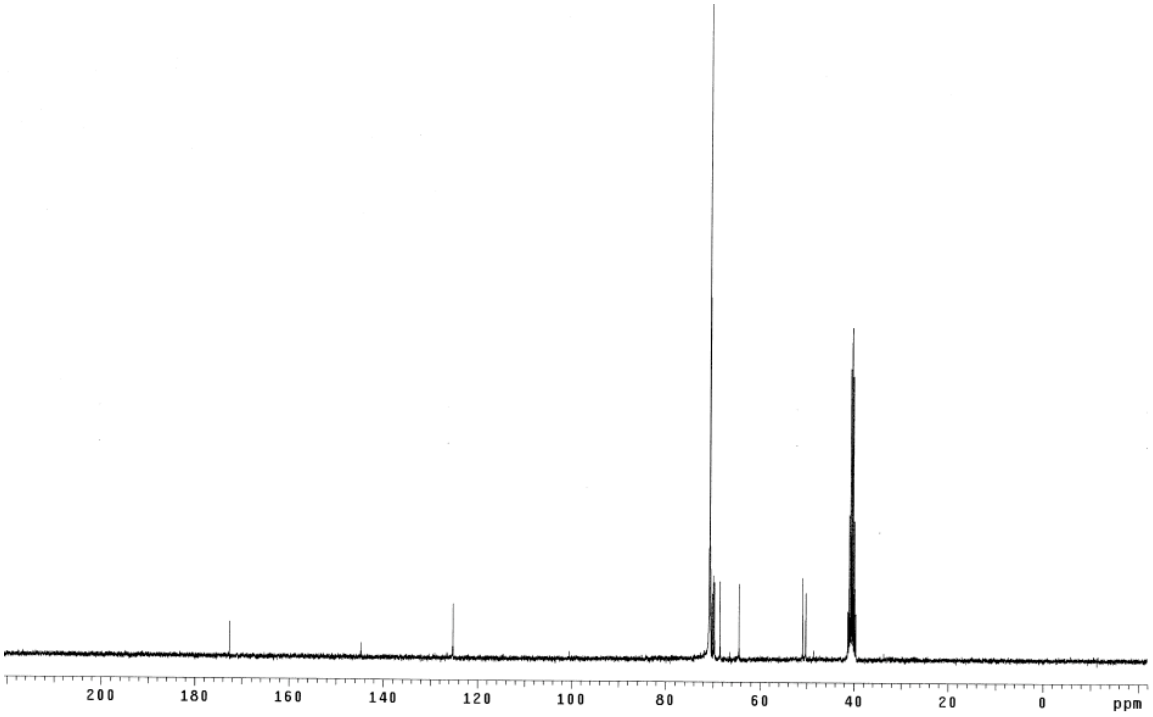

^{13}C NMR (DMSO-d_6)

Propargylated trifluoromethane-BODIPY (22)

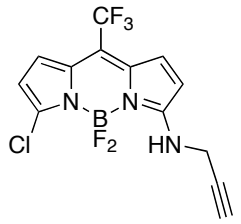

To a solution of dichloro-BODIPY **9**[57] (300 mg, 0.91 mmol) in CH_3CN (24 mL) was added propargyl amine (100 mg, 1.82 mmol) dissolved in CH_3CN (6.0 mL) dropwise at 25 ºC. The reaction mixture was stirred at 25 ºC for 30 min and the solvents were evaporated under the reduced pressure. The residual material was purified by short flash chromatography eluting with 10 to 20 % EtOAc/hexanes to afford product as a orange solid. R_f 0.5 (20 % EtOAc/hexanes). ^{1}H NMR (500 MHz, $CDCl_3$) δ 7.48 (d, 1H, J = 3.0 Hz), 6.95 (bs, 1H), 6.84 (s, 1H), 6.50 (d, 1H, J = 5.5 Hz), 6.27 (d, 1H, J = 4.0 Hz), 4.23 (dd, 2H, J = 6.0, 2.5 Hz), 2.44 (t, 1H, J = 2.5 Hz); ^{13}C NMR (125 MHz, $CDCl_3$) δ 162.7, 135.7, 132.8, 131.5, 126.9, 126.0, 123.8, 121.6, 120.5, 114.0, 76.7, 74.7, 34.4; MS (ESI) m/z 346.02 $(M–H)^–$.

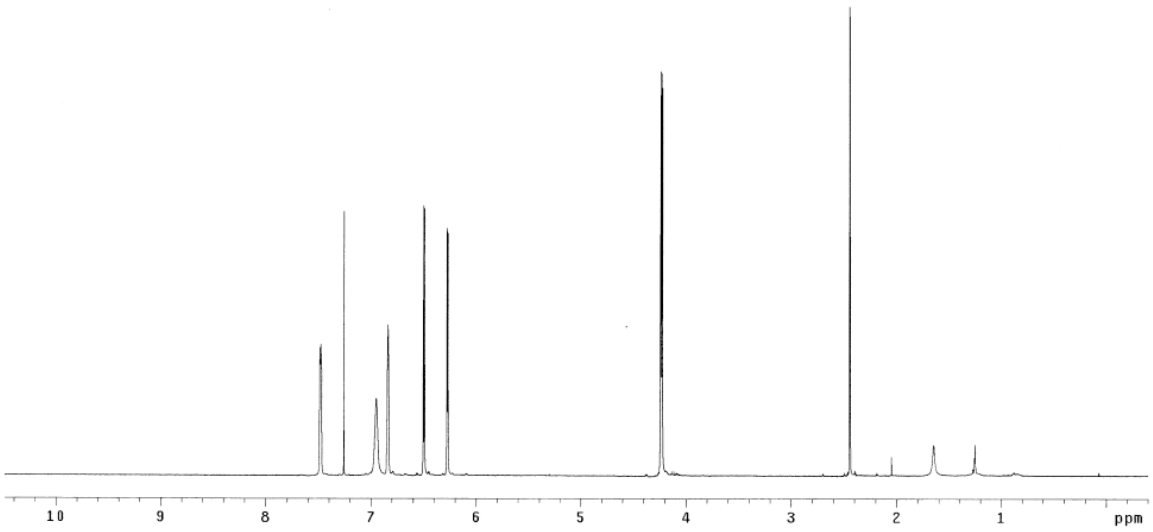

^{1}H NMR ($CDCl_3$)

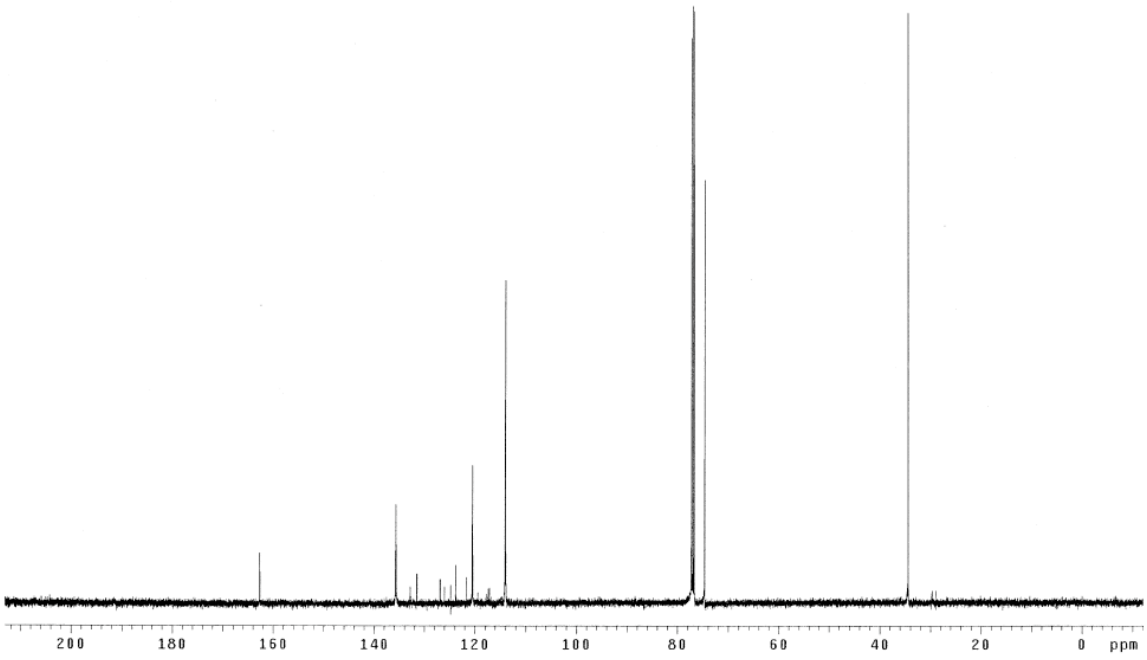

^{13}C NMR ($CDCl_3$)

Triazole-decorated oligoethylene glycol trifluoromethane-BODIPY (23)

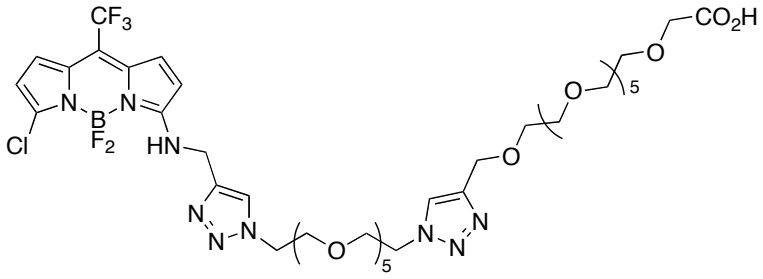

Copper powder (18 mg, 0.288 mmol), $CuSO_4$ (58 mL, 0.058 mmol, 1M in H_2O) and H_2O (10.0 mL) were added to a solution of mono-azido ethylene glycol **14** (245 mg, 0.345 mmol) and propargylated-BODIPY **22** (100 mg, 0.288 mmol) in THF (10.0 mL). The reaction mixture was stirred at 25 ºC for 24 h under nitrogen. The solvents were evaporated under the reduced pressure and the residual material was purified by flash chromatography eluting with 100 % EtOAc then 30 to 90 % MeOH/CH_2Cl_2 (columned 2 times) to afford product as a orange oil (233 mg, 76 %). R_f 0.2 (10 % MeOH/CH_2Cl_2 with iodine stain). ^{1}H NMR (500 MHz, CD_3OD) δ 8.01 (s, 1H), 7.87 (s, 1H), 7.33-7.31 (m, 1H), 6.87 (d, 1H, J = 5.5 Hz), 6.29 (t, 1H, J = 2.5 Hz), 6.08 (d, 1H, J = 4.0 Hz), 4.80 (s, 2H), 4.62 (s, 2H), 4.55 (t, 4H, J = 5.0 Hz), 3.89 (s, 2H), 3.86 (q, 4H, J = 5.0 Hz), 3.67-3.61 (m, 24H), 3.59-3.51 (m, 16H); ^{13}C NMR (125 MHz, $CDCl_3$) δ 174.3, 163.4, 144.6, 143.2, 135.3, 133.7, 129.1, 126.5, 124.4, 124.1, 124.0, 118.5, 116.4, 113.1, 70.50, 70.43 (3C), 70.40 (3C), 70.34 (3C), 70.28 (2C), 70.26, 70.11, 69.99, 69.84, 69.78, 69.61, 69.59, 69.50, 69.39, 69.32, 69.28, 69.16, 64.3, 50.3, 50.1, 40.2; MS (MALDI) m/z 1080.29 $(M+Na)^+$.

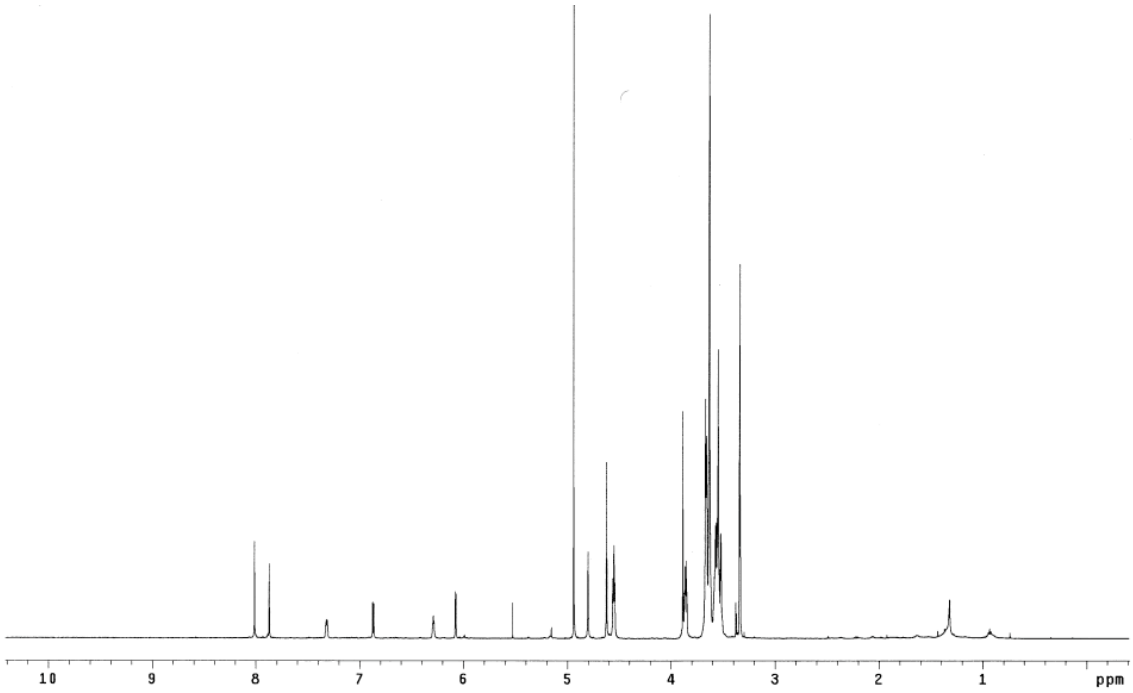

^{1}H NMR (CD_3OD)

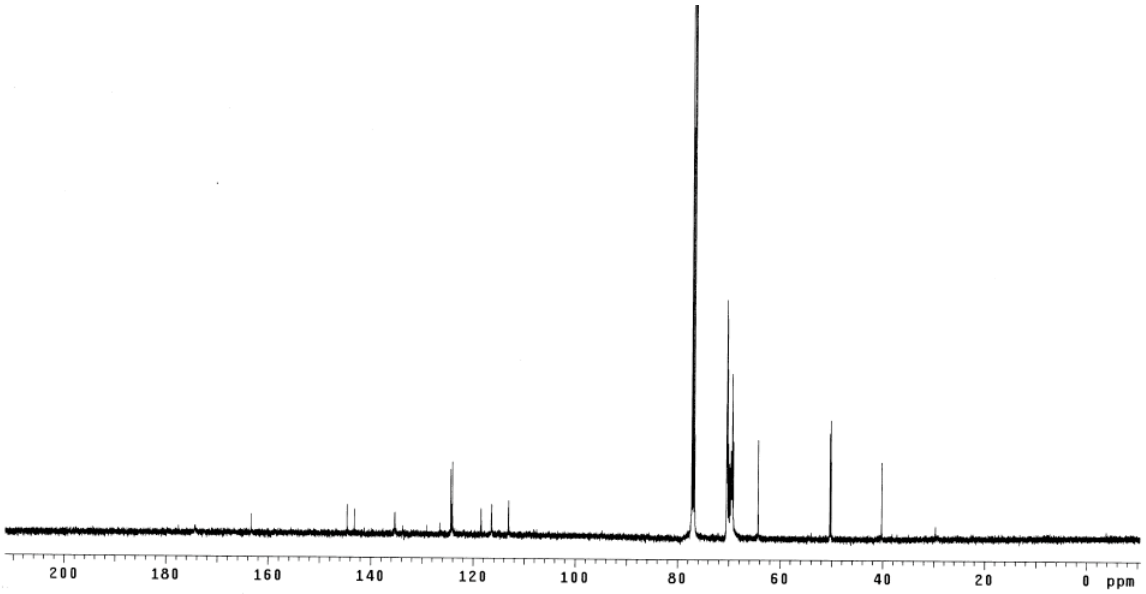

^{13}C NMR ($CDCl_3$)

Mono-silylated triethylene glycol (38)[85]

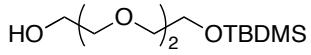

To a solution of triethylene glycol (10.0 g, 66.6 mmol) and *t*-butyldimethylsilyl chloride (11.0 g, 73.3 mmol) in CH_2Cl_2 (100 mL) was added DMAP (0.81 g, 6.66 mmol) and Et_3N (10.2 ml, 73.3 mmol) at 0 ºC. The reaction mixture was stirred at 0 ºC for 10 min and then warmed up to 25 ºC and stirred for 12 h. The reaction mixture was concentrated under reduced pressure and the residual material was purified by flash chromatography eluting with 20–50 % EtOAc/hexanes to afford triethylene glycol mono-TBDMS (8.9 g, 51 %) as a pale blue liquid. R_f 0.5 (50 % EtOAc/hexanes, iodine stain). ^{1}H NMR (500 MHz, $CDCl_3$) δ 3.76 (t, 2H, J = 4.7 Hz), 3.73–3.70 (m, 2H), 3.65 (t, 4H, J = 0.6 Hz), 3.60 (t, 2H, J = 4.7 Hz), 3.55 (t, 2H, J = 5.7 Hz), 0.88 (s, 9H), 0.05 (s, 6H); ^{13}C NMR (125 MHz, $CDCl_3$) δ 72.6, 72.4, 70.7, 70.4, 62.6, 61.7, 25.9, 18.3, –5.3; MS (CI) m/z 265.1 $(M+H)^+$.

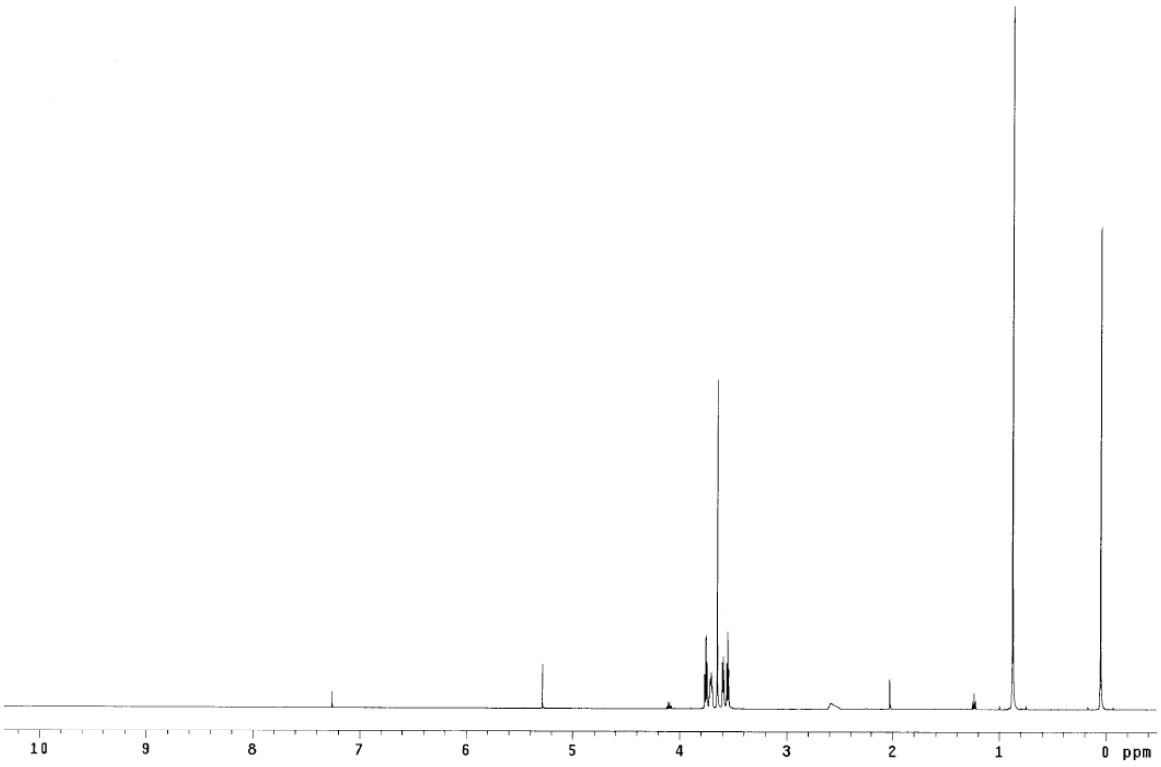

^{1}H NMR ($CDCl_3$)

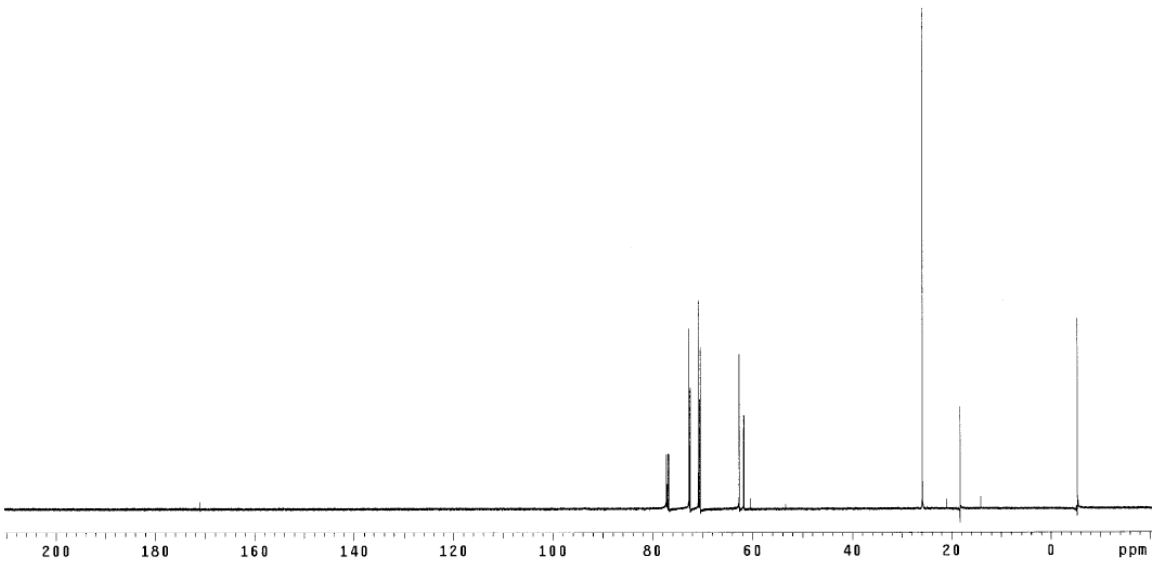

^{13}C NMR ($CDCl_3$)

Mono-silylated triethylene glycol tosylate (39)[86]

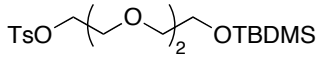

To a solution of triethylene glycol mono-TBDMS **38** (3.0 g, 11.3 mmol), Et_3N (3.2 mL, 22.7 mmol) and Me_3N•HCl (0.11 g, 1.13 mmol) in CH_3CN (15 mL) was added *p*-toluenesulfonyl chloride (3.24 g, 17.0 mmol) in CH_3CN (10 mL) dropwise at 0 ºC over 5 min. This solution was stirred at 25 ºC for 12 h and the reaction was quenched by the addition of water (15 mL). The aqueous phase was extracted with EtOAc (3 x 20 mL) and the combined organic layer was dried over Na_2SO_4, concentrated under reduced pressure. The residual material was purified by flash chromatography eluting with 10–30 % EtOAc/hexanes to afford compound (4.4 g, 92 %) as a colorless liquid. R_f 0.4 (20 % EtOAc/hexanes). ^{1}H NMR (500 MHz, $CDCl_3$) δ 7.79 (d, 2H, J = 8.2 Hz), 7.33 (d, 2H, J = 8.2 Hz), 4.15 (t, 2H, J = 4.9 Hz), 3.73 (t, 2H, J = 5.4 Hz), 3.68 (t, 2H, J = 4.9 Hz), 3.60–3.54 (m, 4H), 3.51 (t, 2H, J = 5.4 Hz), 2.43 (s, 3H), 0.87 (s, 9H), 0.04 (s, 6H); ^{13}C NMR (125 MHz, $CDCl_3$) δ 144.7, 132. 9, 129.8, 127.9, 72.6, 70.7, 70.6, 69.2, 68.6, 62.6, 25.9, 21.6, 18.3, –5.3; MS (CI) m/z 419.2 $(M+H)^+$.

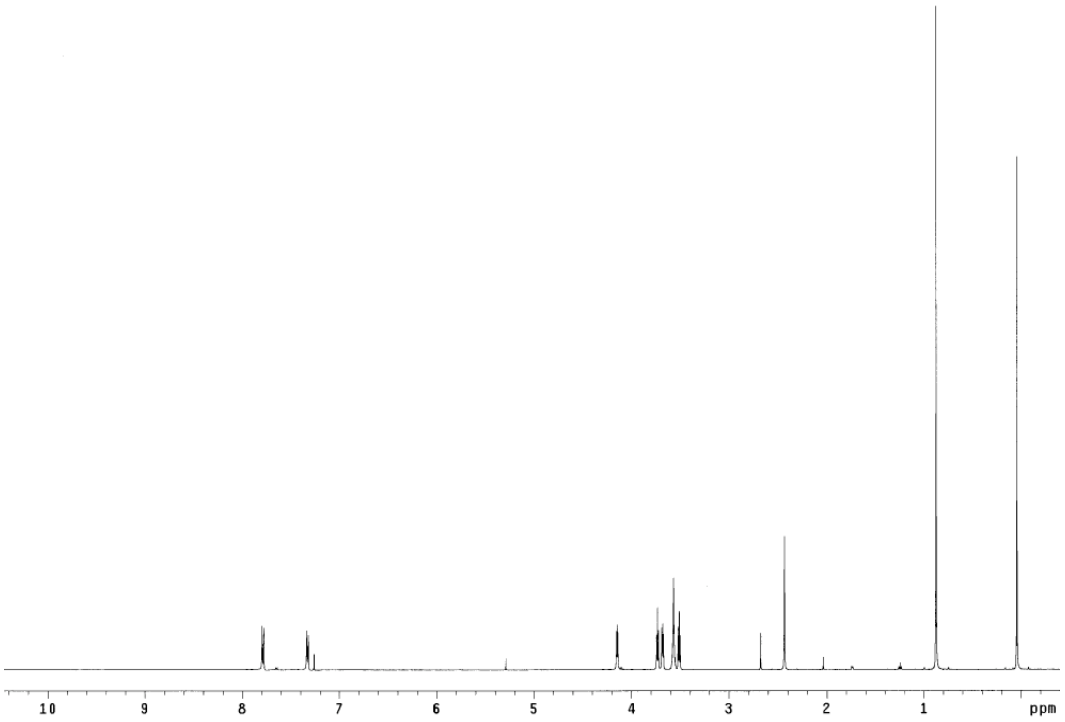

^{1}H NMR ($CDCl_3$)

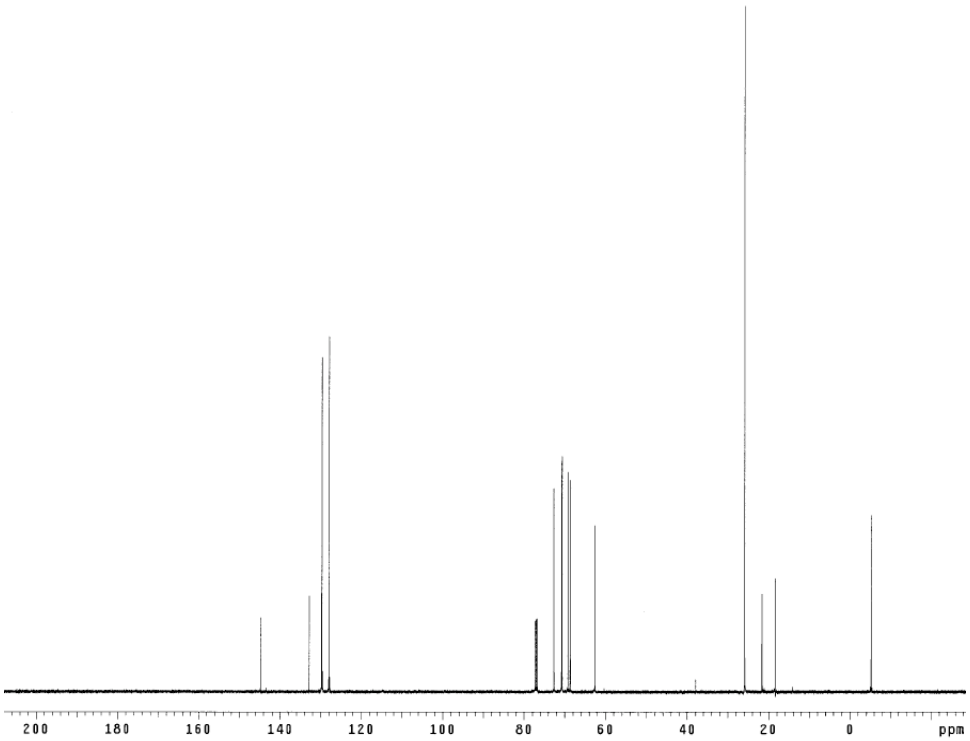

^{13}C NMR ($CDCl_3$)

TBDMS-protected naphthol derivative (40)

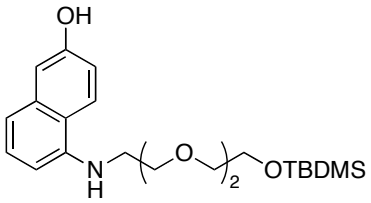

A solution of 5-amino-2-naphthol (0.31 g, 1.95 mmol), tosylated-silylated triethylene glycol **39** (1.47 g, 3.51 mmol) and K_2CO_3 (0.54 g, 3.90 mmol) in DMF (15 mL) was heated at 100 ºC for 7 h. This solution was cooled to room temperature and water (20 mL) was added. The aqueous layer was extracted with EtOAc (4 x 12 mL) and the combined organic layer was dried over Na_2SO_4 and concentrated under reduced pressure. The residual material was purified by flash chromatography eluting with 10–20 % EtOAc/hexanes to afford product (0.61 g, 77 %) as a colorless viscous oil. R_f 0.4 (30 % EtOAc/hexanes). ^{1}H NMR (500 MHz, $CDCl_3$) δ 7.73 (d, 1H, J = 9.0 Hz), 7.24 (t, 1H, J = 7.7 Hz), 7.19 (d, 1H, J = 8.3 Hz), 7.14 (dd, 1H, J = 9.0, 2.5 Hz), 7.09 (d, 1H, J = 2.5 Hz), 6.65 (dd, 1H, J = 7.2, 1.1 Hz), 4.24 (t, 2H, J = 4.9 Hz), 3.93 (t, 2H, J = 4.9 Hz), 3.79–3.74 (m, 4H), 3.72–3.70 (m, 2H), 3.58 (t, 2H, J = 5.5 Hz), 0.89 (s, 9H), 0.07 (s, 6H); ^{13}C NMR (125 MHz, $CDCl_3$) δ 156.7, 142.0, 135.7, 127.0, 122.4, 119.0, 118.1, 117.7, 108.1, 107.4, 72.7, 70.9, 70.8, 69.7, 67.3, 62.7, 25.9, 18.4, –5.3; MS (ESI) m/z 406.26 $(M+H)^+$.

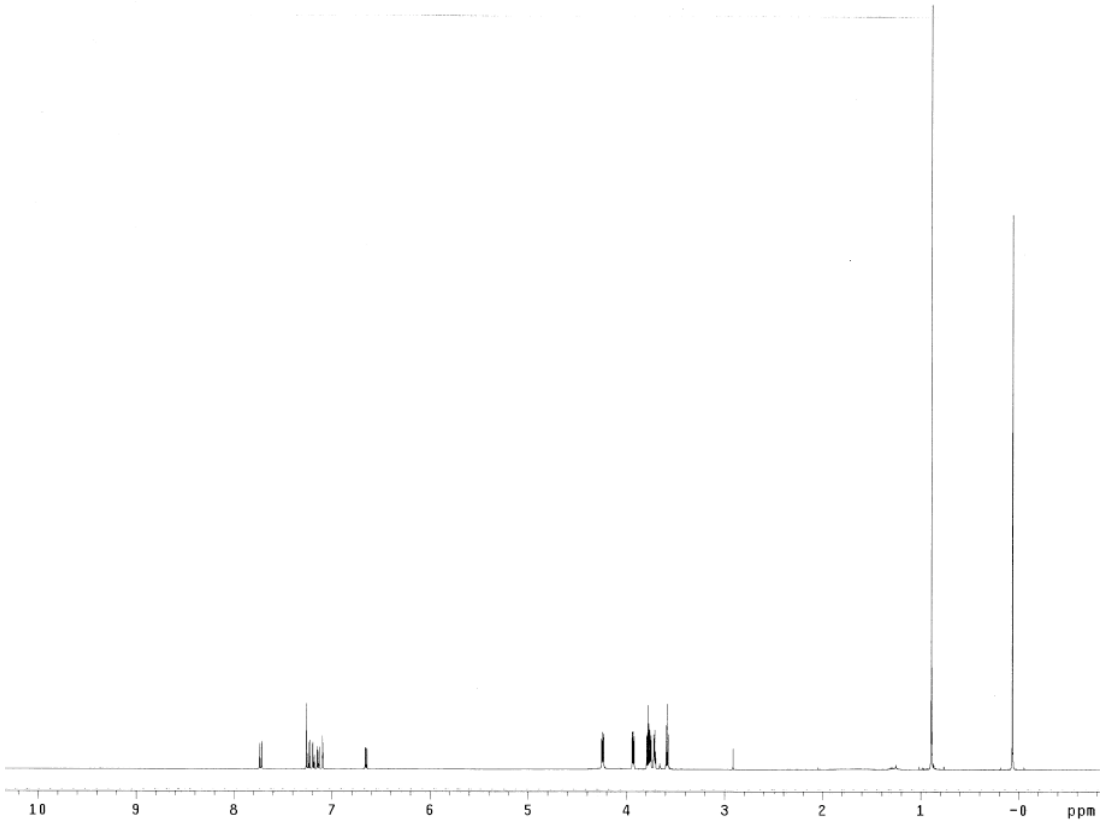

^{1}H NMR ($CDCl_3$)

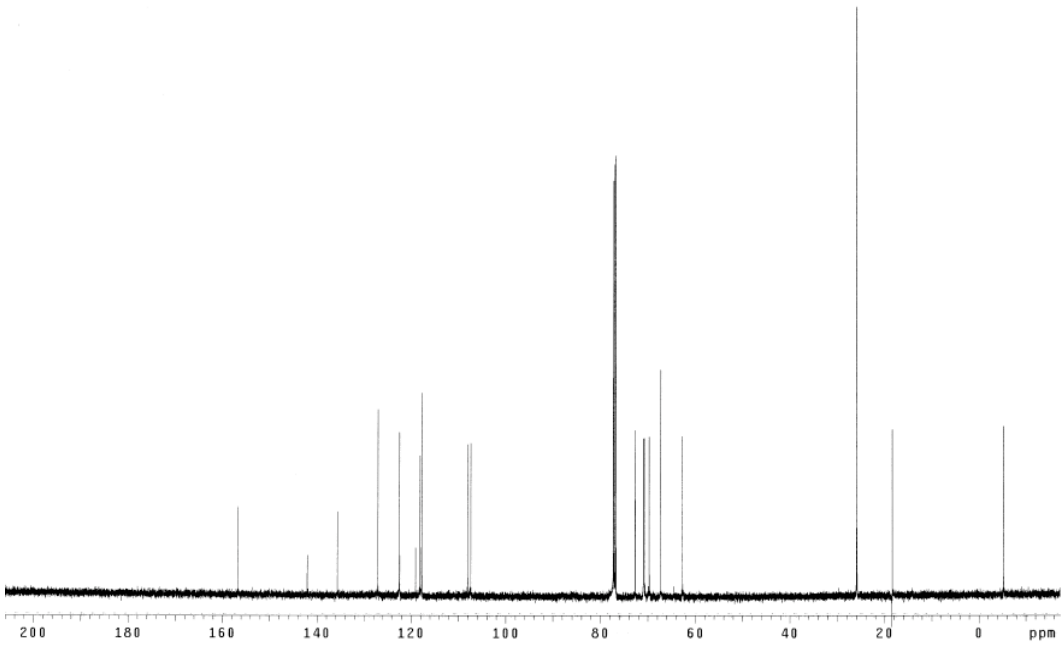

^{13}C NMR ($CDCl_3$)

Naphthol derivative (37b)

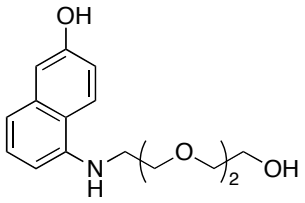

To a solution of TBDMS-protected amino-naphthol **40** (0.61 g, 1.5 mmol) in THF (10 mL) was added TBAF (1.8 mL, 1.8 mmol, 1.0 M in THF) dropwise at 0 ºC. This solution was warmed up to 25 ºC and stirred for 1 h. The reaction mixture was concentrated under reduced pressure at 35 ºC. The residual material was purified by flash chromatography eluting with 80 % EtOAc/hexanes then with 100 % EtOAc to afford product (0.43 g, 98 %) as a gray viscous oil. R_f 0.4 (EtOAc). ^{1}H NMR (500 MHz, $CDCl_3$) δ 7.72 (d, 1H, J = 9.2 Hz), 7.24 (t, 1H, J = 7.7 Hz), 7.18 (d, 1H, J = 8.3 Hz), 7.13 (dd, 1H, J = 9.2, 2.6 Hz), 7.09 (d, 1H, J = 2.4 Hz), 6.64 (dd, 1H, J = 7.3, 1.2 Hz), 4.24 (t, 2H, J = 4.8 Hz), 3.92 (t, 2H, J = 4.8 Hz), 3.77–3.71 (m, 6H), 3.62 (t, 2H, J = 4.5 Hz); ^{13}C NMR (125 MHz, $CDCl_3$) δ 156.6, 142.1, 135.6, 127.0, 122.5, 119.0, 118.0, 117.5, 108.0, 107.4, 72.5, 70.8, 70.3, 69.7, 67.2, 61.7; MS (ESI) m/z 292.15 $(M+H)^+$.

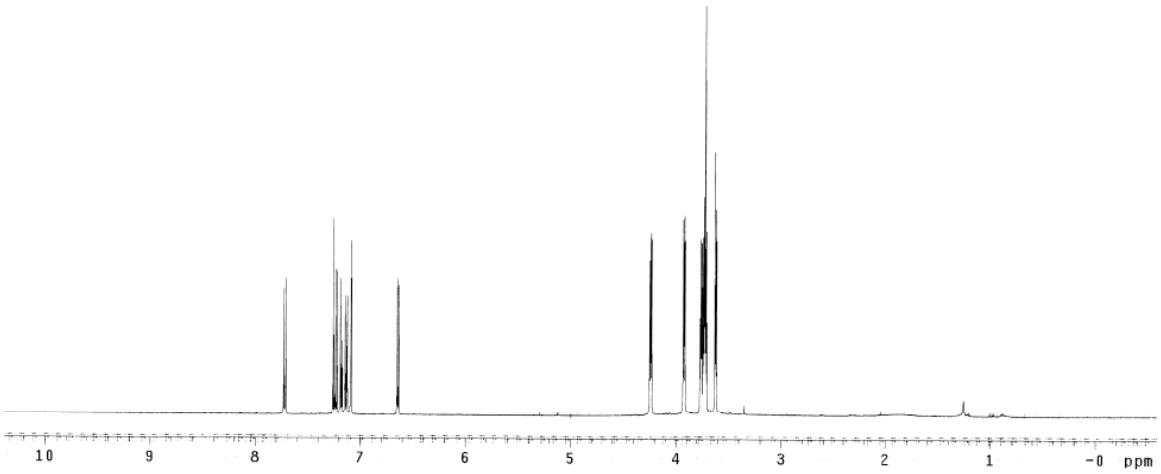

^{1}H NMR ($CDCl_3$)

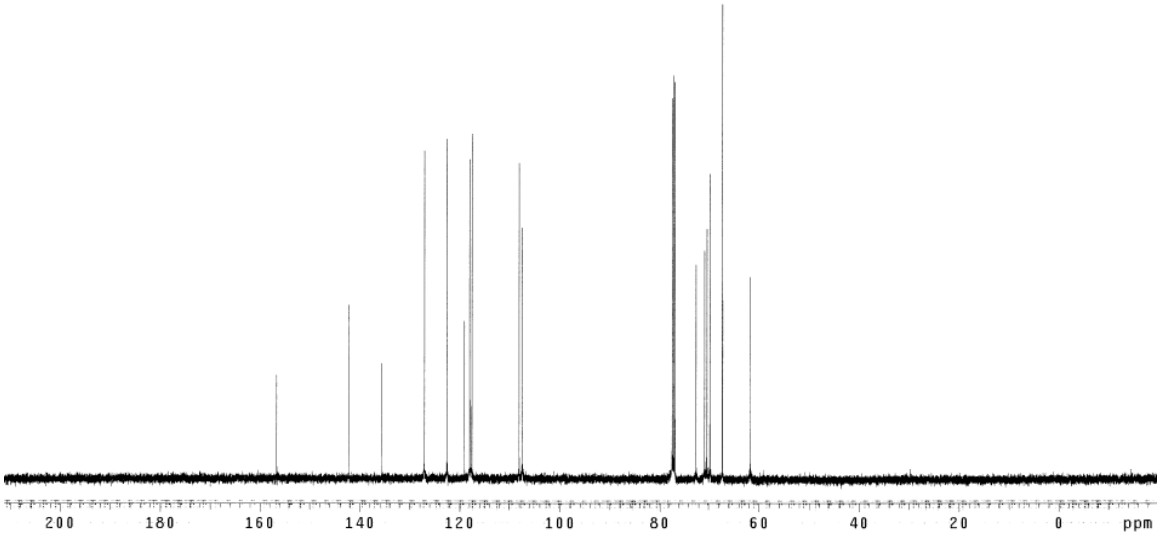

^{13}C NMR ($CDCl_3$)

APPENDIX B

EXPERIMENTAL DATA FOR CHAPTER III

4-Iodo-2-methoxymethylbenzoate (50)

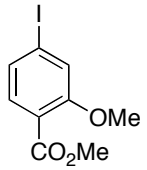

A solution of 2-hydroxy-4-iodobenzoic acid (4.0 g, 15.2 mmol), iodomethane (9.7 g, 68.2 mmol) and K_2CO_3 (9.4 g, 68.2 mmol) in acetone (90 mL) was refluxed at 60 ºC for 20 h. The reaction mixture was cooled to room temperature, filtered and the solvents were concentrated under the reduced pressure. Water (50 mL) was added and aqueous layer was extracted with EtOAc (1 x 40 mL). The organic layer was washed with sat. $NaHCO_3$ (1 x 40 mL) and brine (1 x 40 mL) and dried over Na_2SO_4. The solvents were evaporated and the residue was purified by flash chromatography eluting with 10 % EtOAc/hexanes to afford product as a yellow oil (4.0 g, 91 %). R_f 0.5 (20 % EtOAc/hexanes). ^{1}H NMR (500 MHz, $CDCl_3$) δ 7.48 (d, 1H, J = 8.1 Hz), 7.33 (d, 1H, J = 8.1 Hz), 7.30 (s, 1H), 3.88 (s, 3H), 3.86 (s, 3H); ^{13}C NMR (125 MHz, $CDCl_3$) δ 166.0, 159.1, 132.7, 129.4, 121.5, 119.4, 100.0, 56.2, 52.1; MS (ESI) m/z 292.97 $(M+H)^+$.

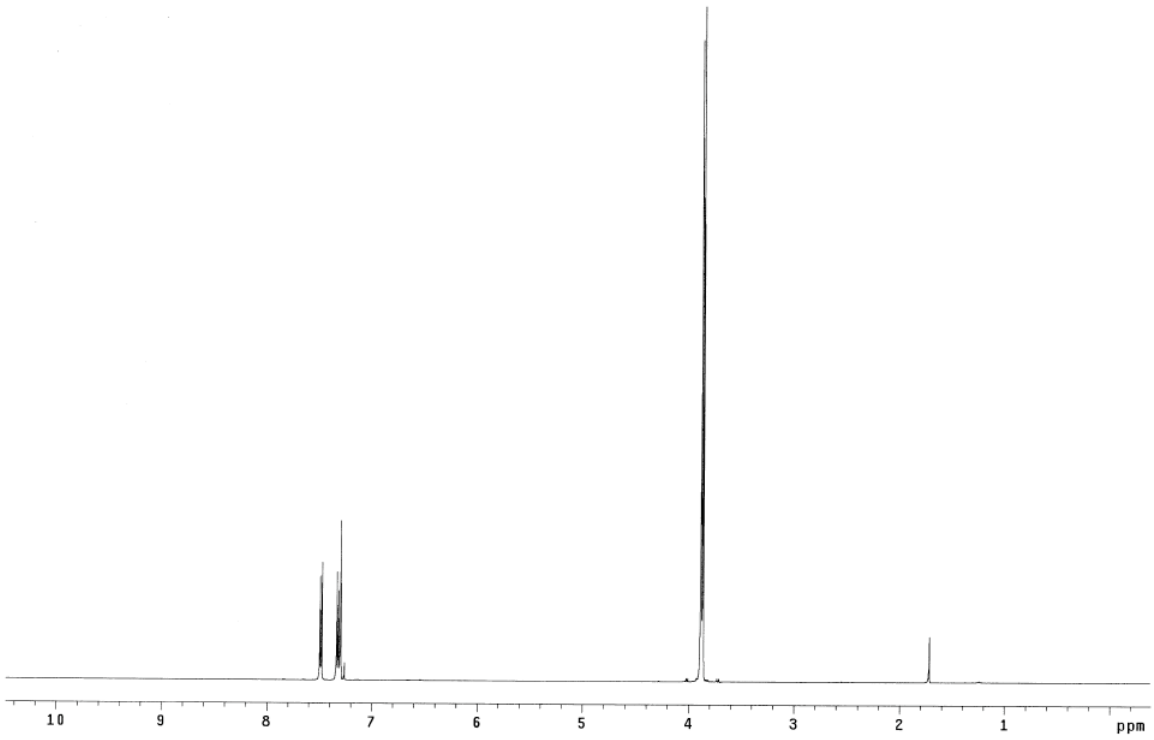

^{1}H NMR ($CDCl_3$)

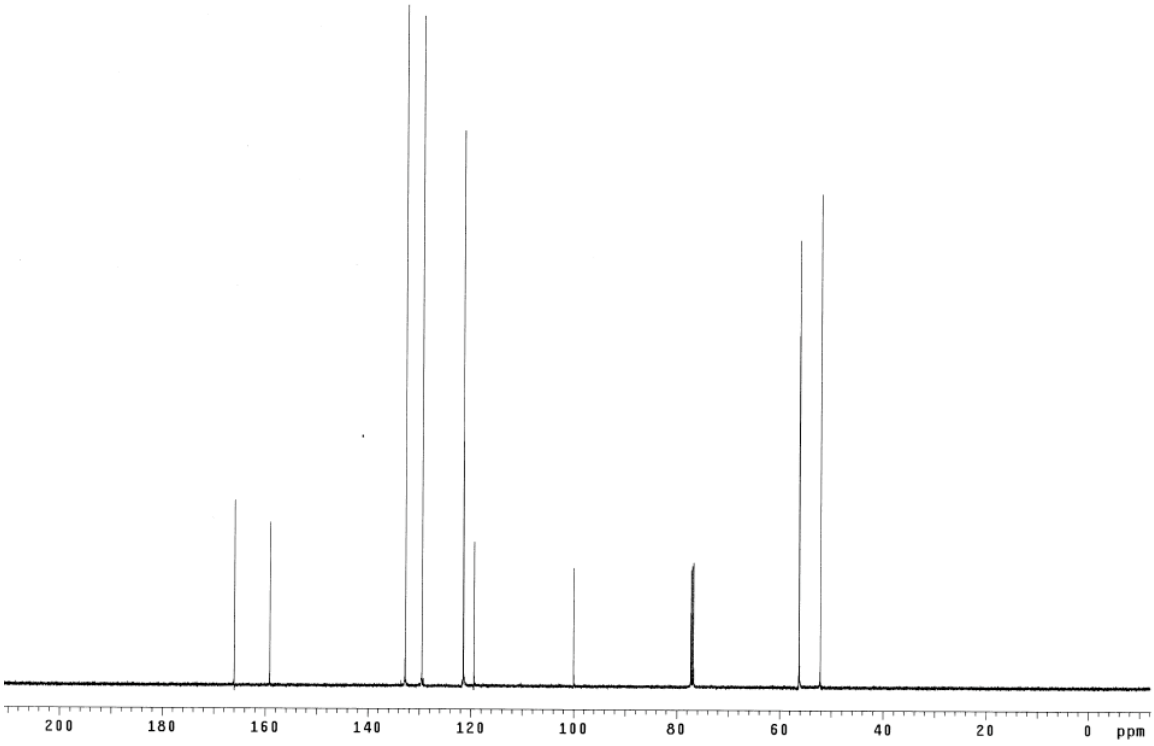

^{13}C NMR ($CDCl_3$)

4-Iodo-2-methoxybenzylalcohol (51)

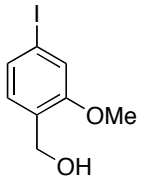

To a solution of methyl ester **50** (3.3 g, 11.2 mmol) in THF (70 mL) was added DIBAL (33.7 mL, 33.7 mmol) dropwise at –78 ºC. The reaction mixture was stirred at 25 ºC for 13 h. The reaction was quenched by the slow addition of sat. NH_4Cl at 0 ºC. The reaction mixture was filtered and aqueous layer was extracted with EtOAc (5 x 250 mL). The combined organic layer was dried over Na_2SO_4 and concentrated under the reduced pressure to afford pure product as a colorless oil (2.9 g, 98 %). R_f 0.5 (30 % EtOAc/hexanes). ^{1}H NMR (300 MHz, $CDCl_3$) δ 7.29 (dd, 1H, J = 8.0, 1.5 Hz), 7.17 (d, 1H, J = 1.5 Hz), 7.00 (d, 1H, J = 8.0 Hz), 4.61 (s, 1H), 3.84 (s, 3H); ^{13}C NMR (125 MHz, $CDCl_3$) δ 157.7, 129.9, 129.8, 128.8, 119.5, 93.2, 61.3, 55.5; MS (ESI) m/z 270.98 $(M+Li)^+$.

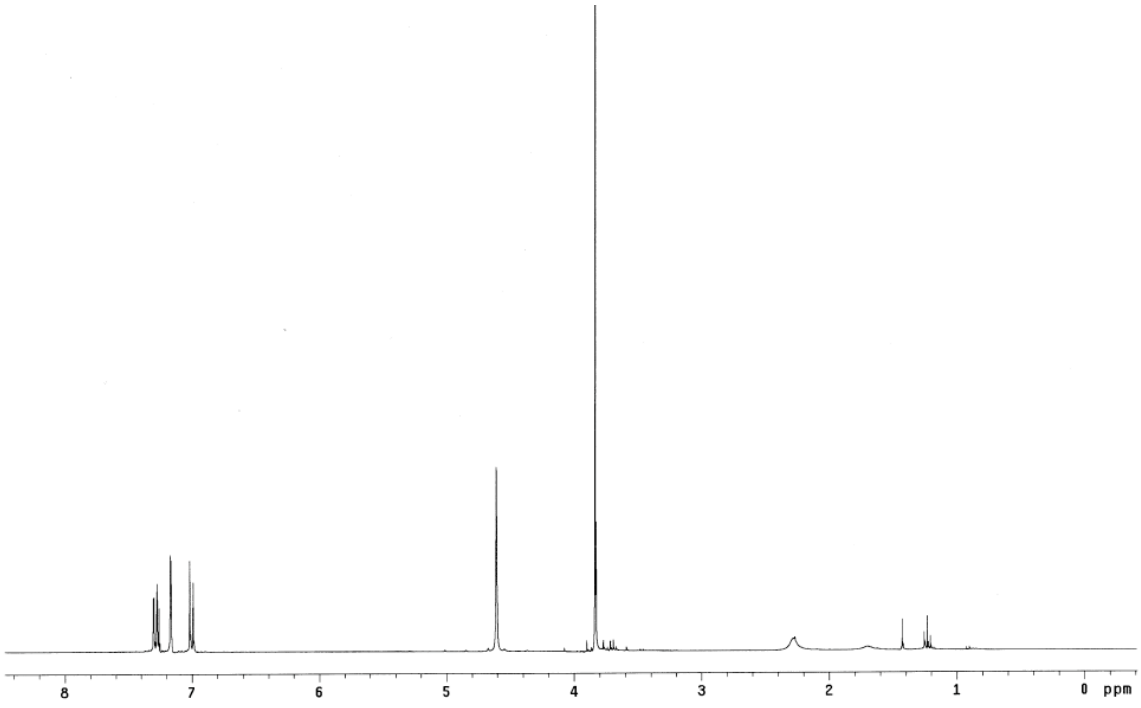

^{1}H NMR ($CDCl_3$)

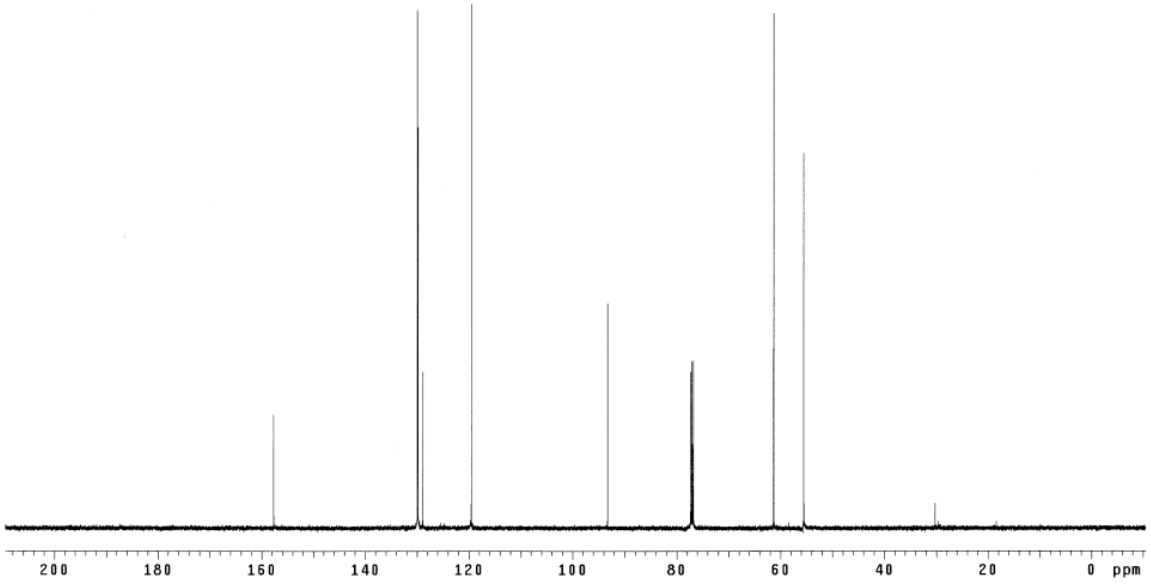

^{13}C NMR ($CDCl_3$)

4-Iodo-2-methoxybenzaldehyde (52)

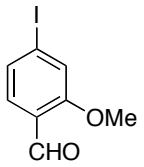

To a slurry of pyridinium chlorochromate (2.7 g, 12.5 mmol) in CH_2Cl_2 (70 mL) was added a solution of alcohol **51** (2.2 g, 8.3 mmol) in CH_2Cl_2 (20 mL) dropwise at 25 ºC. The reaction mixture was stirred at 25 ºC for 2 h. The reaction mixture was filtered through celite and washed with ether. The solvents were concentrated under the reduced pressure and the residue was purified by flash chromatography eluting with 10 % EtOAc/hexanes to afford product as an off-white solid (2.0 g, 91 %). R_f 0.8 (20 % EtOAc/hexanes). ^{1}H NMR (500 MHz, $CDCl_3$) δ 10.40 (s, 1H), 7.51 (d, 1H, J = 8.0 Hz), 7.41 (dd, 1H, J = 8.0, 1.5 Hz), 7.36 (d, 1H, J = 1.5 Hz), 3.92 (s, 3H); ^{13}C NMR (125 MHz, $CDCl_3$) δ 189.1, 161.4, 130.3, 129.5, 124.2, 121.3, 103.4, 56.0; MS (ESI) m/z 262.95 $(M+H)^+$.

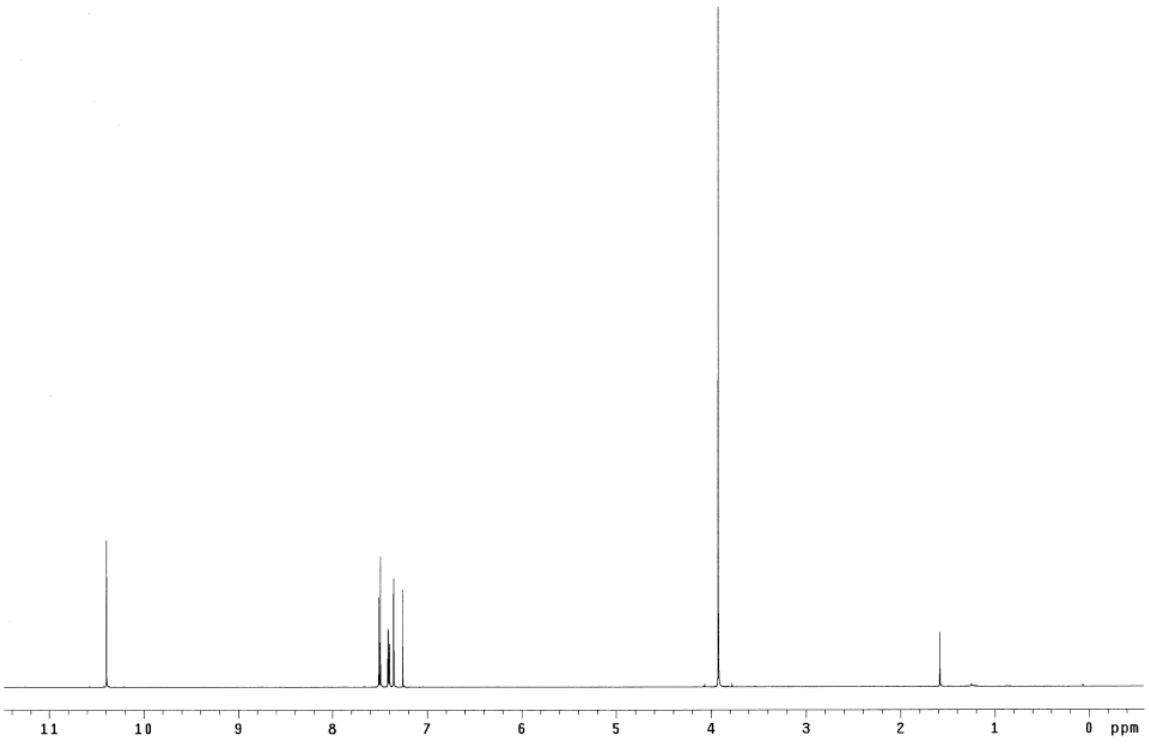

^{1}H NMR ($CDCl_3$)

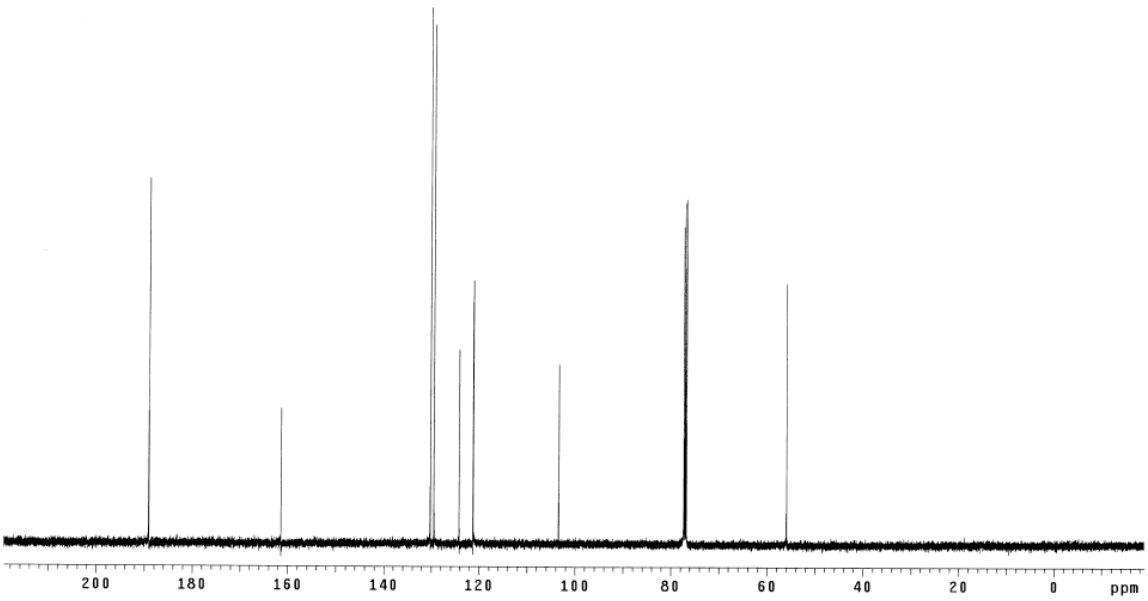

^{13}C NMR ($CDCl_3$)

4-Iodo-2-methoxy tetramethyl-BODIPY (53)

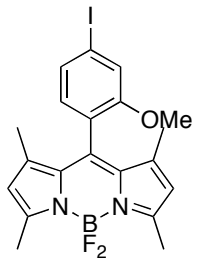

A solution of aldehyde **52** (1.3 g, 5.0 mmol), 2,4-dimethylpyrrole (1.1 g, 11.0 mmol) and one drop of TFA in CH_2Cl_2 (30 mL) was stirred at 25 ºC under nitrogen for 1.5 h. Then chloranil (1.5 g, 6.0 mmol) was added to a reaction mixture and the reaction was stirred at 25 ºC for 40 min under air. The reaction mixture was filtered through celite and washed with CH_2Cl_2 and the solvents were evaporated. The residue was purified by flash chromatography (aluminum oxide, activated, basic) eluting with CH_2Cl_2 and 10 % EtOAc/CH_2Cl_2. The obtained orange solids were dissolved in toluene (20 mL) and Et_3N (2.1 mL, 150 mmol) was added and stirred at 25 ºC for 10 min. BF_3•Et_2O (3.2 mL, 25.0 mmol) was added and stirred at 25 ºC for 20 h. The reaction mixture was diluted with CH_2Cl_2 (30 mL) and washed with water (3 x 30 mL). The organic layer was dried over Na_2SO_4 and evaporated. The residue was purified by flash chromatography eluting with 5 % EtOAc/hexanes to afford product as a orange solid (813 mg, 34 %). R_f 0.5 (10 % EtOAc/hexanes). ^{1}H NMR (500 MHz, $CDCl_3$) δ 7.44 (dd, 1H, J = 8.0, 1.5 Hz), 7.31 (d, 1H, J = 1.5 Hz), 6.87 (d, 1H, J = 8.0 Hz), 5.97 (s, 2H), 3.76 (s, 3H), 2.54 (s, 6H), 1.46 (s, 6H); ^{13}C NMR (125 MHz, $CDCl_3$) δ 156.8, 155.2, 142.3, 137.3, 131.2, 130.8, 130.7, 123.6, 121.0, 120.6, 95.2, 55.9, 14.5, 14.0; MS (MALDI) m/z 479.76 $(M)^+$.

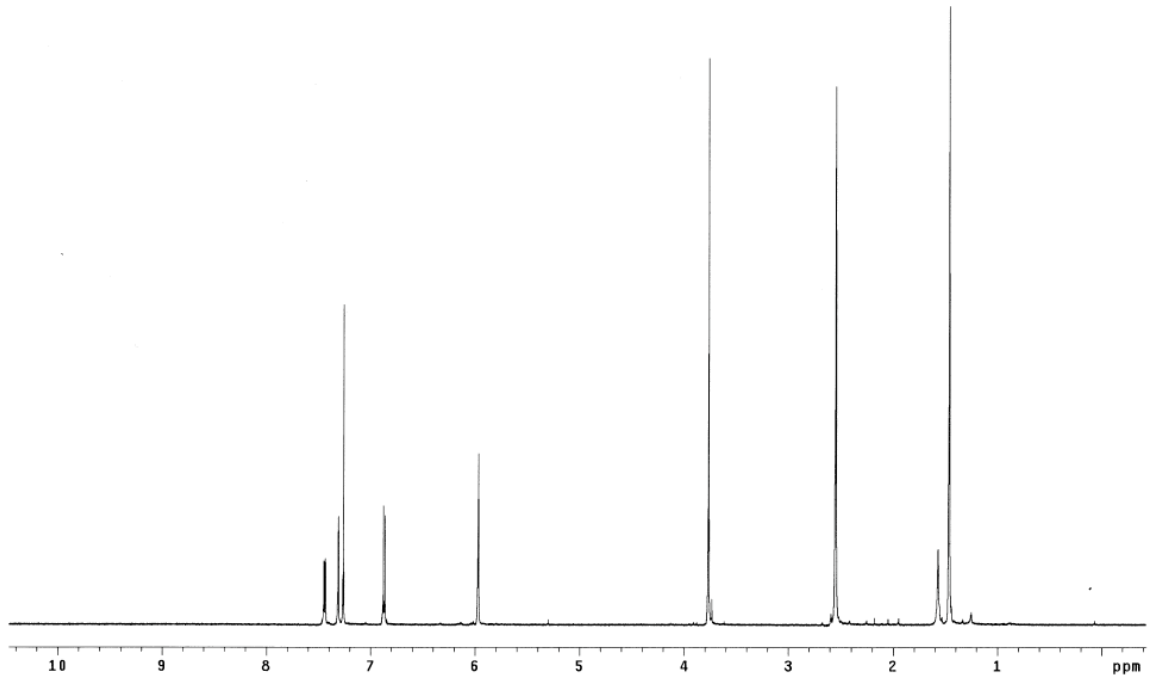

^{1}H NMR ($CDCl_3$)

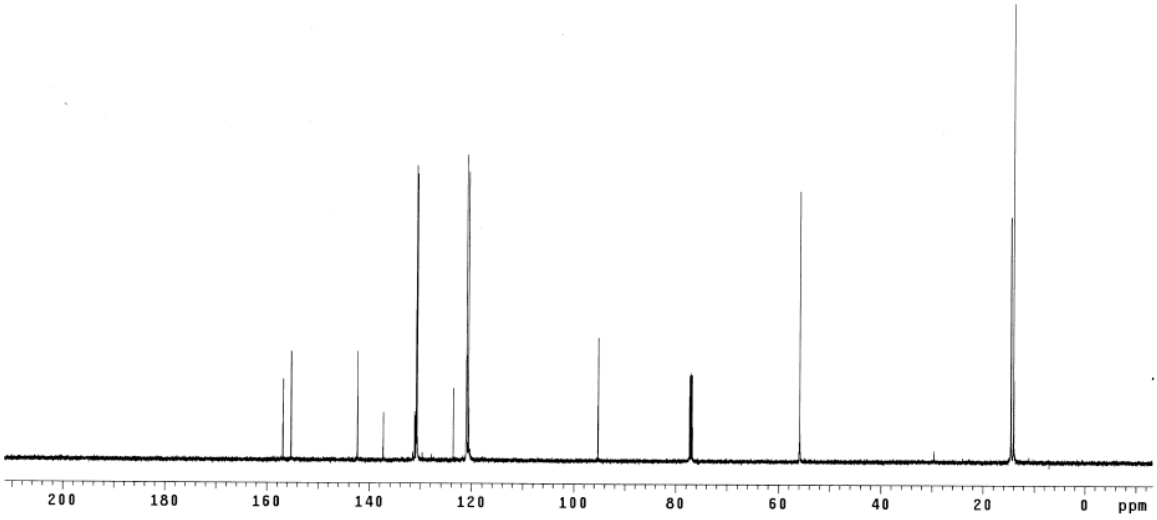

^{13}C NMR ($CDCl_3$)

4-Trimethysilyl-ethynyl tetramethyl-BODIPY (54)

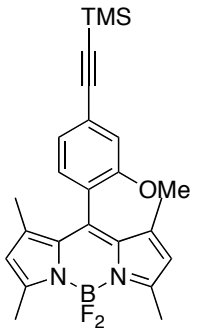

A solution of 4-iodo BODIPY **53** (0.6 g, 1.2 mmol), trimethylsilyl acetylene (1.2 g, 12.4 mmol), $PdCl_2(PPh_3)_2$ (88 mg, 0.12 mmol), CuI (24 mg, 0.12 mmol) and Et_3N (1.7 mL, 12.5 mmol) in THF (15 mL) was stirred at 25 ºC for 12 h. The solvents were concentrated under the reduced pressure. The residue was purified by flash chromatography eluting with 3 % EtOAc/hexanes to afford product as orange solids (548 mg, 97 %). R_f 0.4 (10 % EtOAc/hexanes). ^{1}H NMR (500 MHz, $CDCl_3$) δ 7.22 (dd, 1H, J = 7.7, 1.5 Hz), 7.084 (d, 1H, J = 1.5 Hz), 7.081 (d, 1H, J = 7.7 Hz), 5.96 (s, 2H), 3.78 (s, 3H), 2.54 (s, 6H), 1.44 (s, 6H), 0.28 (s, 9H); ^{13}C NMR (125 MHz, $CDCl_3$) δ 156.2, 155.2, 142.4, 137.9, 131.3, 129.5, 125.3, 125.2, 124.6, 120.9, 114.4, 104.3, 95.4, 55.7, 14.6, 14.0, –0.12; MS (MALDI) m/z 450.28 $(M)^+$.

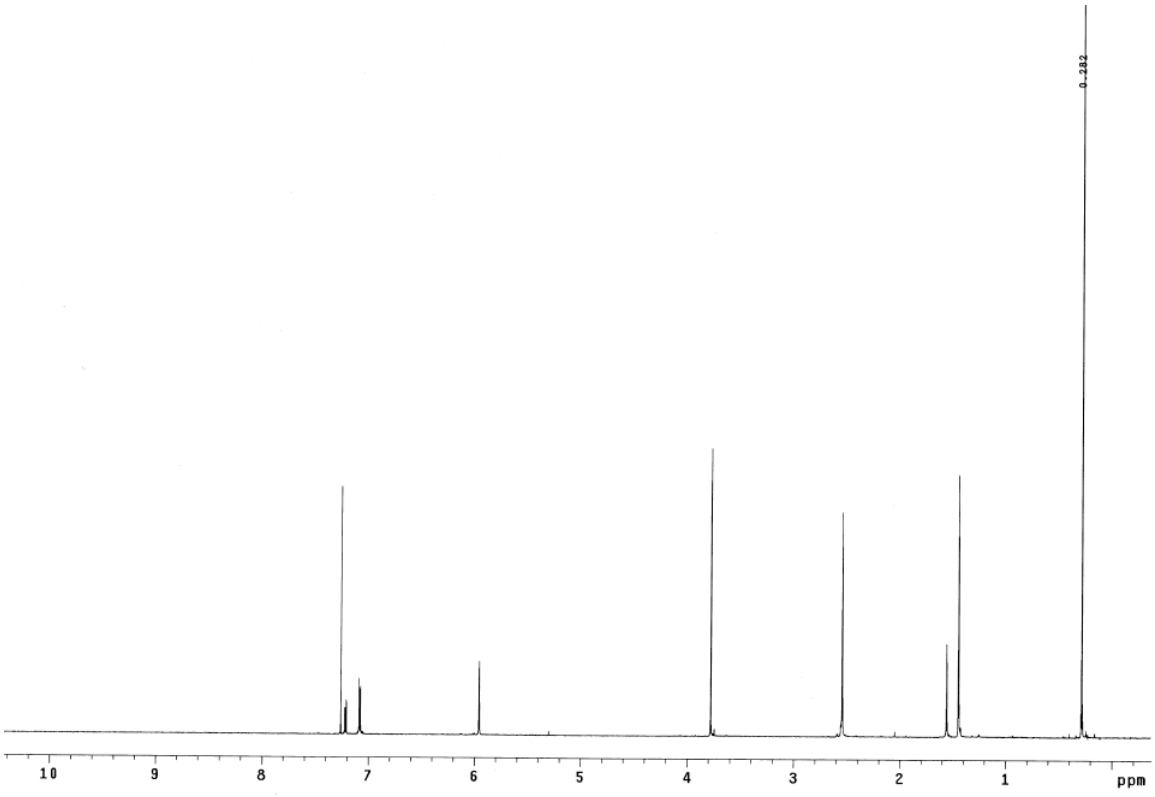

^{1}H NMR ($CDCl_3$)

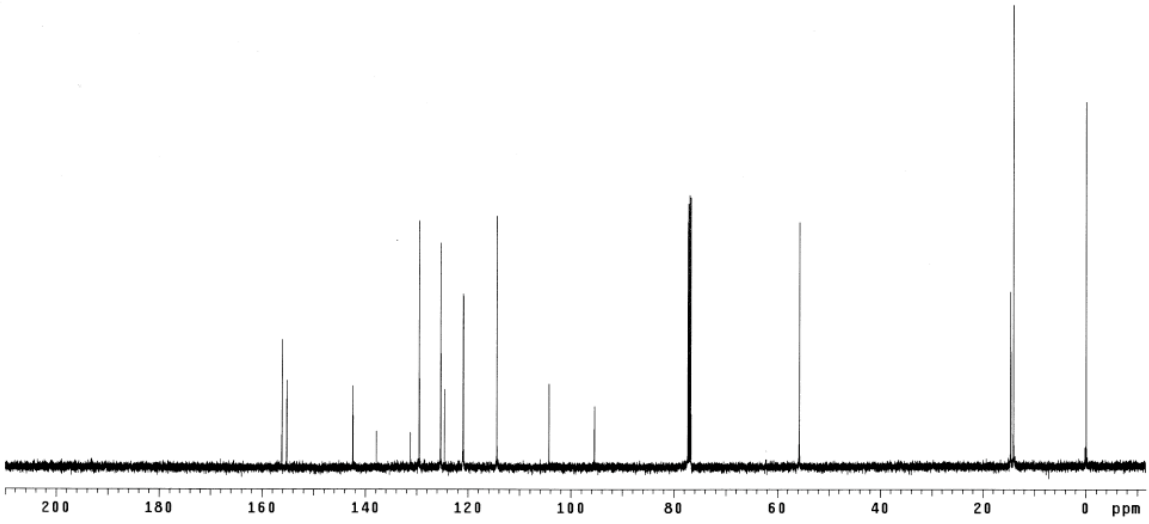

^{13}C NMR ($CDCl_3$)

4-Ethynyl tetramethyl-BODIPY (55)

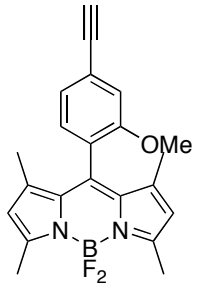

To a solution of TMS-protected BODIPY **54** (500 mg, 1.1 mmol) in THF (20 mL) was added TBAF (1.3 mL, 1.3 mmol, 1 M in THF) dropwise at –78 ºC. After the stirring at –78 ºC for 5 min, the reaction was quenched with water (20 mL) and aqueous layer was extracted with CH_2Cl_2 (3 x 10 mL). The combined organic layer was washed with water (1 x 15 mL) and dried over Na_2SO_4. The solvents were concentrated under the reduced pressure and the residue was purified by short flash chromatography eluting with 3 % EtOAc/hexanes to afford product as orange solids (388 mg, 92 %). R_f 0.4 (20 % EtOAc/hexanes). ^{1}H NMR (500 MHz, $CDCl_3$) δ 7.24 (dd, 1H, J = 7.7, 1.0 Hz), 7.107 (d, 1H, J = 7.7 Hz), 7.105 (d, 1H, J = 1.0 Hz), 5.97 (s, 2H), 3.78 (s, 3H), 3.18 (s, 1H), 2.55 (s, 6H), 1.45 (s, 6H); ^{13}C NMR (125 MHz, $CDCl_3$) δ 156.2, 155.2, 142.4, 137.7, 131.2, 129.6, 125.4, 124.9, 124.3, 121.0, 114.6, 83.0, 78.2, 55.7, 14.6, 14.0; MS (MALDI) m/z 378.28 $(M)^+$.

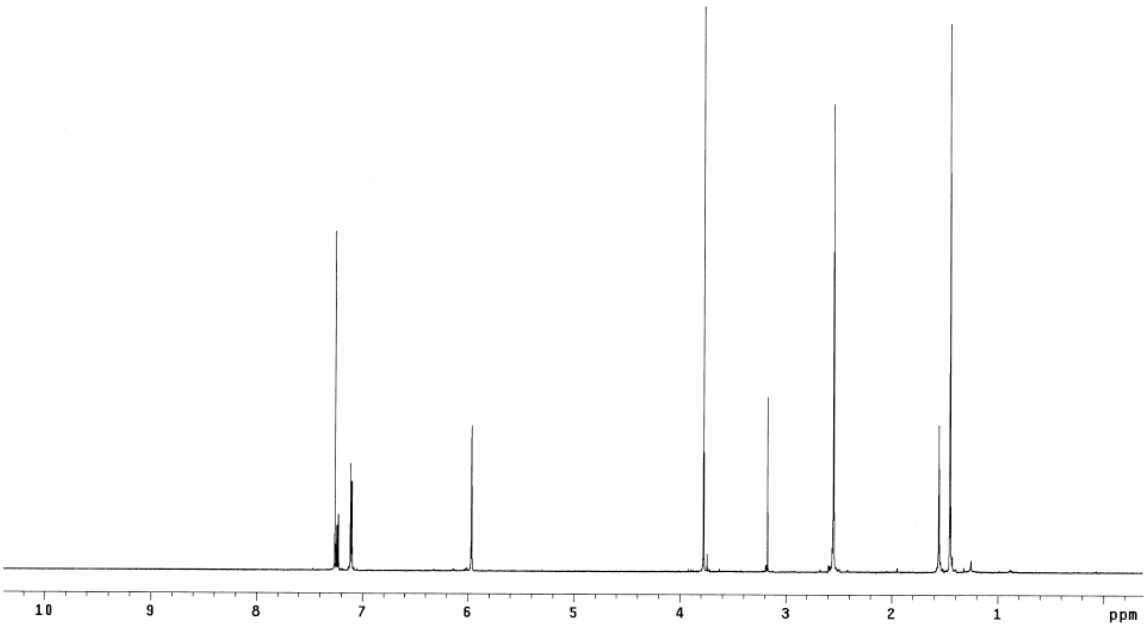

^{1}H NMR ($CDCl_3$)

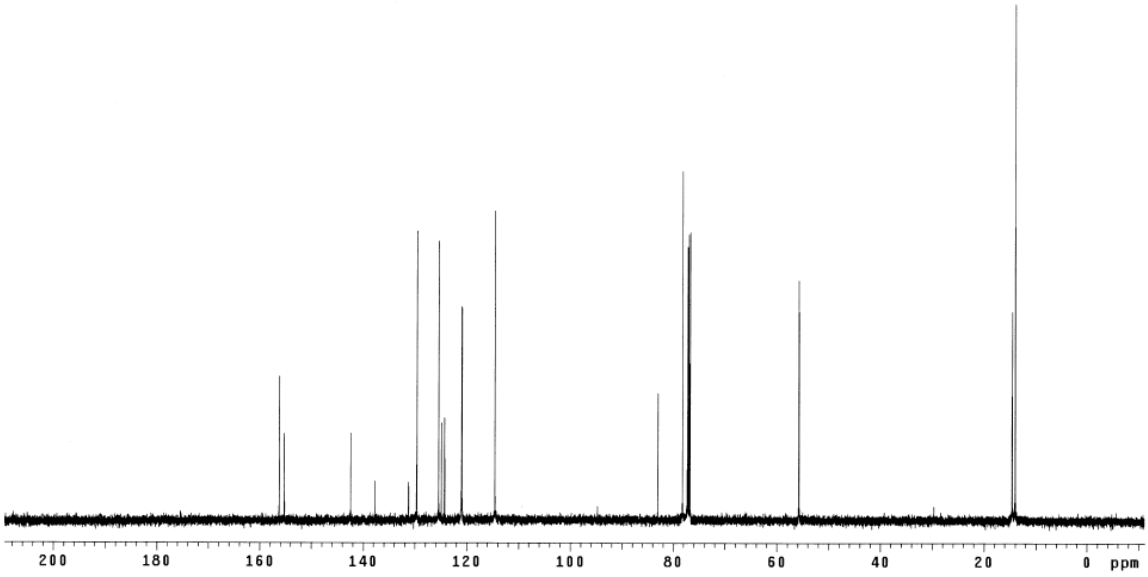

^{13}C NMR ($CDCl_3$)

4-Iodo tetramethyl-BODIPY (57)

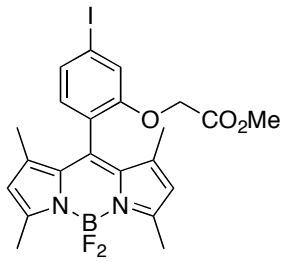

A solution of aldehyde **56** (600 mg, 1.9 mmol), 2,4-dimethylpyrrole (392 mg, 4.1 mmol) and one drop of TFA in CH_2Cl_2 (20 mL) was stirred at 25 ºC under nitrogen for 1 h. Then chloranil (553 mg, 2.2 mmol) was added to a reaction mixture and the reaction was stirred at 25 ºC under air for 40 min. The reaction mixture was filtered through celite and washed with CH_2Cl_2 and solvents were evaporated. The residue was purified by flash chromatography (aluminum oxide, activated, basic) eluting with CH_2Cl_2 and 10 % EtOAc/CH_2Cl_2. The obtained orange solids were dissolved in toluene (15 mL) and Et_3N (0.8 mL, 5.6 mmol) was added and stirred at 25 ºC for 10 min. BF_3•Et_2O (1.2 mL, 9.4 mmol) was added and stirred at 25 ºC for 20 h. The reaction mixture was diluted with CH_2Cl_2 (20 mL) and washed with water (3 x 20 mL). The organic layer was dried over Na_2SO_4 and evaporated. The residue was purified by flash chromatography eluting with 5 to 10 % EtOAc/hexanes to afford product as orange solids (275 mg, 27 %). R_f 0.4 (20 % EtOAc/hexanes). ^{1}H NMR (500 MHz, $CDCl_3$) δ 7.48 (d, 1H, J = 8.0 Hz), 7.08 (s, 1H), 6.91 (d, 1H, J = 8.0 Hz), 5.98 (s, 2H), 4.62 (s, 2H), 3.76 (s, 3H), 2.54 (s, 6H), 1.53 (s, 6H); ^{13}C NMR (125 MHz, $CDCl_3$) δ 168.5, 155.5, 155.1, 142.7, 136.7, 131.6, 131.2, 123.9, 121.1 (2C), 120.9, 94.8, 64.7, 52.3, 14.6, 14.0; MS (MALDI) m/z 537.96 $(M)^+$.

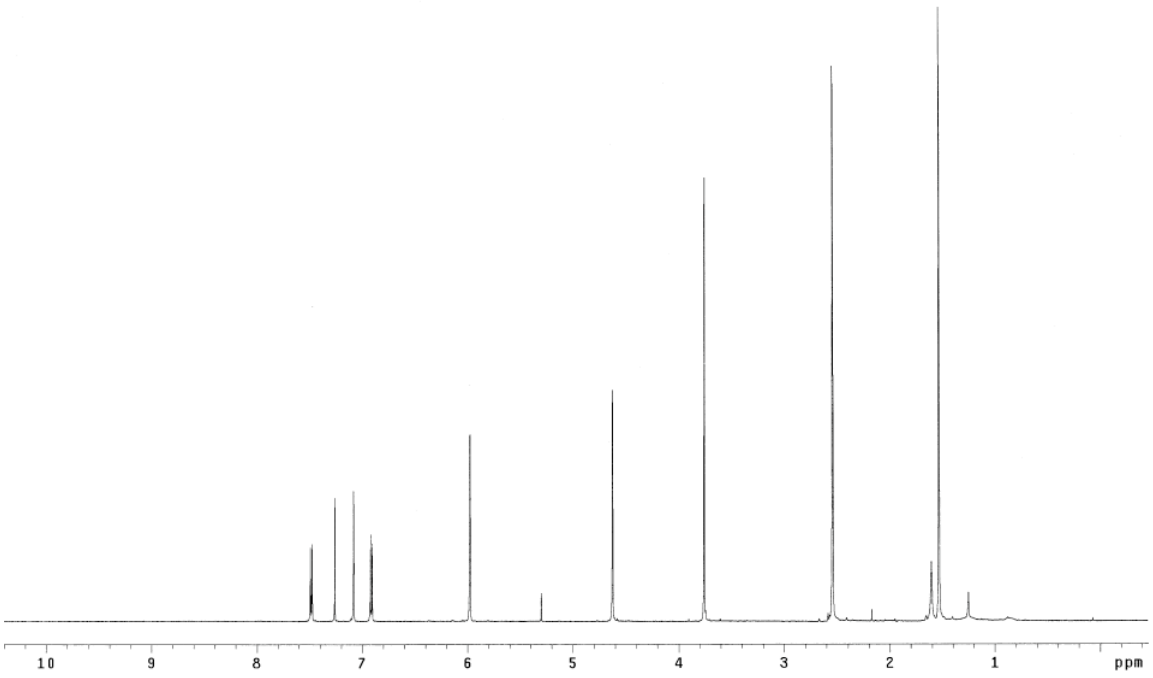

^{1}H NMR ($CDCl_3$)

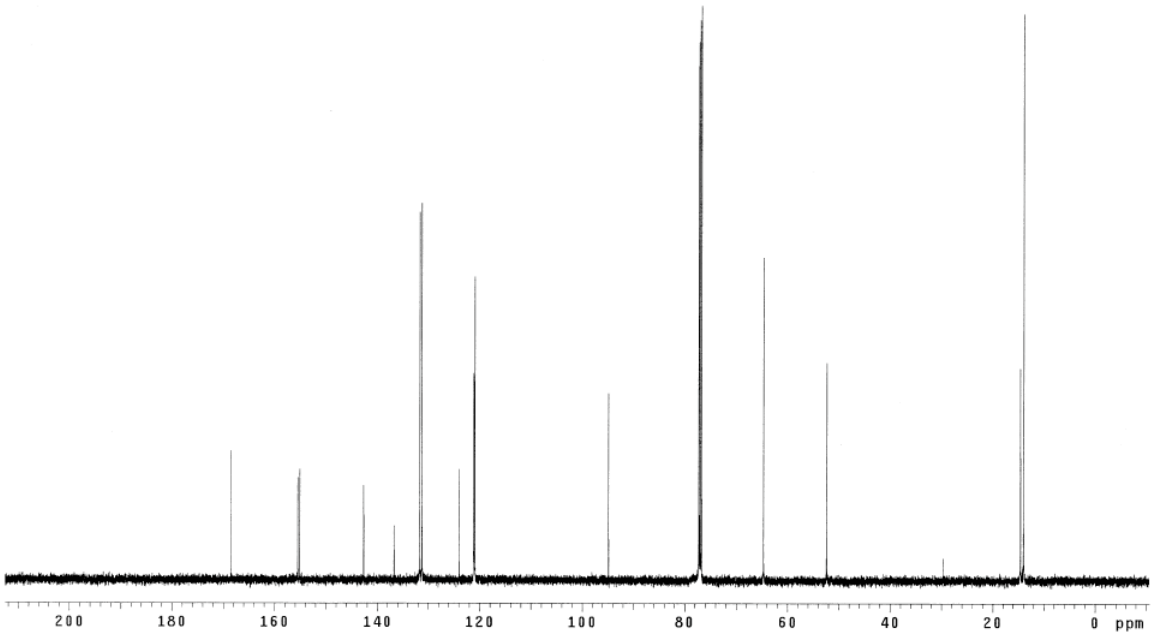

^{13}C NMR ($CDCl_3$)

4-Iodo tetramethyl-BODIPY carboxylic acid (58)

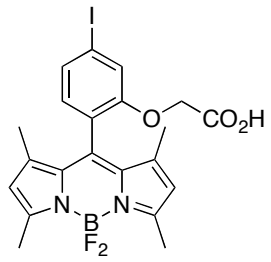

A solution of 4-iodo BODIPY **57** (80 mg, 0.15 mmol) and K_2CO_3 (62 mg, 0.45 mmol) in MeOH/THF/H_2O (2.5 mL, 2.5 mL, 1.0 mL, respectively) was stirred at 25 ºC for 24 h. The organic solvents were only evaporated and H_2O (5.0 mL) was added. The aqueous solution was acidified with 0.1 N HCl to reach pH 2 and extracted with CH_2Cl_2 (3 x 10 mL). The combined organic layer was dried over Na_2SO_4 and concentrated under the reduced pressure to afford pure product as a brown solid (78 mg, 99 %). R_f 0.1 (20 % EtOAc/hexanes). ^{1}H NMR (500 MHz, acetone-d_6) δ 7.62 (dd, 1H, J = 13.0, 2.5 Hz), 7.47 (d, 1H, J = 2.5 Hz), 7.09 (d, 1H, J = 13.0 Hz), 6.13 (s, 2H), 4.90 (s, 2H), 2.53 (s, 6H), 1.62 (s, 6H); ^{13}C NMR (125 MHz, acetone-d_6) δ 170.6, 157.2, 156.7, 144.5, 139.4, 132.9, 132.8, 125.0, 123.1, 122.6 (2C), 96.3, 65.9, 15.3, 14.9; MS (ESI) m/z 523.06 $(M–H)^-$.

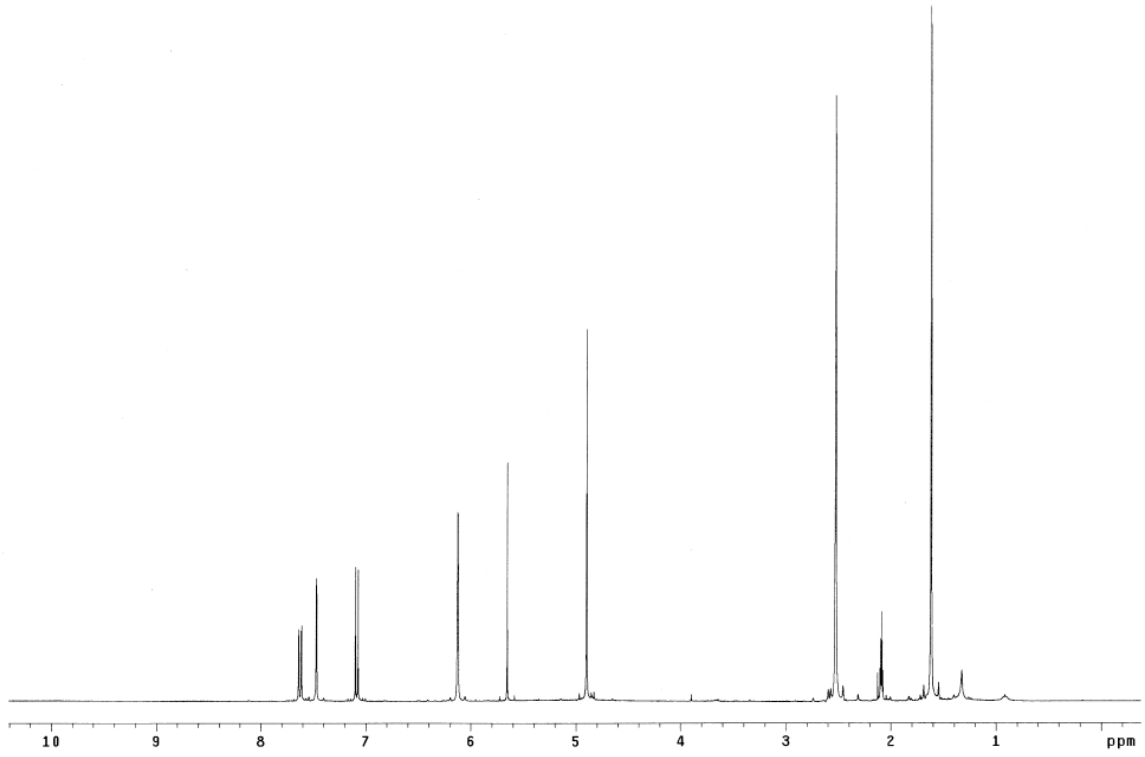

^{1}H NMR (acetone-d_6)

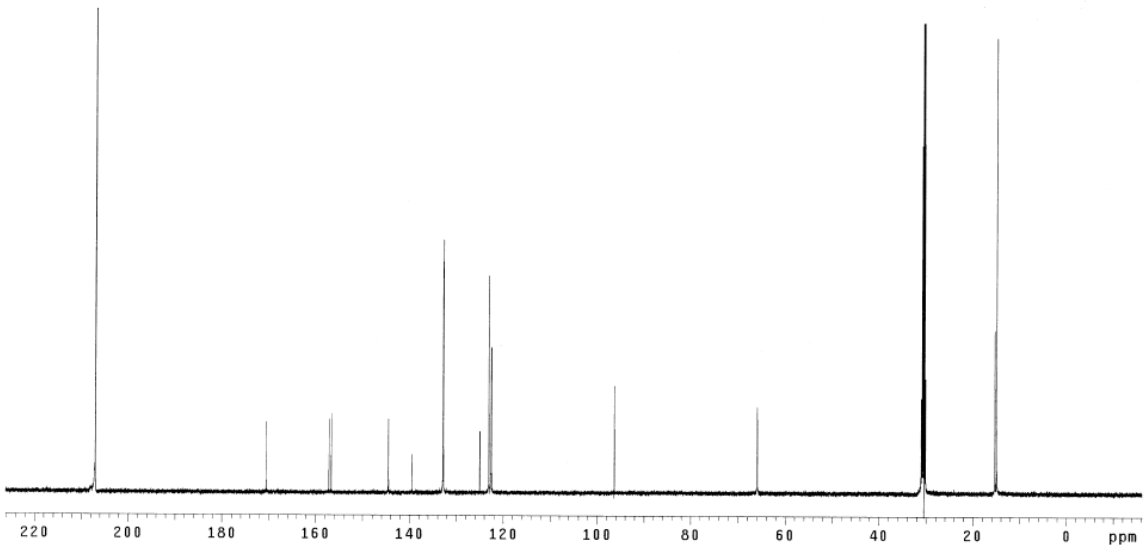

^{13}C NMR (acetone-d_6)

5-Iodo tetramethyl-BODIPY (60)

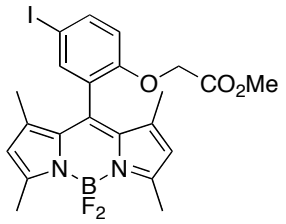

A solution of 5-iodobenzaldehyde **59** (640 mg, 2.0 mmol, *provided by Mr. Liangxing Wu*), 2,4-dimethylpyrrole (419 mg, 2.2 mmol) and one drop of TFA in CH_2Cl_2 (20 mL) was stirred at 25 ºC under nitrogen for 1.5 h. Then chloranil (590 mg, 1.2 mmol) was added to a reaction mixture and the reaction was stirred at 25 ºC for 40 min under air. The reaction mixture was filtered through celite and washed with CH_2Cl_2 and solvents were evaporated. The residue was purified by flash chromatography (aluminum oxide, activated, basic) eluting with CH_2Cl_2 and 10 % EtOAc/CH_2Cl_2. The obtained orange solids were dissolved in toluene (15 mL) and Et_3N (0.83 mL, 6.0 mmol) was added and stirred at 25 ºC for 10 min. BF_3•Et_2O (1.27 mL, 10.0 mmol) was added and stirred at 25 ºC for 19 h. The reaction mixture was diluted with CH_2Cl_2 (20 mL) and washed with water (3 x 20 mL). The organic layer was dried over Na_2SO_4 and evaporated. The residue was purified by flash chromatography eluting with 5 to 20 % EtOAc/hexanes to afford product as orange solids (414 mg, 38 %). R_f 0.2 (5 % EtOAc/hexanes). ^{1}H NMR (500 MHz, $CDCl_3$) δ 7.69 (dd, 1H, J = 8.5, 2.5 Hz), 7.52 (d, 1H, J = 2.5 Hz), 6.55 (d, 1H, J = 8.5 Hz), 5.99 (s, 2H), 4.62 (s, 2H), 3.73 (s, 3H), 2.54 (s, 6H), 1.55 (s, 6H); ^{13}C NMR (125 MHz, $CDCl_3$) δ 168.7, 155.6, 154.7, 142.7, 139.1, 138.2, 135.9, 131.2, 126.4, 121.1, 113.6, 83.8, 64.6, 52.3, 14.6, 14.0; MS (MALDI) m/z 538.13 $(M)^+$.

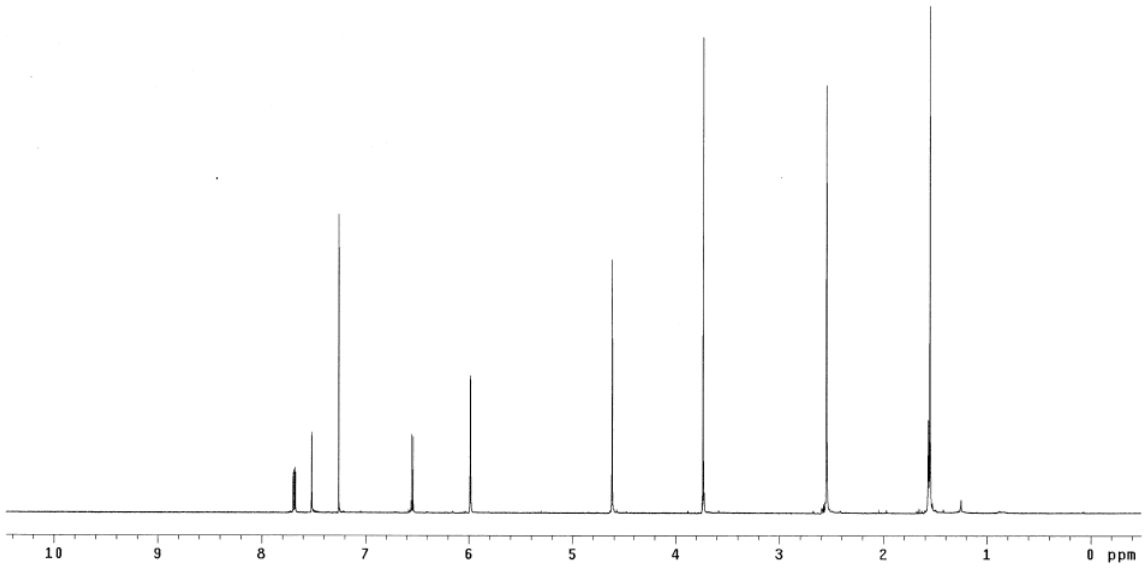

^{1}H NMR ($CDCl_3$)

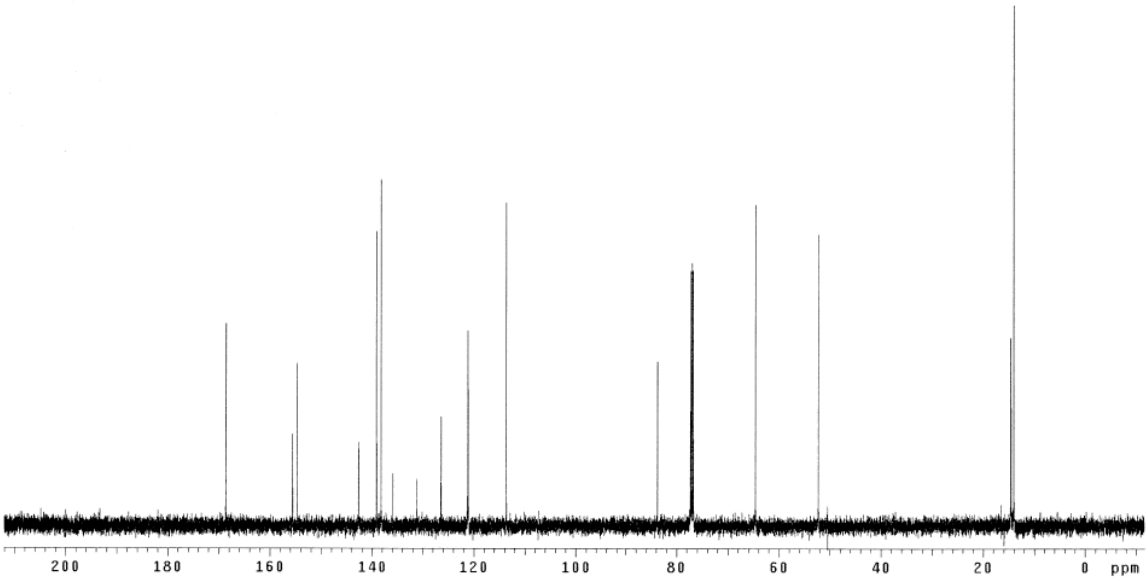

^{13}C NMR ($CDCl_3$)

5-Trimethylsilyl-ethynyl tetramethyl-BODIPY (61)

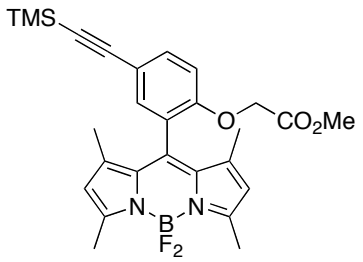

A solution of 5-iodo BODIPY **60** (350 mg, 0.65 mmol), trimethylsilyl acetylene (639 mg, 6.50 mmol), $PdCl_2(PPh_3)_2$ (46 mg, 0.065 mmol), CuI (12 mg, 0.065 mmol) and Et_3N (0.91 mL, 6.50 mmol) in THF (8.0 mL) was stirred at 25 ºC for 12 h. The reaction mixture was concentrated under the reduced pressure. The residue was purified by flash chromatography eluting with 5 to 10 % EtOAc/hexanes to afford product as orange solids (312 mg, 94 %). R_f 0.4 (20 % EtOAc/hexanes). ^{1}H NMR (500 MHz, $CDCl_3$) δ 7.50 (dd, 1H, J = 8.5, 2.0 Hz), 7.34 (d, 1H, J = 2.0 Hz), 6.69 (d, 1H, J = 8.5 Hz), 5.97 (s, 2H), 4.64 (s, 2H), 3.73 (s, 3H), 2.54 (s, 6H), 1.54 (s, 6H), 0.22 (s, 9H); ^{13}C NMR (125 MHz, $CDCl_3$) δ 168.7, 155.4, 154.7, 142.7, 136.7, 134.1, 133.5, 131.3, 124.2, 121.0, 117.4, 111.4, 103.5, 94.3, 64.7, 52.2, 14.6, 14.0, -0.1; MS (MALDI) m/z 508.32 $(M)^+$.

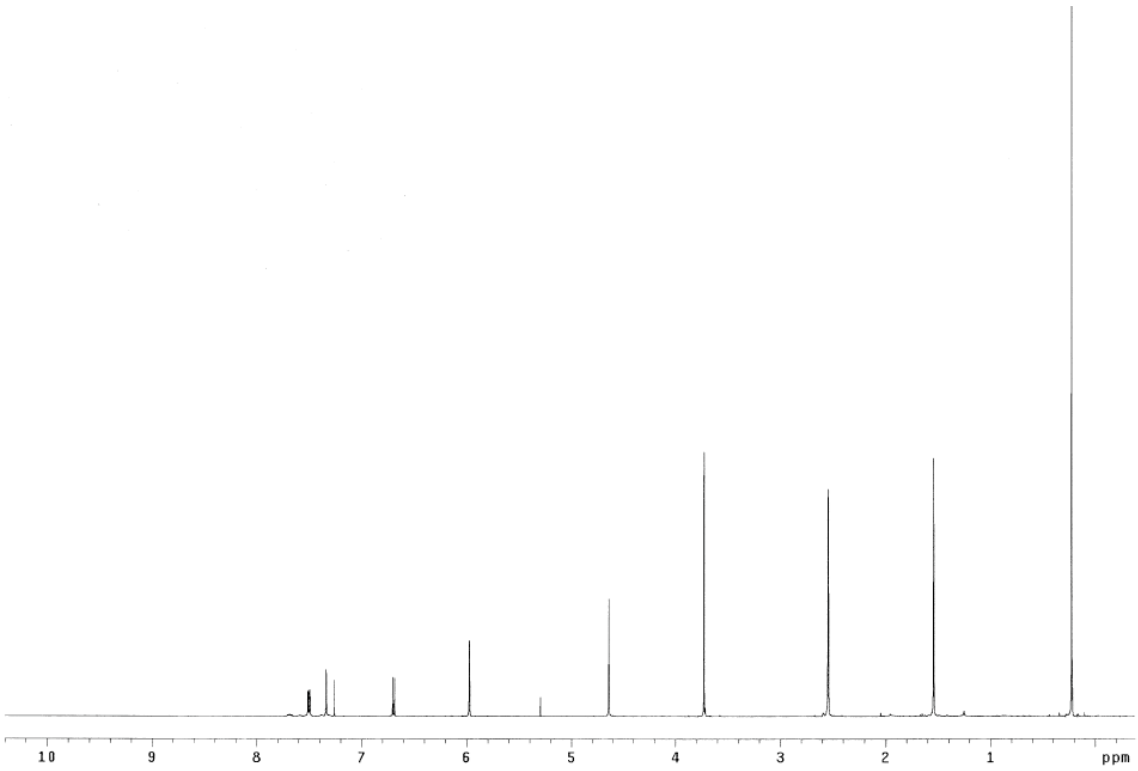

^{1}H NMR ($CDCl_3$)

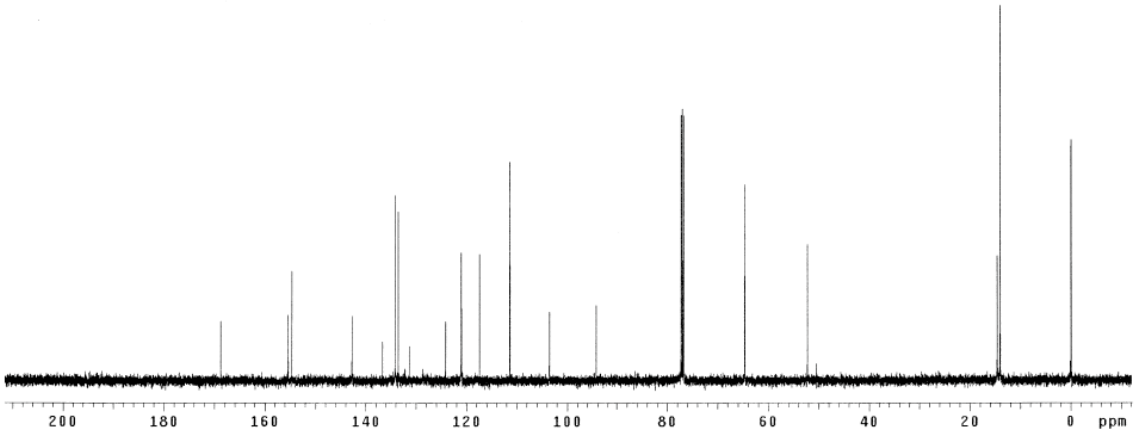

^{13}C NMR ($CDCl_3$)

5-Ethynyl tetramethyl-BODIPY (62)

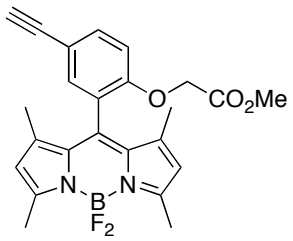

To a solution of TMS-protected BODIPY **61** (212 mg, 0.42 mmol) in THF (8.0 mL) was added TBAF (0.5 mL, 0.50 mmol, 1 M in THF) dropwise at –78 ºC. After the stirring at –78 ºC for 5 min, the reaction was quenched with water (10 mL) and aqueous layer was extracted with CH_2Cl_2 (3 x 10 mL). The combined organic layer was washed with water (1 x 10 mL) and dried over Na_2SO_4. The solvents were concentrated under the reduced pressure and the residue was purified by short flash chromatography eluting with 10 to 15 % EtOAc/hexanes to afford product as orange solids (137 mg, 75 %). R_f 0.5 (30 % EtOAc/hexanes). ^{1}H NMR (500 MHz, $CDCl_3$) δ 7.54 (dd, 1H, J = 8.5, 2.5 Hz), 7.36 (d, 1H, J = 2.5 Hz), 6.72 (d, 1H, J = 8.5 Hz), 5.98 (s, 2H), 4.65 (s, 2H), 3.74 (s, 3H), 3.05 (s, 1H), 2.55 (s, 6H), 1.54 (s, 6H); ^{13}C NMR (125 MHz, $CDCl_3$) δ 168.7, 155.5, 154.9, 142.7, 136.5, 134.4, 133.7, 131.3, 124.3, 121.1, 116.2, 111.5, 82.2, 77.4, 64.7, 52.3, 14.6, 13.9; MS (MALDI) m/z 436.26 $(M)^+$.

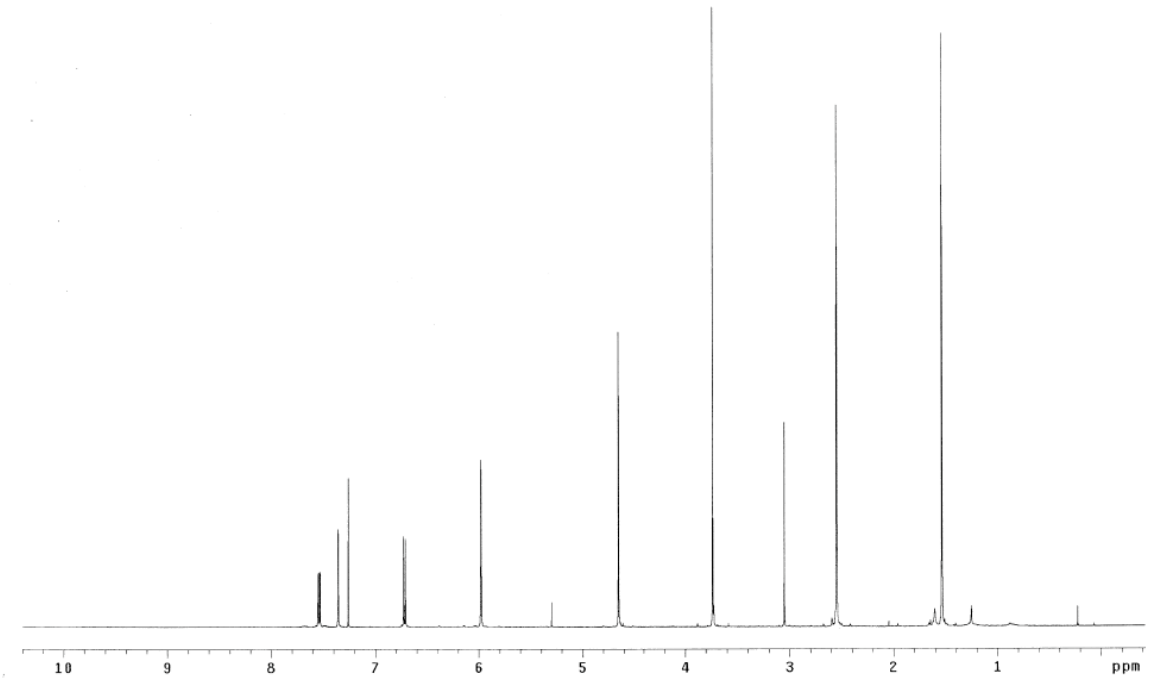

^{1}H NMR ($CDCl_3$)

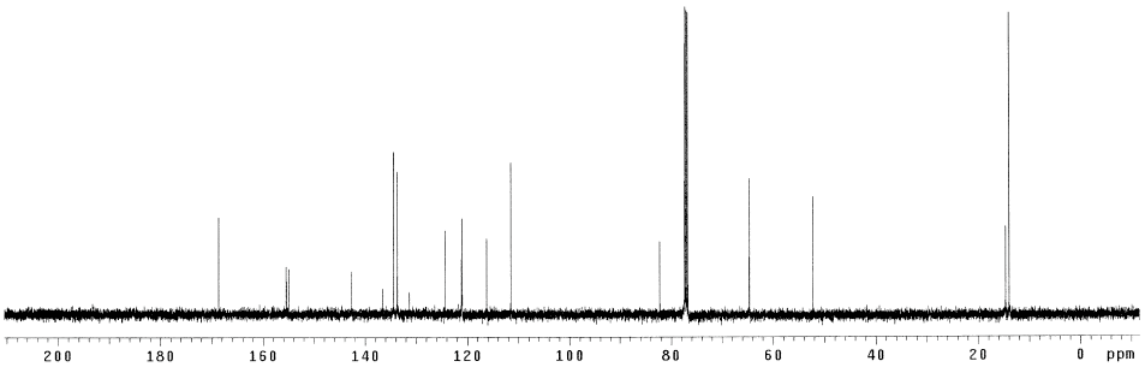

^{13}C NMR ($CDCl_3$)

5-Ethynyl tetramethyl-BODIPY carboxylic acid (63)

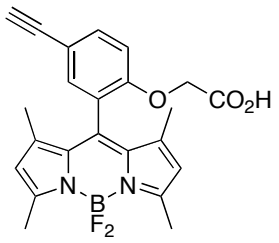

A solution of 5-ethynyl BODIPY **62** (70 mg, 0.16 mmol) and K_2CO_3 (67 mg, 0.48 mmol) in MeOH/THF/H_2O (2.5 mL, 2.5 mL, 1.0 mL, respectively) was stirred at 25 ºC for 12 h. The organic solvents were only evaporated and H_2O (5.0 mL) was added. The aqueous solution was acidified with 0.1 N HCl to reach pH 2 and extracted with CH_2Cl_2 (3 x 10 mL). The combined organic layer was dried over Na_2SO_4 and concentrated under the reduced pressure to afford pure product as a dark brown solid (68 mg, 99 %). R_f 0.1 (50 % EtOAc/hexanes). ^{1}H NMR (300 MHz, acetone-d_6) δ 7.68 (dd, 1H, J = 9.0, 2.1 Hz), 7.45 (d, 1H, J = 2.1 Hz), 7.13 (d, 1H, J = 9.0 Hz), 6.14 (s, 2H), 4.89 (s, 2H), 3.67 (s, 1H), 2.54 (s, 6H), 1.61 (s, 6H); ^{13}C NMR (75 MHz, acetone-d_6) δ 170.5, 157.1, 156.7, 144.6, 139.2, 136.0, 134.7, 132.9, 125.5, 122.6, 117.6, 114.2, 83.9, 79.8, 65.8, 15.3, 14.9; MS (MALDI) m/z 422.23 $(M)^+$.

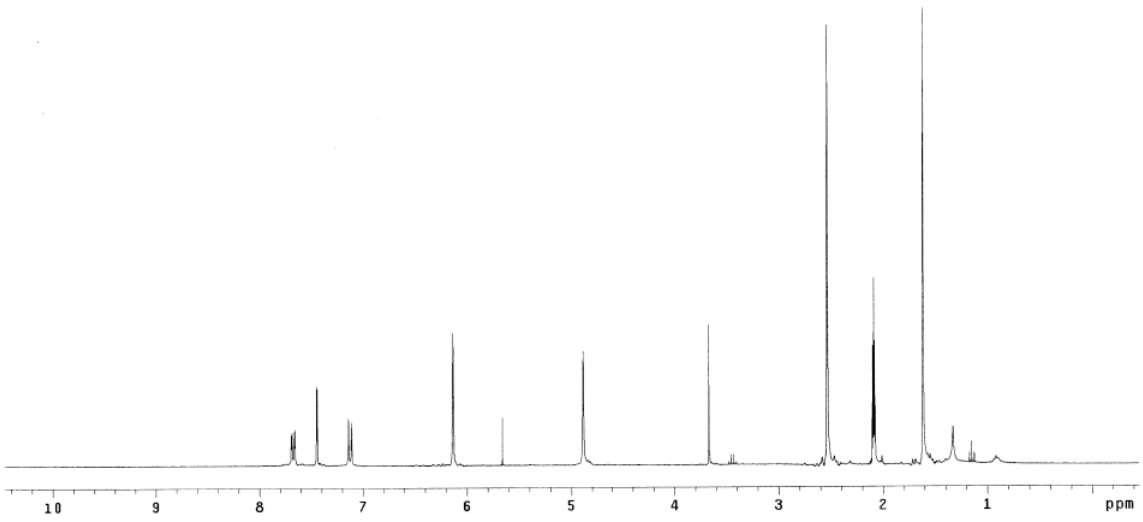

^{1}H NMR (acetone-d_6)

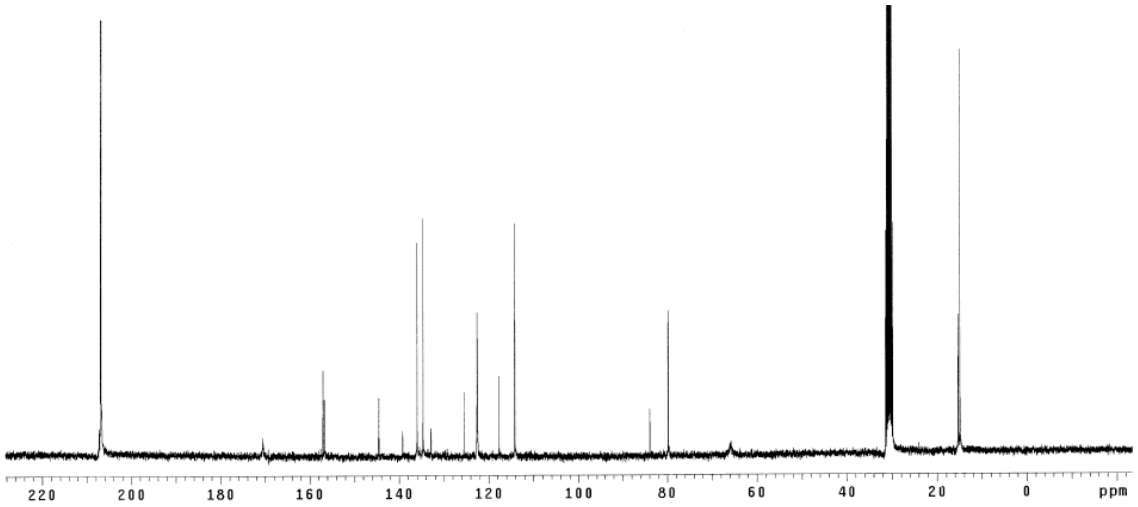

^{13}C NMR (acetone-d_6)

1,2,3,3-Tetramethyl-3*H*-indolium iodide (68)[107]

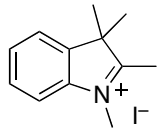

A solution of 2,3,3-trimethylindolenine (3.0 g, 18.8 mmol) and iodomethane (3.2 g, 22.6 mmol) in toluene (60 mL) was heated at 80 ºC for 48 h. The reaction mixture was cooled to room temperature and the solvent was concentrated under the reduced pressure. The residue was suspended in hexanes (100 mL), sonicated for 10 min and filtered off to afford product as a brown solid (5.4 g, 95 %). ^{1}H NMR (500 MHz, DMSO-d_6) δ 7.96-7.95 (m, 1H), 7.88-7.86 (m, 1H), 7.68-7.64 (m, 2H), 4.01 (s, 3H), 2.81 (s, 3H), 1.57 (s, 6H); ^{13}C NMR (125 MHz, DMSO-d_6) δ 196.9, 143.1, 142.5, 130.3, 129.8, 124.3, 116.1, 54.9, 35.7, 22.6, 15.1.

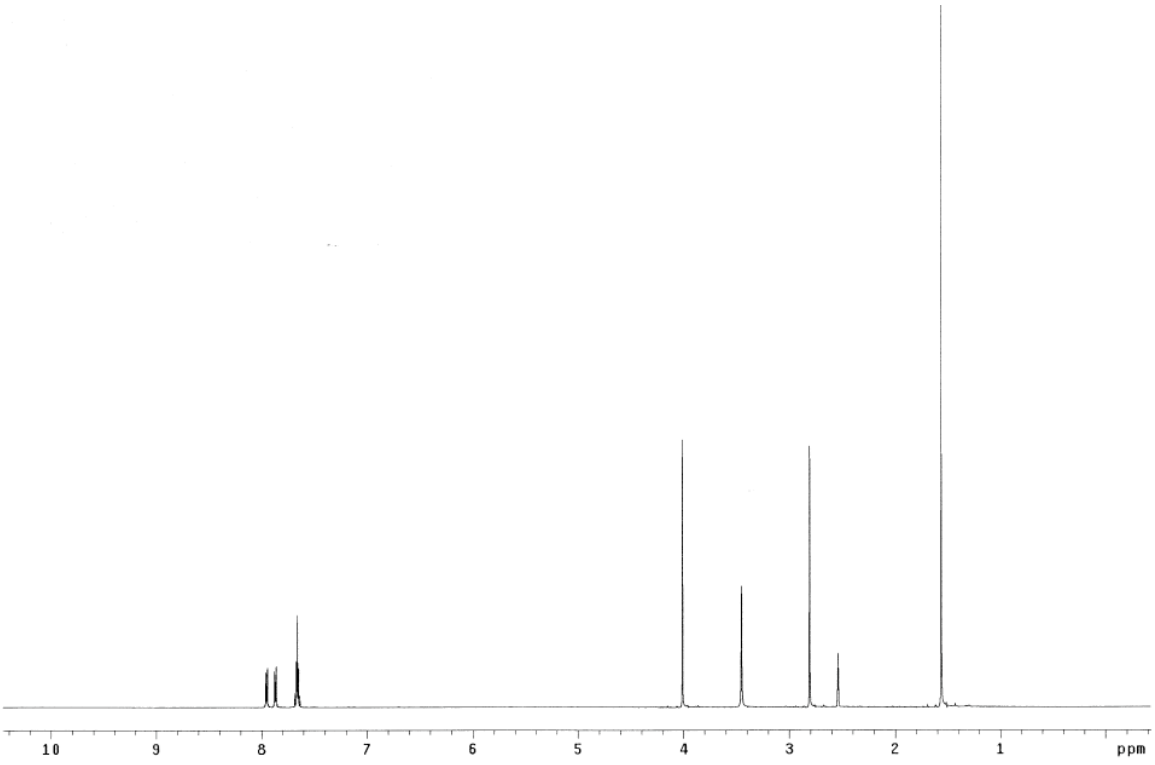

^{1}H NMR (DMSO-d_6)

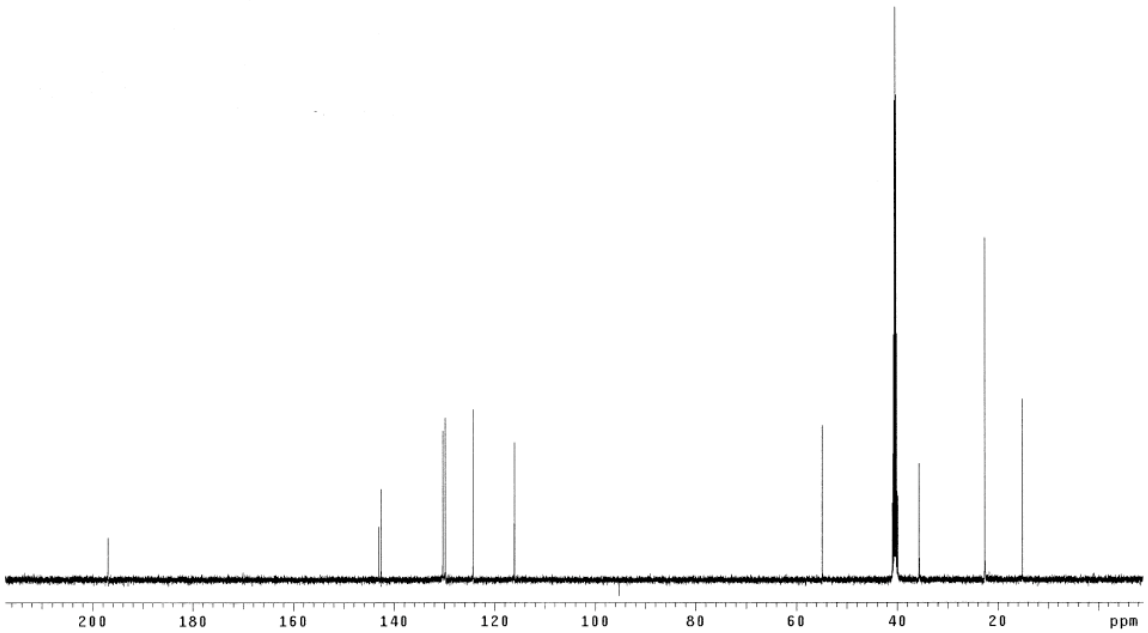

^{13}C NMR (DMSO-d_6)

1-(5-Carboxypentyl)-2,3,3-tetramethyl-3*H*-indolium bromide (76)[108]

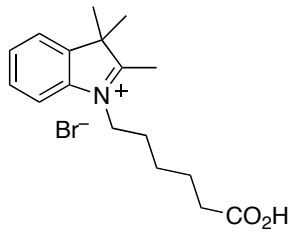

6-Bromohexanoic acid (3.7 g, 18.8 mmol) was added to a solution of 2,3,3-trimethylindolenine (3.0 g, 18.8 mmol) in nitromethane (10 mL). The reaction mixture was heated at 80 ºC for 24 h. The reaction mixture was cooled to room temperature and triturated with ether (60 mL). The precipitate was filtered off and washed with ether to afford product as a purple solid (3.3 g, 49 %). ^{1}H NMR (300 MHz, DMSO-d_6) δ 8.03-8.00 (m, 1H), 7.90-7.87 (m, 1H), 7.68-7.65 (m, 2H), 4.49 (t, 2H, J = 7.9 Hz), 2.88 (s, 3H), 2.27 (t, 2H, J = 7.1 Hz), 1.93-1.83 (m, 2H), 1.65-1.53 (m, 2H), 1.57 (s, 6H), 1.51-1.43 (m, 2H); ^{13}C NMR (75 MHz, DMSO-d_6) δ 198.1, 176.5, 143.4, 142.4, 131.2, 130.7, 125.1, 116.9, 55.8, 49.0, 34.9, 28.4, 26.9, 25.5, 23.6, 15.4.

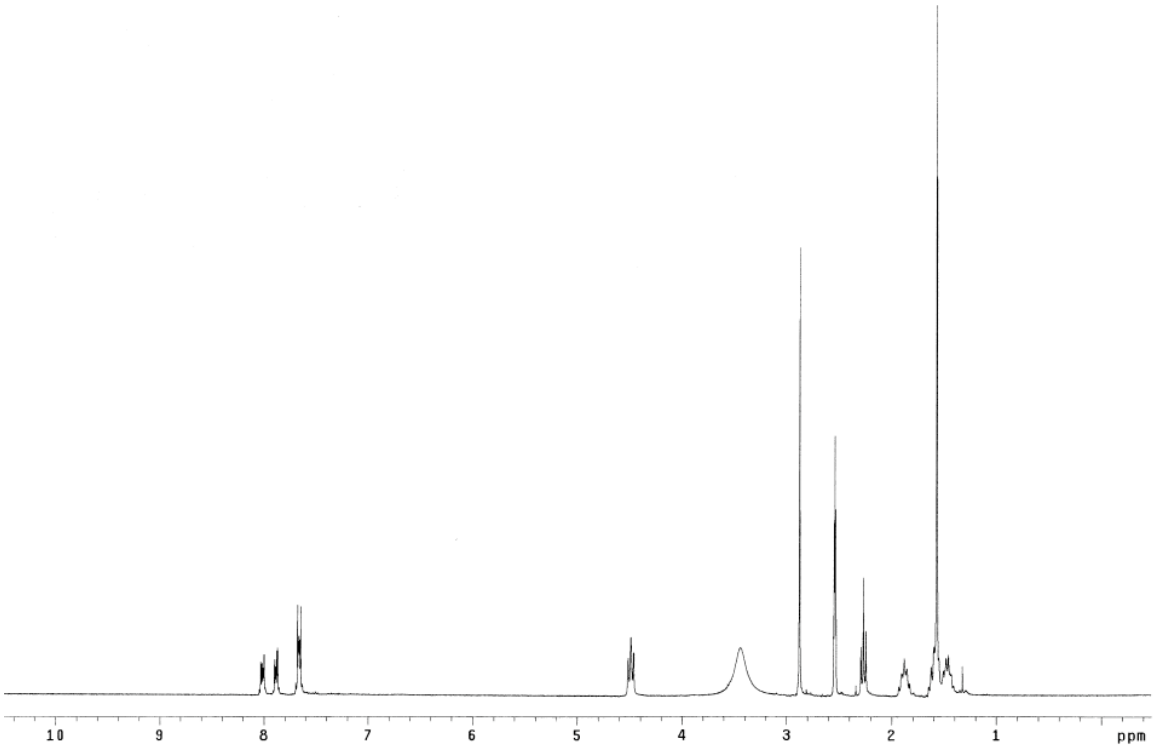

^{1}H NMR (DMSO-d_6)

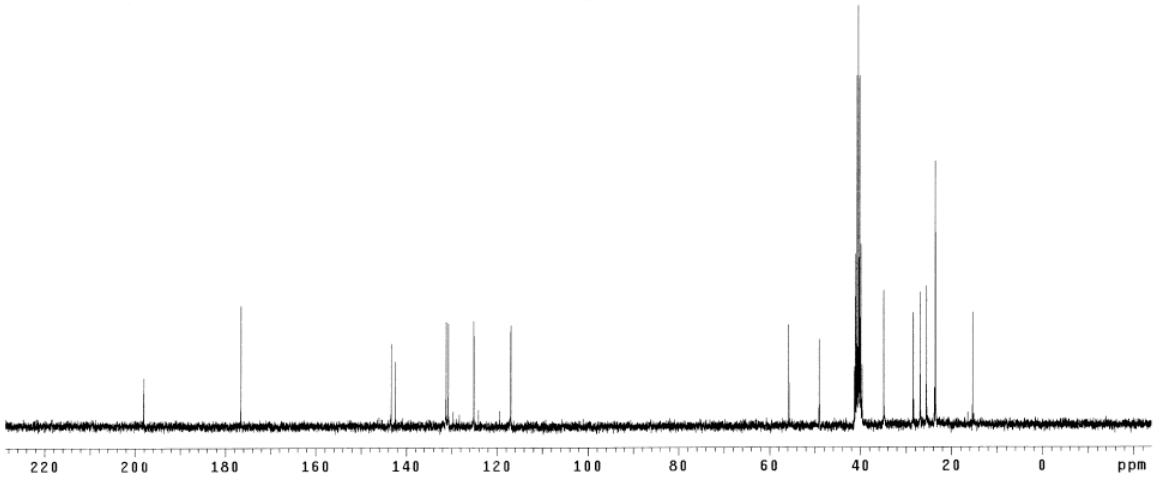

^{13}C NMR (DMSO-d_6)

Cyanine 3 (73a)[108]

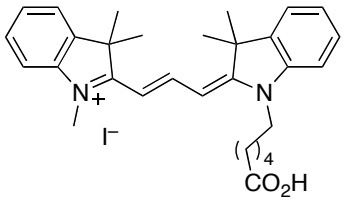

A solution of indolium bromide **76** (100 mg, 0.28 mmol) and *N*,*N*'-diphenylformamidine (66 mg, 0.34 mmol) in Ac_2O (1.5 mL) was heated at 120 ºC for 30 min. The reaction mixture was cooled to room temperature and a solution of indolium iodide **68** (102 mg, 0.34 mmol) in pyridine (1.5 mL) was added. The reaction mixture was stirred at 25 ºC for 1 h. Ether (100 mL) was added and dark red oil was obtained after the remove of ether. The residue was purified by flash chromatography eluting with 100 % EtOAc and 2 % to 10 % MeOH/CH_2Cl_2 to afford product as a dark red foam (106 mg, 64 %). R_f 0.3 (10 % MeOH/CH_2Cl_2). ^{1}H NMR (500 MHz, $CDCl_3$) δ 8.42 (t, 1H, J = 13.4 Hz), 7.40-7.35 (m, 4H), 7.27-7.22 (m, 4H), 7.18 (d, 1H, J = 13.5 Hz), 7.14 (dd, 1H, J = 8.3, 3.5 Hz), 4.21 (t, 2H, J = 7.5 Hz), 3.80 (s, 3H), 2.45 (t, 2H, J = 7.0 Hz), 1.91-1.85 (m, 2H), 1.78-1.63 (m, 4H), 1.71 (s, 6H), 1.70 (s, 6H); ^{13}C NMR (125 MHz, $CDCl_3$) δ 178.1, 174.2, 173.5, 150.7, 142.6, 141.9, 140.5, 140.4, 128.9, 128.8, 125.3 (2C), 122.1, 122.0, 110.9, 110.8, 105.0, 104.4, 48.9, 48.8, 44.7, 33.9, 32.8, 28.14, 28.07, 27.1, 26.1, 24.4.

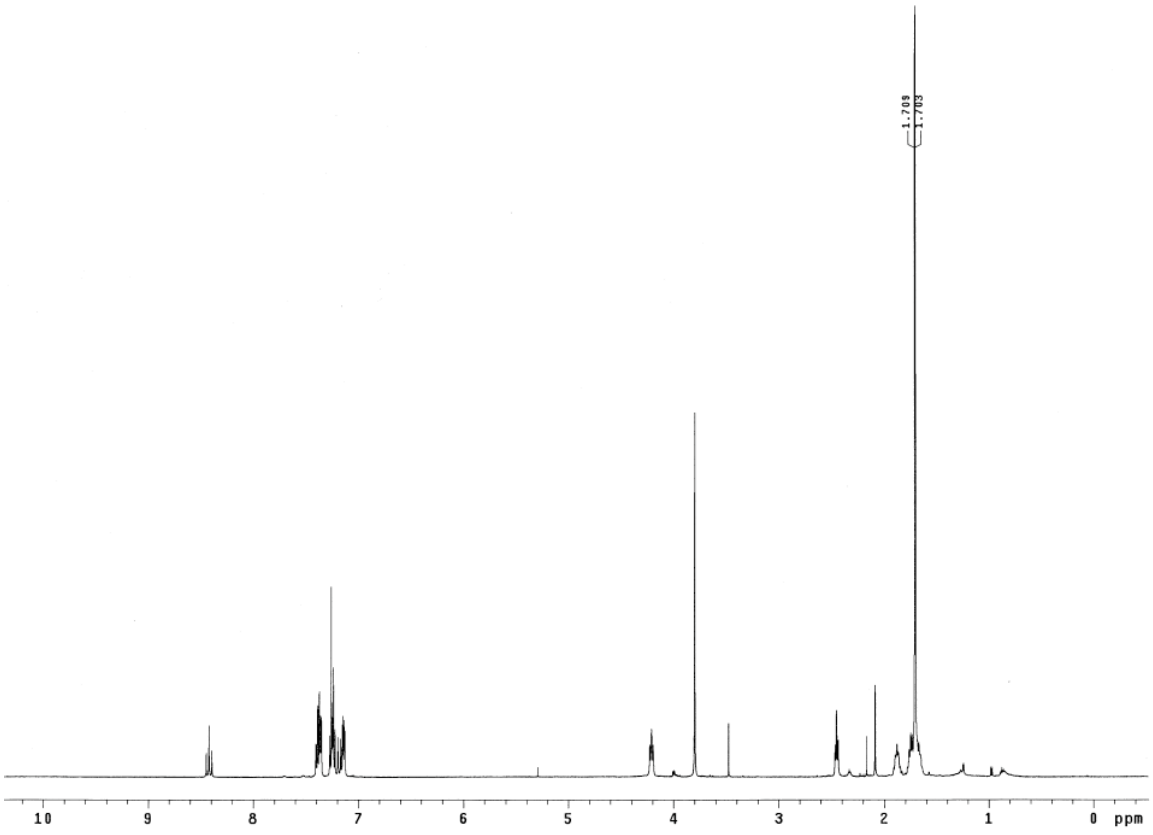

^{1}H NMR ($CDCl_3$)

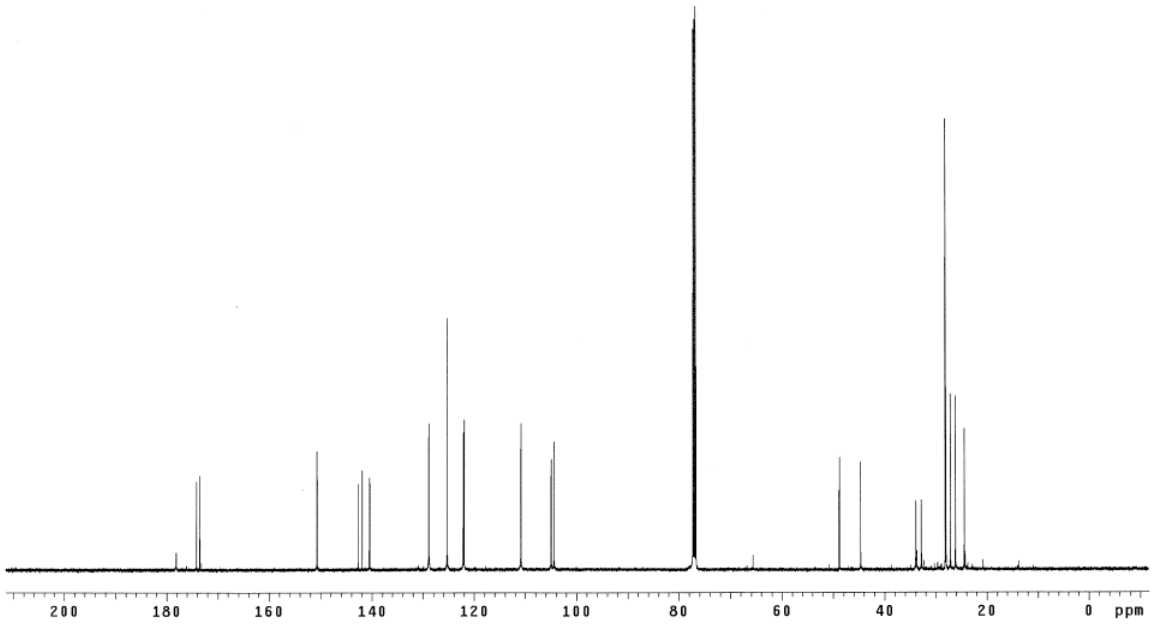

^{13}C NMR ($CDCl_3$)

5-Iodo cyanine 3 (74a)

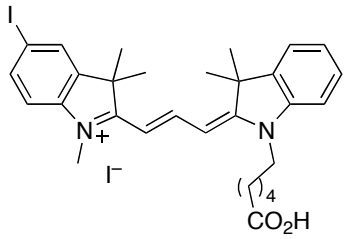

A solution of indolium bromide **76** (170 mg, 0.48 mmol) and *N*,*N*'-diphenylformamidine (113 mg, 0.58 mmol) in Ac_2O (2 mL) was heated at 120 ºC for 30 min. The reaction mixture was cooled to room temperature and a solution of indolium iodide **78** (287 mg, 0.67 mmol) in pyridine (7 mL) was added. The reaction mixture was stirred at 25 ºC for 24 h. Ether (100 mL) was added and the reaction mixture was filtered off to afford dark red solids. The residue was purified by flash chromatography eluting with 100 % EtOAc and 4 % to 10 % MeOH/CH_2Cl_2 to afford product as a dark red solid (213 mg, 62 %). R_f 0.4 (10 % MeOH/CH_2Cl_2). ^{1}H NMR (500 MHz, $CDCl_3$) δ 8.40 (t, 1H, *J* = 13.0 Hz), 7.70 (dd, 1H, *J* = 8.3, 1.5 Hz), 7,61 (d, 1H, *J* = 1.5 Hz), 7.43-7.38 (m, 2H), 7.28 (t, 1H, *J* = 7.5 Hz), 7.21 (d, 2H, *J* = 13.5 Hz), 7.16 (d, 1H, *J* = 8.0 Hz), 6.91 (d, 1H, *J* = 8.0 Hz), 4.24 (t, 2H, *J* = 8.0 Hz), 3.76 (s, 3H), 2.47 (t, 2H, *J* = 6.5 Hz), 1.93-1.87 (m, 2H), 1.80-1.65 (m, 4H), 1.72 (s, 6H), 1.70 (s, 6H); ^{13}C NMR (125 MHz, $CDCl_3$) δ 178.1, 174.3, 172.7, 150.7, 142.6, 142.5, 141.8, 140.7, 137.7, 131.0, 129.0, 125.7, 122.2, 112.5, 111.3, 105.3, 104.8, 88.2, 49.1, 48.5, 44.9, 33.9, 32.9, 29.6, 28.1, 27.2, 26.1, 24.4; MS (ESI) m/z 583.18 $(M)^+$.

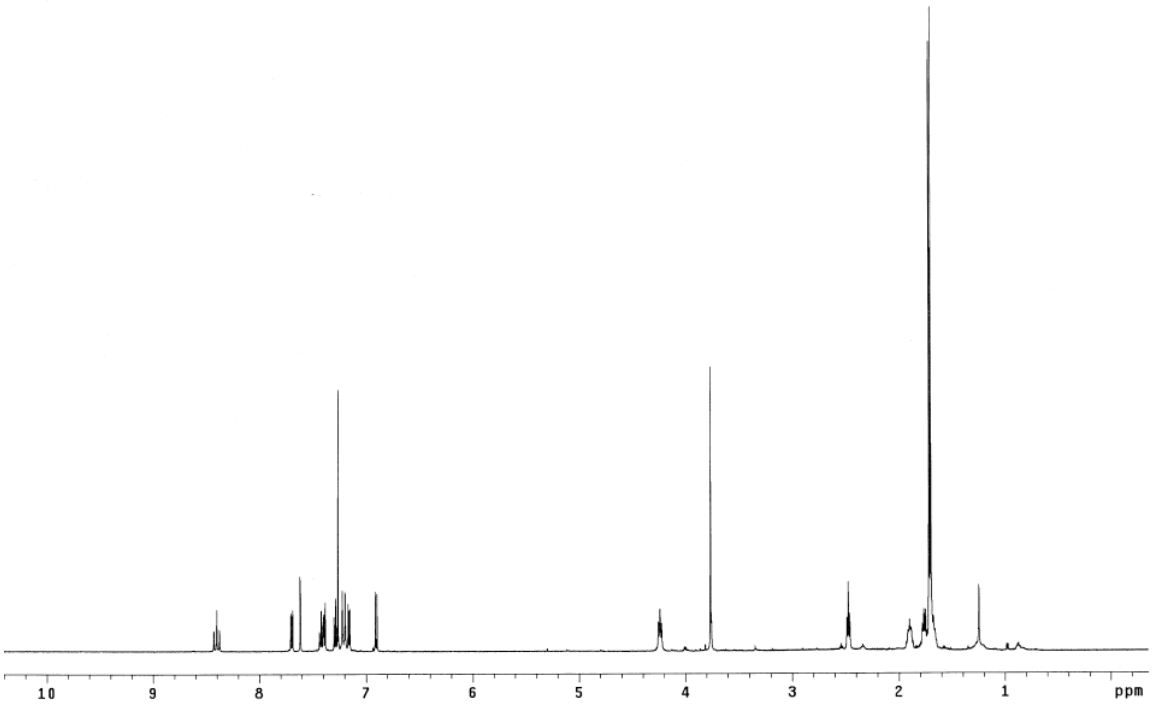

^{1}H NMR ($CDCl_3$)

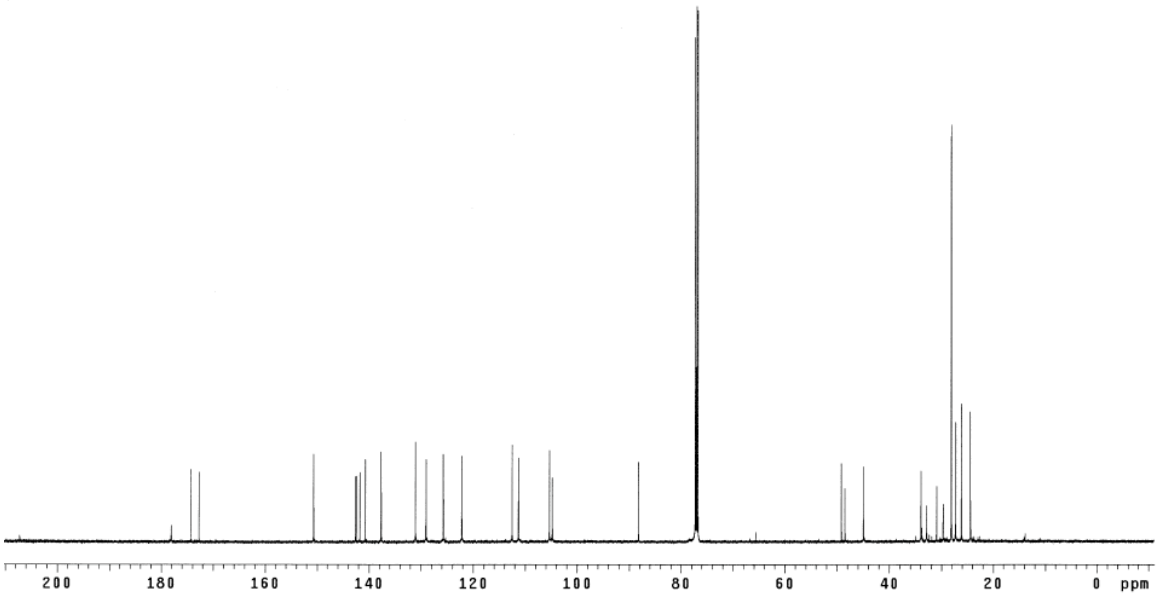

^{13}C NMR ($CDCl_3$)

Hemicyanine intermediate (79)

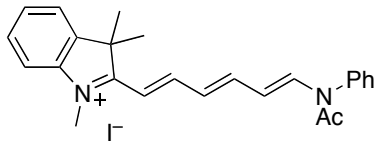

Indolium iodide **68** (1.0 g, 3.3 mmol) and glutaconaldehydedianil hydrochloride (1.4 g, 5.0 mmol) were added to a solution of Ac_2O (5.0 mL) and pyridine (5.0 mL). The reaction mixture was stirred at 25 ºC for 40 min. Ether (200 mL) was added and the reaction mixture was filtered off to afford dark red oil. The residue was purified by flash chromatography eluting with 100 % EtOAc and 4 % to 10 % MeOH/CH_2Cl_2 to afford product as a dark brown solid (1.48 g, 90 %). R_f 0.5 (10 % MeOH/CH_2Cl_2). ^{1}H NMR (300 MHz, $CDCl_3$) δ 8.17 (d, 1H, J = 13.8 Hz), 7.90-7.81 (m, 1H), 7.64-7.46 (m, 8H), 7.20-7.17 (m, 3H), 6.94 (m, 1H), 5.45-5.37 (m, 1H), 4.21 (s, 3H), 1.97 (s, 3H), 1.72 (s, 6H); ^{13}C NMR (75 MHz, $CDCl_3$) δ 180.5, 169.4, 155.9, 151.6, 142.5, 141.5, 141.0, 137.8, 130.7, 130.1, 129.9, 129.4, 128.8, 128.1, 122.4, 113.9, 113.7, 113.5, 51.4, 35.9, 27.1, 23.4; MS (ESI) m/z 371.21 $(M)^+$.

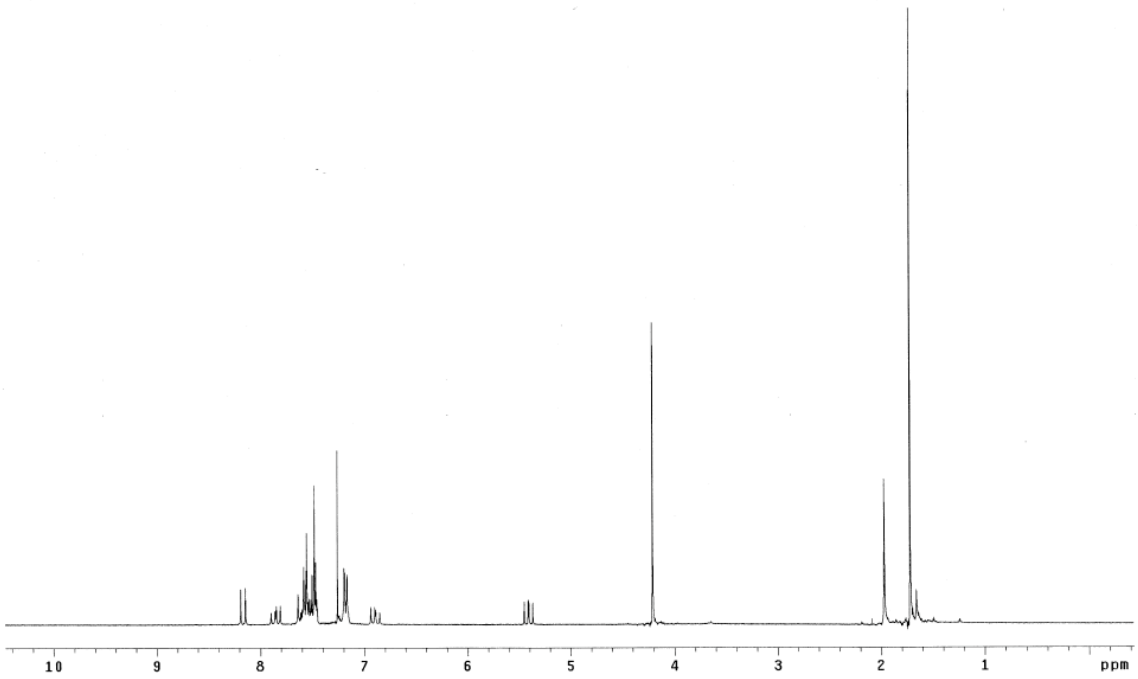

^{1}H NMR ($CDCl_3$)

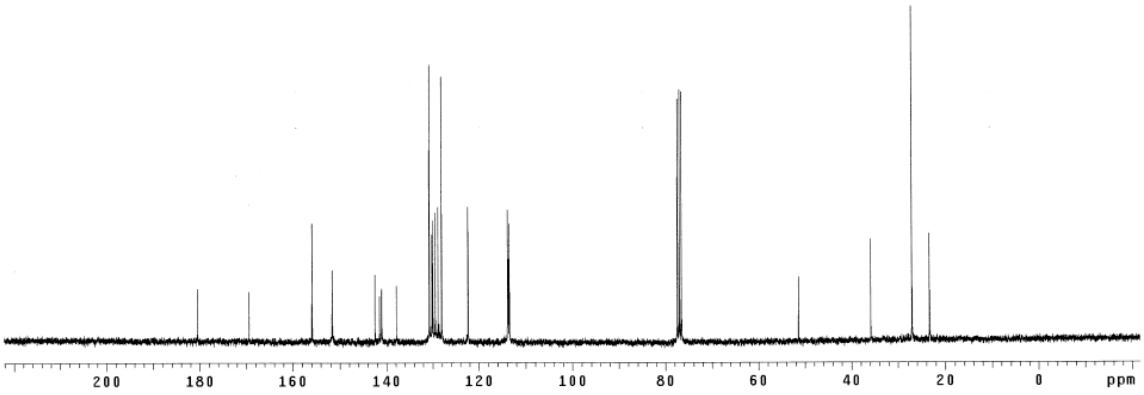

^{13}C NMR ($CDCl_3$)

Cyanine 7 (73c)

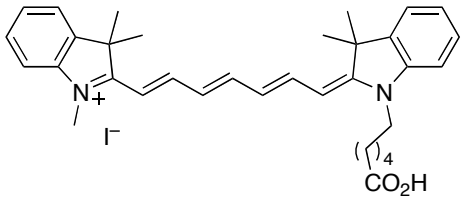

Indolium bromide **76** (200 mg, 0.56 mmol) was added to a solution of hemicyanine **79** (281 mg, 0.56 mmol) in pyridine (6.0 mL). The reaction mixture was stirred at 50 ºC for 1 h. After cooling to room temperature, ether (100 mL) was added and the reaction mixture was filtered off to afford dark green solids. The residue was purified by flash chromatography eluting with 100 % EtOAc and 2 % to 10 % MeOH/CH_2Cl_2 to afford product as a purple solid (280 mg, 78 %). R_f 0.5 (10 % MeOH/CH_2Cl_2). ^{1}H NMR (500 MHz, DMSO-d_6) δ 7.95-7.88 (m, 2H), 7.83-7.78 (m, 1H), 7.63-7.61 (m, 2H), 7.46-7.39 (m, 4H), 7.29-7.24 (m, 2H), 6.57 (q, 2H, J = 12.5 Hz), 6.38 (dd, 2H, J = 13.5, 4.0 Hz), 4.09 (t, 2H, J = 7.0 Hz), 3.63 (s, 3H), 2.24 (t, 2H, J = 7.0 Hz), 1.75-1.68 (m, 2H), 1.67 (s, 6H), 1.66 (s, 6H), 1.62-1.56 (m, 2H), 1.45-1.39 (m, 2H); ^{13}C NMR (125 MHz, DMSO-d_6) δ 175.4, 172.9, 171.8, 157.0, 152.1, 151.8, 150.6, 143.8, 143.2, 141.9, 129.42, 129.36, 126.2, 125.6, 125.4, 124.9, 123.4, 123.3, 112.0, 111.9, 105.1, 104.5, 49.6, 49.5, 44.3, 34.5, 32.1, 28.2, 28.0, 27.7, 26.7, 25.2; MS (ESI) m/z 509.32 $(M)^+$.

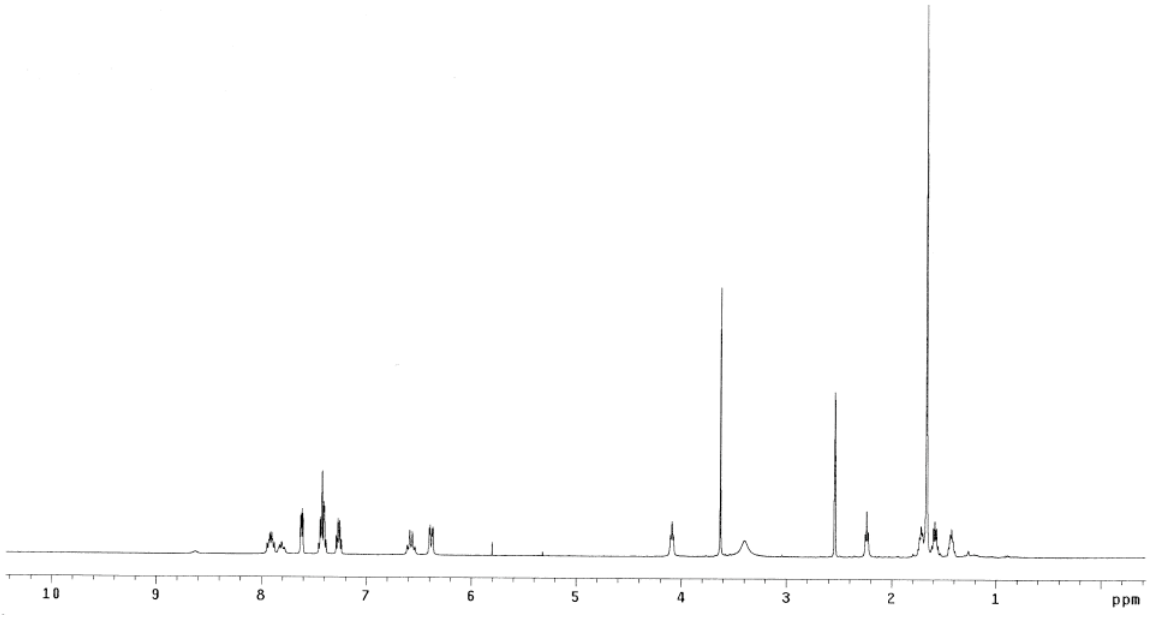

^{1}H NMR (DMSO-d_6)

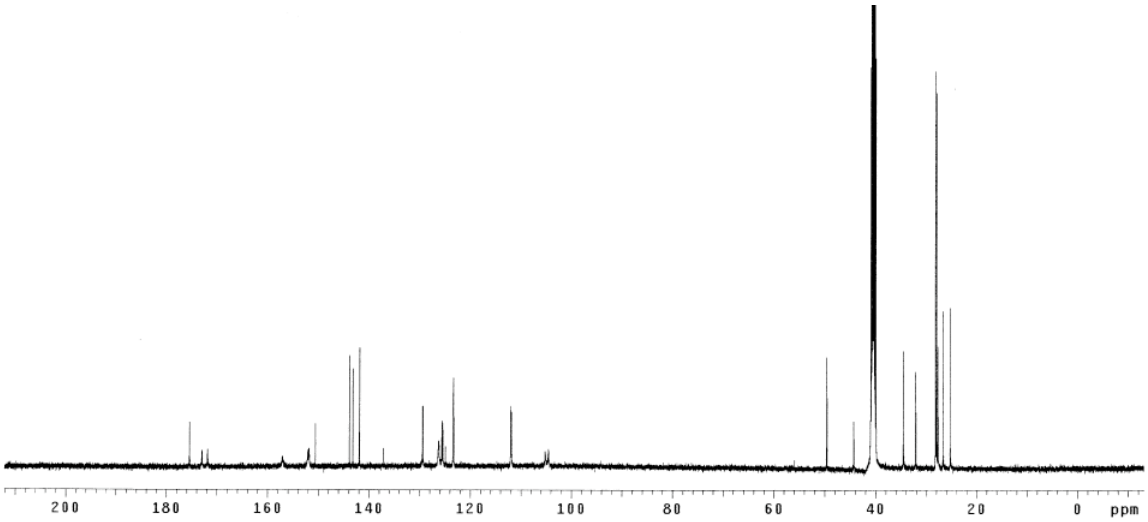

^{13}C NMR (DMSO-d_6)

5-Iodo hemicyanine (80)

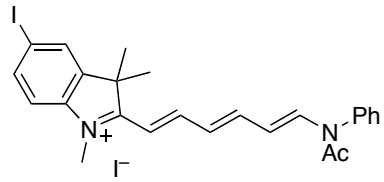

Indolium iodide **78** (300 mg, 0.70 mmol) and glutaconaldehydedianil hydrochloride (300 mg, 1.05 mmol) were added to a solution of Ac_2O (3.0 mL) and pyridine (3.0 mL). The reaction mixture was stirred at 25 ºC for 1 h. Ether (100 mL) was added and the reaction mixture was filtered off to afford dark brown solids. The residue was purified by flash chromatography eluting with 100 % EtOAc and 1 % to 5 % MeOH/CH_2Cl_2 to afford product as a dark brown solid (327 mg, 74 %). R_f 0.4 (10 % MeOH/CH_2Cl_2). ^{1}H NMR (500 MHz, $CDCl_3$) δ 8.20 (d, 1H, J = 14.0 Hz), 7.88-7.82 (m, 2H), 7.77 (d, 1H, J = 1.5 Hz), 7.60-7.54 (m, 4H), 7.24 (d, 2H, J = 8.5 Hz), 7.20-7.18 (m, 2H), 6.92-6.87 (m, 1H), 5.46-5.41 (m, 1H), 4.18 (s, 3H), 1.98 (s, 3H), 1.72 (s, 6H); ^{13}C NMR (125 MHz, $CDCl_3$) δ 179.7, 169.5, 156.6, 152.6, 144.2, 141.8, 141.4, 138.5, 137.8, 131.6, 130.8, 130.7, 130.1, 128.1, 115.3, 113.8, 113.7, 93.7, 51.2, 35.5, 27.2, 23.4; MS (ESI) m/z 497.11 $(M)^+$.

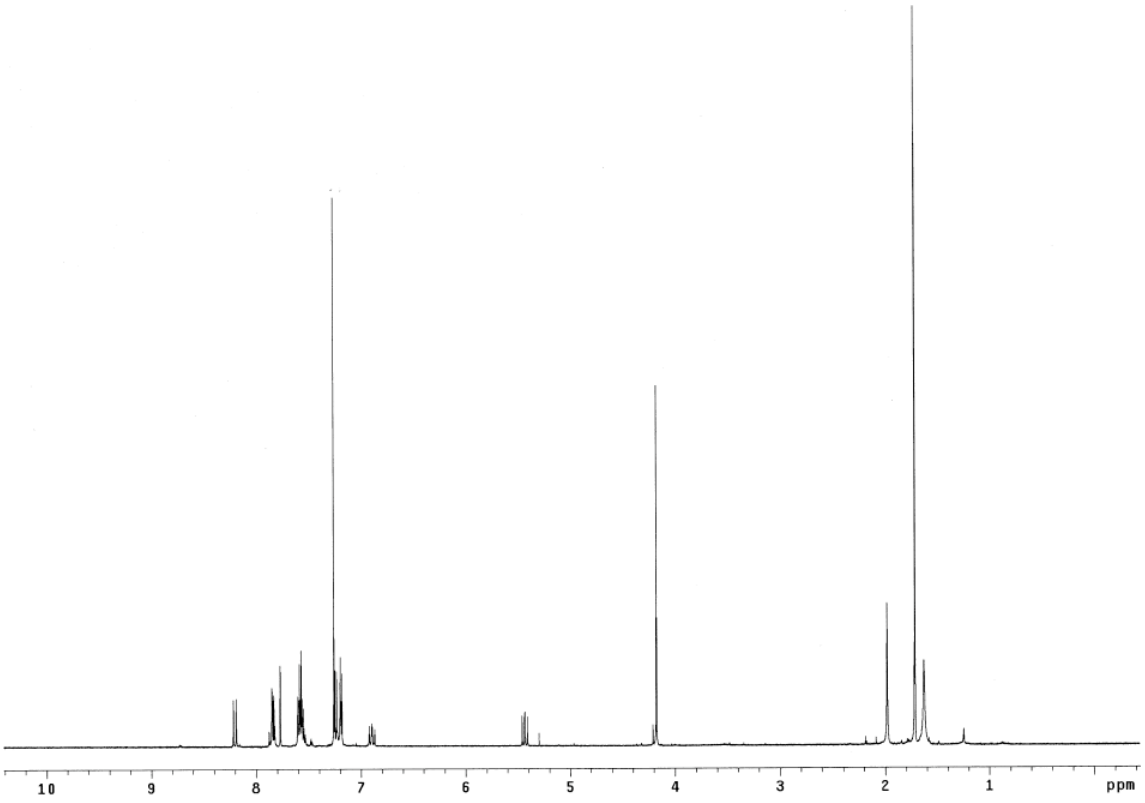

^{1}H NMR ($CDCl_3$)

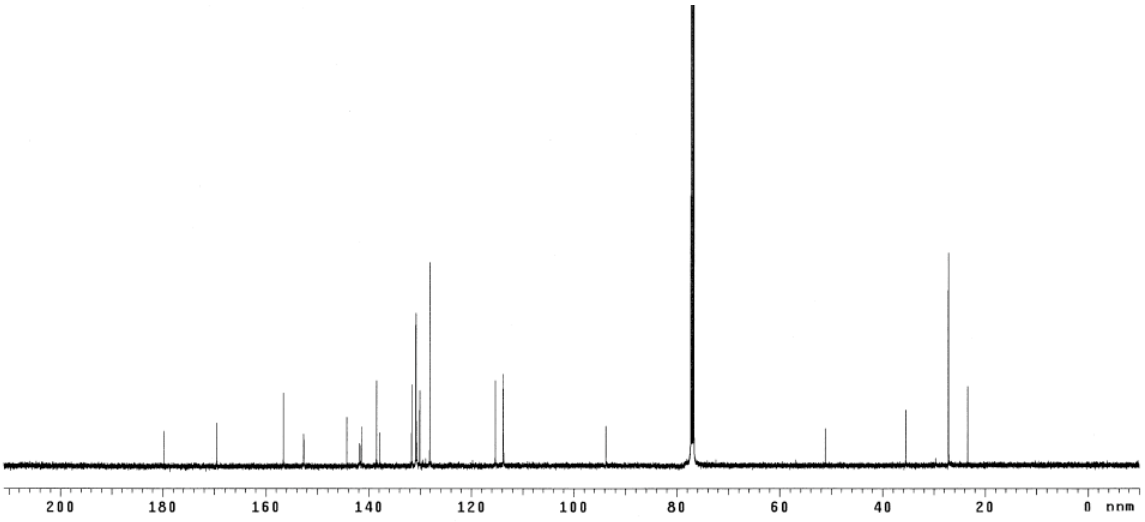

^{13}C NMR ($CDCl_3$)

5-Iodo cyanine 7 (74c)

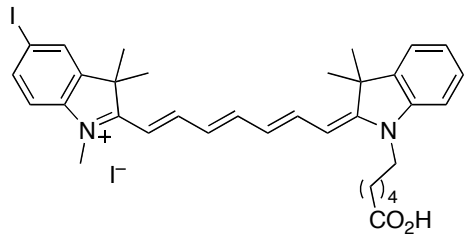

Indolium bromide **76** (150 mg, 0.42 mmol) was added to a solution of 5-iodo hemicyanine **80** (264 mg, 0.42 mmol) in pyridine (5.0 mL). The reaction mixture was stirred at 50 ºC for 1.5 h. After cooling to room temperature, ether (100 mL) was added and the reaction mixture was filtered off to afford dark green solids. The residue was purified by flash chromatography eluting with 100 % EtOAc and 5 % to 10 % MeOH/CH_2Cl_2 to afford product as a purple solid (234 mg, 72 %). R_f 0.5 (10 % MeOH/CH_2Cl_2). ^{1}H NMR (500 MHz, DMSO-d_6) δ 7.97 (t, 1H, J = 13.0 Hz), 7.95 (d, 1H, J = 1.5 Hz), 7.86-7.77 (m, 2H), 7.73 (dd, 1H, J = 10.0, 1.5 Hz), 7.66 (d, 1H, J = 7.5 Hz), 7.50-7.44 (m, 2H), 7.32 (t, 1H, J = 7.5 Hz), 7.17 (d, 1H, J = 8.5 Hz), 6.62 (t, 1H, J = 13.0 Hz), 6.57-6.51 (m, 2H), 6.23 (d, 1H, J = 13.0 Hz), 4.16 (t, 2H, J = 7.0 Hz), 3.52 (s, 3H), 2.23 (t, 2H, J = 7.5 Hz), 1.76-1.70 (m, 2H), 1.68 (s, 6H), 1.65 (s, 6H), 1.61-1.55 (m, 2H), 1.46-1.40 (m, 2H); ^{13}C NMR (125 MHz, $CDCl_3$) δ 177.9, 173.2, 168.8, 156.7, 153.0, 149.4, 143.0, 142.6, 141.8, 141.3, 137.2, 131.0, 128.8, 127.3, 126.8, 125.7, 122.3, 111.5, 111.2, 105.7, 103.1, 86.8, 49.6, 48.2, 44.8, 33.9, 31.8, 28.0, 27.9, 27.3, 26.2, 24.4; MS (ESI) m/z 635.21 $(M)^+$.

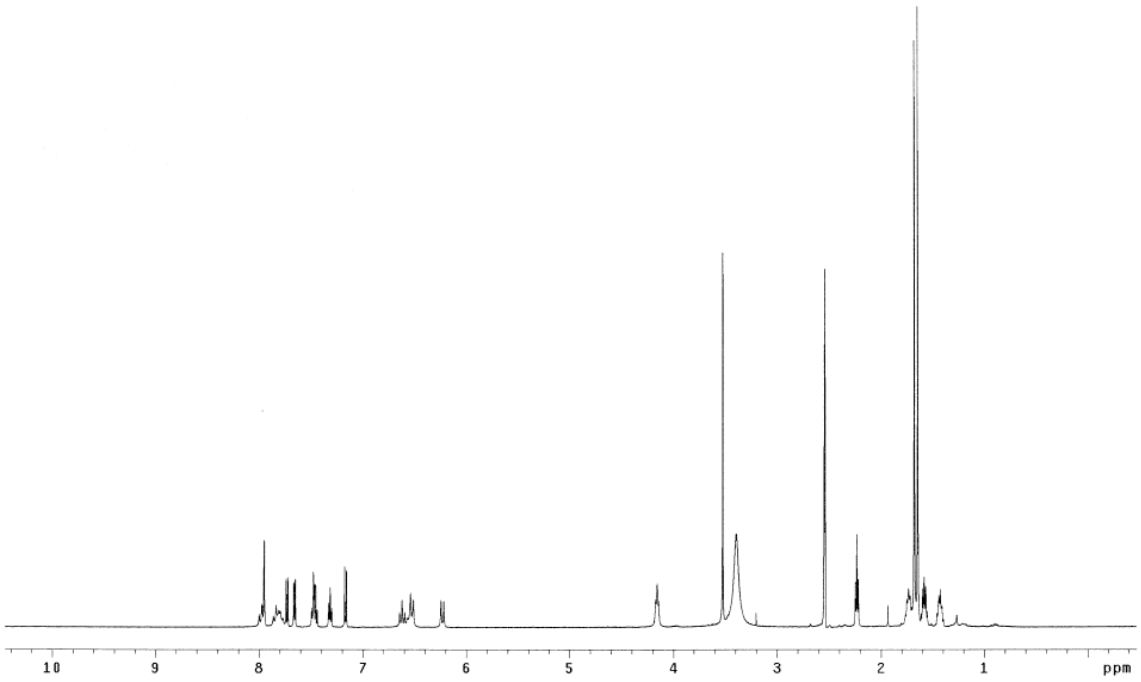

^{1}H NMR (DMSO-d_6)

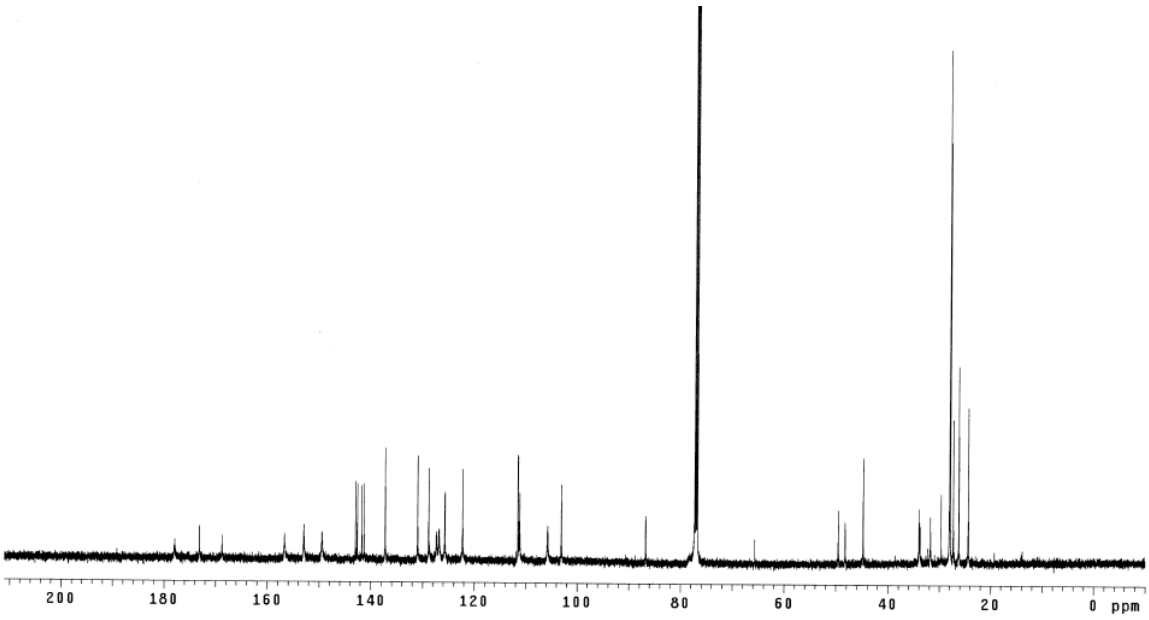

^{13}C NMR ($CDCl_3$)

TBET cassette based on Cy3 (75a)

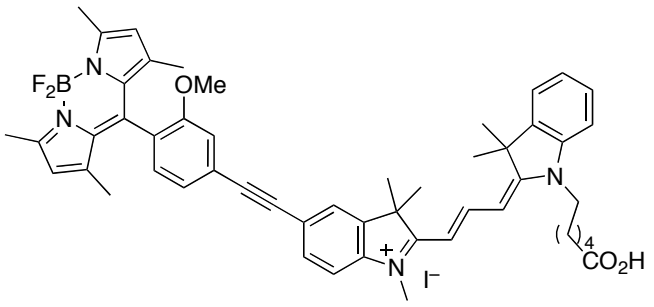

A solution of 5-iodo-Cy3 **74a** (70 mg, 0.099 mmol), 4-ethynyl BODIPY **55** (63 mg, 0.17 mmol), $Pd(PPh_3)_4$ (23 mg, 0.020 mmol), CuI (3.8 mg, 0.020 mmol) in DMF (4.0 mL) was freeze-pump-thawed at –78 ºC (x 3 times). Et_3N (70 mL, 0.49 mmol) was added to a solution and the reaction mixture was stirred at 40 ºC for 45 min under nitrogen. Ether (100 mL) was added to a reaction mixture and reaction mixture was filtered off to afford dark red solid. The residue was purified by flash chromatography eluting with 100 % EtOAc and 10 to 50 % MeOH/CH_2Cl_2 to afford product as a dark red solid (43 mg, 45 %). R_f 0.5 (10 % EtOAc/hexanes). ^{1}H NMR (500 MHz, $CDCl_3$) δ 8.40 (t, 1H, J = 13.2 Hz), 7.59 (d, 1H, J = 8.5 Hz), 7.51 (s, 1H), 7.43-7.38 (m, 2H), 7.30-7.27 (m, 2H), 7.16-7.13 (m, 4H), 7.04 (d, 1H, J = 13.0 Hz), 6.91 (d, 1H, J = 13.0 Hz), 5.97 (s, 2H), 4.15 (br, 2H), 3.81 (s, 3H), 3.79 (s, 3H), 2.63 (br, 2H), 2.55 (s, 6H), 1.90 (br, 2H), 1.86-1.83 (m, 2H), 1.74 (s, 6H), 1.73 (s, 6H), 1.67-1.61 (m, 2H), 1.48 (s, 6H); ^{13}C NMR (125 MHz, $CDCl_3$) δ 175.9, 174.3, 173.6, 156.4, 155.2, 150.6, 142.9, 142.4, 141.7, 140.7, 140.6, 137.8, 132.7, 131.3, 129.7, 129.0, 125.7, 125.2, 125.1, 124.8, 124.5, 122.2, 121.0, 119.3, 114.0, 111.2, 110.9, 105.3, 105.1, 90.0, 89.8, 55.8, 49.2, 48.6, 44.7, 34.5, 32.3, 28.16, 28.13, 26.5, 26.0, 24.2, 14.6, 14.0; MS (MALDI) m/z 833.29 $(M)^+$.

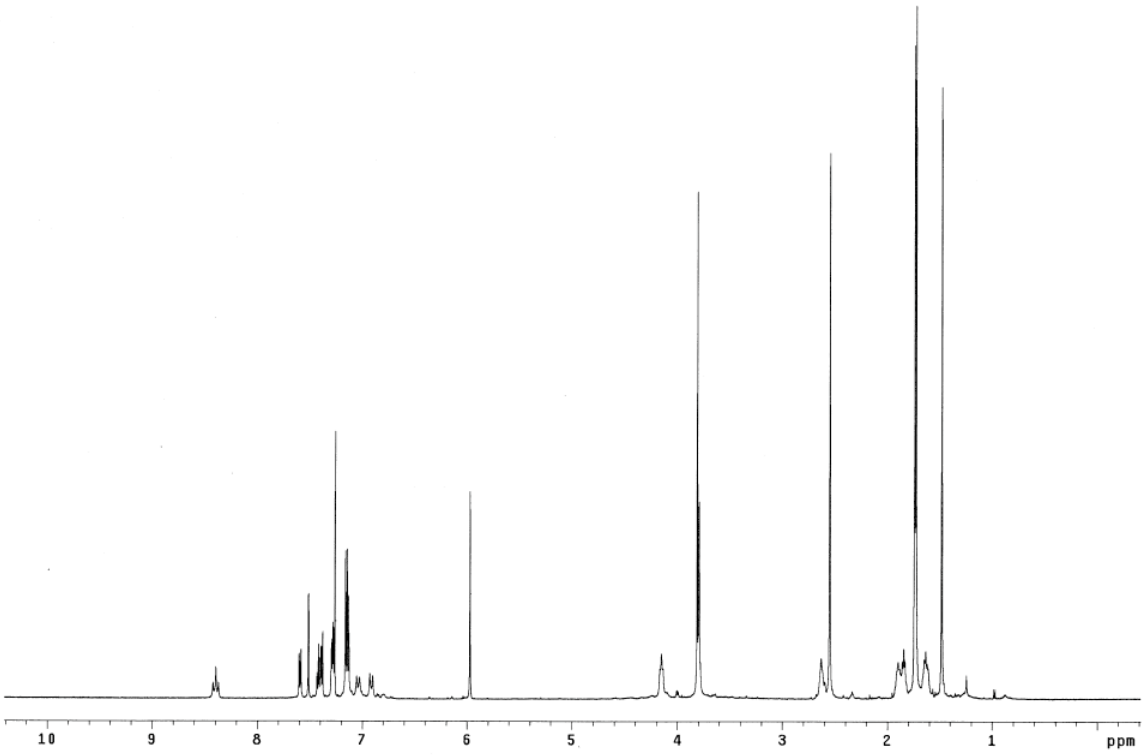

^{1}H NMR ($CDCl_3$)

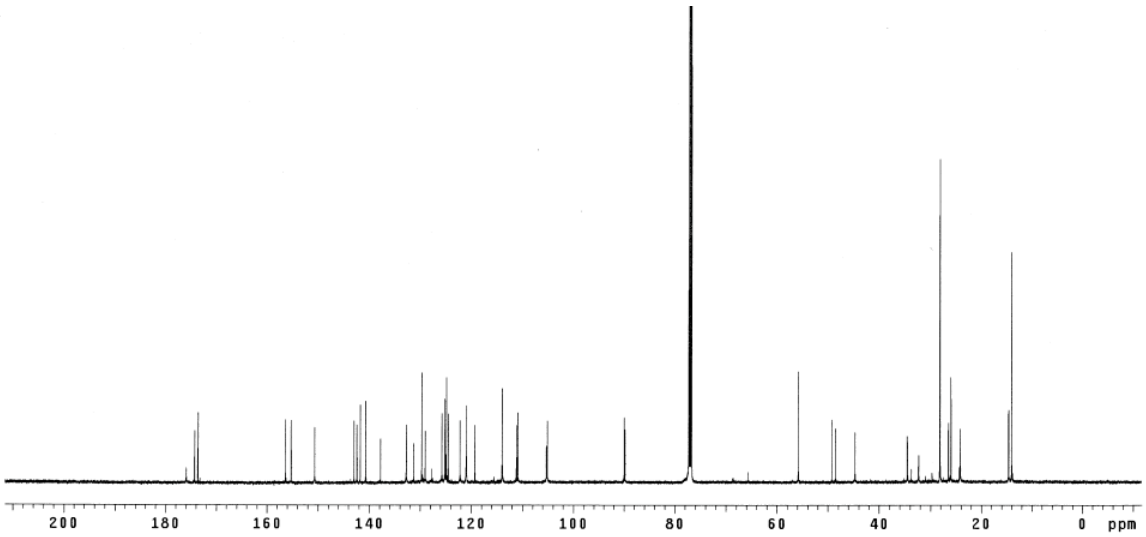

^{13}C NMR ($CDCl_3$)

TBET cassette based on Cy7 (75c)

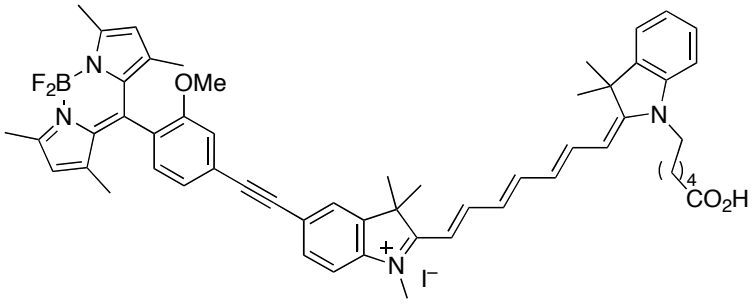

A solution of 5-iodo-Cy7 **74c** (80 mg, 0.10 mmol), 4-ethynyl BODIPY **55** (67 mg, 0.18 mmol), $Pd(PPh_3)_4$ (24 mg, 0.021 mmol), CuI (4 mg, 0.021 mmol) in DMF (4.0 mL) was freeze-pump-thawed at –78 ºC (x 3 times). Et_3N (70 mL, 0.49 mmol) was added to a solution and the reaction mixture was stirred at 40 ºC for 45 min under nitrogen. Ether (100 mL) was added to a reaction mixture and reaction mixture was filtered off to afford dark red solids. The residue was purified by flash chromatography eluting with 100 % EtOAc and 10 to 50 % MeOH/CH_2Cl_2 to afford product as a dark green solid (35 mg, 33 %). R_f 0.5 (10 % EtOAc/hexanes). ^{1}H NMR (500 MHz, CD_3OD) δ 8.07 (t, 1H, J = 12.0 Hz), 7.88 (t, 1H, J = 12.0 Hz), 7.66-7.61 (m, 2H), 7.58 (t, 2H, J = 7.5 Hz), 7.48 (t, 1H, J = 7.5 Hz), 7.42 (d, 1H, J = 8.0 Hz), 7.37-7.33 (m, 3H), 7.22-7.19 (m, 2H), 6.66 (t, 1H, J = 13.0 Hz), 6.59 (t, 1H, J = 13.0 Hz), 6.50 (d, 1H, J = 14.5 Hz), 6.17 (d, 1H, J = 13.0 Hz), 6.09 (s, 2H), 4.21 (t, 2H, J = 7.5 Hz), 3.88 (s, 3H), 3.55 (s, 3H), 2.52 (s, 6H), 2.36 (t, 2H, J = 7.5 Hz), 1.91-1.85 (m, 2H), 1.75 (s, 6H), 1.74-1.69 (m, 2H), 1.73 (s, 6H), 1.55 (s, 6H), 1.54-1.50 (m, 2H); ^{13}C NMR (125 MHz, DMSO-d_6) δ 175.3, 174.7, 169.8, 157.0, 155.7, 154.0, 149.8, 144.8, 143.1, 142.7, 142.6, 141.9, 139.2, 133.1, 131.6, 130.6, 129.6, 127.3, 126.7, 126.6, 126.4, 126.1, 125.5, 124.1, 123.6, 122.2 (2C), 117.4, 115.3, 112.9, 111.3, 106.9, 104.0, 92.1, 89.9, 57.0, 50.4, 48.7, 44.9, 34.5, 31.7, 28.2, 28.0, 27.9, 26.6, 25.2, 15.2, 14.6; MS (MALDI) m/z 885.35 $(M)^+$.

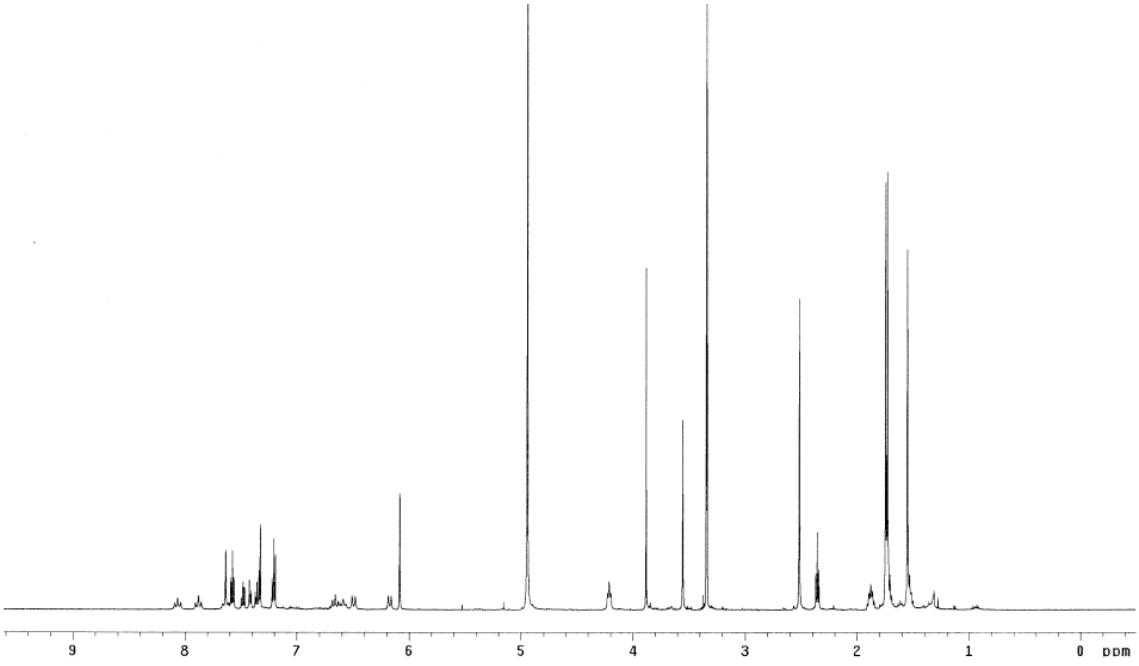

^{1}H NMR (CD_3OD)

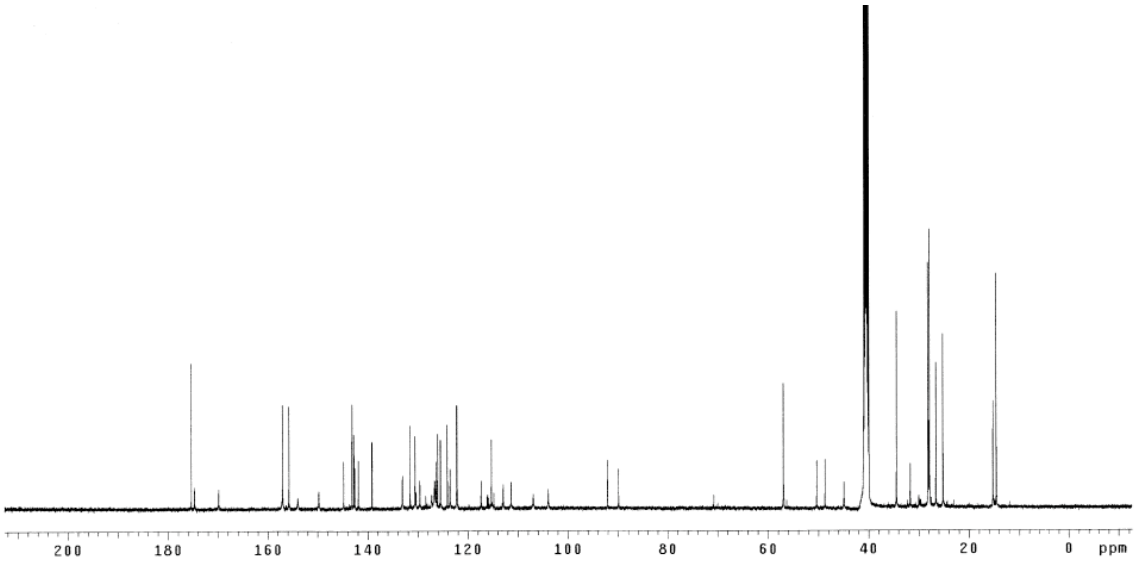

^{13}C NMR (DMSO-d_6)

APPENDIX C

EXPERIMENTAL DATA FOR CHAPTER IV

4-Bromomethyl-3-nitro *tert*-butyl-benzoate (89)

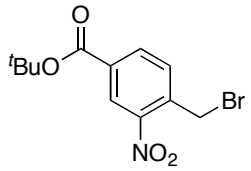

To a solution of 4-bromomethyl-3-nitrobenzoic acid (5.0 g, 0.019 mol), ^{t}BuOH (1.85 g, 0.025 mol) and DMAP (235 mg, 0.0019 mol) in CH_2Cl_2 (50 mL) was added DIC (3.26 mL, 0.021 mol) at 0 ºC. The reaction mixture was stirred at 25 ºC for 2.5 h. The reaction mixture was filtered and the solvent was evaporated. The residue was purified by short flash chromatography eluting with 15 % EtOAc/hexanes to afford product as a yellow solid (3.4 g, 56 %). R_f 0.9 (20 % EtOAc/hexanes). ^{1}H NMR (500 MHz, $CDCl_3$) δ 8.57 (s, 1H), 8.19 (d, 1H, J = 8.0 Hz), 7.63 (d, 1H, J = 8.0 Hz), 4.83 (s, 2H), 1.61 (s, 9H); ^{13}C NMR (125 MHz, $CDCl_3$) δ 163.3, 148.2, 136.8, 134.3, 134.0, 132.9, 126.7, 83.2, 28.41, 28.34; MS (CI) m/z 316.1 $(M+H)^{+}$.

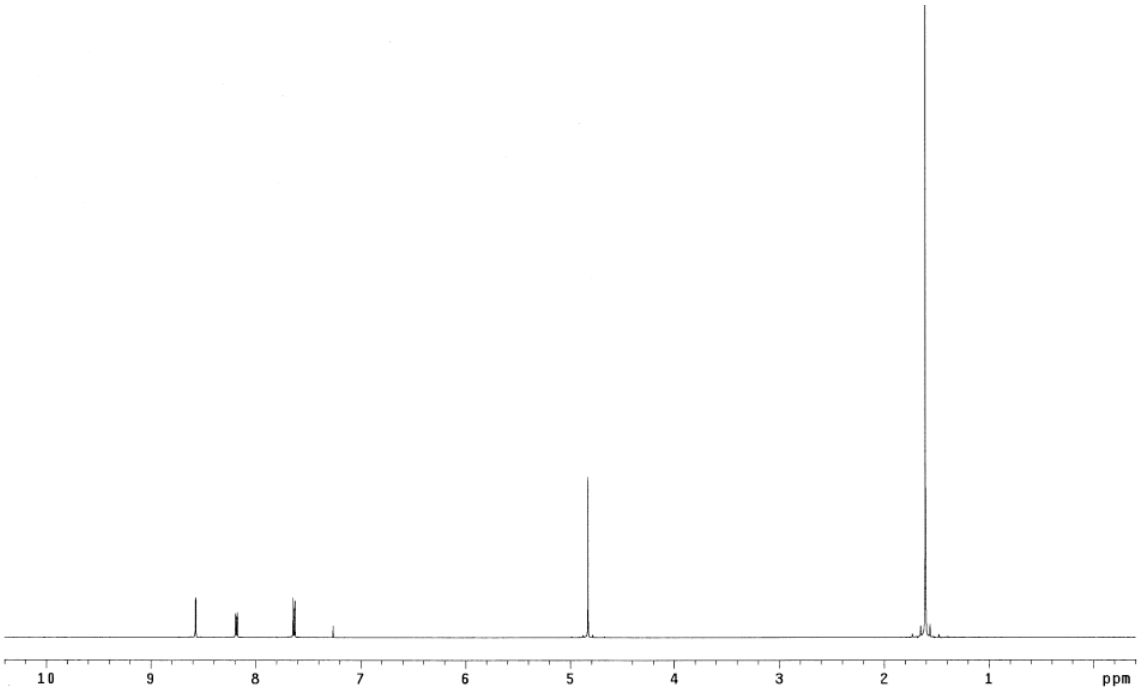

^{1}H NMR ($CDCl_3$)

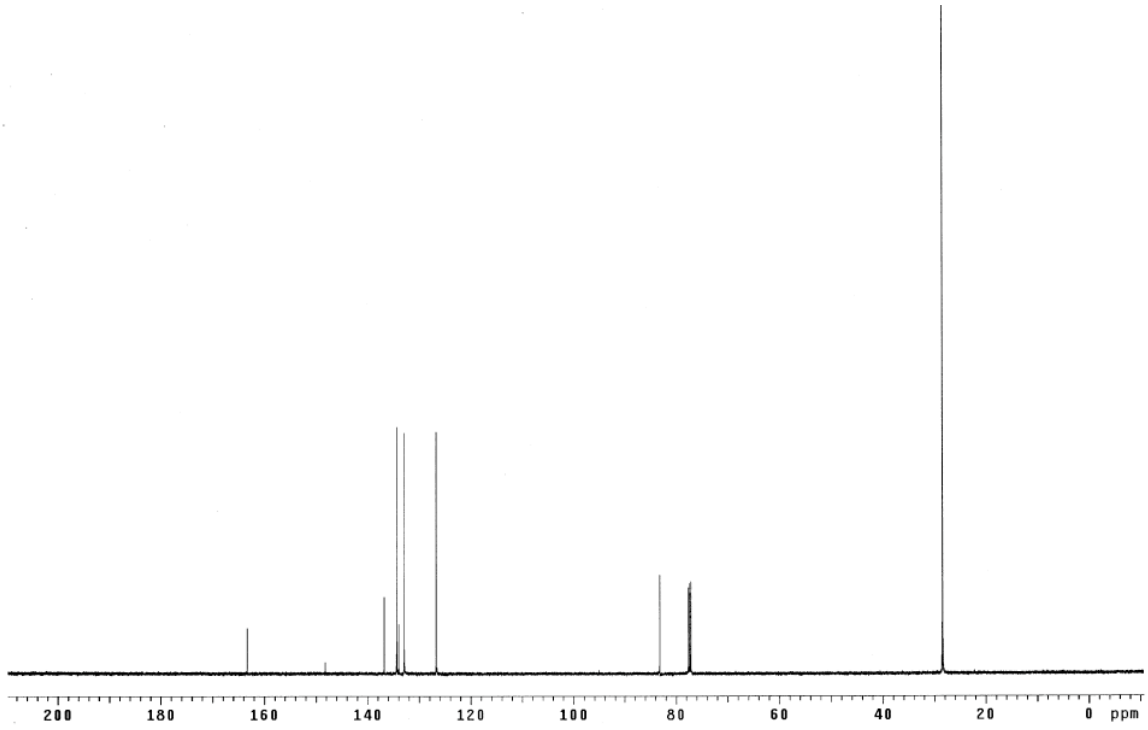

^{13}C NMR ($CDCl_3$)

Photo linker (90)

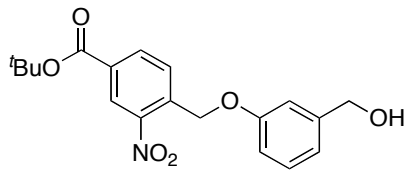

A solution of *tert*-butyl ester **89** (802 mg, 2.54 mmol), 3-hydroxybenzyl alcohol (300 mg, 2.42 mmol) and K_2CO_3 (835 mg, 6.04 mmol) in acetone (16 mL) was stirred at 25 ºC for 12 h in dark (2 batches). The reaction mixture was filtered and the solvent was evaporated. The residue was purified by flash chromatography eluting with 15 to 25 % EtOAc/hexanes to afford product as a light yellow solid (1.8 g, quantitative). R_f 0.4 (30 % EtOAc/hexanes). ^{1}H NMR (500 MHz, $CDCl_3$) δ 8.61 (d, 1H, J = 2.0 Hz), 8.16 (dd, 1H, J = 8.0, 2.0 Hz), 7.87 (d, 1H, J = 8.0 Hz), 7.01-7.17 (m, 1H), 6.92-6.89 (m, 2H), 6.79 (dd, 1H, J = 8.0, 2.0 Hz), 5.42 (s, 2H), 4.58 (d, 2H, J = 5.5 Hz), 1.81 (t, 1H, J = 5.5 Hz), 1.53 (s, 9H); ^{13}C NMR (125 MHz, $CDCl_3$) δ 163.7, 158.4, 147.0, 143.2, 138.2, 134.7, 132.9, 130.2, 128.9, 126.3, 120.4, 114.2, 113.6, 83.0, 67.0, 65.3, 28.4; MS (CI) m/z 360.3 $(M+H)^+$.

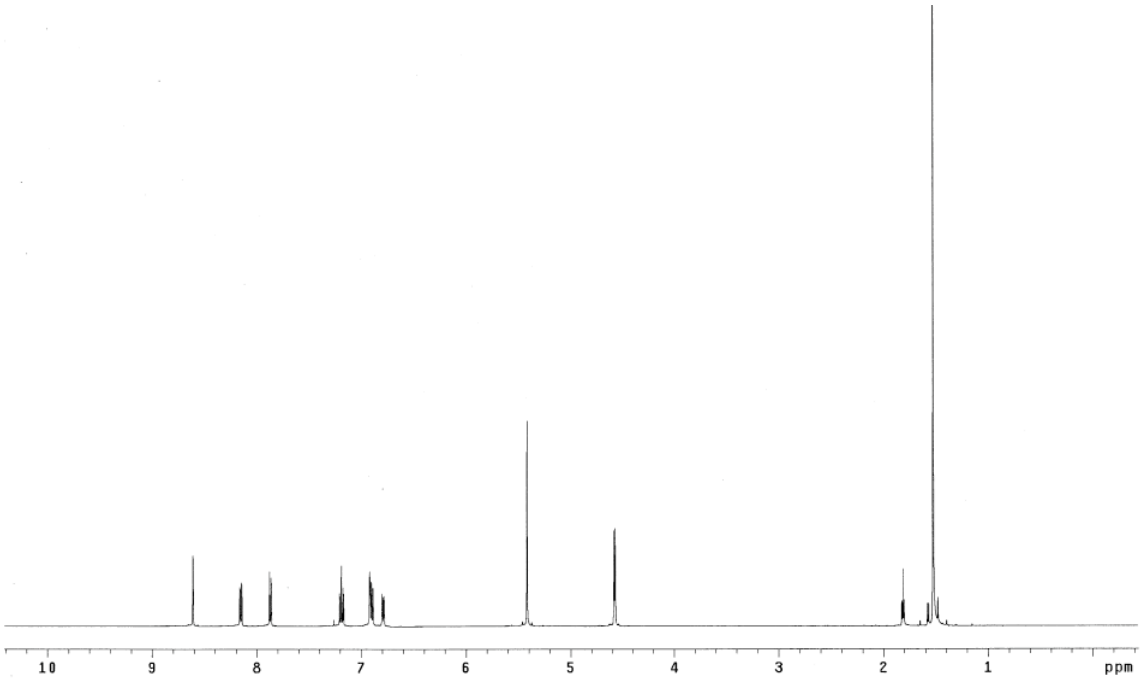

^{1}H NMR ($CDCl_3$)

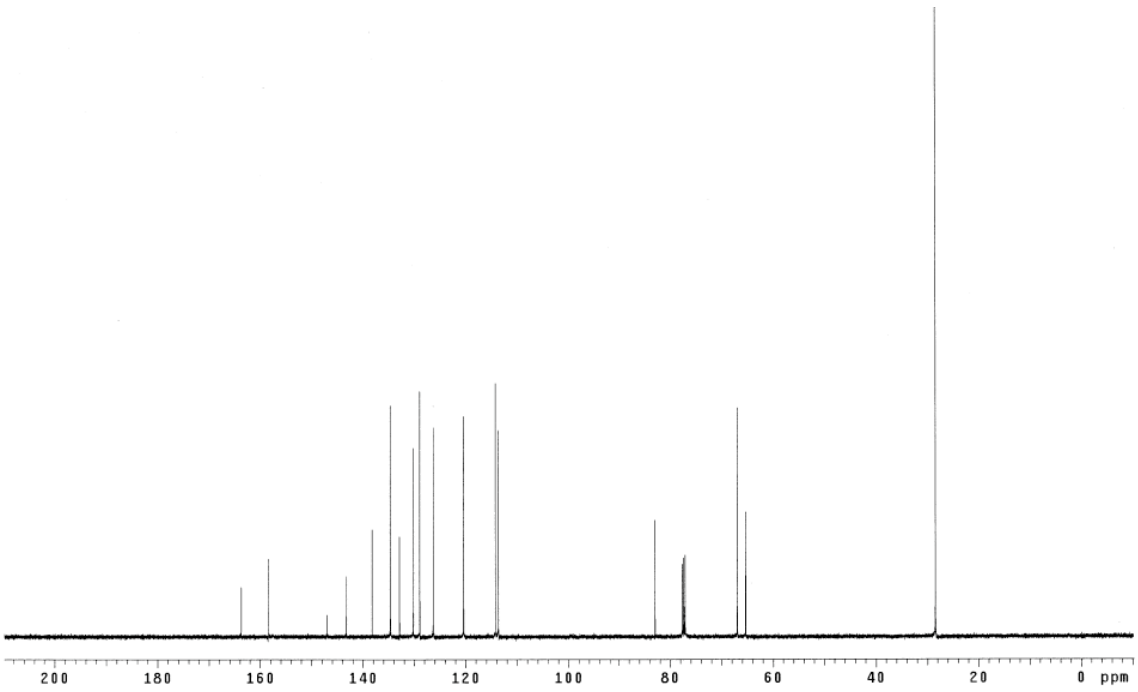

^{13}C NMR ($CDCl_3$)

Photo linker (91)

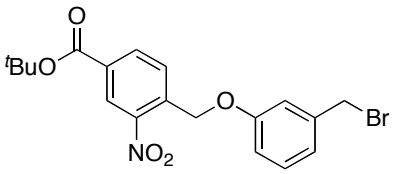

To a solution of alcohol **90** (1.0 g, 2.78 mmol) and PPh_3 (803 mg, 3.06 mmol) in CH_2Cl_2 (30 mL) was added carbon tetrabromide (1.02 g, 3.06 mmol) at 0 ºC. The reaction mixture was stirred at 25 ºC for 24 h in dark. The solvent was concentrated under the reduced pressure. The residue was purified by short flash chromatography eluting with 10 % EtOAc/hexanes to afford product as a light yellow solid (1.02 g, 86 %). R_f 0.4 (10 % EtOAc/hexanes). ^{1}H NMR (500 MHz, acetone-d_6) δ 8.66 (d, 1H, J = 2.0 Hz), 8.34 (dd, 1H, J = 8.0, 1.5 Hz), 8.06 (d, 1H, J = 8.0 Hz), 7.36 (t, 1H, J = 8.0 Hz), 7.22 (t, 1H, J = 2.0 Hz), 7.14 (d, 1H, J = 8.0 Hz), 7.05 (dd, 1H, J = 8.0, 2.0 Hz), 5.64 (s, 2H), 4.66 (s, 2H), 1.66 (s, 9H); ^{13}C NMR (125 MHz, acetone-d_6) δ 163.7, 158.9, 148.0, 140.6, 138.2, 134.5, 133.2, 130.6, 129.8, 125.9, 123.0, 116.2, 115.5, 82.7, 67.2, 33.8, 28.0; MS (APCI) m/z 422.1 $(M+H)^+$.

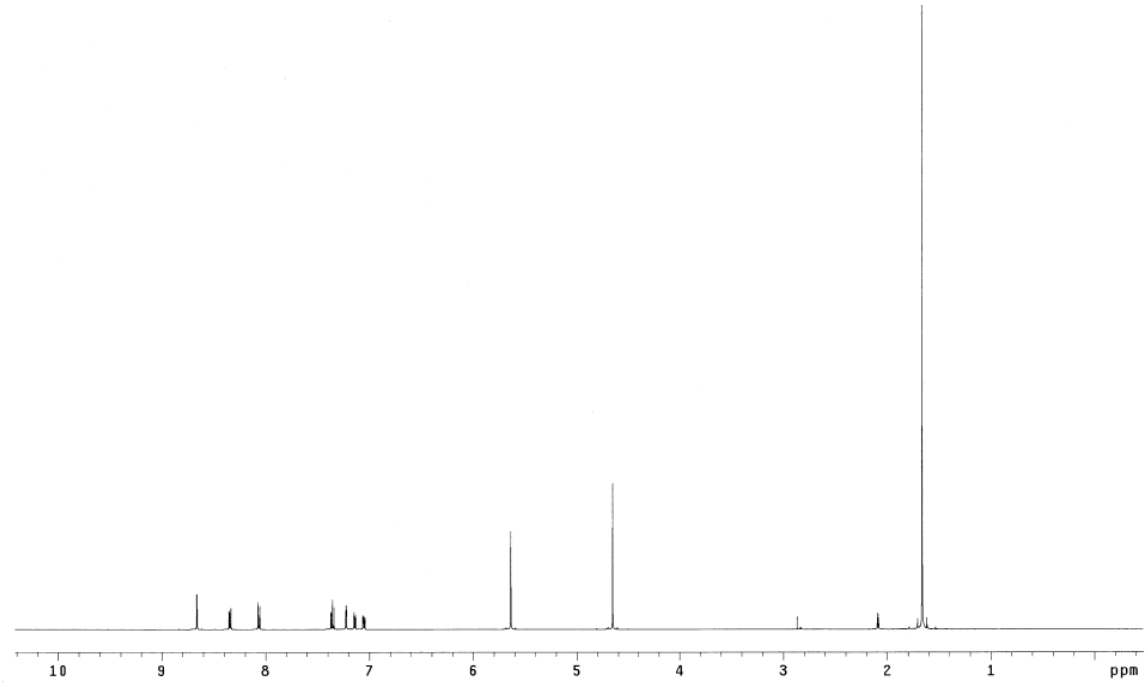

^{1}H NMR (acetone-d_6)

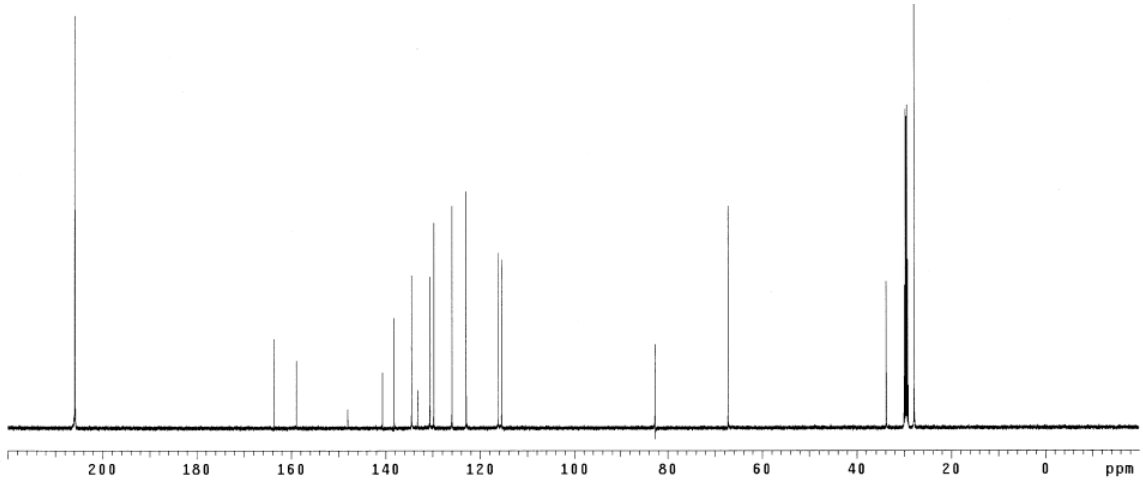

^{13}C NMR (acetone-d_6)

Dimethylester Nile Red derivative (93)

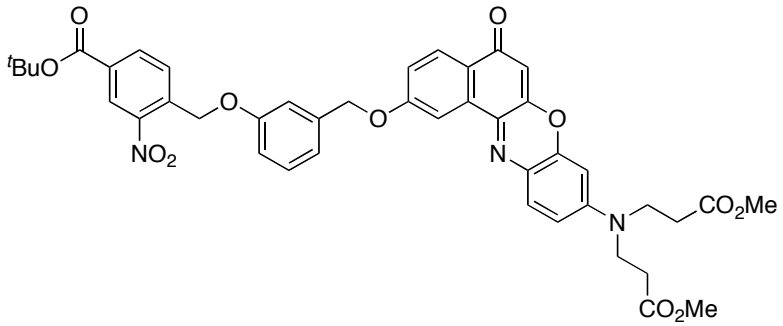

A solution of benzylbromide **91** (244 mg, 0.577 mmol), Nile Red **92** (200 mg, 0.444 mmol, *provided by Mr. Jiney Jose*) and Cs_2CO_3 (289 mg, 0.888 mmol) in acetone (20 mL) was refluxed at 70 ºC for 5 h under nitrogen. After the cooling to room temperature, small amount of silica gel was added to a solution and the solvent was evaporated. The obtained dark red powder was purified by flash chromatography eluting with 20 to 50 % EtOAc/hexanes to afford product as a red solid (199 mg, 57 %). R_f 0.7 (60 % EtOAc/hexanes). ^{1}H NMR (300 MHz, DMSO-d_6) δ 8.54 (d, 1H, J = 1.8 Hz), 8.27 (dd, 1H, J = 8.0, 1.8 Hz), 8.10 (s, 1H), 8.09 (d, 1H, J = 8.0 Hz), 7.96 (d, 1H, J = 8.0 Hz), 7.68 (d, 1H, J = 8.0 Hz), 7.43-7.37 (m, 2H), 7.26 (s, 1H), 7.19 (d, 1H, J = 7.5 Hz), 7.06 (dd, 1H, J = 9.0, 2.0 Hz), 6.88 (dd, 1H, J = 9.0, 2.0 Hz), 6.78 (d, 1H, J = 2.0 Hz), 6.26 (s, 1H), 5.62 (s, 2H), 5.34 (s, 2H), 3.78 (t, 4H, J = 7.2 Hz), 3.66 (s, 6H), 2.70 (t, 4H, J = 7.2 Hz), 1.61 (s, 9H); MS (MALDI) m/z 793.17 $(M+H)^+$. ^{13}C NMR was difficult to obtain because of poor solubility of compound **93** in any organic solvents.

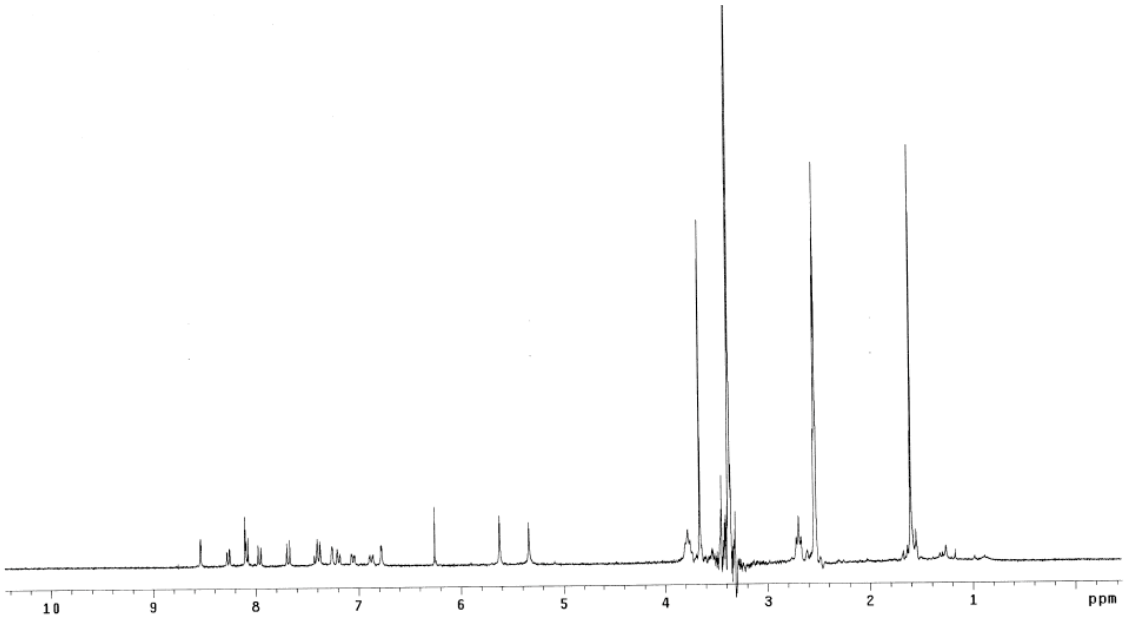

^{1}H NMR (DMSO-d_6)

Carboxylic acid Nile red derivative (94)

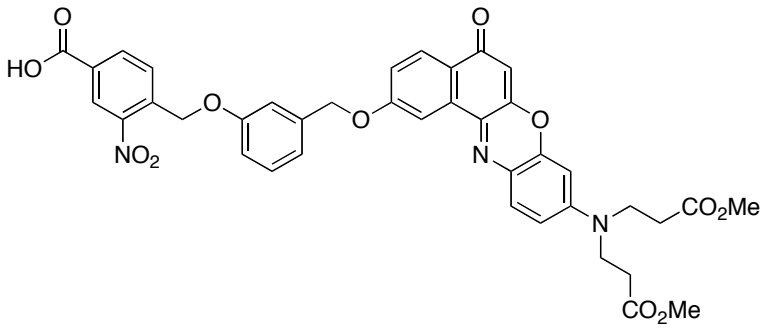

To a solution of Nile Red derivative **93** (171 mg, 0.216 mmol) in CH_2Cl_2 (22 mL) was added 2,6-lutidine (0.06 mL, 0.54 mmol) and then added TMSOTf (0.42 mL, 2.16 mmol) dropwise at 0 ºC. The reaction mixture was stirred at 25 ºC for 30 h under nitrogen. The solvent was evaporated at 30 ºC and EtOAc (30 mL) was added to this residue. The organic layer was washed with water (1 x 30 mL) and brine (1 x 30 mL). The organic layer was dried over Na_2SO_4 and small amount of silica gel was added to this solution and the solvent was concentrated under the reduced pressure. The obtained dark red powder was purified by flash chromatography eluting with 70 % EtOAc/hexanes and 5 to 20 % MeOH/EtOAc to afford product as a dark red solid (123 mg, 77 %). R_f 0.5 (10 % MeOH/EtOAc). ^{1}H NMR (300 MHz, DMSO-d_6) δ 8.54 (d, 1H, J = 1.2 Hz), 8.22 (dd, 1H, J = 8.0, 1.2 Hz), 8.11 (s, 1H), 8.09 (d, 1H, J = 8.0 Hz), 7.77 (d, 1H, J = 8.0 Hz), 7.68 (d, 1H, J = 8.0 Hz), 7.42-7.37 (m, 2H), 7.26 (s, 1H), 7.18 (d, 1H, J = 7.5 Hz), 7.04 (dd, 1H, J = 9.0, 1.8 Hz), 6.88 (dd, 1H, J = 9.0, 1.8 Hz), 6.77 (d, 1H, J = 2.4 Hz), 6.25 (s, 1H), 5.53 (s, 2H), 5.33 (s, 2H), 3.78 (t, 4H, J = 7.2 Hz), 3.66 (s, 6H), 2.70 (t, 4H, J = 7.2 Hz); MS (MALDI) m/z 737.13 $(M+H)^+$. ^{13}C NMR was difficult to obtain because of poor solubility of compound **94** in any organic solvents.

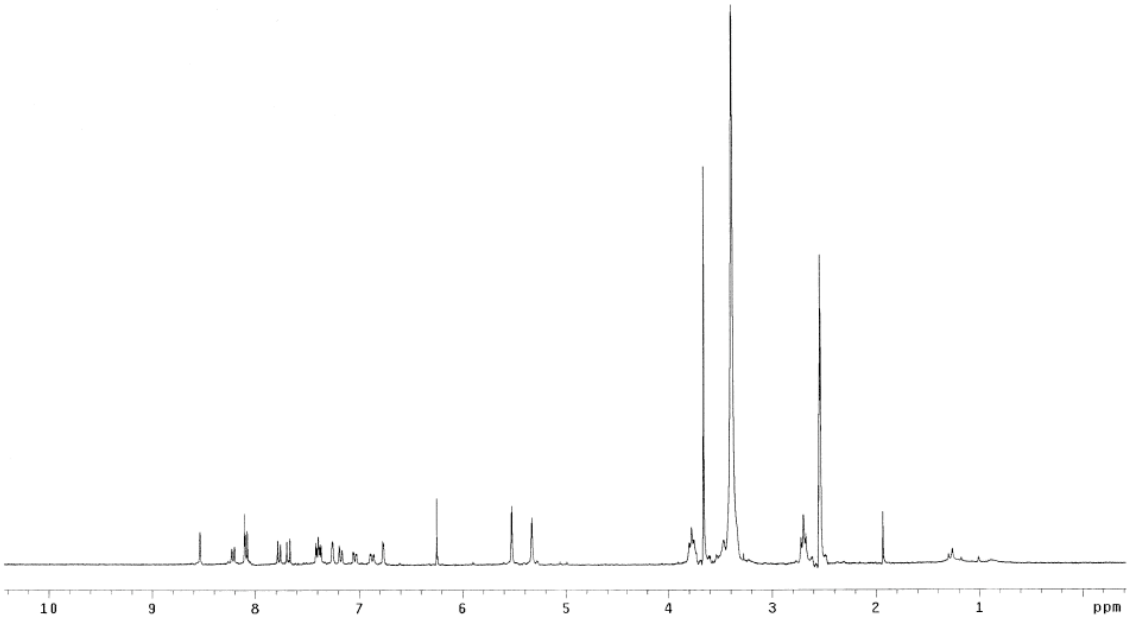

^{1}H NMR (DMSO-d_6)

3-(*tert*-butyldiphenylsilyloxy)benzaldehyde (97)

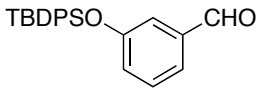

To a solution of 3-hydroxybenzaldehyde (3.0 g, 0.025 mol) and imidazole (2.5 g, 0.037 mol) in DMF (40 mL) was added TBDPSCl (8.1 g, 0.030 mol) at 25 ºC. The reaction was stirred at 25 ºC for 3.5 h. Water (50 mL) was added to a reaction mixture and the aqueous layer was extracted with EtOAc (3 x 20 mL). The combined organic layer was dried over Na_2SO_4 and concentrated in vacuo. The residual material was purified by flash chromatography eluting with 100 % hexanes and 5 % EtOAc/hexanes to afford product as a colorless oil (8.0 g, 90 %). R_f 0.6 (10 % EtOAc/hexanes). ^{1}H NMR (500 MHz, CD_3OD) δ 9.78 (s, 1H), 7.75-7.73 (m, 4H), 7.48-7.38 (m, 8H), 7.29-7.26 (m, 1H), 7.03 (dd, 1H, J = 10.0, 2.5 Hz), 1.13 (s, 9H); ^{13}C NMR (125 MHz, CD_3OD) δ 193.5, 157.6, 139.3, 136.6, 133.3, 131.4, 131.1, 129.1, 127.1, 124.3, 120.6, 27.0, 20.2; MS (CI) m/z 361.2 $(M+H)^+$.

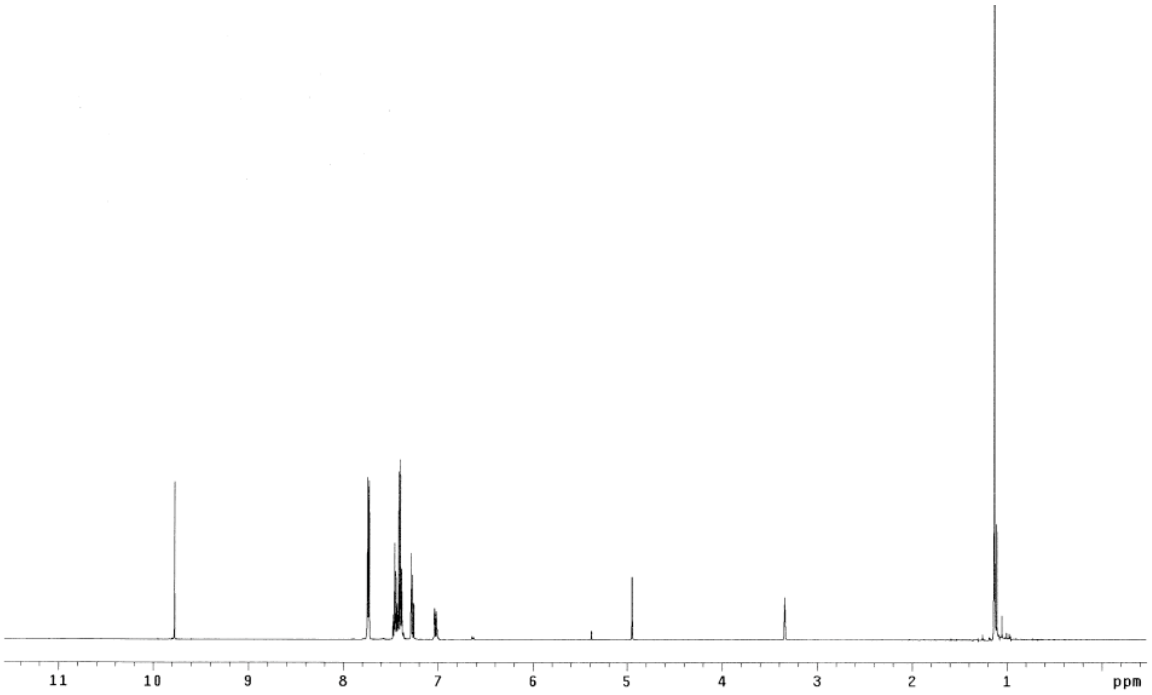

^{1}H NMR (CD_3OD)

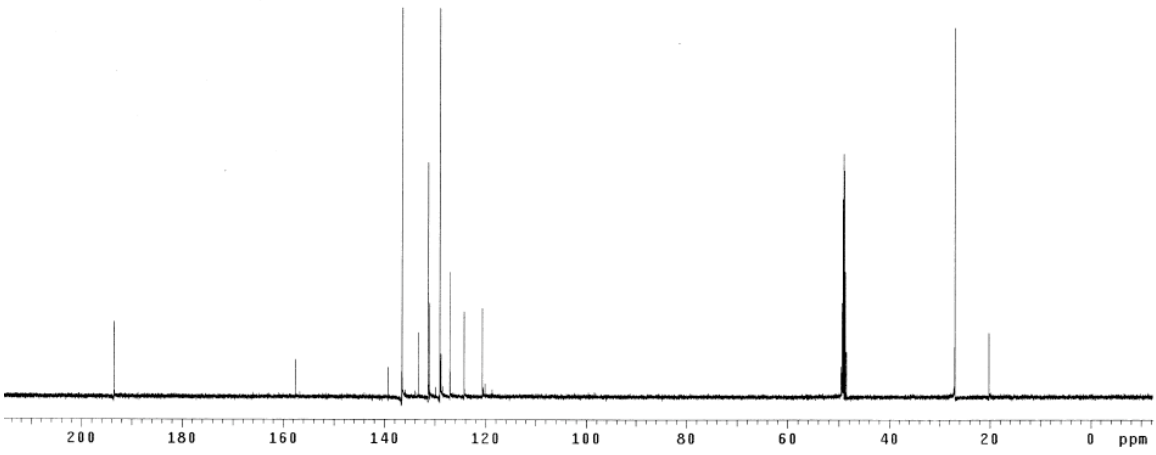

^{13}C NMR (CD_3OD)

3-(*tert*-butyldiphenylsilyloxy)benzylalcohol (98)

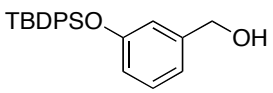

To a solution of TBDPS-protected-hydroxybenzaldehyde **97** (6.3 g, 0.017 mol) in MeOH (120 mL) was slowly added $NaBH_4$ (793 mg, 0.021 mol) at 0 ºC. The reaction was stirred at 25 ºC for 1 h. Water (30 mL) was added to a reaction mixture and MeOH was only evaporated under reduced pressure. The aqueous layer was extracted with EtOAc (5 x 50 mL) and the combined organic layer was dried over Na_2SO_4 and concentrated in vacuo to afford pure product as a colorless oil (6.2 g, 98 %). R_f 0.4 (20 % EtOAc/hexanes). ^{1}H NMR (500 MHz, CD_3OD) δ 7.75 (dd, 4H, J = 5.0, 1.5 Hz), 7.47-7.44 (m, 2H), 7.41-7.38 (m, 4H), 7.03 (t, 1H, J = 8.0 Hz), 6.89-6.87 (m, 2H), 6.60 (dd, 1H, J = 8.0, 3.0 Hz), 4.45 (s, 2H), 1.11 (s, 9H); ^{13}C NMR (125 MHz, CD_3OD) δ 157.0, 144.3, 136.6, 134.0, 131.1, 130.1, 128.9, 120.8, 119.5, 119.2, 64.8, 27.0, 20.2; MS (CI) m/z 363.3 $(M+H)^+$.

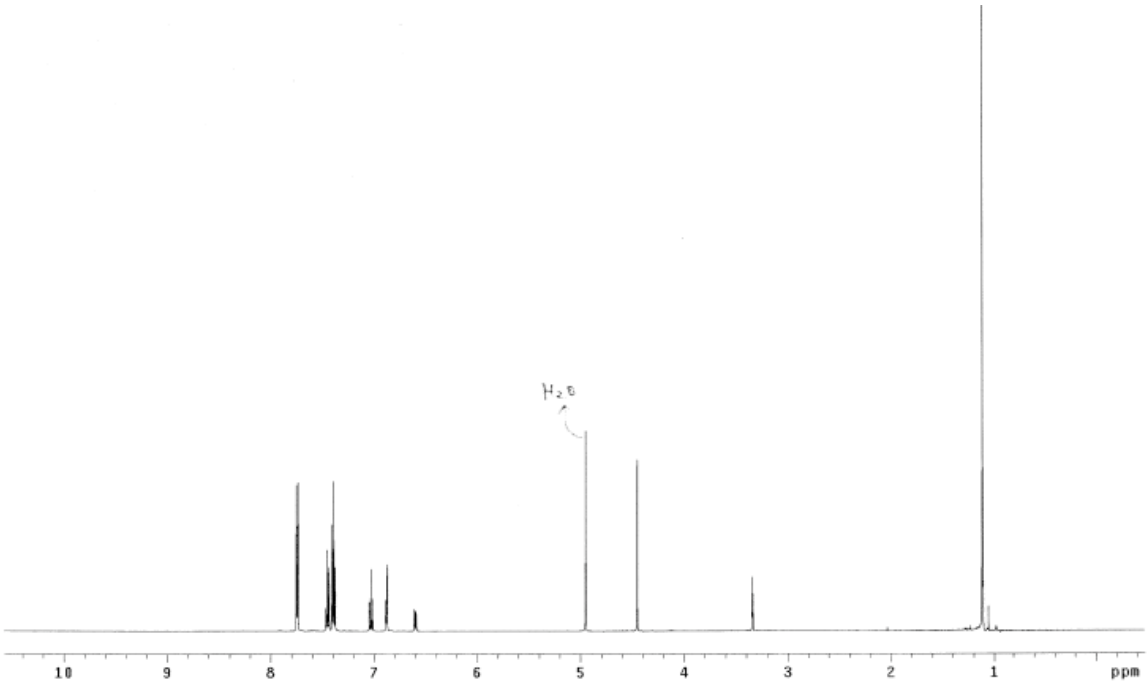

^{1}H NMR (CD_3OD)

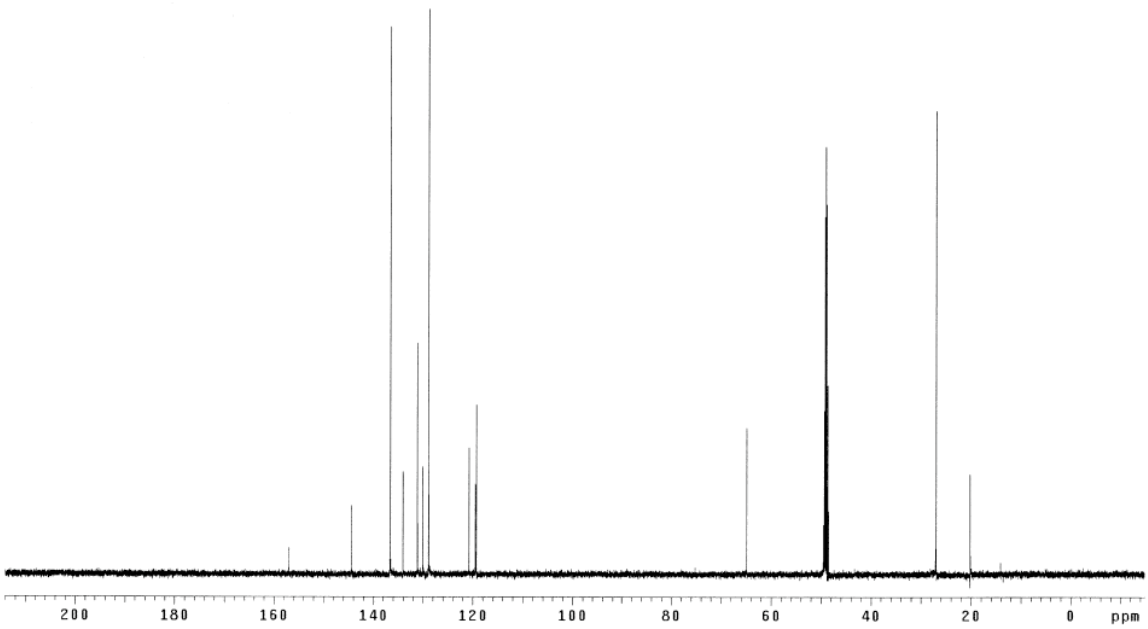

^{13}C NMR (CD_3OD)

3-(*tert*-butyldiphenylsilyloxy)benzylbromide (99)

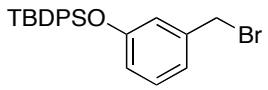

To a solution of alcohol **98** (6.19 g, 0.017 mol) and PPh_3 (4.93 g, 0.019 mol) in CH_2Cl_2 (120 mL) was added carbon tetrabromide (6.23 g, 0.019 mol) at 0 ºC. The reaction was stirred at 25 ºC for 19 h under nitrogen. The solvent was evaporated under the reduced pressure and the residual material was purified by flash chromatography eluting with 100 % hexanes and 10 % EtOAc/hexanes to afford product as a colorless oil (6.0 g, 83 %). R_f 0.7 (10 % EtOAc/hexanes). ^{1}H NMR (500 MHz, CD_3OD) δ 7.74-7.72 (m, 4H), 7.47-7.44 (m, 2H), 7.41-7.38 (m, 4H), 7.03 (t, 1H, J = 8.0 Hz), 6.91 (d, 1H, J = 8.0 Hz), 6.85 (t, 1H, J = 2.5 Hz), 6.65 (dd, 1H, J = 8.0, 2.5 Hz), 4.35 (s, 2H), 1.12 (s, 9H); ^{13}C NMR (125 MHz, CD_3OD) δ 157.0, 140.9, 136.6, 133.8, 131.2, 130.4, 128.9, 123.0, 121.5, 120.7, 33.6, 27.0, 20.2; MS (CI) m/z 425.2 $(M+H)^+$.

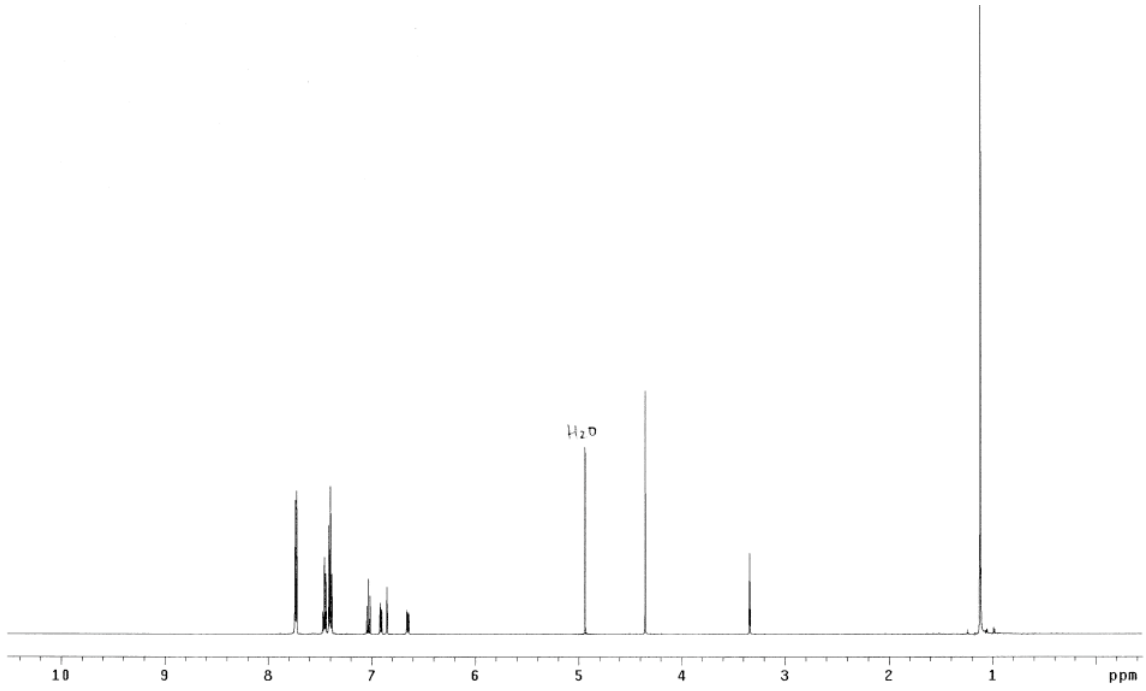

^{1}H NMR (CD_3OD)

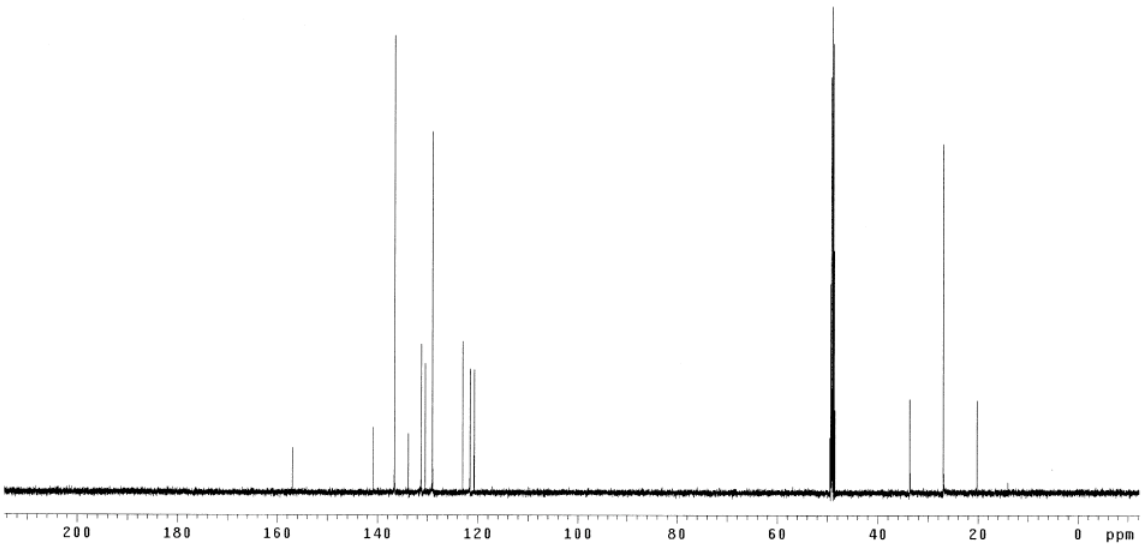

^{13}C NMR (CD_3OD)

Silyloxy Nile Red derivative (100)

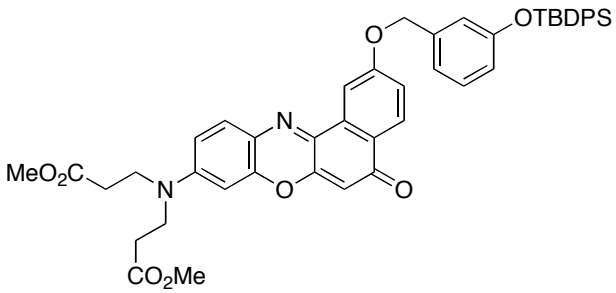

A solution of Nile Red dimethylester **92** (350 mg, 0.78 mmol, *provided by Mr. Jiney Jose*), benzylbromide **99** (1.7 g, 3.89 mmol) and Cs_2CO_3 (2.5 g, 7.77 mmol) in acetone (20 mL) was refluxed at 70 ºC for 3.5 h. After cooling to room temperature, the solvent was evaporated under the reduced pressure and the residual material was purified by flash chromatography (2 times column) eluting with 20 to 50 % EtOAc/hexanes to afford product as a red oil (236 mg, 38 % yield, 90 % purity). R_f 0.6 (60 % EtOAc/hexanes). ^{1}H NMR (500 MHz, DMSO-d_6) δ 8.04 (d, 1H, J = 8.5 Hz), 7.96 (d, 1H, J = 2.5 Hz), 7.69-7.68 (m, 4H), 7.64 (d, 1H, J = 9.0 Hz), 7.53-7.48 (m, 2H), 7.46-7.43 (m, 4H), 7.24 (dd, 1H, J = 8.5, 2.5 Hz), 7.19 (t, 1H, J = 7.5 Hz), 7.06 (d, 1H, J = 7.5 Hz), 6.99 (s, 1H), 6.85 (dd, 1H, J = 9.0, 2.5 Hz), 6.75 (d, 1H, J = 2.5 Hz), 6.69 (dd, 1H, J = 8.0, 2.5 Hz), 6.23 (s, 1H), 5.20 (s, 2H), 3.77 (t, 4H, J = 7.0 Hz), 3.66 (s, 6H), 2.59 (t, 4H, J = 7.0 Hz), 1.06 (s, 9H); MS (MALDI) m/z 796.13 $(M+H)^+$.

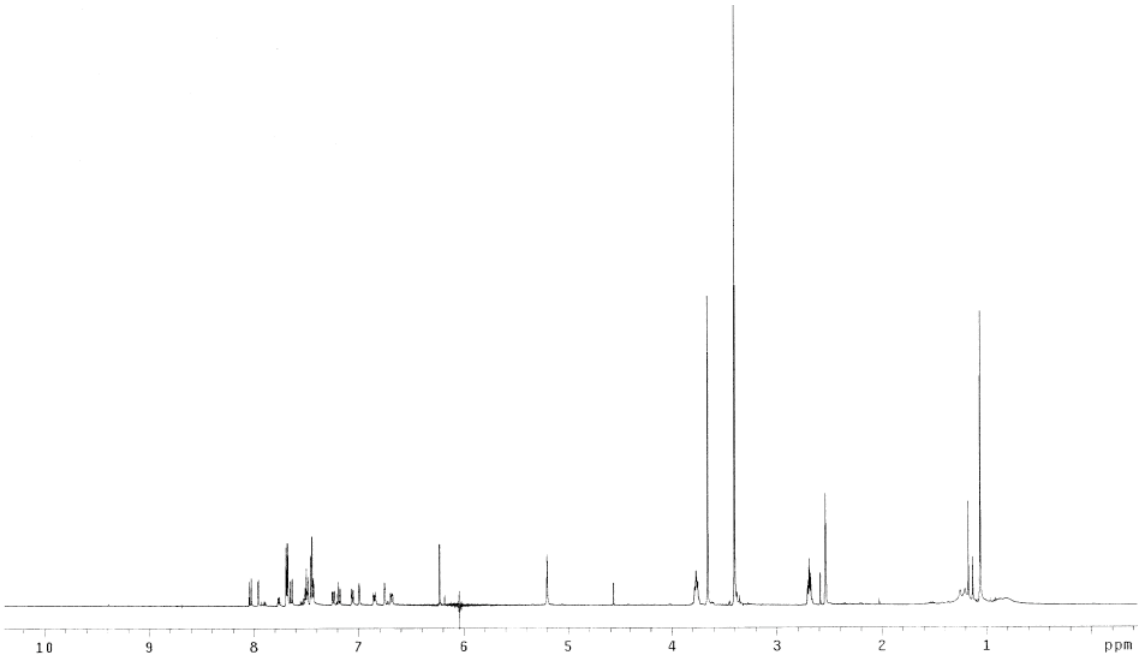

^{1}H NMR (DMSO-d_6)

Hydroxy Nile Red derivative (101)

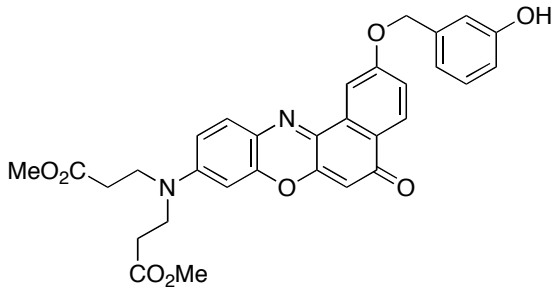

To a solution of TBDPS-protected Nile Red dimethylester **100** (236 mg, 0.297 mmol) in THF (20 mL) was added TBAF (0.36 mL, 0.356 mmol, 1 M in THF) dropwise at 0 ºC. After the stirring for 10 min, the solvent was evaporated under the reduced pressure at 35 ºC. The residual dark red material was purified by flash chromatography eluting with 40 to 70 % EtOAc/hexanes to afford product as a red solid (116 mg, 70 % yield, 90 % purity). R_f 0.3 (70 % EtOAc/hexanes). ^{1}H NMR (300 MHz, DMSO-d_6) δ 9.54 (s, 1H), 8.10 (d, 1H, J = 8.0 Hz), 8.08 (s, 1H), 7.69 (d, 1H, J = 8.0 Hz), 7.39 (dd, 1H, J = 8.4, 2.4 Hz), 7.24 (t, 1H, J = 7.5 Hz), 6.98-6.96 (m, 2H), 6.89 (dd, 1H, J = 8.4, 2.4 Hz), 6.78-6.75 (m, 2H), 6.25 (s, 1H), 5.28 (s, 2H), 3.78 (t, 4H, J = 7.5 Hz), 3.66 (s, 6H), 2.70 (t, 4H, J = 7.5 Hz); MS (MALDI) m/z 558.08 $(M+H)^+$.

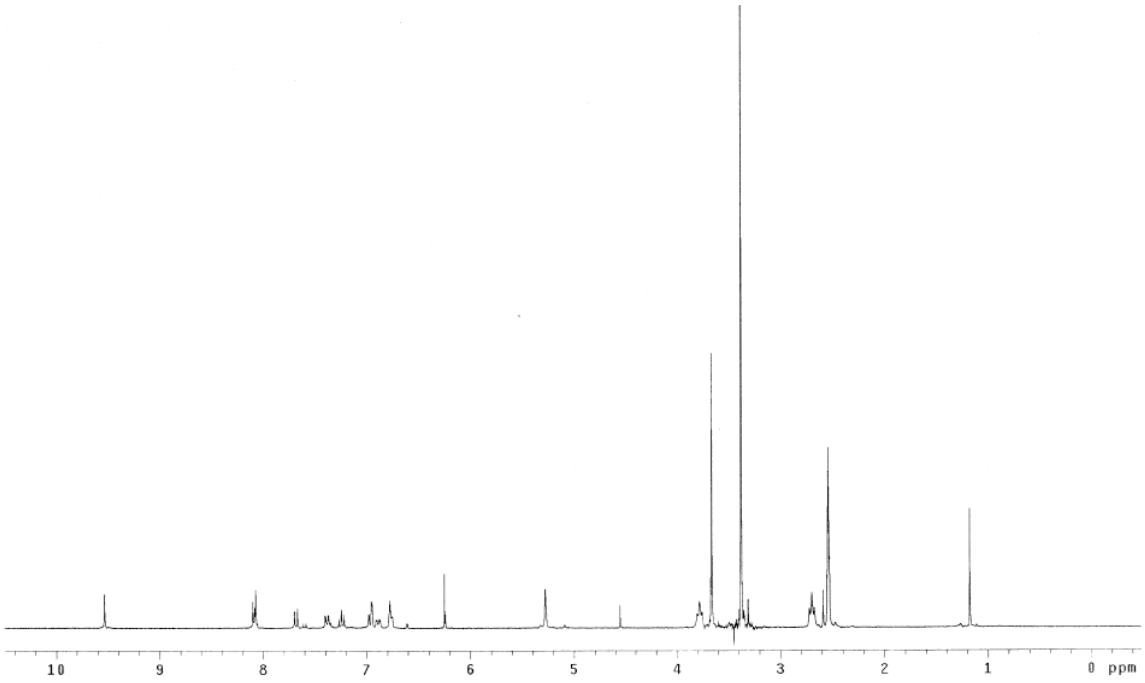

^{1}H NMR (DMSO-d_6)

Nile Red derivative (102)

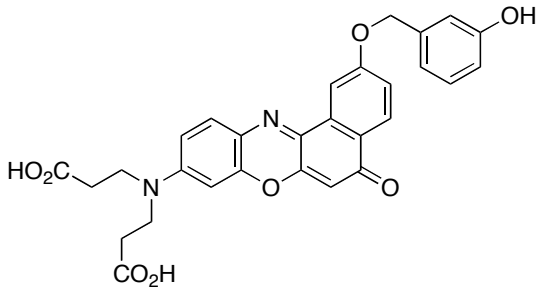

A solution of Nile Red dimethylester **101** (50 mg, 0.090 mmol) and K_2CO_3 (99 mg, 0.719 mmol) in 1:1 MeOH/H_2O (5 mL:5 mL) was stirred at 40 ºC for 12 h. MeOH was only evaporated and water (5 mL) was added to a solution. The aqueous layer was extracted with EtOAc (3 x 10 mL) and the aqueous layer was acidified with 1 N HCl to reach pH 2. The aqueous layer was again extracted with EtOAc (2 x 10 mL) and the combined organic layer was dried over Na_2SO_4. The solvent was concentrated under the reduced pressure to afford product as a red solid (36 mg, 77 %). R_f 0.1 (100 % EtOAc). ^{1}H NMR (300 MHz, DMSO-d_6) δ 9.54 (s, 1H), 8.08 (d, 1H, J = 6.5 Hz), 8.07 (s, 1H), 7.67 (d, 1H, J = 9.0 Hz), 7.38 (dd, 1H, J = 9.0, 2.5 Hz), 7.23 (d, 1H, J = 7.8 Hz), 6.98-6.95 (m, 2H), 6.90-6.86 (m, 1H), 6.79-6.73 (m, 2H), 6.24 (s, 1H), 5.27 (s, 2H), 3.76 (t, 4H, J = 7.0 Hz), 2.61 (t, 4H, J = 7.0 Hz); ^{13}C NMR (75 MHz, DMSO-d_6) δ 182.5, 173.8, 162.0, 158.5, 152.7, 151.5, 147.2, 140.3, 138.9, 134.4, 131.8, 130.5, 128.3, 126.0, 125.2, 119.3, 119.2, 115.9, 115.4, 111.2, 108.0, 105.4, 97.8, 70.5, 47.5, 32.8; MS (ESI) m/z 527.15 $(M–H)^–$.

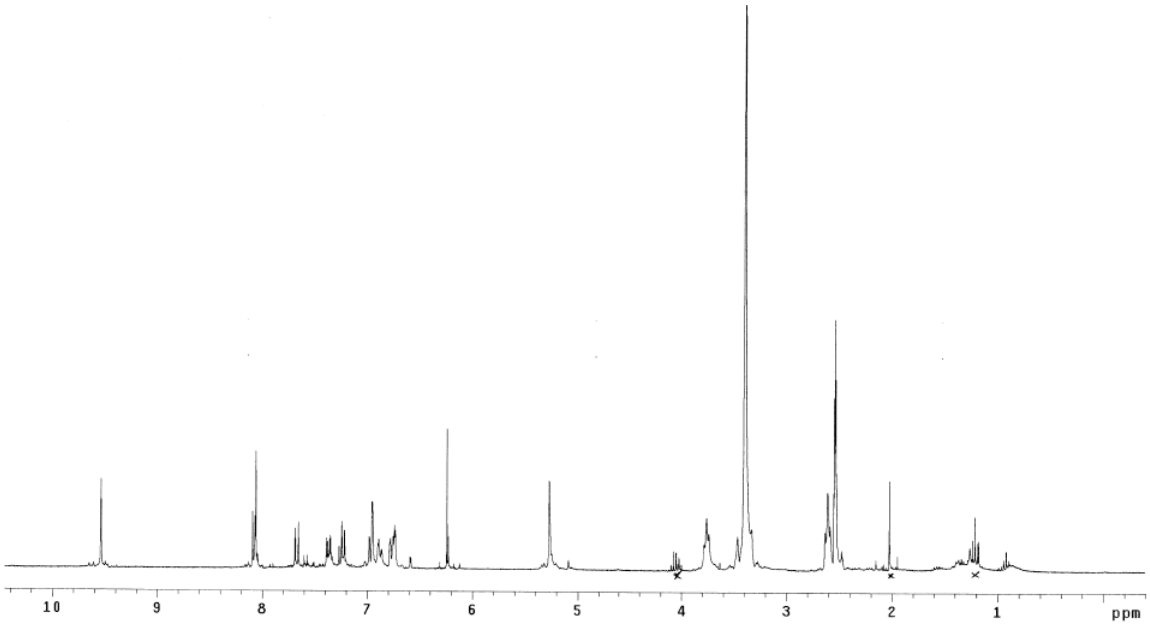

^{1}H NMR (DMSO-d_6)

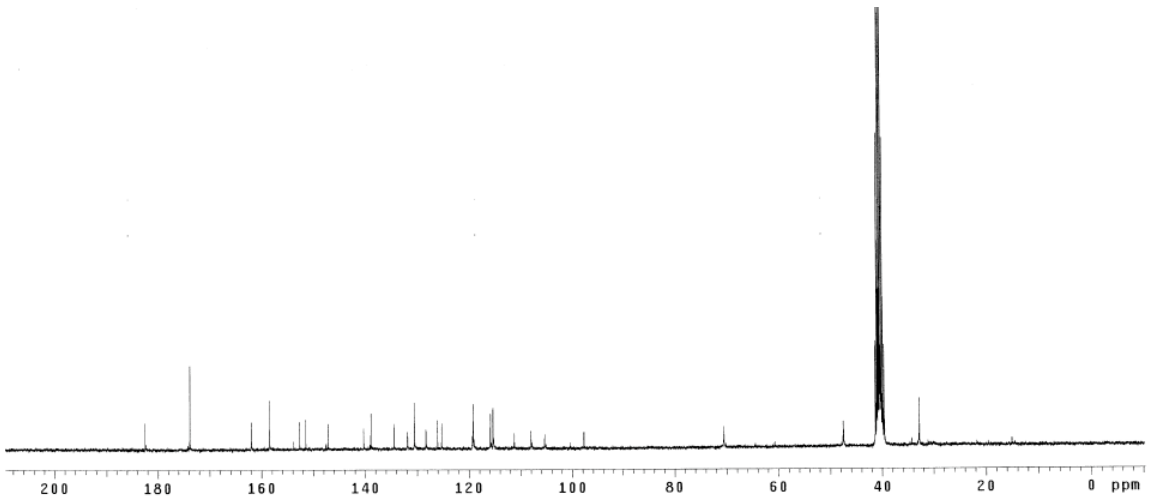

^{13}C NMR (DMSO-d_6)

4-Benzyloxy-3-methoxybenzaldehyde (104)[149]

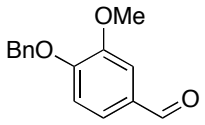

A solution of vanillin (30 g, 0.197 mol), benzyl bromide (25.8 mL, 0.217 mol) and K_2CO_3 (27.3 g, 0.197 mol) in acetone (400 mL) was refluxed at 66 ºC for 20 h and then this reaction mixture was added into DI water (400 mL). Acetone was only evaporated and aqueous phase was extracted with EtOAc (3 x 200 mL). The combined organic layer was dried over Na_2SO_4 and concentrated under the reduced pressure. The residue was purified by flash chromatography eluting with 10 % to 40% EtOAc/hexanes to afford product as a colorless crystals (43.6 g, 91 %). R_f 0.7 (40 % EtOAc/hexanes). ^{1}H NMR (500 MHz, $CDCl_3$) δ 9.83 (s, 1H), 7.45-7.43 (m, 3H), 7.40-7.37 (m, 3H), 7.34-7.31 (m, 1H), 6.98 (d, 1H, J = 8.5 Hz), 5.25 (s, 2H), 3.95 (s, 3H); ^{13}C NMR (125 MHz, $CDCl_3$) δ 190.9, 153.5, 150.0, 135.9, 130.2, 128.7, 128.2, 127.1, 126.6, 112.2, 109.2, 70.8, 56.0.

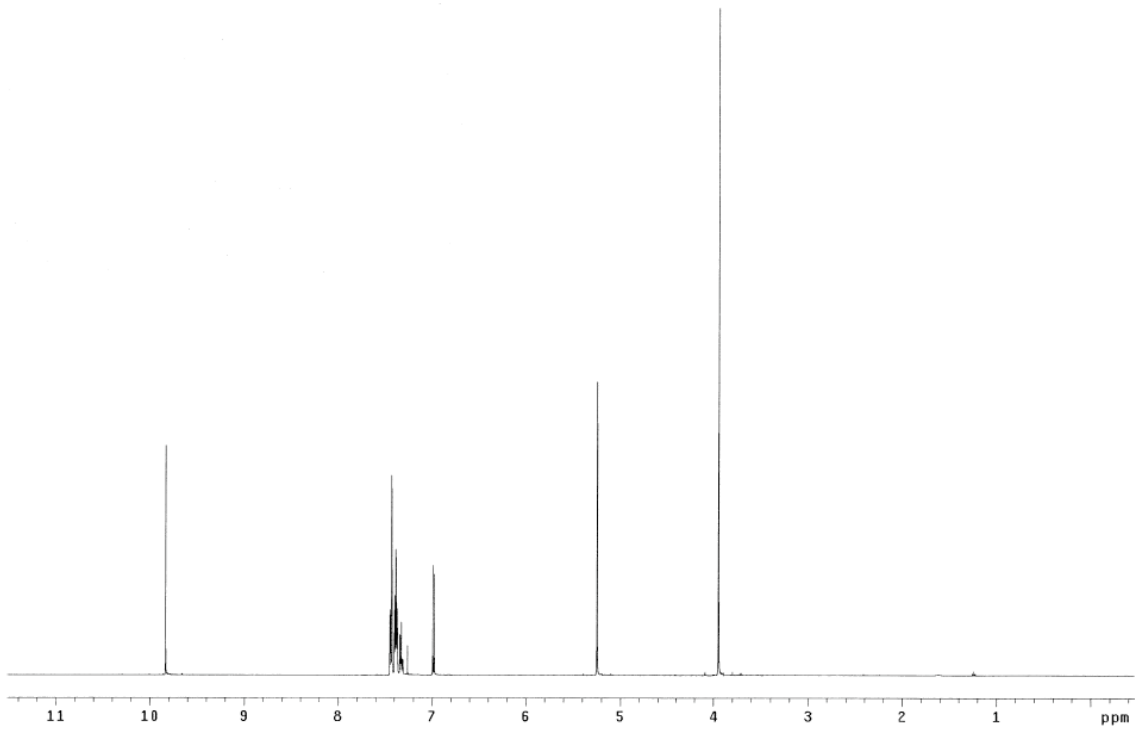

^{1}H NMR ($CDCl_3$)

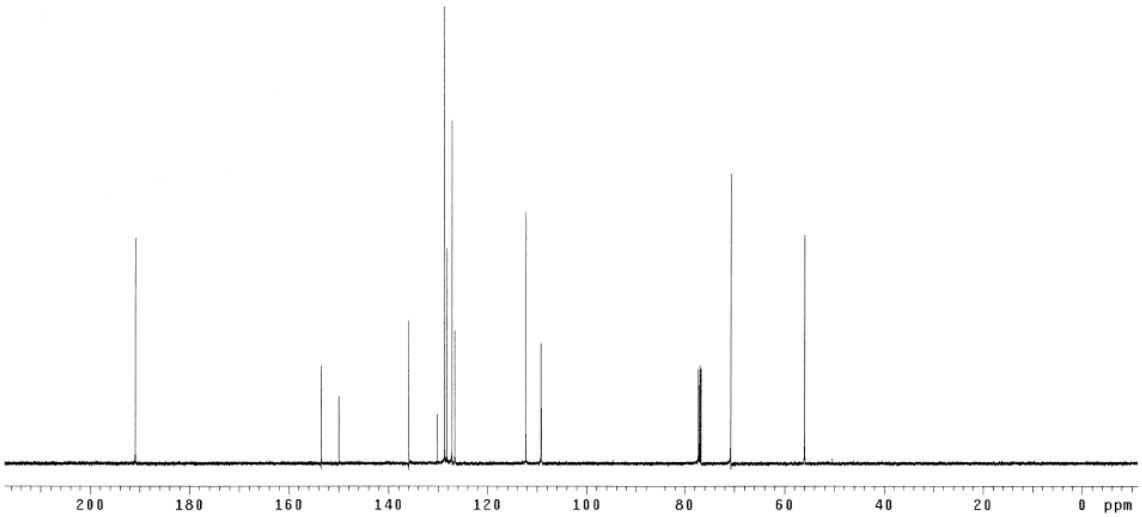

^{13}C NMR ($CDCl_3$)

4-Benzyloxy-5-methoxy-2-nitrobenzaldehyde (105)[149]

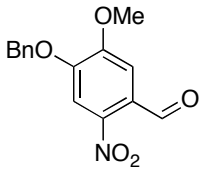

Powdered *O*-benzylvanillin **104** (10 g, 41.3 mmol) was slowly added to nitric acid (50 mL) at 0 ºC for 10 min. The reaction mixture was stirred at 0 ºC for 2 h. The precipitates were filtrated and the collected brown solid was recrystallized from ethyl acetate to afford product as a yellow crystals (6.2 g, 52 %). ^{1}H NMR (500 MHz, $CDCl_3$) δ 10.4 (s, 1H), 7.67 (s, 1H), 7.47-7.45 (m, 2H), 7.43-7.40 (m, 3H), 7.38-7.35 (m, 1H), 5.27 (s, 2H), 4.02 (s, 3H); ^{13}C NMR (125 MHz, $CDCl_3$) δ 187.8, 153.6, 151.3, 143.5, 134.7, 128.9, 128.7, 127.6, 125.6, 110.0, 108.8, 71.5, 56.7.

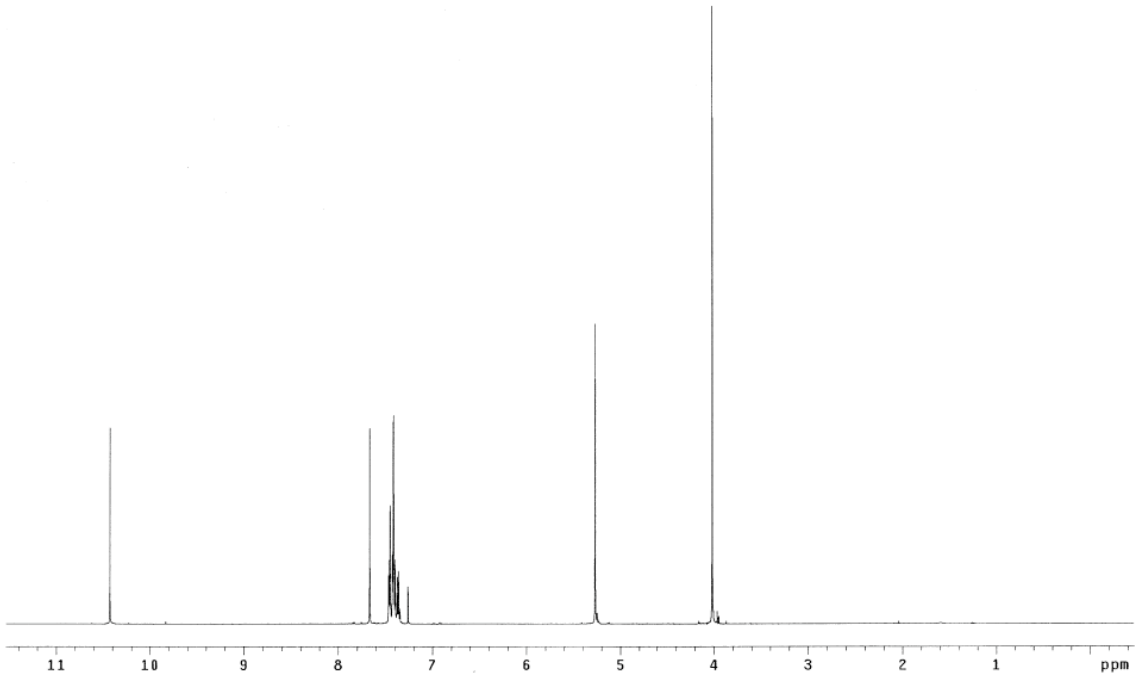

^{1}H NMR ($CDCl_3$)

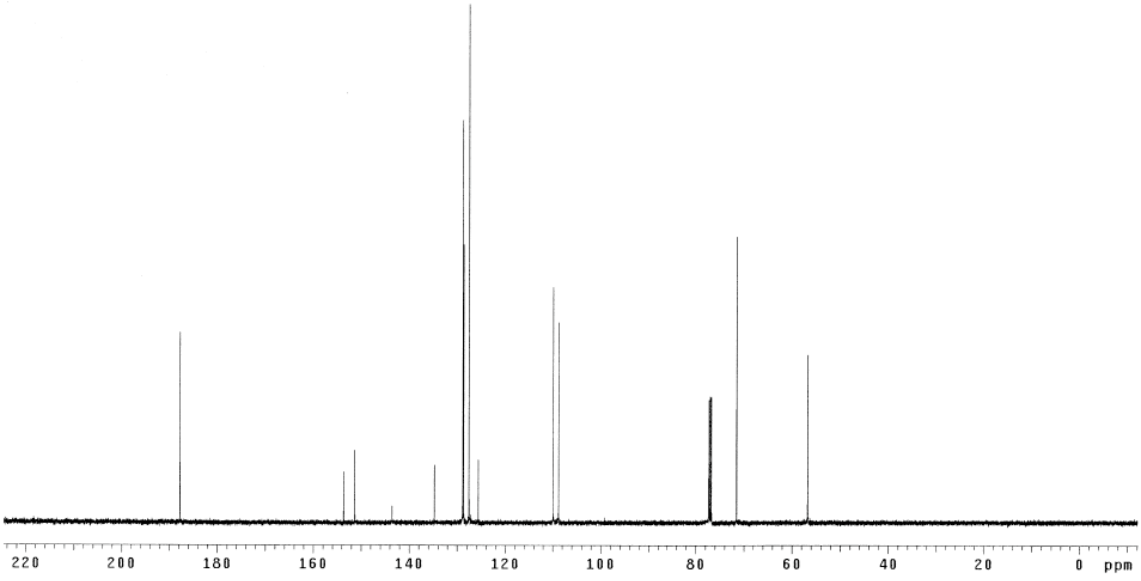

^{13}C NMR ($CDCl_3$)

4-Hydroxy-5-methoxy-2-nitrobenzaldehyde (106)[149]

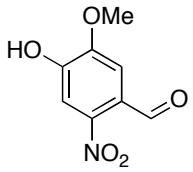

A mixture of *O*-benzyl-6-nitrovanillin **105** (6.0 g, 20.9 mmol) and acetic acid (40 mL) was stirred at 85 ºC and 48 % hydrobromic acid (11 mL) was added by auto syringe for 10 min. The reaction mixture was stirred at 85 ºC for 1 h and cooled to room temperature. The precipitates were filtrated and washed with hexanes to afford product as a yellow crystals (3.5 g, 86 %). R_f 0.4 (40 % EtOAc/hexanes). ^{1}H NMR (500 MHz, DMSO-d_6) δ 11.1 (br, 1H), 10.2 (s, 1H), 7.52 (s, 1H), 7.36 (s, 1H), 3.97 (s, 3H); ^{13}C NMR (125 MHz, DMSO-d_6) δ 189.3, 152.8, 152.0, 144.7, 124.4, 112.0, 111.5, 57.3.

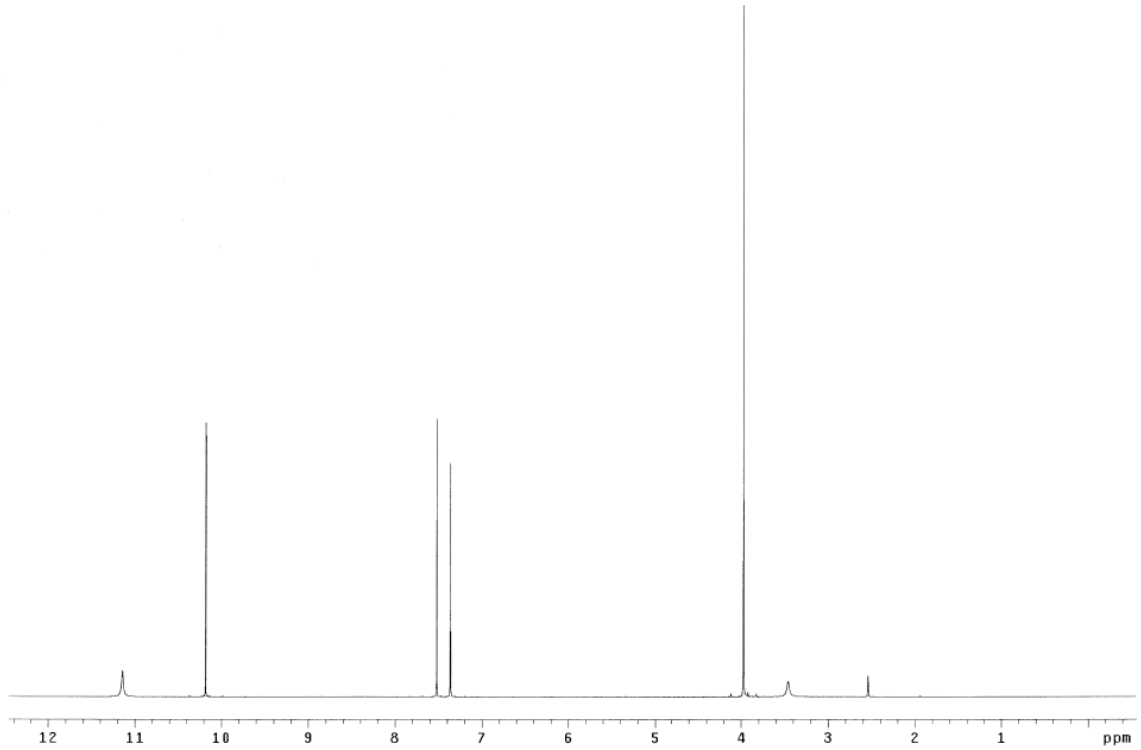

^{1}H NMR (DMSO-d_6)

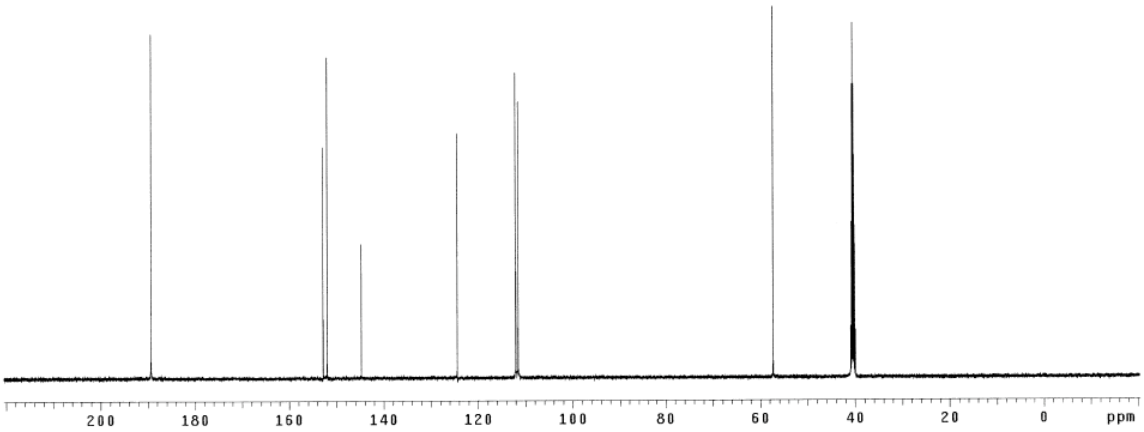

^{13}C NMR (DMSO-d_6)

4-(Hydroxymethyl)-2-methoxy-5-nitrophenol (107)[135]

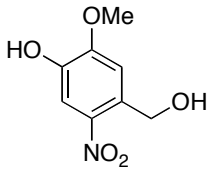

Aldehyde **106** (2.0 g, 10.1 mmol) was added in 1:1 THF/EtOH (25 mL:25 mL) at 0 ºC. Sodium borohydride (0.77 g, 20.3 mmol) was slowly added into the solution. The reaction mixture was stirred at 25 ºC for 17 h and poured into DI water (50 mL) carefully. THF and EtOH were only evaporated and aqueous layer was extracted with EtOAc (15 x 30 mL). The combined organic layer was washed with water (1 x 50 mL) and brine (1 x 50 mL) and dried over Na_2SO_4. The solvents were concentrated under the reduced pressure to afford product as a yellow solid (1.9 g, 95 %). R_f 0.2 (40 % EtOAc/hexanes). ^{1}H NMR (500 MHz, DMSO-d_6) δ 9.97 (s, 1H), 7.59 (s, 1H), 7.37 (s, 1H), 5.55 (t, 1H, J = 5.0 Hz), 4.83 (d, 2H, J = 5.0 Hz), 3.94 (s, 3H); ^{13}C NMR (125 MHz, DMSO-d_6) δ 153.8, 145.9, 139.3, 133.5, 112.3, 110.9, 61.2, 57.0.

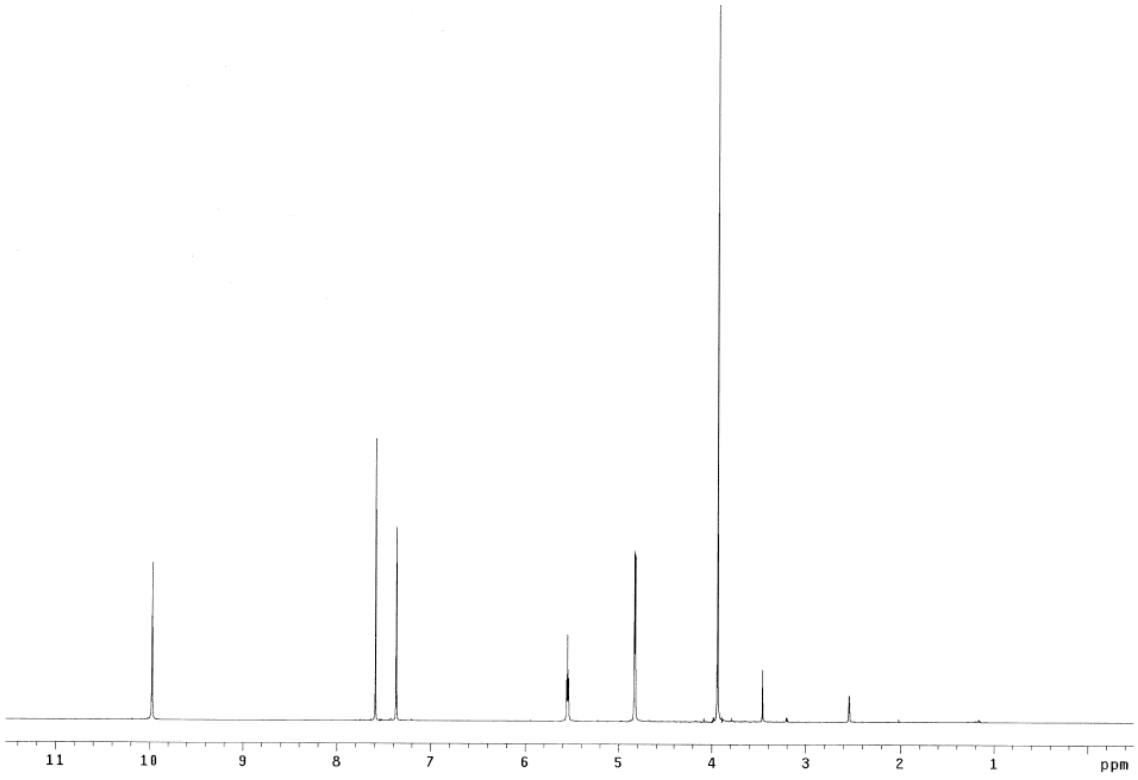

^{1}H NMR (DMSO-d_6)

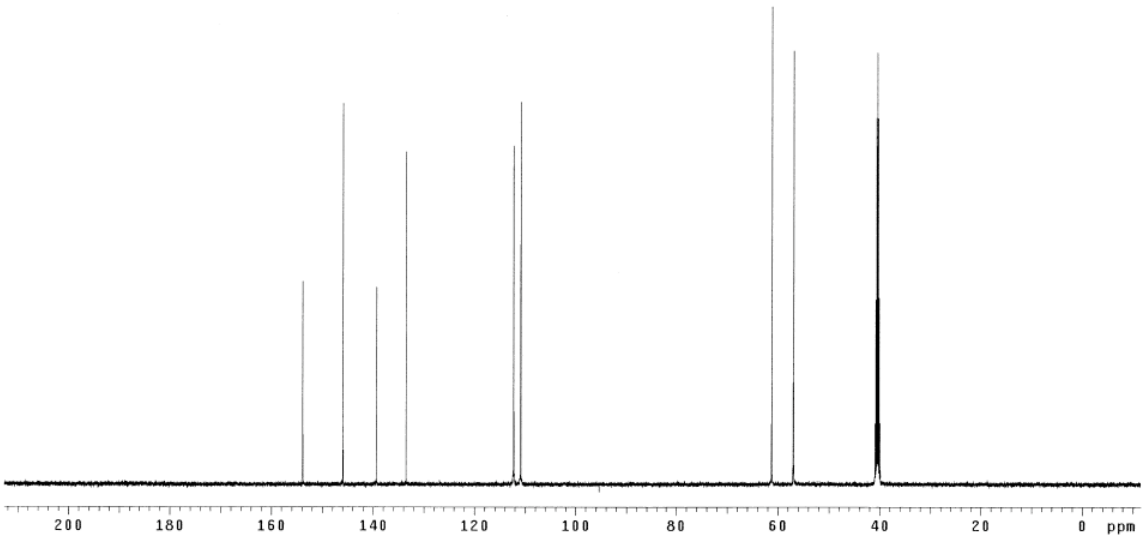

^{13}C NMR (DMSO-d_6)

tert-Butyl 2-(4-(hydroxymethyl)-2-methoxy-5-nitrophenoxy)acetate (108)

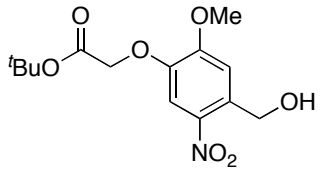

A solution of photolinker **107** (1.0 g, 5.0 mmol), *tert*-butylbromoacetate (1.48 mL, 10.0 mmol) and K_2CO_3 (1.7 g, 12.6 mmol) in CH_3CN (50 mL) was stirred at 70 ºC for 2.5 h. The reaction mixture was cooled to room temperature and filtered to remove K_2CO_3. The solvents were concentrated under the reduced pressure and the residue was purified by flash chromatography eluting with 20 % to 50 % EtOAc/hexanes to afford product as a yellow solid (1.5 g, 95 %). R_f 0.5 (50 % EtOAc/hexanes). ^{1}H NMR (500 MHz, $CDCl_3$) δ 7.61 (s, 1H), 7.22 (s, 1H), 4.96 (s, 2H), 4.64 (s, 2H), 3.99(s, 3H), 1.49 (s, 9H); ^{13}C NMR (125 MHz, $CDCl_3$) δ 166.9, 154.2, 145.9, 139.2, 133.5, 111.2, 109.9, 83.1, 66.2, 62.6, 56.5, 28.0; MS (ESI) m/z 320.13 $(M+Li)^+$.

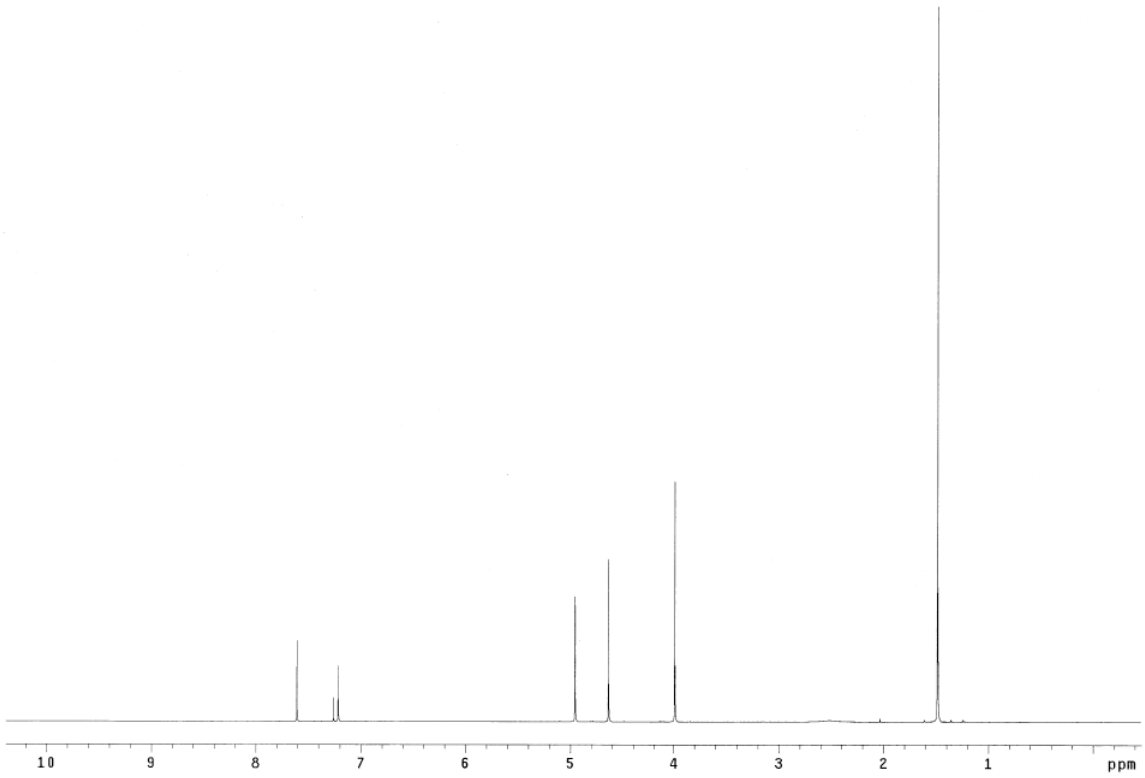

^{1}H NMR ($CDCl_3$)

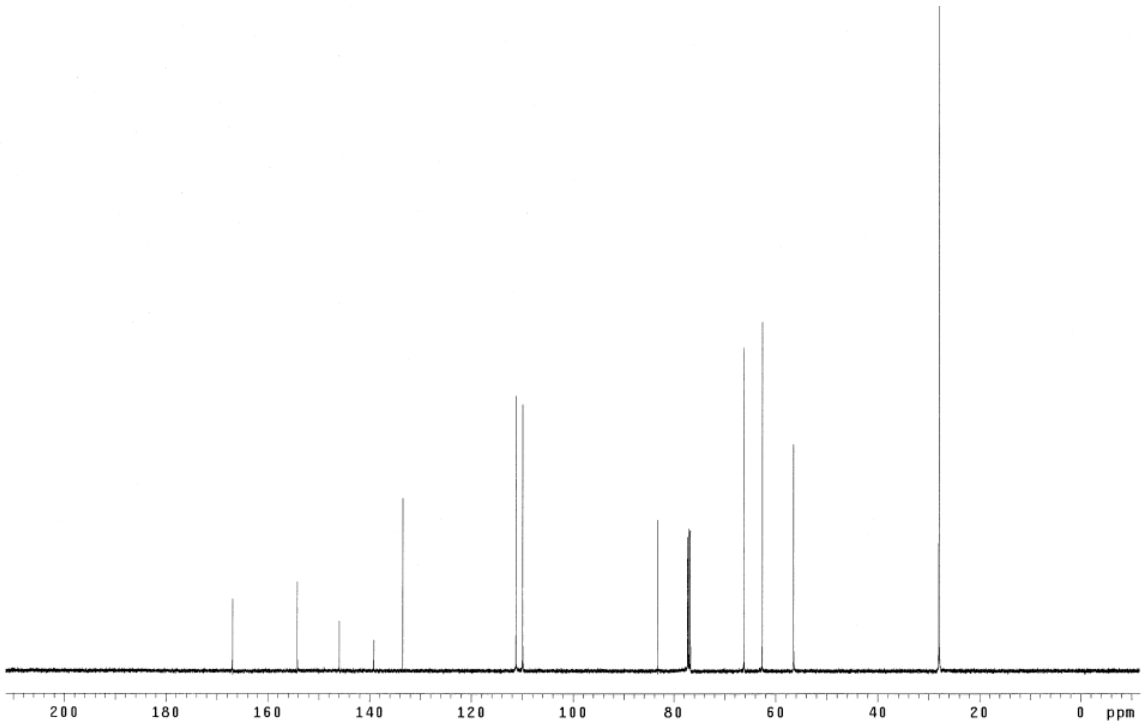

^{13}C NMR ($CDCl_3$)

Photolinker (109a)

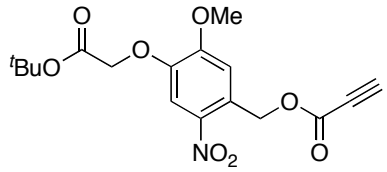

Photolinker **108** (1.2 g, 3.83 mmol) was dissolved in CH_2Cl_2 (50 mL) and then DIC (725 mg, 5.75 mmol) and DMAP (47 mg, 0.38 mmol) were added to this solution at 0 ºC. After stirring at 0 ºC for 15 min, propiolic acid (402 mg, 5.75 mmol) dissolved in CH_2Cl_2 (10 mL) was added. The reaction mixture was stirred at 25 ºC for additional 4 h. The solvents were concentrated under the reduced pressure at 35 ºC and the residue was purified by flash chromatography eluting with 15 to 30 % EtOAc/hexanes to afford product as a yellow semi-solid (1.17 g, 84 %). R_f 0.5 (30 % EtOAc/hexanes). ^{1}H NMR (500 MHz, $CDCl_3$) δ 7.64 (s, 1H), 7.05 (s, 1H), 5.62 (s, 2H), 4.65 (s, 2H), 4.00 (s, 3H), 2.99 (s, 1H), 1.48 (s, 9H); ^{13}C NMR (125 MHz, $CDCl_3$) δ 166.7, 153.9, 151.9, 146.5, 139.3, 126.6, 110.7, 109.9, 83.2, 75.9, 74.0, 66.1, 64.5, 56.5, 28.0; MS (ESI) m/z 372.13 $(M+Li)^+$.

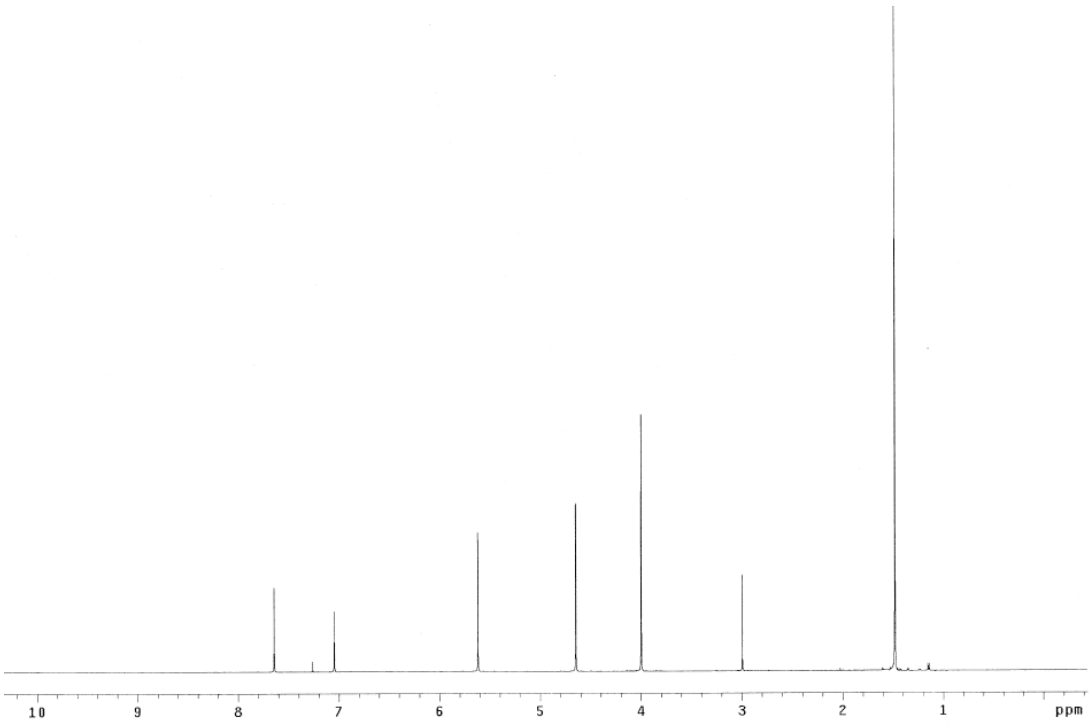

^{1}H NMR ($CDCl_3$)

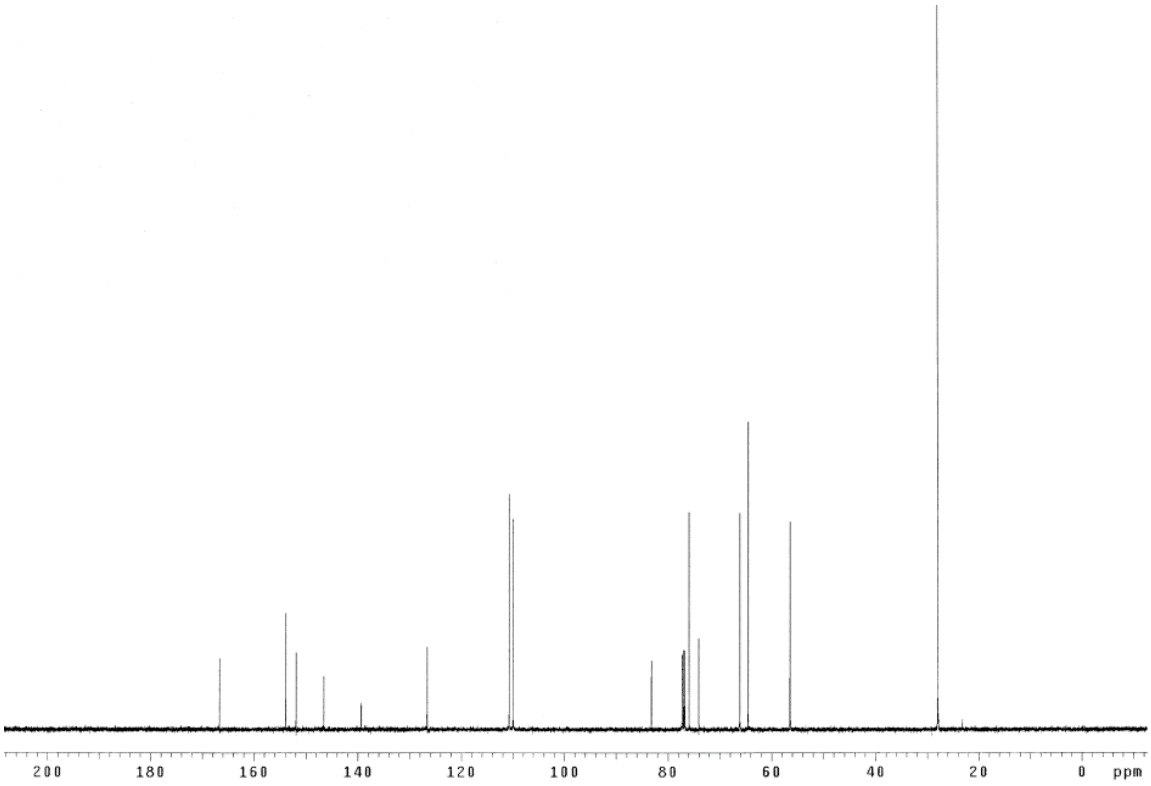

^{13}C NMR ($CDCl_3$)

Carboxylate photolinker (110a)

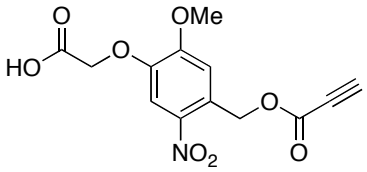

A solution of photolinker **109a** (100 mg, 0.27 mmol) in 1:1 TFA/CH_2Cl_2 (1.0 mL:1.0 mL) was stirred at 25 ºC for 1 h. The reaction mixture was flashed with nitrogen to remove TFA and CH_2Cl_2 at 25 ºC for overnight. Pure product was obtained as an off-white solid (90 mg, quantitative yield). ^{1}H NMR (500 MHz, DMSO-d_6) δ 7.70 (s, 1H), 7.32 (s, 1H), 5.52 (s, 2H), 4.92 (s, 2H), 4.71 (s, 1H), 3.97 (s, 3H); ^{13}C NMR (125 MHz, DMSO-d_6) δ 170.6, 154.1, 152.8, 147.7, 140.9, 125.7, 114.3, 110.7, 80.8, 75.3, 66.1, 65.6, 57.4; MS (ESI) m/z 308.05 $(M–H)^-$.

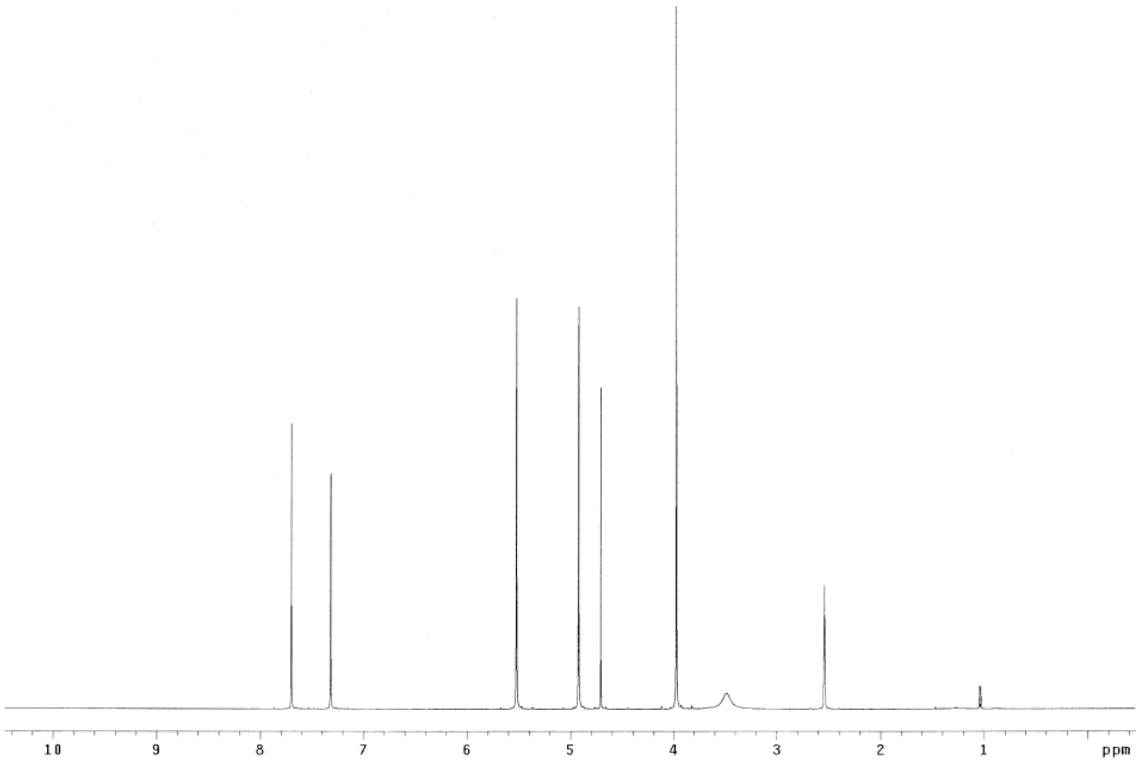

^{1}H NMR (DMSO-d_6)

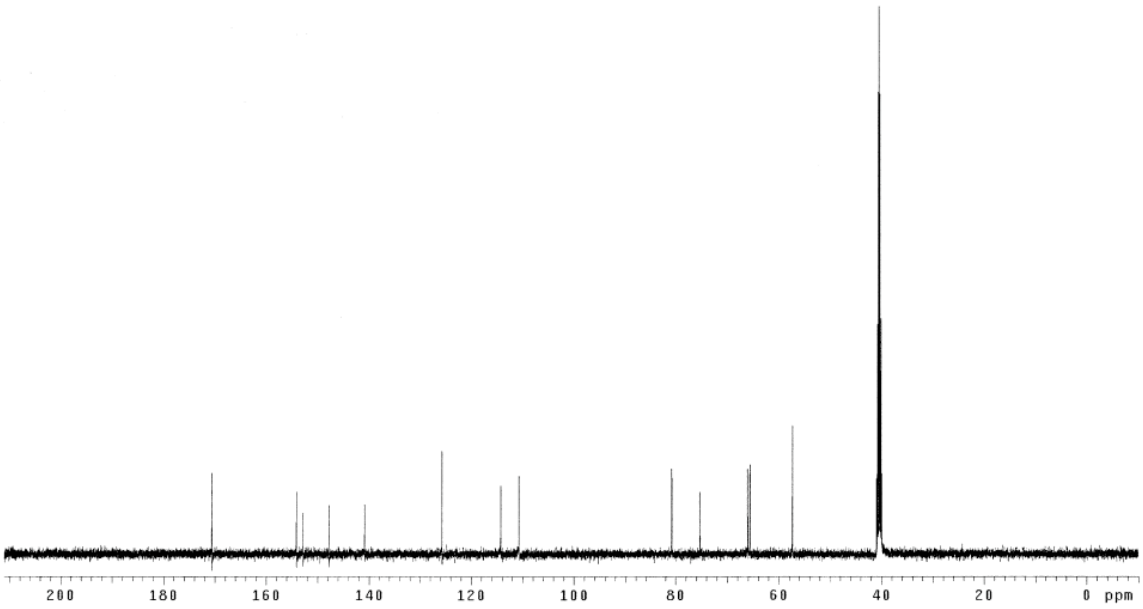

^{13}C NMR (DMSO-d_6)

Photolinker (109b)

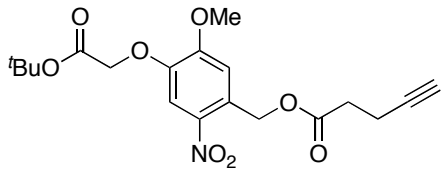

Photolinker **108** (100 mg, 0.319 mmol) was dissolved in CH_2Cl_2 (4.0 mL) and then DIC (40 mg, 0.319 mmol) and DMAP (3.9 mg, 0.032 mmol) were added to this solution at 0 ºC. After stirring at 0 ºC for 15 min, 4-pentynoic acid (31 mg, 0.319 mmol) dissolved in CH_2Cl_2 (2.0 mL) was added. The reaction mixture was stirred at 25 ºC for additional 3 h. The solvents were concentrated under the reduced pressure at 35 ºC and the residue was purified by flash chromatography eluting with 10 to 30 % EtOAc/hexanes to afford product as a colorless oil (115 mg, 91 %, 95 % purity). R_f 0.3 (30 % EtOAc/hexanes). ^{1}H NMR (500 MHz, $CDCl_3$) δ 7.63 (s, 1H), 7.05 (s, 1H), 5.55 (s, 2H), 4.65 (s, 2H), 3.99 (s, 3H), 2.70-2.66 (m, 2H), 2.58-2.54 (m, 2H), 1.98 (t, 1H, J = 2.5 Hz), 1.49 (s, 9H); ^{13}C NMR (125 MHz, $CDCl_3$) δ 171.0, 166.7, 153.8, 146.3, 139.5, 127.8, 110.9, 109.9, 83.2, 82.2, 69.3, 66.1, 63.4, 56.5, 33.3, 28.0, 14.3; MS (ESI) m/z 400.16 $(M+Li)^+$.

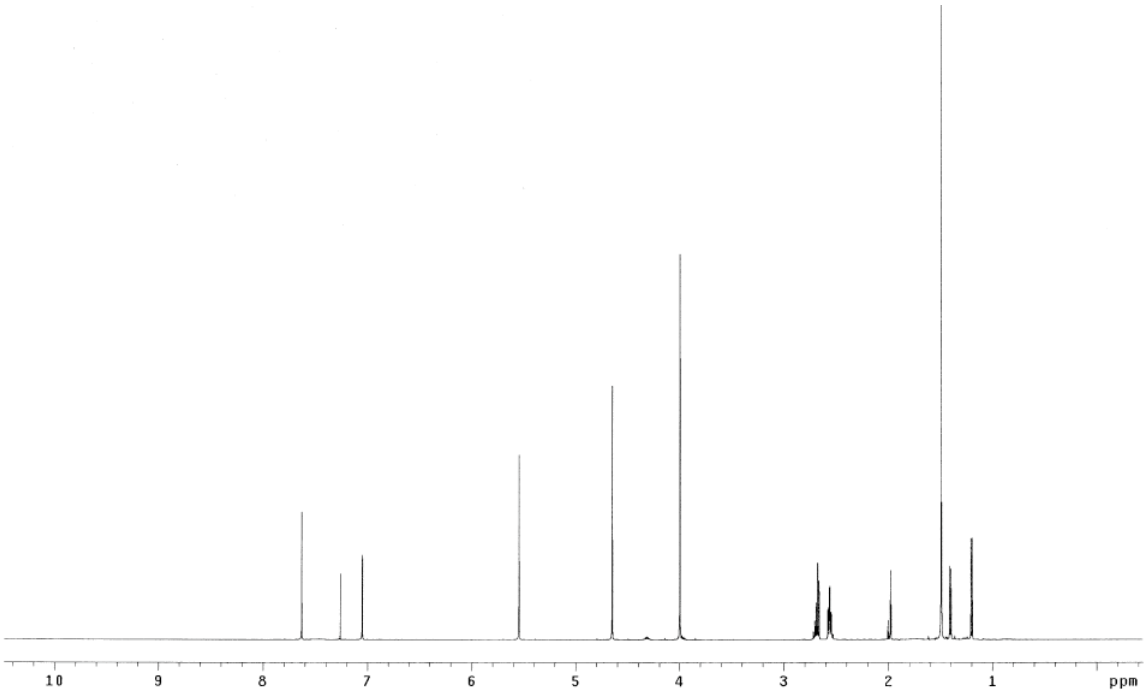

^{1}H NMR ($CDCl_3$)

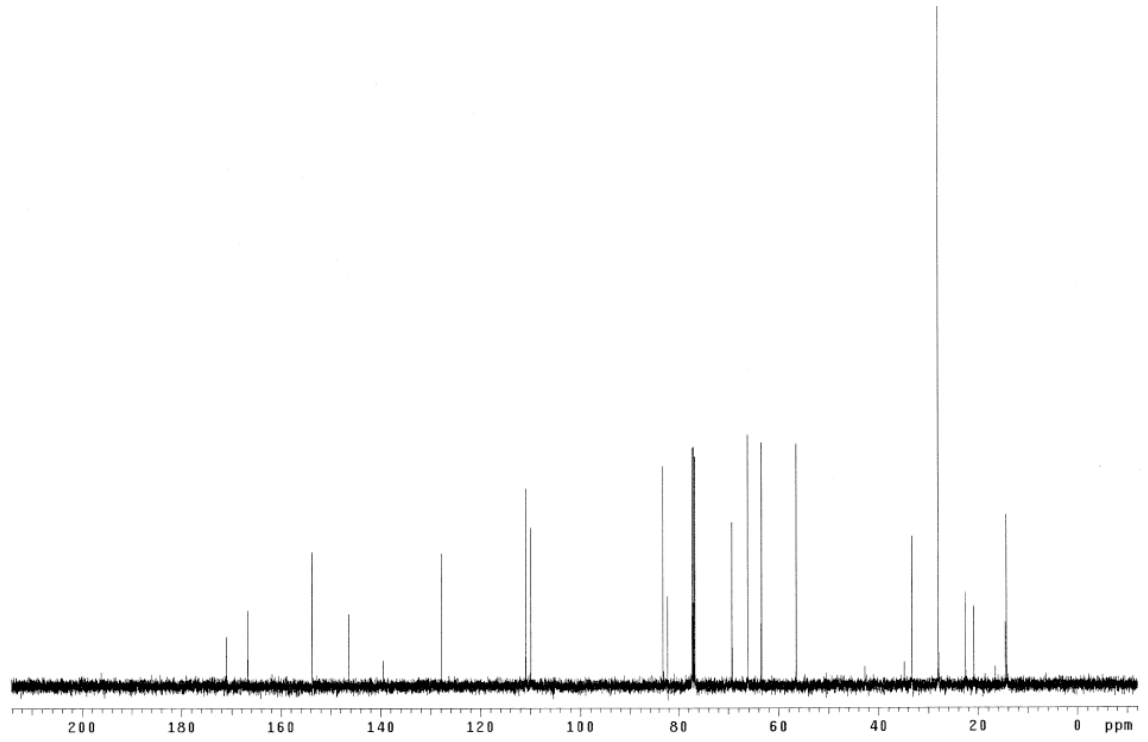

^{13}C NMR ($CDCl_3$)

Carboxylate photolinker (110b)

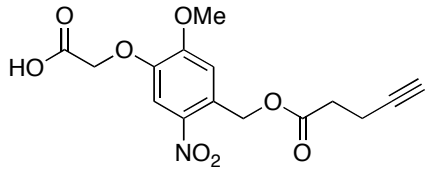

A solution of photolinker **109b** (94 mg, 0.24 mmol) in 1:1 TFA/CH_2Cl_2 (1.5 mL:1.5 mL) was stirred at 25 ºC in dark for 1 h. The reaction mixture was flashed with nitrogen to remove TFA and CH_2Cl_2 at 25 ºC for overnight. Pure product was obtained as a yellow solid (83 mg, quantitative yield). R_f 0.2 (100 % EtOAc). ^{1}H NMR (500 MHz, DMSO-d_6) δ 7.54 (s, 1H), 7.20 (s, 1H), 5.44 (s, 2H), 4.48 (s, 2H), 3.95 (s, 3H), 2.88 (t, 1H, J = 2.5 Hz), 2.67 (t, 2H, J = 7.0 Hz), 2.50-2.47 (m, 2H); ^{13}C NMR (125 MHz, DMSO-d_6) δ 172.0, 171.0, 154.2, 148.4, 140.3, 126.5, 112.2, 110.1, 84.0, 72.7, 68.2, 63.8, 57.2, 33.6, 14.7; MS (ESI) m/z 336.02 $(M–H)^-$.

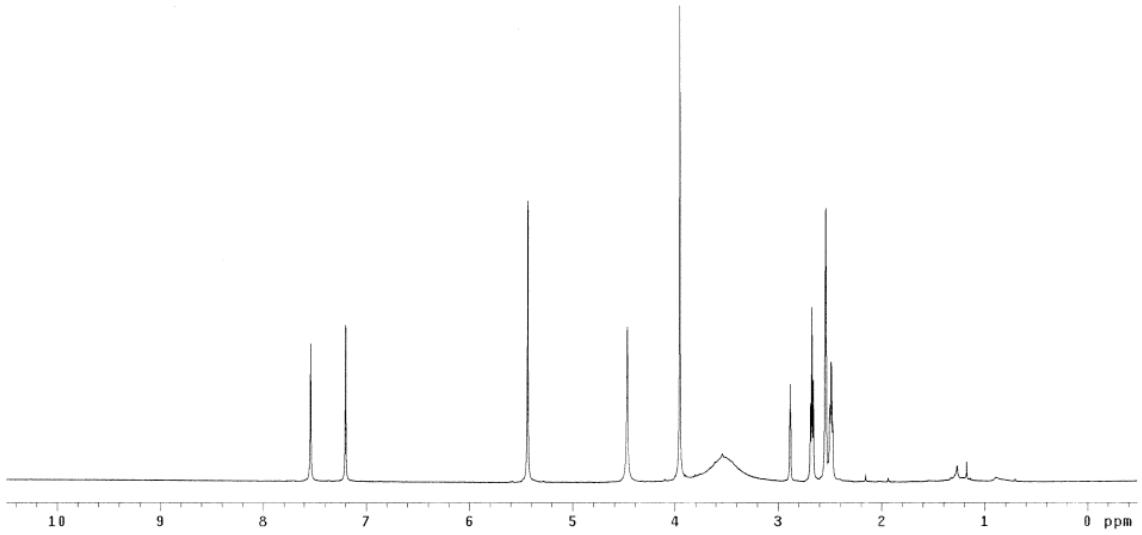

^{1}H NMR (DMSO-d_6)

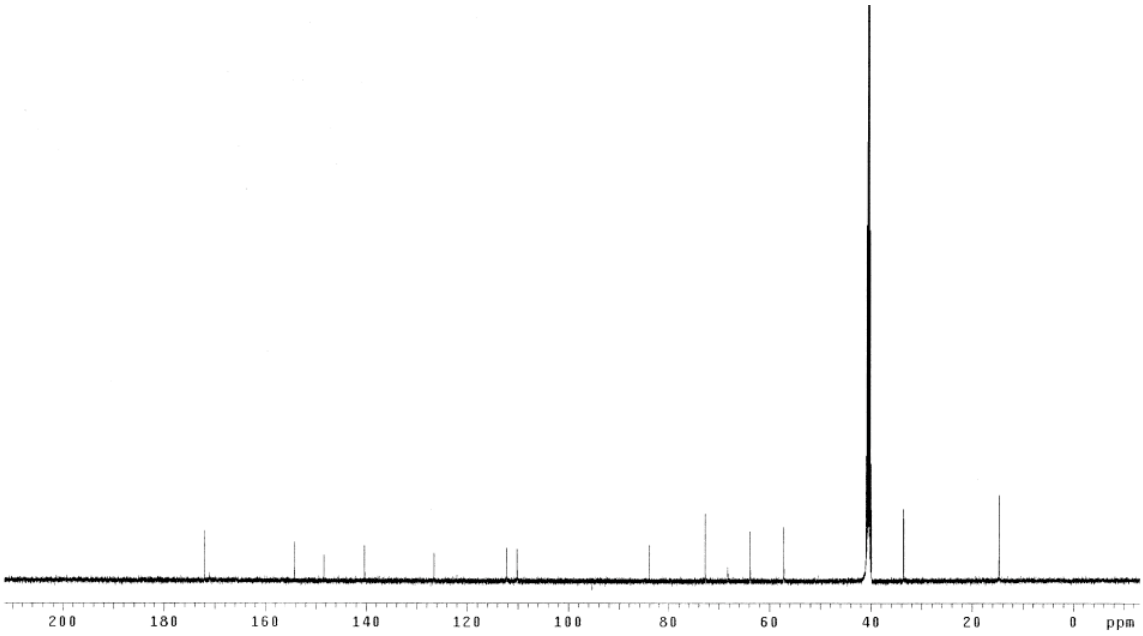

^{13}C NMR (DMSO-d_6)

Azidomethyl benzene (111)[150]

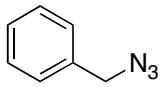

A solution of benzylbromide (1.0 g, 5.85 mmol) and sodium azide (760 mg, 11.7 mmol) in DMSO (6.0 mL) was stirred at 25 ºC for 2 h. Water (10 mL) was added into reaction mixture and aqueous phase was extracted with EtOAc (5 x 4 mL). The combined organic layer was dried over Na_2SO_4 and concentrated under the reduced pressure at 35 ºC. The residual material was purified by flash chromatography eluting with 100 % hexanes to 10 % EtOAc/hexanes to afford product as a colorless oil (636 mg, 82 %). R_f 0.7 (20 % EtOAc/hexanes). ^{1}H NMR (500 MHz, $CDCl_3$) δ 7.44-7.34 (m, 5H), 4.36 (s, 2H); ^{13}C NMR (125 MHz, $CDCl_3$) δ 135.3, 128.8, 128.2, 128.1, 54.7.

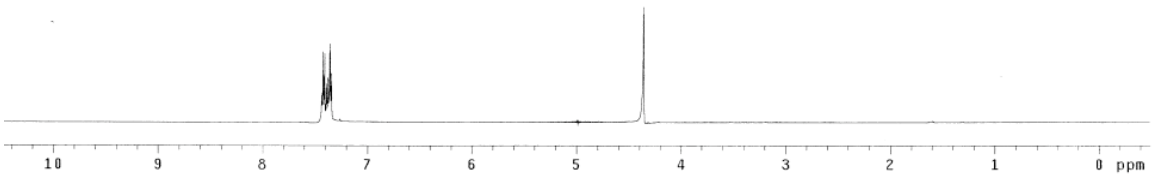

^{1}H NMR ($CDCl_3$)

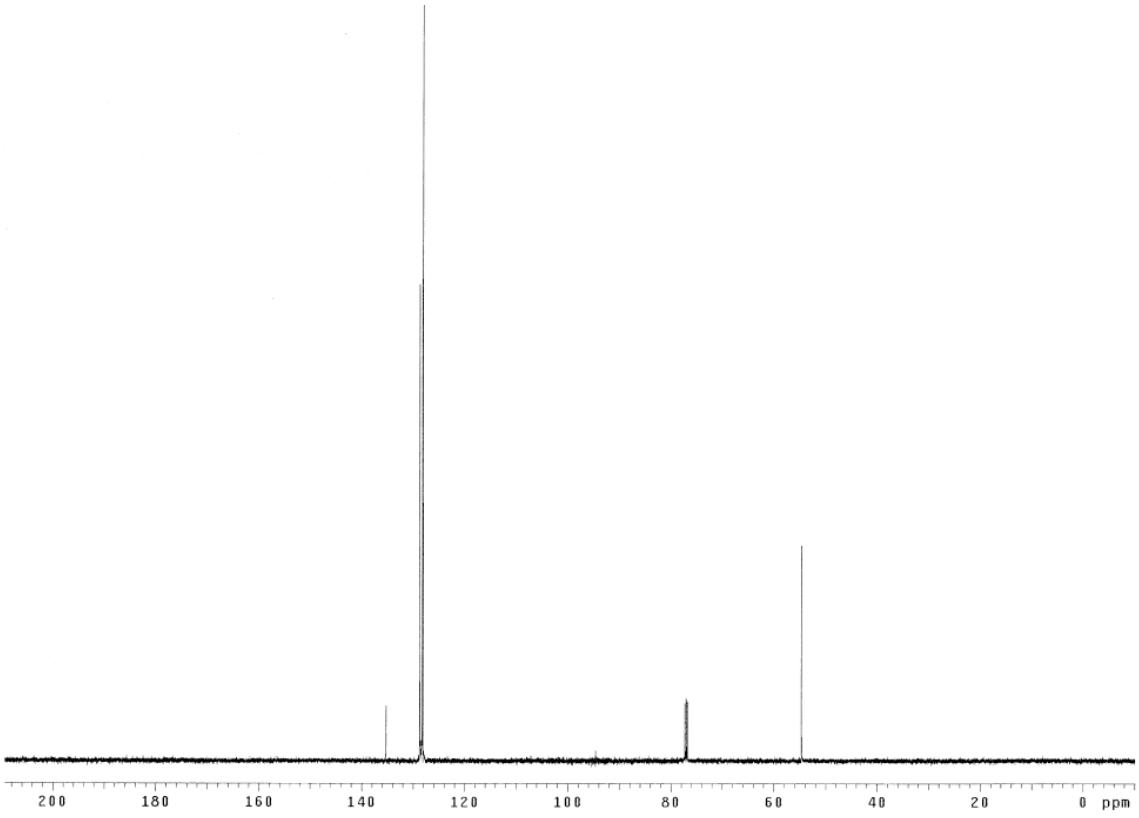

^{13}C NMR ($CDCl_3$)

Triazole (112)

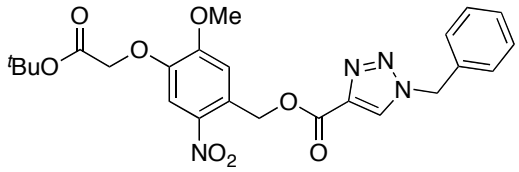

A solution of photolinker **109a** (78 mg, 0.21 mmol), benzylazide **111** (43 mg, 0.32 mmol), $CuSO_4$ (43 mL, 0.043 mmol, 1M in H_2O) and sodium ascorbate (0.5 mL, 1.07 mmol, 2M in H_2O) in THF/^{i}PrOH/H_2O (2 mL:1 mL:1 mL, respectively) was stirred at 25 ºC for 22 h in dark. Water (10 mL) was added into reaction mixture and aqueous layer was ectracted with EtOAc (5 x 5 mL). The combined organic layer was dried over $MgSO_4$ and concentrated under the reduced pressure. The residual material was purified by flash chromatography eluting with 40 to 60 % EtOAc/hexanes to afford product as a colorless solid (72 mg, 68 %). R_f 0.2 (40 % EtOAc/hexanes). ^{1}H NMR (500 MHz, DMSO-d_6) δ 9.01 (s, 1H), 7.69 (s, 1H), 7.44-7.38 (m, 6H), 5.70 (s, 2H), 5.65 (s, 2H), 4.90 (s, 2H), 3.95 (s, 3H), 1.47 (s, 9H); ^{13}C NMR (125 MHz, $CDCl_3$) δ 166.8, 160.0, 154.0, 146.4, 140.0, 139.3, 133.4, 129.4, 129.3, 128.3, 127.9, 127.8, 110.9, 109.9, 83.1, 66.2, 63.5, 56.5, 54.6, 28.0; MS (ESI) m/z 499.19 $(M+H)^+$.

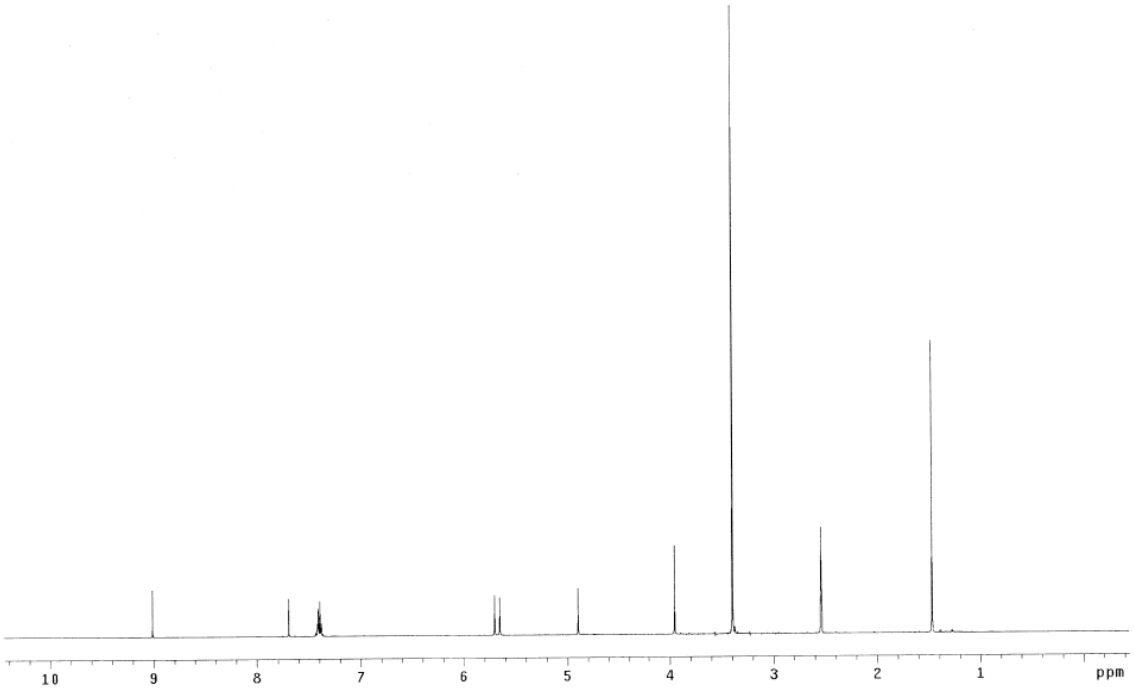

^{1}H NMR (DMSO-d_6)

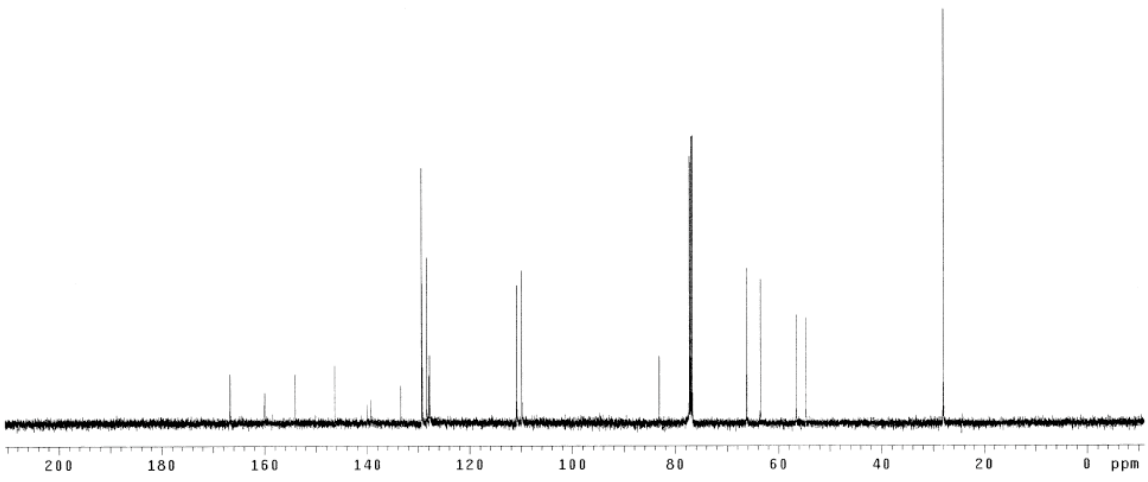

^{13}C NMR ($CDCl_3$)

Azidolysine derivative (134)

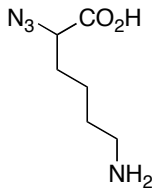

A solution of Boc-protected azido lysine **121** (500 mg, 1.84 mmol, *provided by Ms. Eunhwa Ko*) in 1:1 TFA/CH_2Cl_2 (3 mL:3 mL) was stirred at 25 ºC for 1.5 h. The reaction mixture was flashed with nitrogen to remove TFA and CH_2Cl_2 at 25 ºC for overnight. Pure product was obtained as a brown oil (320 mg, quantitative yield). ^{1}H NMR (500 MHz, DMSO-d_6) δ 9.03 (s, 1H), 7.87 (bs, 2H), 4.15 (q, 1H, J = 3.0 Hz), 2.84-2.80 (m, 2H), 1.81-1.63 (m, 2H), 1.63-1.55 (m, 2H), 1.45-1.38 (m, 2H); ^{13}C NMR (125 MHz, DMSO-d_6) δ 172.8, 62.1, 39.6, 31.3, 27.6, 23.3; MS (ESI) m/z 173.09 $(M+H)^+$.

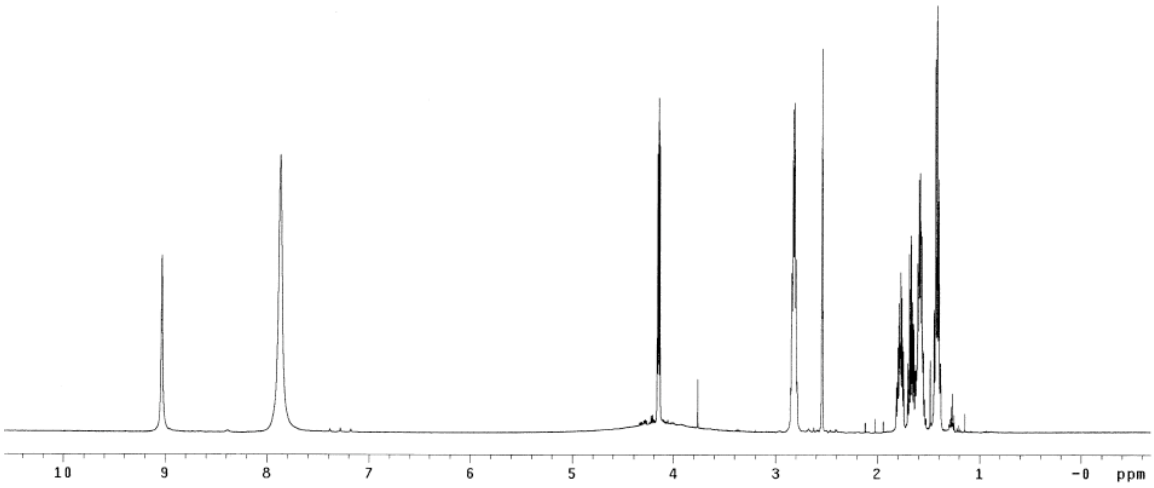

^{1}H NMR (DMSO-d_6)

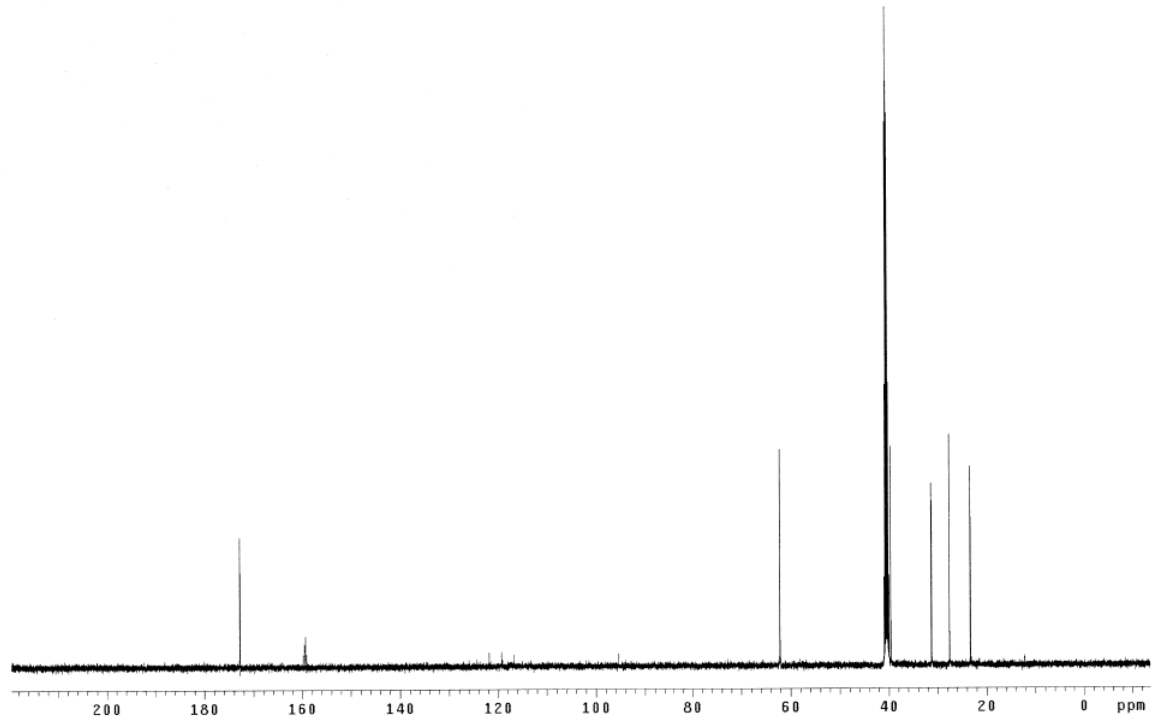

^{13}C NMR (DMSO-d_6)

BODIPY derivative (137)

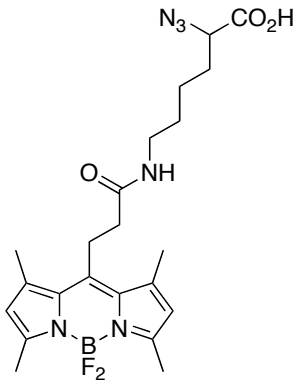

A solution of tetramethyl BODIPY **135** (200 mg, 0.625 mmol, provided by *Mr. Cliferson Thivierge*), *N*-hydroxysuccinimide (72 mg, 0.625 mmol) and *N,N'*-diisopropylcarbodiimide (79 mg, 0.625 mmol) in DMF (4.0 mL) was stirred at 25 ºC for 24 h under nitrogen. A solution of azido lysine **134** (183 mg, 1.06 mmol) in DMF (2.0 mL) and DIPEA (0.44 mL, 2.50 mmol) was added to a reaction mixture and the reaction was stirred at 25 ºC for additional 16 h. The solvents were evaporated under reduced pressure and the residue was purified by flash chromatography eluting with 100 % EtOAc and 10 % to 30 % MeOH/EtOAc (columned 2 times) to afford product as a orange semi-solid (225 mg, 76 %). R_f 0.3 (100 % EtOAc). ^{1}H NMR (500 MHz, CD_3OD) δ 6.18 (s, 2H), 3.78 (q, 1H, J = 4.0 Hz), 3.38 (t, 2H, J = 4.5 Hz), 3.22 (t, 2H, J = 6.5 Hz), 2.53 (s, 6H), 2.48 (s, 6H), 1.89-1.83 (m, 1H), 1.77-1.69 (m, 1H), 1.58-1.42 (m, 5H), 1.37-1.32 (m, 1H); ^{13}C NMR (75 MHz, DMSO-d_6) δ 170.8, 154.3, 146.7, 142.0, 131.6, 122.7, 64.6, 39.4, 37.4, 32.2, 29.7, 26.1, 25.1, 24.4, 17.0, 15.1; MS (ESI) m/z 473.15 $(M–H)^-$.

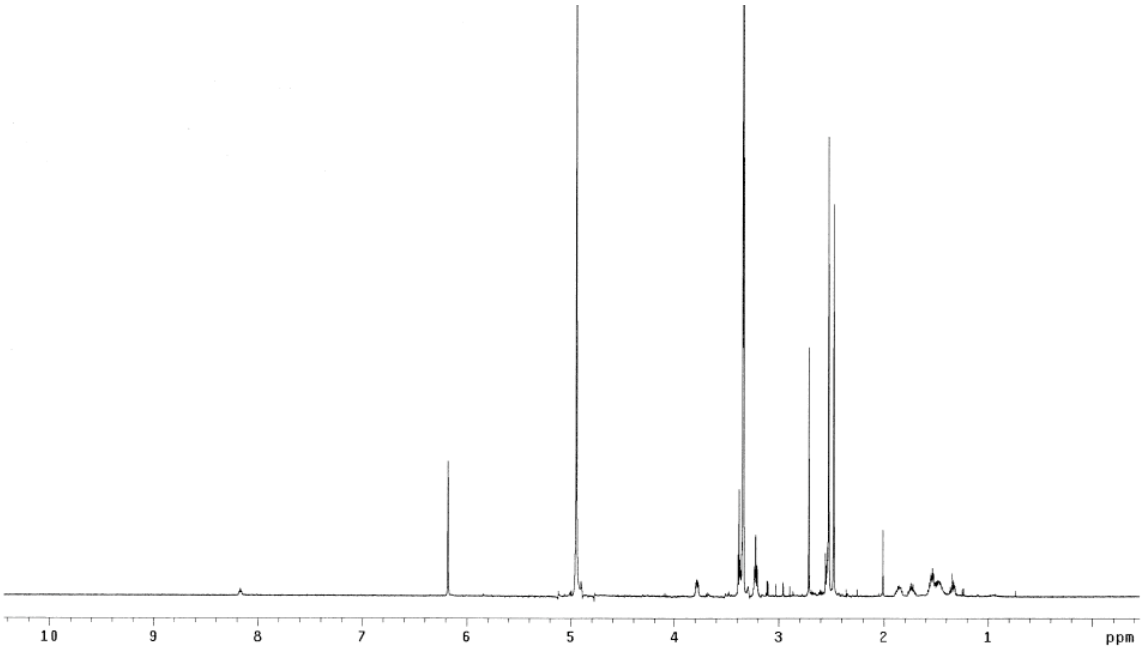

^{1}H NMR (CD_3OD)

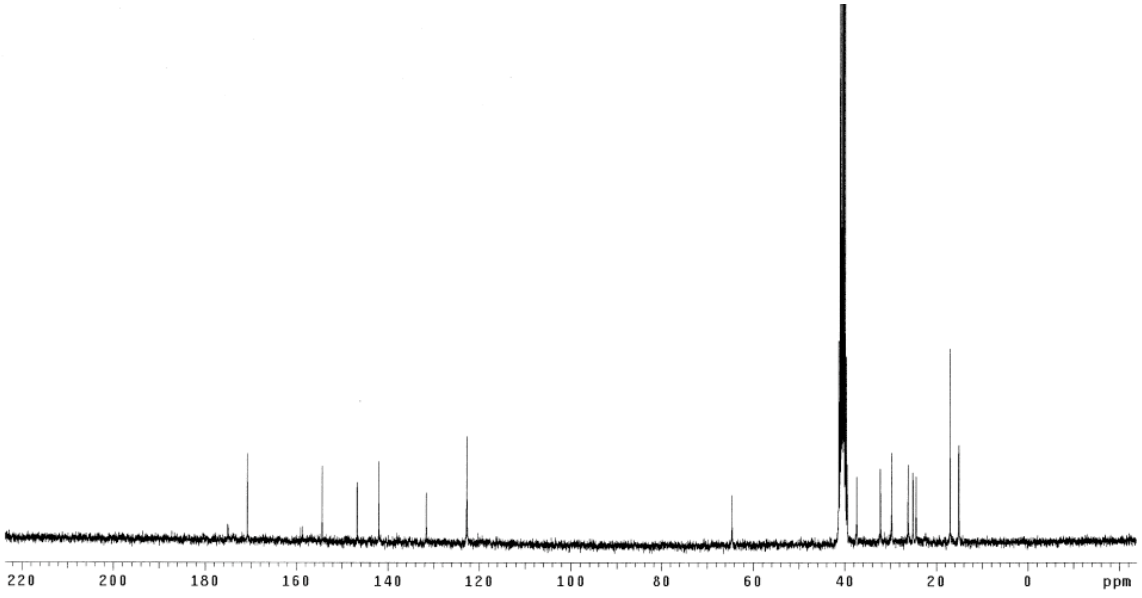

^{13}C NMR (DMSO-d_6)

Propargyl tosylate (142)[152]

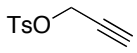

Propargyl alcohol (2.8 g, 50.0 mmol) and TsCl (11.4 g, 60 mmol) were added in ether (50 mL) at 0 ºC. KOH (14.0 g, 250.0 mmol) was added in 10 portions and the reaction mixture was stirred at 0 ºC for 1 h and at 25 ºC for 4 h. Cold water (25 mL) was added at 0 ºC and aqueous layer was extracted with ether (2 x 25 mL). The combined organic layer was washed with brine (1 x 25 mL) and dried over Na_2SO_4. The solvents were concentrated under the reduced pressure to afford product as a brown liquid (8.7 g, 83 %). ^{1}H NMR (300 MHz, $CDCl_3$) δ 7.81 (d, 2H, *J* = 8.5 Hz), 7.35 (d, 2H, *J* = 8.5 Hz), 4.69 (d, 2H, *J* = 2.5 Hz), 2.47 (t, 1H, *J* = 2.5 Hz), 2.45 (s, 3H); ^{13}C NMR (75 MHz, $CDCl_3$) δ 145.2, 132.8, 129.8, 128.1, 77.3, 75.3, 57.3, 21.6.

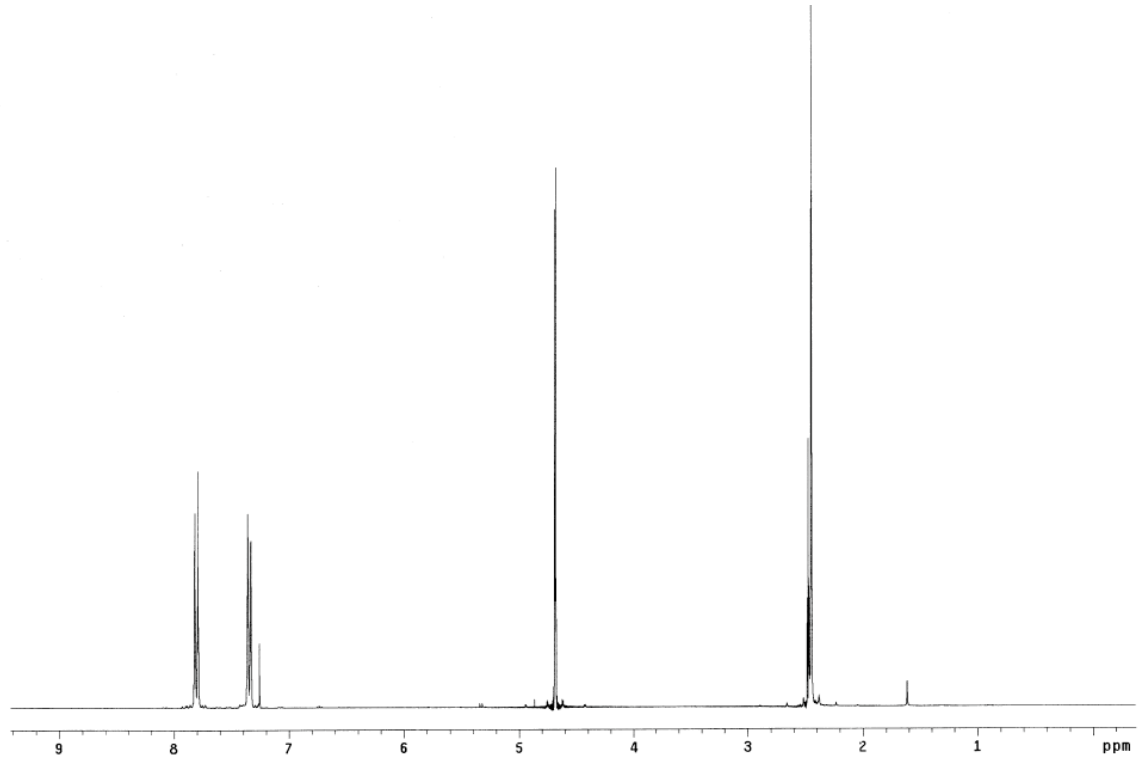

^{1}H NMR ($CDCl_3$)

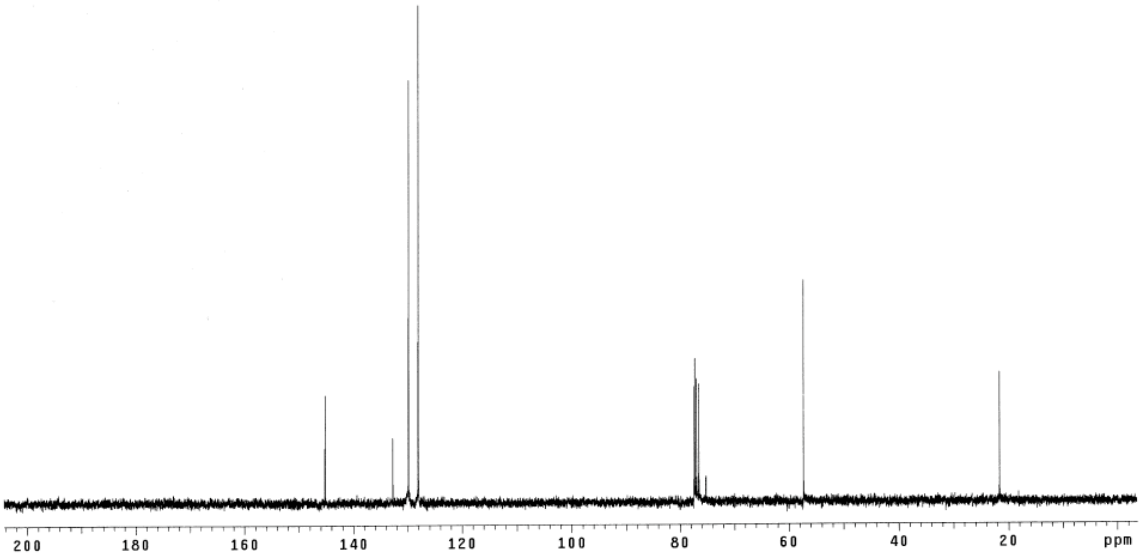

^{13}C NMR ($CDCl_3$)

Mono-propargyl resorcinol (143)[151]

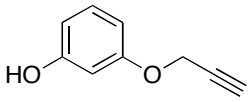

A solution of resorcinol (2.0 g, 18.2 mmol) and K_2CO_3 (1.6 g, 11.8 mmol) in acetone (20 mL) was stirred at 25 ºC for 5 min. A solution of propargyl tosylate **142** (1.9 g, 9.1 mmol) in acetone (10 mL) was added dropwise for 5 min and the reaction mixture was refluxed at 65 ºC for 7 h. The reaction mixture was filtrated and the solvents were evaporated. The residue was purified by flash chromatography eluting with 10 % to 20 % EtOAc/hexanes to afford product as a colorless oil (723 mg, 54 %). R_f 0.4 (30 % EtOAc/hexanes). ^{1}H NMR (500 MHz, $CDCl_3$) δ 7.15 (t, 1H, J = 7.6 Hz), 6.59-6.56 (m, 1H), 6.51-6.48 (m, 2H), 4.65 (d, 2H, J = 2.3 Hz), 2.53 (t, 1H, J = 2.3 Hz); ^{13}C NMR (125 MHz, $CDCl_3$) δ 158.7, 156.5, 130.2, 108.8, 107.2, 102.5, 78.3, 75.7, 55.8.

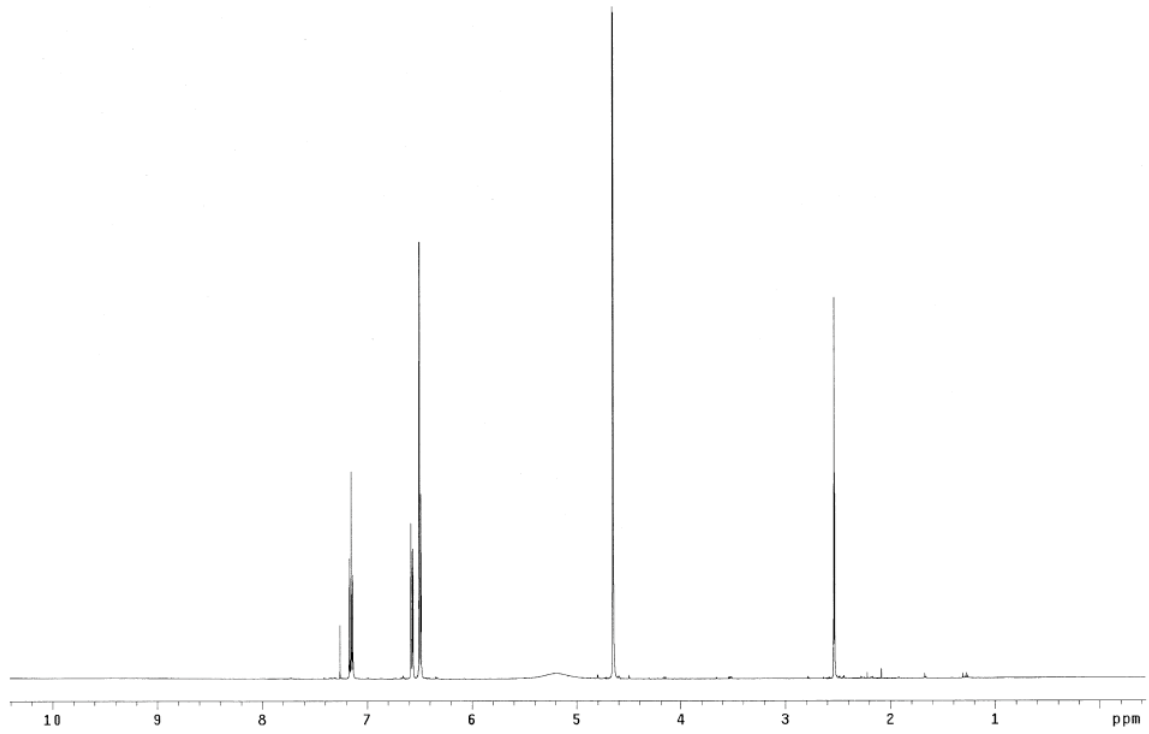

^{1}H NMR ($CDCl_3$)

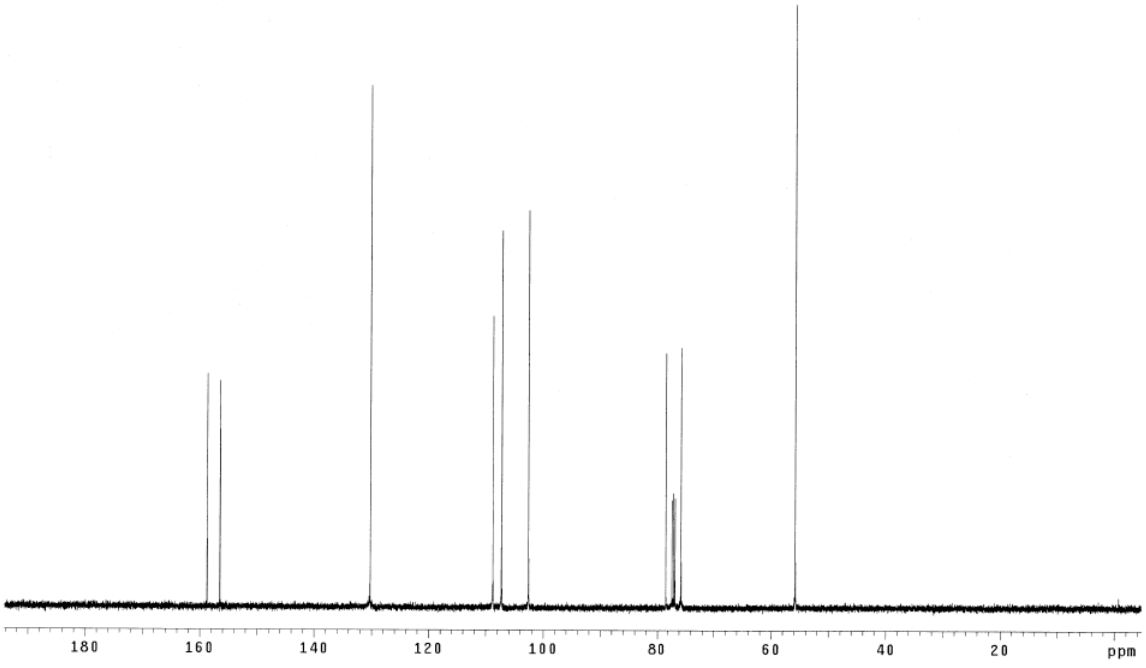

^{13}C NMR ($CDCl_3$)

Tosylate (144)

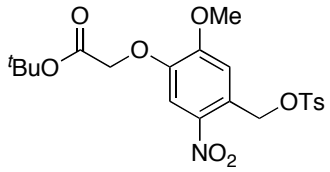

Photolinker **108** (300 mg, 0.96 mmol), Et_3N (0.27 mL, 1.92 mmol) and Me_3N•HCl (9 mg, 0.096 mmol) were added in CH_3CN (9.0 mL) at 0 ºC. A solution of TsCl (237 mg, 1.24 mmol) in CH_3CN (3.0 mL) was then added by syringe and the reaction mixture was stirred at 0 ºC for 20 min. The reaction was quenched with water (15 mL) at 0 ºC and the aqueous layer was extracted with EtOAc (3 x 15 mL). The combined organic layer was washed with water (1 x 10 mL) and brine (1 x 10 mL). The organic layer was dried over Na_2SO_4 and solvents were concentrated under the reduced pressure to afford pure product as a yellow solid (429 mg, 99 %). R_f 0.5 (20 % EtOAc/hexanes). ^{1}H NMR (500 MHz, $CDCl_3$) δ 7.84 (d, 2H, J = 8.3 Hz), 7.60 (s, 1H), 7.37 (d, 2H, J = 8.3 Hz), 7.16 (s, 1H), 5.46 (s, 2H), 4.63 (s, 2H), 3.98 (s, 3H), 2.45 (s, 3H), 1.48 (s, 9H); ^{13}C NMR (125 MHz, $CDCl_3$) δ 166.6, 154.2, 146.5, 145.3, 138.6, 132.5, 130.0, 127.9, 126.6, 110.1, 109.8, 83.2, 68.5, 66.2, 56.6, 28.0, 21.6; MS (ESI) m/z 474.14 $(M+Li)^+$.

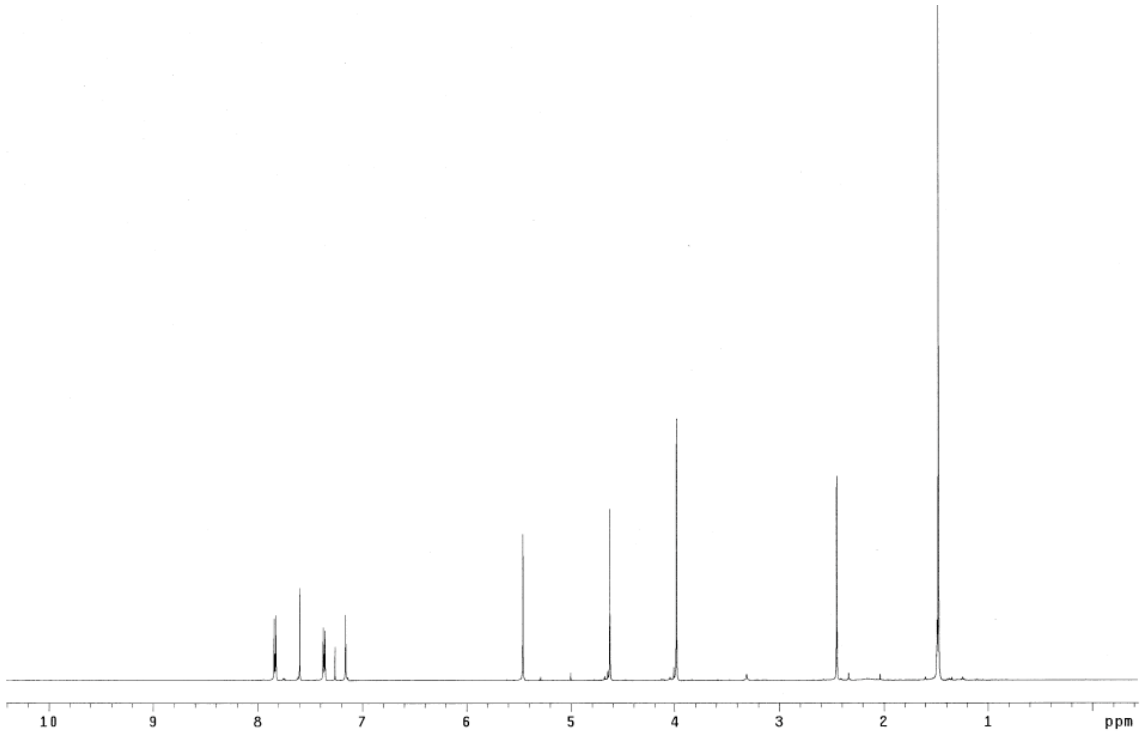

^{1}H NMR ($CDCl_3$)

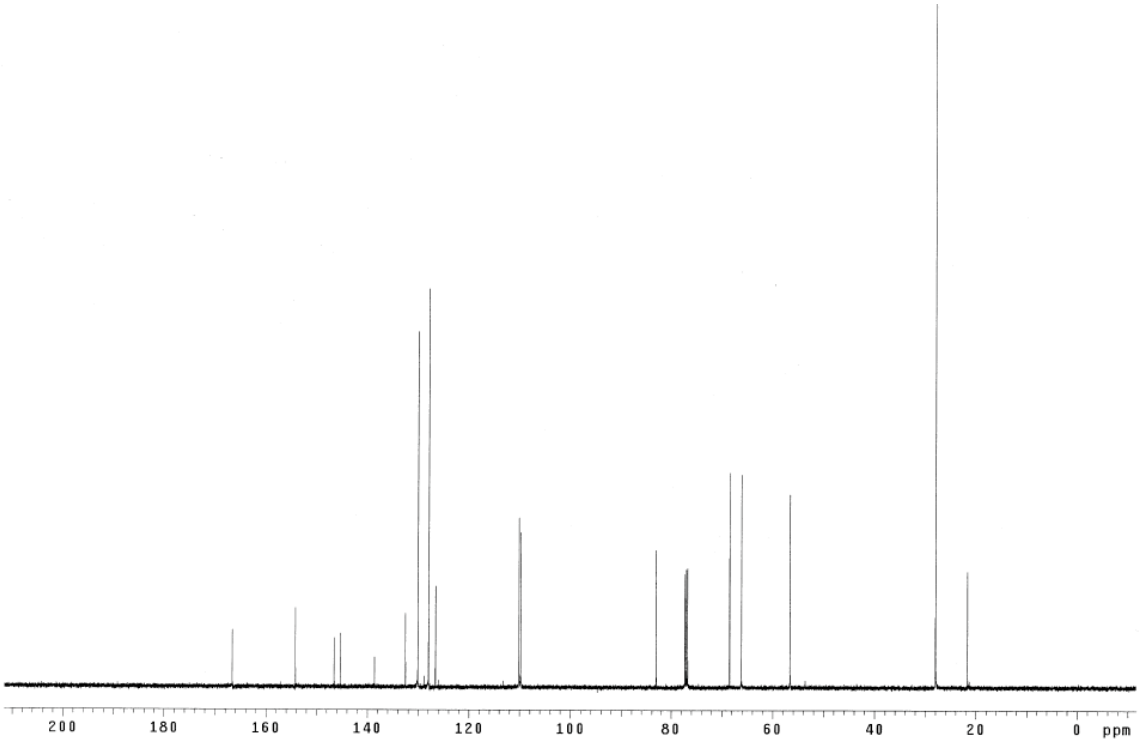

^{13}C NMR ($CDCl_3$)

Propargylated photolinker (145)

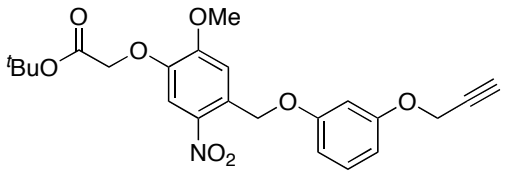

A solution of tosylate **144** (303 mg, 0.65 mmol), propargyl-resorcinol **143** (80 mg, 0.54 mmol) and K_2CO_3 (149 mg, 1.08 mmol) in acetone (10 mL) was stirred at 25 ºC in dark for 6 h. The reaction mixture was filtrated and the solvents were evaporated. The residue was purified by flash chromatography eluting with 30 % to 80 % CH_2Cl_2/hexanes to afford product as a yellow solid (230 mg, 96 %). R_f 0.3 (70 % CH_2Cl_2/hexanes). ^{1}H NMR (500 MHz, $CDCl_3$) δ 7.68 (s, 1H), 7.34 (s, 1H), 7.22 (t, 1H, J = 8.8 Hz), 6.65-6.61 (m, 3H), 5.47 (s, 2H), 4.67 (d, 2H, J = 2.4 Hz), 4.65 (s, 2H), 3.95 (s, 3H), 2.52 (t, 1H, J = 2.4 Hz), 1.50 (s, 9H); ^{13}C NMR (125 MHz, $CDCl_3$) δ 166.8, 159.1, 158.8, 154.2, 145.9, 138.6, 130.3, 130.1, 109.9, 109.8, 108.1, 107.6, 102.5, 83.1, 78.3, 75.6, 67.1, 66.2, 56.4, 55.8, 28.0; MS (ESI) m/z 444.17 $(M+H)^+$.

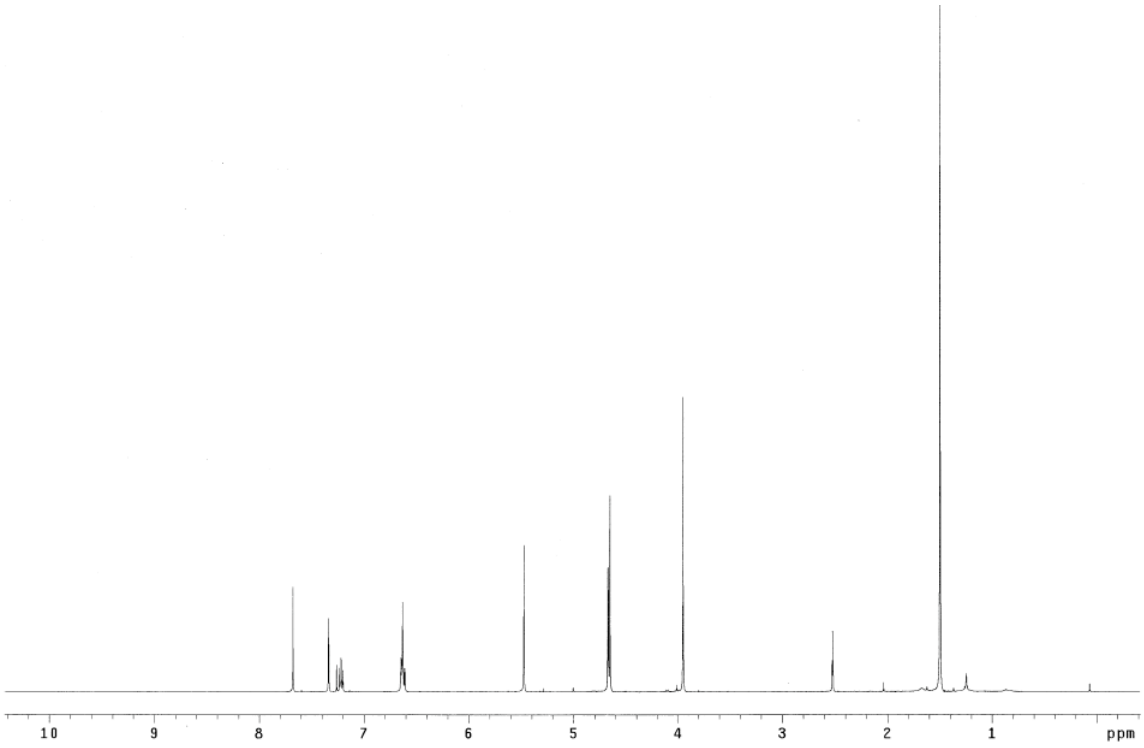

^{1}H NMR ($CDCl_3$)

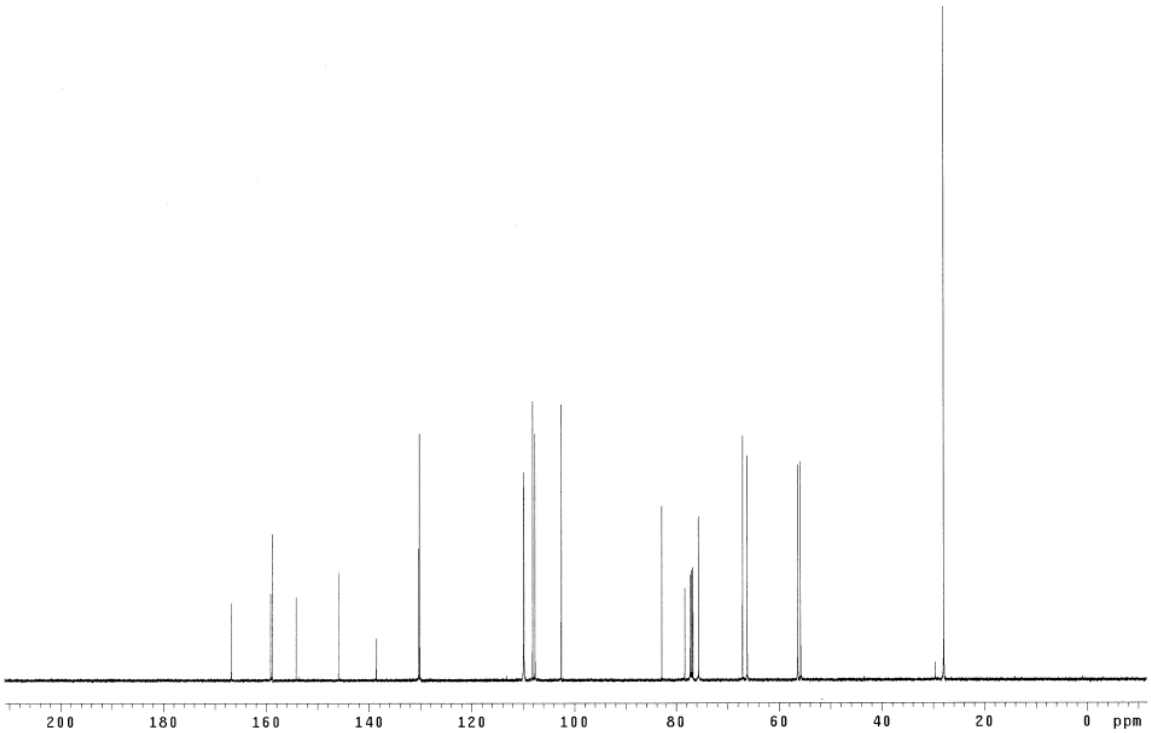

^{13}C NMR ($CDCl_3$)

Photolinker (146)

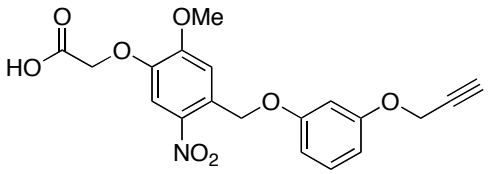

A solution of photolinker **145** (57 mg, 0.13 mmol) in 1:1 TFA/CH_2Cl_2 (1.5 mL:1.5 mL) was stirred at 25 ºC in dark for 1 h. The reaction mixture was flashed with nitrogen to remove TFA and CH_2Cl_2 at 25 ºC for overnight. Pure product was obtained as a light brown solid (53 mg, quantitative yield). R_f 0.2 (40 % EtOAc/hexanes). ^{1}H NMR (500 MHz, acetone-d_6) δ 7.81 (s, 1H), 7.46 (s, 1H), 7.28 (t, 1H, J = 7.6 Hz), 6.74-6.72 (m, 2H), 6.69-6.67 (m, 1H), 5.51 (s, 2H), 4.95 (s, 2H), 4.81 (d, 2H, J = 2.4 Hz), 4.00 (s, 3H), 3.11 (t, 1H, J = 2.4 Hz), ; ^{13}C NMR (125 MHz, acetone-d_6) δ 170.5, 161.2, 160.7, 155.8, 148.1, 141.1, 131.7, 130.7, 112.7, 112.1, 109.38, 109.35, 103.9, 80.4, 77.8, 68.4, 67.0, 57.5, 57.1; MS (APCI) m/z 387.87 $(M+H)^+$.

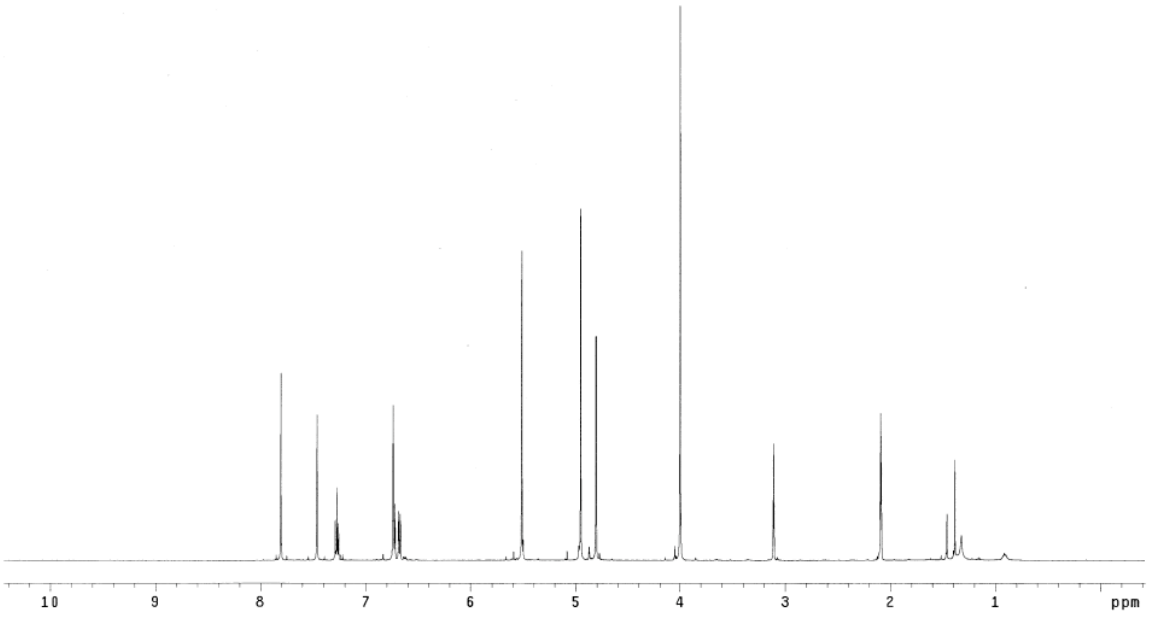

^{1}H NMR (acetone-d_6)

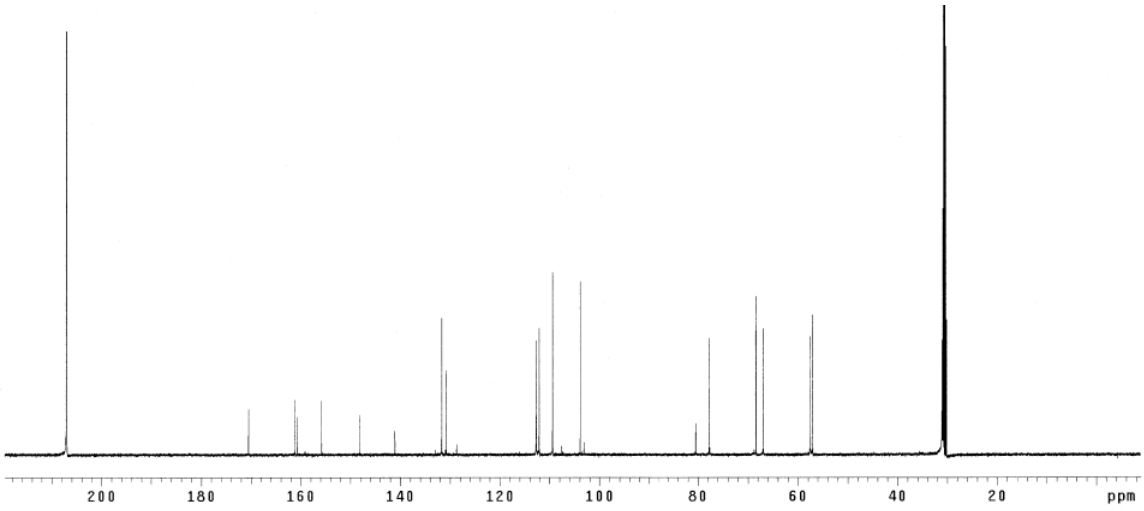

^{13}C NMR (acetone-d_6)

APPENDIX D

PROCEDURES OF SOLID-PHASE SYNTHESIS AND PHOTOLYSIS FOR CHAPTER IV

Solid-supported Nile Red derivatives (95-PEGA and 95-CPG)

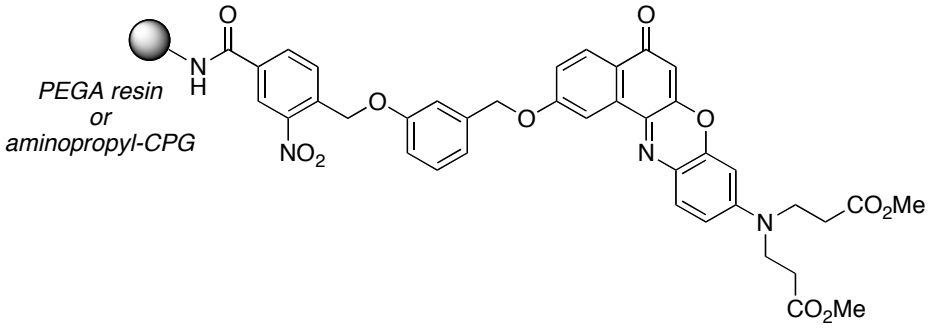

Solid-supported Nile Red derivative ***95-PEGA***

PEGA resin (700 mg, 0.020 mmol, 5 wt % in MeOH, 0.59 mmol/g) was washed with DMF (4 x 3 mL). A solution of Nile Red derivative **94** (30 mg, 0.041 mmol), DIC (13 mg, 0.102 mmol), DMAP (0.2 mg, 0.002 mmol) and PEGA resin (washed with DMF) in DMF (2 mL) was shaken in reaction vessel at 25 ºC in dark for 24 h. Excess amount of chemicals were washed off with DMF (5 x 2 mL), MeOH (5 x 2 mL), acetone (5 x 2 mL) and CH_2Cl_2 (5 x 2 mL), then PEGA resin was dried under the vacuum to afford purple beads (**95-PEGA**). Ninhydrin test resulted in about 50 % conversion (purple and brown beads). Resin was shaken with Ac_2O and pyridine in CH_2Cl_2 (2 mL) for 2 h. Excess chemicals were washed off with CH_2Cl_2 (3 x 5 mL), MeOH (3 x 5 mL), CH_2Cl_2 (3 x 5 mL), ether (3 x 5 mL). Then ninhydrin test gave brown beads (negative).

Solid-supported Nile Red derivative ***95-CPG***

A solution of Nile Red derivative **94** (36 mg, 0.049 mmol), DIC (10 mg, 0.081 mmol), DMAP (0.2 mg, 0.002 mmol) and aminopropyl-CPG (100 mg, 0.016 mmol,

0.162 mmol/g) in DMF (2 mL) was shaken in reaction vessel at 25 ºC in dark for 24 h. Excess amount of chemicals were washed off with DMF (10 x 3 mL), MeOH (10 x 3 mL), acetone (3 x 3 mL) and CH_2Cl_2 (3 x 3 mL), then CPG was dried under the vacuum to afford purple beads (**95-CPG**). Then ninhydrin test gave brown beads (negative).

Solid-supported Nile red derivative (96-PEGA and 96-CPG)

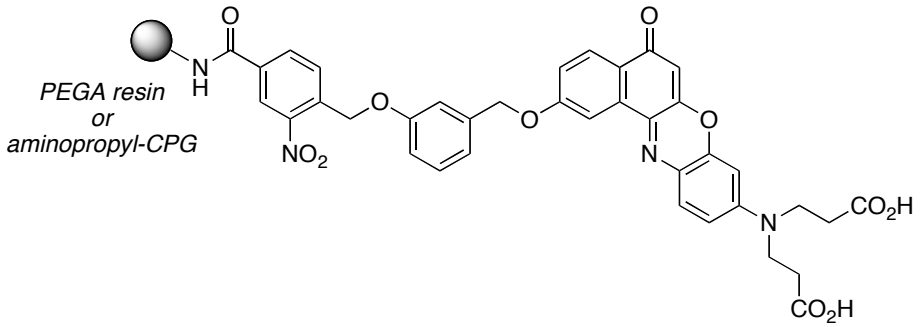

Solid-supported Nile Red derivative ***96-PEGA***

A solution of **95-PEGA** (35 mg, 0.020 mmol) and K_2CO_3 (28 mg, 0.205 mmol) in 1:1 MeOH/H_2O (1 mL:1 mL) was shaken in round bottom flask at 40 ºC in dark for 24 h. Excess amount of chemicals were washed off with H_2O (3 x 2 mL), MeOH (3 x 2 mL), CH_2Cl_2 (3 x 2 mL) and ether (3 x 2 mL), then PEGA resin was dried under the vacuum to afford purple beads (**96-PEGA**).

Solid-supported Nile Red derivative ***96-CPG***

A solution of **95-CPG** (30 mg, 0.0049 mmol) and K_2CO_3 (6.7 mg, 0.049 mmol) in 4:1 MeOH/H_2O (0.8 mL:0.2 mL) was shaken in reaction vessel at 25 ºC in dark for 24 h. Excess amount of chemicals were washed off with H_2O (3 x 3 mL), MeOH (3 x 3 mL), CH_2Cl_2 (3 x 3 mL) and ether (3 x 3 mL), then beads were dried under the vacuum to afford light pink beads (**96-CPG**).

CPG-supported photolinker (115)

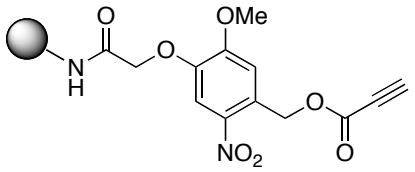

A solution of photolinker **110a** (25 mg, 0.081 mmol), DIC (20 mg, 0.162 mmol), DMAP (0.4 mg, 0.0032 mmol) and CPG (100 mg, 0.0162 mmol, loading: 0.162 mmol/g) in DMF (2 mL) was shaken in reaction vessel at 25 ºC in dark for 24 h. Excess chemicals were washed off with DMF (5 x 2 mL), MeOH (5 x 2 mL) and CH_2Cl_2 (5 x 2 mL), then beads were dried under the vacuum to afford orange beads (compound **115**). Ninhydrin test gave negative results (brown beads).

Model compound (117)

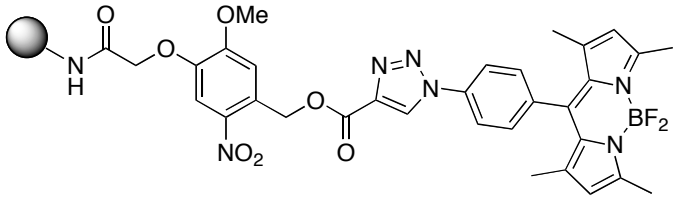

A solution of CPG-support photolinker **115** (20 mg, 0.0032 mmol), 4-azido-BODIPY **116** (3.5 mg, 0.0097 mmol, *provided by Mrs. Lingling Li*), $CuSO_4$ (0.6 μL, 0.6 μmol, 1 M in H_2O), and sodium ascorbate (8.1 μL, 0.016 mmol, 2 M in H_2O) in 4:1:1 THF/^{i}PrOH/H_2O (1 mL:0.25 mL:0.25 mL, respectively) was shaken in reaction vessel at 25 ºC in dark for 24 h. Excess chemicals were washed off with H_2O (5 x 2 mL), MeOH (5 x 2 mL), THF (5 x 2 mL) and CH_2Cl_2 (5 x 2 mL), then beads were dried under the vacuum to afford brown beads (compound **117**).

CPG-supported photolinker (120)

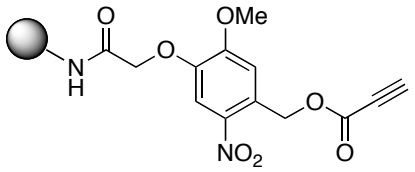

A solution of photolinker **110a** (14 mg, 0.045 mmol), DIC (5.6 mg, 0.045 mmol), DMAP (0.2 mg, 0.0018 mmol) and CPG (100 mg, 0.0089 mmol, pore size: 1000 Å, loading: 0.089 mmol/g) in DMF (2 mL) was shaken in reaction vessel at 25 ºC in dark for 24 h. Excess chemicals were washed off with DMF (5 x 2 mL), MeOH (5 x 2 mL) and CH_2Cl_2 (5 x 2 mL), then beads were dried under the vacuum to afford light yellow beads (compound **120**). Ninhydrin test gave negative results (brown beads).

CPG-supported triazole (122)

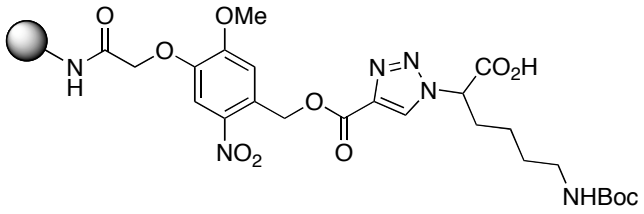

A solution of CPG-support **120** (111 mg, 0.0099 mmol, loading: 0.089 mmol/g), azido-lysine derivative **121** (8.0 mg, 0.030 mmol), $CuSO_4$ (5.0 μL, 5.0 μmol, 1 M in H_2O) and sodium ascorbate (25 μL, 49 μmol, 2 M in H_2O) in 5:1 THF/H_2O (total volume 2 mL) was shaken in reaction vessel at 25 ºC in dark for 24 h. Excess chemicals were washed off with H_2O (5 x 2 mL), MeOH (5 x 2 mL), THF (5 x 2 mL) and CH_2Cl_2 (5 x 2 mL), then beads were dried under the vacuum to afford colorless beads (compound **122**).

CPG-supported lysine derivative (123)

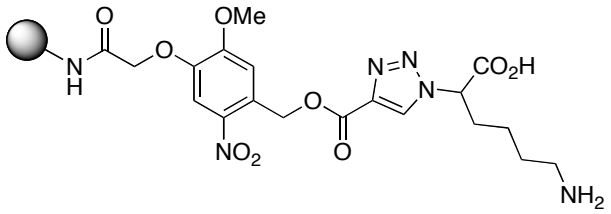

A solution of CPG-supported triazole **122** (101 mg, 0.009 mmol, loading: 0.089 mmol/g) in 50 % TFA/CH_2Cl_2 (1 mL:1 mL) was shaken in reaction vessel at 25 ºC in dark for 2 h. The obtained beads were washed with CH_2Cl_2 (5 x 2 mL), then beads were dried under the vacuum to afford colorless beads (compound **123**). Ninhydrin test gave positive results (purple beads).

CPG-supported Nile Red derivative (126)

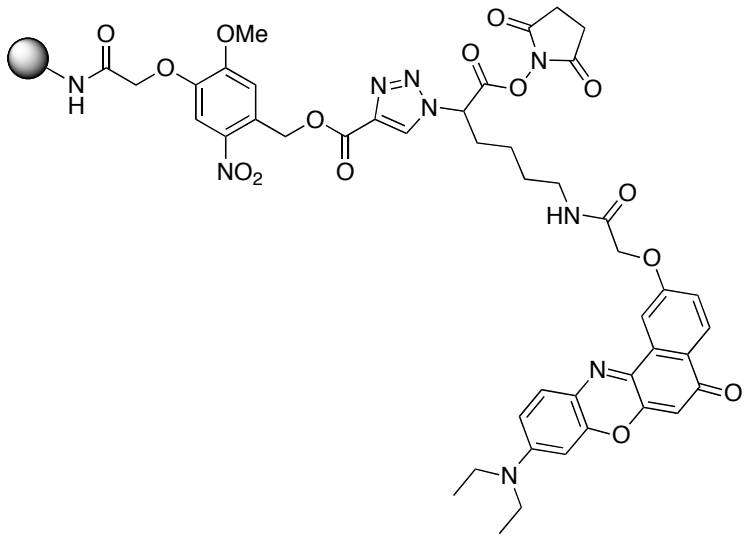

A solution of Nile Red derivative **124** (17 mg, 0.043 mmol), NHS (4.7 mg, 0.041 mmol) and DIC (5.2 mg, 0.041 mmol) in DMF (2 mL) was stirred at 25 ºC for 24 h. Reaction was followed by TLC (100 % conversion after 24 h). Crude compound **125** (1 mL) was shaken with CPG-supported lysine **123** (50 mg, 0.0045 mmol), DIPEA (2.9 mg, 0.022 mmol), DMAP (0.1 mg, 0.9 mmol) in additional DMF (1 mL) in reaction vessel at 25 ºC in dark for 24 h. The beads were washed with DMF (7 x 2 mL), MeOH (7 x 2 mL) and CH_2Cl_2 (7 x 2 mL), then dried under the vacuum to afford purple beads. A solution of beads (20 mg), NHS (2.0 mg, 0.018 mmol) and DIC (2.2 mg, 0.018 mmol) in DMF (2 mL) was shaken in reaction vessel at 25 ºC in dark for 24 h. The beads were washed with DMF (5 x 2 mL) and CH_2Cl_2 (5 x 2 mL) and dried under the vacuum to afford purple beads (compound **126**).

CPG-supported dye-ubiquitin conjugate (127)

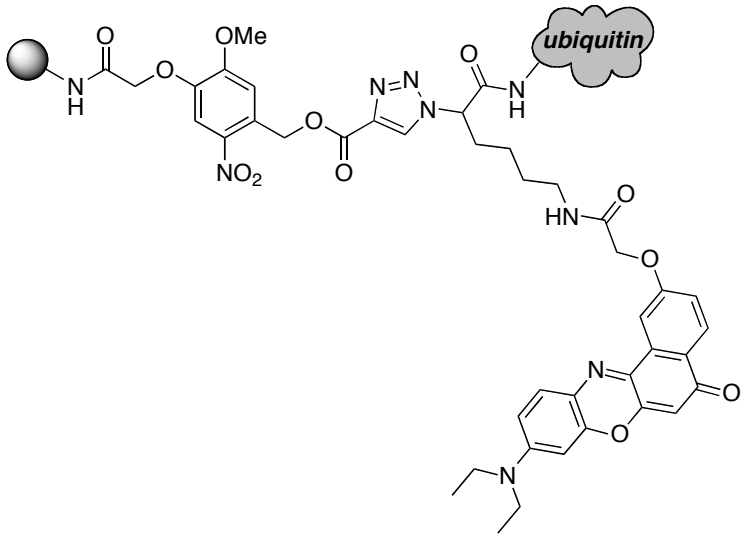

A solution of CPG-supported Nile Red derivative **126** (19 mg, 0.0017 mmol) and ubiquitin (7.2 mg, 0.85 mmol) in pH 8.3 sodium bicarbonate buffer (0.5 mL) was shaken in reaction vessel at 25 ºC in dark for 4 h. CPG was washed with pH 8.3 buffer (5 x 2 mL) and H_2O (5 x 2 mL) to afford CPG-supported dye-protein conjugate **127** and the beads were directly used for next photocleavage reaction.

CPG-support succinimide (130)

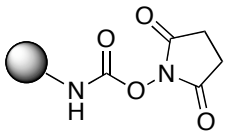

A solution of LCAA CPG (300 mg, 0.029 mmol, pore size: 1000 Å, loading: 0.097 mmol/g), *N,N'*-disuccinimidyl carbonate (37 mg, 0.146 mmol) and DIPEA (19 mg, 0.146 mmol) in DMF (5.0 mL) was shaken in reaction vessel at 25 ºC in dark for 5 h. CPG was washed with DMF (5 x 2 mL), EtOH (3 x 2 mL) and pH 7.4 phosphate buffer (3 x 2 mL) to afford colorless beads (compound **130**). These beads were directly used for next reaction.

BSA-coated CPG (131)

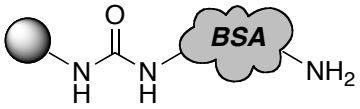

A solution of CPG-supported succinimide **130** (300 mg, 0.029 mmol, loading: 0.097 mmol/g) and BSA (60 mg, 0.87 mmol) in pH 7.4 phosphate buffer (6.0 mL) was shaken in reaction vessel at 25 ºC in dark for 16 h. CPG was washed with pH 7.4 phosphate buffer (5 x 2 mL), H_2O (5 x 2 mL), EtOH (5 x 2 mL) and ether (5 x 2 mL) then dried under vacuum to afford BSA-coated CPG (**131**) as colorless beads. Ninhydrin test gave positive result (purple bead).

CPG-support photolinker (132)

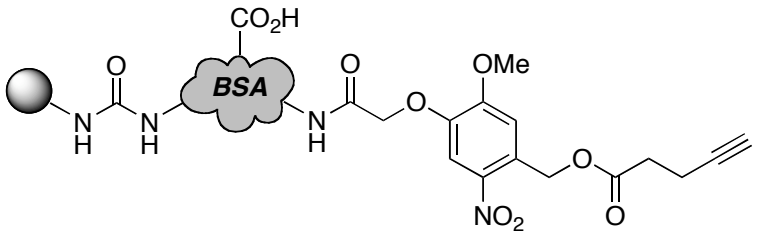

A solution of BSA-coated CPG **131** (100 mg, 0.0097 mmol, loading: 0.097 mmol/g), photolinker **110b** (6.5 mg, 0.019 mmol), DIC (3.7 mg, 0.029 mmol) and DMAP (1.2 mg, 0.0097 mmol) in DMF (2.0 mL) was shaken in reaction vessel at 25 ºC in dark for 24 h. CPG was washed with DMF (5 x 2 mL), EtOH (5 x 2 mL) and ether (3 x 2 mL) to afford BSA-coated CPG (**132)** as light orange beads.

CPG-support photolinker (133)

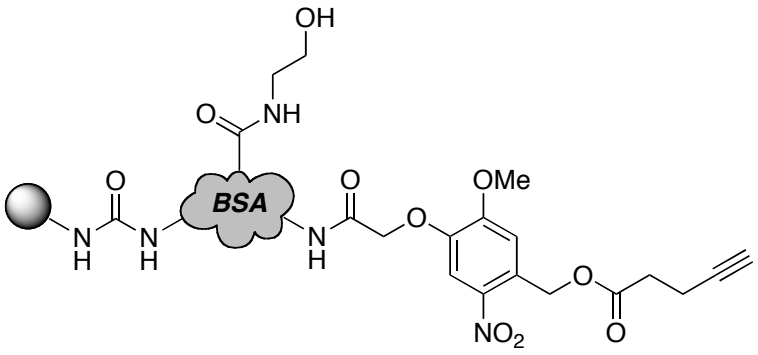

Capping of carboxylic acid for aspartate and glutamate

A solution of BSA-coated CPG **132** (100 mg, 0.0097 mmol, loading: 0.097 mmol/g), NHS (11 mg, 0.1 mmol) and DIC (12 mg, 0.1 mmol) in DMF (1.5 mL) was shaken in reaction vessel at 25 ºC in dark for 12 h. CPG was washed with DMF (3 x 2 mL). The beads were shaken with ethanolamine (3.0 mg, 0.05 mmol) and DIPEA (13 mg, 0.1 mmol) in DMF (2.0 mL) at 25 ºC in dark for 6 h. CPG was washed with DMF (5 x 2

mL), EtOH (5 x 2 mL) and ether (3 x 2 mL) and dried under the vacuum to afford light orange beads (compound **133**).

CPG-support BODIPY (138)

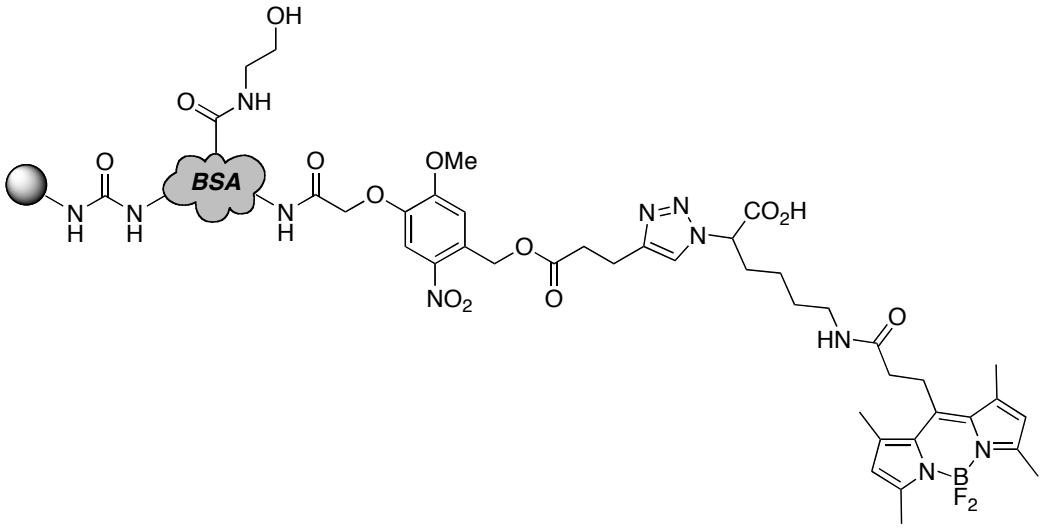

A solution of CPG-supported photolinker **133** (100 mg, 0.0097 mmol, loading: 0.097 mmol/g), BODIPY derivative **137** (14 mg, 0.029 mmol), $CuSO_4$ (4.9 μL, 4.9 μmol, 1 M in H_2O) and sodium ascorbate (24 μL, 49 μmol, 2 M in H_2O) in 5:1 THF/H_2O (total volume 2 mL) was shaken in reaction vessel at 25 ºC in dark for 30 h. Excess chemicals were washed off with H_2O (10 x 2 mL), DMF (10 x 2 mL), THF (5 x 2 mL), EtOH (5 x 2 mL) and ether (5 x 2 mL), then beads were dried under the vacuum to afford light green beads (compound **138**).

CPG-support dye-ubiquitin conjugate (139)

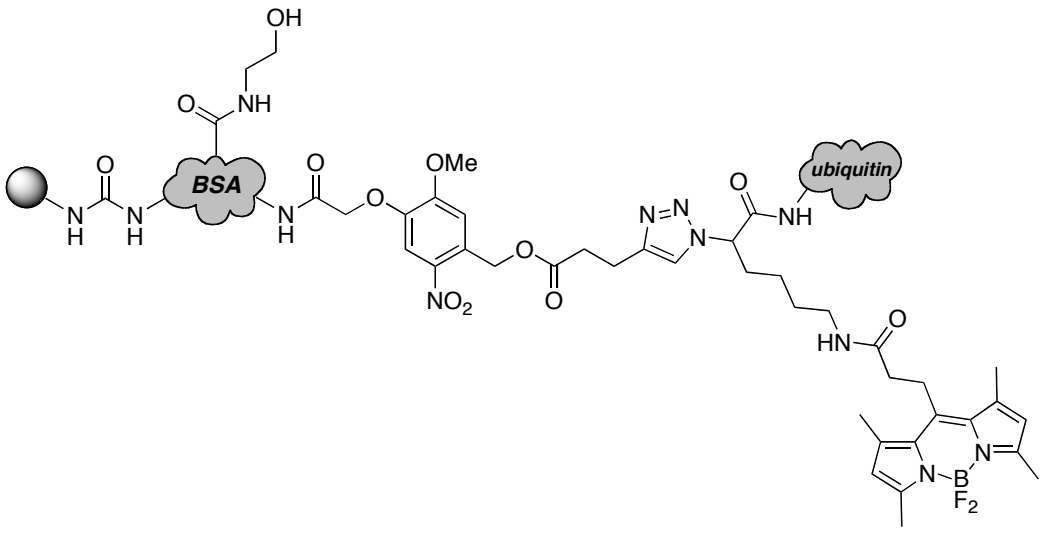

A solution of CPG-supported BODIPY **138** (63 mg, 0.0061 mmol), NHS (7.0 mg, 0.061 mmol) and DIC (7.7 mg, 0.061 mmol) in DMF (1 mL) was shaken in reaction vessel at 25 ºC in dark for 16 h. The beads were washed with DMF (5 x 2 mL) and ether (3 x 2 mL) and dried under the vacuum to afford light orange beads (succinimidyl ester of **138**). A solution of these beads (56 mg, 0.0054 mmol) and ubiquitin (9.3 mg, 1.1 mmol) in pH 8.3 sodium bicarbonate buffer (0.7 mL) was shaken in reaction vessel at 25 ºC in dark for 4.5 h. CPG was washed with pH 8.3 buffer (7 x 2 mL), H_2O (7 x 2 mL), EtOH (5 x 2 mL) and ether (3 x 2 mL), and dried under the vacuum to afford CPG-supported dye-protein conjugate (**139**) as light orange beads. These beads were used for next photocleavage reaction.

CPG-supported photolinker (147)

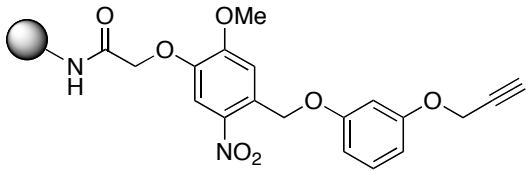

A solution of photolinker **146** (11 mg, 0.029 mmol), DIC (3.7 mg, 0.029 mmol), DMAP (0.2 mg, 0.002 mmol) and LCAA CPG (100 mg, 0.0097 mmol, pore size: 1000 Å, loading: 0.097 mmol/g) in DMF (2 mL) was shaken in reaction vessel at 25 ºC in dark for 24 h. CPG was washed with DMF (5 x 2 mL), MeOH (3 x 2 mL), CH_2Cl_2 (3 x 2 mL) and ether (3 x 2 mL), then dried under the vacuum to afford colorless beads. Ninhydrin test gave positive results (purple beads). Therefore, the beads were capped with Ac_2O (2.0 mg, 0.019 mmol) and pyridine (1.5 mg, 0.019 mmol) in CH_2Cl_2 (1.5 mL) for 2 h. The beads were washed with CH_2Cl_2 (5 x 2 mL) and ether (5 x 2 mL), and dried under the vacuum to afford colorless beads (compound **147**). Ninhydrin test gave negative results (brown beads).

CPG-supported BODIPY derivative (148)

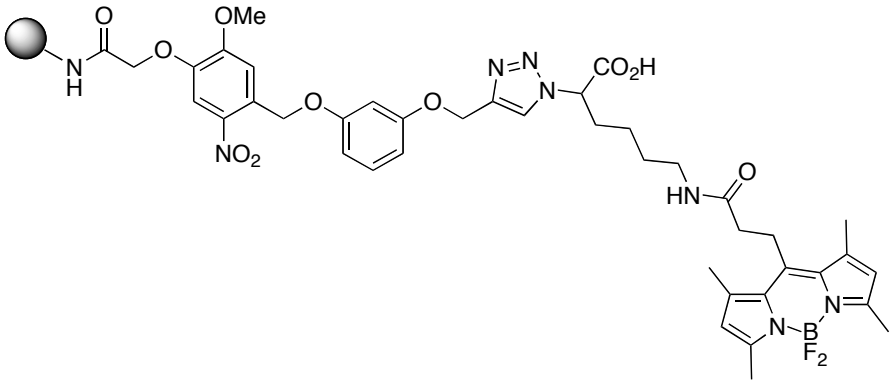

A solution of CPG-support photolinker **147** (50 mg, 0.0049 mmol, loading: 0.097 mmol/g), BODIPY derivative **137** (6.9 mg, 0.015 mmol), $CuSO_4$ (2.4 μL, 2.4 μmol, 1 M in H_2O) and sodium ascorbate (12 μL, 24 μmol, 2 M in H_2O) in 5:1 THF/H_2O (total volume 2 mL) was shaken in reaction vessel at 25 ºC in dark for 24 h. Excess chemicals were washed off with H_2O (10 x 2 mL), DMF (10 x 2 mL), THF (5 x 2 mL), MeOH (5 x 2 mL), CH_2Cl_2 (3 x 2 mL) and ether (3 x 2 mL), then beads were dried under the vacuum to afford orange beads (compound **148**).

CPG-supported BODIPY derivative (149)

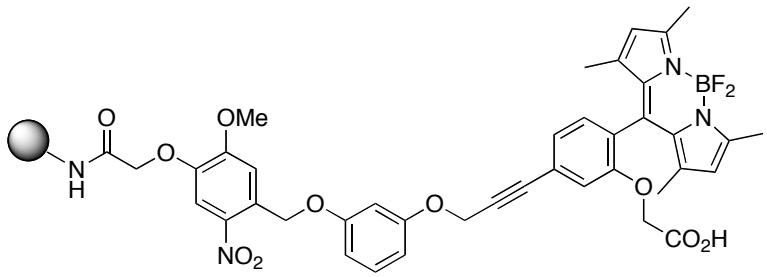

A solution of CPG-support photolinker **147** (40 mg, 3.9 μmol), 4-iodo BODIPY **41** (6.1 mg, 12 μmol), $PdCl_2(PPh_3)_2$ (0.8 mg, 1.2 μmol), CuI (0.2 mg, 1.2 μmol) and Et_3N (5.4 μL, 39 μmol) in THF (1 mL) was shaken in reaction vessel at 25 ºC for 24 h. CPG was washed with THF (10 x 2 mL), CH_3CN (10 x 2 mL), CH_2Cl_2 (5 x 2 mL) and ether (5 x 2 mL), then dried under the vacuum to afford light brown beads (compound **149**).

CPG-support succinimide (150)

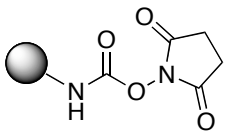

A solution of LCAA CPG (300 mg, 0.050 mmol, pore size: 500 Å, loading: 0.165 mmol/g), *N,N'*-disuccinimidyl carbonate (63 mg, 0.248 mmol) and DIPEA (32 mg, 0.248 mmol) in DMF (5.0 mL) was shaken in reaction vessel at 25 ºC in dark for 5 h. CPG was washed with DMF (5 x 2 mL), EtOH (3 x 2 mL) and pH 7.4 phosphate buffer (3 x 2 mL) to afford colorless beads (compound **150**). These beads were directly used for next reaction.

BSA-coated CPG (151)

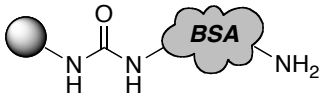

A solution of CPG-support succinimide **150** (300 mg, 0.050 mmol, loading: 0.165 mmol/g) and BSA (103 mg, 1.5 mmol) in pH 7.4 phosphate buffer (6.0 mL) was shaken in reaction vessel at 25 ºC in dark for 16 h. CPG was washed with pH 7.4 phosphate buffer (5 x 2 mL), H_2O (5 x 2 mL), EtOH (5 x 2 mL) and ether (5 x 2 mL) then dried under vacuum to afford BSA-coated CPG (**151**) as colorless beads. Ninhydrin test gave positive result (purple bead).

BSA-CPG with diazobenzene linker (153)

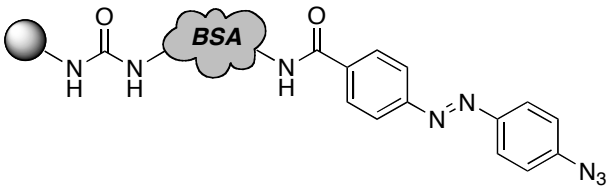

A solution of diazobenzene linker **152** (13 mg, 0.050 mmol, *provided by Mr. Jiney Jose*), DIC (6.2 mg, 0.050 mmol), DMAP (0.4 mg, 0.003 mmol) and BSA-coated CPG **151** (100 mg, 0.0165 mmol, pore size: 500 Å, loading: 0.165 mmol/g) in DMF (2 mL) was shaken in reaction vessel at 25 ºC in dark for 24 h. CPG was washed with DMF (5 x 2 mL), EtOH (5 x 2 mL) and ether (5 x 2 mL), then dried under the vacuum to afford orange beads (compound **153**). Ninhydrin test gave negative result (brown bead).

BSA-CPG with diazobenzene linker (154)

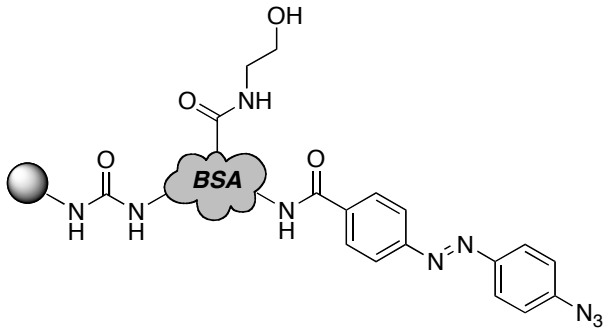

Capping of carboxylic acid for aspartate and glutamate

A solution of BSA-coated CPG **153** (50 mg, 0.008 mmol, loading: 0.165 mmol/g), NHS (9.5 mg, 0.083 mmol) and DIC (10 mg, 0.083 mmol) in DMF (2.0 mL) was shaken in reaction vessel at 25 ºC in dark for 5 h. CPG was washed with DMF (5 x 2 mL). The beads were shaken with ethanolamine (2.5 mg, 0.041 mmol) and DIPEA (11 mg, 0.083

mmol) in DMF (2.0 mL) at 25 ºC in dark for 5 h. CPG was washed with DMF (5 x 2 mL), EtOH (3 x 2 mL) and ether (3 x 2 mL) and dried under the vacuum to afford light orange beads (compound **154**).

BSA-CPG with BODIPY derivative (155)

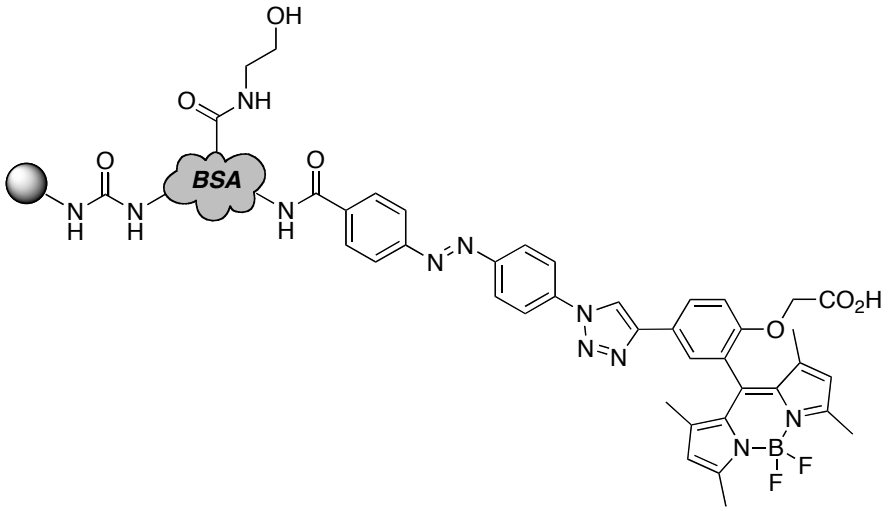

A solution of BSA-CPG diazobenzene linker **154** (30 mg, 0.0050 mmol, loading: 0.165 mmol/g), BODIPY derivative **46** (2.1 mg, 0.0050 mmol), $CuSO_4$ (2.5 μL, 2.5 μmol, 1 M in H_2O) and sodium ascorbate (13 μL, 25 mmol, 2 M in H_2O) in 5:1 THF/H_2O (total volume 2 mL) was shaken in reaction vessel at 25 ºC in dark for 24 h. Excess chemicals were washed off with H_2O (10 x 2 mL), DMF (10 x 2 mL), THF (5 x 2 mL), EtOH (5 x 2 mL) and ether (5 x 2 mL), then the beads were dried under the vacuum to afford dark brown beads (compound **155**).

CPG-support diazobenzene linker (156)

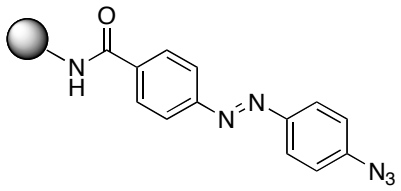

A solution of diazobenzene linker **152** (13 mg, 0.050 mmol), DIC (6.2 mg, 0.050 mmol), DMAP (0.4 mg, 0.003 mmol) and LCAA CPG (100 mg, 0.0165 mmol, pore size: 500 Å, loading: 0.165 mmol/g) in DMF (2 mL) was shaken in reaction vessel at 25 ºC in dark for 24 h. CPG was washed with DMF (5 x 2 mL), EtOH (5 x 2 mL) and ether (5 x 2 mL), then dried under the vacuum to afford orange beads (compound **156**). Ninhydrin test gave negative result (brown bead). IR (solid state): ν (cm^{-1}) 1072, 1655, 2125.

CPG-support BODIPY derivative (157)

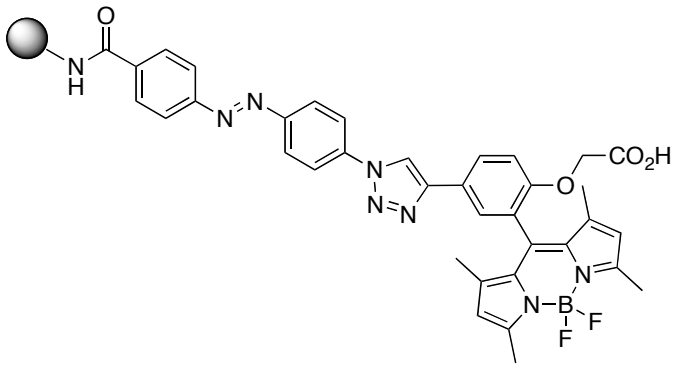

A solution of CPG-diazobenzene **156** (50 mg, 0.008 mmol, loading: 0.165 mmol/g), BODIPY derivative **46** (6.1 mg, 0.015 mmol), $CuSO_4$ (2.0 μL, 2.0 mmol, 1 M in H_2O) and sodium ascorbate (12 μL, 24 μmol, 2 M in H_2O) in 5:1 THF/H_2O (total volume 2 mL) was shaken in reaction vessel at 25 ºC in dark for 24 h. Excess chemicals were

washed off with H_2O (10 x 2 mL), DMF (10 x 2 mL), THF (5 x 2 mL), EtOH (5 x 2 mL) and ether (3 x 2 mL), then beads were dried under the vacuum to afford brown beads (compound **157**). IR (solid state): a peak at 2125 cm^{-1} (N_3 stretch) was not seen.

General Procedure for Photolysis of Compounds (96-CPG), (112), (117), (127), and (139)

Strip UV light designed to emit at 360 nm (Southern New England Ultraviolet Company) was used for all photochemical reactions. Compound (**96-CPG**, **112**, **117**, **127**, or **139**) (10 mg), ethanolamine (10 eq.), solvent (MeOH or CH_3CN; 0.5 mL), and small magnetic spin bar were added into quartz cuvette. Quartz cuvette was set inside of photo reactor; the distance between cuvette and light is 0.5 cm. Then the reaction was irradiated at 360 nm with continuous stirring. In photolysis of solid-phase, beads were filtered off after the reaction and then the obtained solution was analyzed by CE, MALDI, and LCMS.

APPENDIX E

FLUORESCENT DYE TERMINATORS FOR DNA SEQUENCING

6.1 DNA Sequencing

The most important property of DNA molecules is their nucleoside sequence. Until the late 1970s, determining the sequence of a nucleic acid containing even five or ten nucleotides was difficult and very laborious. In 1977, two new techniques of DNA sequencing were developed. One was by Maxam and Gilbert,[154] the other was by Sanger.[155] Their methods made possible the sequencing of even larger DNA molecules with an ease unimagined just a few decades ago. In both Sanger and Maxam-Gilbert sequencing, the general principle is to reduce the DNA to four sets of labeled fragments. The reaction producing each set is base-specific, so that the lengths of the fragments correspond to positions in the DNA sequence where a certain base occurs.

The Sanger method for DNA sequencing is the most widely used technique in high throughput analysis. The basis of this method is the use of four different dideoxynucleoside triphosphates (ddNTP) which are ddATP, ddTTP, ddGTP and ddCTP and the use of four different deoxynucleoside triphosphate (dNTP) which are dATP, dTTP, dGTP and dCTP reducing the DNA to four sets of labeled fragments (Figure 6.1).

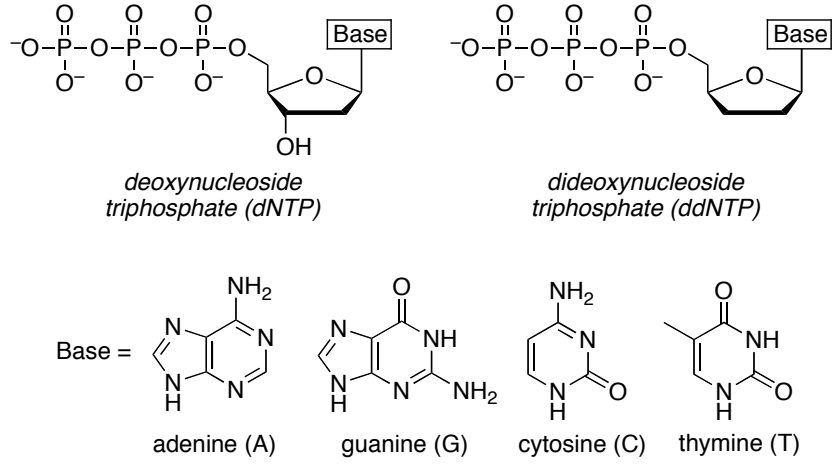

Figure 6.1. Structures of deoxynucleotides and dideoxynucleotides.

DNA polymerases require both a primer (a short oligonucleotide strand), to which nucleotides are added, and a template strand to guide selection of each new nucleotide. In cells, the 3'-hydroxy group of the primer reacts with an incoming deoxynucleoside triphosphate (dNTP) to form a new phosphodiester bond. The Sanger sequencing procedure uses dideoxynucleoside triphosphate (ddNTP) analogs (Figure 6.1) to interrupt DNA synthesis. When a ddNTP is inserted in place of a dNTP, strand elongation is halted after the analog is added because of the lack of 3'-hydroxy group needed for the next step to do DNA synthesis.

The DNA to be sequenced is used as the template strand, and a short primer, radioactively or fluorescently labeled, is annealed to it. After DNA polymerase is performed, each fragments are separated by different-sized using electrophoresis gel and the sequence can be read directly from an autoradiogram of the gel (Figure 6.2). Because shorter DNA fragments migrate faster and the fragments near the bottom of the gel represent the nucleotide positions closest to the primer (the 5' end), the sequence is read from bottom to top.

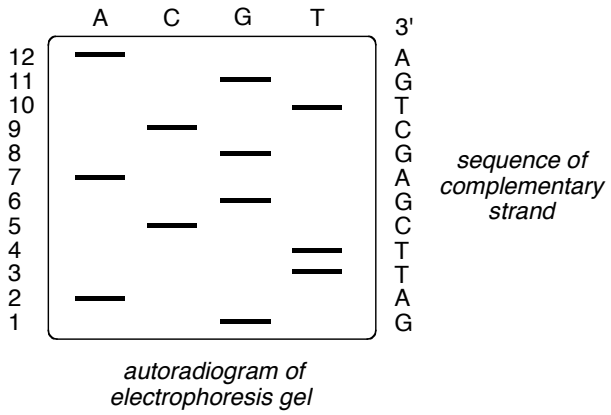

Figure 6.2. Representative autoradiogram of electrophoresis gel.

Each ddNTP used in the Sanger method can be linked to a fluorescent molecule that gives all the fragments terminating in that nucleotide a particular color. Therefore, four dNTPs and four ddNTPs labeled by fluorescent tags are required to do this procedure.

The resulting colored DNA fragments are applied to a capillary gel and subjected to electrophoresis to separate each fragment. All fragments of a given length migrate through the capillary gel in a single peak, and each peak with color is detected using a laser beam. The DNA sequence is read by determining the sequence of colors in the peaks as they pass the detector. Then these information are directly monitored to a computer. Therefore, this automated DNA sequencing method give the unknown DNA sequence much faster.

6.2 Syntheses of ddT and ddC

Four modified dideoxynucleosides (adenosine, guanosine, cytidine and thymidine) are definitely necessary to prepare four nucleoside triphosphates (Figure 6.3). 2', 3'-Dideoxy-8-deazaiodoadenosine **160** has been synthesized by one of our group members, and 2',3'-dideoxy-8-deazaiodoguanosine **161** was a gift from an other group. These compounds are extremely difficult to make. In the following section, the synthesis of 2',3'-dideoxy-5-iodouridine **163** and 2',3'-dideoxy-5-iodocytidine **162** will be described.

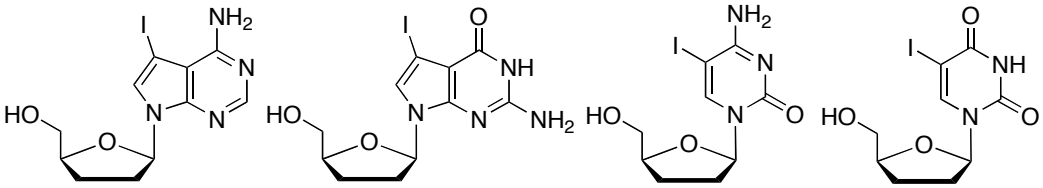

160
7-iodo-adenosine (**A**)
(*from other member*)

161
7-iodo-guanosine (**G**)
(*gift from other group*)

162
5-iodo-cytidine (**C**)

163
5-iodo-thymidine (**T**)

Figure 6.3. Structures of four iodo-dideoxynucleosides.

2',3'-Dideoxy-5-iodouridine **163** was synthesized from commercially available uridine. 5'-Hydroxy-group of uridine was selectively protected with trityl-group to give compound **164**. This **164** was reacted with 1,1'-thiocarbonyldiimidazole (TCDI) followed by the reaction with trimethylphosphite to afford olefin **166** (*Corey-Winter olefination*).[156-158] Trityl-group of olefin **166** was deprotected under the acidic condition to give compound **167**. This olefin was then hydrogenated with palladium catalyst to afford 2',3'-dideoxyuridine **168**. Compound **168** was iodinated with iodine-monochloride[159] to form 2',3'-dideoxy-5-iodouridine **163** and this was obtained in 6 steps and 10 % overall yield (Scheme 6.1).

Scheme 6.1. Synthesis of 2',3'-dideoxy-5-iodouridine **163**.

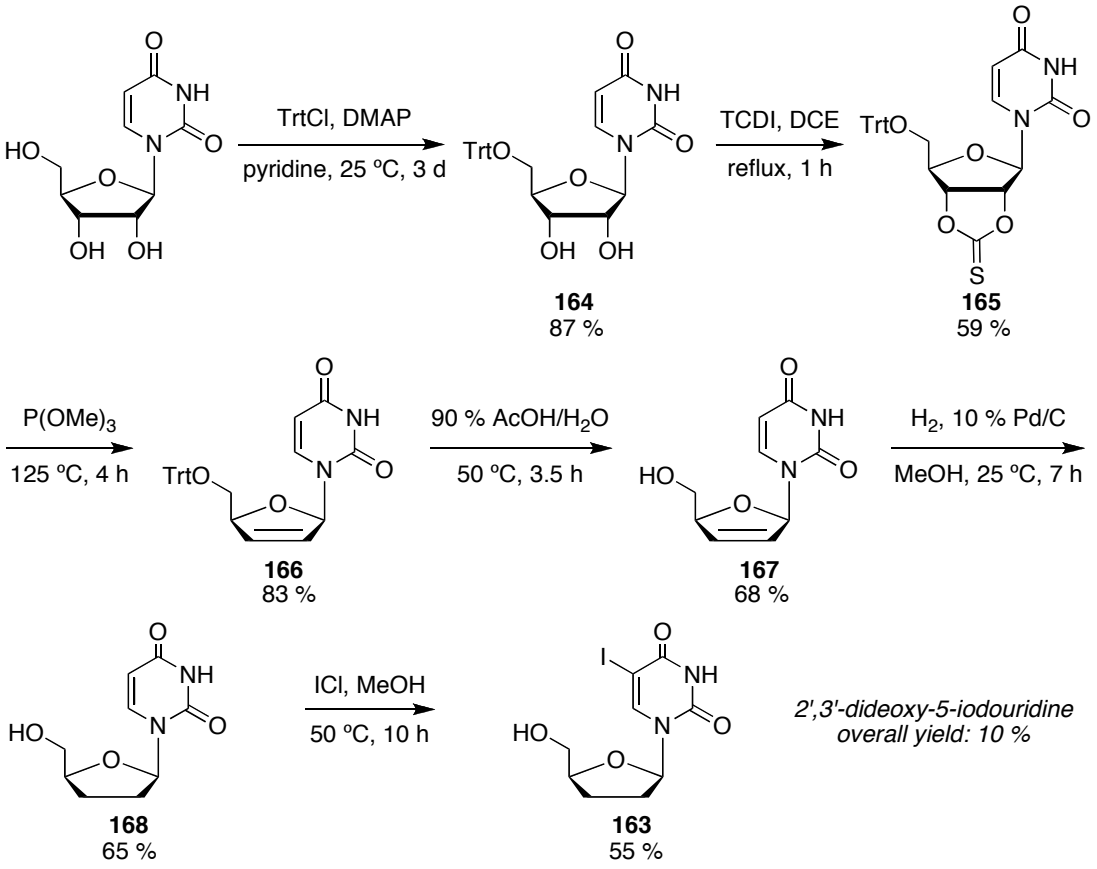

2',3'-Dideoxy-5-iodocytidine **162** was synthesized from commercially available cytidine. The acetylation of cytidine followed by the protection of 5'-hydroxy-group by TBDMS-group afforded compound **170**.[160-162] Dihydroxy-groups of compound **170** was reacted with MsCl to give dimesylates **171**.[60] The reaction of dimesylate **171** with telluride dianion generated by tellurium and Et_3BHLi (Super-Hydride) afforded olefin **172**.[163] The TBDMS-group was then deprotected with TBAF to form alcohol **173**. The hydrogenation of olefin **173** followed by the deprotection of acetyl-group and the iodination afforded the final product, 2',3'-dideoxy-5-iodocytidine **162** and this was obtained in 8 steps and 18 % overall yield (Scheme 6.2).

Scheme 6.2. Synthesis of 2',3'-dideoxy-5-iodocytidine **162**.

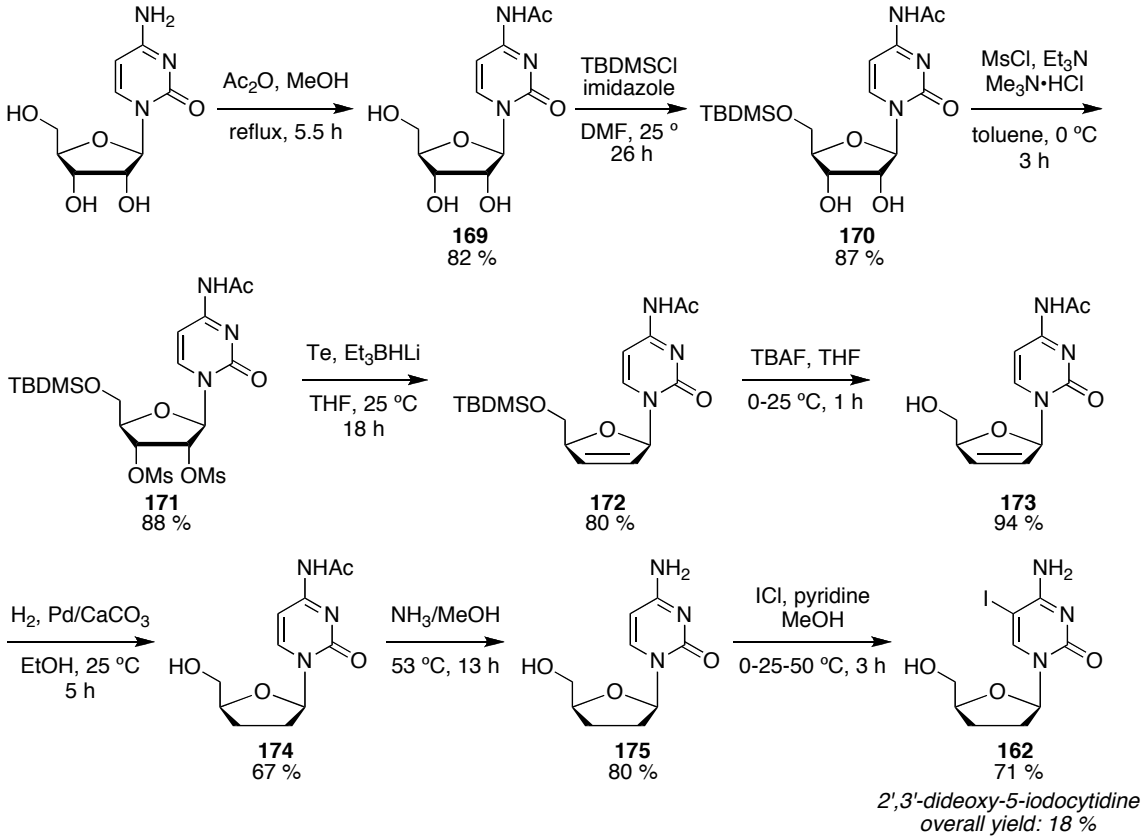

6.3 Syntheses of Nucleoside Triphosphates

Nucleotides have three characteristic components: (i) a nitrogenous base, (ii) a pentose, and (iii) a phosphate. Triphosphate which has three phosphate in its structure, is useful compound to make DNA strand. However, it is difficult to make those compounds and to date, only two methods have been developed to synthesize them: the Kovacs method[164] and the Eckstein method.[165] In previous work from our group, the Eckstein protocol has consistently given better yields and cleaner reaction mixtures than the Kovacs method (Figure 6.4). Therefore, this method was chosen to synthesize the modified nucleoside triphosphates so far.

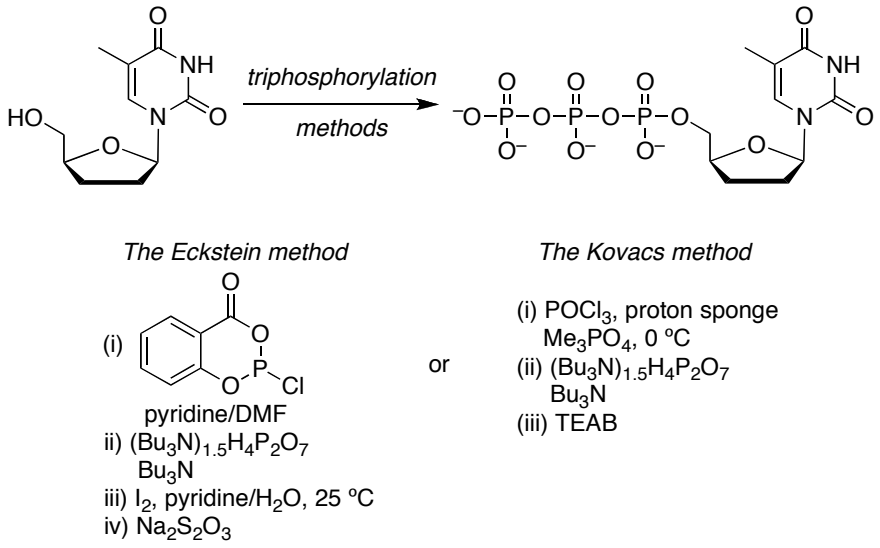

Figure 6.4. Triphosphorylation of dideoxynucleosides via *Eckstein* or *Kovacs* method.

We now have in our hand the four dideoxyiodo nucleosides and can start making the corresponding triphosphates. ddIATP, ddIUTP and ddICTP were first synthesized via the Eckstein method.

Dideoxyiodo nucleosides were treated with 2-chloro-4*H*-1,3,2-benzodioxa-phosphorin-4-one, tributylammonium pyrophosphate and iodine for oxidation (Scheme

5.3).[165] Triphosphorylation of 2',3'-dideoxy-5-iodouridine **163** gave its triphosphate **177** (ddIUTP) in 55 % yield. However, it was difficult to obtain the 2',3'-dideoxy-8-deazaiodoadenosine triphosphate **176** (ddIATP) and 2',3'-dideoxy-5-iodocytidine triphosphate **178** (ddICTP) (trace and 9 % yield, respectively; >90 % purity). This is probably due to the presence of the reactive amine-group in the DNA bases. It is therefore necessary to improve the reaction conditions or purification method for the synthesis of these triphosphates.

For the purification of triphosphates, ion exchange chromatography was used as a common method. After the reaction was performed, the reaction mixture was applied to a DEAE (diethylaminoethyl) Sephadex column and eluted with 0 to 1.0 M lithium chloride or TEAB (triethylammonium bicarbonate).

Scheme 6.3. Triphosphorylation of dideoxyiodo adenosine, cytidine, and uridine.

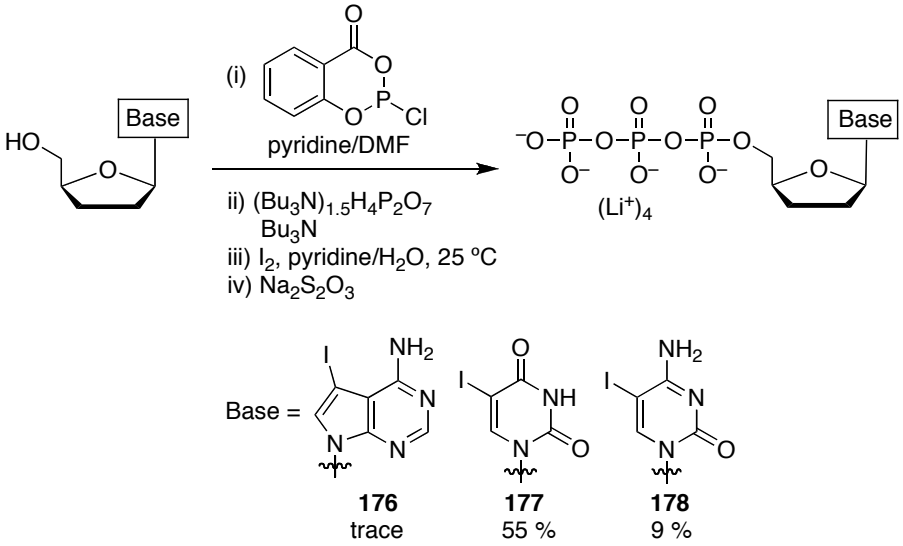

6.4 Synthesis of Control Compound for DNA Sequencing

Before attempting four nucleoside triphosphates with TBET cassette, we synthesized a model compound **183**. Fluorescein derivative was chosen as a probe instead of cassette. 6-Carboxyfluorescein diacetate **179** (*synthesized from 6-carboxyfluorescein*) was activated with NHS and EDCI in DMF followed by the addition of propargy amine and base to afford crude material of alkyne **181**. This crude material containing diacetate **181** was deprotected with K_2CO_3 to give 6-carboxyfluorescein derivative **182** (Scheme 6.4). Compounds **180** and **181** were not isolated due to the difficult chromatographic separation.

Scheme 6.4. Synthesis of fluorescein derivative **182**.

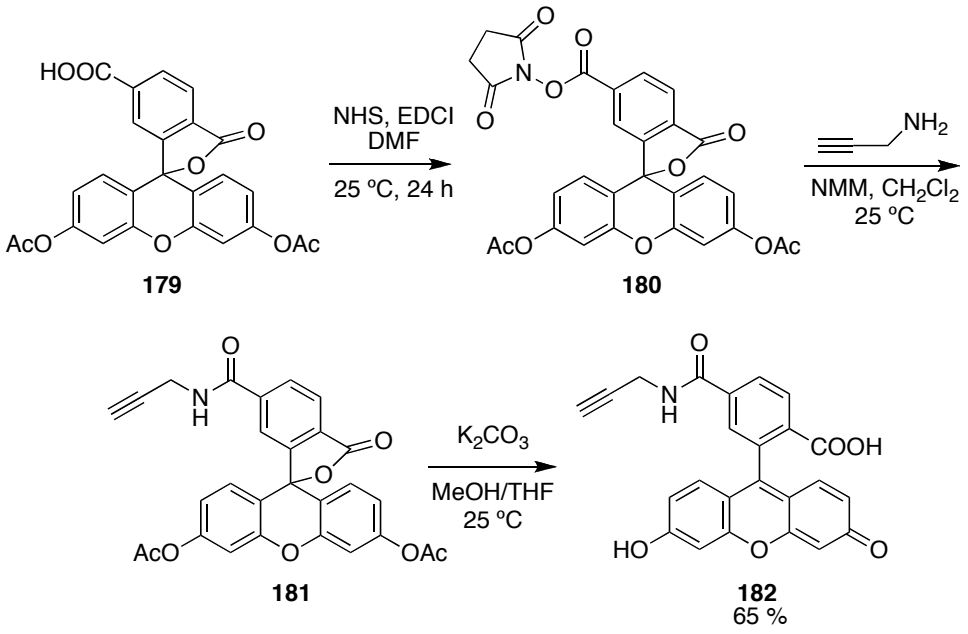

A propargylic 6-carboxyfluorescein **182** and ddIUTP **177** were reacted via Sonogashira coupling in phosphate buffer at 25 ºC. Preparative HPLC purification was used to purify target molecule **183** (reverse phase C18-column, H_2O/CH_3CN) (Scheme 6.5).

Scheme 6.5. Synthesis of model nucleotide compound **183**.

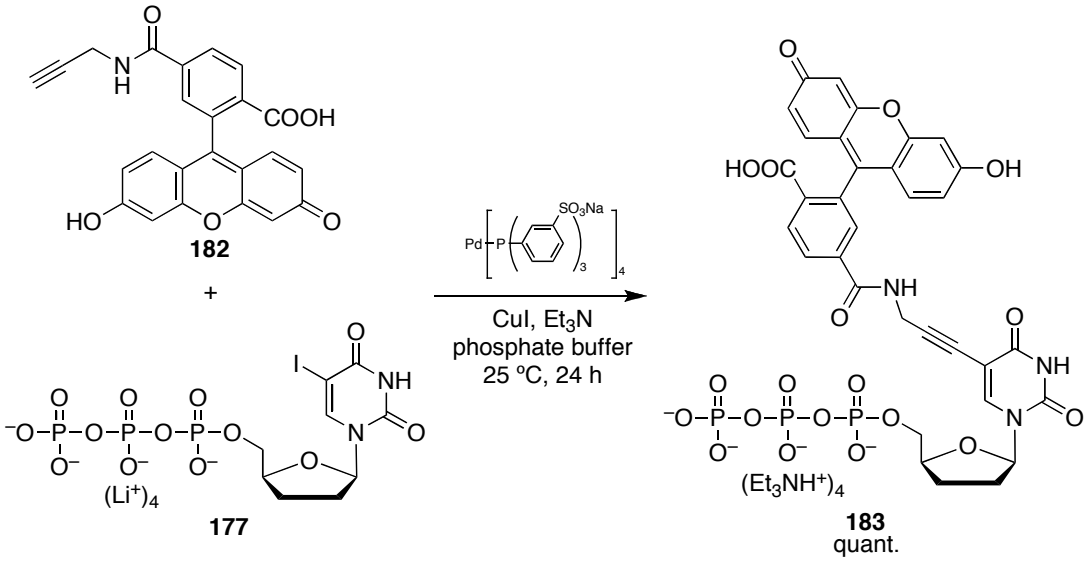

6.5 Synthesis of TBET Cassette for DNA sequencing

Previous work in our group has shown that longer linker gives better effect for the incorporation to DNA.[166] Moreover, if it is water-soluble, it should help the water-solubility of dye-terminators. The azide **25** has been synthesized in our laboratories from commercially available hexaethylene glycol (Scheme 6.6). This **25** was alkylated followed by the protection of alkyne by TBDMS-group to afford **185**. The azido-group of **185** was transferred to primary amine **186** *via* Staudinger ligation.

Scheme 6.6. Synthesis of TBDMS-protected amino-hexaethylene glycol **186**.

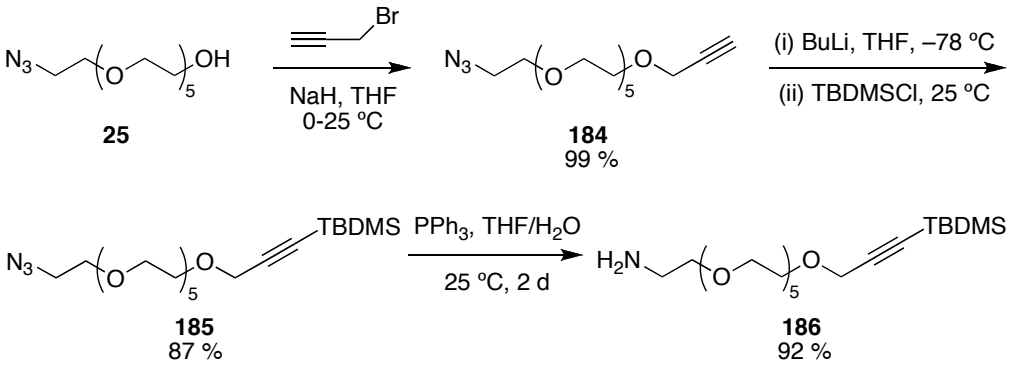

3-Bromo-5-iodobenzoic acid chloride **187** was synthesized from its benzoic acid. This acid chloride **187** was coupled with ethylene glycol linker **186** to afford compound **188** in 93 % yield (Scheme 6.7).

Scheme 6.7. Synthesis of modified ethylene glycol linker **188**.

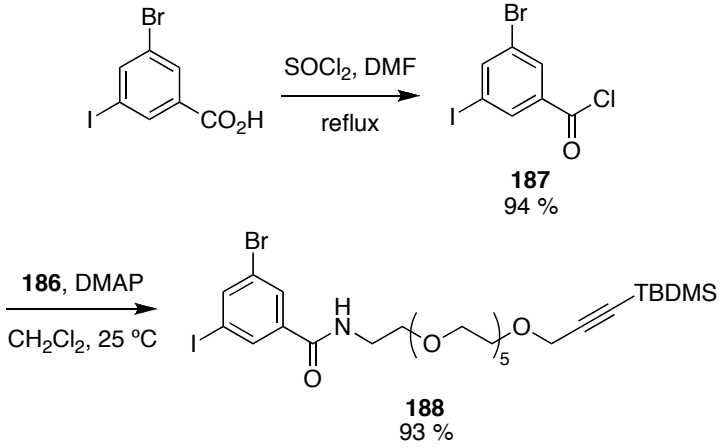

5-Bromofluorescein diacetate **189** was previously synthesized in our group.[38] This 5-isomer **189** was reacted with trimethylsilyl acetylene *via* Sonogashira coupling followed by the deprotection of TMS-group with TBAF to give 5-ethynylfluorescein diacetate **191** in 70 % yield (Scheme 6.8).

Scheme 6.8. Synthesis of 5-ethynylfluorescein diacetate **191**.

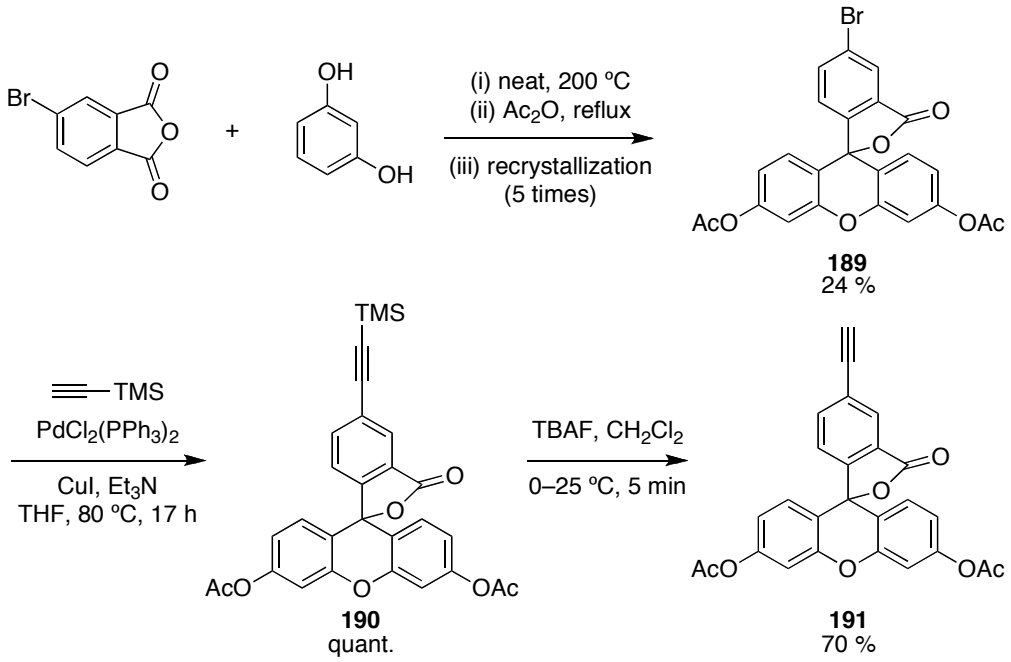

The ethylene glycol linker **188** and 5-ethynylfluorescein diacetate **191** were reacted *via* the palladium-catalyzed cross coupling (Sonogashira) to afford dye **192** in 80 % yield (Scheme 6.9). The first cross-coupling reaction with iodine worked smoothly at 25 ºC and the chromatographic purification was not hard because of clean reaction. However, the second cross-coupling with bromine resulted in a messy reaction under the Sonogashira and Suzuki conditions, even though we tried to use several different palladium catalysts and different reaction conditions (temperature, solvents and equivalents). This is due to the reactivity of bromine and less stability of **192**. The coupling reaction at higher temperature (above 90 ºC) was attempted, but it led to the decomposition of molecule **192**.

Scheme 6.9. Synthesis of precursor **192** for TBET cassette.

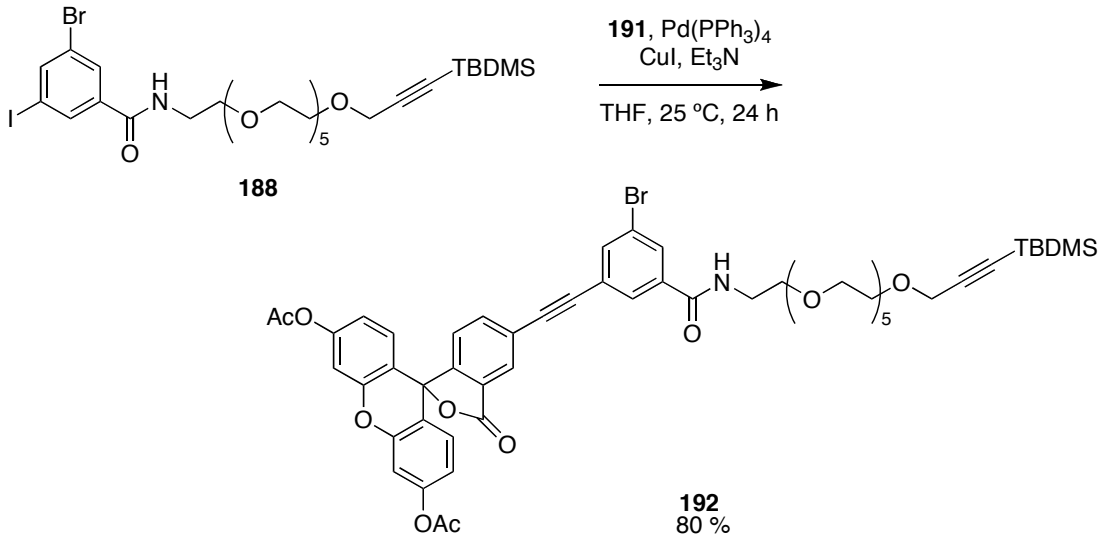

APPENDIX F

RELATED ATTEMPTED REACTIONS

7.1 Synthesis of Water-soluble Rosamine Dye

We also attempted to make rosamine derivative **199** as an acceptor fragment for synthesizing TBET cassette. Dye **199** has iodine on 5-positon to couple with ethynyl-donor component. Compound **199** has two carboxylic acids to increase water-solubility and act as a handle for attachment of biomolecules. First of all, *m*-anisidine was chosen as a starting material and this was reacted with acetone and catalytic amount of iodine to afford cyclized anisidine **193**. Compound **193** was alkylated with bromo methylacetate to give ester **194** in 98 % yield (Scheme 7.1). The deprotection of methyl ester was attempted using BBr_3, however, the reaction was messy and purification was difficult.

Scheme 7.1. Synthesis of cyclized anisidine **194**.

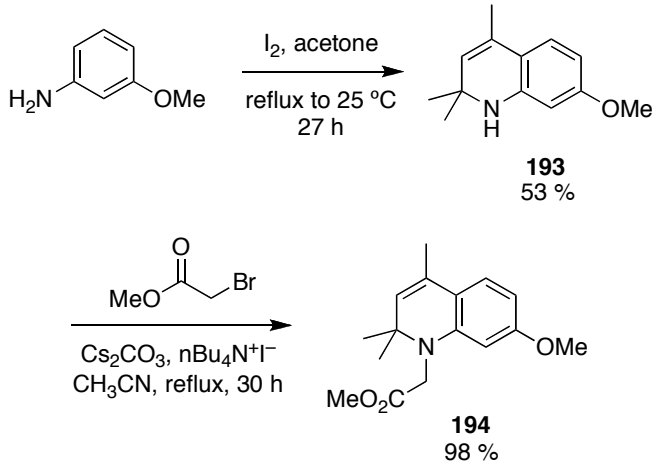

We planed an other synthetic route to make cyclized aminophenol. The synthesis was started from 3-aminophenol and this was first protected with TBDMS-group to afford compound **195**. Protected-aminophenol **195** was cyclized with acetone and cat. iodine followed by the alkylation to give compound **197**. The TBDMS-group was first deprotected with TBAF, however, it resulted in the decomposition of molecule **197**.

Deprotection with Cs_2CO_3 in DMF/H_2O at 25 ºC afforded product **198** and this method was previously reported by Wang *et al*.[167] Finally, the condensation reaction of **198** and iodo-benzaldehyde **35** was carried out with several acids (sulfonic acid, trifluoromethane sulfonic acid, methanesulfonic acid, and TFA), but all cases resulted in messy reaction and it was really difficult to purify (Scheme 7.2). Further investigation of reaction conditions could be possible, however, this kind of cyclized rosamine dye synthesis usually gives low yields and purification is difficult, because many side-products are formed in condensation step.[168,169]

Scheme 7.2. Synthesis of 5-iodo rosamine derivative **199**.

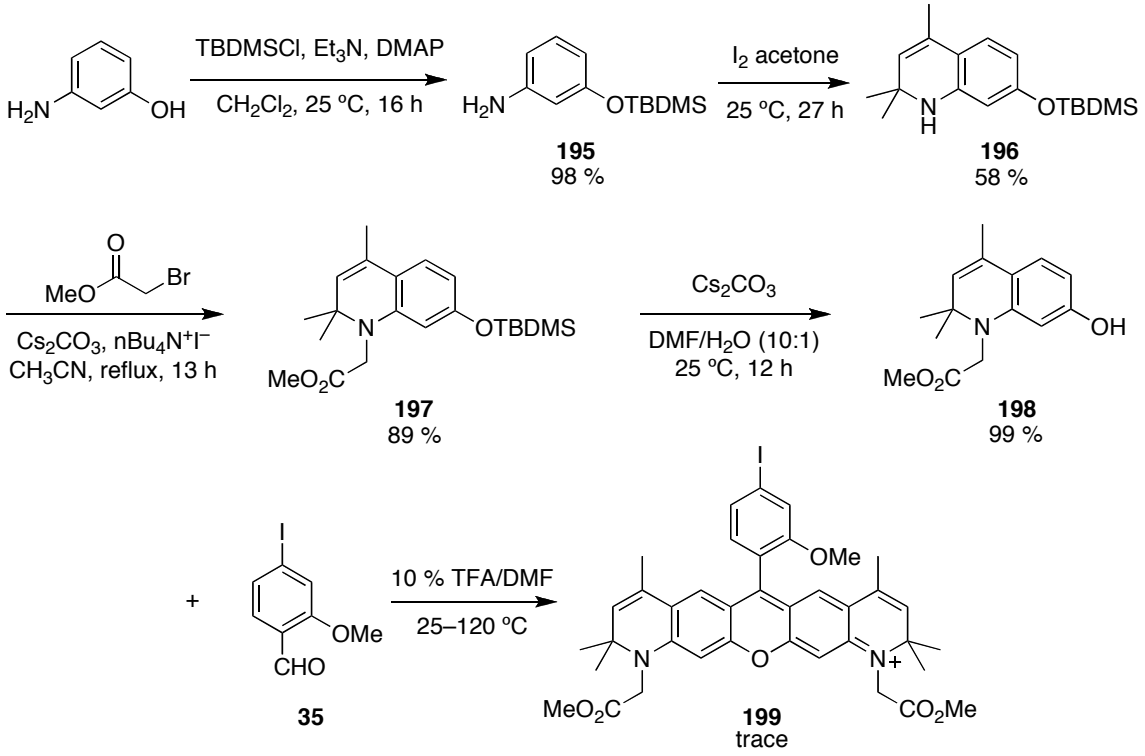

7.2 Synthesis of Water-soluble Nile Blue Derivative

We have expertise in synthesis of functionalized ethylene glycol linkers. We tried to make oligoethylene glycol modified Nile Blue derivative to increase water-solubility of dye and photophysical properties in aqueous media. Hexaethylene glycol was first

mono-protected with PMB-group to give compound **200**.[58] Alkylation of ethylene glycol **200** followed by click reaction with azido ethylene glycol **25** afforded triazole-decorated ethylene glycol **202** in 94 % yield. Primary alcohol of **202** was tosylated to afford ethylene glycol derivative **203** (Scheme 7.3).

Scheme 7.3. Synthesis of triazole-decorated oligoethylene glycol **203**.

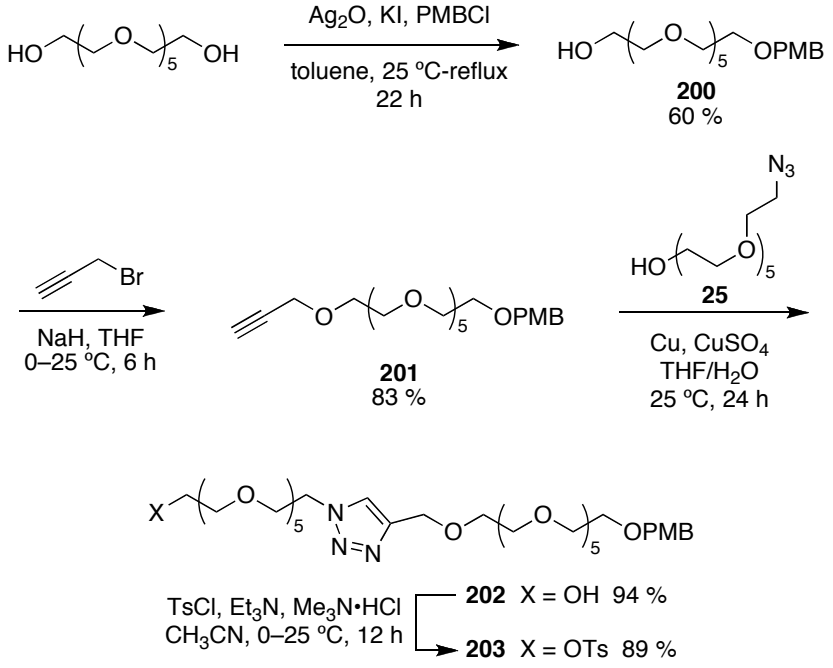

Next, the Eastern part of Nile Blue was synthesized in three steps as shown in Scheme 7.4. 5-Amino-2-naphthol was protected with TBDMS-group followed by the alkylation to give functionalized aminonaphthol **205**. Compound **205** was deprotected with TBAF to afford product **206** in moderate yield.

Scheme 7.4. Synthesis of functionalized aminonaphthol derivative **206**.

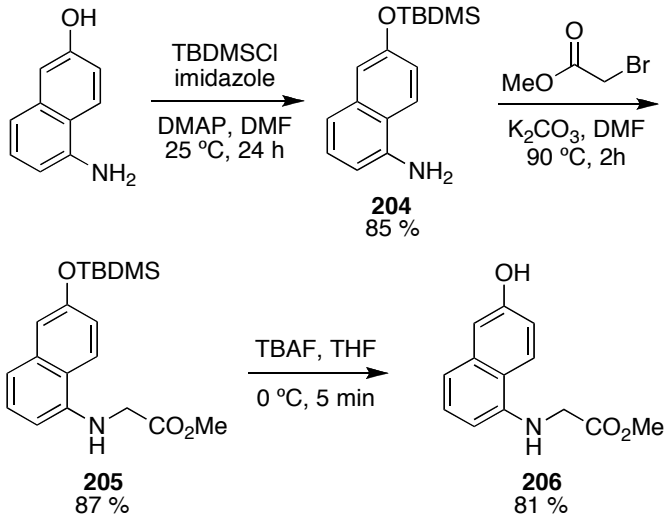

Scheme 7.5 represents the synthesis of water-soluble Nile Blue derivative **209**. At first, aminonaphthol **206** and ethylene glycol **203** will be reacted via simple S_N2 reaction. The condensation reaction of compound **207** and nitroso dialkyl-aminophenol **208** followed by the deprotection of methyl ester will afford final product **209** (Scheme 7.5).

Scheme 7.5. Plan for the synthesis of water-soluble Nile Blue derivative **209**.

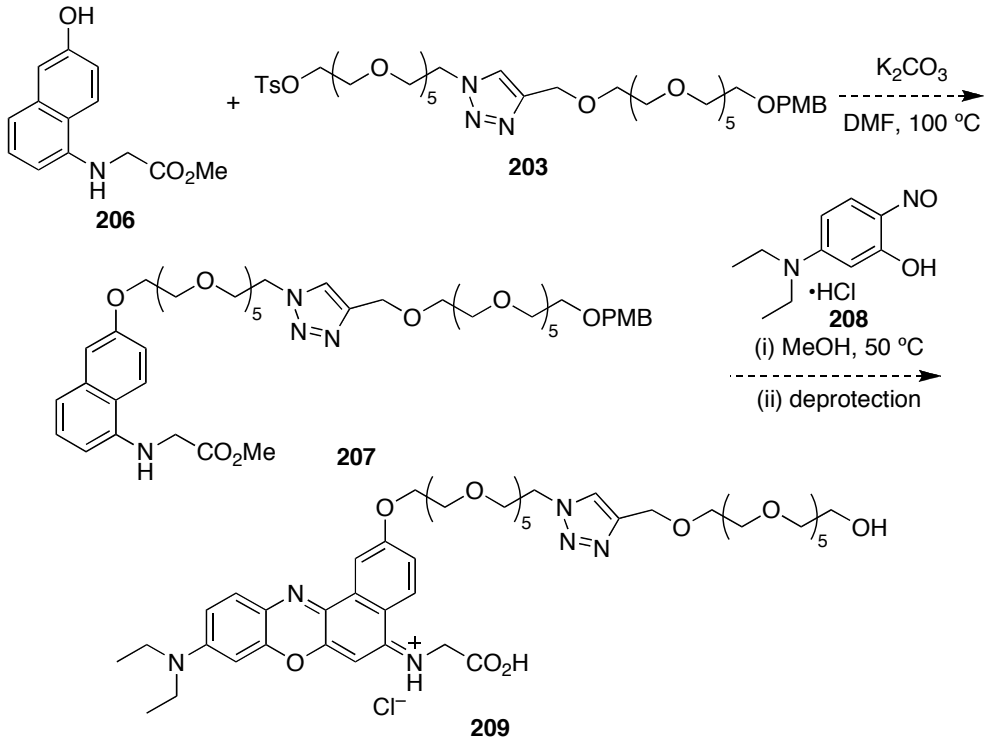

7.3 Photolysis of Triazole-mediated Photolinker

Surprisingly, only one example of photochemical reaction for heterocyclic compounds have been found.[170] *o*-Nitrobenzyl group was introduced into the imidazole side chain of histidine and this compound was photo-cleaved by a irradiation with mercury lamp. We focused on the photolysis of triazole moiety and activated *o*-nitrobenzyl group was used for this study. 5-Methoxy-2-nitrobenzyl alcohol was brominated to give compound **210** and bromine was then transferred to azide to afford compound **211**. Azide **211** was cyclyzed with phenylacetylene via 2+3 cycloaddition to give triazole **212** in 84 % yield. Triazole **212** was irradiated with simple strip UV light or mercury lamp and the reaction was followed by TLC. However, even after long irradiation periods , the reaction was not completed and mass spectrometry did not detect any desired compound (Scheme 7.6).

Scheme 7.6. Synthesis of triazole **212** and its photolysis.

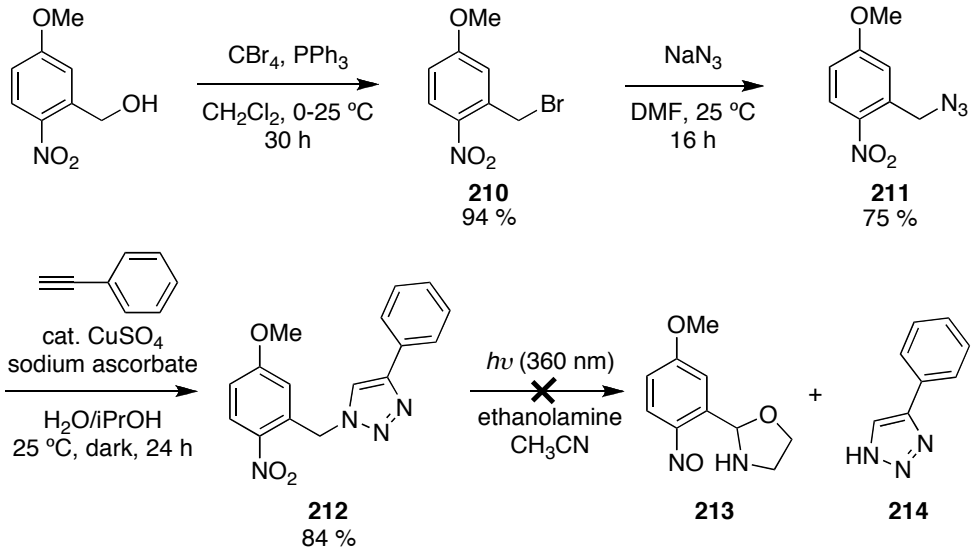

APPENDIX G

EXPERIMENTAL DATA FOR APPENDIX E & F

5'-Tritylated Nucleoside (164)

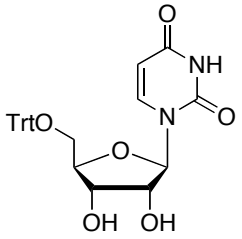

A solution of uridine (15.0 g, 0.061 mol), trityl chloride (51.0 g, 0.183 mol) and DMAP (2.98 g, 0.024 mol) in pyridine (100 mL) was stirred at 25 ºC for 3 d. The solvents were evaporated under the reduced pressure and the residual material was purified by flash chromatography eluting with 100 % CH_2Cl_2, 70 % EtOAc/hexanes and 100 % EtOAc to afford product as a colorless solid (25.9 g, 87 %). R_f 0.4 (100 % EtOAc). ^{1}H NMR (500 MHz, CD_3OD) δ 8.00 (d, 1H, J = 8.5 Hz), 7.45 (d, 6H, J = 8.0 Hz), 7.34-7.25 (m, 9H), 5.91 (d, 1H, J = 3.5 Hz), 5.27 (d, 1H, J = 8.0 Hz), 4.44 (t, 1H, J = 5.5 Hz), 4.28-4.26 (m, 1H), 4.14-4.12 (m, 1H), 3.53-3.45 (m, 2H); ^{13}C NMR (125 MHz, CD_3OD) δ 166.0, 152.1, 144.8, 142.3, 129.9, 129.0, 128.4, 102.4, 91.0, 88.6, 84.2, 76.0, 70.9, 63.7; MS (ESI) m/z 493.20 $(M+Li)^+$.

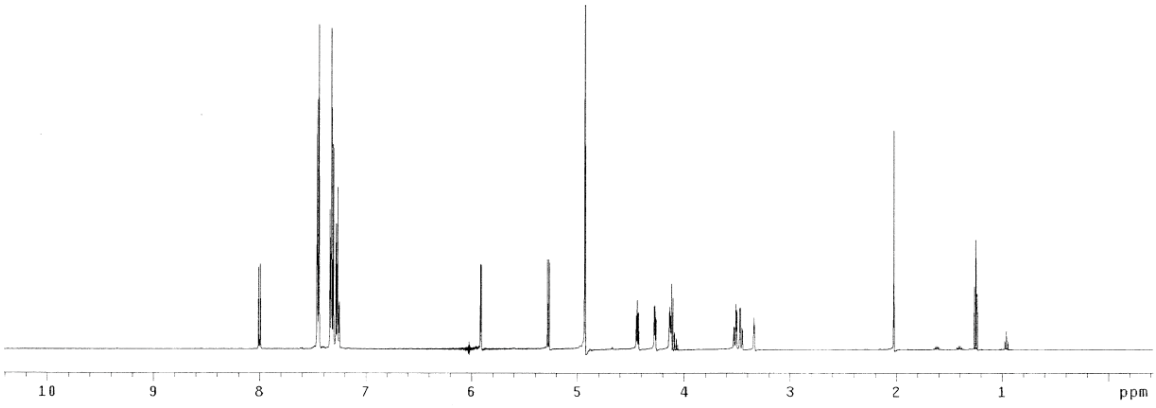

^{1}H NMR (CD_3OD)

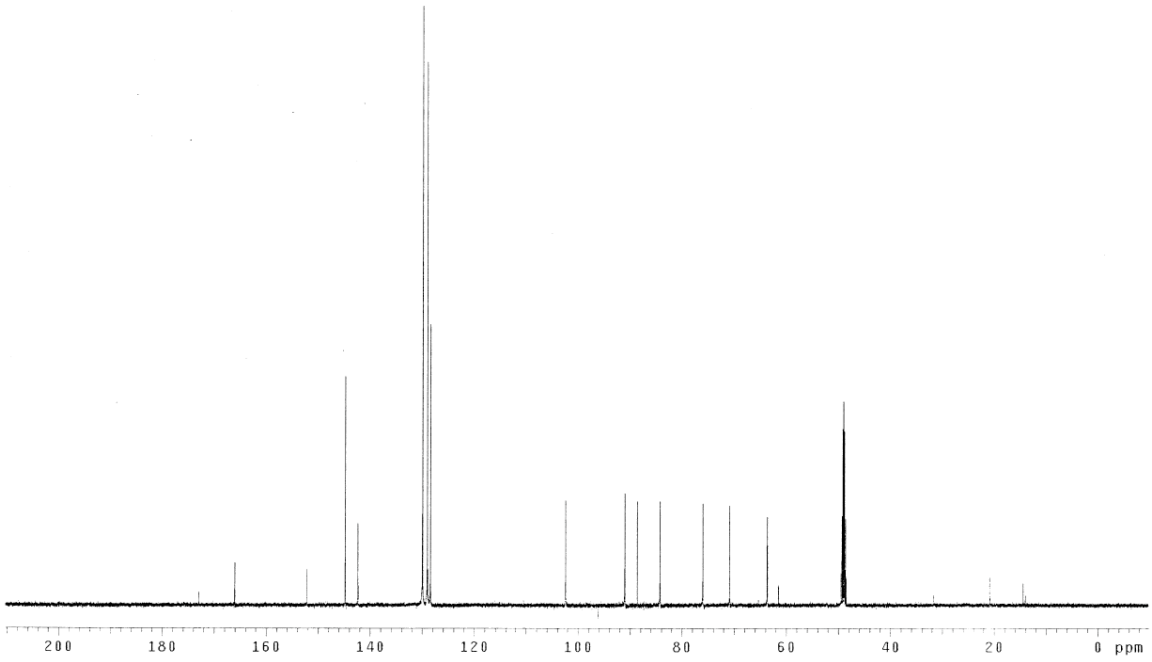

^{13}C NMR (CD_3OD)

Thiocarbonate derivative (165)

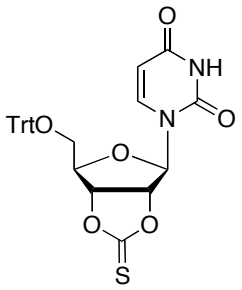

A solution of 5'-tritylated uridine **164** (10.0 g, 0.021 mol) and 1,1'-thiocarbonyldiimidazole (TCDI) (4.05 g, 0.023 mol) in 1,2-dichloroethane (160 mL) was refluxed at 97 ºC for 1 h. The solvents were evaporated under the reduced pressure and the residual material was purified by flash chromatography eluting with 100 % ether and 70 % EtOAc/hexanes to afford product as a colorless solid (6.4 g, 59 %). R_f 0.5 (60 % EtOAc/hexanes). ^{1}H NMR (500 MHz, DMSO-d_6) δ 11.50 (d, 1H, J = 2.0 Hz), 7.81 (d, 1H, J = 8.0 Hz), 7.42-7.28 (m, 15H), 6.10 (s, 1H), 6.03 (dd, 1H, J = 8.0, 1.0 Hz), 5.71 (dd, 1H, J = 10.0, 2.5 Hz), 5.62 (q, 1H, J = 3.5 Hz), 4.48-4.45 (m, 1H), 3.46-3.42 (m, 1H), 3.25 (dd, 1H, J = 10.0, 5.0 Hz); ^{13}C NMR (125 MHz, DMSO-d_6) δ 191.1, 164.2, 151.3, 144.8, 144.4, 129.1, 128.9, 128.1, 102.9, 93.9, 89.8, 87.2, 87.1, 86.8, 64.7; MS (ESI) m/z 535.13 $(M+Li)^+$.

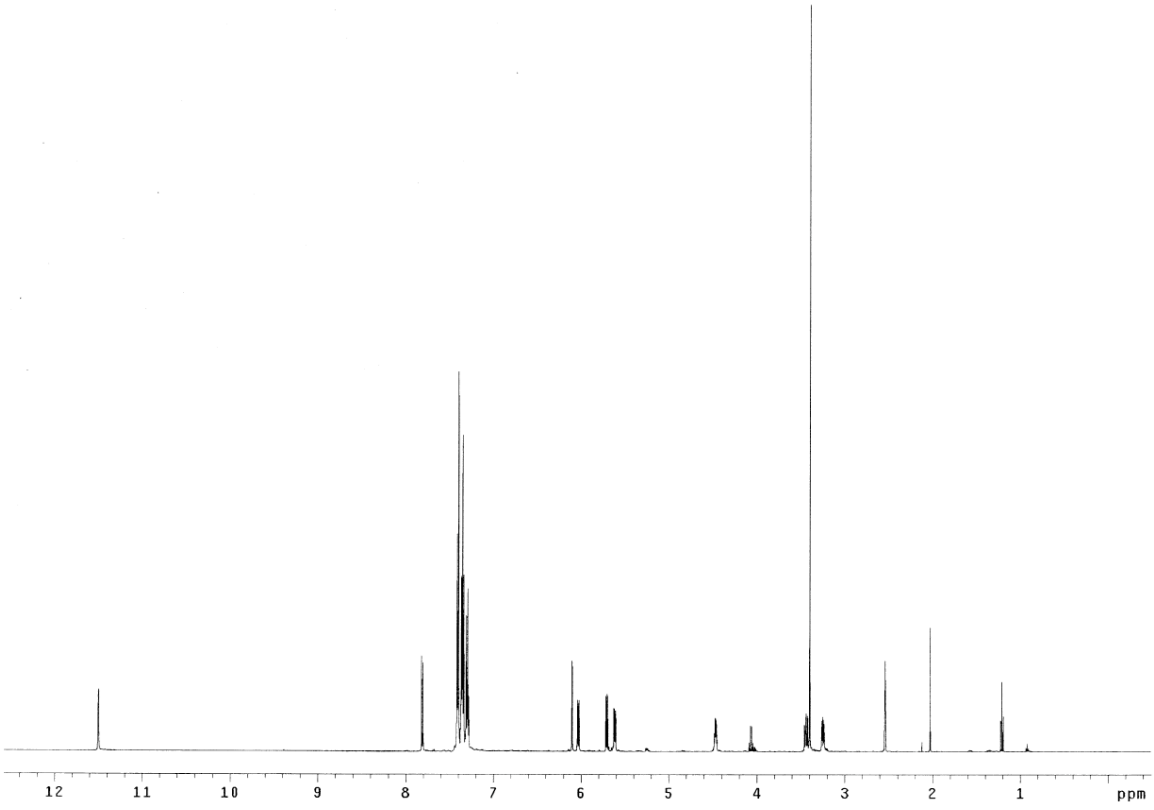

^{1}H NMR (DMSO-d_6)

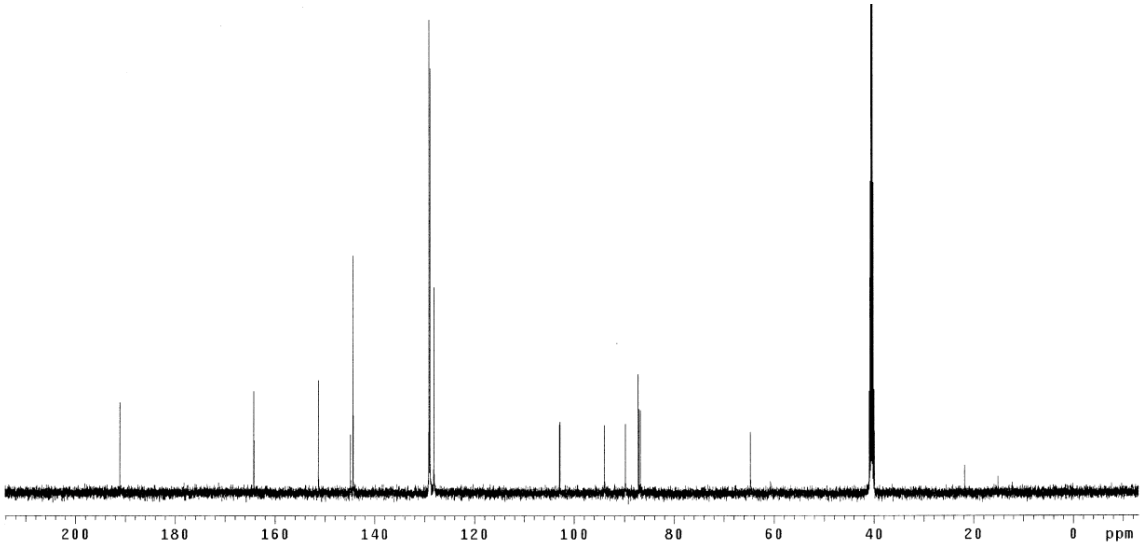

^{13}C NMR (DMSO-d_6)

2', 3'-Dedihydro Nucleoside (166)

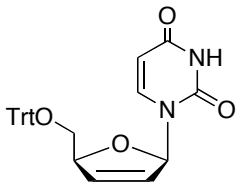

Method A (thermal condition)

A solution of thiocarbonate **165** (5.89 g, 0.011 mol) in trimethylphosphite (40 mL) was refluxed at 125 ºC for 4 h under nitrogen. The solvents were evaporated under the reduced pressure and the residual material was purified by flash chromatography eluting with 70 % EtOAc/hexanes to afford product as a light yellow solid (4.15 g, 83 %).

Method B (microwave)

A solution of thiocarbonate **165** (100 mg, 0.19 mmol) in trimethylphosphite (2.0 mL) was irradiated with microwave reactor at 130 ºC for 20 min (sealed tube). The solvents were evaporated under the reduced pressure and the residual material was purified by flash chromatography eluting with 70 % EtOAc/hexanes to afford product as a light yellow solid (82 mg, 96 %).

R_f 0.6 (70 % EtOAc/hexanes). ^{1}H NMR (500 MHz, DMSO-d_6) δ 11.44 (s, 1H), 7.60 (d, 1H, J = 8.0 Hz), 7.38-7.29 (m, 15H), 6.86-6.85 (m, 1H), 6.58 (d, 1H, J = 6.0 Hz), 6.05 (d, 1H, J = 5.5 Hz), 4.97 (bs, 1H), 4.95 (d, 1H, J = 8.0 Hz), 3.37-3.33 (m, 1H), 3.16 (dd, 1H, J = 10.8, 2.5 Hz); ^{13}C NMR (75 MHz, $CDCl_3$) δ 163.5, 150.7, 143.0, 141.2, 134.3, 128.7, 127.9, 127.3, 126.3, 102.2, 89.6, 87.3, 85.9, 64.4; MS (ESI) m/z 459.19 $(M+Li)^+$.

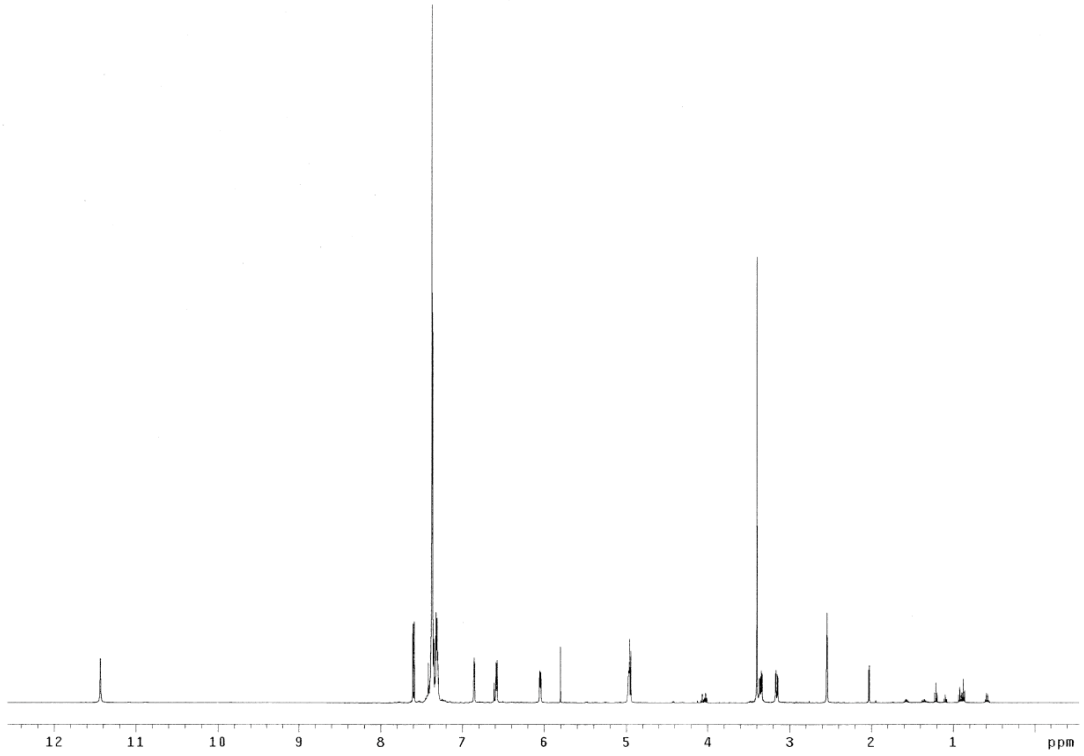

^{1}H NMR (DMSO-d_6)

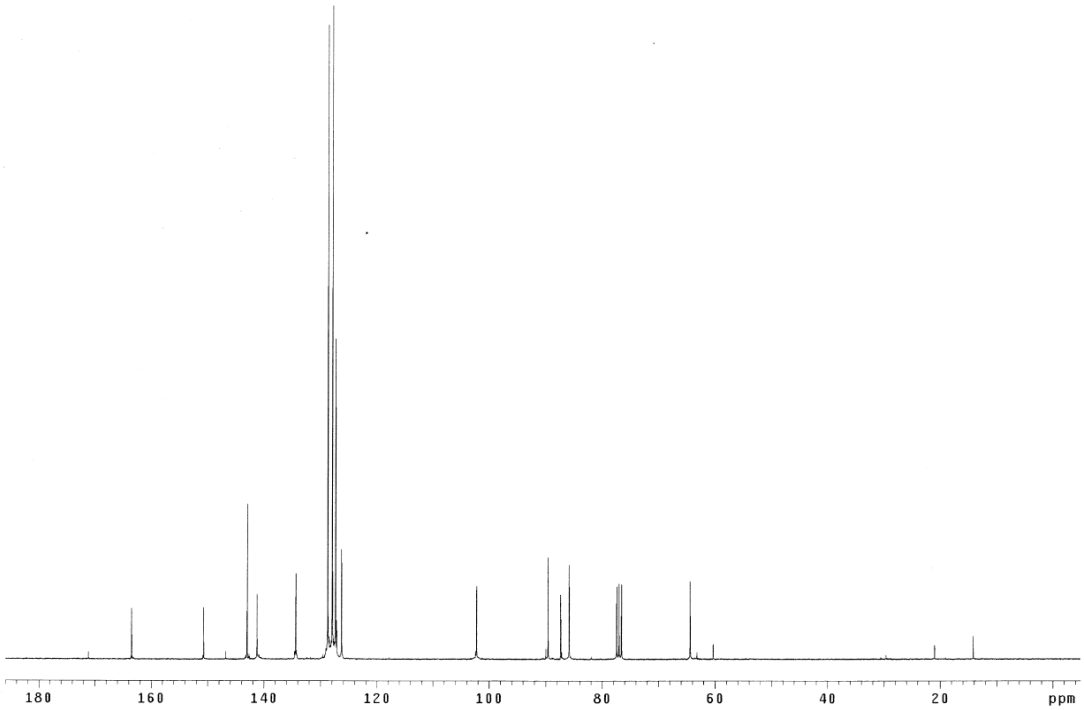

^{13}C NMR ($CDCl_3$)

2', 3'-Dedihydro-5'-hydroxy Nucleoside (167)

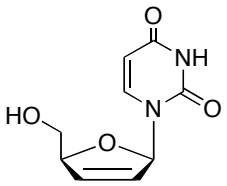

A solution of olefin **166** (4.15 g, 9.17 mmol) in 90 % AcOH in H_2O (AcOH:72 mL, H_2O:8 mL) was heated at 50 ºC for 3.5 h under nitrogen. The solvents were evaporated under the reduced pressure and the residual material was purified by flash chromatography eluting with 5 % to 15 % MeOH/$CHCl_3$ to afford product as a colorless solid (1.31 g, 68 %). R_f 0.2 (10 % MeOH/$CHCl_3$). ^{1}H NMR (500 MHz, DMSO-d_6) δ 11.37 (s, 1H), 7.79 (d, 1H, J = 8.0 Hz), 6.85 (s, 1H), 6.44 (d, 1H, J = 6.0 Hz), 5.96 (d, 1H, J = 5.5 Hz), 5.63 (d, 1H, J = 8.0 Hz), 5.04 (t, 1H, J = 5.0 Hz), 4.82 (bs, 1H), 3.62 (t, 2H, J = 4.5 Hz); ^{13}C NMR (125 MHz, DMSO-d_6) δ 164.3, 151.8, 142.1, 136.1, 126.8, 102.6, 90.1, 88.4, 63.2; MS (APCI) m/z 211.0 $(M+H)^+$, 421.0 $(2M+H)^+$.

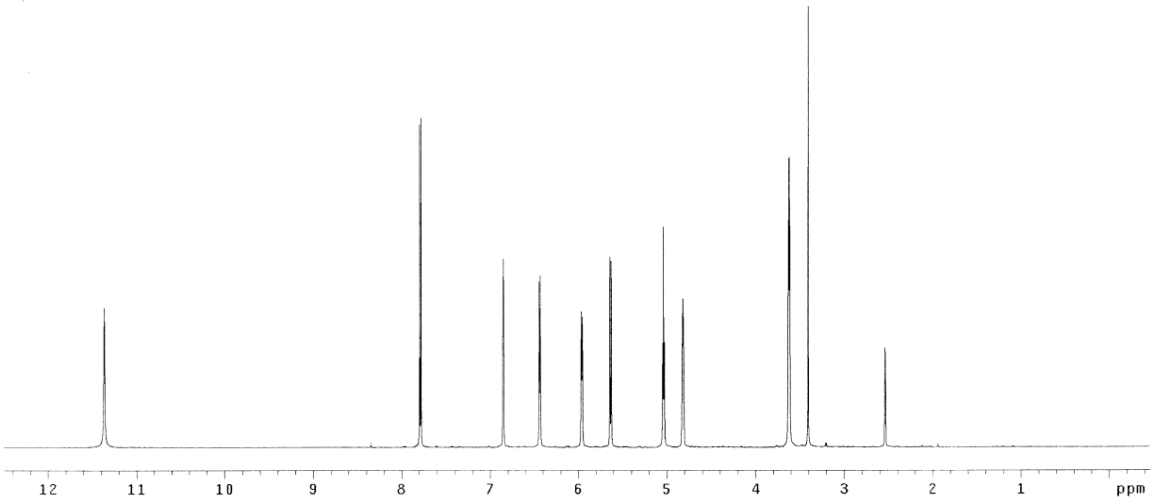

^{1}H NMR (DMSO-d_6)

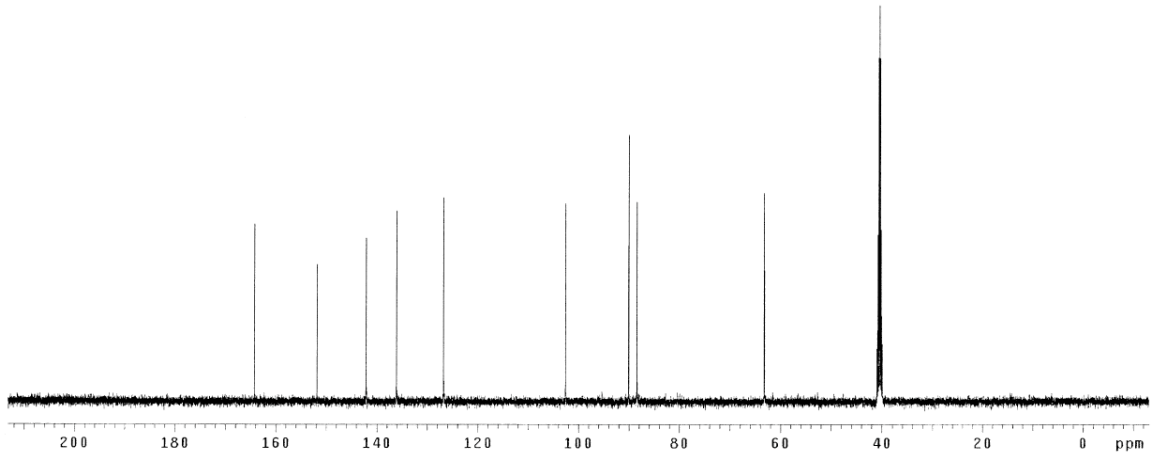

^{13}C NMR (DMSO-d_6)

2', 3'-Dideoxyuridine (168)[159]

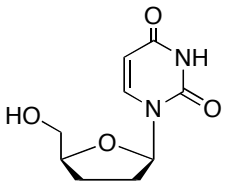

A solution of olefin **167** (200 mg, 0.95 mmol) and 10 % Pd/C (101 mg, 0.95 mmol) in MeOH (8.0 mL) with hydrogen balloon was stirred at 25 ºC for 7 h. The reaction mixture was filtered with silica-pad and washed with MeOH. The solvents were evaporated under the reduced pressure and the residual material was purified by flash chromatography eluting with 5 to 10 % MeOH/$CHCl_3$ to afford product as a colorless solid (132 mg, 65 %). R_f 0.2 (10 % MeOH/$CHCl_3$). ^{1}H NMR (300 MHz, DMSO-d_6) δ 11.30 (bs, 1H), 7.98 (d, 1H, J = 8.0 Hz), 5.98 (q, 1H, J = 3.0 Hz), 5.62 (d, 1H, J = 8.0 Hz), 5.07 (t, 1H, J = 5.4 Hz), 4.09-4.02 (m, 1H), 3.74-3.67 (m, 1H), 3.59-3.53 (m, 1H), 2.37-2.25 (m, 1H), 2.04-1.82 (m, 3H); ^{13}C NMR (75 MHz, DMSO-d_6) δ 164.0, 151.1, 141.3, 101.7, 85.8, 82.3, 62.7, 32.5, 25.5.

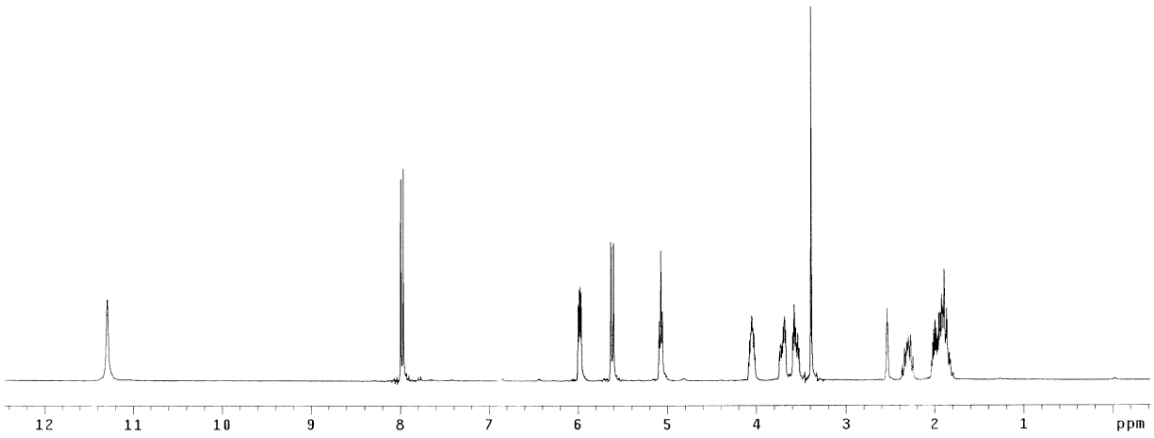

^{1}H NMR (DMSO-d_6)

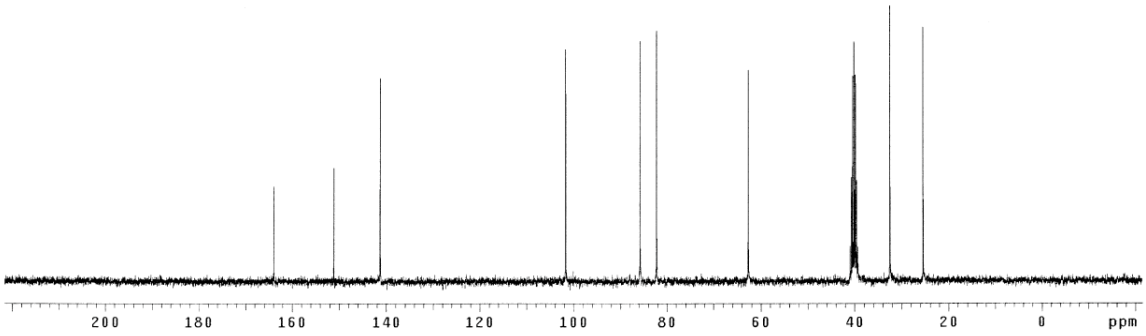

^{13}C NMR (DMSO-d_6)

2', 3'-Dideoxy-5-iodouridine (163)[159]

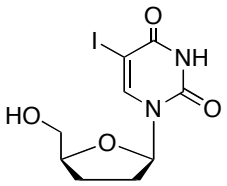

2',3'-Dideoxyuridine **168** (103 mg, 0.49 mmol) was dissolved in MeOH (5.0 mL) and iodine monochloride (0.68 mL, 0.68 mmol, 1 M in CH_2Cl_2) was added to a solution dropwise. The reaction mixture was heated at 50 ºC for 10 h. After cooling to room temperature, sat. $Na_2S_2O_3$ was added to a reaction mixture dropwise until orange color disappeared (12 drops). The white precipitates were filtered off with celite and the solvents were evaporated under the reduced pressure. The residual material was purified by flash chromatography eluting with 10 % MeOH/$CHCl_3$ to afford product as a colorless solid (90 mg, 55 %). R_f 0.2 (10 % MeOH/$CHCl_3$). ^{1}H NMR (500 MHz, DMSO-d_6) δ 11.67 (s, 1H), 8.63 (s, 1H), 5.92 (dd, 1H, J = 6.5, 3.0 Hz), 5.28 (t, 1H, J = 5.0 Hz), 4.10-4.07 (m, 1H), 3.81-3.77 (m, 1H), 3.58-3.54 (m, 1H), 2.33-2.26 (m, 1H), 2.08-2.03 (m, 1H), 1.94-1.85 (m, 2H); ^{13}C NMR (75 MHz, DMSO-d_6) δ 161.6, 151.1, 146.2, 86.8, 83.1, 69.1, 62.1, 33.5, 24.8.

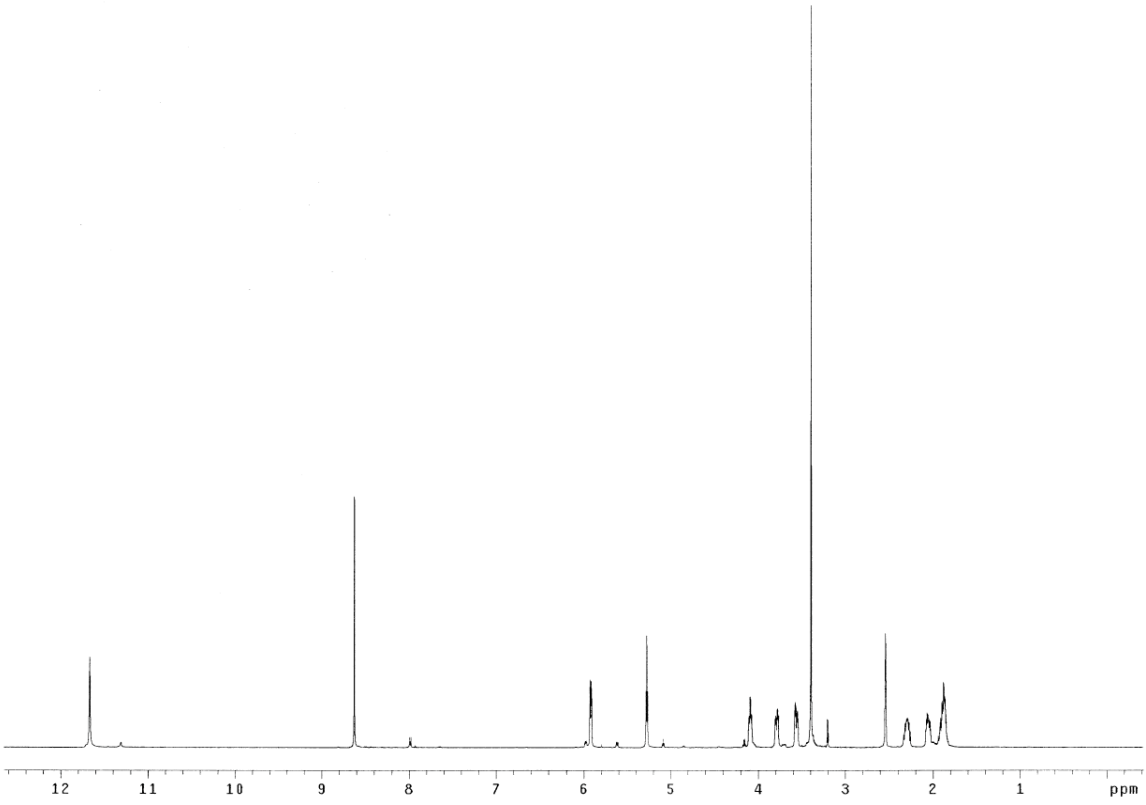

^{1}H NMR (DMSO-d_6)

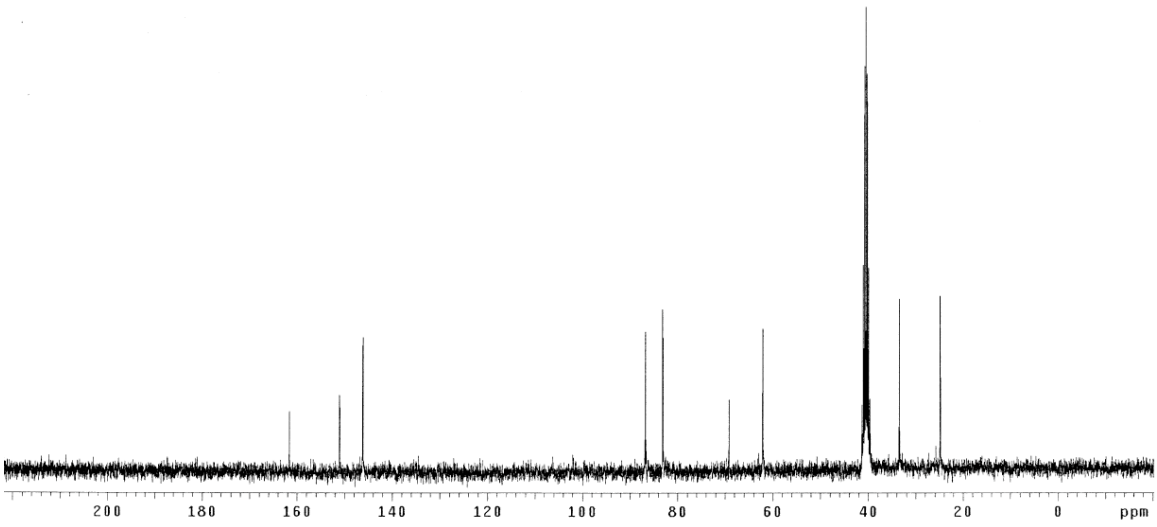

^{13}C NMR (DMSO-d_6)

_N_-Acetyl cytidine (169)[160]

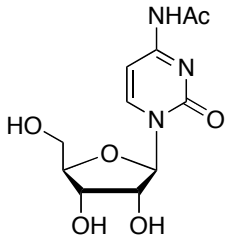

Cytidine (40 g, 0.16 mol) was suspended in MeOH (800 mL) and the solution was refluxed at 90 ºC for 1.5 h under nitrogen. Ac_2O (160 mL, 1.69 mol) was added to a solution with addition funnel over a period of 1 h. The reaction mixture was refluxed for additional 3 h. After cooling to room temperature, precipitates were filtered to afford product as a colorless solid (38.4 g, 82 %). R_f 0.7 (20 % MeOH/CH_2Cl_2). ^{1}H NMR (500 MHz, DMSO-d_6) δ 10.93 (s, 1H), 8.46 (d, 1H, J = 7.5 Hz), 7.22 (d, 1H, J = 7.5 Hz), 5.81 (d, 1H, J = 3.0 Hz), 5.54 (d, 1H, J = 5.0 Hz), 5.21 (t, 1H, J = 5.0 Hz), 5.11 (d, 1H, J = 6.0 Hz), 4.02-3.97 (m, 2H), 3.94-3.92 (m, 1H), 3.79-3.75 (m, 1H), 3.65-3.61 (m, 1H), 2.13 (s, 3H); ^{13}C NMR (125 MHz, DMSO-d_6) δ 172.0, 163.3, 155.6, 146.4, 96.1, 91.1, 85.1, 75.5, 69.6, 60.8, 25.3; MS (ESI) m/z 308.07 $(M+Na)^+$.

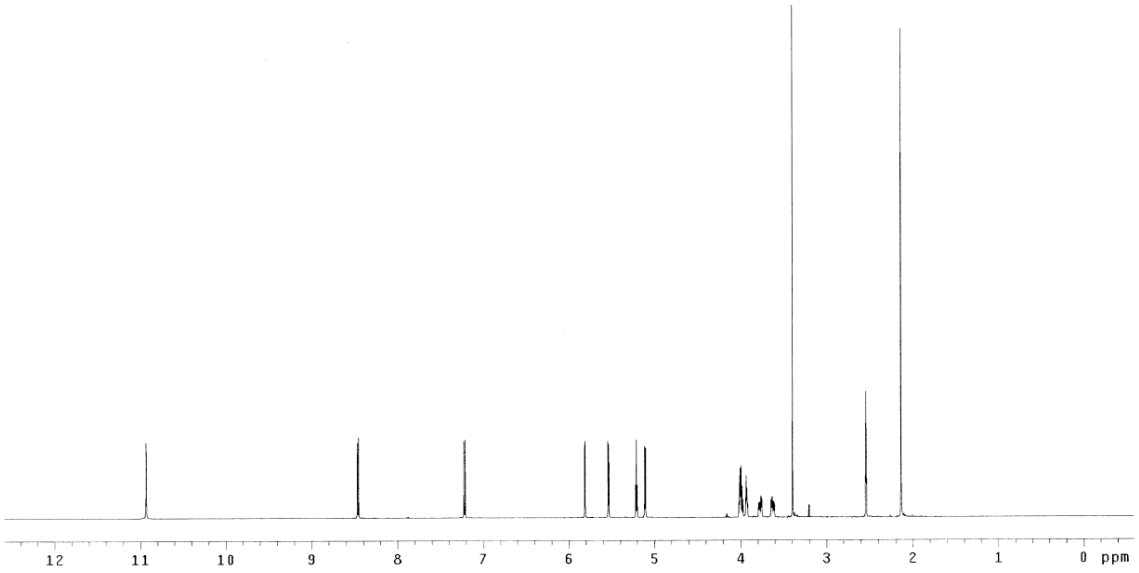

^{1}H NMR (DMSO-d_6)

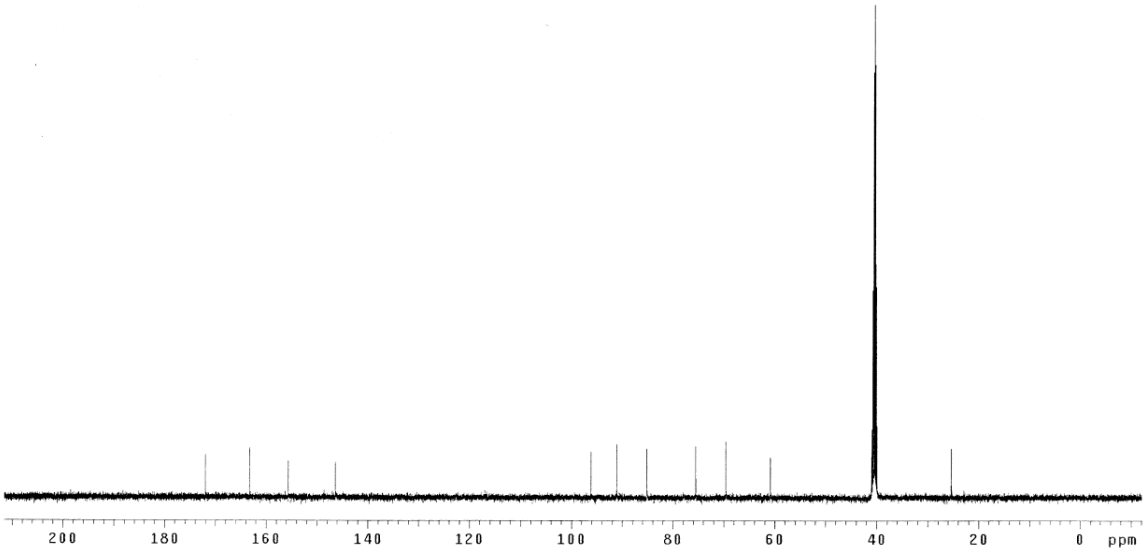

^{13}C NMR (DMSO-d_6)

5'-Silylated cytidine (170)[161]

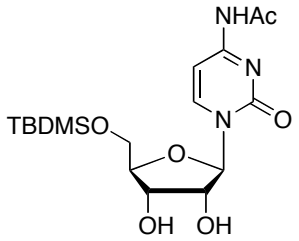

To a solution of *N*-acetyl cytidine **169** (30 g, 0.105 mol) and imidazole (19.3 g, 0.284 mol) in DMF (600 mL) was added TBDMSCl (20.6 g, 0.137 mol) slowly. The reaction mixture was stirred at 25 ºC for 26 h. The solvents were evaporated under reduced pressure and the residual material was purified by flash chromatography eluting with 100 % EtOAc and 5 to 10 % MeOH/$CHCl_3$ to afford product as a colorless solid (36.4 g, 87 %). R_f 0.1 (100 % EtOAc). ^{1}H NMR (500 MHz, DMSO-d_6) δ 10.95 (s, 1H), 8.37 (d, 1H, J = 7.5 Hz), 7.23 (d, 1H, J = 8.0 Hz), 5.80 (d, 1H, J = 2.0 Hz), 5.65 (d, 1H, J = 5.0 Hz), 5.13 (d, 1H, J = 5.0 Hz), 4.00 (d, 1H, J = 10.0 Hz), 3.99-3.98 (m, 3H), 3.81 (d 1H, J = 10.0 Hz), 2.13 (s, 3H), 0.93 (s, 9H), 0.133 (s, 3H), 0.126 (s, 3H); ^{13}C NMR (125 MHz, DMSO-d_6) δ 172.1, 163.3, 155.5, 145.5, 96.0, 91.2, 84.3, 75.6, 69.1, 62.5, 26.8, 25.4, 19.1, -4.56, -4.62; MS (ESI) m/z 400.19 $(M+H)^+$.

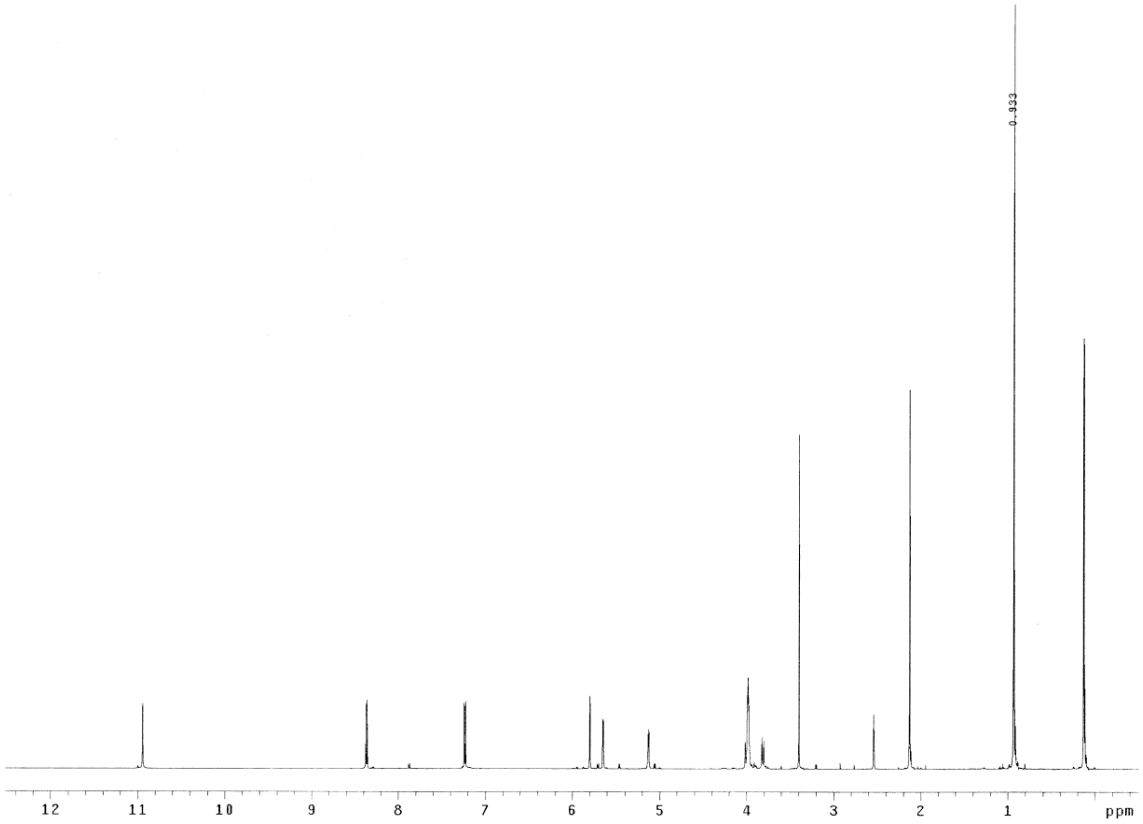

^{1}H NMR (DMSO-d_6)

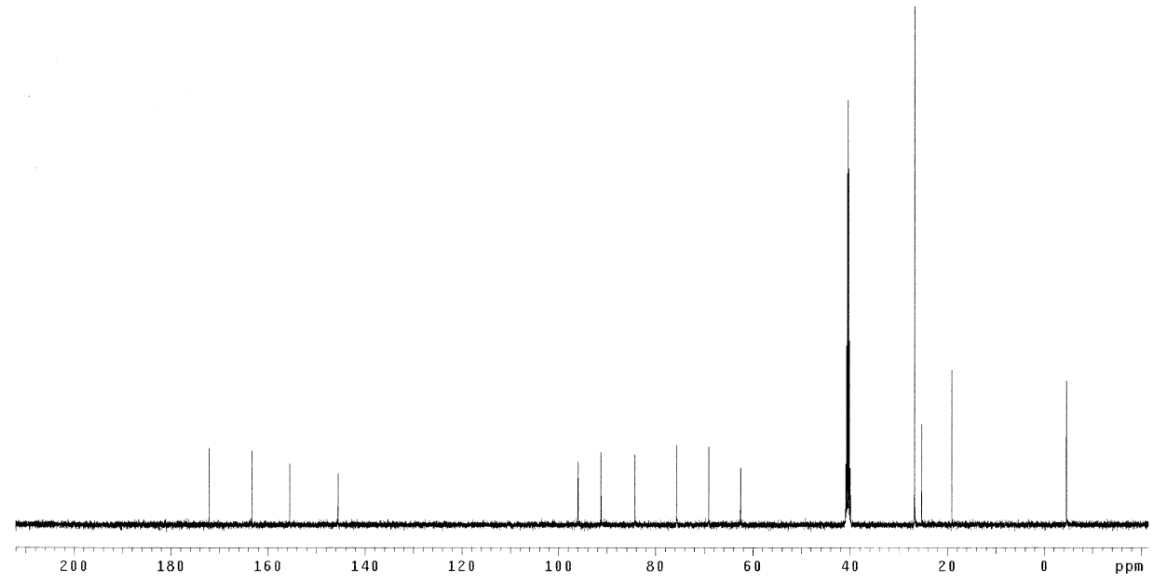

^{13}C NMR (DMSO-d_6)

2', 3'-Dimesyl Nucleoside (171)

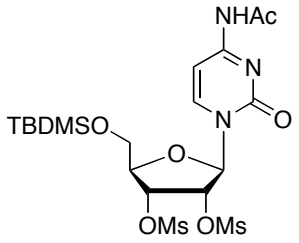

5'-Silylated cytidine **170** (10 g, 25.0 mmol), Et_3N (14.0 mL, 100.1 mmol) and Me_3N•HCl (1.2 g, 12.5 mmol) were added in toluene (100 mL) at 0 ºC. A solution of MsCl (7.8 mL, 100.1 mmol) in toluene (60 mL) was then added by syringe over a period of 10 min. The reaction mixture was stirred at 0 ºC for 3 h. The reaction was quenched with water (60 mL) at 0 ºC and the aqueous layer was extracted with EtOAc (3 x 60 mL). The organic layer was dried over $MgSO_4$ and solvent was concentrated under the reduced pressure. The residue was purified by flash chromatography eluting with 50 % EtOAc/hexanes and 100 % EtOAc to afford product as a yellow solid (12.3 g, 88 %). R_f 0.5 (100 % EtOAc). ^{1}H NMR (500 MHz, DMSO-d_6) δ 9.04 (d, 1H, J = 7.5 Hz), 8.16 (d, 1H, J = 7.5 Hz), 7.01 (d, 1H, J = 6.0 Hz), 6.00 (d, 1H, J = 6.0 Hz), 5.66 (s, 1H), 4.75 (s, 1H), 3.67-3,64 (m, 1H), 3.50 (s, 3H), 3.43-3.40 (m, 1H), 2.36 (s, 3H), 2.29 (s, 3H), 0.87 (s, 9H), -0.01 (s, 6H); ^{13}C NMR (125 MHz, DMSO-d_6) δ 172.6, 166.1, 161.1, 147.9, 105.6, 93.5, 89.9, 89.4, 83.4, 61.5, 40.7, 38.7, 26.7, 25.8, 18.8, -2.2; MS (ESI) m/z 556.11 $(M+H)^+$.

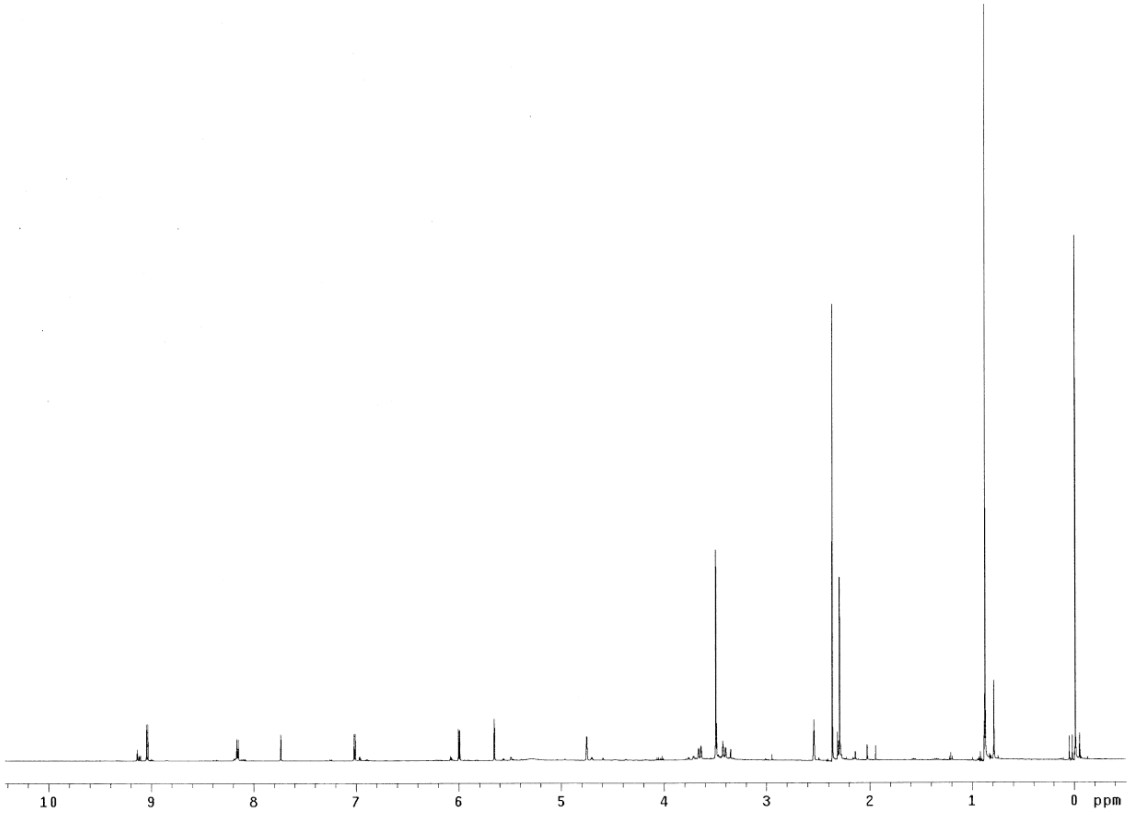

^{1}H NMR (DMSO-d_6)

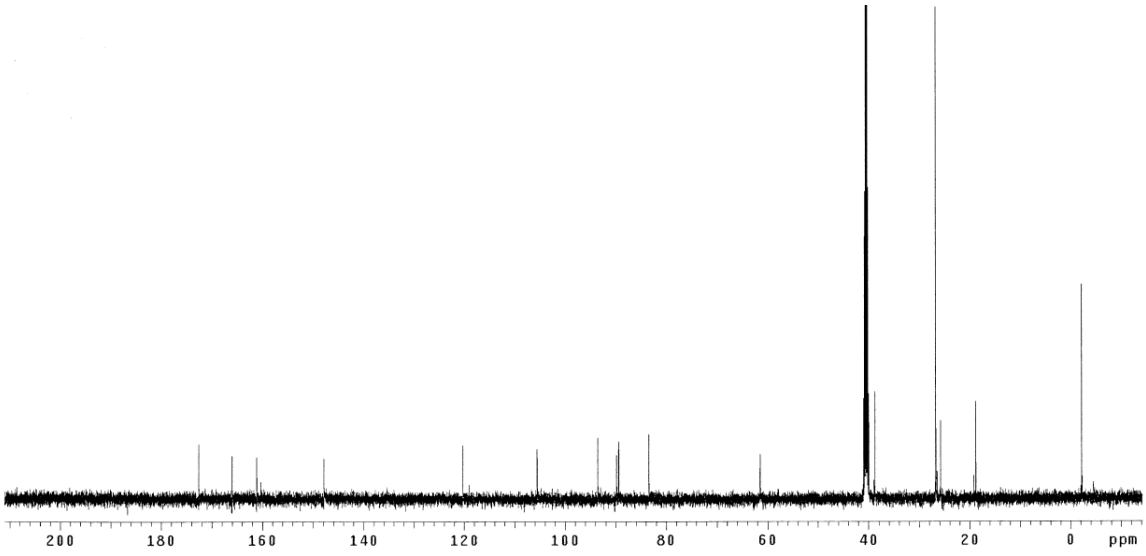

^{13}C NMR (DMSO-d_6)

2', 3'-Dedihydro Nucleoside (172)

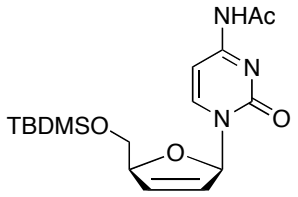

Tellurium (1.8 g, 14.1 mmol) and Et_3BHLi (30.2 mL, 30.2 mmol, 1 M in THF) were stirred at 40 ºC for 30 min under nitrogen. To this solution, dimesylate **171** (3.73 g, 6.7 mmol) dissolved in THF (70 mL) was added by syringe. The reaction mixture was stirred at 25 ºC for 18 h. The solvent was evaporated under reduced pressure at 25 ºC and the residual material was purified by flash chromatography eluting with 100 % EtOAc and 5 to 10 % MeOH/$CHCl_3$ to afford product as a colorless solid (1.95 g, 80 %). R_f 0.2 (100 % EtOAc). ^{1}H NMR (500 MHz, DMSO-d_6) δ 8.16 (d, 1H, J = 7.5 Hz), 7.21 (d, 1H, J = 7.5 Hz), 6.91 (bs, 1H), 6.42 (d, 1H, J = 6.0 Hz), 6.05 (d, 1H, J = 6.0 Hz), 4.94 (bs, 1H), 3.90-3.82 (m, 2H), 2.13 (s, 3H), 0.88 (s, 9H), 0.07 (s, 3H), 0.06 (s, 3H); ^{13}C NMR (125 MHz, DMSO-d_6) δ 172.1, 163.5, 155.8, 146.4, 135.0, 127.7, 96.5, 91.6, 88.4, 65.1, 26.8, 25.4, 19.1, -4.47, -4.52; MS (ESI) m/z 366.16 $(M+H)^+$.

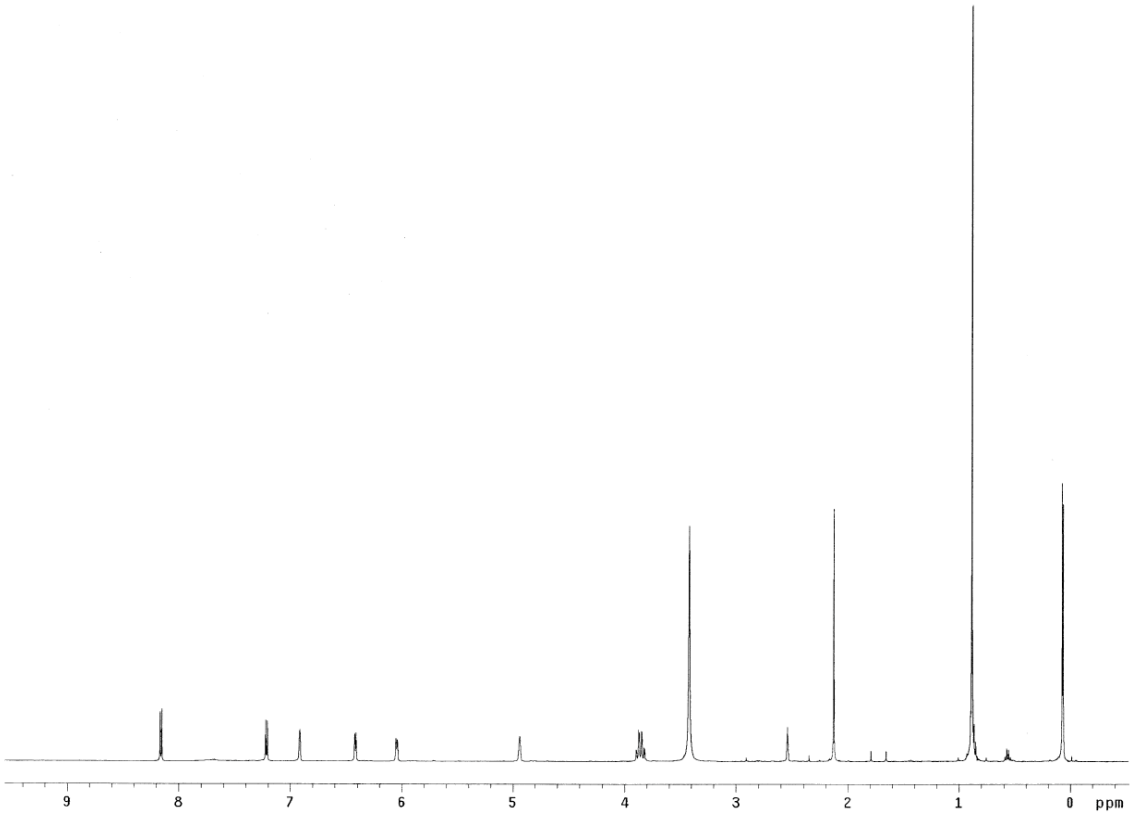

^{1}H NMR (DMSO-d_6)

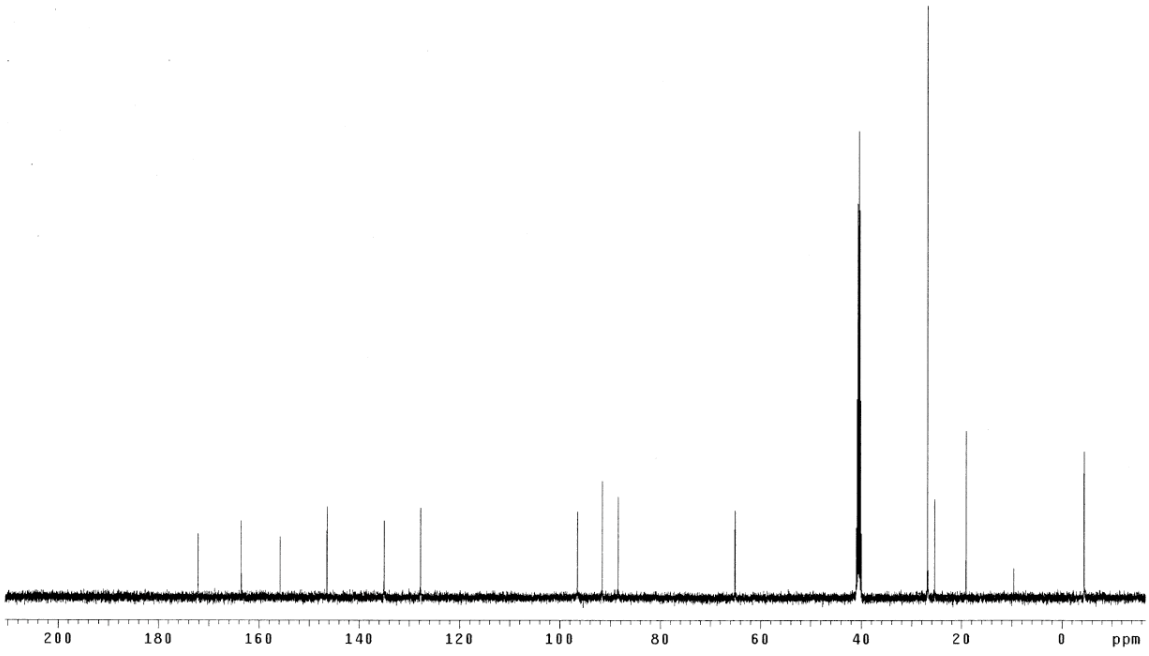

^{13}C NMR (DMSO-d_6)

2', 3'-Dedihydro-5'-hydroxy Nucleoside (173)

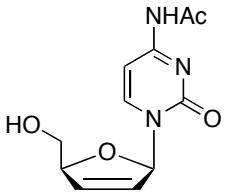

To a solution of olefin **172** (3.9 g, 10.7 mmol) in THF (100 mL) was added TBAF (12.8 mL, 12.8 mmol, 1 M in THF) at 0 ºC. The reaction mixture was stirred at 25 ºC for 1 h. The solvent was evaporated under reduced pressure at 25 ºC. The residual material was purified by flash chromatography eluting with 100 % $CHCl_3$ then 5 % MeOH/$CHCl_3$ to afford product as a colorless solid (2.54 g, 94 %). R_f 0.3 (10 % MeOH/$CHCl_3$). ^{1}H NMR (300 MHz, DMSO-d_6) δ 10.93 (s, 1H), 8.25 (d, 1H, J = 7.5 Hz), 7.20 (d, 1H, J = 7.5 Hz), 6.92-6.91 (m, 1H), 6.45-6.42 (m, 1H), 6.04-6.01 (m, 1H), 5.09 (t, 1H, J = 5.5 Hz), 4.91-4.88 (m, 1H), 3.66-3.63 (m, 2H), 2.13 (s, 3H); ^{13}C NMR (75 MHz, DMSO-d_6) δ 172.0, 163.5, 155.9, 146.9, 135.6, 127.2, 96.4, 91.7, 88.9, 63.2, 25.4; MS (ESI) m/z 252.08 $(M+H)^+$.

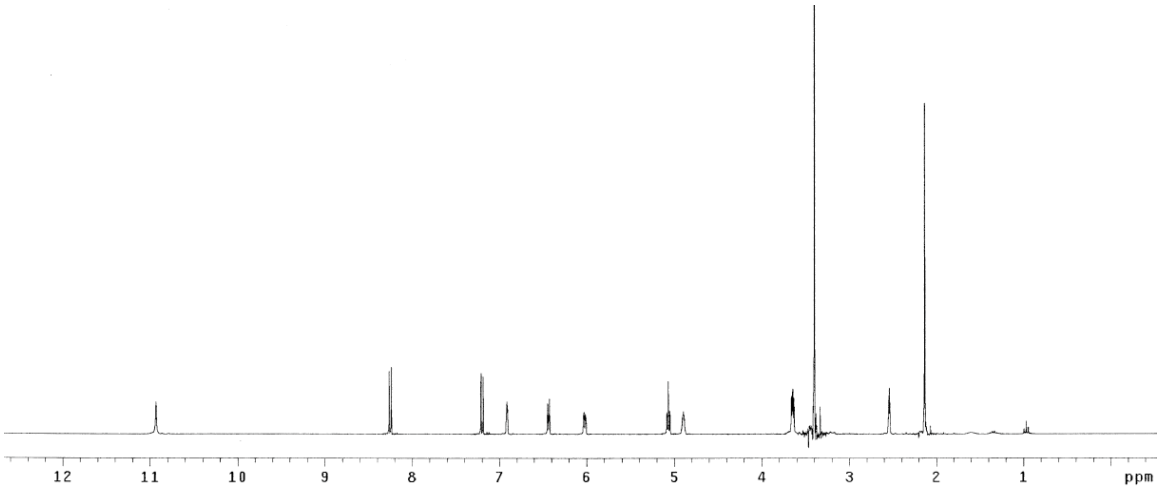

^{1}H NMR (DMSO-d_6)

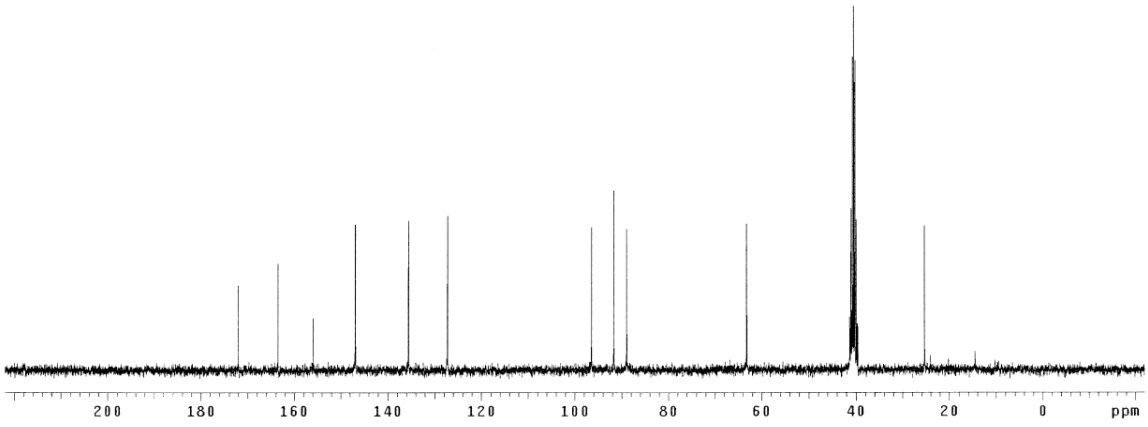

^{13}C NMR (DMSO-d_6)

2', 3'-Dideoxy-5'-hydroxy Nucleoside (174)

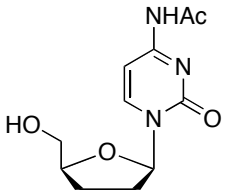

A solution of olefin **173** (500 mg, 1.99 mmol) and $Pd/CaCO_3$ (420 mg, 10 mol %) in EtOH (50 mL) with hydrogen balloon was stirred at 25 ºC for 5 h (2 batches). The two reaction batches were combined and filtered with celite and washed with EtOH. The solvent was evaporated under the reduced pressure and the residual material was purified by flash chromatography eluting with 10 to 15 % $MeOH/CHCl_3$ to afford product as a colorless solid (678 mg, 67 %). R_f 0.3 (10 % $MeOH/CHCl_3$). ^1H NMR (500 MHz, CD_3OD) δ 8.66 (d, 1H, J = 7.5 Hz), 7.45 (d, 1H, J = 7.5 Hz), 6.06 (dd, 1H, J = 5.0, 2.0 Hz), 4.27-4.23 (m, 1H), 3.99-3.96 (m, 1H), 3.77-3.74 (m, 1H), 2.58-2.50 (m, 1H), 2.20 (s, 3H), 2.16-2.11 (m, 1H), 2.00-1.88 (m, 2H); ^{13}C NMR (125 MHz, CD_3OD) δ 173.0, 164.2, 158.0, 146.5, 97.3, 89.5, 84.6, 63.1, 34.5, 25.0, 24.5; MS (ESI) m/z 253.82 $(M+H)^+$.

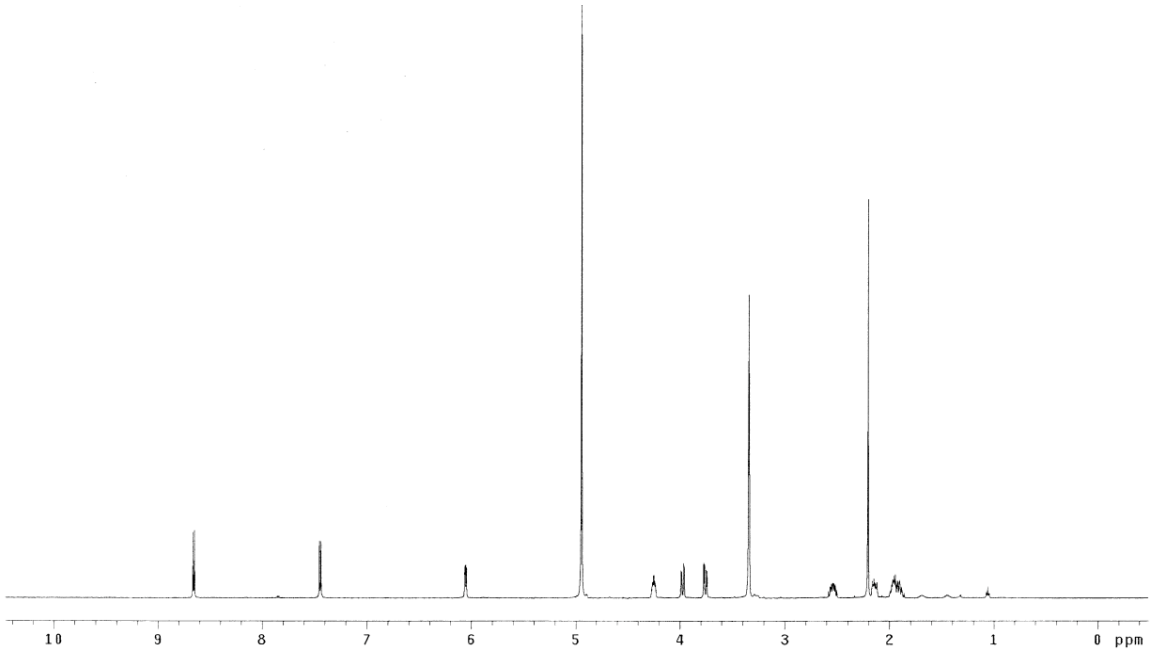

^{1}H NMR (CD_3OD)

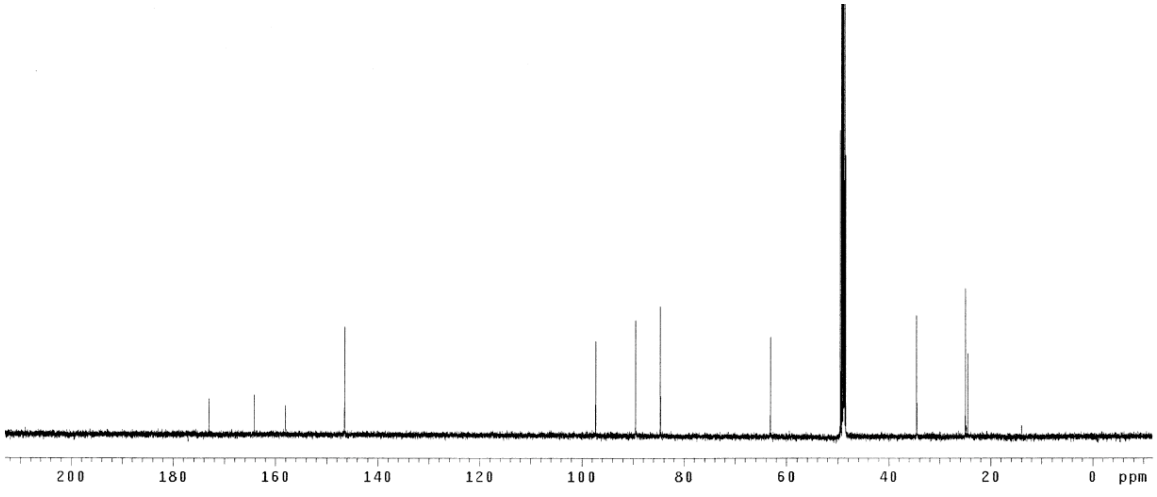

^{13}C NMR (CD_3OD)

2', 3'-Dideoxycytidine (175)[157]

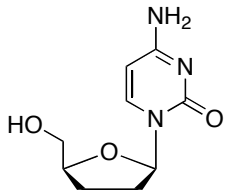

A solution of *N*-acetyl dideoxycytidine (678 mg, 2.68 mmol) in 30 mL of NH_3 (7 N in MeOH) in pressure vessel was stirred at 53 ºC for 13 h. After cooling to room temperature, the solvent was evaporated under the reduced pressure. The residual material was recrystallized from MeOH/CH_2Cl_2/hexanes to afford product as a colorless solid (451 mg, 80 %). R_f 0.5 (20 % MeOH/CH_2Cl_2). ^{1}H NMR (300 MHz, DMSO-d_6) δ 7.94 (d, 1H, J = 7.5 Hz), 7.12 (br, 2H), 5.98-5.95 (m, 1H), 5.72 (d, 1H, J = 7.5 Hz), 5.05 (t, 1H, J = 5.0 Hz), 4.07-4.00 (m, 1H), 3.74-3.67 (m, 1H), 3.60-3.53 (m, 1H), 2.35-2.21 (m, 1H), 1.93-1.75 (m, 3H); ^{13}C NMR (75 MHz, DMSO-d_6) δ 166.6, 156.2, 142.0, 94.2, 86.7, 82.5, 63.1, 33.4, 25.7.

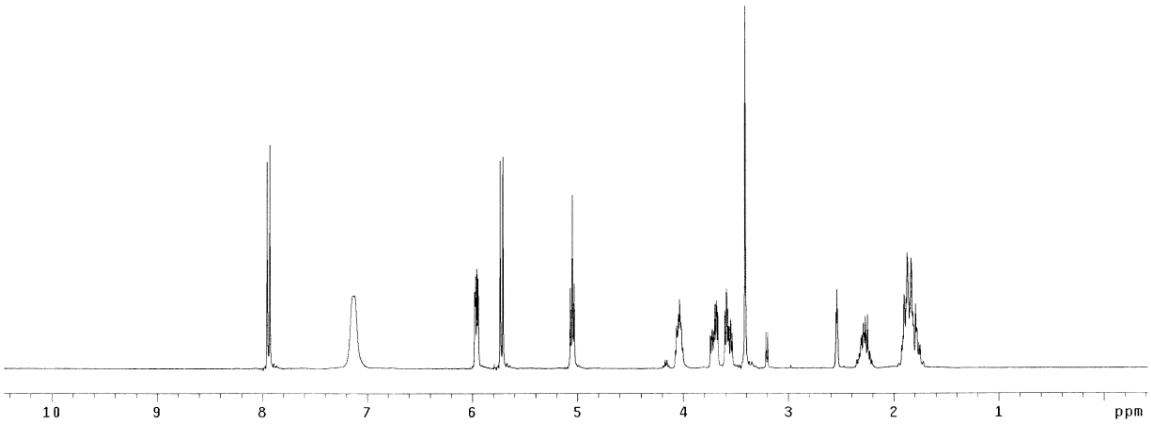

^{1}H NMR (DMSO-d_6)

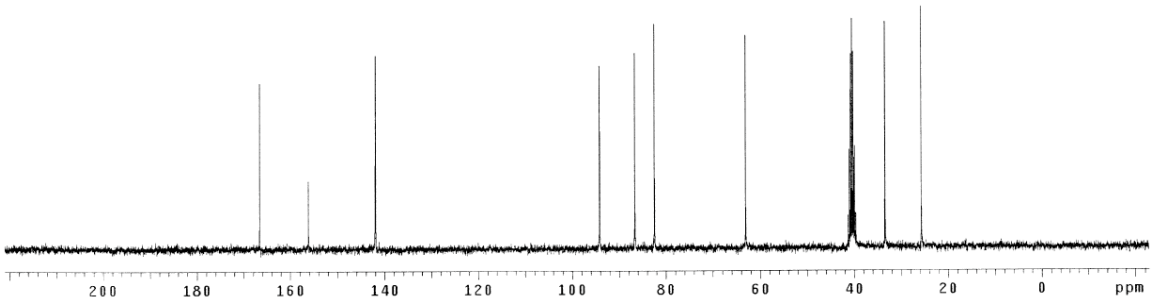

^{13}C NMR (DMSO-d_6)

2', 3'-Dideoxy-5-iodocytidine (162)[171]

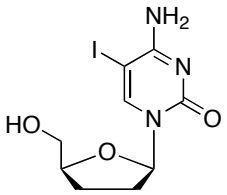

2',3'-Dideoxycytidine **175** (200 mg, 0.95 mmol) and pyridine (0.15 mL, 1.89 mmol) were dissolved in MeOH (16.0 mL) and iodine monochloride (1.33 mL, 1.33 mmol, 1 M in CH_2Cl_2) was added to a solution dropwise at 0 ºC. The reaction mixture was stirred at 0 ºC for 30 min, 25 ºC for 30 min and 50 ºC for 2 h under nitrogen. After cooling to room temperature, the solvent was evaporated under the reduced pressure. The residual material was purified by flash chromatography eluting with 10 to 15 % MeOH/CH_2Cl_2 to afford product (>90 % purity). This impure material was recrystallized from MeOH/ CH_2Cl_2/hexanes to afford pure product as a colorless solid (225 mg, 71 %). R_f 0.7 (20 % MeOH/CH_2Cl_2). ^{1}H NMR (300 MHz, DMSO-d_6) δ 8.54 (s, 1H), 7.76 (br, 1H), 6.57 (br, 1H), 5.89 (q, 1H, J = 6.3, 2.4 Hz), 5.23 (t, 1H, J = 5.0 Hz), 4.10-4.05 (m, 1H), 3.82-3.76 (m, 1H), 3.60-3.53 (m, 1H), 2.36-2.23 (m, 1H), 1.97-1.80 (m, 3H); ^{13}C NMR (75 MHz, DMSO-d_6) δ 164.7, 154.9, 148.3, 87.1, 83.1, 62.1, 56.5, 34.0, 24.7.

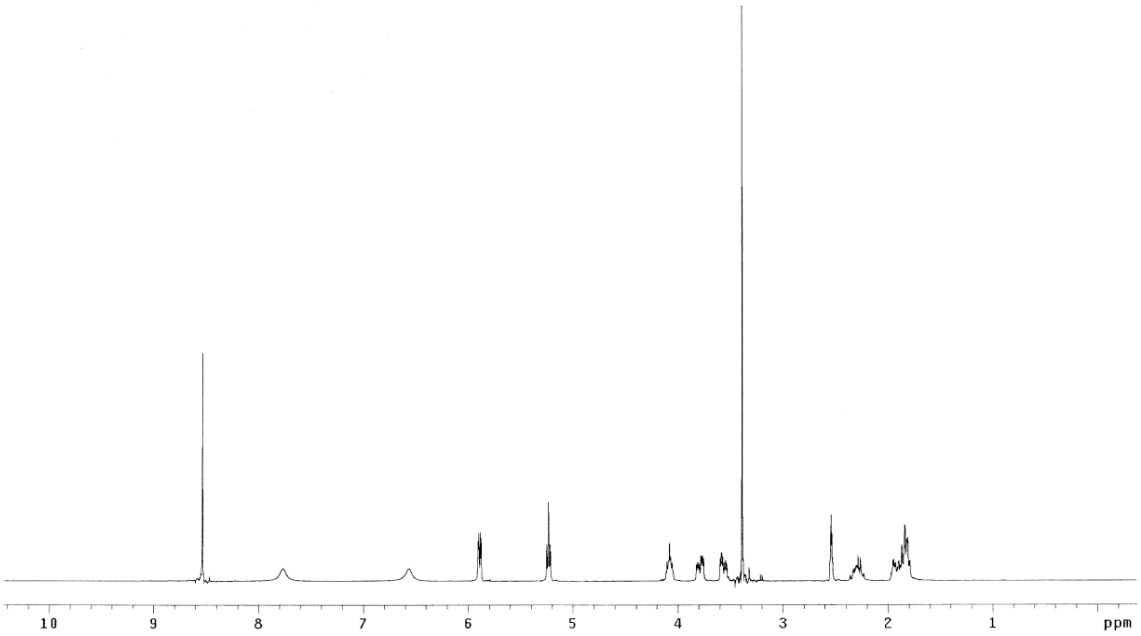

^{1}H NMR (DMSO-d_6)

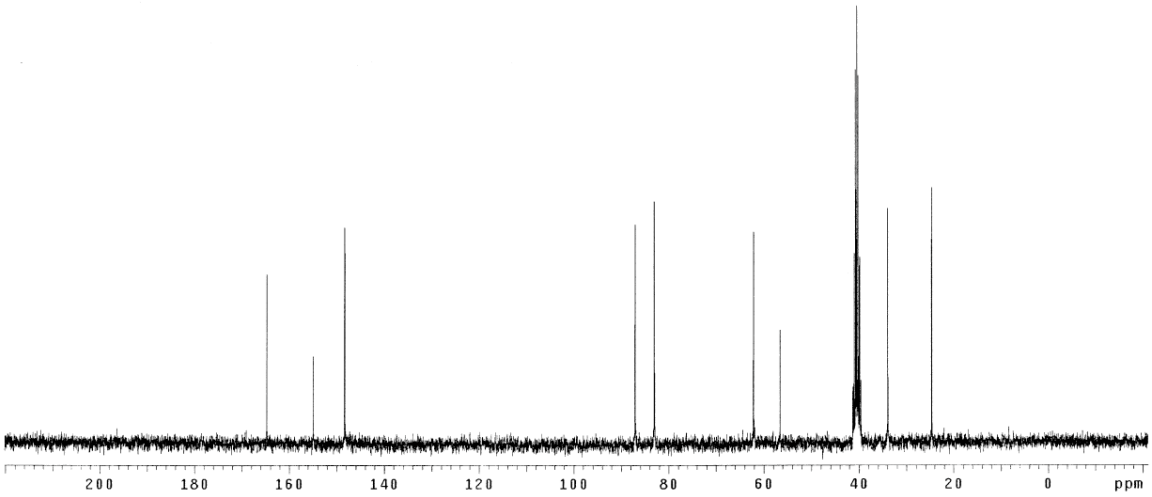

^{13}C NMR (DMSO-d_6)

2',3'-Dideoxy-5-iodouridine triphosphate (177)[166]

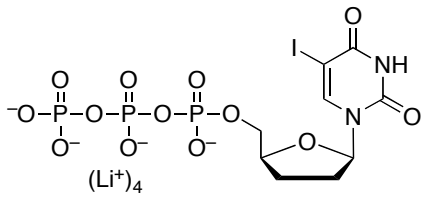

2',3'-Dideoxy-5-iodouridine **163** (50 mg, 0.148 mmol) was taken in round bottom flask and dissolved in dry pyridine (2 mL) then concentrated *in vacuo* three times then dissolved in 1 mL 1:4 pyridine/DMF. 2-Chloro-4*H*-1,3,2-benzodioxa-phosphorin-4-one (36 mg, 0.178 mol) was added as a solution in DMF (300 μL), and the reaction was stirred at 25 ºC under nitrogen for 10 min. Tributylammonium pyrophosphate (108 mg, 0.237 mmol) dissolved in DMF (500 μL) and distilled tributylamine (115 mg, 0.622 mmol) were simultaneously added into the reaction mixture. The reaction was stirred at 25 ºC for 10 min. Iodine (60 mg, 0.237 mmol) was added as a solution in 3 mL 95:5 pyridine/H_2O. The reaction was stirred at 25 ºC for additional 20 min. Sodium thiosulfate was added dropwise as a saturated aqueous solution (*ca.* 15 drops) until the iodine color disappeared. The reaction mixture was concentrated *in vacuo* then partitioned between CH_2Cl_2 (10 mL) and water (10 mL). The layers were separated and the organic extracts were discarded. The crude reaction mixture was dissolved in 10 mL water then applied to a DEAE Sephadex column (1 x 30 cm) and eluted with 0 to 1 M lithium chloride. The absorbance of the elute was monitored at 310 nm. The desired product eluted approximately 0.5 M LiCl. Fractions containing product were concentrated *in vacuo* at 25 ºC and the product was precipitated from acetone to afford 2',3'-dideoxy-5-iodouridine triphosphate **177** as an off-white solid (tetralithium salt, 49 mg, 55 %). ^{1}H NMR (300 MHz, D_2O) δ 8.22 (s, 1H), 6.08 (dd, 1H, J = 6.5, 3.0 Hz), 4.45-4.38 (m, 1H), 4.34-4.24 (m, 1H), 4.19-4.10 (m, 1H), 2.51-2.40 (m, 1H), 2.21-2.11 (m, 2H), 2.04-1.93 (m, 1H); ^{31}P NMR (121 MHz, D_2O) δ –6.5 (d, 1P, J = 24.3 Hz), –11.8 (d, 1P, J = 18.3 Hz), –21.5 (t, 1P, J = 18.3 Hz).

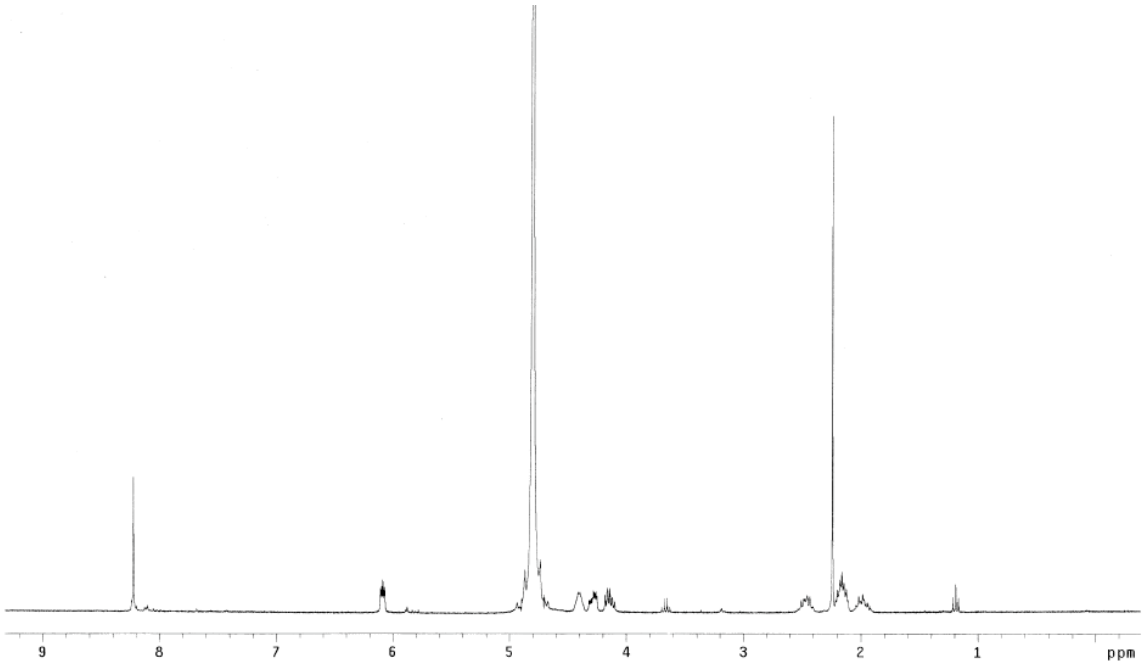

^{1}H NMR (D_2O)

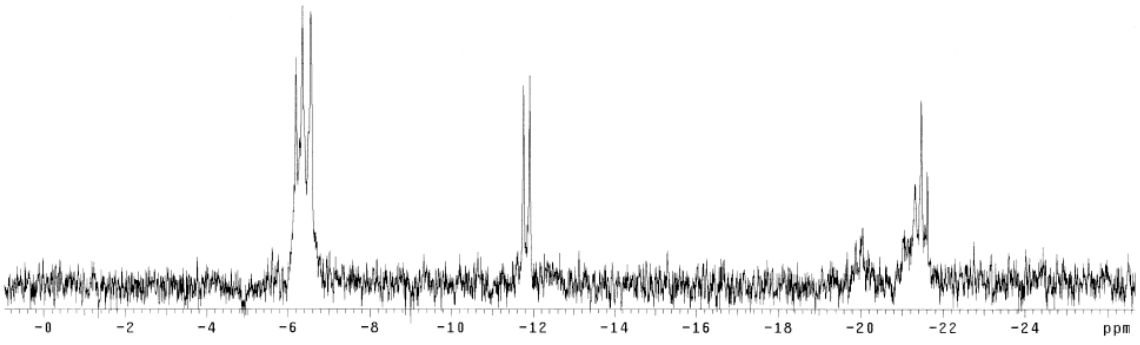

^{31}P NMR (D_2O)

Nucleoside Triphosphate (183)

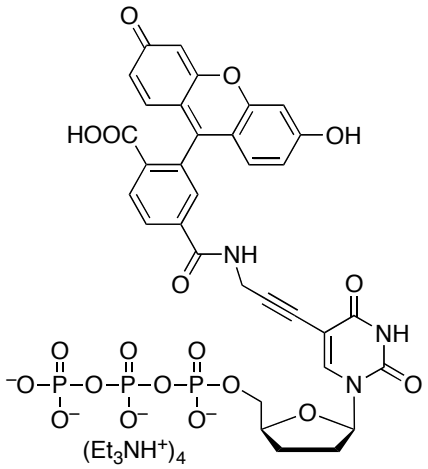

A solution of 6-propargylated carboxyfluorescein **182** (14 mg, 33.2 μmol), 2',3'-dideoxy-5-iodouridine triphosphate tetralithium salt **177** (10 mg, 16.6 μmol), water-soluble palladium catalyst (4 mg, 1.7 μmol), CuI (0.3 mg, 1.7 μmol), and Et_3N (84 mg, 830 μmol) in degassed 0.3 M phosphate buffer (800 μL, pH 7.2) was stirred at 25 ºC for 24 h under nitrogen. The product was purified by preparative HPLC then concentrated *in vacuo* to afford the title compound **183** as a fluffy yellow-orange solid (tetra(triethylammonium) salt, 32 mg, quantitative, >95 % purity). ^{1}H NMR (300 MHz, D_2O) δ 8.96 (s, 1H), 8.13 (d, 2H, J = 6.1 Hz), 8.05 (s, 1H), 7.78 (s, 1H), 7.29 (d, 2H, J = 9.0 Hz), 6.92-6.80 (m, 3H), 6.20-6.16 (m, 1H), 4.72 (s, 2H), 4.58-4.50 (m, 1H), 4.49-4.41 (m, 1H), 4.35-4.28 (m, 1H), 3.24 (q, 24H, J = 7.3 Hz), 2.70-2.57 (m, 1H), 2.24-2.09 (m, 2H), 1.98-1.91 (m, 1H), 1.32 (t, 36H, J = 7.3 Hz); ^{31}P NMR (121 MHz, 0.1 M EDTA in D_2O) δ –9.5 (d, 1P, J = 19.4 Hz), –10.1 (d, 1P, J = 18.6 Hz), –21.8 (t, 1P, J = 18.6 Hz); MS (ESI) m/z 431.10 $(M–2H)^{–2}$.

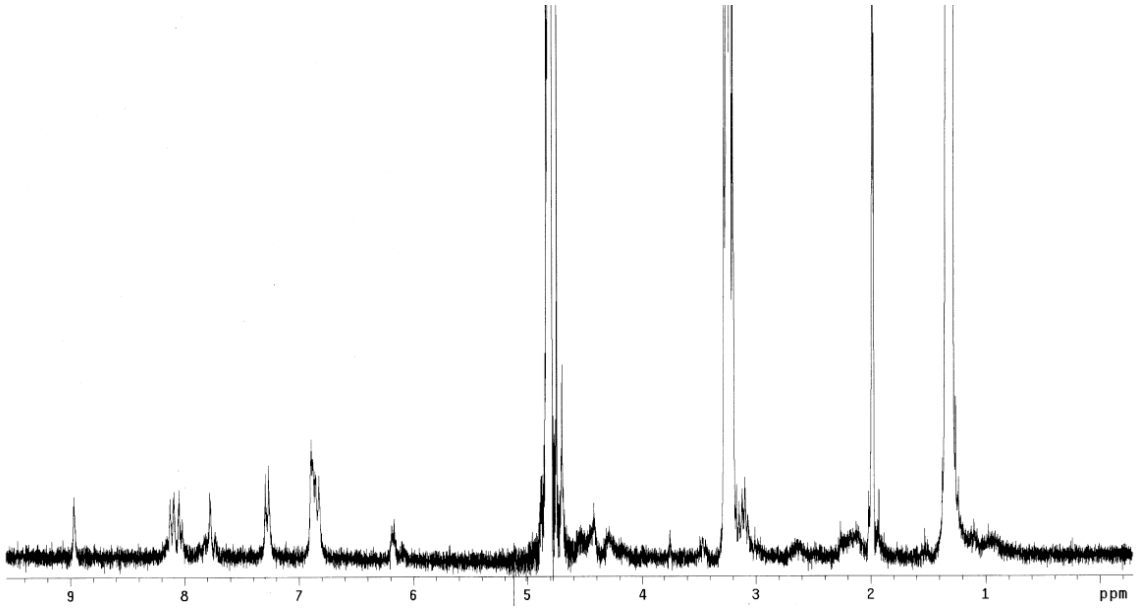

^{1}H NMR (D_2O)

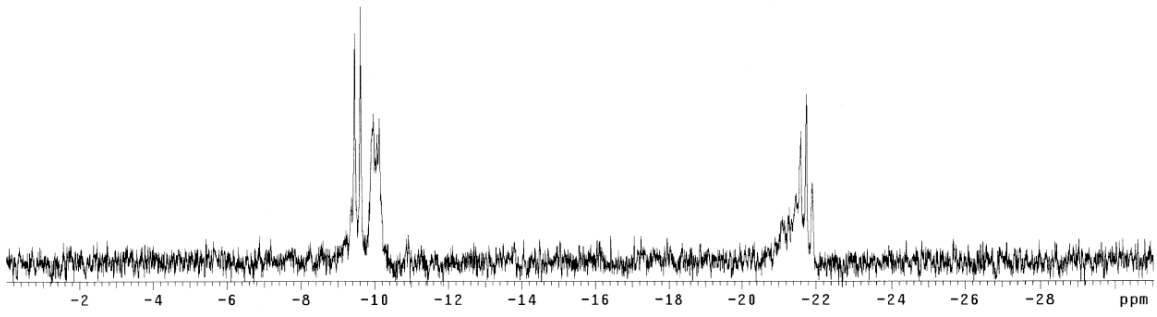

^{31}P NMR (D_2O)

Propargylated hexaethylene glycol mono-azide (184)[172]

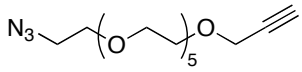

To a solution of hexaethylene glycol mono-azide **25** (8.55 g, 0.028 mol) in THF (210 mL) was slowly added NaH (1.56 g, 0.039 mol, 60 % in mineral oil) at 0 ºC. After the stirring for 40 min, propargyl bromide (6.2 g, 0.042 mol, 80 % w/w in toluene) was added dropwise at 0ºC. The reaction mixture was stirred at 25 ºC for 18 h. MeOH (40 mL) was added dropwise to a reaction mixture at 0ºC and H_2O (150 mL) was added. The aqueous layer was extracted with CH_2Cl_2 (7 x 150 mL) and the combined organic layer was dried over Na_2SO_4. The solvents were concentrated under the reduced pressure and the residual material was purified by flash chromatography eluting with 100 % CH_2Cl_2 and then 30 to 50 % acetone/EtOAc to afford product **184** as a yellow oil (9.6 g, 99 %). R_f 0.5 (20 % acetone/EtOAc, with iodine stain). ^{1}H NMR (300 MHz, $CDCl_3$) δ 4.20-4.19 (m, 2H), 3.68-3.64 (m, 22H), 3.38 (t, 2H, J = 4.8 Hz), 2.43 (t, 1H, J = 1.8 Hz).

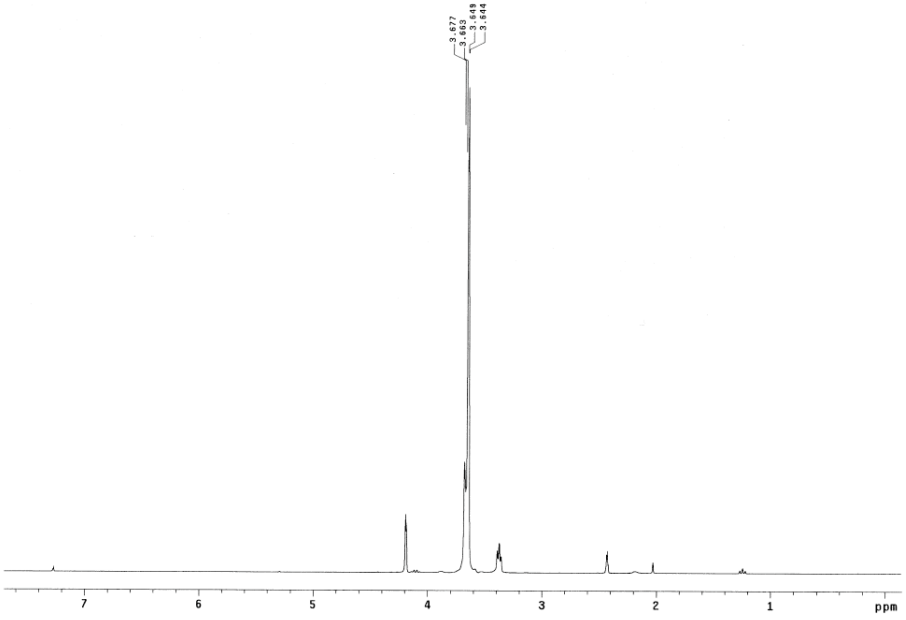

^{1}H NMR ($CDCl_3$)

Silylated, hexaethylene glycol mono-azide (185)

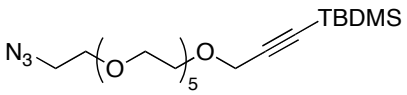

To a solution of propargylated ethylene glycol **184** (5.0 g, 14.5 mmol) in THF (175 mL) was added ^{n}BuLi (11.8 mL, 18.9 mmol, 1 M in hexane) dropwise at –78 ºC. After the stirring for 30 min, a solution of TBDMSCl (3.5 g, 23.2 mmol) in THF (50 mL) was added to a reaction dropwise (*note: concentration is important for this reaction*). The reaction mixture was stirred at 25 ºC for 5 h. MeOH (5 mL) was added dropwise to a reaction mixture at 0ºC and H_2O (100 mL) was added. The aqueous layer was extracted with CH_2Cl_2 (7 x 100 mL) and the combined organic layer was dried over Na_2SO_4. The solvents were concentrated under the reduced pressure and the residual material was purified by flash chromatography eluting with 100 % CH_2Cl_2 and then 60 to 80 % EtOAc/hexanes to afford product as a colorless oil (5.8 g, 87 %). R_f 0.3 (50 % EtOAc/hexanes, with iodine stain). ^{1}H NMR (300 MHz, $CDCl_3$) δ 4.17 (s, 2H), 3.65-3.62 (m, 22H), 3.35 (t, 2H, J = 5.0 Hz), 0.90 (s, 9H), 0.07 (s, 6H); ^{13}C NMR (75 MHz, $CDCl_3$) δ 102.1, 89.5, 70.64 (2C), 70.61 (3C), 70.57 (3C), 70.52 (3C), 70.3, 70.0, 68.8, 59.1, 50.6, 26.0,16.4, -4.7; MS (ESI) m/z 466.27 $(M+Li)^+$.

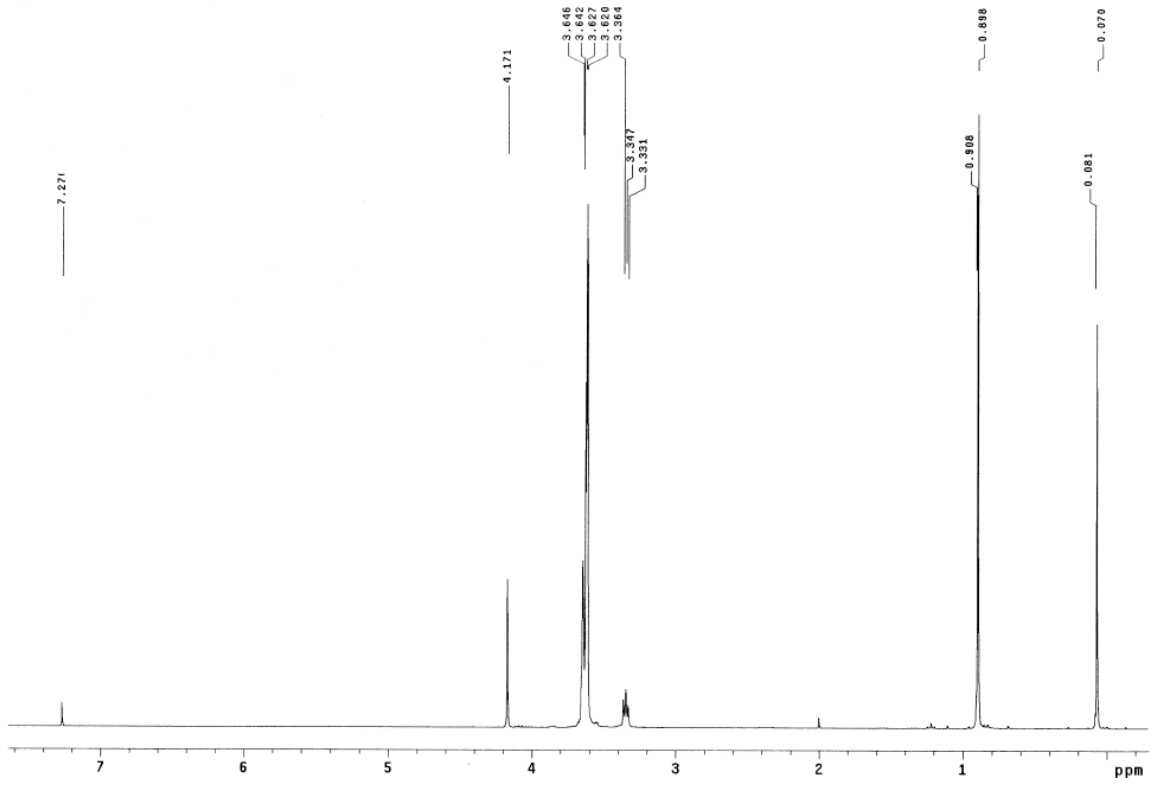

^{1}H NMR ($CDCl_3$)

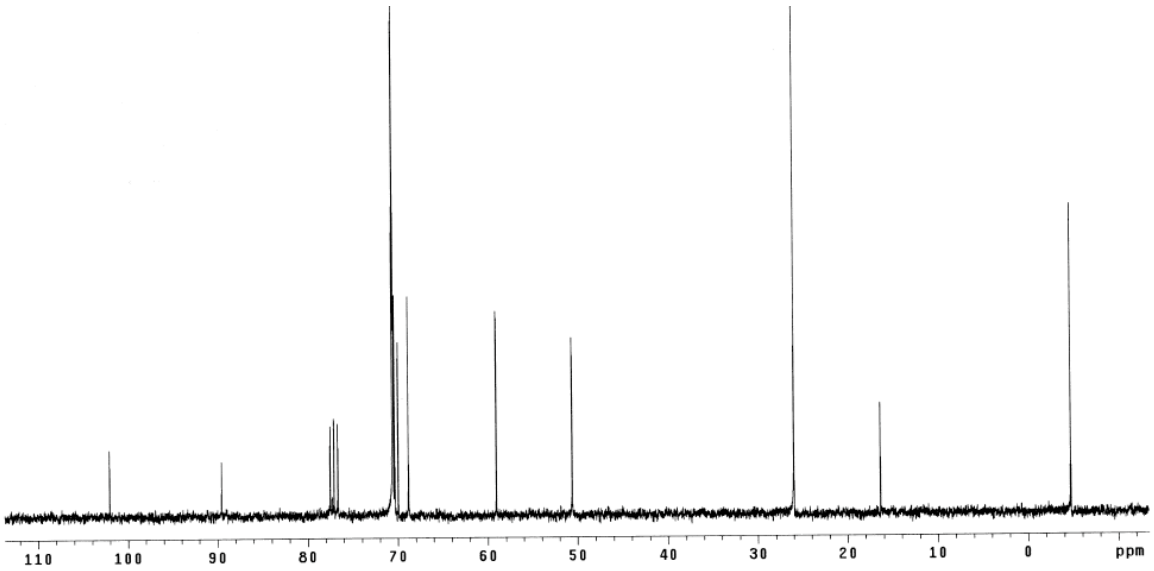

^{13}C NMR ($CDCl_3$)

Silylated, aminohexaethylene glycol (186)

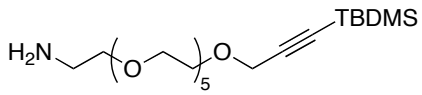

Triphenylphosphine (5.08 g, 19.4 mmol) was added to a solution of azido-ethylene glycol **185** (4.05 g, 8.8 mmol) in 9:1 THF/H_2O (81 mL: 9 mL) at 25 ºC. The reaction mixture was stirred at 25 ºC for 48 h. The solvent was concentrated under the reduced pressure and the residual material was purified by short flash chromatography eluting with 100 % EtOAc and 100 % MeOH to afford product as a yellow oil (3.5 g, 92 %). R_f 0.1 (100 % MeOH with iodine stain). ^{1}H NMR (300 MHz, $CDCl_3$) δ 4.21 (s, 2H), 3.68-3.61 (m, 20H), 3.53 (t, 2H, J = 4.7 Hz), 2.88 (t, 2H, J = 4.7 Hz), 0.93 (s, 9H), 0.11 (s, 6H); ^{13}C NMR (75 MHz, $CDCl_3$) δ 101.6, 70.11 (4C), 70.06 (3C), 69.92 (3C), 69.8, 68.4, 58.7, 41.2, 25.5, 15.9, -5.2; MS (ESI) m/z 434.31 $(M+H)^+$.

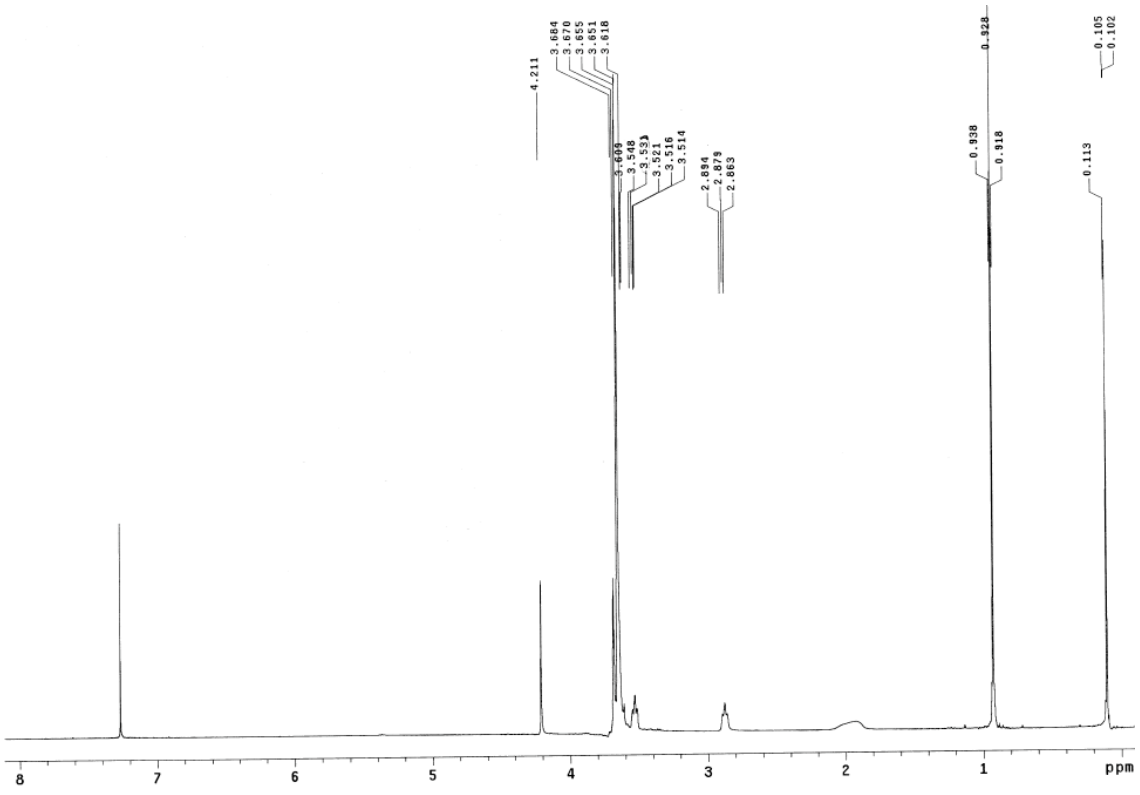

^{1}H NMR ($CDCl_3$)

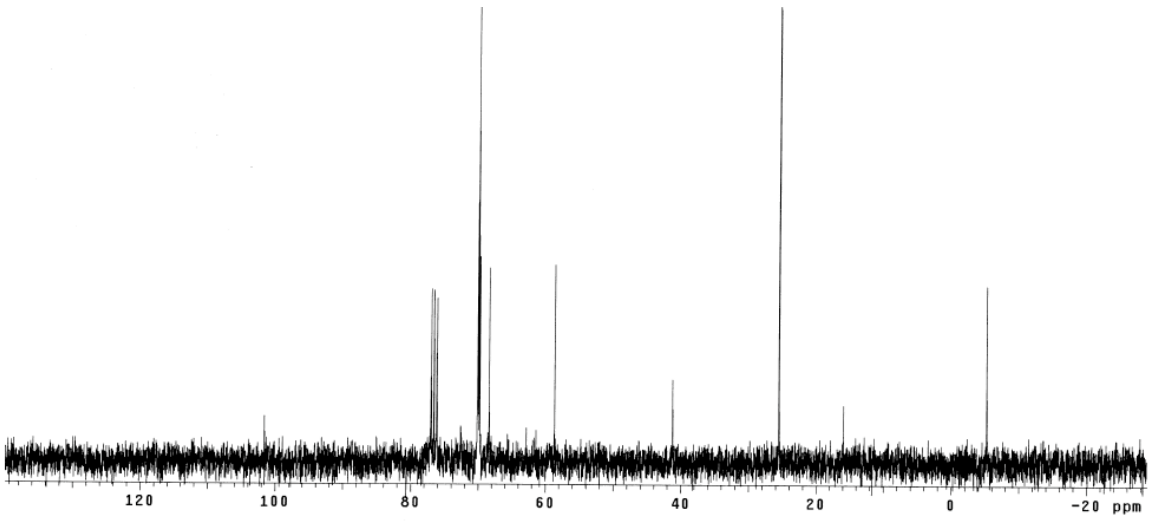

^{13}C NMR ($CDCl_3$)

3-Bromo-5-iodobenzoic acid chloride (187)

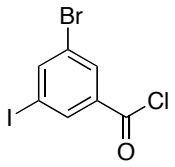

A solution of 3-bromo-5-iodobenzoic acid (5.0 g, 0.015 mol), thionylchloride (47 mL) and DMF (5 drops) was refluxed at 90 ºC for 12 h. The excess of thionylchloride was distilled off with benzene. After the distillation, the residual material (5.5 g) was dissolved in EtOAc and hexanes. The white precipitate was filtered off and the solvent was evaporated under the reduced pressure and the residue was dried under the vacuum to afford pure product as brown solid (4.97 g, 94 %). R_f 0.9 (100 % EtOAc). ^{1}H NMR (500 MHz, $CDCl_3$) δ 8.34 (t, 1H, J = 1.5 Hz), 8.19 (t, 1H, J = 1.5 Hz), 8.15 (t, 1H, J = 1.5 Hz); ^{13}C NMR (125 MHz, $CDCl_3$) δ 165.8, 145.9, 138.3, 136.0, 133.2, 123.5, 94.4; MS (GCMS) m/z 345 $(M+H)^+$.

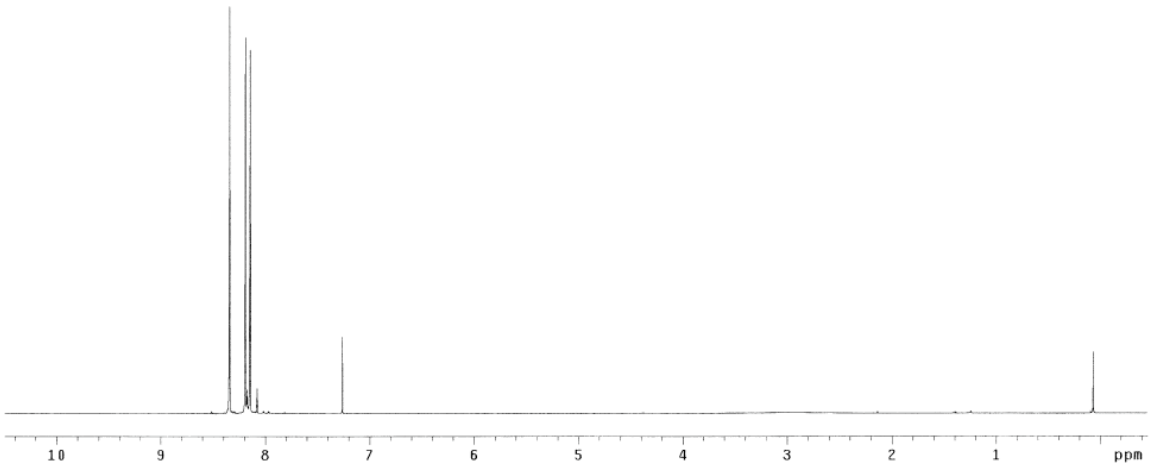

^{1}H NMR ($CDCl_3$)

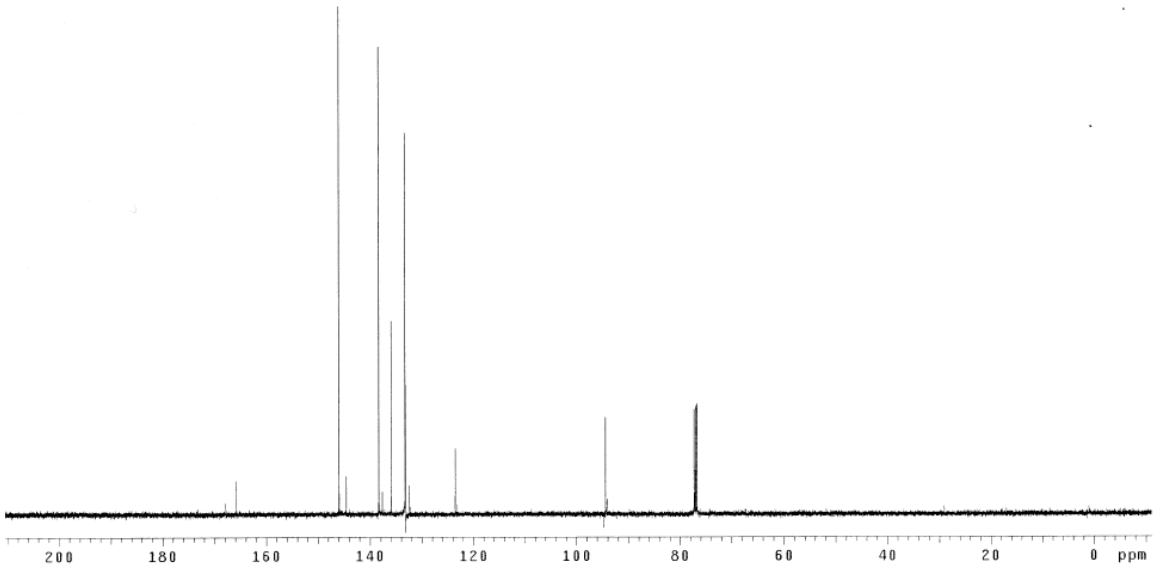

^{13}C NMR ($CDCl_3$)

Silylated, hexaethylene glycol linker (188)

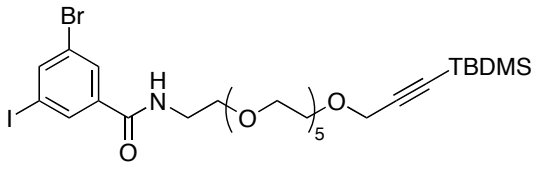

To a solution of acid chloride **187** (2.54 g, 7.36 mmol) in CH_2Cl_2 (60 mL) was added a solution of silylated-aminohexaethylene glycol **186** (3.51 g, 8.09 mmol) in CH_2Cl_2 (20 mL) and DMAP (988 mg, 8.09 mmol) at 0 ºC. The reaction mixture was stirred at 25 ºC for 24 h. The solvent was evaporated under the reduced pressure and the residue was purified by flash chromatography eluting with 100 % CH_2Cl_2 and 100 % EtOAc to afford product as a yellow oil (5.1 g, 93 %). R_f 0.5 (100 % EtOAc with iodine stain). ^{1}H NMR (500 MHz, $CDCl_3$) δ 8.10 (t, 1H, J = 1.5 Hz), 7.95-7.93 (m, 2H), 7.30 (br, 1H), 4.18 (s, 2H), 3.66-3.59 (m, 24H), 0.91 (s, 9H), 0.09 (s, 6H); ^{13}C NMR (125 MHz, $CDCl_3$) δ 164.6, 142.0, 137.9, 135.0, 129.8, 123.0, 101.9, 94.2, 89.7, 70.49, 70.47, 70.45 (2C), 70.43 (4C), 70.3, 70.1, 69.6, 68.8, 59.1, 40.1, 26.0, -4.7; MS (ESI) m/z 748.14 $(M+Li)^+$.

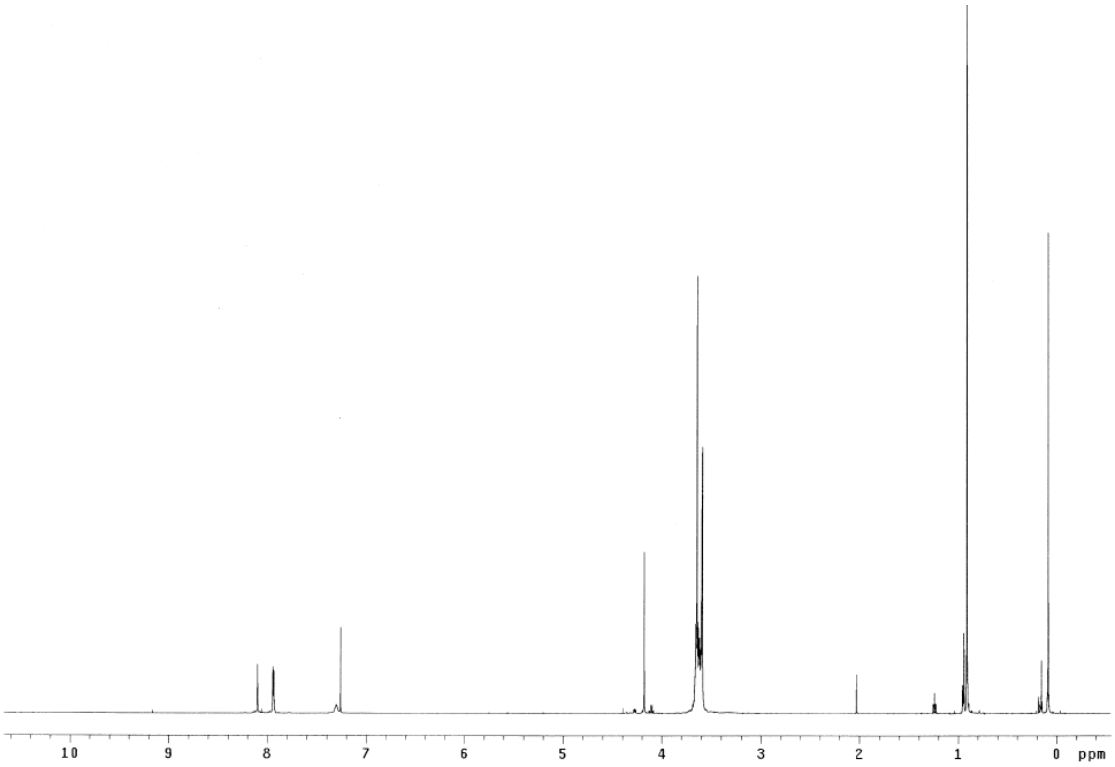

^{1}H NMR ($CDCl_3$)

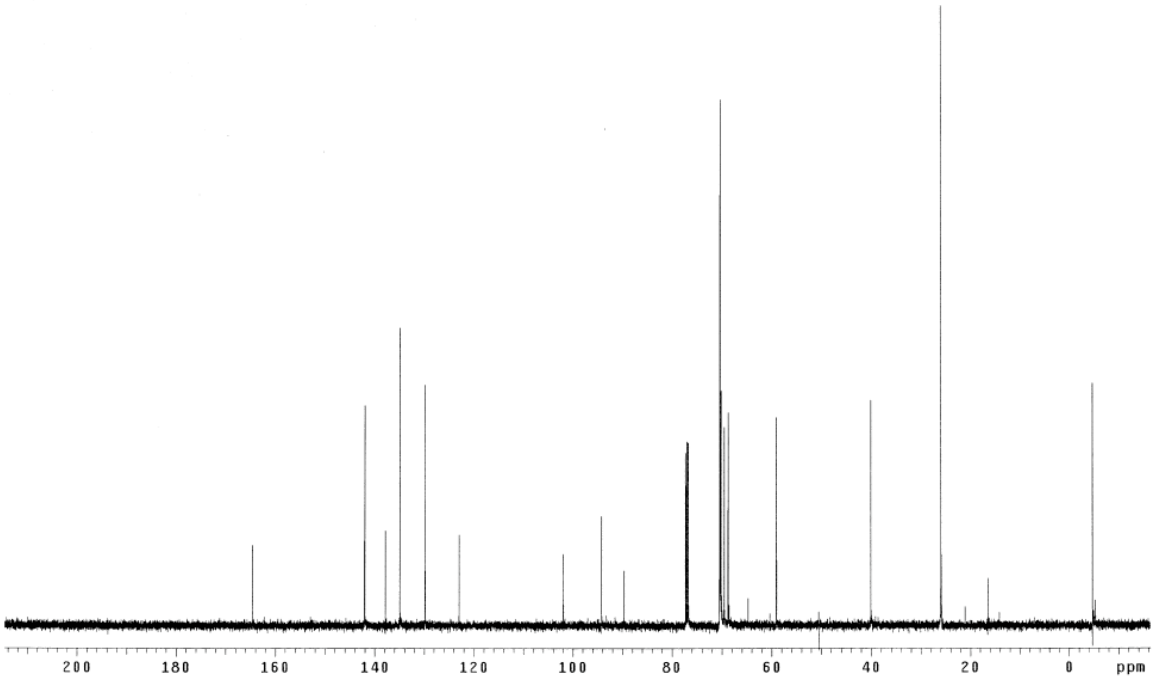

^{13}C NMR ($CDCl_3$)

Fluorescein derivative (192)

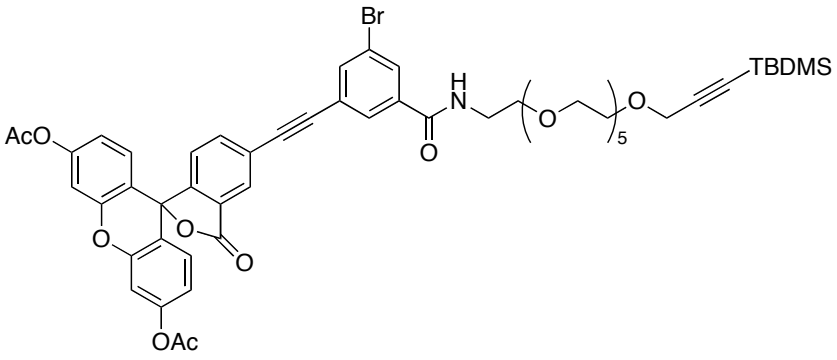

5-Ethynyl fluorescein diacetate **191** (1.60 g, 3.64 mmol), $Pd(PPh_3)_4$ (191 mg, 0.17 mmol), CuI (32 mg, 0.17 mmol) were taken in 200 mL round bottom flask and vacuum-pump-thawed (x 3 times). To this flask, a solution of ethylene glycol linker **188** (2.46 g, 3.31 mmol) in THF (40 mL) and Et_3N (4.6 mL, 33.13 mmol) was added. The reaction mixture was stirred at 25 ºC for 24 h. The solvent was evaporated under the reduced pressure and the residue was purified by flash chromatography eluting with 100 % CH_2Cl_2 and 80 % EtOAc/hexanes, and then 100 % EtOAc to afford product as a semi-yellow solid (2.8 g, 80 %). R_f 0.5 (100 % EtOAc). ^{1}H NMR (500 MHz, $CDCl_3$) δ 8.13 (m, 1H), 7.99 (t, 1H, J = 1.5 Hz), 7.96 (t, 1H, J = 1.5 Hz), 7.80 (d, 1H, J = 1.5 Hz), 7.79-7.78 (m, 1H), 7.24 (t, 1H, J = 5.5 Hz), 7.18 (d, 1H, J = 8.0 Hz), 7.09-7.08 (m, 2H), 6.85-6.81 (m, 4H), 4.17 (s, 2H), 3.68-3.58 (m, 24H), 2.30 (s, 6H), 0.90 (s, 9H), 0.08 (s, 6H); ^{13}C NMR (125 MHz, $CDCl_3$) δ 168.7, 168.0, 165.1, 152.4, 152.1, 151.4, 138.2, 136.7, 136.6, 130.7, 129.2, 128.8, 128.1, 126.5, 124.8, 124.4, 124.3, 122.3, 117.8, 115.8, 110.4, 101.9, 89.6, 89.4, 89.1, 81.7, 70.44, 70.43 (2C), 70.39 (4C), 70.3, 70.1, 69.5, 68.7, 59.0, 40.0, 25.9, 21.0, 16.4, -4.8; MS (MALDI) m/z 1054.37 $(M+H)^+$.

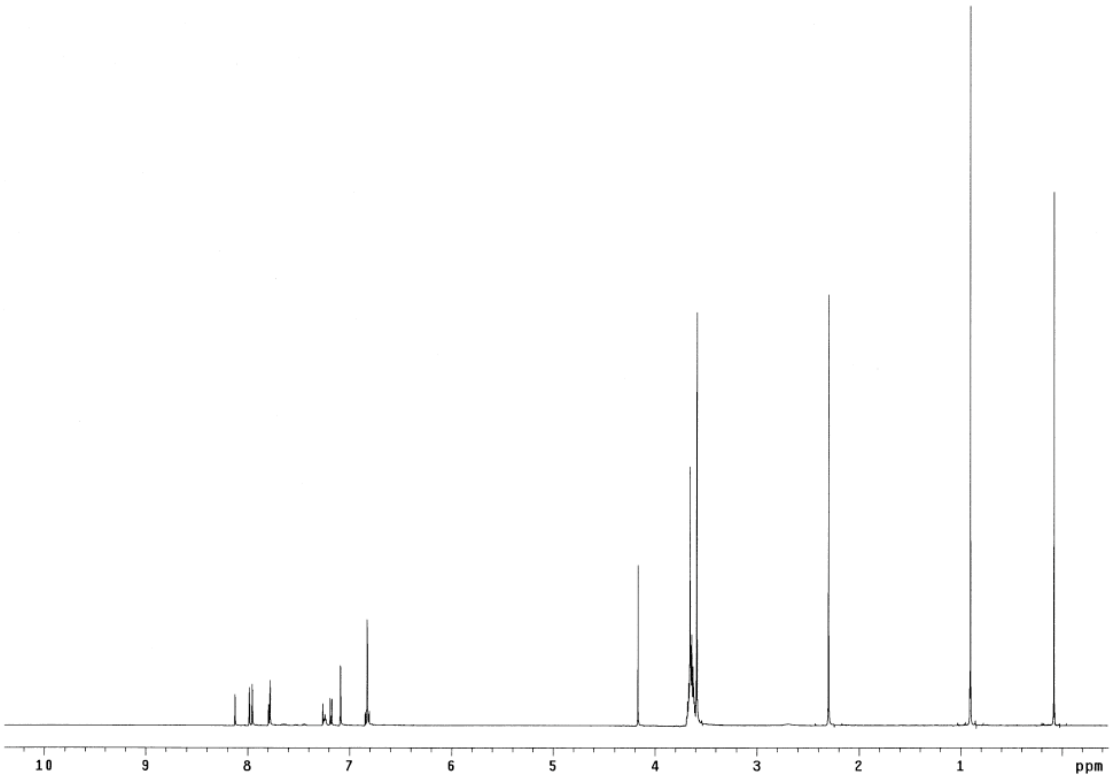

^{1}H NMR ($CDCl_3$)

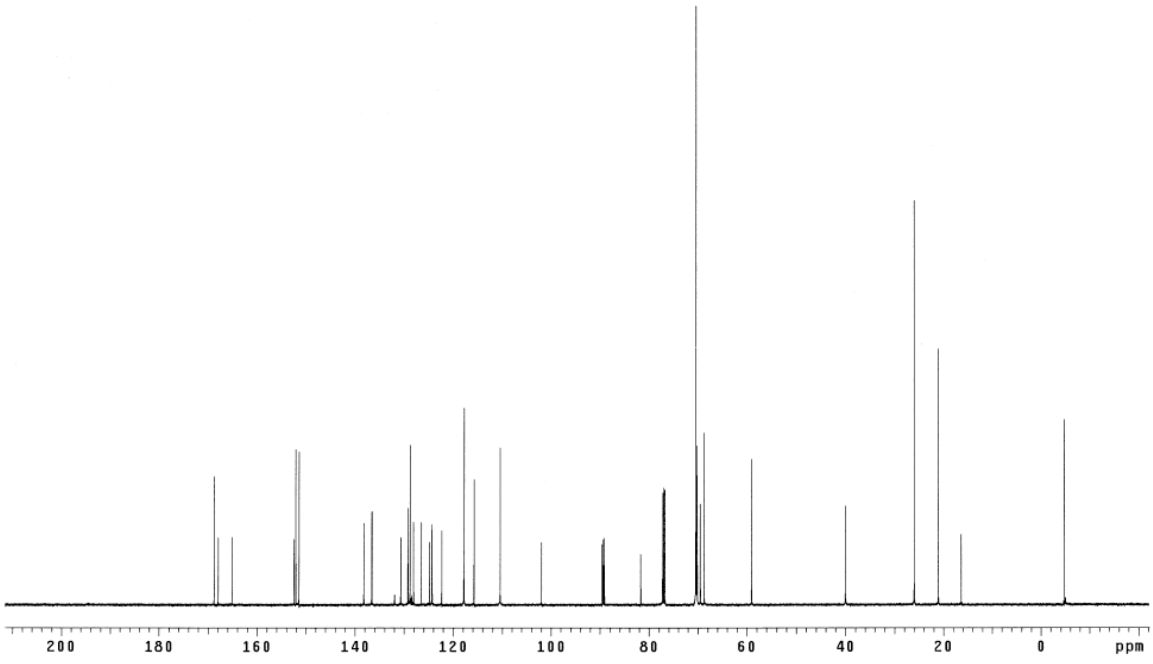

^{13}C NMR ($CDCl_3$)

Cyclized anisidine (193)

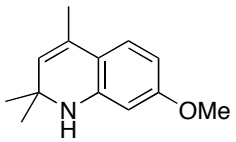

A solution of *m*-anisidine (3.0 g, 24.4 mmol) and iodine (216 mg, 0.85 mmol) in acetone (40 mL) was refluxed at 66 ºC for 1 h and stirred at 25 ºC for 12 h. The solvent was evaporated and the residual material was purified by flash chromatography eluting with 100 % hexanes and 4 % EtOAc/hexanes to afford product as an off-white solid (2.6 g, 53 %). R_f 0.6 (10 % EtOAc/hexanes). ^{1}H NMR (500 MHz, $CDCl_3$) δ 6.99 (d, 1H, J = 8.0 Hz), 6.21 (dd, 1H, J = 8.0, 2.5 Hz), 6.03 (d, 1H, J = 2.5 Hz), 5.20 (s, 1H), 3.76 (s, 3H), 1.97 (s, 3H), 1.27 (s, 6H); ^{13}C NMR (125 MHz, $CDCl_3$) δ 160.1, 144.6, 128.1, 125.9, 124.6, 115.3, 102.2, 98.5, 55.0, 51.9, 31.0, 18.6; MS (ESI) m/z 204.14 $(M+H)^+$.

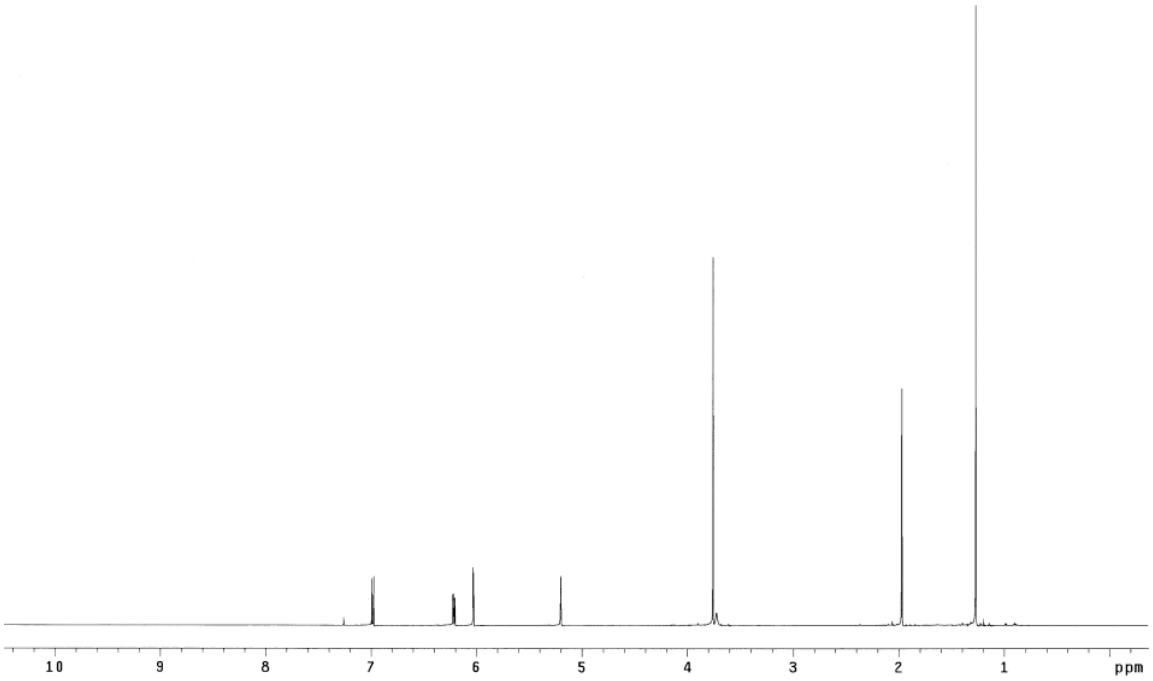

^{1}H NMR ($CDCl_3$)

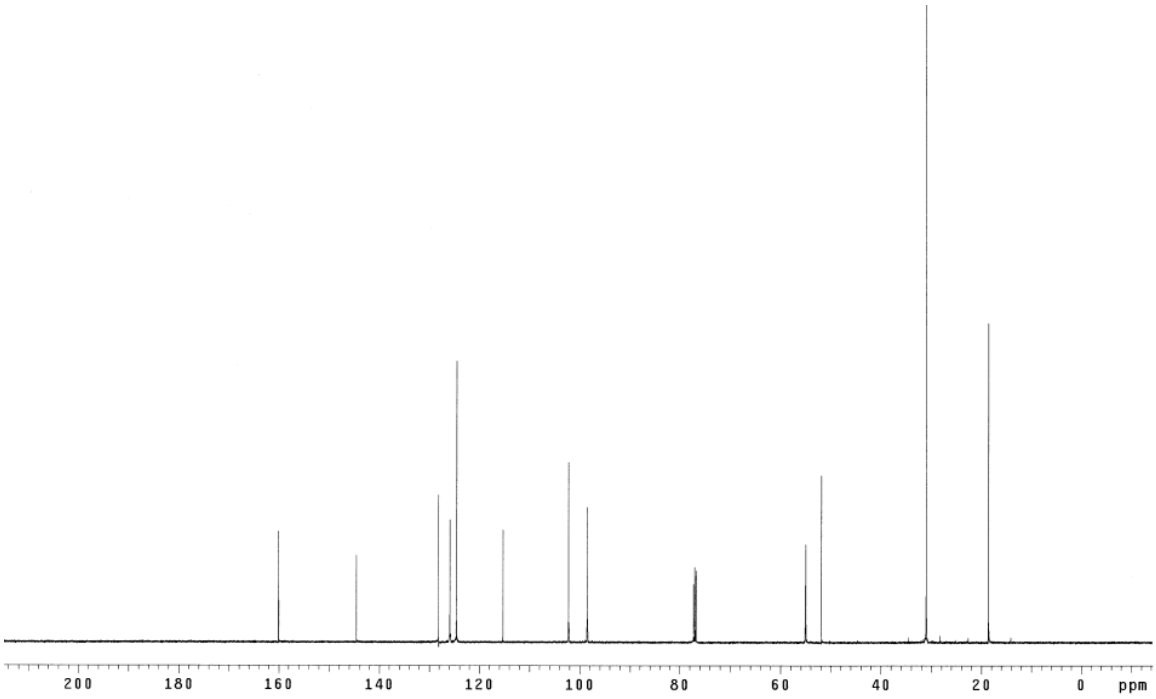

^{13}C NMR ($CDCl_3$)

_N_-Alkylated, cyclized anisidine (194)

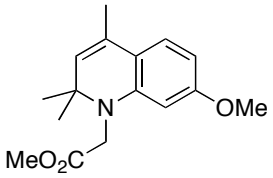

A solution of cyclized anisidine **193** (1.0 g, 4.92 mmol), Cs_2CO_3 (8.0 g, 24.6 mmol), methyl bromoacetate (5.3 g, 34.4 mmol), and *tetra*-n-butylammonium iodide (2.0 g, 5.41 mmol) in CH_3CN (15.0 mL) was refluxed at 93 ºC for 30 h. After cooling to room temperature, the reaction mixture was filtered and washed with acetone and then the solvent was evaporated. The residual material was purified by flash chromatography eluting with 100 % hexanes and 5 % EtOAc/hexanes to afford product as a yellow oil (1.32 g, 98 %). R_f 0.4 (10 % EtOAc/hexanes). ^{1}H NMR (500 MHz, $CDCl_3$) δ 6.98 (d, 1H, J = 8.5 Hz), 6.19 (dd, 1H, J = 8.5, 2.5 Hz), 5.85 (d, 1H, J = 2.5 Hz), 5.14 (s, 1H), 4.00 (s, 2H), 3.75 (s, 3H), 3.74 (s, 3H), 1.96 (s, 3H), 1.32 (s, 6H); ^{13}C NMR (125 MHz, $CDCl_3$) δ 171.8, 160.4, 144.7, 127.2, 126.5, 124.5, 116.2, 100.1, 97.3, 57.0, 55.0, 52.2, 46.5, 28.9, 18.8; MS (ESI) m/z 276.15 $(M+H)^+$.

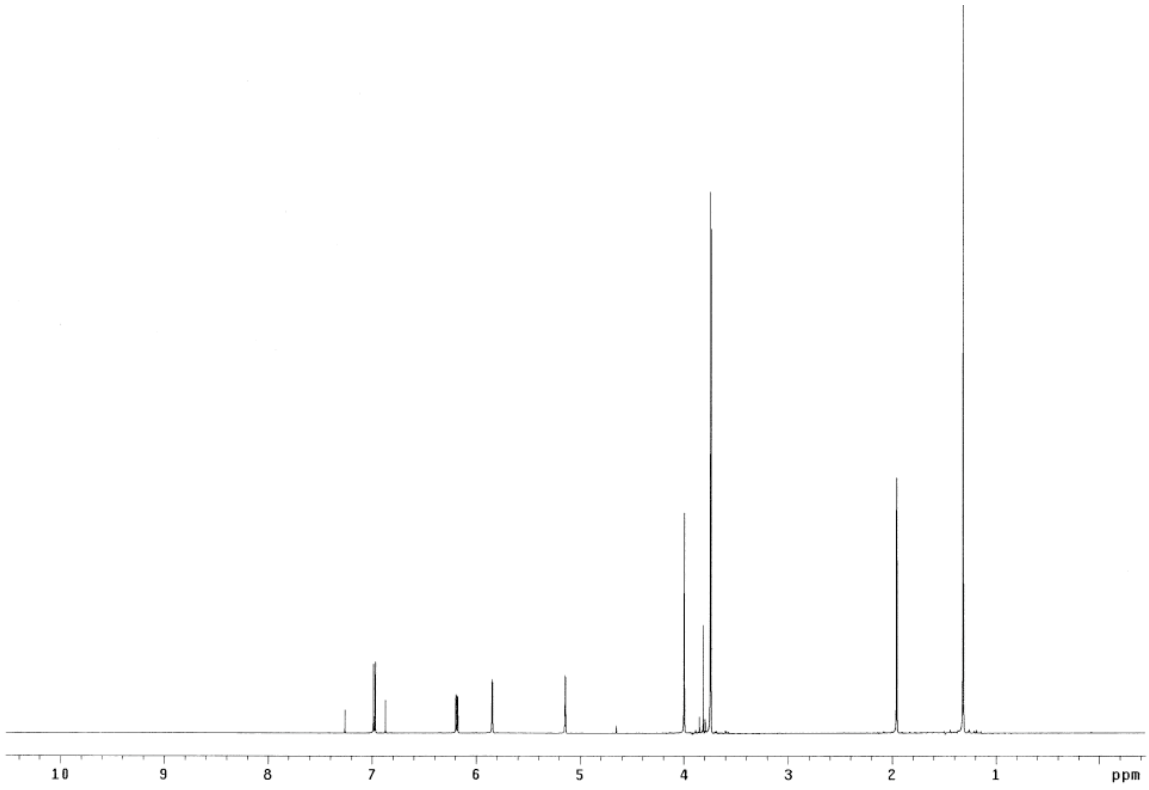

^{1}H NMR ($CDCl_3$)

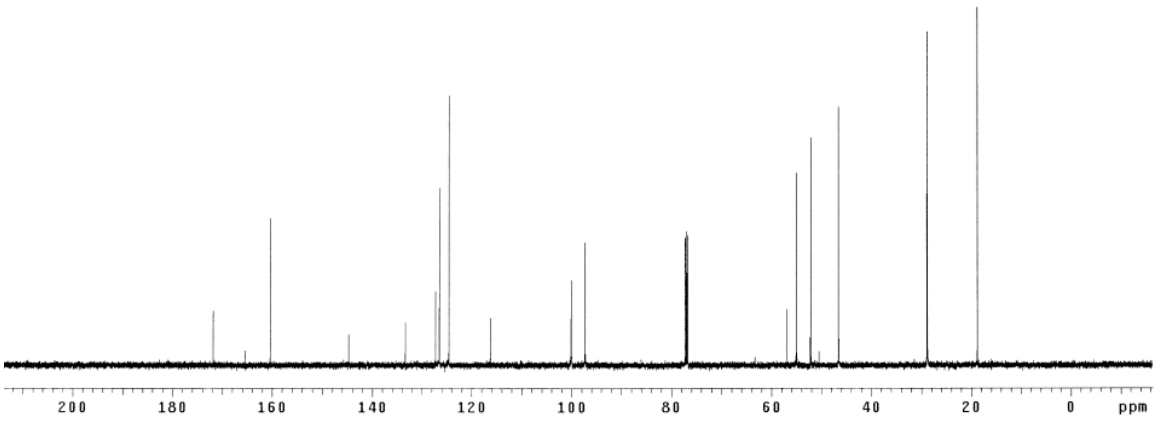

^{13}C NMR ($CDCl_3$)

3-(*tert*-Butyldimethylsilyloxy)aniline (195)

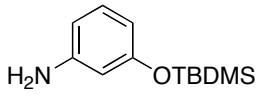

To a solution of 3-aminophenol (10 g, 0.092 mol) and TBDMSCl (15.2 g, 0.10 mol) in CH_2Cl_2 (150 mL) was added Et_3N (14.0 mL, 0.10 mol) and DMAP (1.1 g, 0.009 mol) at 0 ºC. The reaction was warmed to room temperature and stirred at 25 ºC for 16 h. Water (150 mL) was added to a reaction mixture and the aqueous layer was extracted with CH_2Cl_2 (3 x 150 mL). The combined organic layer was dried over Na_2SO_4 and concentrated under the reduced pressure. The residual material was purified by flash chromatography eluting with 10 to 30 % EtOAc/hexanes to afford product as a colorless oil (20.1 g, 98 %, 95 % purity). R_f 0.7 (20 % EtOAc/hexanes). ^{1}H NMR (500 MHz, $CDCl_3$) δ 7.00 (t, 1H, J = 8.0 Hz), 6.33-6.30 (m, 1H), 6.28-6.26 (m, 1H), 6.22-6.21 (m, 1H), 0.98 (s, 9H), 0.19 (s, 6H); ^{13}C NMR (125 MHz, $CDCl_3$) δ 156.6, 147.3, 129.9, 110.6, 108.6, 107.2, 25.6, 18.1, -4.4; MS (ESI) m/z 224.14 $(M+H)^+$.

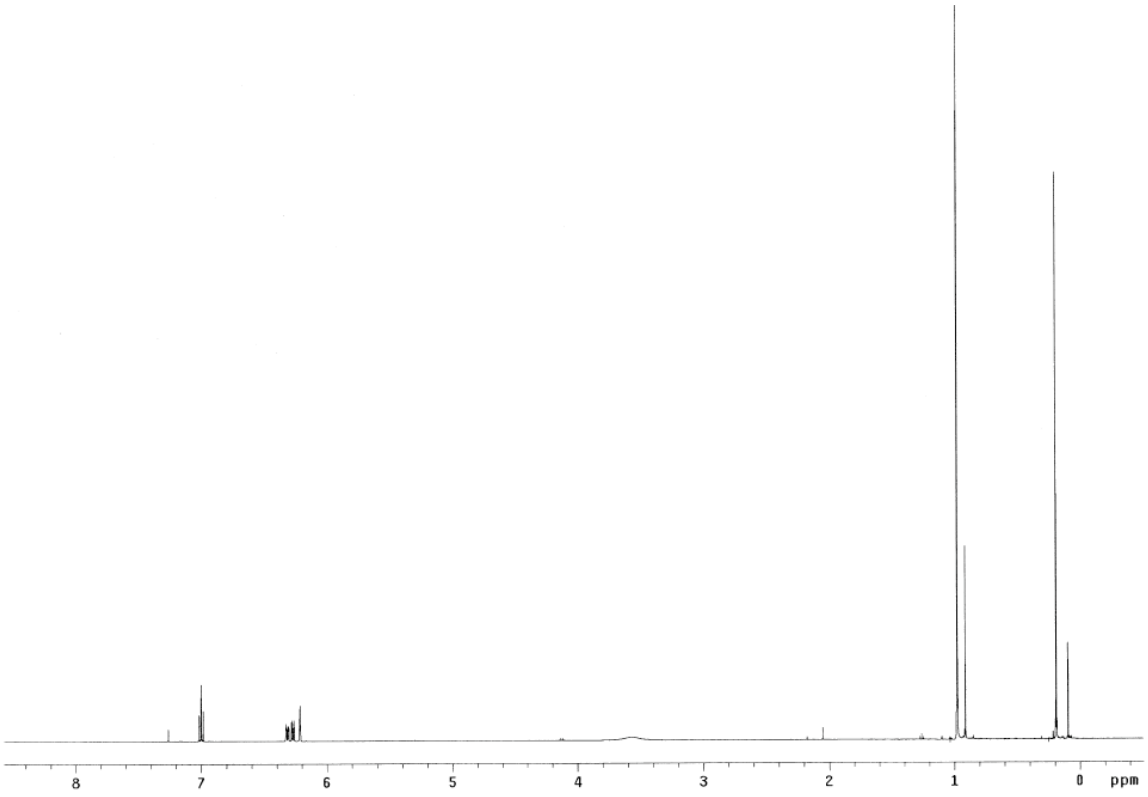

^{1}H NMR ($CDCl_3$)

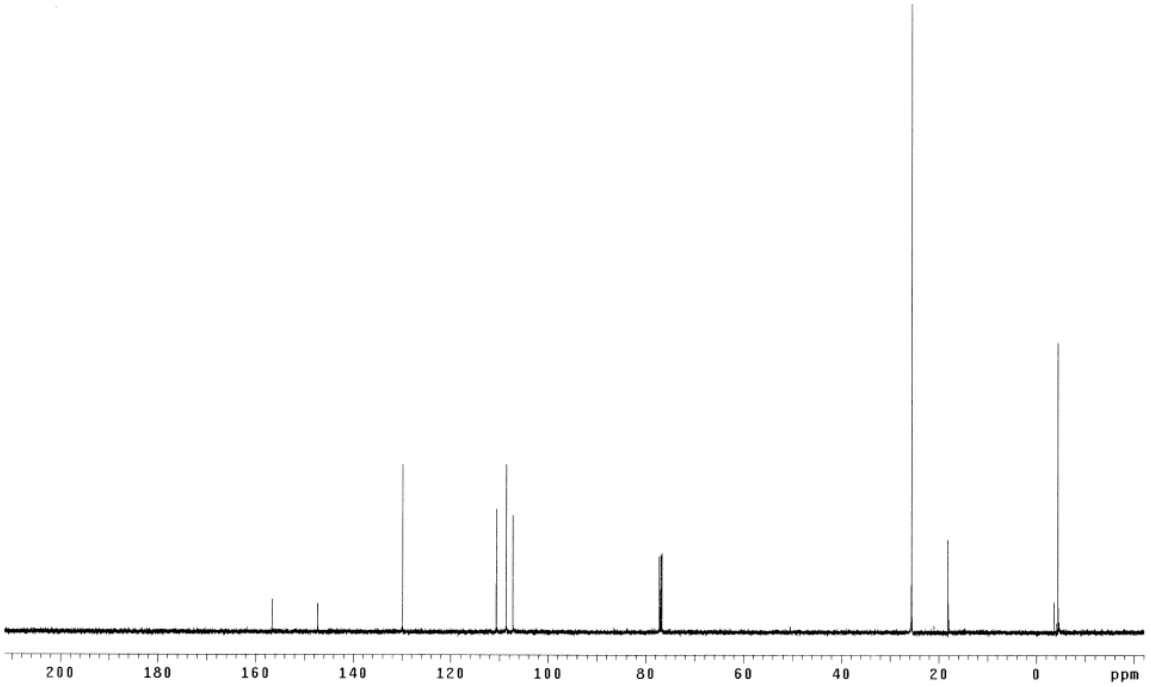

^{13}C NMR ($CDCl_3$)

Silylated, dihydroquinoline (196)

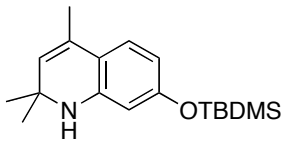

A solution of TBDMS-protected 3-aminophenol **195** (17.3 g, 77.4 mmol) and iodine (688 mg, 27.1 mmol) in acetone (300 mL) was stirred at 25 ºC for 27 h. The solvent was evaporated under the reduced pressure at 35 ºC and the residual material was purified by flash chromatography eluting with 100 % hexanes and 3 to 4 % EtOAc/hexanes to afford product as a brown oil (13.7 g, 58 %). R_f 0.9 (10 % EtOAc/hexanes). ^{1}H NMR (500 MHz, $CDCl_3$) δ 6.91 (d, 1H, J = 8.0 Hz), 6.14 (dd, 1H, J = 8.0, 2.5 Hz), 5.98 (d, 1H, J = 2.5 Hz), 5.19 (s, 1H), 1.96 (s, 3H), 1.26 (s, 6H), 0.98 (s, 9H), 0.19 (s, 6H); ^{13}C NMR (125 MHz, $CDCl_3$) δ 156.3, 144.8, 128.6, 126.3, 124.7, 116.1, 109.1, 104.9, 52.1, 31.1, 26.0, 18.8, 18.4, -4.1; MS (ESI) m/z 304.21 $(M+H)^+$.

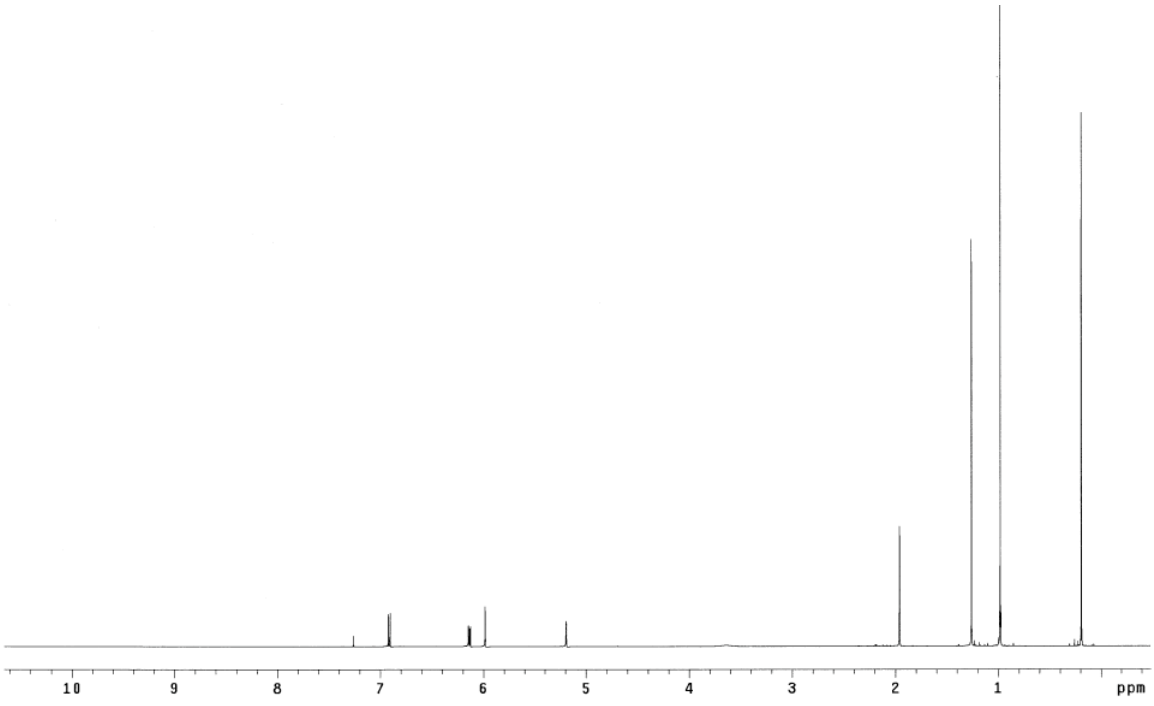

^{1}H NMR ($CDCl_3$)

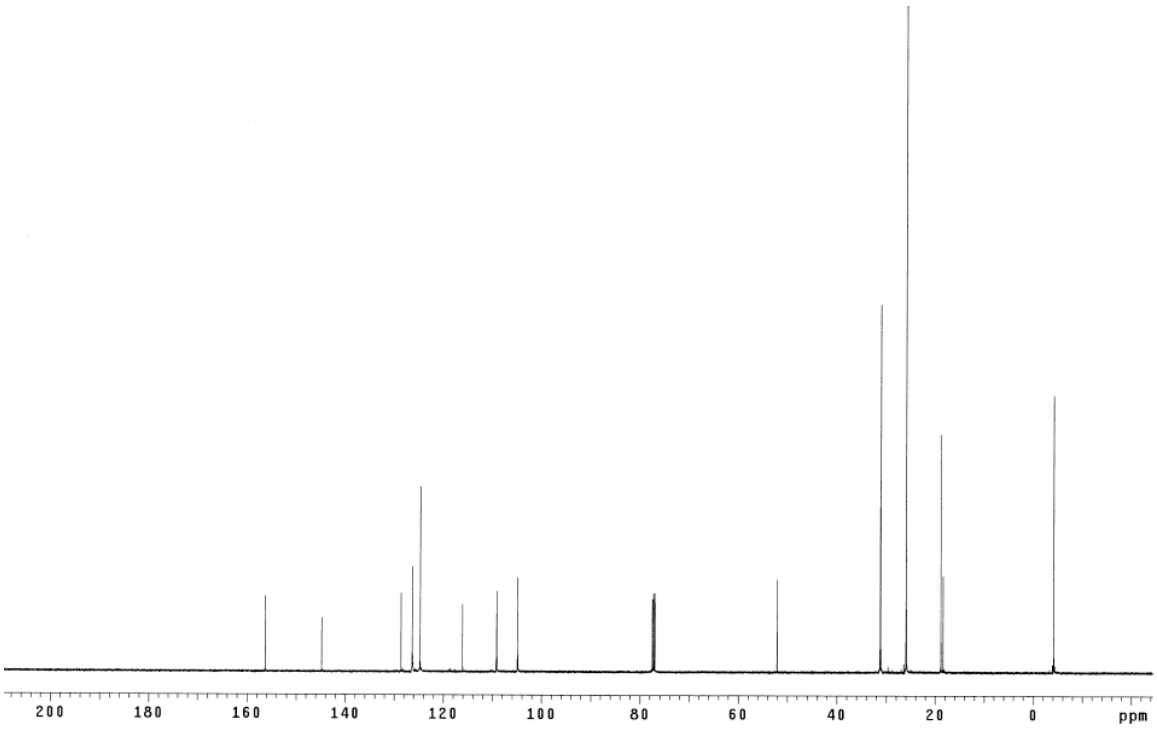

^{13}C NMR ($CDCl_3$)

_N_-Alkylate dihydroquinoline (197)

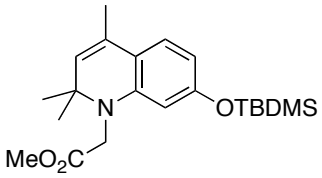

A solution of TBDMS-protected dihydroquinoline **196** (3.0 g, 9.88 mmol), Cs_2CO_3 (16.1 g, 49.4 mmol), methyl bromoacetate (10.6 g, 69.2 mmol), and *tetra*-n-butylammonium iodide (4.7 g, 12.8 mmol) in CH_3CN (50.0 mL) was refluxed at 93 ºC for 13 h. After cooling to room temperature, the reaction mixture was filtered and washed with acetone and then the solvent was evaporated. The residual material was purified by flash chromatography eluting with 100 % hexanes and 2 % EtOAc/hexanes to afford product as a yellow oil (3.3 g, 89 %). R_f 0.4 (10 % EtOAc/hexanes). ^{1}H NMR (500 MHz, $CDCl_3$) δ 6.91 (d, 1H, J = 8.0 Hz), 6.13 (dd, 1H, J = 8.0, 2.0 Hz), 5.76 (d, 1H, J = 2.0 Hz), 5.12 (s, 1H), 3.96 (s, 2H), 3.73 (s, 3H), 1.94 (s, 3H), 1.31 (s, 6H), 0.96 (s, 9H), 0.16 (s, 6H); ^{13}C NMR (125 MHz, $CDCl_3$) δ 171.9, 156.4, 144.6, 127.4, 126.4, 124.5, 116.4, 107.8, 102.4, 57.0, 52.1, 46.6, 28.9, 25.7, 18.8, 18.2, -4.5; MS (ESI) m/z 376.22 $(M+H)^+$.

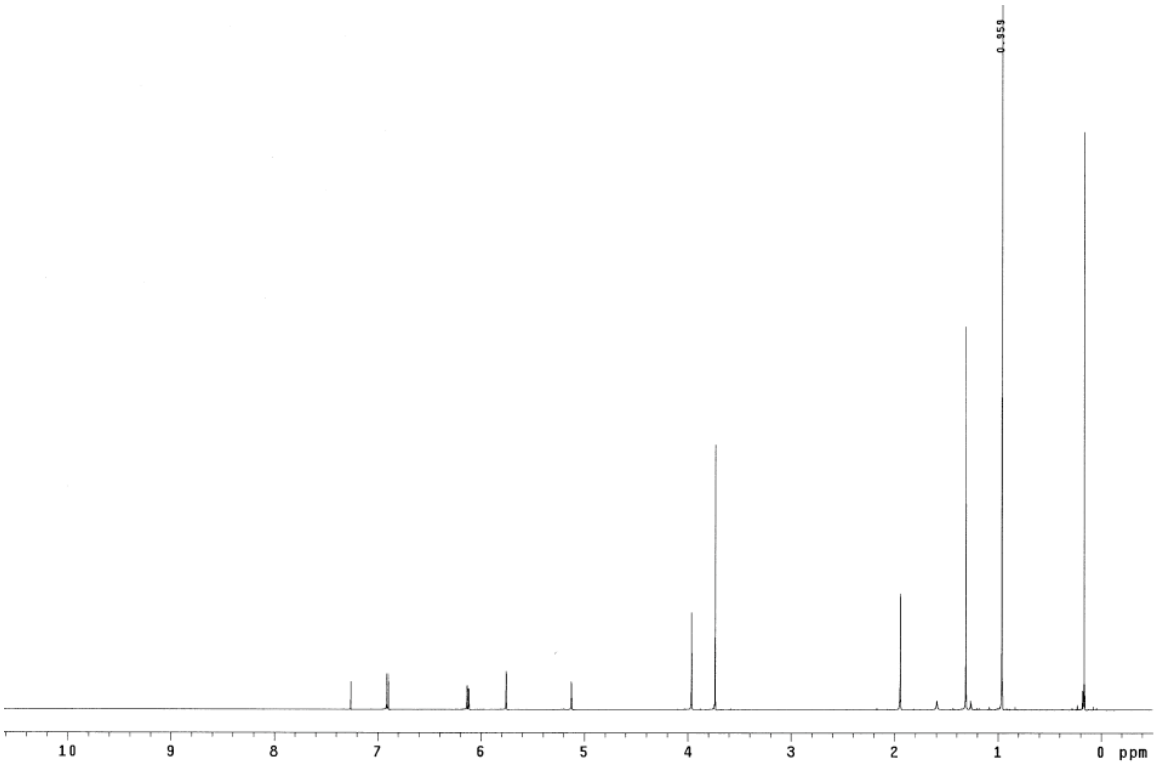

^{1}H NMR ($CDCl_3$)

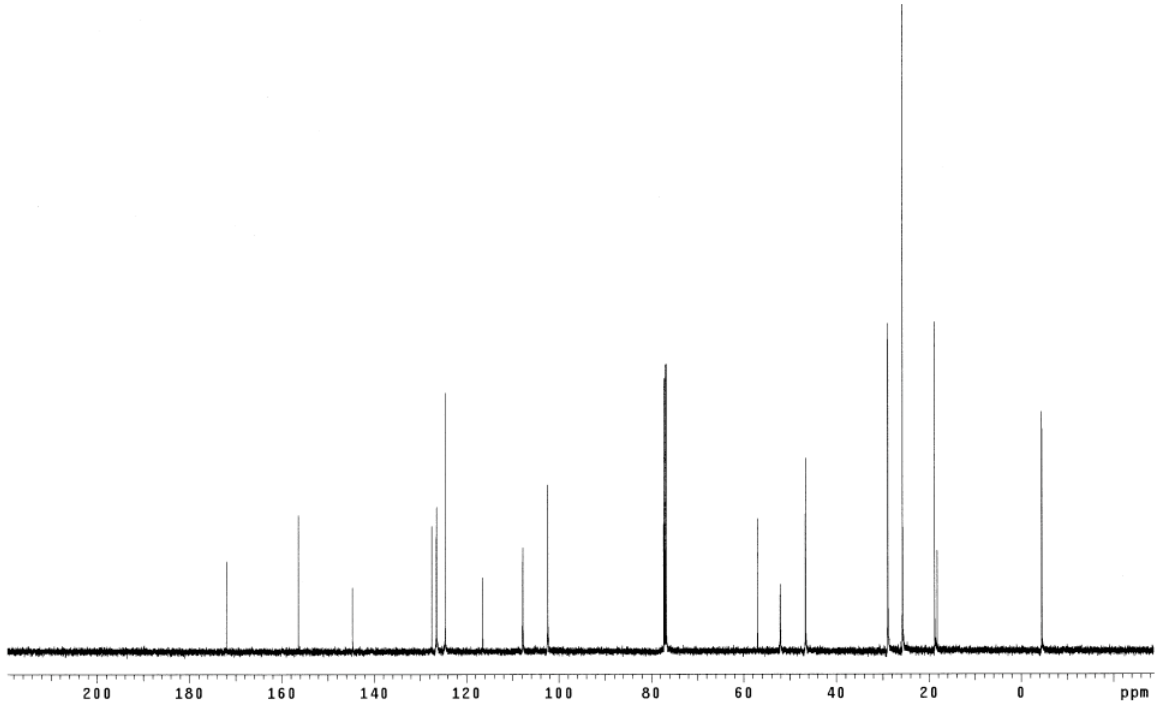

^{13}C NMR ($CDCl_3$)

_N_-Alkylated dihydroquinoline (198)

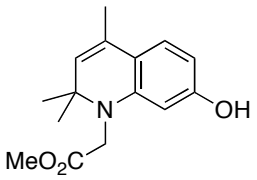

A solution of TBDMS-protected dihydroquinoline **197** (716 mg, 1.91 mmol) and Cs_2CO_3 (621 mg, 1.91 mmol) in 10:1 DMF/H_2O (2.0 mL/0.2 mL) was stirred at 25 ºC for 12 h. The reaction mixture was diluted with Et_2O (15 mL) and the organic layer was washed with brine (1 x 5 mL). This aqueous layer was back-extracted with Et_2O (1 x 5 mL) and EtOAc (3 x EtOAc). The combined organic layer was dried over Na_2SO_4 and concentrated under the reduced pressure. The residual material was purified by flash chromatography eluting with 100 % hexanes and 10 to 20 % EtOAc/hexanes to afford product as a yellow oil (493 mg, 99 %). R_f 0.5 (40 % EtOAc/hexanes). ^{1}H NMR (500 MHz, $CDCl_3$) δ 6.91 (d, 1H, J = 8.0 Hz), 6.11 (dd, 1H, J = 8.0, 2.0 Hz), 5.78 (d, 1H, J = 2.0 Hz), 5.36 (bs, 1H), 5.12 (s, 1H), 3.99 (s, 2H), 3.74 (s, 3H), 1.94 (s, 3H), 1.31 (s, 6H); ^{13}C NMR (125 MHz, $CDCl_3$) δ 172.3, 156.5, 145.0, 127.3, 126.1, 124.9, 115.9, 102.9, 97.5, 57.0, 52.3, 46.6, 28.9, 18.8; MS (APCI) m/z 262.14 $(M+H)^+$.

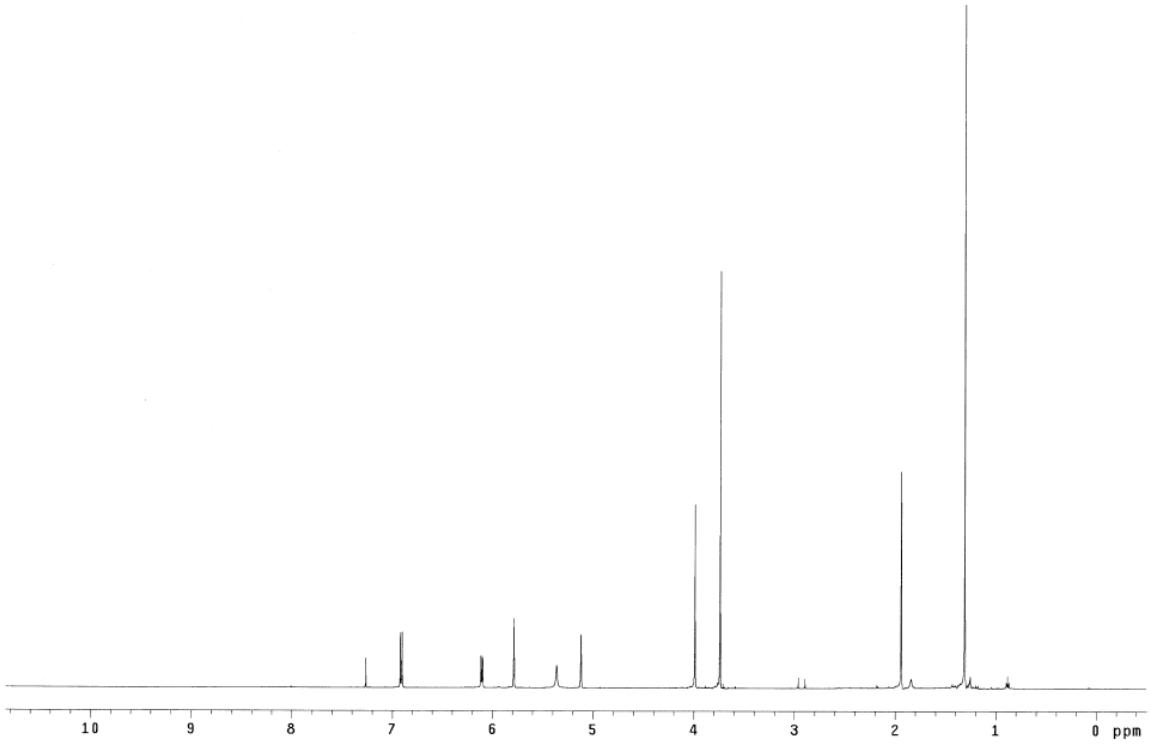

^{1}H NMR ($CDCl_3$)

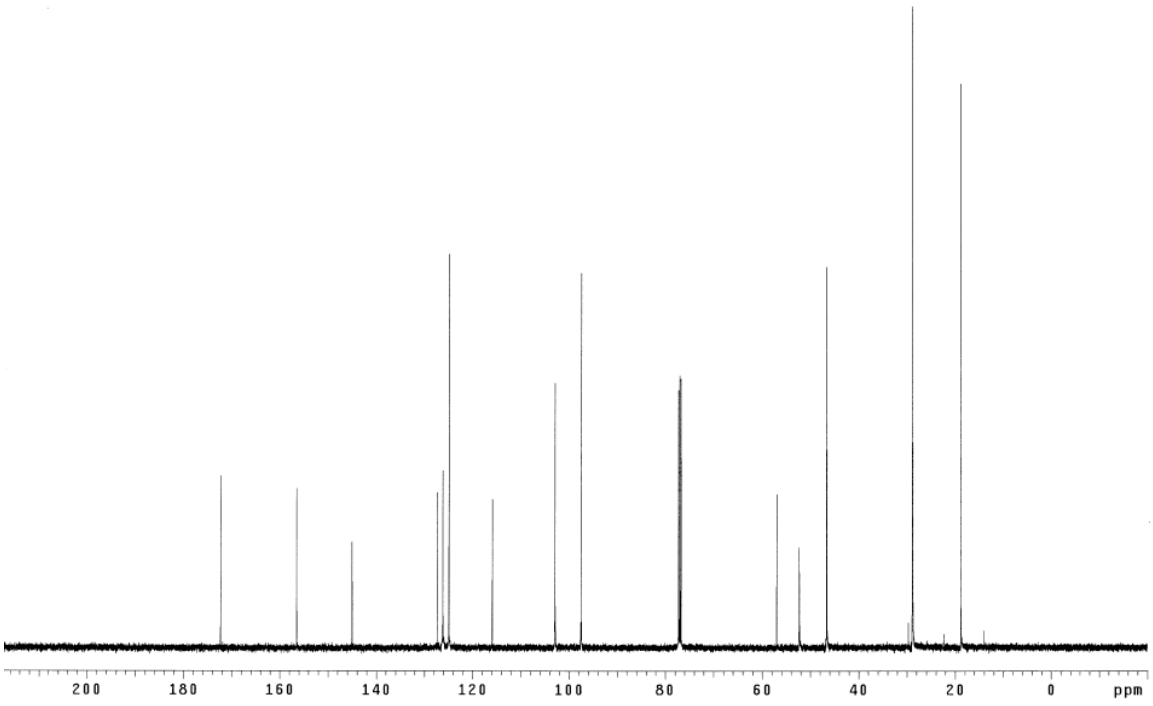

^{13}C NMR ($CDCl_3$)

p-Methoxybenzyl hexaethylene glycol (200)[58]

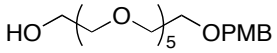

To a solution of hexaethylene glycol (4.3 g, 15.2 mmol), Ag_2O (5.29 g, 22.8 mmol) and potassium iodide (1.52 g, 9.14 mmol) in toluene (40 mL) was added *p*-methoxybenzyl chloride (2.62 g, 16.8 mmol) dropwise at 25 ºC. The reaction mixture was refluxed at 120 ºC for 22 h. After cooling to room temperature, the reaction was filtered through celite and washed with EtOAc. The solvent was evaporated and the residual material was purified by flash chromatography eluting with 50 % EtOAc/hexanes, 100 % EtOAc and 50 % acetone/EtOAc to afford product as a yellow oil (3.68 g, 60 %). R_f 0.1 (100 % EtOAc with iodine stain). ^{1}H NMR (500 MHz, $CDCl_3$) δ 7.25 (d, 2H, J = 8.5 Hz), 6.85 (d, 2H, J = 8.5 Hz), 4.48 (s, 2H), 3.79 (s, 3H), 3.79-3.69 (m, 2H), 3.67-3.64 (m, 18H), 3.60-3.57 (m, 4H); ^{13}C NMR (125 MHz, $CDCl_3$) δ 159.1, 130.2, 129.3, 113.7, 72.8, 72.5, 70.6, 70.53, 70.51 (3C), 70.49 (2C), 70.46, 70.3, 69.0, 61.7, 55.2; MS (ESI) m/z 409.24 $(M+Li)^+$.

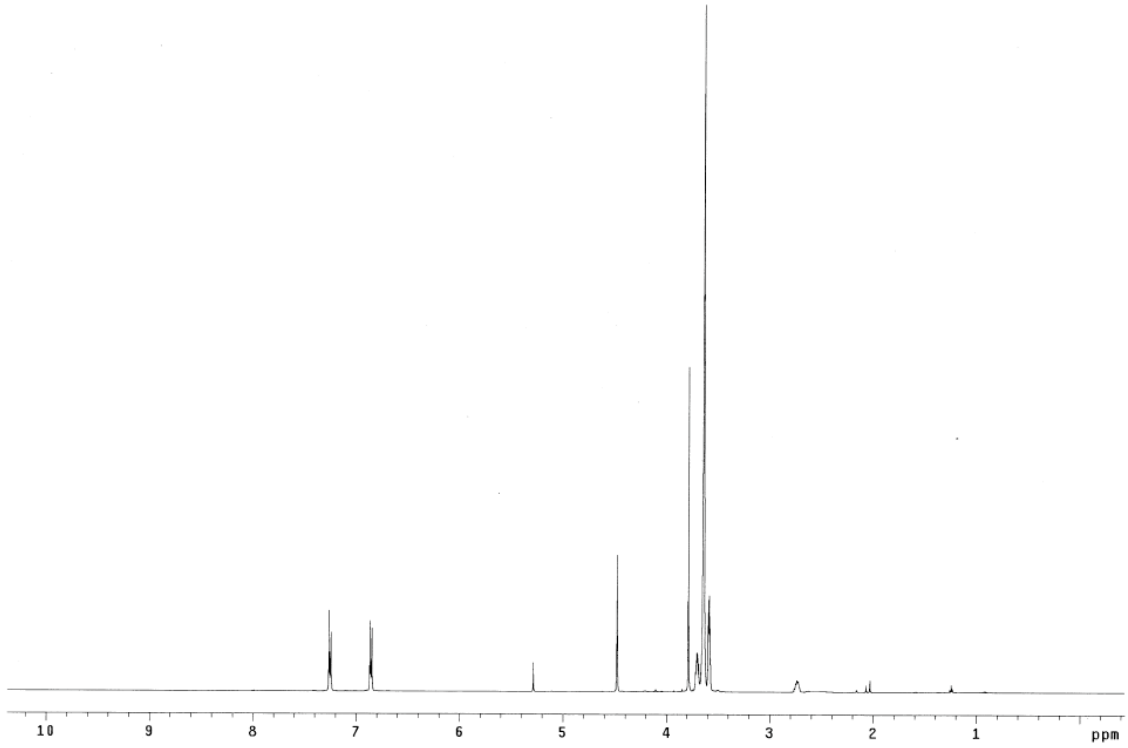

^{1}H NMR ($CDCl_3$)

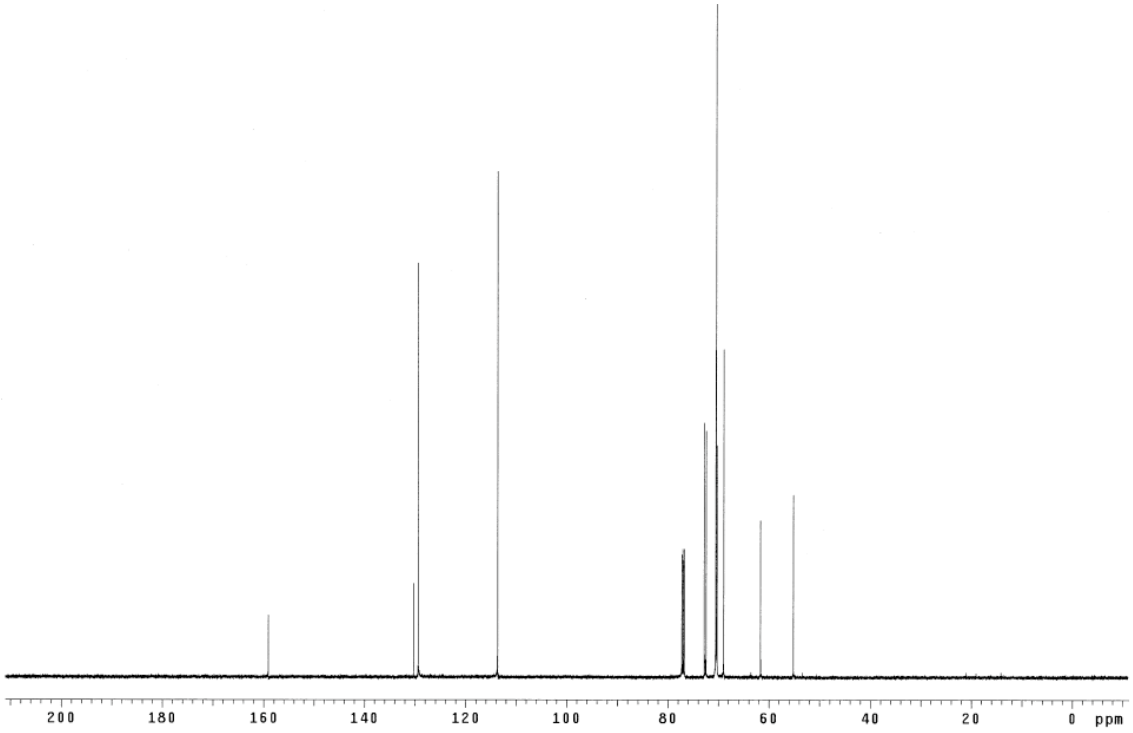

^{13}C NMR ($CDCl_3$)

Propargylated hexaethylene glycol (201)

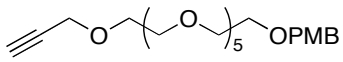

Sodium hydride (278 mg, 6.96 mmol, 60 % in mineral oil) was slowly added to a solution of mono-PMB-protected hexaethylene glycol **200** (2.0 g, 4.97 mmol) in THF (15 mL) at 0 ºC. The reaction was stirred at 0 ºC for 30 min, then propargyl bromide (1.1 g, 7.45 mmol, 80 % w/w in toluene) was added dropwise. After the stirring at 0 ºC for 30 min, the reaction mixture was warmed to room temperature and stirred at 25 ºC for additional 6 h. MeOH (1 mL) was added carefully at 0 ºC and water (5 mL) was added. The aqueous layer was extracted with CH_2Cl_2 (5 x 20 mL) and the combined organic layer was dried over $MgSO_4$ and concentrated under the reduced pressure. The residue was purified by flash chromatography eluting with 50 % EtOAc/hexanes and 100 % EtOAc to afford product as a yellow oil (1.81 g, 83 %). R_f 0.5 (100 % EtOAc with iodine stain). ^{1}H NMR (500 MHz, $CDCl_3$) δ 7.26 (d, 2H, J = 8.5 Hz), 6.87 (d, 2H, J = 8.5 Hz), 4.49 (s, 2H), 4.20 (d, 2H, J = 2.5 Hz), 3.80 (s, 3H), 3.70-3.64 (m, 22H), 3.60-3.58 (m, 2H), 2.43 (t, 1H, J = 2.5 Hz); ^{13}C NMR (125 MHz, $CDCl_3$) δ 159.1, 130.3, 129.4, 113.7, 79.6, 74.5, 72.8, 70.6, 70.57 (2C), 70.54 (6C), 70.4, 69.1, 69.0, 58.4, 55.2; MS (ESI) m/z 447.26 $(M+Li)^+$.

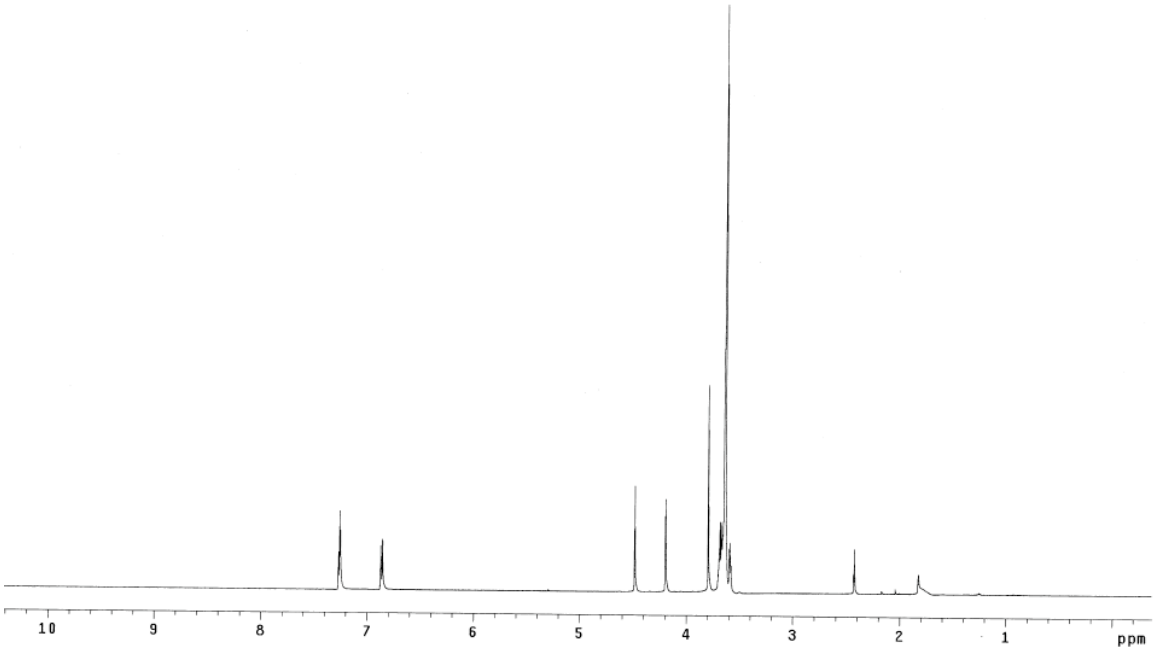

^{1}H NMR ($CDCl_3$)

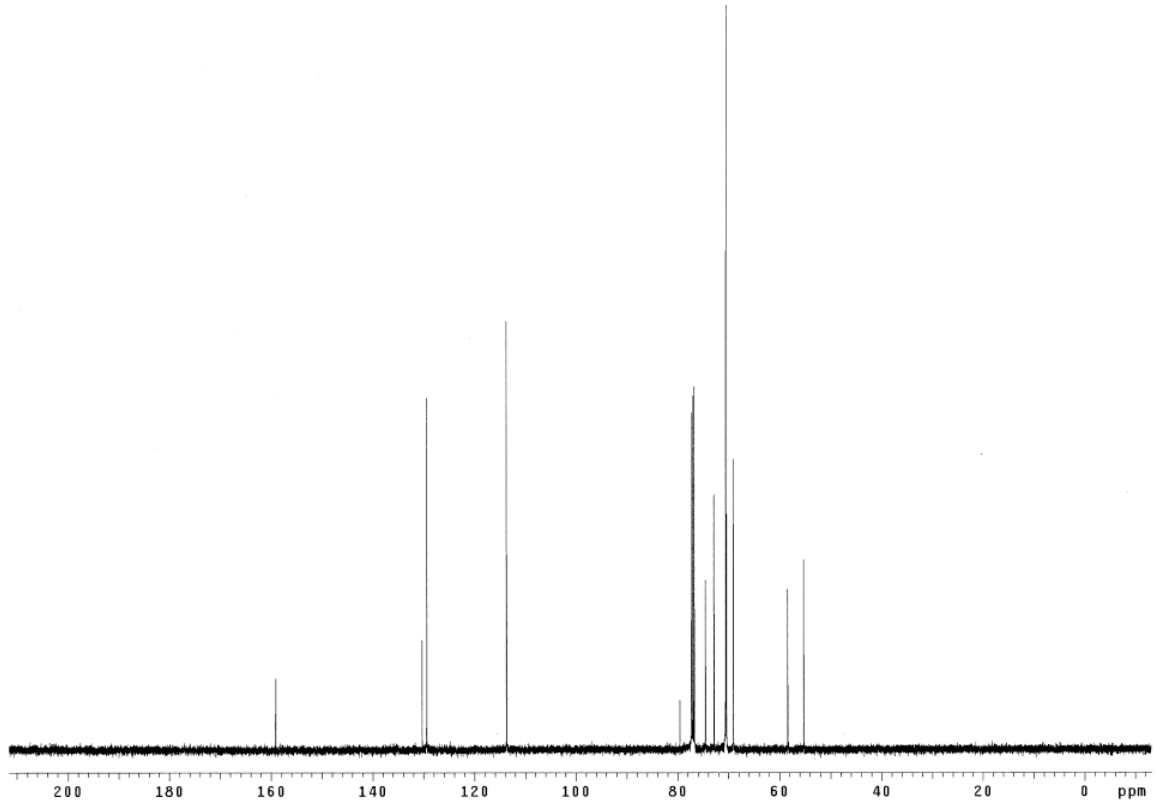

^{13}C NMR ($CDCl_3$)

Triazole-decorated oligoethylene glycol (202)

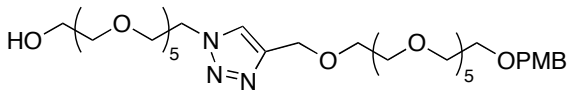

Copper powder (244 mg, 3.84 mmol), $CuSO_4$ (0.77 mL, 0.77 mmol, 1M in H_2O) and H_2O (12 mL) were added to a solution of hexaethylene glycol mono-azide **25** (1.18 g, 3.84 mmol) and propargylated hexaethylene glycol **201** (2.2 g, 4.99 mmol) in THF (12 mL). The reaction mixture was stirred at 25 ºC for 24 h under nitrogen. The solvents were evaporated under the reduced pressure and the residual material was purified by flash chromatography eluting with 50 % acetone/EtOAc, 100 % acetone and 5 to 10 % MeOH/CH_2Cl_2 to afford product as a yellow oil (2.7 g, 94 %). R_f 0.2 (50 % acetone/EtOAc with iodine stain). ^{1}H NMR (300 MHz, $CDCl_3$) δ 7.75 (s, 1H), 7.26 (d, 2H, J = 9.0 Hz), 6.86 (d, 2H, J = 9.0 Hz), 4.67 (s, 2H), 4.53 (t, 2H, J = 5.1 Hz), 4.48 (s, 2H), 3.86 (t, 2H, J = 5.1 Hz), 3.79 (s, 3H), 3.73-3.57 (m, 44H); ^{13}C NMR (125 MHz, $CDCl_3$) δ 158.9, 144.6, 130.1, 129.2, 123.7, 113.5, 72.6, 72.4, 70.4, 70.32 (8C), 70.26 (8C), 70.0, 69.4, 69.2, 68.8, 64.3, 61.4, 55.1, 50.0; MS (ESI) m/z 748.44 $(M+H)^+$.

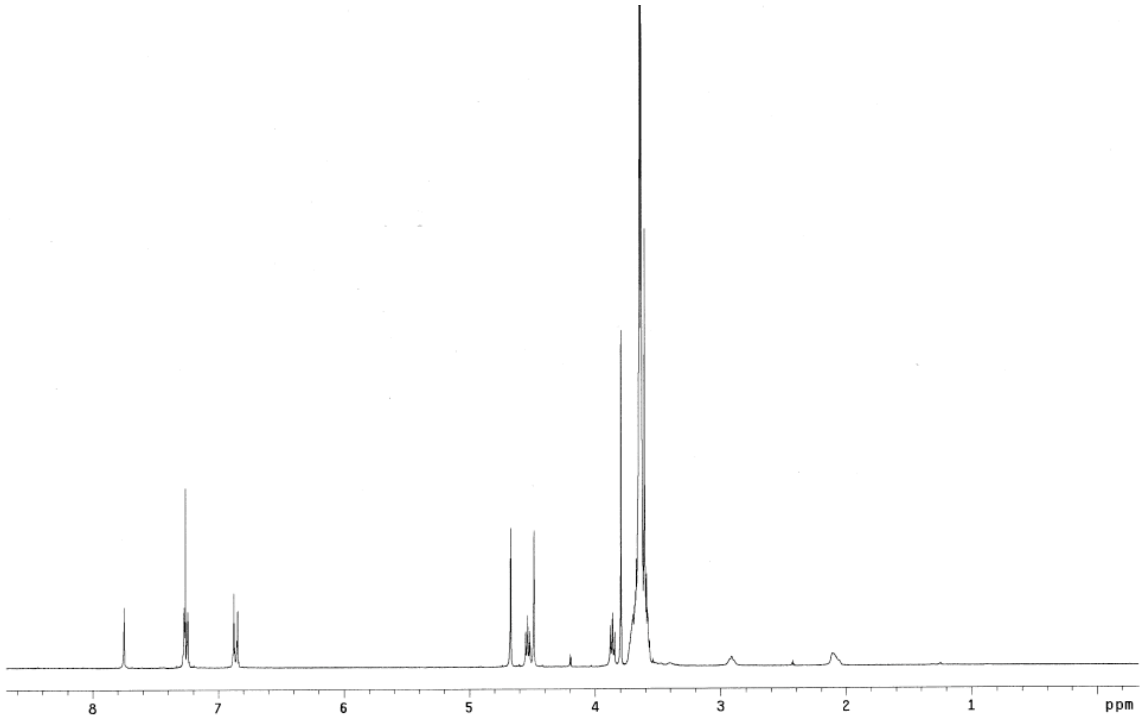

^{1}H NMR ($CDCl_3$)

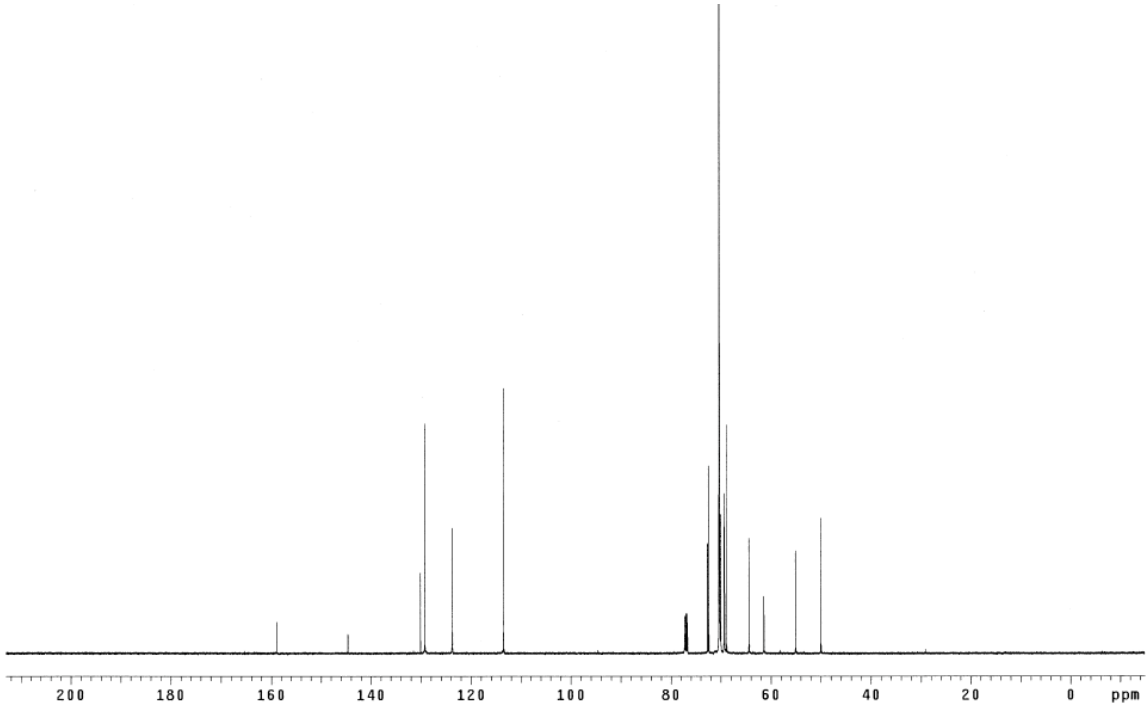

^{13}C NMR ($CDCl_3$)

Triazole-decorated oligoethylene glycol (203)

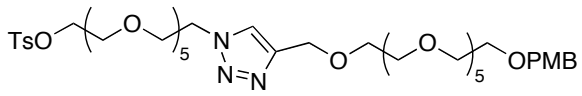

Triazole-decorated oligoethylene glycol **202** (1.5 g, 2.01 mmol), Et_3N (0.56 mL, 4.01 mmol) and Me_3N•HCl (19 mg, 0.20 mmol) were added in CH_3CN (20 mL) at 0 ºC. A solution of TsCl (574 mg, 3.01 mmol) in CH_3CN (12 mL) was then added by syringe and the reaction mixture was stirred at 0 ºC for 10 min and 12 h at 25 ºC. The reaction was quenched with water (12 mL) and the aqueous layer was extracted with EtOAc (3 x 20 mL). The combined organic layer was dried over $MgSO_4$ and solvents were concentrated under the reduced pressure. The residue was purified by flash chromatography eluting with 50 % acetone/EtOAc and then 100 % acetone to afford product as a brown oil (1.6 g, 89 %). R_f 0.3 (50 % acetone/EtOAc with iodine stain). ^{1}H NMR (300 MHz, $CDCl_3$) δ 7.74 (d, 2H, J = 8.0 Hz), 7.72 (s, 1H), 7.30 (d, 2H, J = 8.0 Hz), 7.22 (d, 2H, J = 9.0 Hz), 6.82 (d, 2H, J = 9.0 Hz), 4.62 (s, 2H), 4.48 (t, 2H, J = 5.0 Hz), 4.44 (s, 2H), 4.10 (t, 2H, J = 5.0 Hz), 3.82 (t, 2H, J = 5.0 Hz), 3.75 (s, 3H), 3.65-3.53 (m, 42H), 2.40 (s, 3H); ^{13}C NMR (125 MHz, $CDCl_3$) δ 158.9, 144.7, 132.7, 130.1, 129.7, 129.2, 127.8, 123.7, 113.5, 72.7, 70.5, 70.43, 70.39, 70.37, 70.34 (10C), 70.28 (3C), 70.25, 69.4, 69.3, 69.1, 68.9, 68.5, 64.4, 55.1, 50.0, 21.5 (1 carbon is missing for aromatic region); MS (ESI) m/z 902.45 $(M+H)^+$.

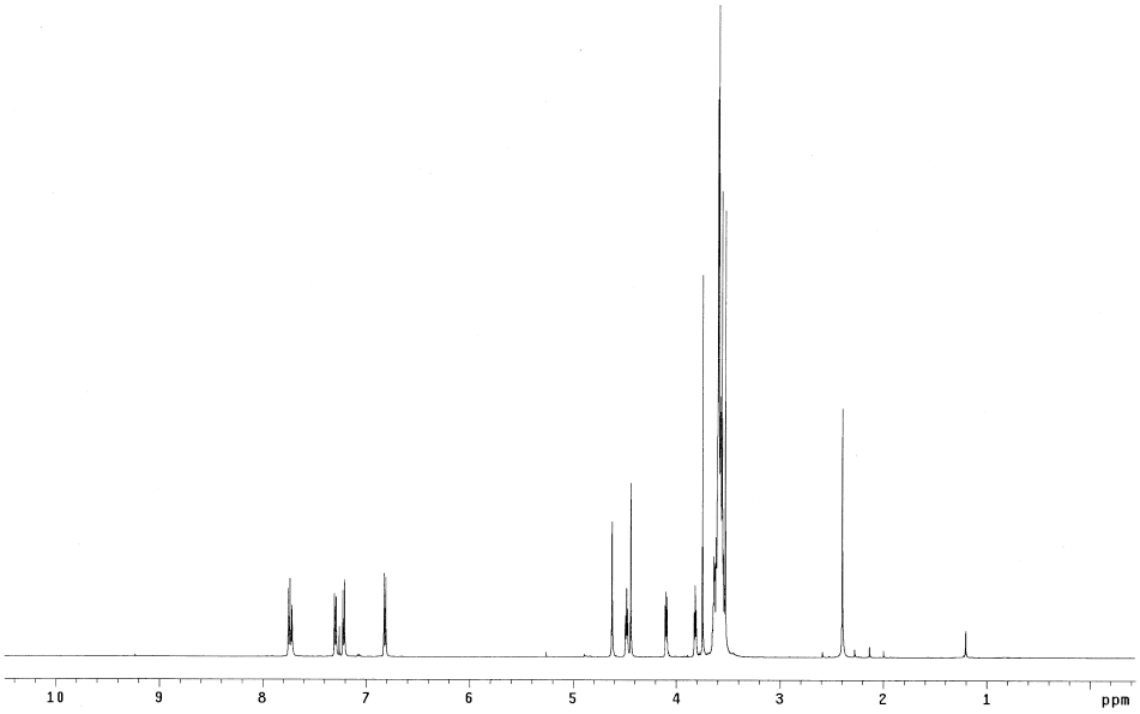

^{1}H NMR ($CDCl_3$)

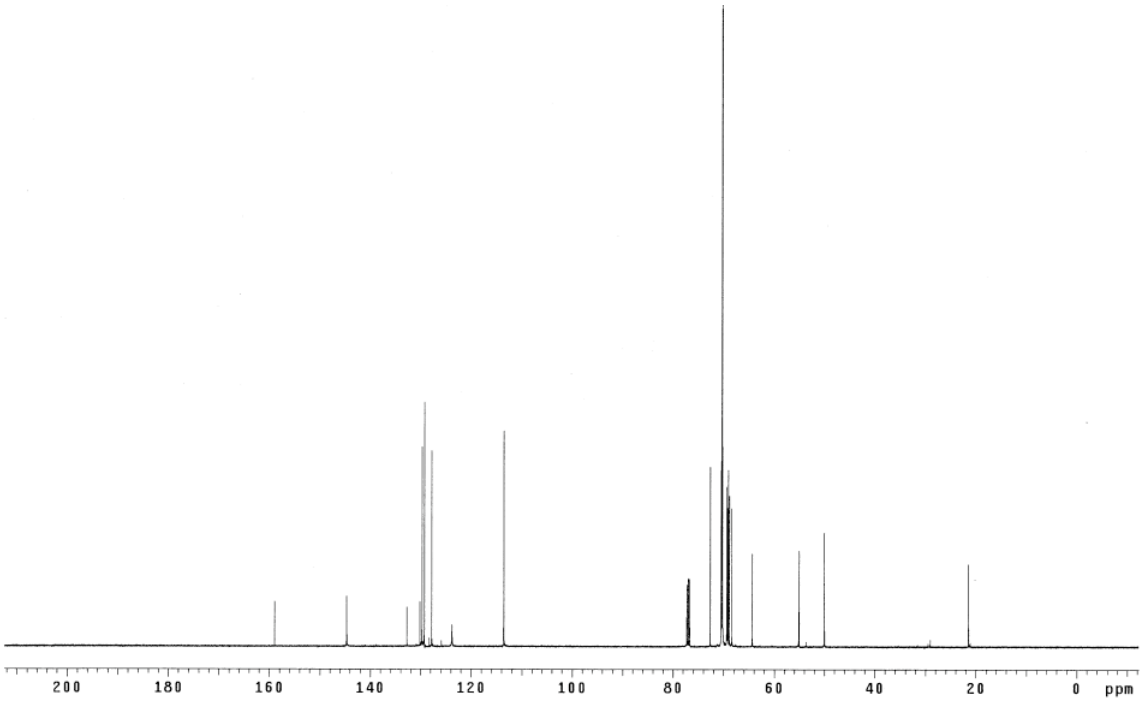

^{13}C NMR ($CDCl_3$)

Silylated, aminonaphthol (204)

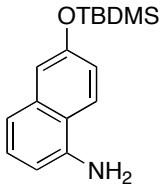

To a solution of 5-amino-2-naphthol (1.0 g, 6.28 mmol) and TBDMSCl (1.04 g, 6.91 mmol) in DMF (7.0 mL) was added DMAP (77 mg, 0.63 mmol) and imidazole (470 mg, 6.91 mmol) at 0 ºC. The reaction mixture was stirred at 25 ºC for 24 h. Water (15 mL) was added to a reaction mixture and the aqueous layer was extracted with EtOAc (3 x 5 mL). The combined organic layer was dried over $MgSO_4$ and concentrated under the reduced pressure. The residual material was purified by flash chromatography eluting with 100 % hexanes and 10 % EtOAc/hexanes to afford product as a brown oil (1.47 g, 85 %). R_f 0.8 (50 % EtOAc/hexanes). ^{1}H NMR (300 MHz, $CDCl_3$) δ 7.75 (d, 1H, J = 9.0 Hz), 7.31-7.28 (m, 1H), 7.23-7.21 (m, 2H), 7.10 (dd, 1H, J = 9.0, 2.4 Hz), 6.69 (dd, 1H, J = 7.2, 1.5 Hz), 1.08 (s, 9H), 0.31 (s, 6H); ^{13}C NMR (75 MHz, $CDCl_3$) δ 153.5, 142.1, 135.8, 126.8, 122.3, 120.7, 119.4, 117.9, 115.6, 107.9, 25.7, 18.3, -4.4; MS (ESI) m/z 274.17 $(M+H)^+$.

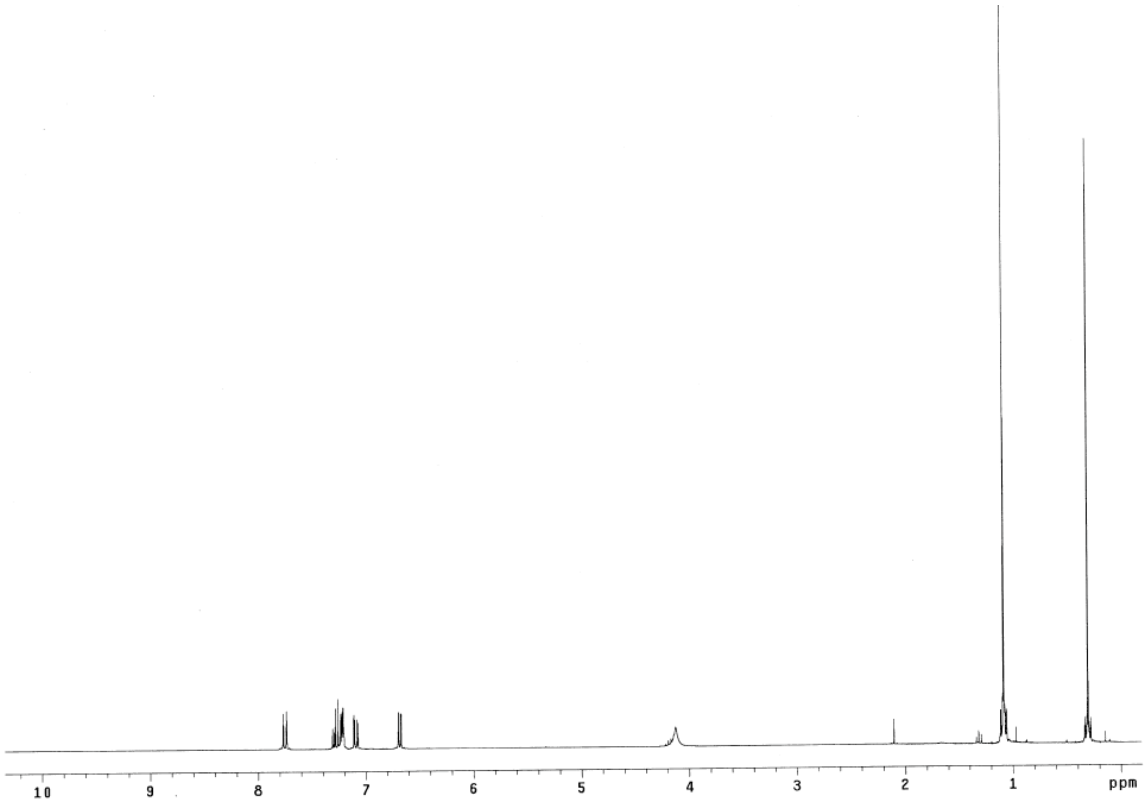

^{1}H NMR ($CDCl_3$)

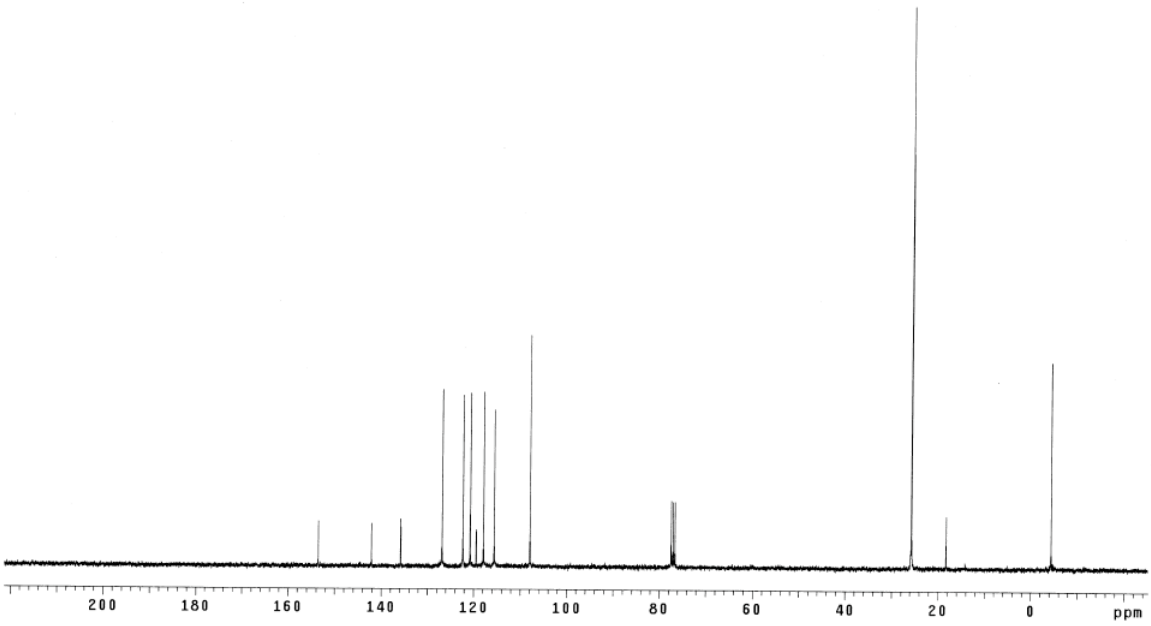

^{13}C NMR ($CDCl_3$)

_N_-Alkylated aminonaphthol (205)

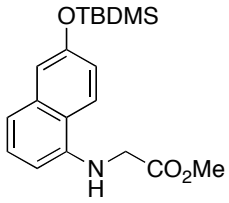

A solution of TBDMS-protected 5-amino-2-naphthol **204** (1.19 g, 4.35 mmol), K_2CO_3 (902 mg, 6.53 mmol) and methyl bromoacetate (999 mg, 6.53 mmol in DMF (20 mL) was heated at 90 ºC for 2 h. After cooling to room temperature, the reaction mixture was filtered and washed with acetone and then the solvent was evaporated. The residual material was purified by flash chromatography eluting with 100 % hexanes and 5 to 7 % EtOAc/hexanes to afford product as a light brown solid (1.31 g, 87 %). R_f 0.6 (20 % EtOAc/hexanes). ^{1}H NMR (500 MHz, $CDCl_3$) δ 7.81 (d, 1H, J = 9.0 Hz), 7.31-7.26 (m, 1H), 7.17-7.14 (m, 2H), 7.06 (dd, 1H, J = 9.0, 2.0 Hz), 6.35 (d, 1H, J = 7.5 Hz), 4.07 (s, 2H), 3.84 (s, 3H), 1.03 (s, 9H), 0.25 (s, 6H); ^{13}C NMR (125 MHz, $CDCl_3$) δ 171.6, 153.6, 142.3, 135.7, 126.9, 121.6, 120.7, 119.1, 117.3, 115.8, 102.8, 52.4, 45.8, 25.7, 18.3, -4.4; MS (ESI) m/z 346.17 $(M+H)^+$.

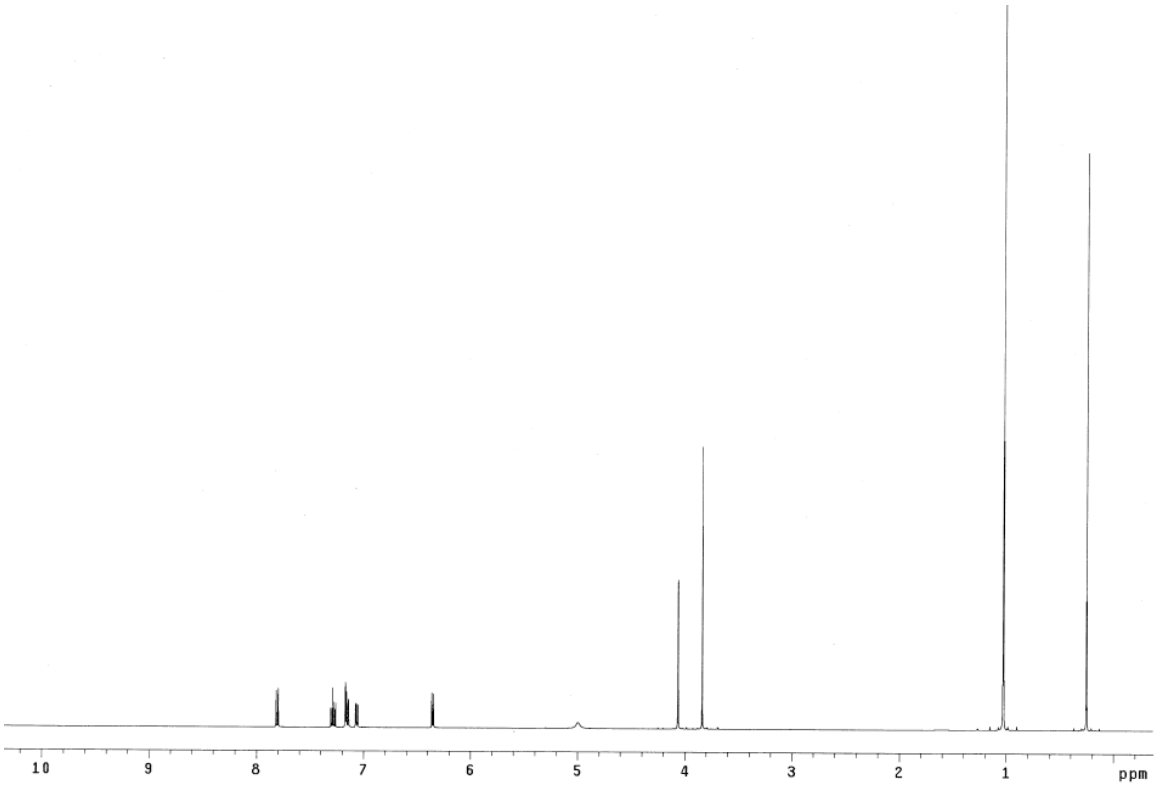

^{1}H NMR ($CDCl_3$)

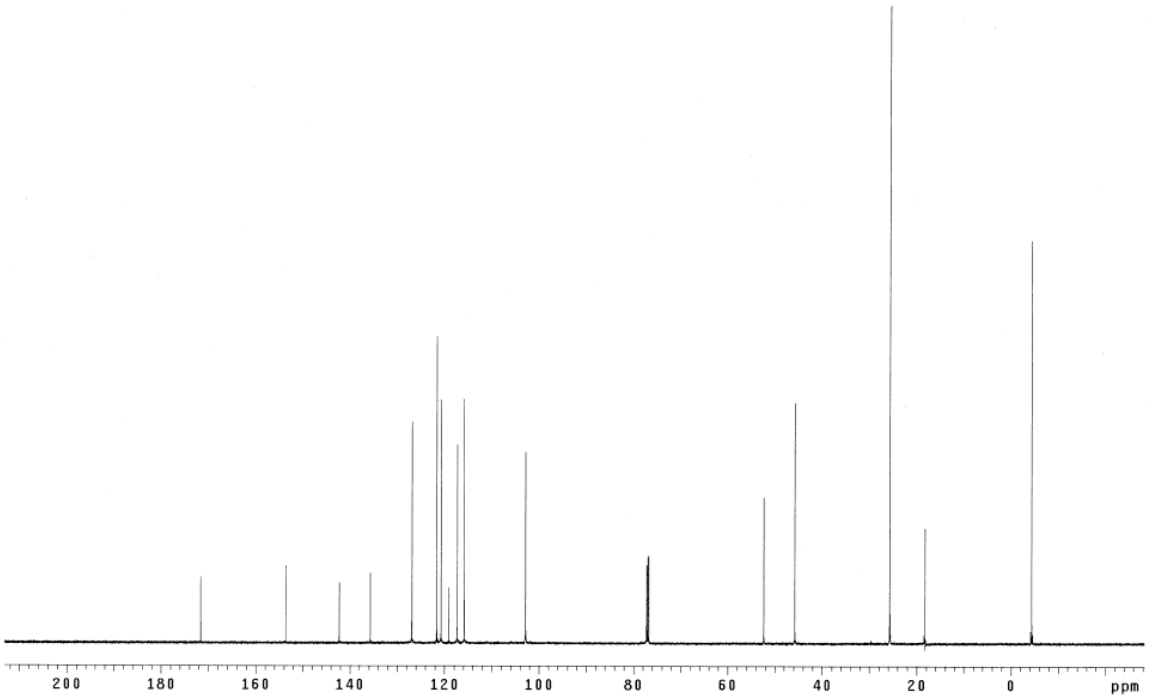

^{13}C NMR ($CDCl_3$)

_N_-Alkylated aminonaphthol (206)

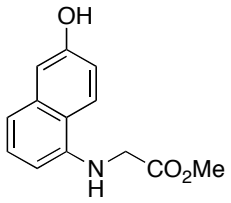

To a solution of *N*-alkylated 5-amino-2-naphthol **205** (600 mg, 1.74 mmol) in THF (20 mL) was added TBAF (1.9 mL, 1.91 mmol, 1 M in THF) dropwise at 0 ºC. The reaction mixture was stirred at 0 ºC for 5 min. The solvent was evaporated at 35 ºC and the residual material was purified by short flash chromatography eluting with 30 to 50 % EtOAc/hexanes to afford product as a yellow solid (327 mg, 81 %). R_f 0.5 (40 % EtOAc/hexanes). ^{1}H NMR (500 MHz, CD_3OD) δ 7.91 (d, 1H, J = 9.0 Hz), 7.19 (t, 1H, J = 8.0 Hz), 7.05-7.02 (m, 3H), 6.26 (d, 1H, J = 7.5 Hz), 4.11 (s, 2H), 3.78 (s, 3H); ^{13}C NMR (125 MHz, CD_3OD) δ 174.0, 156.3, 144.6, 137.6, 127.9, 123.5, 119.8, 117.4 (2C), 110.7, 102.7, 52.5, 46.4; MS (ESI) m/z 232.10 $(M+H)^+$.

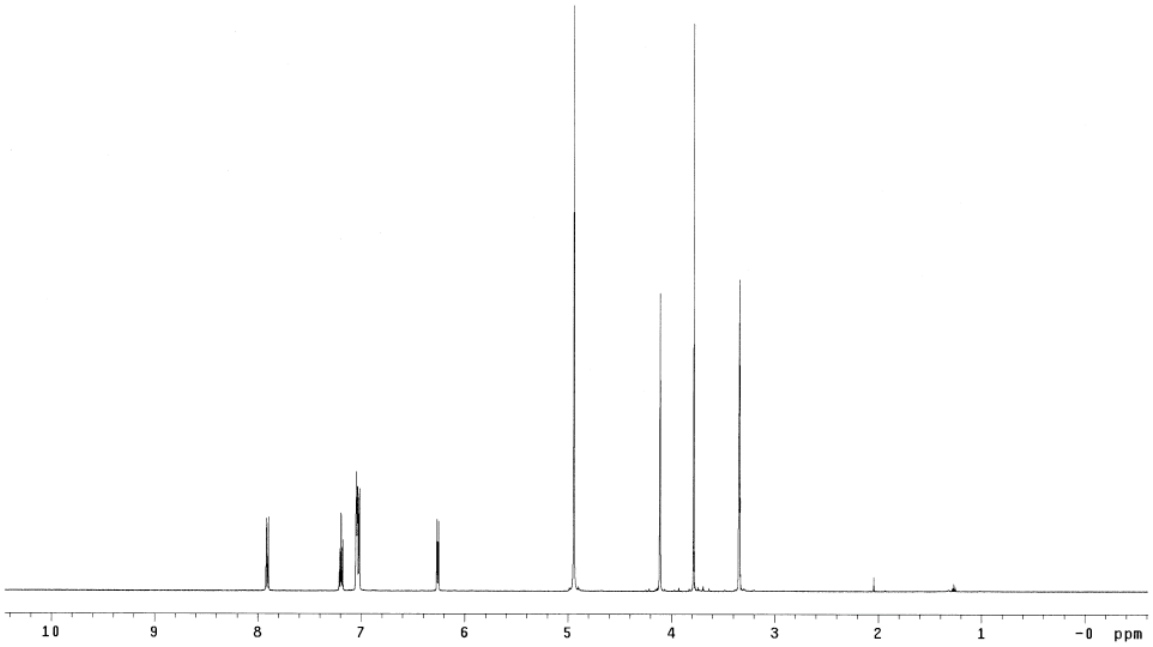

^{1}H NMR (CD_3OD)

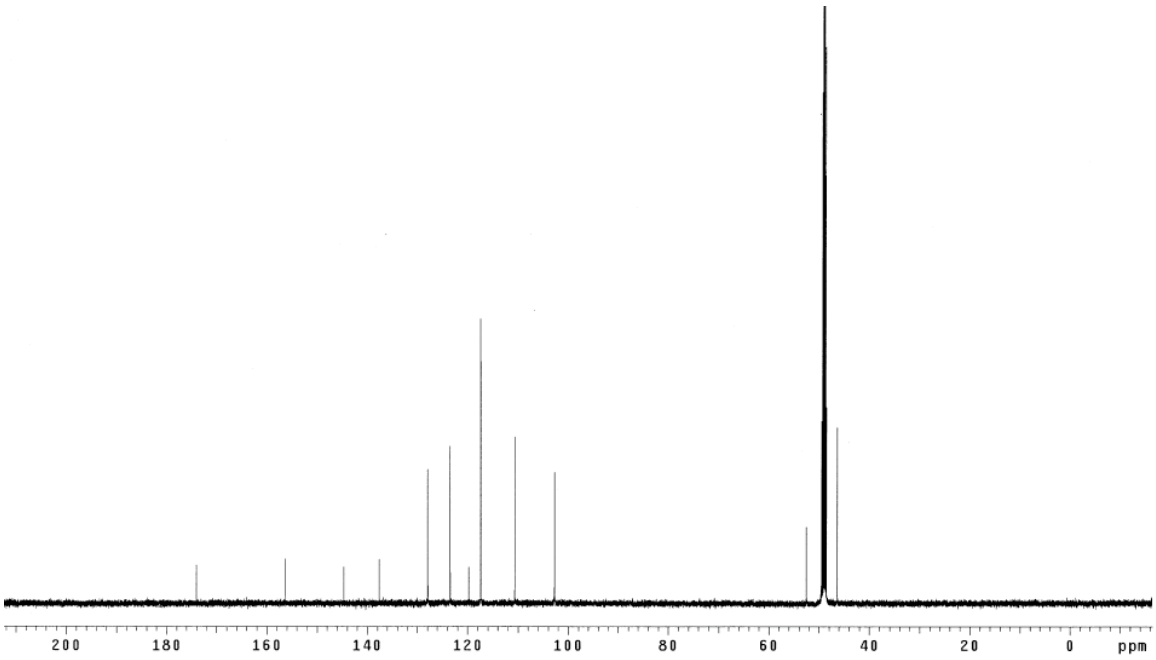

^{13}C NMR (CD_3OD)

5-Methoxy-2-nitrobenzyl bromide (210)

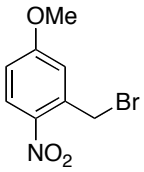

To a solution of 5-methoxy-2-nitrobenzyl alcohol (1.02 g, 5.57 mmol) and PPh_3 (1.75 g, 66.8 mmol) in CH_2Cl_2 (20 mL) was added carbon tetrabromide (2.22 g, 66.8 mmol) at 0 ºC. The reaction mixture was stirred at 25 ºC for 30 h. The solvent was evaporated under the reduced pressure and the residual material was purified by flash chromatography eluting with 100 % hexanes and 5 to 10 % EtOAc/hexanes to afford product as a brown solid (1.29 g, 94 %). R_f 0.7 (30 % EtOAc/hexanes). ^{1}H NMR (500 MHz, $CDCl_3$) δ 8.13 (d, 1H, J = 9.0 Hz), 7.01 (d, 1H, J = 2.5 Hz), 6.91 (dd, 1H, J = 9.0, 2.5 Hz), 4.85 (s, 2H), 3.91 (s, 3H); ^{13}C NMR (125 MHz, $CDCl_3$) δ 163.4, 140.6, 135.6, 128.4, 117.6, 114.0, 56.0, 29.9; MS (CI) m/z 245.2 $(M+H)^+$.

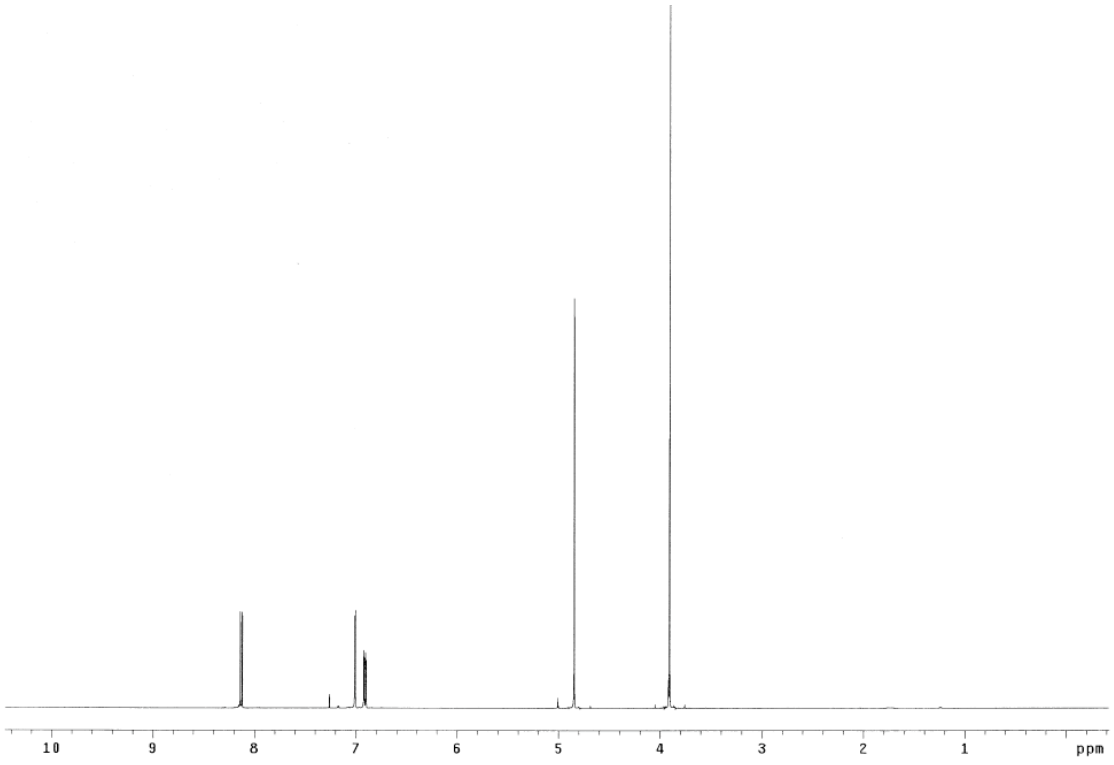

^{1}H NMR ($CDCl_3$)

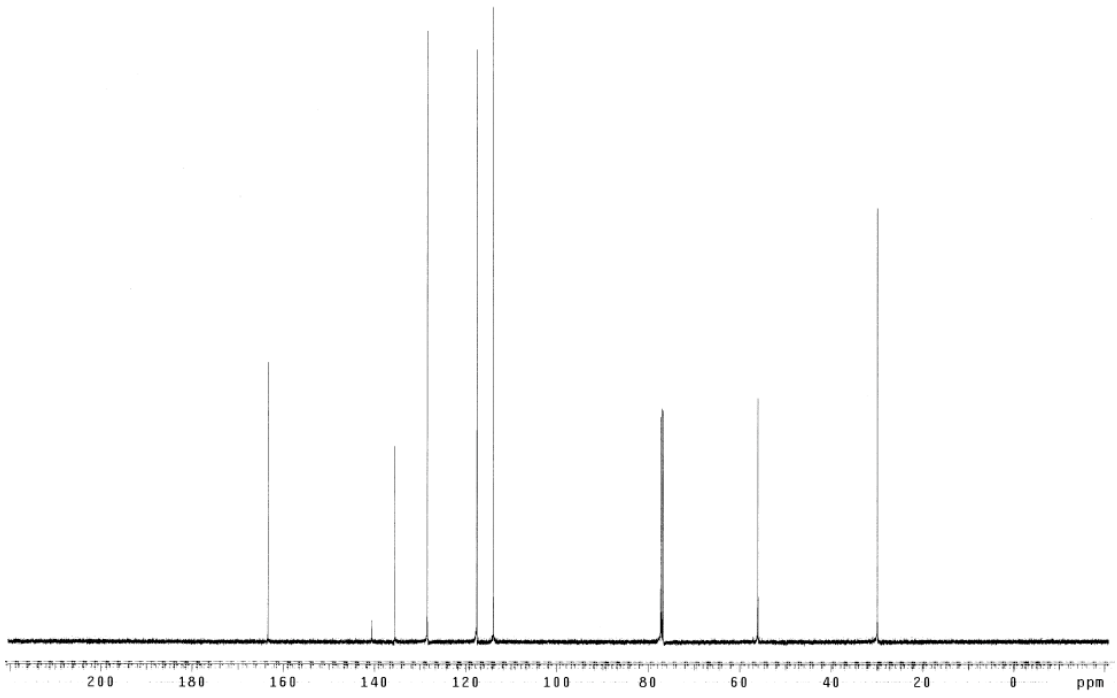

^{13}C NMR ($CDCl_3$)

5-Methoxy-2-nitrobenzyl azide (211)

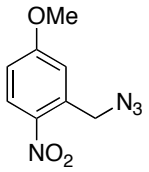

A solution of 5-methoxy-2-nitrobenzyl bromide **210** (280 mg, 1.14 mmol) and sodium azide (148 mg, 2.28 mmol) in DMF (2.0 mL) was stirred at 25 ºC for 16 h. The reaction was quenched with water (5 mL) and the aqueous layer was extracted with EtOAc (7 x 2 mL). The combined organic layer was dried over Na_2SO_4 and concentrated under the reduced pressure at 30 ºC. The residual material was purified by flash chromatography eluting with 100 % hexanes to 5 % EtOAc/hexanes to afford product as a colorless oil (177 mg, 75 %). R_f 0.6 (20 % EtOAc/hexanes). ^{1}H NMR (500 MHz, $CDCl_3$) δ 8.19 (d, 1H, J = 9.0 Hz), 7.13 (d, 1H, J = 3.0 Hz), 6.91 (dd, 1H, J = 9.0, 3.0 Hz), 4.89 (s, 2H), 3.93 (s, 3H); ^{13}C NMR (125 MHz, $CDCl_3$) δ 163.9, 140.2, 134.9, 128.1, 114.6, 113.2, 56.0, 52.4; MS (CI) m/z 209.0 $(M+H)^+$.

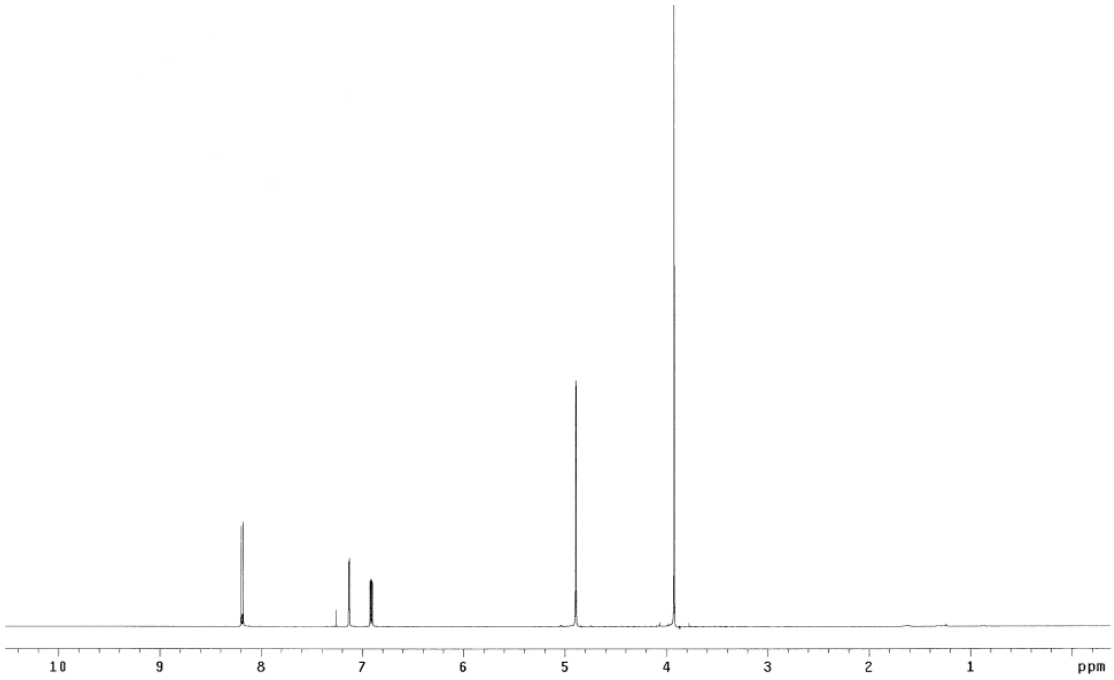

^{1}H NMR ($CDCl_3$)

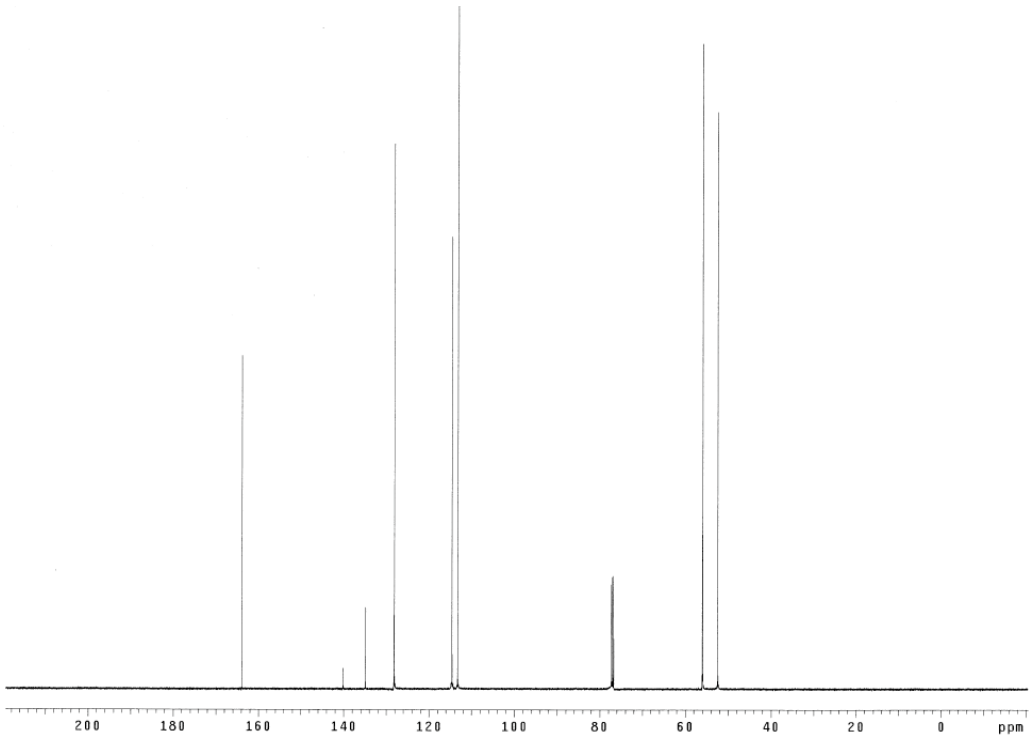

^{13}C NMR ($CDCl_3$)

Triazole derivative (212)

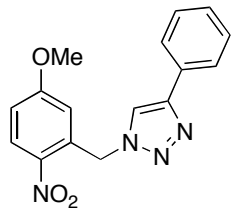

A solution of 5-methoxy-2-nitrobenzyl azide **211** (122 mg, 0.586 mmol), phenylacetylene (120 mg, 1.17 mmol), $CuSO_4$ (0.12 mL, 0.117 mmol, 1M in H_2O) and sodium ascorbate (1.46 mL, 2.93 mmol, 2 M in H_2O) in ^{i}PrOH (1.0 mL) was stirred at 25 ºC for 24 h in dark. Water (5 mL) was added to a reaction mixture and the aqueous layer was extracted with EtOAc (5 x 5 mL). The combined organic layer was dried over Na_2SO_4 and concentrated under the reduced pressure to afford pure product as an off-white solid (152 mg, 84 %). R_f 0.5 (40 % EtOAc/hexanes). ^{1}H NMR (300 MHz, $CDCl_3$) δ 8.23 (d, 1H, J = 9.3 Hz), 7.95 (s, 1H), 7.84 (d, 2H, J = 7.2 Hz), 7.46-7.32 (m, 3H), 6.94 (dd, 1H, J = 9.3, 2.7 Hz), 6.54 (d, 1H, J = 2.7 Hz), 6.01 (s, 2H), 3.81 (s, 3H); ^{13}C NMR (75 MHz, $CDCl_3$) δ 164.4, 148.5, 140.5, 134.1, 130.5, 129.1, 128.63, 128.59, 126.0, 120.9, 115.7, 114.2, 56.3, 51.8; MS (ESI) m/z 311.12 $(M+H)^+$.

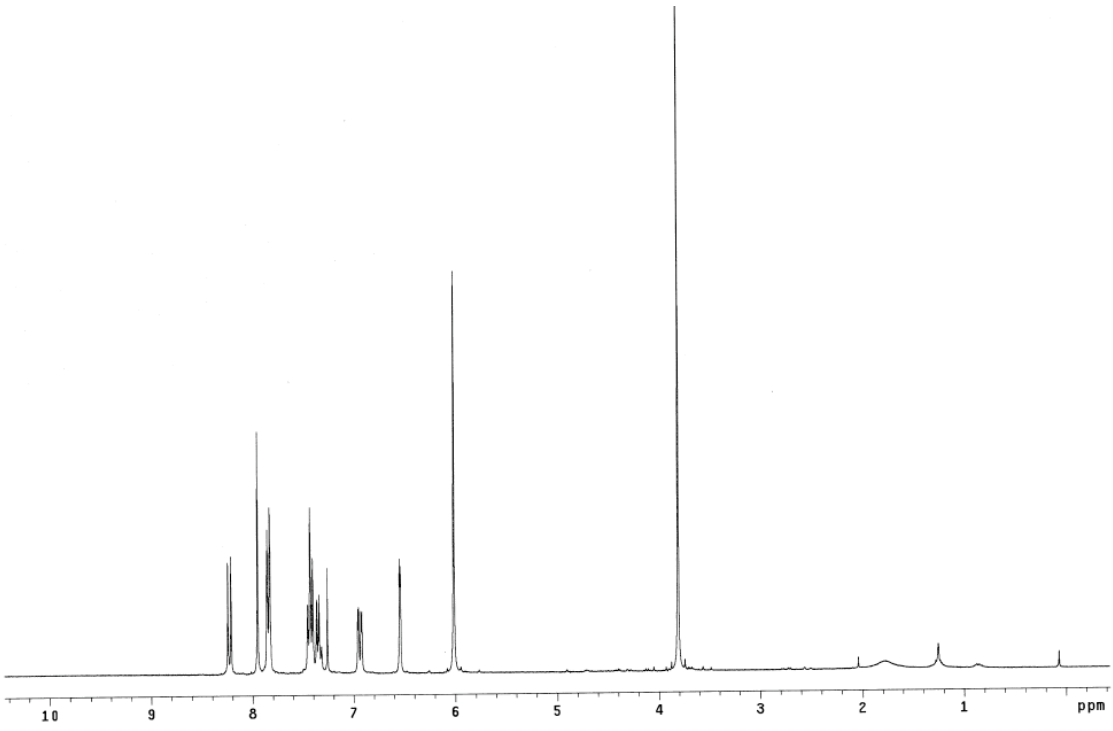

^{1}H NMR ($CDCl_3$)

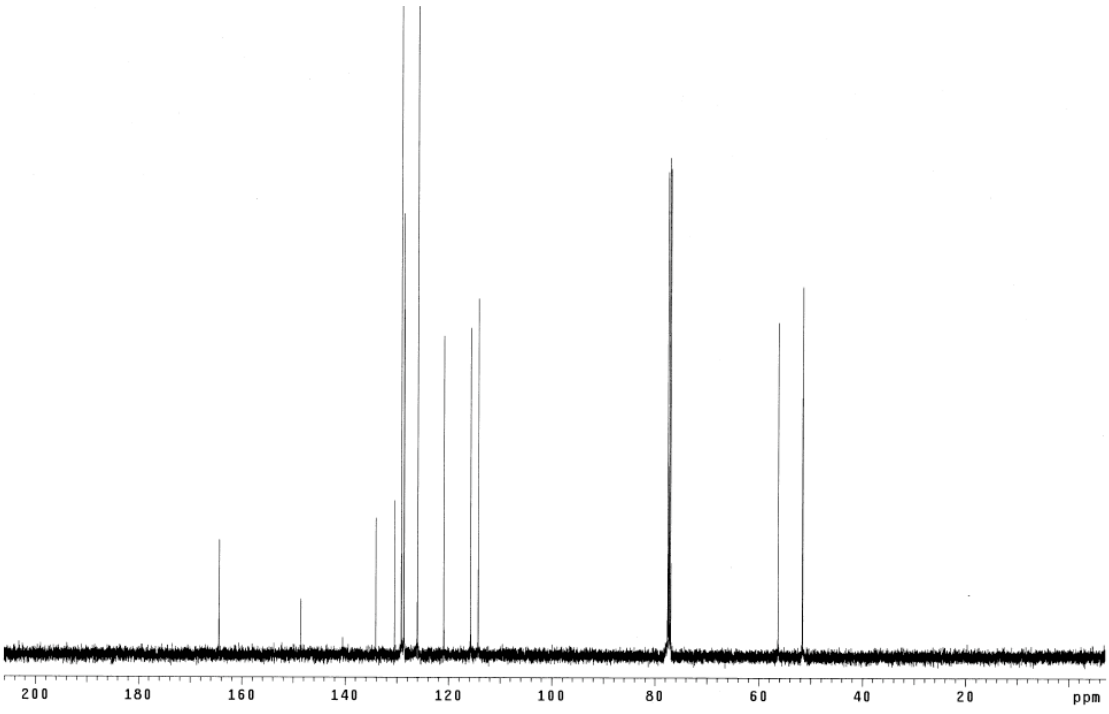

^{13}C NMR ($CDCl_3$)

Phenyl-triazole derivative (214)[173]

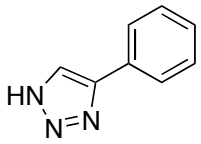

A solution of sodium azide (131 mg, 2.01 mmol) in DMSO (2.0 mL) was heated at 85 ºC. Then, a solution of *trans*-β-nitrostyrene (150 mg, 1.01 mmol) in DMSO (7 mL) was added dropwise over a period of 4 h. The reaction mixture was cooled to room temperature and water (10 mL) was added slowly. The aqueous layer was extracted with EtOAc (3 x 5 mL) and the combined organic layer was dried over Na_2SO_4 and concentrated under the reduced pressure. The residual material was purified by flash chromatography eluting with 100 % hexanes to 30 % EtOAc/hexanes to afford product as a colorless solid (119 mg, 82 %). R_f 0.5 (50 % EtOAc/hexanes). ^{1}H NMR (500 MHz, CD_3OD) δ 8.18 (s, 1H), 7.86 (d, 2H, J = 7.5 Hz), 7.48-7.45 (m, 2H), 7.40-7.37 (m, 1H); ^{13}C NMR (125 MHz, CD_3OD) δ 130.0, 129.5, 126.9 (3 carbons overlapping).

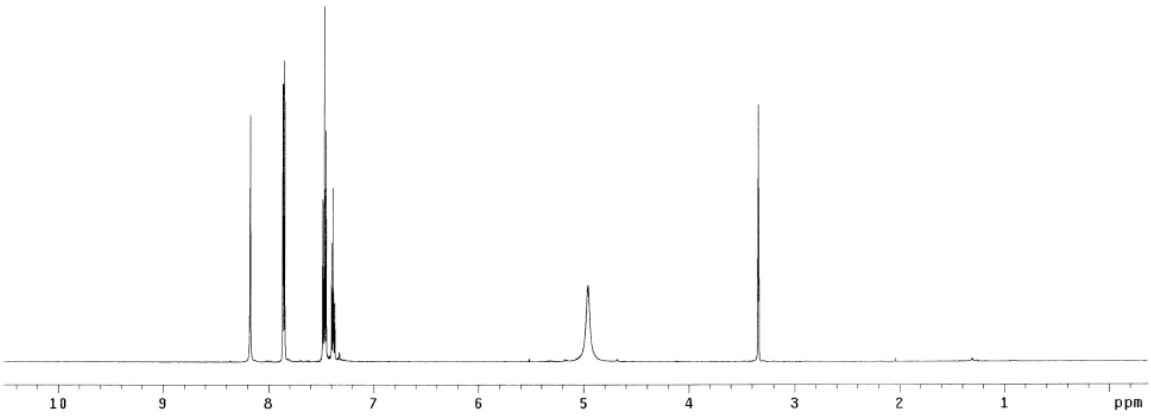

^{1}H NMR (CD_3OD)

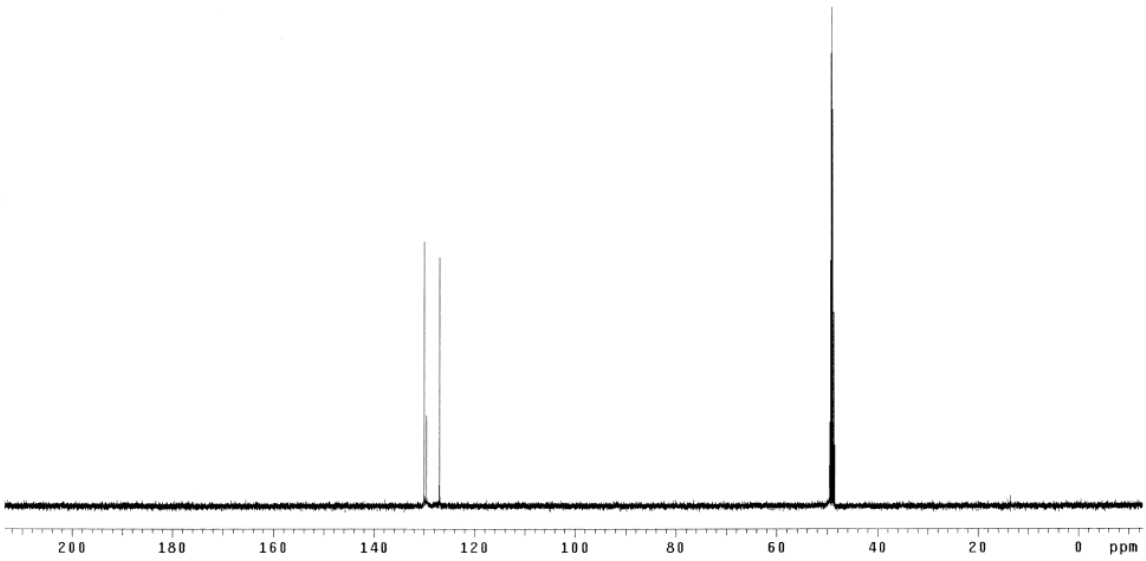

^{13}C NMR (CD_3OD)

VITA

Name:		Yuichiro Ueno
Permanent Address:		25-39 Suizenji Ko-en Kumamoto City, Kumamoto 862-0956, Japan
Education:	2002-2009	Ph.D., Chemistry, Texas A&M University College Station, TX, U.S.A.
	2000-2002	M.S., Chemistry, Fukuoka University Fukuoka City, Fukuoka, Japan
	1996-2000	B.S., Chemistry, Fukuoka University Fukuoka City, Fukuoka, Japan